Regulatory T cells in experimental solid organ transplantation

Thomas Chan

Green Templeton College



And

Nuffield Department of Surgical Sciences,

University of Oxford

A thesis submitted in partial fulfilment of the requirements for the degree of Doctor of Philosophy

2018

Acknowledgments

I would like to dedicate this thesis to the late Dr. Andrew Bushell who provided me invaluable guidance throughout this D.Phil.

I would like to thank Prof. Kathryn Wood for giving me the opportunity to work in the Transplantation Research Immunology Group and her constructive criticisms on my thesis draft.

I would like to thank Dr. Gang Feng who initially developed the IFN-γ conditioning protocol in which my thesis is founded; Dr. Joanna Hester for her guidance in the laboratory.

Dr. Lai Mun Wang at the Department of Cellular Pathology has been invaluable for advice on the histological analysis. I would also like to acknowledge Dr. Carolyn Carr, Dr. Rhys Evans and Professor Kieran Clarke for their collaboration with the *in vivo* magnetic resonance imaging work.

This work would not be possible without the financial support provided by the National Medical Research Council and the National Research Foundation in Singapore.

I would like to personally thank A/Prof. Henry Ho, Dr. Ng Lay Guat and A/Prof. Weber Lau in the Department of Urology at the Singapore General Hospital for allowing me to have the time-off for the completion of this thesis.

I would like to thank Prof. Chris Sauer for his guidance and support especially towards the submission of this thesis.

Family life in Oxford would not be more fruitful without my friendship with Gillian Kinnear, Karen English, Ryoichi Goto and Masaaski Zaitsu and their families. I would also like to thank Wallace Tan and Wayne Mooney for their constant support in the UK.

Finally, I would like give my gratitude to my family for their relentless support throughout my academic career.

Disclaimer

The experimental work was carried out at the Transplantation Research Immunology Group, Nuffield Department of Surgical Sciences, University of Oxford, between October 2008 and October 2012. Owing to unforeseen circumstances in relation to the return to full-time clinical training in Singapore, this thesis was written in 2018, which was 6 years after the completion of all experiments. I acknowledge that the application of the data presented in this thesis may have limited impact in the current rapidly-growing field in transplantation.

Thesis Abstract

Regulatory T cells in experimental solid organ transplantation

Thomas Chan, Green Templeton College, D.Phil. in Surgical Sciences,

Michaelmas Term 2018

Clinical transplantation outcome has been improved significantly over the last few decades by powerful immunosuppressive drugs. However, transplant recipients are subjected to non-specific immunosuppression, which increases the risks of malignancy, opportunistic infections, and drug associated toxicities. Alternative strategies that provide more selective immunosuppression are currently being investigated. The possibility of harnessing regulatory T cells as cellular therapeutic agents has been proposed based on the evidence obtained from a number of pre-clinical studies.

We have developed an *in vitro* protocol that could generate an enriched population of $CD4^+$ $Foxp3^+$ regulatory T cells (IFN-γ Treg) by stimulating $CD4^+$ T cells with allogeneic APC in the presence of exogenous IFN-γ. We found that these Treg could suppress alloresponses following adoptive transfer to immunodeficient, as well as immunocompetent hosts in the presence of a sub-optimal costimulation blockade treatment *in vivo*. When compared to Treg generated by other *in vitro* protocols, IFN-γ Treg appeared to be superior in their suppressive function on a cell-to-cell basis. Alloantigen-driven IFN-γ Treg prolong allograft survival in a dose-dependent manner. More importantly, Treg delivered prior to the transplant resulted in the induction of tolerance but they had no impact on graft survival when given post-transplant.

We demonstrated that IFN-γ Treg control alloresponses via the action of CTLA-4 and are partially dependent on IL-10 *in vivo*. Using an *in vitro* suppression assay, we showed that IFN-γ Treg controlled the proliferation of naïve $CD4^+CD25^-$ T cells *in vitro*. Tolerance was only partially reversed following the depletion of IFN-γ Treg suggesting that the persistence of IFN-γ Treg was not a prerequisite for the induction of tolerance long-term, but that tolerance was maintained via infectious tolerance *in vivo*. However, IFN-γ Treg were less efficacious in controlling memory responses in sensitized recipients compared to naïve hosts at a given cell dose.

IFN-γ Treg were more resistant to expansion in response to polyclonal or allogeneic stimulation in the presence of exogenous IL-2 compared to naturally-occurring Treg (nTreg) *in vitro*. However, at the same cell dose, IFN-γ Treg were more potent than freshly-isolated nTreg or expanded nTreg. Cryopreservation is a permissible solution to various logistic issues; however, Treg function could be discounted following the freeze and thaw processes. Activation status of Treg appeared to be crucially important for their suppressive function and we found that activated nTreg were equally effective in controlling allograft rejection in immunocompetent recipients as IFN-γ Treg, in the presence a sub-optimal costimulation blockade. Furthermore we developed a novel *in vivo* magnetic resonance imaging technique that provided a non-invasive method to assess graft function.

In conclusion, we propose that alloantigen-driven Treg are potential candidates as alternative to nTreg for controlling allograft rejection after transplantation.

Abbreviations

7AAD	7-Aminoactinomycin D
AICD	Activation induced cell death
ABMR	Antibody mediated rejection
AIRE	Autoimmune regulator
AP-1	Activing-protien-1 (AP-1)
APC	Antigen-presenting cells / Allophycocyanin
BM-APC	Bone marrow-derived antigen-presenting cells
BM-DC	Bone marrow-derived dendritic cells
CAV	Chronic allograft vasculopathy
CD	Cluster of differentiation
CFSE	Carboxyfluorescein diacetate succinimidyl ester
cLN	Contralateral lymph nodes
CNI	Calcineurin inhibitors
CO	Cardiac output
CP-1	CAMPATH-1H
CTLA-4	Cytotoxic T-lymphocyte-associated antigen-4
CTLA-4Ig	Cytotoxic T-lymphocyte-associated antigen-4 immunoglobulin fusion protein
DC	Dendritic cells
dLN	Draining lymph nodes
DMSO	Dimethyl sulfoxide
DSA	Donor specific antibody
DST	Donor-specific transfusion
ECG	Electrocardiogram
EDV	End diastolic volume

EF	Ejection fraction
ESV	End systolic volume
FACS	Fluorescence-activated cell sorting
FCS	Fetal calf serum
FDA	Food and drug administration
FITC	Fluorscein isothiocynate
Foxp3	Forkhead box protein 3
GFP	Green fluorescent protein
GITR	Glucocorticoid-induced tumour necrosis factor receptor family-related gene
GM-CSF	Granulocyte macrophage-colony stimulating factor
GMP	Good manufacturing practice
GVHD	Graft-versus-host disease
H2	Mouse histocompatibility system 2
HLA	Human leukocyte antigen
HR	Heart rate
IDO	Indoleamine-2,3-dioxygenase
IL	Interleukin
IFN-γ	Interferon-γ
IFN-γ Treg	Interferon-γ conditioned Treg
Ig	Immunoglobulin
iTreg	Inducible regulatory T cells
i.p.	Intraperitoneal
i.v.	Intravenous
IVC	Inferior vena cava
KI	Knock-in

LAG-3	Lymphocyte activation gene 3
LFA-1	Lymphocyte function-associated antigen 1
LPS	Lipopolysaccharide
mAb	Monoclonal antibody
MACS	Magnetic-activated cell sorting
mBM-DC	Mature bone marrow-derived dendritic cells
MHC	Major histocompatibility complex
MLR	Mixed lymphocyte reactions
MMF	Mycophenolate mofetil
MRI	Magnetic Resonance Imaging
MST	Median survival time
mTOR	Mammalian target of rapamycin
NFAT	Nuclear factor of activated T cells
NF-κB	Nuclear factor κB
NK	Natural killer cells
n.s.	Not statistically significant
nTreg	Naturally-occurring regulatory T cells
PA	Pulmonary artery
PB	Pacific blue
PBMC	Peripheral blood mononuclear cells
PBS	Phosphate buffered saline
PD-1	Programme cell death 1
PD-L1	Programme cell death ligand 1
PE	R-Phycoerythrin
Pe-Cy7	R-Phycoerythrin-Cyanine 7

PerCP	Peridin-chlorophyll-protein
PI	Proliferation index
PKC	Protein kinase C
PMN	Polymorph nuclear cells
PS	Palpation score
PTLD	Post-transplant lymphoproliferative disorders
PV	Pulmonary vein
RAG	Recombination activating gene
RPMI	Roswell Park Memorial Institute
RVCO	Right ventricular cardiac output
RVEDV	Right ventricular end diastolic volume
RVEF	Right ventricular ejection fraction
RVSV	Right ventricular stroke volume
s.c.	Subcutaneous
SD	Standard deviation
SV	Stroke volume
SVC	Superior vena cava
TCR	T cell receptor
TIM-3	T cell immunoglobulin and mucin domain 3
TGF-β	Transforming growth factor-beta
Tm	Memory T cells
TNF	Tumour necrosis factor
Treg	Regulatory T cells
TSDR	Treg-specific demethylated region
WT	Wild type

Table of contents

		Acknowledgements……..	**i**
		Disclaimer……	**ii**
		Thesis abstract……..	**iii**
		Abbreviations……	**iv-vii**
		Table of contents……	**viii-xviii**
Chapter 1		**Introduction**	**1**
1.1.		**Modern history of clinical solid organ transplantation**	**1**
	1.1.1.	*Transplantation Pioneers-the Nobel Prize laureates……*	**1**
	1.1.2.	*Immunosuppressive therapeutics era in transplantation…….*	**2**
	1.1.2.1.	*Preclude to calcineurin inhibitors……..*	**2**
	1.1.2.2.	*Current immunosuppressive drugs in transplantation……*	**4**
	1.1.2.3.	*Novel immunosuppressive drugs……..*	**5**
	1.1.2.4.	*Latest development of surgical management in transplantation……..*	**7**
1.2.		**Mechanisms of transplant rejection**	**10**
	1.2.1.	*Hyperacute rejection……*	**10**
	1.2.2.	*Acute rejection……*	**10**
	1.2.2.1.	*Innate immunity in allotransplantation……*	**10**
	1.2.2.2.	*Adaptive immune responses in allotransplantation……*	**13**
	1.2.2.2.1.	*Allorecognition……..*	**13**

	1.2.2.2.2.	*Alloreactive T cell activation*……..	**18**
	1.2.2.2.2.1.	*Signal 1-TCR activation*……..	**18**
	1.2.2.2.2.2.	*Signal 2-costimulation signals*……..	**18**
	1.2.2.2.2.3.	*Signal 3-CD4$^+$ T cell differentiation and proliferation*……	**20**
	1.2.2.2.3.	*Activation of CD8 T cells*……..	**24**
	1.2.2.3.	*T cell memory response*……	**24**
	1.2.2.4.	*Antibody-mediated rejection*……..	**27**
	1.2.3.	*Chronic allograft rejection*……	**28**
1.3.		**Immunological tolerance**	**30**
	1.3.1.	*Central tolerance*……..	**30**
	1.3.2.	*Peripheral tolerance*……..	**31**
	1.3.2.1.	*CD4$^+$CD25$^+$ Regulatory T cells*……..	**32**
	1.3.2.2.	*Foxp3 transcription factor and Treg*……	**33**
	1.3.2.3.	*Stability and plasticity of Foxp3$^+$ Treg*……	**35**
	1.3.2.4.	*Thymic development of naturally-occurring Treg*……	**38**
	1.3.2.5.	*Inducible Treg*……	**39**
	1.3.2.6.	*Contrasting between nTreg and iTreg*……	**40**
	1.3.2.7.	*Mechanisms of action of Treg*……..	**43**
	1.3.2.8.	*Latest development of immune checkpoint regulators in tolerance*……	**46**
	1.3.2.8.1.	*CTLA-4*……..	**46**
	1.3.2.8.2.	*Other immune checkpoint regulators*……	**47**

	1.3.2.8.3.	*Immune checkpoint regulators and oncology……..*	**48**
1.4.		**Harnessing Regulatory T cells as therapeutic agents in transplantation**	**49**
	1.4.1.	*First ex vivo generated Treg protocol……*	**50**
	1.4.2.	*First large scale human Treg expansion protocol……..*	**50**
	1.4.3.	*In vitro generated Treg using allogeneic APC as stimulators….*	**51**
	1.4.4.	*In vitro generated Treg with designated allospecificities…….*	**52**
	1.4.5.	*In vitro generated Treg suppress alloresponses in immunocompetent recipients……*	**53**
	1.4.6.	*Current development of Treg clinical trials in transplantation.*	**55**
1.5.		**Thesis Aims and Objectives**	**57**
Chapter 2		**<u>Materials and Methods</u>**	**58**
2.1.		**Experimental mice**	**58**
2.2.		**Experimental surgical procedures**	**60**
	2.2.1.	*Anaesthesia, analgesics and recovery from anaesthesia…….*	**60**
	2.2.2.	*Skin transplantation……*	**60**
	2.2.2.1.	*Donor mice……*	**60**
	2.2.2.2.	*Recipient mice……*	**61**
	2.2.3.	*Second skin graft transplantation……..*	**61**
	2.2.4.	*Heterotopic heart transplantation……*	**62**
	2.2.4.1.	*Donor mice……*	**62**

	2.2.4.2.	*Recipient mice*……	**63**
2.3.		**Experimental non-surgical procedures**	**65**
	2.3.1.	*Administration of pharmacological reagents*……	**65**
	2.3.2.	*Adoptive cell transfer*……	**65**
	2.3.3.	*Blood sampling*……	**65**
	2.3.4.	*In vivo generation of CD44^{hi} memory T cells*……	**66**
2.4.		***In vivo* Magnetic Resonance Imaging**	**66**
2.5.		**Organ/tissue harvest and histopathology examination**	**68**
	2.5.1.	*Spleen, lymph nodes*……	**68**
	2.5.2.	*Heart graft harvesting in heterotopic heart transplant recipients*……	**68**
	2.5.3.	*Skin graft harvesting in skin transplant recipients*……	**69**
	2.5.4.	*Histopathology*……	**69**
	2.5.4.1.	*Tissue frozen sections preparation*……	**69**
	2.5.4.2.	*Haematoxylin and Eosin staining protocol*……	**69**
	2.5.4.3.	*Elastin Van Gieson staining protocol*……	**70**
	2.5.4.4.	*Immunohistochemistry protocol*……	**70**
2.6.		**Reagents**	**72**
	2.6.1.	*Monoclonal antibodies*……	**72**
	2.6.2.	*Monoclonal antibody from culturing hybridomas*……	**75**
	2.6.3.	*Cytokines and growth factors*……	**75**
	2.6.4.	*Pharmacological agents*……	**76**

	2.6.5.	*Concanavalin A supernatant production……*	**76**
2.7.		**Cell isolation, purification and culture**	**77**
	2.7.1.	*Cell culture……*	**77**
	2.7.2.	*Single cell preparation……..*	**77**
	2.7.3.	*$CD4^+$ T cells enrichment protocol……..*	**78**
	2.7.4.	*$CD4^+CD25^+$ and $CD4^+CD25^-$ cell isolation protocol……..*	**78**
	2.7.5.	*Bone marrow cell isolation……..*	**79**
	2.7.6.	*Modulated BM-APC generation……*	**79**
	2.7.7	*Mature BM-DC generation……..*	**80**
	2.7.8.	*$CD11c^+$ and $CD11c^-$ BM-APC isolation……*	**80**
2.8.		***In vitro* alloantigen-driven Treg generation protocols**	**81**
	2.8.1.	*IFN-γ conditioning Treg generation protocol……*	**81**
	2.8.2.	*TGF-β/IL-2 Treg generation protocol……*	**82**
	2.8.3.	*Cliostamide Treg generation protocol……*	**82**
2.9.		**Cryopreservation of leucocytes**	**83**
	2.9.1.	*Freezing media for BM-APC……..*	**83**
	2.9.2.	*Freezing media for lymphocytes……..*	**83**
2.10.		***In vitro* Treg expansion protocol**	**83**
	2.10.1.	*Anti-CD3/CD28 bead-based protocol……*	**83**
	2.10.1.1.	*Invitrogen® protocol……*	**84**
	2.10.1.2.	*Miltenyi® protocol……*	**84**
	2.10.2.	*APC-based protocol……*	**85**

	2.10.3.	*Plate-bound antiCD-3/CD28 antibody-based protocol……*	**85**
2.11.		***In vitro* Treg activation**	**86**
2.12.		**Cell labeling with CFSE, PKH26, eFluor® 670 dyes**	**86**
	2.12.1.	*CFSE fluorescent dye……*	**86**
	2.12.2.	*PKH26 fluorescent dye……*	**87**
	2.12.3.	*eFluor® 670 cell proliferation dye ……*	**87**
2.13.		***In vitro* Treg suppression assay**	**88**
	2.13.1.	*Beads as stimulators……*	**88**
	2.13.2.	*Allogeneic BM-APC as stimulators……*	**88**
	2.13.3	*Proliferation index calculations……*	**89**
2.14.		**Flow cytometry**	**90**
	2.14.1.	*Cell surface staining……*	**90**
	2.14.2	*Intracellular staining (Foxp3, Helios, CTLA-4)……*	**90**
	2.14.3.	*Intracellular cytokine signaling (IL-10)……*	**91**
	2.14.4.	*Cell enumeration with counting beads……*	**91**
	2.14.5.	*FACS cell sorting……*	**91**
2.15.		**Statistical analysis**	**92**
Chapter 3		***In vitro* generated Regulatory T cells prolonged allograft survival in immunocompetent recipients**	**93**
3.1.		**Introduction**	**93**

3.2.		**Results**	**94**
	3.2.1.	**The IFN-γ conditioning protocol is a robust system that enriches for a dominant $CD4^+Foxp3^+$ alloantigen-experienced Treg population**.....	**94**
	3.2.2.	**IFN-γ Treg prevented skin graft rejection in an adoptive transfer model**.....	**97**
	3.2.3.	**Optimization of IFN-γ conditioning protocol**.....	**100**
	3.2.3.1.	*Enhancing alloantigen stimulation in the culture system*.....	**101**
	3.2.3.2.	*Increasing the overall cell density in the IFN-γ conditioning protocol did not improve quality or the quantity of the output Treg population*.....	**105**
	3.2.3.3.	*Phenotypic features of BM-APC affected by incubation in a 24-well plate versus a petridish*.....	**108**
	3.2.3.4.	*Differentiation status of allogeneic BM-APC altered by GM-CSF and TGF-β*.....	**112**
	3.2.3.5.	*Frozen BM-APC could be utilized as a single batch to reduce variation of IFN-γ protocol conversion rate*.....	**118**
	3.2.3.6.	*$CD11c^+$ BM-APC were not essential for the enrichment for $Foxp3^+$ IFN-γ Treg*.....	**126**
	3.2.4.	**Rationale of using adjunctive immunosuppressive therapy in immunocompetent recipients**.....	**129**
	3.2.5.	**Treg therapy in combination with a sub-optimal abatacept regimen prevent allograft rejection in immunocompetent mice**.....	**133**
	3.2.6.	**IFN- γ Treg dosing strategies**.....	**138**

	3.2.6.1.	*Graft protection manifested in a dose-dependent manner…..*	**138**
	3.2.6.2.	*Timing of IFN-γ Treg delivery critically affected graft outcome……..*	**144**
	3.2.7.	**Comparison between IFN-γ Treg and adaptive Treg generated by other established protocols**……	**149**
3.3.		**Discussion**	**154**
Chapter 4		**Suppression of allograft rejection by *in vitro* generated Treg - Mechanisms of action**	**160**
4.1.		**Introduction**	**160**
4.2.		**Results**	**162**
	4.2.1.	**IFN-γ Treg mediated suppression of alloresponses through CTLA-4**……	**162**
	4.2.2.	**IFN-γ Treg mediated suppressive function partially dependent on the IL-10-IL-10R pathway**……	**167**
	4.2.3.	**IFN-γ Treg suppressed the proliferation of alloreactive effector T cells *in vitro***……	**172**
	4.2.4.	**Persistence of infused IFN-γ Treg was essential to maintain dominant suppression via infectious tolerance**……	**191**
	4.2.5.	**Treg therapy was less effective in controlling memory responses *in vivo***……	**218**
4.3.		**Discussion**	**223**
Chapter 5		**Expansion of regulatory T cells**	**228**

5.1.		**Introduction**	**228**
5.2.		**Results**	**230**
	5.2.1.	**Expansion of IFN-γ Treg**……..	**230**
	5.2.1.1.	*Expanding IFN-γ Treg with anti-CD3/28 antibody-conjugated beads*……..	**230**
	5.2.1.2.	*Expansion of IFN-γ Treg using allogeneic mature BM-DC*……..	**246**
	5.2.1.3.	*Expansion of IFN-γ Treg using other potential T cell proliferation stimuli*……..	**251**
	5.2.1.4.	*Expansion of cryopreserved IFN-γ Treg with anti-CD3/CD28 beads plus rapamycin*……..	**255**
	5.2.1.5.	*Expansion of cryopreserved IFN-γ Treg with mature BM-DC…*	**259**
	5.2.1.6.	*Ultra-purification of Foxp3$^+$ IFN-γ Treg*……..	**262**
	5.2.1.7.	*Cryopreserved IFN-γ Treg retained Foxp3 expression and suppressive function in vivo*……..	**269**
	5.2.2.	**Revisiting CD4$^+$CD25$^+$ nTreg**……..	**276**
	5.2.2.1.	*Freshly-isolated CD4$^+$CD25$^+$ nTreg*……..	**276**
	5.2.2.2.	*Expansion of nTreg using anti-CD3/CD28 antibody-conjugated beads*……..	**282**
	5.2.2.3.	*nTreg expansion incorporated with other 'Treg-favourable soluble growth factors'*……..	**286**
	5.2.2.4.	*Expansion of MACS-isolated versus FACS-sorted nTreg*……..	**292**
	5.2.2.5.	*Expansion of doubly-sorted nTreg*……	**297**

	5.2.3.	**Treg expanded efficiently using a plate-bound anti-CD3/28 antibody protocol**……	**303**
	5.2.4.	**Suppressive function of expanded nTreg *in vivo***……..	**316**
	5.2.5.	**Activation alone could fully equip nTreg to function *in vivo***..	**320**
5.3.		**Discussion**	**342**
Chapter 6		**Novel bio-imaging for the evaluation of graft outcome**	**350**
6.1.		**Introduction**	**350**
6.2.		**Results**	**351**
	6.2.1.	**Magnetic resonance imaging in experimental heterotopic heart transplantation**……..	**351**
	6.2.2.	**Rationale of non-invasive graft assessment technique**…….	**352**
	6.2.3.	**In vivo MRI experimental set up**……..	**353**
	6.2.4.	**Pilot in vivo MRI of heterotopic heart allograft** …….	**360**
	6.2.5.	**IFN-γ Treg therapy preserved right ventricular function of allograft in a dose-dependent manner**……	**371**
	6.2.6.	**IFN-γ Treg therapy preserved right ventricular function of allograft when delivered at optimal timing**……..	**382**
	6.2.7.	**Comparison in vivo MR imaging versus traditional histopathological assessment of graft outcome**……	**394**
	6.2.7.1.	*Haematoxylin and Eosin staining*……..	**394**
	6.2.7.2.	*Chronic allograft vasculopathy*……	**397**
	6.2.7.3.	*Immunohistochemistry*……..	**400**

6.3.	**Discussion**	**408**
Chapter 7	**General Discussion**	**410**
Chapter 8	**Conclusion**	**422**
Chapter 9	**References**	**423**

Chapter 1 Introduction

1.1 Modern history of clinical solid organ transplantation

1.1.1 Transplantation Pioneers- the Nobel Prize laureates

Transplantation of organs, in terms of an autograft (self), homograft (non-self same species) or even xenograft (different species) has been documented dating back in ancient history according to various manuscripts and paintings[1]. However, the era of modern transplantation only began in the early twentieth century after a number of pioneer transplant surgeons succeeded in pursuing what was once regarded as an impossible task[2]. Alexis Carrel earned his Nobel Prize in 1912 for his work on vascular anastomosis suturing technique, which not only revolutionized clinical surgery but also laid down the foundation for transplant surgery[3]. Since then, extensive work on experimental transplantation was carried out, which showed that autografts were accepted, but without much success in transplanting allografts (homografts donated from genetically distinct human individuals). In 1933 Yuri Yurijevich Voronoy performed the first human-to-human cadaveric kidney transplantation, but because of the long organ retrieval time and transplantation across a mismatched blood group the graft was rejected promptly[4]. Interestingly, pathology assessment of the rejected allograft revealed that the donor renal vessels were patent suggesting that graft failure was not simply due to a technical failure. In the 1950s, René Küss pioneered the technique of extraperitoneal implantation of kidney allografts by anastomosing their vascular supply to the iliac vessels in the pelvis and an uretero-neocystostomy for urine drainage, which still remains the standard procedure[5].

The immunological basis of organ transplantation came to light stemming from the seminal studies of transplants between genetically identical and dispared individuals. The unique

anatomical features in fraternal twin cows first described by John Hunter[6], and later by Frank Lillie[7] and Ray Owen[8], who collectively suggested that the placental circulation allows the transfer of haematopoietic leucocytes between them *in utero*. The development of chimerism in these animals, thus the co-existence of two genetically distinct haematopoetic populations had important implications in graft acceptance. This chimerism persisted in their adulthood, which prevented the rejection of homografts transplanted between fraternal twins. Inspired by these findings, Peter Medawar tested the hypothesis that tolerance could be acquired in early life *in vivo*. Their group provided the first experimental evidence that fetal mice inoculated with donor-specific tissues *in utero* led to the tolerance of donor tissues as well as donor-specific skin graft transplanted later in adulthood.[9]. Their work in tolerance was rewarded with the award of the Nobel Prize to Peter Medawar in 1960 and it has become the landmark study of transplantation immunology. One year later, the breakthrough in clinical transplantation finally emerged as the first successful kidney transplant in humans between two genetically identical twins was carried out by Joseph Murray[10,11], who subsequently received the Nobel Prize for his contribution in Medicine.

1.1.2 Immunosuppressive therapeutics era in transplantation

1.1.2.1 Preclude to calcineurin inhibitors

The second important milestone of modern clinical transplantation was the beginning of the immunosuppressive therapeutics era[12]. Extrapolating from the use of radiation therapy in malignant diseases, the initial experience with total body irradiation indicated that while allograft survival could be modestly extended in unmodified recipients, it was often associated

with a significant acute post-radiation syndrome[13]. Fractionated or unfractionated total lymphoid irradiation had also been used in combination with corticosteroids as an adjunct therapy post-transplantation[14-16]. However, this cumbersome modality of treatment has been superseded by highly efficacious pharmacological immunosuppressive drugs. 6-mercaptopurine (6-MP), an anti-proliferative drug was first shown to delay allograft rejection modestly in transplant models[17,18], but its analogue-azathioprine appeared to be a more promising candidate which extended allograft survival significantly, when combined with prednisolone[19]. Around the same time, anti-lymphocyte serum (ALS) was developed as another permissive adjunct immunosuppressive therapy[20], which paved the way for future antibody-based immunosuppressive agents. The striking discovery of cyclosporine, a calcinerin inhibitor, revolutionized the clinical transplantation of kidneys and other organs[21-23]. However, its narrow therapeutic window, intrinsic nephrotoxicity, risks of development of lymphomas and other malignancies, cardiovascular and metabolic diseases, and opportunistic infections have baffled many clinicians in the post-operative care of transplant patients. Nevertheless, due to its efficacy, numerous transplant centres around the world adopted cyclosporine as the chief immunosuppressive drug [24]. Solid organ transplantation has since become the treatment of choice for many end-stage organ diseases.

1.1.2.2 Current immunosuppressive drugs in transplantation

Newer immunosuppressive agents have been developed and approved since the mid-90s. Combination immunosuppressive therapies have been employed as a strategy with the aims of achieving optimal graft outcome and minimizing adverse drug reactions at the same time. In addition, drug substitution or 'drug minimization' has also been developed, for example early withdrawal of corticosteroids being the strategy to reduce systemic steroidal side-effects[25,26]. Tacrolimus (FK506), a new member of calcineurin inhibitors (CNI) appeared to be superior to cyclosporine in terms of graft outcome and patient survival in various organ transplant settings, but inferior to cyclosporine in terms of side-effect profiles according to several systematic reviews and meta-analyses[27-31]. Similarly, mycophenolate mofetil (MMF), a new anti-proliferative drug was shown to be superior to azathioprine in terms of its efficacy, however, with a balance of side-effect profiles[32-35]. Mammalian target of rapamycin (mTOR) inhibitors such as rapamycin (sirolimus) and everolimus have also been compared with standard CNI and MMF. mTOR inhibitors were shown to have a comparable clinical outcome and a lower incidence of *de novo* malignancies, but they have been associated with a higher rate of metabolic and wound complications[36-42]. Induction ablative therapies using anti-CD25 monoclonal antibody (basiliximab and daclizumab), anti-thymocyte globulin and more recently, alemtuzumab (CAMPATH-1H) have been implemented to provide maximal immunosuppressive effects with the greatest impact at the time of transplantation in order to prevent acute rejection in the hope of reducing the dose or withdrawal of certain drugs in due course depending on the individual patient's risk profiles for rejection[43-47].

Technological advances in the detection of anti-human leukocyte antigen (HLA) antibodies provided the opportunity to pre-treat highly-sensitized recipients in anticipated HLA/ABO-incompatible transplantation, or to treat new onset of acute and chronic antibody-mediated rejection (ABMR) in the form of bortezomib[48], rituximab (anti-CD20 monoclonal antibody)[49,50], intravenous immunoglobulin (IVIG)[51] and plasmaphoresis[52-54].

Despite the rapid development of immunosuppressive agents in the last few decades, their pan-immunosuppressive action increases the risk of the development of opportunistic bacterial, viral, fungal and parasitic infectious diseases[55-57], de novo malignancies[58,59] and post-transplant lymphoproliferative disorders (PTLD)[60]. Immunosuppressive drugs can also lead to significant long-term morbidities secondary to cardiovascular and metabolic complications[61,62]. Patients' non-compliance to medication is often related to drug adverse effects. Changes of dosages, drug formulations and therapeutic drug monitoring tools have been proposed to improve patients' adherence to therapy, which will have a definitive impact on long-term graft outcome[63-69].

1.1.2.3 Novel immunosuppressive drugs

More recently, novel classes of immunosuppressive therapeutics have been tested in preclinical studies and are now being investigated for their roles in clinical transplantation[70,71]. A new CNI-voclosporin (ISA 247) was designed to possess enhanced potency and a lower drug metabolite load. Voclosporin has been shown to be non-inferior to tacrolimus in terms of acute rejection rates and a lower rate of new onset of diabetes in a phase II study[72]. With the new

understanding of the molecular pathways involving mTOR1 and mTOR2 complexes, new mTOR kinase inhibitors with strong activities against both complexes are being investigated[73].

Agents that block the costimulation pathway for T cell activation and proliferation have been studied extensively in the last two decades and they have been envisaged to have a very promising translational potential in clinical transplantation [74-76]. Belatacept (LEA29Y) is a second generation of Cytotoxic T-lymphocyte-associated protein 4 Immunoglobulin (CTLA-4 Ig), which consists of a fusion protein of the humanized CTLA-4 domain that blocks the costimulatory signals between CD80/CD86 (also known as B7.1/B7.2) and CD28 on APC and T cell, respectively. The BENEFIT trials demonstrated a significant impact of belatacept in patient survivals, as well as long-term graft function compared to cyclosporine-based protocols[77-81]. Of interest, the unexpected increased rate of significant acute rejection seen in the high-dose intensity arm of belatacept has sparked new investigations to revisit the complex costimulatory pathways[82,83]. ASKP1240, a costimulation blockade agent of the CD40-CD40Ligand (CD154) pathway which has completed a phase I trial recently showed limited toxicities[84].

Eculizumab is a monoclonal antibody which inhibits complement activation and in turn suppresses antibody responses. Only a few case studies demonstrated that eculizumab could attenuate ABMR[85-87].

YSPSL (rPSGL-Ig) is composed of the fusion of a humanized P-selectin domain and immunoglobulin that acts by blocking the adhesion of leukocytes and reduces ischaemic-reperfusion injury. A recent phase II trial, however, showed that there were no differences in the incidence of patients requiring dialysis secondary to delayed graft function between the treatment group and the placebo control[88].

A few promising therapeutic agents initially showed good results *in vivo* but have failed to advance beyond phase II trials. Sotrastaurin (AEB071) is a protein kinase C inhibitor of the signal transduction pathway for T cell activation and proliferation. The initial experience of this drug in phase II trials showed increased rates of rejection in the sotrastaurin arm of the studies rendering the premature termination of the trials[89-91]. Tofacitinib (CP-6905501) is another signal transduction pathway inhibitor which acts to inhibit interleukin-2 (IL-2)-driven T cell proliferation via JAK (Janus kinases). It demonstrated promising results in preventing acute and chronic rejection, however, it was associated with a higher risk of serious viral infections, haematological toxicities and PTLD[92,93]. Efaluzimab is a monoclonal antibody that binds to LFA-1 (lymphocyte function-associated antigen 1) for the inhibition of leukocyte migration. A phase I/II trial showed that it caused a higher incidence of PTLD compared to standard treatment arms, but more importantly, because of its association with progressive multi-focal leukoencephalopathy (PML) it has since been withdrawn[94,95]. Alefacept is a fusion of humanized LFA-3 domain costimulation inhibitor of CD2, which completed a phase II study in renal transplant. It was found to have higher rate of *de novo* malignancies compared to standard treatment and it has since been withdrawn by the manufacturer in 2011.

1.1.2.4 Latest development of surgical management in transplantation

Long-term graft outcome has not changed significantly over the last few decades despite the development of these immunosuppressive agents. However, a small number of patients achieved operational tolerance after a period of time in which immunosuppressive agents could

be withdrawn; up to 8% and 20% in kidney and liver transplantation respectively[96-98]. By exploiting this platform, it provides an invaluable opportunity not only to study the mechanisms of tolerance but it also provides important clinical information with regards to the tolerant state. In order to optimize immunosuppressive therapeutics for individualized immunosuppressive regimens, to predict rejection episodes and to define the state of operational tolerance for withdrawal of drugs, investigators have been looking at biomarkers as a means of a non-invasive method to survey the immunological status of transplant recipients[99-107].

Surgical management in transplantation has improved significantly on the backbone of a multi-disciplinary approach. Advanced molecular technology enables optimal HLA-matching between organ donors and potential recipients registered in different transplant centres across a large geographical area[108]. DNA-based molecular tissue typing and solid-phase immunoassays (Luminex technique) have superseded traditional cell-based serological assays and mixed-lymphocyte reactions (MLR). Complex alloantibody profiles can be detected using current methodology that enables clinicians to stratify risk of rejection in potential recipients and to prescribe pre-transplant conditioning regimen in sensitized patients appropriately[109]. Revised organ procurement procedures and preservation technique, as well as pre-operative recipient conditioning and various induction protocols have gained important ground in the pre-operative management of transplant patients[110,111].

In terms of surgical procedures, the basic surgical principle of transplant surgery has not changed dramatically over the years. However, surgical skills and modern technology has improved the standard of living donor organ surgery in which the warm ischaemia time has greatly reduced in laparoscopic donor nephrectomy, which benefits both donor and the

recipients[112]. Indeed, the contemporary long-term graft survival of living donor renal transplantation has reached 90% at 5 years and 80% at 10 years in comparison to 87% and 77% in deceased donor renal transplants in the UK[113]. More recently, robotic-assisted laparoscopic nephrectomy/kidney implantation has also gained debatable attention[114,115].

Post-operatively, renal transplant patients usually undergo speedy recovery because of a combination of effort from a team of nephrologists, specialist nurses, pharmacists, physiotherapists and transplant coordinators. Furthermore, improved radiological expertise and imaging technique, as well as safety of image-guided biopsy protocols aid to diagnose acute rejection promptly and allow timely treatment[116].

Major clinical advances over the last few decades have made transplantation of kidney, liver, heart and lung the treatment of choice of terminal organ failure. More complex transplant procedures have been reported including composite transplantation of face and limbs in recent years[117,118]. With much progress in clinical transplantation, more scientific questions have been generated and the drawing board has been geared back towards the study of the mechanisms of rejection and tolerance and to search for tools in achieving the holy-grail in transplant immunology.

1.2 Mechanisms of transplant rejection

1.2.1 Hyperacute rejection

Transplant rejection is conventionally classified into hyperacute, acute and chronic rejection according to the tempo of rejection episodes that occur following surgery. Hyperacute rejection occurs within minutes of establishing perfusion of the allograft. The mechanisms of hyperacute rejection are often related to ABO blood group incompatibility or the presence of pre-formed anti-donor HLA antibodies in sensitized recipients. These antibodies are capable of activating the complement system efficiently and trigger the secretion of Von Willebrand factor from endothelial cells. Platelet aggregation and activation of the coagulation cascade ultimately then lead to intravascular thrombosis[119]. Rapid graft loss occurs intraoperatively as evident by the presence of macroscopic ischaemic features promptly after revascularization is completed. Hyperacute rejection is now a rare clinical entity because of advanced pre-operative matching and treatment, however it occurs in untreated recipients in xenotransplantation because of the recognition of αGal antigens across phylogenentically different species[120].

1.2.2 Acute rejection

1.2.2.1 Innate immunity in allotransplantation

Acute rejection occurs between days and months following transplantation. Alloantigen-specific mechanisms elicited by the adaptive immune system play a crucial role in acute graft rejection. However, the first level of defense - the innate immune system, cannot be overlooked. The innate immune system reacts in an alloantigen-non-specific fashion and it has been linked to the

initiation of the adaptive immune response. A brief summary of these pathways is outlined below.

Secondary to surgical stress, trauma, ischaemia-reperfusion injury and infection, a 'danger signal' is triggered and DAMPs (damage associated molecular patterns) /PAMPs (pathogen associated molecular patterns) are released[121]. In the context of transplantation, these chemical mediators are recognized by toll-like receptors (TLR) which belong to a family of pattern-recognition receptors expressed by donor passenger leukocytes, such as dendritic cells (DC). The activation of donor DC and other antigen-presenting cells (APC) triggers the upregulation of costimulatory signals and the secretion of pro-inflammatory cytokines in the local microenvironment. Mature donor APC then migrate to recipient's secondary lymphoid tissue and activate naïve T cells. Ultimately, the graft is infiltrated with activated alloreactive $CD4^+$ and $CD8^+$ T effector cells, and other effectors of the innate immune system such as macrophages and polymorph nuclear cells (PMNs) that mediate graft damage.

Macrophages may be activated and differentiate into classically-activcated or alternatively-activated subsets which enage in different aspects in transplant rejection. Upon activation via IFN-γ and TLRs, M1 macrophages (classically-activated macrophages) mediate proinflammatory responses in ischaemic reperfusion injury, acute rejection and chronic rejection via the secretion of a variety of inflammatory mediators such as TNF-α, IL-1 and IL-6. M2 macrophages (alternatively-activated macrophages), on the other hand, have been shown to possess immune regulatory properties. In the presence of IL-10, M2 macrophages mediate anti-inflammatory action. Interestingly, this phenotypic differentiation has been shown to be plastic. Thus, depending on the context in which macrophages encounter either proinflammatory or anti-inflammatory pathyway will be activated[122].

The recruitment of immune cells to the site of action is mediated by the expression of chemokines and their corresponding receptors. CCR5 and CXCR3 are implicated in both acute and chronic rejection[123]. A combination of CCR5 and CXCR3 blockade was shown to be able to prolong allograft survival long-term *in vivo*[124,125]. The complement system is also activated following ischaemia-reperfusion injury and the release of DAMPs and PAMPs, which in turn activate DC to promote antigen processing and presentation for T cell immunity.

The activated complement cascade modulates alloreactive T cell activation and differentiation and contributes to the activation of alloreactive B cells which promotes allograft rejection[126]. Three complement pathways could be activated: classical, alternative and lectin pathway which converge to a final common pathway that ultimately leads to membrane attack complex (MAC) that causes cytotoxicity. Besides, soluble and split proteins associated with the complement cascade have been well documented to be involved in chemoattraction, opsonization of antibodies and activation of macrophages and neutrophils[126,127]. Blocking the upstream activation of the complement system using a C1 esterase inhibitor was shown to dampen inflammatory responses in an ischaemia-reperfusion model[128]. An anti-CD5aR antibodies such as eculizumab ***(Chapter 1.1.2.3)***, were shown to be able to delay graft rejection *in vivo*[129,130]. More recently, blockade of C3aR and C5aR have been shown to be implicated in the modulation of regulatory T cell function[131,132]. Complements are responsible for the production of alloantibody *in vivo*[133] and an anti-C5 convertase antibody has been shown to reduce the incidence of ABMR[85].

The implication of Natural Killer (NK) cells in transplantation has attracted much attention recently because of the new understanding of the role of NK cells in both acute and chronic ABMR. NK cells are important components of the innate immune system that recognize self and

non-self via their activating and inhibitory receptors specific to MHC Class I molecules. The absence or a suboptimal self-MHC class I recognition, NK cells are activated which leads to their release of proinflammatory cytokines that mediates antibody-dependent cellular cytotoxicity (ADCC) against target cells, also known as the 'missing self'mechanism of which NK cells discriminate self and non-self. On the other hand, the interaction between the inhibitory receptors and self-MHC class I molecules prevents such autoimmune responses in normal circumstances [134]. In the transplant setting, as circulating NK cells encounter an allograft which lacks self-MHC molecules this leads to the disinhibition of their inhibitory killer cell immunoglobulin-like receptors (iKIR), which in turn activates NK cells to exert their cytotoxic action against non-self tissues[135]. Activated NK cells against allograft produce cytotoxic effector molecules such as granzyme A and B and IFN-γ that mediate rejection, bypassing allorecognition pathways requiring APC and lymphocytes.

1.2.2.2 Adaptive immune responses in allotransplantation

1.2.2.2.1 Allorecognition

Lymphocytes have been known to be involved in rejection processes since the 1930s. Although Medawar et al showed that there was a possibility to acquire tolerance experimentally[9], the intrinsic humoral or cellular immune mechanisms involved in either rejection or tolerance were not described in any detail at that time. We now understand that both T and B cells play a critical role in the mechanisms of alloantigen-specific rejection. Moreover, following the identification of the major and minor histocompatibility complex genes in mice[136-139] and

humans[138], we began to understand the intricate mechanisms of allorecognition better[140,141].

Alloantigens can be recognized by T cells by three non-mutually exclusive mechanisms: direct, indirect and the semi-direct pathways[142,143]. In the direct pathway ***(Figure 1.2.2.2.1.i)***, T cells bearing allospecific T cell receptors (TCR) recognize intact MHC (major histocompatibilty complex) molecules or MHC-peptide complexes on donor passenger APC which have migrated to secondary lymphoid organs. This pathway is often linked to acute rejection because of the availability of donor derived passenger leukocytes in early stage of transplantation. Both $CD4^+$ and $CD8^+$ T allospecific T cells may be activated via the direct allorecognition pathway. Pietra et al showed that immunodeficient mice would not reject heart allografts unless they were transplanted with allografts lacking MHC class II molecules, demonstrating that $CD4^+$ T cells with direct allospecificity are important in mediating acute rejection[144]. In fact, in these situations where $CD8^+$ cells and indirect allorecogntion were absent, it demonstrated that the direct allorecogition pathway alone could lead to graft rejection. The high determinant density and the multiple binary complex model suggest that both allo-peptide and allo-MHC molecules drive direct allorecognition, which results in a high precursor frequency of T cells with direct allospecificity in an individual[143,145]. The high determinant density theory describes that alloreactive T cells recognize polymorphisms in the allogeneic MHC molecules directly, whereas the multiple binary complex model describes the recognition of the presented peptide in the MHC-peptide binding groove. As a result, a polyclonal T cell response is triggered causing acute allograft rejection.

The indirect pathway ***(Figure 1.2.2.2.1.ii)*** involves alloantigens being processed and presented as short peptides in the context of recipient MHC class I or II molecules to alloreactive $CD8^+$ and $CD4^+$ T cells, respectively. Following transplantation, foreign cellular materials and donor MHC molecules may be phagocytosed by recipient APC. These processed donor peptides are presented to allorective T cells by recipient APC in a self-MHC restriction fashion. Lechler et al showed that allosensitization occurred in the absence of donor passenger leukocytes, which was restored after the introduction of donor APC[146,147]. Benichou et al later confirmed that alloreactive T cells reacted to allogeneic MHC peptides presented by host's APC using a skin graft model[148]. Unlike the direct pathway, the indirect pathway has been proposed to be involved in chronic allograft rejection given the time taken for donor antigen processing and presentation and diminished number of passenger leucocytes over time. However, it has been shown that in the absence of a direct response, the indirect pathway alone can also result in acute rejection[149].

The third allorecognitiion pathway-the semi-direct pathway has been proposed for many years with the speculation that cell-to-cell contact between donor and recipient APC could lead to transfer of allo-MHC molecules ***(Figure 1.2.2.2.1.iii)***. It has been found that the acquisition and transfer of MHC molecules from donor APC to recipient APC could lead to T cell allorecognition of 'cross-dressing' of MHC class I and class II molecules *in vivo*[150]. Lechler's group demonsrated that recipient cells have the ability to acquire donor MHC molecules that present and activate allospecific T cells[151]. It has been described as recipient APC present intact or processed donor MHC molecules to both alloreactive $CD4^+$ and $CD8^+$ T cells. Several mechanisms of the transfer of MHC molecules have been proposed: 1) secreted exosomes that bear MHC

molecules derived from donor APC could be processed and presented by recipient APC[152]; 2) released exosomes are transported to the secondary lymphoid tissues where donor MHC molecules are fused directly with recipient APC[153]; 3) direct molecule transfer between donor and recipient APC can also occur, thus the acquisition of donor MHC by recipient APC[154]. More recently, Harper et al showed that a CD8 response could be generated by the semi-direct pathway. Allografts lacking APC were rejected in a recipient secondary lymphoid tissue-dependent manner. Recipient DC acquire MHC from the allograft and present as intact MHC molecules to $CD8^+$ T cells and present processed alloantigens to $CD4^+$ T cells via the indirect pathway at the same time. This provides the T cell help from $CD4^+$ to $CD8^+$ T cells for their effector function[155]. Morelli et al demonstrated the presence of recipient DC which captured donor MHC and APC costimulatory signals located in the drainng lymphoid organs in transplant recipients. Despite the lack of abundant passenger leucocytes, a strong alloresponse against donor MHC was found[156]. Symth et al also demonstrated the acquisition of MHC-peptide complexes by recipients' cells could confer CD8-mediated rejection in this semi-direct pathway[157]. These studies have shed some light into the precise mechanism of the semi-direct allorecognition pathway. The latest development of the semi-direct alloantigen recognition pathway is summarized in a concise review by Gonzalez-Nolasco et al[158]. In essence, donor MHC antigen—containing extracellular vesicles could be released by transplanted allografts. Allogeneic MHC antigens are captured by recipient APC, which are capable to present these 'intact' donor MHC molecules on their cell surface. Recipient T cells are then activated via this cross-dressed, or called semi-direct alloantigen recognition pathway.

Figure 1.2.2.2.1 Alloantigen recognition pathways

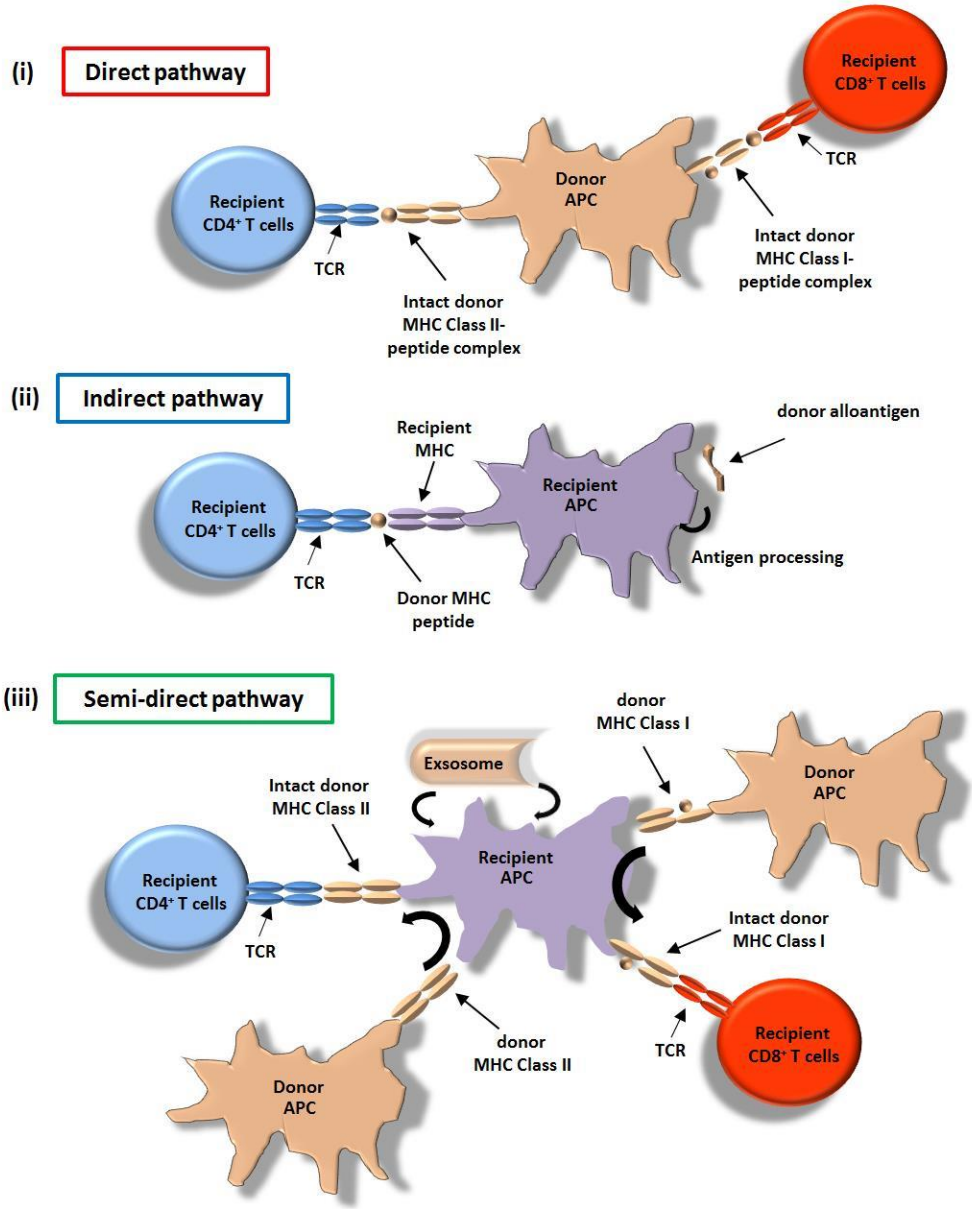

Figure 1.2.2.2.1. Alloantigen recognition pathways. (i) Direct pathway: Recipient alloreactive $CD4^+$ and $CD8^+$ T cells recognize alloantigens in the context of intact MHC class I or II molecules expressed on donor APC, respectively. **(ii) Indirect pathway**: Recipient alloreactive $CD4^+$ T cells recognize processed alloantigens presented by recipient APC in the context of recipient-MHC Class II molecules **(iii) Semi-direct pathway:** Recipient alloreactive $CD4^+$ or $CD8^+$ T cells recognize intact or processed donor MHC presented by recipient APC.

1.2.2.2.2 Alloreactive T cell activation

1.2.2.2.2.1 Signal 1 - TCR activation

Naïve $CD4^+$ and $CD8^+$ T cells are required to be activated in order to differentiate into various subsets of effector T helper cells and cytotoxic T cells to mediate their immune responses against allografts. Antigen stimulation provides the first signal, often referred to 'Signal 1', for initial T cell activation via the TCR/CD3 complex ***(Figure 1.2.2.2.2.i)***. The TCR/CD3 complex interacts with the immunoreceptor tyrosine-based activation motifs (ITAMs) to allow transmission of signal transduction via adaptor proteins, such as ZAP-70[159]. This in turn triggers three distinct signal transduction pathways: calcium-calcineurin pathway[160], RAS-mitogen-activated protein (MAP) kinase pathway[161] and protein kinase C (PKC) pathway[162], which activate nuclear factor of activated T cells (NFAT), activing-protien-1 (AP-1) and nuclear factor NF-κB, respectively. These signals cause upregulation of the surface expression of CD154 (CD40 ligand), CD25, as well as the secretion of IL-2.

1.2.2.2.2.2 Signal 2 - costimulation signals

T cells require a second signal, costimulation, provided by APC for full activation. In the absence of costimulation T cells will be anergized[163] ***(Figure 1.2.2.2.2.ii)***. It was first described by Jenkins and Schwartz that T cells were rendered into a state of unresponsiveness or anergy when cultured with APC lacking costimulation signals[164]. The molecular mechanisms underpinning T cell anergy have been described and reviewed in the literature[165-167]. The summation of the signals through antigen, costimulation and growth factor receptors will

dictate should this T cell proceed to clonal expansion. Following activation via the TCR without costimulation signals, NFAT nuclear translocaion occurs in the absence of AP-1, which results in a reduction of the transcription of *IL-2* and other cytokines genes as well as downregulation of cell cycle. In addition, it has been shown that *IL-2* mRNA is rendered stable in the absence of costimulation. Anergic T cells were shown to express transcription factors that maintain themselves within the anergic state, e.g. *Egr2*, *Egr3*, *Dgka* and *Cblb* genes. In addition, mTOR protein kinase has been shown to be responsible for sensing of metabolic demands following T cell activation and upregulating metabolic machinery in preparation for cell differentiation, other than its role in the integration of positive and negative costimulatory signals. Thus, suboptimal activation of the mTOR-AKT pathway as a result of the lack of costimulation via CD28 could render these T cells metabolic anergic in which they fail to meet the metabolic demand for cell division and differentiation upon activation[168,169]. There are also negative regulatory mechanisms to the proximal TCR signal transduction. For example, the activity of Fyn tyrosine kinase with the ζ chain of TCR/CD3 complex was shown to be increased in anergic T clones; whereas the association of Lck tyrosine kinase with ζ chain of TCR/CD3 complex was increased with cosimulation of CD28 was delivered upon TCR activation[170,171]. Epigenetically, there are also mechanisms in which T cells activated via TCR without further costimulation experienced epigenetic regulation and were dissuaded from clonal expansion[172].

In the last 20 years, a number of costimulatory molecules have been identified and sub-divided into three main groups: the integrins, the immunoglobulin superfamily and the TNFR/TNF family[173]. These pathways can provide a positive signal that promotes cell differentiation and proliferation (e.g. the CD28-CD80/86 pathway); or provide a negative signal that results in the arrest of an immune response (e.g. the CTLA-4-CD80/CD86 pathway). The summation of these positive and negative costimulatory signals is pivotal in determining the outcome of T cell

responses[174] and these potential therapeutic targets have been studied extensively in the last two decades[75,175].

1.2.2.2.2.3 Signal 3 - $CD4^+$ T cell differentiation and proliferation

A third signal is required for the propagation of T cell differentiation and proliferation ***(Figure 1.2.2.2.2.iii)***. T cell growth factors, primarily IL-2 but also other common γ-chain cytokines (such as IL-4, IL-7, IL-9, IL-15 and IL-21) bind to their corresponding receptors and form complexes that signal through Janus kinases. These signals in turn activate a number of STAT proteins, which interact with transcription factors for differentiation into distinct T cell subsets[176,177]. Common γ-chain cytokines also signal through phosphoinositide 3 kinase (PI3K) and trigger cell cycle via the mTOR-AKT pathway[178].

Upon recognition of alloantigens presented by APC, $CD4^+$ T cells are activated and differentiated into different subsets of effector T helper cells including Th1, Th2, Th9, Th17, Th22, follicular T helper and regulatory T cells, with respect to the cytokine milieu in the microenvironment[179], ***(see Figure 1.2.2.2.3)***. In the context of an inflammatory condition, in the presence of IFN-γ and IL-12 for example, $CD4^+$ T helper cells expressing the T-bet transcription factor differentiate into Th1 cells, which produce the inflammatory cytokine IFN-γ that primes $CD8^+$ T cells to elicit their cytotoxic effector function. In addition, IFN-γ also activates NK cells and macrophages which can also mediate cytotoxic effects against the graft[180]. In the presence of IL-4, $CD4^+$ T helper cells expressing the GATA-3 transcription factor differentiate into Th2 cells, which attract eosinophils and macrophages to the graft, as well as modulate Th1 responses[181,182]. Th17 differentiation is dependent on the expression of the transcription factor RORγt and the presence of IL-6, IL-21, IL-23 and TGF-β in the microenvironment. Th17 cells secrete IL-17, which stimulates the

recruitment of neutrophils to the site of inflammation, in this setting the allograft[183,184]. Th9 cells have been identified as a new group of T helper cell subset that secretes IL-9. IL-4 and TGF-β have been shown to be required, but no single master transcription factor has been identified for Th9 differentiation. IL-9 recruits mast cells to the site of action which might promote tolerance via Regulatory T cells (Treg), but their effector functions in transplant rejection remains to be fully elucidated.[185] At the same time, $CD4^+$ T helper cells that possess suppressive function-now called Treg are also activated in response to the inflammatory response, which are critically important in the maintenance of tolerance. Naïve T cells differentiate into follicular T helper cells (Tfh) under the influence of IL-6 and TNF, which activate the signal transduction molecule STAT-3, which activate the expression of Bcl-6. Th0 could also differentiate into regulatory phenotypes called regulatory T cells (Treg) in the presence of IL-2 and TGF-β, which will be discussed in more details in ***Chapter 1.3.2***.

Figure 1.2.2.2.2. T cell activation

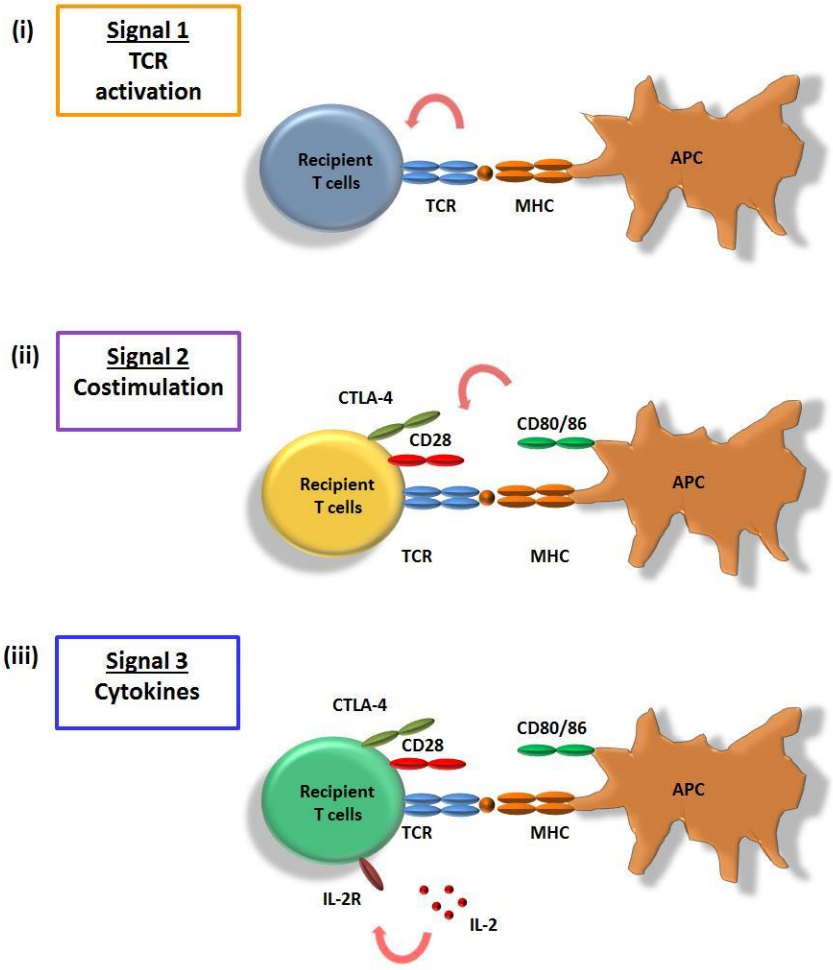

Figure 1.2.2.2.2. Signalling for T cell activation. (i) Signal 1-TCR activation: naive $CD4^+$ and $CD8^+$ T cells recognize alloantigens via their TCR in the context of alloantigen peptide-MHC molecules presented by APC via the alloantigen recognition pathways as shown in ***Figure 1.2.2.2.1***. The TCR/CD3 complex interacts with ITAMs and transmit signals via transduction pathways such as ZAP-70. This in turn triggers down-stream activation signalling pathways such as the calcium-calcineurin, RAS-MAP kinase and protein kinase C pathways. **(ii) Signal 2**-costimulation: costimulatory molecules expressed by APC provide the second signal for activated T cells to promote cell differentiation and proliferation (e.g. CD28/B7 pathway); or a negative signal to inhibit immune responses (e.g. CTLA-4/B7 pathway). (iii) **Signal 3**-cytokine signalling: common γ chain cytokines such as IL-2 bind to their corresponding receptors (e.g. IL-2R) expressed by T cells, which activate a number of STAT proteins and transcription factors that determine subsequent T cell subset differentiation. These signals also activate second messenger PI3K, which triggers cell proliferation via the mTOR and AKT pathways.

Figure 1.2.2.2.3. CD4⁺ T helper cell differentiation

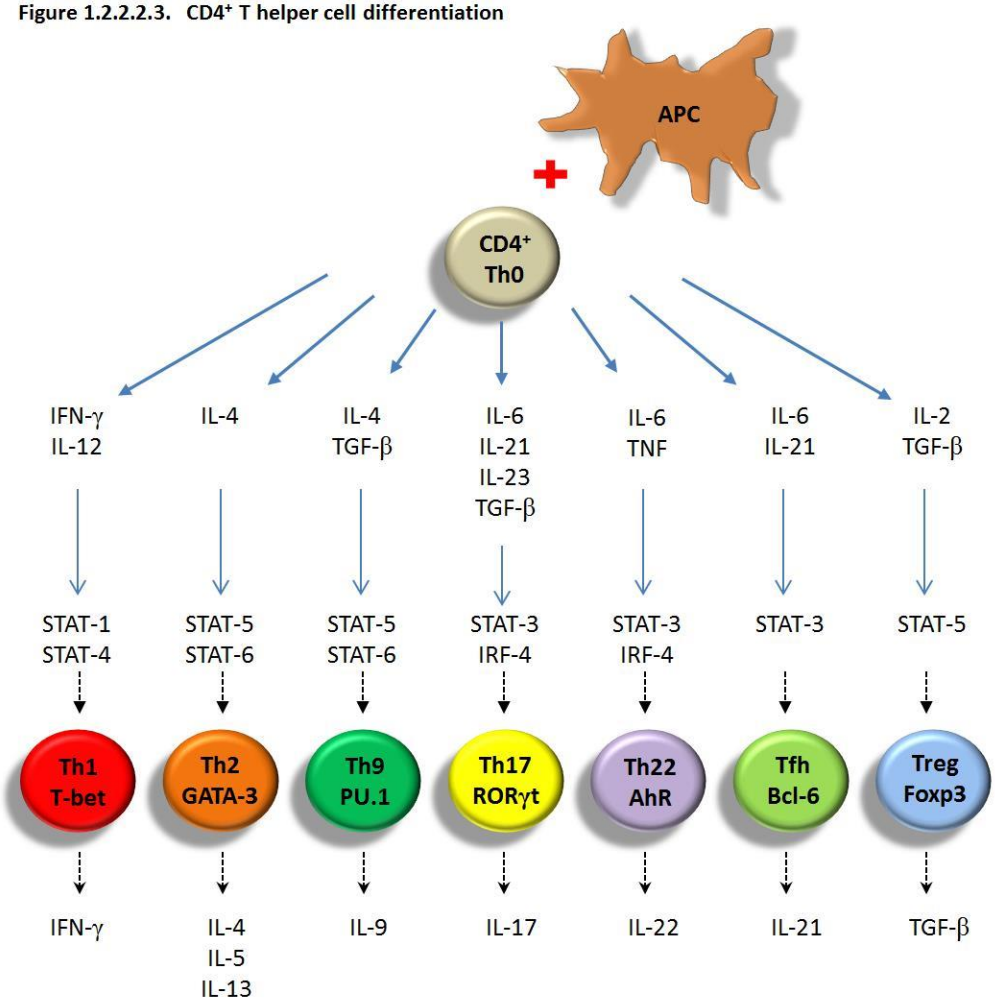

Figure 1.2.2.2.3. CD4⁺ T helper cell differentiation. Schematic diagram illustrates the differentiation of naïve CD4⁺ T cells. Upon on activated by antigen via the TCR **(Signal 1)** and costimulation signals **(Signal 2)** provided by APC, naïve CD4⁺ T helper cells (**Th0**) differentiate into different functional subsets **Th1**, **Th2**, **Th9**, **Th17**, **Th22**, **Tfh** and **Treg** under the regulation of cytokines **(Signal 3)**, transcription factors. Their respective effector function is characterized by their cytokine profiles.

1.2.2.2.3 Activation of CD8 T cells

$CD8^+$ T cells are activated via the recognition of MHC class I-peptide complex and differentiate into effector cytotoxic T lymphocytes (CTL) ***(Figure 1.2.2.2.2)***. $CD8^+$ T cells may be activated by recognizing the MHC class I-peptide complex presented by the same donor passenger leucocytes that activate $CD4^+$ alloreactive T cells. In such microenvironment, $CD4^+$ T cells provide T cell help to $CD8^+$ T cells for further differentiation into CTL. As a result, $CD8^+$ T cells can be activated via the direct and semi-direct allorecognition pathways (see ***Chapter 1.2.2.2.1***). In the context of transplantation, recipient alloreactive $CD8^+$ T cells recognize intact MHC class I molecules expressed by donor APC. The binding affinity of peptide ligands for CD8 TCR gives rise to a variable ligand-binding kinetics that ultimately leads to different signalling outcome. The downstream effect of this 'graded TCR signalling' might have an impact on $CD8^+$ T cell effector function via the modulation of inducible T cell kinase (Itk) and interferon regulatory factor 4 (IRF4)[186], which warrants further investigation.

1.2.2.3 T cell memory response

Memory is a hallmark of the adaptive immune system in which a more efficient and a greater magnitude of immune response is elicited after a primary antigenic challenge. Mature T cells ($CD4^+$ or $CD8^+$ T cells) mature in primary lymphoid organ and continue to develop in the extrathymic phase. These matured resting T cells express low level of CD44, which can readily respond to their specific antigen and develop into antigen-specific memory T cells, expressing high level of CD44[187,188]. The origin of memory T cells has been found to be related to self-reactive T cells. Haluszczak et al provided the evidence that 10-30% of antigen-specific $CD8^+$ T

cells in naïve mice possessed a $CD44^{hi}$ memory phenotype by virtue of using tetramers in their study[189]. Memory T cells (Tm) have enhanced expression of adhesion molecules and a lower threshold for costimulation compared to naïve T cells allowing them to elicit a rapid recall response[190]. It has been proposed that T cells undergro TCR desensitization prior to entering secondary lymphoid tissues. The modulation of TCR signal renders render T cells in check to an activation threshold below the level for entering into cell cycle, thereby quiescent. However, these cells are highly sensitive to profound proliferation in lymphopenic state[190]. Conversion of naïve T cells to memory phenotype has been described in the use of depleting therapy in transplantation[191]. Alloreactive Tm can be generated in sensitized transplant recipients who underwent previous blood transfusions, pregnancies or previous organ transplants. Furthermore, Tm can also be formed as a result of cross-reactivity with environmental pathogens following an infection[192]. More importantly, Tm have been implicated as a barrier to current immunosuppressive treatment in achieving favourable graft outcome long-term[193]. Novel strategies targetting both costimulatory signals and adhesion molecules are currently under consideration in order to overcome this deficit[194,195].

Homeostatic proliferation is a compensatory mechanism as a result of lymphopenia –induced proliferation of T cells in the absence of cognate antigenic stimulation in order to restore the normal T cell numbers in the peripheral compartment[196]. The precise mechanism is largely unknown; however, it has been proposed that the magitude of homeostatic proliferation depends on the degree of lymphopenia. At the cellular level, a strong avidity between TCR and self-MHC-peptide complex was shown to have a positive correlation with homeostatic proliferation of naïve $CD4^{+}$ and $CD8^{+}$ T cells[197]. CD4 and CD8 co-receptors are critically important as $CD4^{-/-}$ or $CD8^{-/-}$ T cells do not undergo homeostatic proliferation[198,199]. Common γ-chain cytokines, especially IL-7 has been strongly associated with the underlying

cellular mechanism of homeostatic proliferation[200]. IL-7-IL-7Rα/common γ–chain receptor heterodimer signals to activate PI3K and the JAK/STAT pathway, downregulate cyclin-dependent kinase inhibitor p27, as well as modulate the expression of anti-apoptotic molecules such as Bcl-1[201]. T cell trafficking via the ligation of CCR7 and CCL21 or CCL19 in secondary lymphoid tissues has also been implicated, interestingly in $CD4^+$ but not $CD8^+$ T cells[202]. On the other hand, homeostatic proliferation of regulatory T cells (Treg) was shown to be IL-2 dependent[203].

The transfer of naïve T cells to lymphopenic hosts (such as $RAG^{-/-}$ or SCID mice), results in the generation of large number of memory phenotypes following homeostatic proliferation. These Tm are capable to respond to low dose antigenic challenge without the coligation of costimulation molecules[204]. The homeostatic proliferation of memory and $CD8^+$ T cells requires both IL-7 and IL-15 signals[205]; however, the control of memory $CD4^+$ T cells homeostasis is less dependent on IL-15 signalling[206]. Although MHC was not a prerequisite for the homeostatic proliferation of memory $CD4^+$ or $CD8^+$ T cells in contrast to naïve T cells[207,208], the effector activity of these cells were altered upon subsequent antigenic challenge.

The consequences of homeostatic proliferation in the clinical setting are that naïve T cells expand in numbers and differentiate into memory phenotype, characterized by the loss of CD62L following homing to secondary lymphoid tissue and the simultaneous upregulation of CD44, which is required for adhesion and trafficking in the periphery. In contrast to antigen-stimulated proliferating cells, activation markers such as CD69 and CD25 are not upregulated[209]. Functionally, T cells undergone homeostatic proliferation have lowered

activation threshold[208], they could respond rapidly and proliferate, and with a greater magnitude with upregulated cytokine secretion and cytotoxic effect[204].

Lymphodepletion with various strategies have significant clinical implications in transplantation because of the different degree and magnitude of homeostatic proliferation giving rise to different characteristic memory T cell population that might contribute to rejection[210]. Potential barrier to successful long-term graft outcome is memory against alloantigens. 40-50% of human peripheral T cells express memory phenotype that often underlines the inability to translate pre-clinical studies to human[211]. These cells readily produce IFN-γ in response to donor alloantigens[212]. In addition, heterologous immunity in which human T cells possess two different TCR (up to 30%) with cross-reactivty against environmental antigens and alloantigens[213], could lead to the generation of allosepcific Tm even prior to the transplant and ultimately resistant to tolerogenic therapy[214].

1.2.2.4 Antibody-mediated rejection

ABMR has received much attention recently because it is less susceptible to conventional anti-lymphocytic therapy[215]. Hyperacute, accelerated and *de novo* ABMR are 3 clinical manifestations of ABMR that share a common complement-dependent effector mechanism leading to graft loss. The presence of preformed high levels of anti-donor HLA antibodies can lead to hyperacute rejection. An accelerated form of ABMR could be seen during the first week post-ABO-incompatible renal transplant. Early graft loss is due to the presence of a low level of preformed anti-HLA antibody follow by a boosted ABMR response. *De novo* ABMR can occur as an early, indolent or late event in non-sensitized patients receiving the first transplant. More

importantly, a complement-independent effector mechanism has also been described recently[135]. The positive correlation between peri-capillary infiltration of NK cells in biopsied specimens and proven donor-specific antibody (DSA) positive ABMR rejection indicated that NK cells are implicated in the complement-independent ABMR. When DSA bind to donor endothelial cells, their Fc portions bind to the FCγRIII receptors expressed on NK cells and simultaneously activate NK cells. Thereby, activated NK cells secrete cytotoxic cytokines such as perforin, granzymes, TNF-α and IFN-γ, which trigger target cells lysis and apoptosis and mediate the action of so-called ADCC[216]. Furthermore, NK cells can also be activated in an antibody-independent fashion via the activation of the NK cell receptors, such as NKG2D, which is implicated in both acute and chronic rejection[135].

1.2.3 Chronic allograft rejection

Chronic or delayed rejection has been the most common form of rejection in recent times because current immunosuppressive drugs are highly effective in preventing and treating acute rejection episodes. Chronic rejection has become the major cause of graft dysfunction and graft loss in transplant patients[217]. A number of immunological and non-immunological factors contribute to the aetiology of chronic allograft rejection. However, it has recently become clear that antibody-mediated mechanisms are pivotal in orchestrating chronic rejection[119,218,219]. DSA could be formed from de novo synthesis or as a result of triggered memory T and B cell responses, which then stimulate innate immune cells to cause graft damage in a complement-dependent or complement-independent manner[220]. In addition, autoantibodies are developed as a consequence of chronic ABMR that could propagate further tissue injuries[221]. DSA can also activate endothelial cells leading to the amplification of the inflammatory actions

of various growth factors such as platelet-derived growth factor (PDGF), epidermal growth factor (EGF), vascular endothelial growth factor receptor (VEFG) and fibroblast growth factor (FGF). Lymphoid neogenesis or the development of new tertiary lymphoid organs in the graft is found to be a unique feature in chronic rejection with infiltrating B cells that are capable of producing DSA[222]. The combination of alloantibodies and local tissue inflammatory insults ultimately leads to proliferation of myofibroblasts, which secrete extracellular matrix and causes fibrosis, a classical histological feature of chronic inflammation. Chronic allograft vasculopathy (CAV) is a prominent feature of chronic rejection characterized by arteritis, intimal smooth muscle proliferation and interstitial fibrosis. In addition, it is associated with peri-vascular infiltration of $CD4^+$ T cells, NK cells and macrophages[223].

The Th17 subset has recently been implicated in chronic rejection because of its relative resistance to CNI treatment and its link between autoimmune and alloimmune responses[184,224]. An array of effector mechanisms is being studied and investigators are currently looking at new targets for the potential treatment of chronic ABMR[225,226].

1.3 Immunological tolerance

Our immune system is equipped with multi-faceted layers of mechanisms to maintain tolerance to self-antigens, but at the same time it preserves an efficient way to defend ourselves against environmental pathogens. T cells differentiate and mature in the thymus from pluripotent haematopoietic stem cells produced in the bone marrow. Stochastic rearrangement of the VDJ genes of TCR gives rise to a T cell repertoire capable of recognizing ubiquitous antigens including self-antigens presented by thymic epithelial cells[227]. Two gross modes of tolerance (central and peripheral tolerance) that are comprised of complex molecular and cellular mechanisms ensure that we could react to almost any environmental antigens, but at the same time we are protected against autoimmunity[228].

1.3.1 Central tolerance

Pluripotent haematopoetic stem cells in the bone marrow differentiate into T cell progenitors and migrate to the thymus for their maturation. As part of their development, T cells undergo positive and negative selection processes for self-MHC restriction and self tolerance. Central tolerance for T cells takes place in the thymus. Immature thymocytes differentiate into double-positive $CD4^+CD8^+$ thymocytes in the thymic cortex under the influence of thymic cortical epithelial cells. Double positive thymocytes bearing TCR with a defined affinity to self-peptide:self-MHC complexes are positively selected, whereas those bind with a strong affinity to self-MHC molecules are deleted and undergo apoptosis. In addition, a special $CD4^+$ lineage T cells are generated by positive selection that express high level of CD25, CTLA-4 and Foxp3 are

called regulatory T cells (Treg), whose important role in the maintenance of peripheral tolerance will be discussed below.

Thymic medullary stromal cells express tissue-specific protein outside the thymus play a crucial role in the negative selection of self-reactive thymocytes and the induction of central tolerance. Expression of tissue-specific proteins on thymic medullary stromal cells is highly regulated by the *Aire* (autoimmune regulator) gene[229]. The importance of the *Aire* gene is demonstrated by the development of multi-organ autoimmunity in *Aire*-deficient mice and autoimmune polyendocrinopathy-candidiasis-ectodermal dystrophy (APECED) in humans with *Aire* mutations. The *Aire* gene functions to activate a number of tissue-specific antigen encoding gene in medullary thymic epithelial cells (mTEC) creating an environment such that autoreactive T cells are deleted by negative selection. However, a small number of autoreactive T cells escape this mechanism but are deleted, anergized or ignored in the periphery. AIRE has been implicated in the generation by shaping the repertoire of Treg via mTEC in the thymus before they are exported in the periphery[230].

1.3.2 Peripheral tolerance

The contribution of AIRE in peripheral tolerance remains to be fully elucidated. Reports have showed that AIRE is also expressed by peripheral lymphoid tissues and DC, which can affect the regulation of TLR expression, maturation status of APC and T cell differentiation[231]. Its role in the regulation of tissue specific antigen expression in peripheral lymphoid tissues in order to eliminate autoreactive T cells shares a similar mechanism as seen in the thymus. AIRE has been proposed to participate in the regulation of the expression of TLR and surface molecules in APC

in vitro. AIRE down-regulates the expression of MHC class II and costimulation molecules on APC, thereby governing T cell activation status, inducing apoptosis of autoreactive T cells and maintaining peripheral tolerance. More importantly, in the last two decades, regulatory T cells (Treg) have been shown to be critical in their role in maintaining tolerance in the periphery[232].

The cellular components of this suppressive mechanism became apparent following the work carried out by Gershon and Kondo in the 1970s and these cells were coined 'Suppressor cells'[233,234]. Accumulated evidence at the time suggested that these 'suppressor cells' belonged to the T cell lineage and were derived from the thymus[235-237].

Hall et al[238] demonstrated the existence of $CD4^+$ T cells with suppressive function in a rat heart transplant model. $CD4^+$ T cells were isolated from tolerized transplant recipients treated with cyclosporine. When these cells were adoptively transferred into irradiated hosts, they prevented allograft rejection mediated by co-transferred a T effector population.

1.3.2.1 $CD4^+CD25^+$ Regulatory T cells

In the 1990s, Sakaguchi et al initially showed that multi-organ autoimmune disease could be induced by reconstitution of athymic mice with $CD4^+CD5^{hi}$ T cells. On the other hand, the co-transfer of $CD4^+CD5^{lo}$ T cells prevented autoimmunity[239]. Similarly, Powrie et al showed that athymic rats reconstituted with splenocytes depleted of $CD4^+CD45RB^{lo}$ T cells developed autoimmunity; and the adoptive transfer of $CD4^+CD45RB^{hi}$ T cells led to autoimmunity[240]. Subsequently, Sakaguchi's group further characterized this distinct $CD4^+$ T cell population which showed that these cells constitutively express the IL-2α chain CD25[241]. They showed that athymic mice reconstituted with splenocytes depleted of $CD4^+CD25^+$ T cells developed

autoimmune disease. By contrast, $CD4^+CD25^+$ T cells could prevent the development of autoimmunity induced by $CD4^+CD25^-$ T cells in these mice[242]. Subsequently, it was shown that $CD4^+CD25^+$ T cells suppress the proliferation and production of IL-2 production by $CD4^+$ T cells *in vitro*[243,244]. Human $CD4^+CD25^+$ T cells were also characterized by various groups and their suppression function was demonstrated *in vitro* [245-250].

$CD4^+CD25^+$ T cells have become known as regulatory T cells or 'Treg'. Identification of Treg using CD25 is not optimal because it has been known for many years that activated T cells also upregulate the expression of CD25. Further characterization has revealed several surface molecules which are either constitutively expressed or upregulated in Treg, for example: CTLA-4[251,252], GITR[253,254] and CD62L[255,256]. However, the expression profile of these molecules also appears to be shared by other activated lymphocytes and is not unique to Treg.

1.3.2.2 Foxp3 transcription factor and Treg

Fork-head box protein 3 (Foxp3) is a transcription factor encoded in the X chromosome. The deficiency of *Foxp3* genes was found to be responsible for the development of the immune dysregulation polyendocrinopathy enteropathy X-linked syndrome (IPEX) in humans[257] and the multi-organ autoimmunity phenotype equivalent in scurfy mice[258]. In 2003, three independent laboratories showed that the Foxp3 transcription factor was the master genes responsible for Treg development and function[259-261]. In addition, forced Foxp3 expression by retroviral transfection of $CD4^+CD25^-$ T cells resulted in the acquisition of Treg phenotype and suppressive function. Since then, Foxp3 expression has been used as the preferred lineage marker for Treg. $CD4^+CD25^+$ $Foxp3^+$ Treg are often referred as naturally-occurring Treg or nTreg.

Of note, other types of regulatory T cells have been described as follow: $CD4^+$ lineages: IL-10-secreting Tr1[262], TGF-β–secreting Th3[263,264], T follicular regulatory cells[265]; non-$CD4^+$ lineages such as $CD8^+$[266], $CD4^-CD8^-$[267], γδ T[268] regulatory cells; other non T cell lineage: B regulatory cells[269], natural killer T cells[270], myeloid-derived suppressor cells[271], and mesenchymal stromal cells[272]. The features of these regulatory immune cells were reviewed individually elsewhere[273] and this thesis will focus on the experimental study of $CD4^+CD25^+Foxp3^+$ Treg. However, as intracellular staining Foxp3 requires cell permeabilization thus leading to cell death, Foxp3 cannot be used as a marker for the isolation of viable Treg. In addition, activated human conventional T cells transiently upregulate Foxp3. Furthermore, the stability of Foxp3 expression on Treg has been questioned recently[274]. Despite these limitations, the combination of CD4, CD25, Foxp3 and CD4, CD25, CD127, CD45RA and Foxp3 are still commonly used for the qualification of mouse and human Treg *ex vivo*, respectively.

Foxp3 genes regulate the transcription of many target genes[275]. Foxp3 also interacts with a number of cofactors. For example, NFAT[276] and RUNX1[277] bind to the promoter region of Foxp3 related gene to elicit Treg function. At the epigenetic level, Foxp3 positively or negatively controls the expression of IL-2, IFN-γ, GITR, CD25 and CTLA-4 via histone deacetylation or acetylation[278,279]. *Foxp3* transcription is governed by the binding of other transcription factors to the conserved non-coding sequences (CNS). CNS1 is thought to play a critical role in the extrathymic development of Treg. The CNS2 region, also known as the TSDR has been shown to be responsible for the maintenance of the expression of Foxp3. CNS3 serves as an epigenetic switch controlling Foxp3 transcription in the initiation of Foxp3 expression as in Treg development in the thymus. [280]

Transcription of the *Foxp3* gene is triggered by the interaction of TCR and costimulatory signals via the activation of RAS-FAF-MAPK signalling pathway[281,282]. On the other hand, IL-2R signalling via the JAKs leads to the phorsphorlation of STAT5, which binds to *Foxp3* promotor and CNS2. Indeed, IL-2 has been shown to play a crucial role in the maintenance of Foxp3 expression[283]. TGF-β is important for extrathymic induction of Treg via the activation of SMAD, which bind to the CNS1 on *Foxp3* gene[284]. On the other hand, IL-6 inhibits Foxp3 expression by interferring the binding of *STAT5* and *Foxp3* gene[285].

1.3.2.3 Stability and plasticity of Foxp3$^+$ Treg

The stability of Foxp3 expression of Treg could be influenced by external and intracellular factors. Under inflammatory conditions, the stability of Treg phenotype might be altered[286,287]. The stability could also be affected by the interaction between the TCR/CD3 and peptide-MHC complex and costimulatory molecules[288,289]. The plasticity of Treg lineage commitment could be determined by the epigenetic status of Treg. Demethylation states of the CpG islands located in the Treg-specific demethylation region (CNS2 as mentioned in ***Chapter 1.3.2.2***) of the Foxp3 locus have been implicated in Treg for the maintenance of their lineage and function[290] ***(see Figure 1.3.2.3.1)***. Furthermore, the plasticity of Treg lineage could be influenced by a complex network of transcription factors. A few transcription factors have been identified to influence Treg lineage plasticity. For example, the expression of T-bet, GATA-3 and RORγt have been reported to be implicated in the differentiation of Foxp3$^+$ Treg into Th1, Th2 and Th17 cells, respectively[291,292]. The expression of Foxp3 in mice has been considered to be more stable compared to human Treg, although cell-fate reporter mice experiments indicated that mouse Treg can lose their Foxp3 expression under certain circumstances and

conversion between Foxp3^{+} and Foxp3^{-} phenotypes can occur[293]. The quest of mechanisms governing the stability and plasticity of Treg continues to create opportunities for therapeutic intervention.

Figure 1.3.2.3.1. Treg plasticity

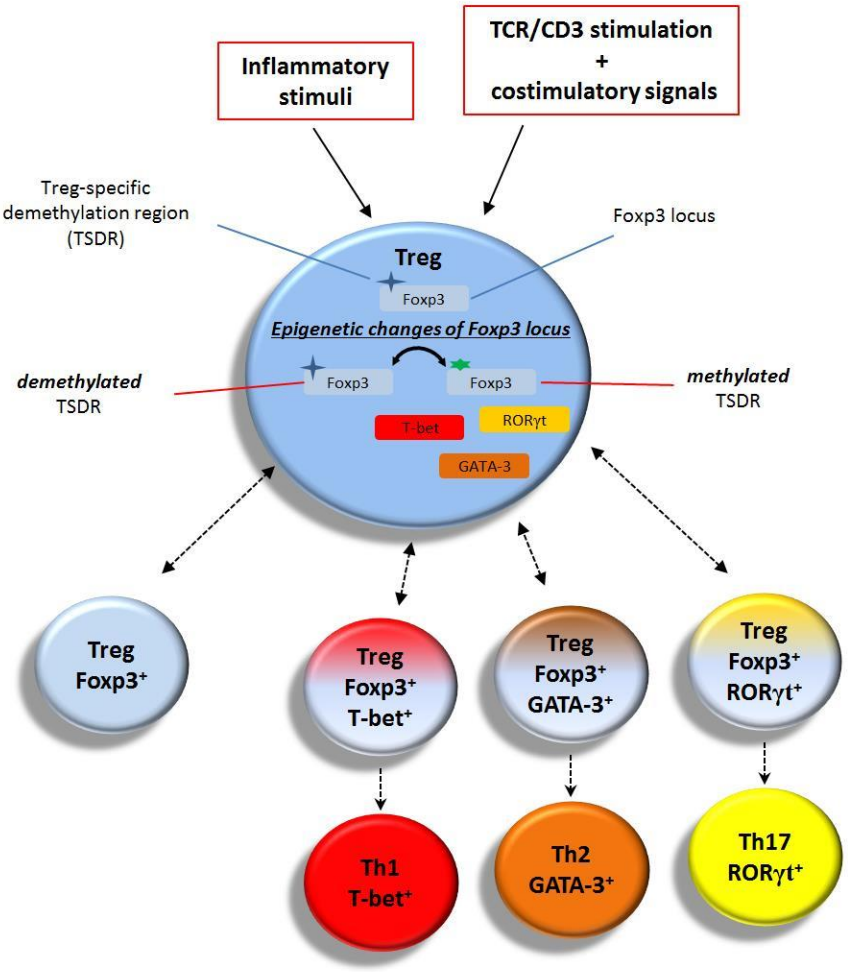

Figure 1.3.2.3.1. Treg plasticity. Treg phenotype and differentiation is dependent on external and internal factors. The plasticity of Treg lineage commitment is determined by the epigenetic status of Treg. The demethylation states of CpG islands located in the Treg-specific demethylation region (TSDR) of the Foxp3 locus are important determinants of the maintenance of Treg lineage and function. T-bet, GATA-3 and RORγt are key transcription factors that have been shown to influence plasticity of Treg differentiation into Th1, Th2 and Th17 effector $CD4^+$T cells, respectively.

1.3.2.4 Thymic development of naturally-occurring Treg

The studies of Treg biology revealed that naturally-occurring Treg (nTreg) develop from thymocytes following positive and negative selection similar to conventional T cells. The proposed two-step model suggests that Treg begin to develop from a preTreg stage, which is followed by the progression to mature Treg after the rearrangement of αβTCR[294]. Double positive and single positive thymocytes begin to express Foxp3 as a result of signals initiated from the high-avidity interactions between TCR and MHC class II, cytokine receptors, and costimulatory molecules in the thymus. Thymic epithelial cells (TEC) are found to be crucial for Treg homeostasis in the thymus. Cortical thymic epithelial cells (cTEC) and CCR7 were found to be implicated in Treg development in the thymic cortex. Medullary thymic epithelial cells (mTEC) and the presence of thymic stromal-derived lymphopoeitin (TSLP) are important for nTreg development in the thymic medulla. At the molecular level, apart from AIRE, the expression of IRF4 has been shown to be critically important in the induction of Treg[295].

AIRE has been implicated in the development of T cells in the thymus. Studies showed that *Aire* deficiency in *Foxp3* knock-out mice exhibited exacerbated autoimmunity as shown by multi-organ damage[296]. *Aire* knock-out mice have a normal number of $CD4^+CD25^+$ T cells, but the Treg subset appeared to be different from wild-type mice[297]. Self antigen presentation by $Aire^+$ mTEC was responsible for the development of Treg repertoire[298]. It has been shown that AIRE promoted the generation of a distinct Treg population that persisted from childhood into adulthood[299]. Furthermore, AIRE was shown to promote Treg enrichment in secondary lymphoid tissues, which might be responsible to promote peripheral tolerance[300].

Mature polyclonal nTreg that have undergone selection processes and developmental checkpoints in the thymus migrate into the periphery and mediate immunomodulation in

secondary lymphoid tissues or non-lymphoid tissues. Recently, t-Treg (thymic-derived Treg) is an analogous term used by some groups to define the developmental origin of nTreg. In unmanipulated experimental models, it is widely accepted that the majority of isolated nTreg are thought to be tTreg because of the small number of autoreactive peripheral Treg (pTreg) and the lack of definitive marker to separate the two. Hence, the bonafide polyclonal nTreg isolated from healthy individuals are thought to be of thymic origin. In this thesis, nTreg obtained from mice in our experimental studies refer to a combination of both t-Treg and pTreg expressing the master gene transcription factor Foxp3.

1.3.2.5 Inducible Treg

Naïve conventional $CD4^+$ T cells are converted to $CD4^+Foxp3^+$ Treg extra-thymically in response to a variety of inflammatory and non-inflammatory conditions *in vivo*, including the induction of Treg by tolerogenic protocols in the context of allotransplantation. Adaptive or induced Treg (iTreg) were interchangeable terms that have been used to describe these populations. Liang et al demonstrated that $CD4^+CD25^-$ T cells are converted to $CD4^+CD25^+$ T cells in a B7 costimulation-dependent manner in congenic thymectomized mice. More importantly, these cells expressed high levels of Foxp3 and controlled the proliferation of $CD4^+CD25^-$ responder T cells *in vitro*[301]. Kretschmer et al showed that naïve $CD4^+CD25^-$ T cells could be converted to $CD4^+CD25^+$ T cells that express high levels of Foxp3 using a combination of minute antigen dosing and a sub-optimal DC activation. Furthermore, the conversion rate of $CD4^+CD25^-$ T cells into iTreg was enhanced by pretreating $CD4^+CD25^-$ T cells with TGF-β *in vitro*[302]. Using GFP (green fluorescent protein) Foxp3 knock-in (KI) reporter mice, Gao et al found that rapamycin facilitated the conversion of $CD4^+GFP^-$ T cells to $CD4^+GFP^+$ T cells *in vivo*[303].

The mechanism underpinning the acquisition of suppressive function in conventional T cells through the action of Treg was demonstrated by Qin et al[304]. They described that under tolerizing conditions, $CD4^+CD25^+$ Treg could confer suppressive function to conventional $CD4^+$ T cells *in vivo* and they coined this process called 'infectious tolerance'. Further studies confirmed that the underlying mechanisms of infectious tolerance was principally contributed by both the presence of iTreg and the conversion of new $Foxp3^+$ phenotypes from naïve $CD4^+$ T cells[305]. A variety of *in vitro* culture protocols have been reported for the generation of iTreg, which will be discussed separately in subsequent sections.

1.3.2.6 Contrasting between nTreg and iTreg

Given the developmental differences between nTreg and iTreg, it has been hypothesized that their consequent specificity, requirement of costimulation and mechanisms of action might be different which could lead to the identification of potential therapeutic targets[306-310]. In order to delineate two Treg populations of different developmental origins, anti-thy1.1 antibody was used to label and isolate thymic-derived $CD4^+CD25^+$ Treg. Using this approach, a member of the Ikaros transcription factor family called Helios was initially found to be expressed preferentially on thymic-derived nTreg, serving a possible specific marker to differentiate between nTreg and iTreg[311-313]. The expression of Helios was shown to be directly proportional to Foxp3 expression and the suppressive function of human nTreg[314-317]. However, Helios was subsequently shown to be merely a marker of cell activation in both mouse and human Treg rather than a lineage marker[318-322]. More recently, Sebastian et al showed that the role of Helios might attribute to a subset of regulatory T cells. More importantly, in

Helios deficient mice, there was a loss of Treg suppressive function, differentiation and survival[317].

nTreg developed in the thymus possess a polyclonal TCR specific to self-antigens as they serve to prevent autoimmunity as they are exported into the periphery[323]. iTreg have a different TCR repertoire depending on the conditions they are generated, possibly due to the cross-reactivity to environmental antigens in the context of inflammatory response secondary to infection[324]. nTreg are thought to be fully functional after being exported from the thymus[325]. On the other hand, iTreg differentiated from naïve $CD4^+$ T cells in the periphery would need to be re-activated to acquire full function[309]. nTreg require CD28-B7 costimulation to acquire fully functional capacity[325]. In contrast, costimulatory signals appeared to have a negative impact of the conversion of non-Treg to Treg in the presence of TGF-β[302] In terms of mechanisms of action, Shevach et al demonstrated that nTreg inhibited the trafficking of T effector cells, whereas antigenic-reactive iTreg suppressed T effector cell priming via the secretion of IL-10[310].

Do nTreg and iTreg have the same therapeutic potential to be translated into the clinic? A number of studies made comparison between nTreg and iTreg that were generated using a variety of protocols *in vitro*. Functionally, iTreg appeared to be more potent than nTreg as illustrated by a number of *in vivo* models. Huang et al showed that iTreg had a higher tolerogenic property than nTreg *in vitro* and *in vivo* using an asthma model[326]. Karlsson et al demonstrated that, on a cell-to-cell basis, iTreg are more potent suppressor cells compared to freshly-isolated nTreg in a colitis model[327]. Interestingly, Harbhai et al found that neither nTreg nor iTreg alone were able to prevent autoimmunity in newborn $Foxp3^{-/-}$ mice, but that nTreg and iTreg could prevent autoimmunity in synergy. More importantly, selective depletion

of iTreg resulted in the resurgence of inflammation suggestive of the important role of iTreg in the maintenance of tolerance in this setting [328]. Kong et al showed that iTreg were superior to nTreg in the control of autoimmune response because the former showed a higher level of stability based on cell number and Foxp3 expression in an arthritis model[329].The caveat of these studies was that none of these studies made an adequate comparison between nTreg and iTreg because of the inherent heterogenicity of cell preparation and the system in which Treg function was tested. On the other hand, iTreg were shown to have a similar suppressive potency compared to nTreg when these experimental conditions were standardized for a reliable comparison[330-334].

1.3.2.7 Mechanisms of action of Treg

It has long been suggested that Treg must be activated in the presence of IL-2 in order to elicit their suppressive function[243,244,335], although it has also been reported that TCR-mediated activation was not a prerequisite for Treg function[336]. *In vivo*, it has been demonstrated that Treg expansion could be preferentially promoted by a sustained low-dose IL-2 treatment[337]. More recently, this low-dose IL-2 strategy was shown to be able to induce an effective, long-term protective effect against allergy in animal models and its effect was Treg-dependent[338]. The importance of antigen specificity in Treg function has consistently been a debatable issue. It is generally believed that antigen-specific Treg are a more potent population compared to polyclonal Treg. Attempts have been made over the years to generate antigen-specific Treg and to test their suppressive capacity *in vivo*[203,339-341]. On the other hand, Treg could confer efficient suppression in the absence of direct antigenic stimulation such as through mechanisms of bystander suppression[335,342], linked suppression[343-345] and infectious tolerance[304,346]. The following summarizes some well characterized mechanisms, although not exclusively, carried out by Treg at multiple levels[347].

The migration of Treg to the site of action was shown to be an integral part for their suppression of effector cells[348]. In addition, Treg obtained from homing receptors E/P selectin-deficient mice were not able to control target cells *in vivo*[349].

A wealth of evidence demonstrated that Treg regulate both the adaptive and innate immune system bearing a variety of effector cells including $CD4^+$ T cells[243], $CD8^+$ T cells[350], NK cells[351], NKT cells[352], B cells[353] and DC[354] via a range of molecular mechanisms. Although initial findings suggested that memory T cell responses are more resistant to suppression by Treg compared to their naïve counterparts in mice and human[355,356],

accumulated evidence have suggested that Treg can limit the generation of memory T cells[357-359] and suppress memory T cell responses[360,361].

Locally, Treg were shown to suppress target T cells by means of preventing the contact between naïve T cells and antigen-specific T cells or APC[362,363]. In addition, Treg were shown to suppress the activation, proliferation and IL-2 production capacity of $CD4^{+}CD25^{-}$ T cells *in vitro[364,365]*. They were also reported to alter expression of various genes in target cells[366]. In immunodeficient animal models, it has been shown that adoptive transferred nTreg inhibit co-transferred T effector cell differentiation and proliferation[367]. On the other hand, nTreg appear to control the trafficking of effector T cells into site of action; whilst antigen-reactive iTreg mediate their suppressive action via their interaction with APC in immunocompetent animals[310].

A cell-to-cell contact between Treg and target cells has been shown to be required for Treg to exert their suppressive function as shown by experiments using transwell systems *in vitro*[243,244]. A number of surface molecules have been implicated in the suppressive mechanism of Treg. CTLA-4 is constitutively expressed on Treg and it contributes to their suppressive function directly by binding to B7 molecules (CD80/CD86) on activated effector T cells, or indirectly by modulating APC function[368]. LAG-3 (Lymphocyte-activation gene 3) is a CD4 homolog that binds to MHC class II molecules on DC which induce downregulation of costimulatory molecules[369]. A second mechanism involving the ligation of CTLA-4 and B7 was described whereby Treg modulate APC function via the induction of indoleamine-2,3-dioxygenase (IDO)[370,371], although this hypothesis has been challenged recently. The expression of CD83 has been linked to various Treg functional markers and it has also been implicated in Treg suppression in a contact-dependent manner[372,373]. Galectin-1 expressing

Treg could lead to cell arrest via the induction of cell cycle arrest and apoptosis[374]. It has been demonstrated that Treg suppress effector responses by inducing target cell apoptosis. Several molecules involving the direct cytolysis have been implicated in this mechanism of Treg suppression including perforin, granzyme and the Fas-FasL pathway[375-377].

Treg exert their suppressive function in the surrounding microenvironment. Treg were initially characterized by their ability to secrete inhibitory cytokines such as TGF-β[378] and IL-10[379] to suppress target cells. More recently, IL-35 was shown to be implicated as a mediator for Treg suppression[380]. Treg mediate suppression by competition of growth factors locally, such as IL-2[381]. It has been shown that Treg either directly transfer cyclic adenosine monophosphate (cAMP) or produce cAMP in the local environment surrounding target cells[382]. The rising cAMP in turn reduces the expression of IL-2 genes. In addition, Treg express high levels of CD39/CD73, which are responsible for the metabolism of ATP and the generation of extracellular adenosine that mediate suppression[383].

An array of mechanisms of action of Treg has been reported. However, owing to the differences amongst different studies in terms of the site of action (lymphoid organs versus non-lymphoid tissues), inflammatory milieu in the microenvironment, antigen load, precursor frequency of the target population, and the activation status of the target cells in different studies, it is believed that there is no single master regulatory mechanism responsible for Treg suppression and that the mechanisms deployed by Treg are context dependent.

1.3.2.8 Latest development of immune checkpoint regulators in tolerance

1.3.2.8.1 CTLA-4

There has been a resurgence of interest in coinhibitory costimulatory molecules in the last few years. Earlier findings affirmed the critical role of CTLA-4 in negative regulation of T cell responses[384,385]. Mice lacking CTLA-4 expression would develop fatal lymphoproliferative disease[386,387]. The negative CTLA-4 intracellular signalling model in T cell activation has remained an intriguing hypothesis for some time. Following T cell activation, CTLA-4 is upregulated and it binds to CD80/CD86 expressed on APC competitively with CD28 to prevent continuous amplified T cell activation. However, T cells obtained from CTLA-$4^{-/-}$ mice were not hyperactive as postulated. Chimera studies demonstrated that CTLA-$4^{-/-}$ cells could be suppressed by CTLA-$4^{+/+}$ cells *in vivo*[388,389]. Later, it was shown that the expression of CD80/CD86 on APC could also be modulated by the action of CTLA-4[370]. An IDO-dependent mechanism was proposed to account for these findings, but this has recently been challenged[390-392]. Alternatively, new insights into the interaction between CTLA-4 and CD80/CD86 appear to provide a solution to the jig-saw puzzle. Walker and Sansom proposed a cell-extrinsic mechanism that Treg elicit their suppressive function via a CTLA-4-mediated trans-endocytosis of B7 molecules on APC. They demonstrated that CTLA-4 captured these costimulatory ligands on APC which were then internalized and transferred to lysozymes for degradation, thereby limiting access of B7 for CD28[393]. Similarly, conventional T cells that express CTLA-4 can also mediate inhibitory function via the same cell extrinsic mechanism[394]. As the use of belatacept in clinical transplantation has become more prevalent, more mechanistic information will be available in the near future.

1.3.2.8.2 Other immune checkpoint regulators

Current studies indicated that the CD28-CTLA-4 pathway ranks the top of the hierarchy of the costimulation cascade in the determination of T cell responses, however, there is extensive overlap and redundancy within this system which involves many other molecules which have been reviewed elsewhere[395]. For instance, programmed cell death protein 1 (PD-1) is another negative costimulatory molecule belonging to the B7 family which is highly expressed on activated T cells[396]. *In vivo* studies demonstrated that PD-1Ig in combination with anti-CD154 antibody led to prolongation of graft survival[397] while blockade of PD-1 resulted in aggravation of graft rejection[398]. More interestingly, the expression of PD-1 ligands on graft tissue appeared to be important in determining graft outcome[399].

The B and T lymphocyte attenuator (BTLA)-Herpesvirus entry mediator (HVEM) pathway can deliver either a stimulatory or an inhibitory costimulatory signal[400]. T cell alloreactivity was enhanced in the absence of BTLA or HVEM. Blockade of BTLA led to accelerated rejection in partially mismatched but not in a fully mismatched allotransplantation model. B7-H4 also belongs to the B7 family and its expression is upregulated in activated DC. Blockade of B7-H4 led to accelerated graft rejection in $CD28^{-/-}$ recipients and a full MHC-mismatched heart transplant model using $CD80^{-/-}$ and $CD86^{-/-}$ animals, suggestive of its non-redundant role in fine tuning T cell responses[401]. V domain-containing Ig suppressor of T cell activation (VISTA) is a PD-1 homolog which negatively regulates T cell responses. Its ability to deliver bidirectional inhibitory signals to APC and T cells simultaneously is a potential therapeutic target in the context of transplantation[400]. Butyrophilin (BTN) or BTN-like molecules are a family of immune checkpoint regulators that belongs to the Ig superfamily that are able to elicit either costimulatory or coinhibitory function. Their role in transplantation remains to be fully

elucidated[400]. Nevertheless, the rapidly growing interests in this exciting field might provide potential translational platforms for novel cellular and pharmacological intervention in clinical transplantation.

1.3.2.8.3 Immune checkpoint regulators and oncology

While the action of coinhibitory molecules is important in the regulation of autoimmunity and allograft rejection, certain tumours were found to evade immune surveillance by means of switching off T cell responses via coinhibitory signals. The effectiveness of unleashing T cell responses against immunogenic tumours by blocking the action of CTLA-4 was clearly evident *in vivo*[402]. Ipilimumab, a humanized anti-CTLA-4 monoclonal antibody has shown promising results in prolonging survivals in patients with advanced melanoma recently[403,404]. Another coinhibitory molecule, programmed cell death protein 1 (PD-1) and its ligand PD-L1 have taken immune checkpoint blockade therapy to another level in oncology[405]. In contrast to CTLA-4, PD-1 appears to play a major role in governing intratumoral effector T cell responses instead of participating in early T cell activation. PD-1 is found to be highly expressed on tumour infiltrating T cells, whereas PD-L1 is found to be highly expressed on the surface of a number of different solid tumours. This PD-1-PD-L1 pathway creates a microenvironment in which tumours evade the host's immunity. Blockade of PD-1[406] or its ligand[407] appears to be a promising avenue to control tumour growth in selected patients with established advanced cancers. As a monotherapy, nivolumab, an anti-PD-1 antibody has shown to have a durable effect in patients with advanced melanoma[408]. Given the complementary mode of action of these two immune checkpoint molecules in the induction of tumour immunity, a combination therapy of anti-CTLA-4 and anti-PD-1 antibody therapy has been employed in clinical trials to investigate their

synergism in the treatment of advanced melanoma[409]. With a wide variety of cellular and molecular mechanisms that present as targets for deliberate manipulation, it has become more appealing to harnessing the immune system to act against specific diseases.

1.4 Harnessing Regulatory T cells as therapeutic agents in transplantation

The immunoregulatory function of Treg has been implicated in various immune conditions such as autoimmunity, infection, malignancy and transplantation[325,410-413]. Clinical transplant outcome has been improved significantly by the development of powerful immunosuppressive drugs. However, transplant patients are subjected to non-specific immunosuppression, which increases the risks of malignancy, opportunistic infections, and drug associated toxicities as mentioned above. Alternative strategies that provide more selective immunosuppression are currently being investigated, and the possibility of harnessing Treg as cellular therapeutic agents has been proposed by several groups based on the evidence obtained from numerous *in vitro* and *in vivo* studies[254,256,414-422].

The basic principle of Treg-based therapy is that Treg are isolated from the patient's peripheral circulation, expanded and/or activated *ex vivo*, and re-infused at an appropriate time relative to transplantation. Given that the number of nTreg in both humans and mice is relatively low (5-10% of the whole $CD4^+$ T cell pool), an *ex vivo* expansion protocol is usually needed, so that sufficient numbers of Treg can be obtained for transfer.

1.4.1 First *ex vivo* generated Treg protocol

Taylor et al demonstrated that *ex vivo* expanded Treg were able to suppress alloresponses in a graft-versus-host disease (GVHD) model[423]. GVHD was induced by reconstituting BALB/c ($H2^d$) SCID (severe combined immune deficiency) mice with $1x10^6$ allogeneic C57BL/6 ($H2^b$) CD25-depleted T cells and all mice died from GVHD after 8 days. $CD4^+CD25^+$ T cells were isolated from naive C57BL/6 mice and cultured with irradiated BALB/c APC for one week, in the presence of IL-2 and TGF-β. Five out of six BALB/c mice that received $1.0x10^6$ C57BL/6 CD25-depleted T cells plus $0.5x10^6$ C57BL/6 $CD4^+CD25^+$ *ex vivo* expanded T cells survived for more than 60 days without any signs of GVHD. This was the first study to clearly demonstrate that *ex vivo* activated Treg can suppress alloresponses *in vivo*, however, it also highlighted the importance of exploring potential avenues to enhance cell yield as the recovery rate of this culture system was only 30% of the initial cell input.

1.4.2 First large scale human Treg expansion protocol

The main problem associated with expanding Treg is that these cells are intrinsically anergic and they respond poorly to stimulation via the TCR. Hoffmann et al addressed this issue by expanding human Treg using CD3/CD28 stimulation plus a high-dose of IL-2, which overcomes Treg anergy[424]. Magnetic-activated Cell Sorting (MACS)-enriched and Fluorescence-Activated Cell Sorting (FACS)-isolated $2x10^4$ $CD4^+CD25^{hi}$ T cells were expanded in cultures with $1.5x10^4$ irradiated mouse Ltk cells (artificial APC) transfected with human CD32, in the presence of anti-CD3 antibody (100ng/ml), anti-CD28 antibody (100ng/ml) and IL-2 (300 U/ml). A 13,000-fold increase in cell yield was observed after 3-4 weeks. Replacing $CD32^+$ Ltk cells, anti-CD3 and anti-

CD28 antibody by anti-CD3/anti-CD28 antibody-conjugated beads, the expansion of $CD4^+CD25^{hi}$ T cells fell to an average of 2800-fold after 3-4 weeks. Although $CD4^+CD25^{hi}$ T cells were expanded less efficiently by beads in this way, their suppressive function was comparable to that expanded by Lkt cells, as shown by their ability to suppress the proliferation of responder cells at similar ratios in MLRs. Nevertheless, without additional human Treg lineage markers, the number of $CD4^+CD25^{hi}$ might be contaminated with a significant number of activated non-Treg.

1.4.3 *In vitro* generated Treg using allogeneic APC as stimulators

The data above suggest that alloreactive Treg are likely to be generated more effectively by employing allogeneic APC as the primary stimulators. Several groups reported the use allogeneic APC and IL-2 in their Treg generation protocols and these *ex vivo* generated Treg invariably prolonged cardiac allograft survival in various models. Zheng et al[425] demonstrated that *ex vivo* generated Treg prolonged cardiac graft survival without additional treatment. Treg were generated by co-culturing DBA/2 ($H2^d$) T cells ($CD4^+$ and $CD8^+$ T cells) with irradiated C57BL/6 ($H2^b$) APC for 5 days, in the presence of IL-2 and TGF-β. $10x10^6$ Treg (mixture of $CD4^+$ and $CD8^+$ T cells) were given to DBA/2 recipients on day-1 and day 5 relative to the day of cardiac transplantation of the same donor and recipient strain combination. This Treg regimen alone, without additional immunosuppressive therapy, prolonged the median survival time (MST) of cardiac allografts to 40 days, compared to 11 days in untreated mice.

Xia et al[426] attempted to use *ex vivo* activated Treg to suppress alloresponses in the presence of a peri-operative depletion therapy (anti-thy1.2 monoclonal antibody specific to recipients). MACS-isolated $CD4^+CD25^+$ T cells ($H2^b$) were stimulated with anti-CD3/CD28 antibody

conjugated beads plus IL-2 and TGF-β for 5 days, then cultured with allogeneic DC ($H2^d$) for 19 days. A single dose of $4x10^7$ *ex vivo* activated Treg immediately after cardiac transplantation ($H2^d$ to $H2^b$) plus anti-thy1.2 mAb conferred long-term graft survival (>100 days). The MST of allografts in mice that were treated with anti-thy1.2 mAb alone was approximately 20 days, although 2 out of 15 mice had long-term graft survival exceeding 100 days. Collectively, these data emphasize that Treg-based therapy, when used alone, may not be able to control a fully-mismatched graft rejection in primary transplant recipients without additional immunosuppressive strategies.

1.4.4 *In vitro* generated Treg with designated allospecificities

Joffre et al[427] generated Treg with direct or dual (direct and indirect) allospecificities by culturing C57BL/6 ($H2^b$) $CD4^+CD25^+$ T cell with irradiated DBA/2 ($H2^d$) or B6D2F1 ($H2b^d$) APC plus IL-2 for two weeks, in order to address the importance of allorecognition pathways in the pathology of graft rejection. C57BL/6 hosts were preconditioned with a sub-lethal dose of irradiation followed by reconstitution of donor-type bone marrow cells ($H2^d$). In the presence of this chimerism, mice that were given Treg generated with direct allospecificity or dual allospecificity (unspecified cell doses) accepted their allografts indefinitely. However, histological examination of allografts harvested 100 days post-transplant from mice that were treated with Treg with direct allospecificity revealed extensive pathological changes such as intimal thickening and cellular infiltration, suggesting that these cells were not able to control chronic rejection. On the other hand, minimal histological changes were seen in allografts harvested from mice that were treated with Treg with dual allospecificity, suggesting that the indirect alloantigen recognition pathway is important in the pathogenesis of chronic rejection.

Tsang et al[428,429] developed a protocol to generate Treg with dual allospecificities that were able to provide long-term graft protection in immunocompetent recipients, when used in conjunction with a peri-operative rapamycin and an anti-CD8 antibody treatment. Treg with direct allospecificity (dTreg) were generated by co-culturing MACS-isolated $CD4^{+}CD25^{+}$ T cells ($H2^{b}$) with allogeneic APC ($H2^{d}$) in the presence of IL-2; whereas Treg with dual allospecificity were generated by transducing dTreg with TCR genes that were specific for $H2K^{d}$ presented by $I\text{-}A^{b}$ MHC class II molecules. Allogeneic heart transplantation was carried out using a BALB/c ($H2^{d}$) to C57BL/6 ($H2^{b}$) strain combination. Recipients were given $1x10^{7}$ Treg on day-1, +7, +14, +21 combined with a maintenance dose of rapamycin plus a peri-operative treatment of anti-CD8 antibody. The MST of allografts in mice that were given anti-CD8 antibody alone was 25 days. Anti-CD8 antibody plus rapamycin prolonged the MST to 50 days. Treg with direct allospecificity plus rapamycin and anti-CD8 antibody prolonged the MST to 80 days, whereas Treg with direct and indirect allospecificity were able to confer long-term graft survival with the MST exceeding 150 days.

1.4.5 *In vitro* generated Treg suppress alloresponses in immunocompetent recipients

At the time of writing, apart from the aforementioned work carried out by Zheng et al[425] and Tsang et al [428,429], there are two other published studies which demonstrated *in vitro* generated Treg could prolong allograft significantly in immunocompetent hosts. Ramondi et al showed that *in vitro* generated Treg combined with a short course of sub-optimal rapamycin led to long-term survival of full MHC-mismatched heterotopic heart allografts. Alloreactive Treg

were generated by stimulating isolated $CD4^+CD25^+$ nTreg ($H2^b$) with immature allogeneic BM-DC ($H2^d$) in the presence of exogenous IL-2 for 10 days *in vitro*. Upon harvesting, $CD11c^+$ BM-DC were removed from the Treg culture by MACS. A sub-optimal rapamycin regimen extended allograft survival from a MST of 11 days to 30 days. On the other hand, rapamycin plus a single dose of $2x10^6$ alloreactive Treg (with a purity of 85% $Foxp3^+$) given on day 7 post-operatively prevented allograft rejection long-term (MST >100 days), whereas rapamycin plus the same number of freshly-isolated $CD4^+CD25^+$ nTreg modestly extended graft survival with a MST of 41 days. Their data demonstrated that the combination of a sub-optimal mTOR inhibitor and alloreactive Treg was able to control allograft rejection in otherwise unmanipulated recipients. More importantly, they have also demonstrated that alloreactive Treg were more potent than polyclonal nTreg in the same setting.

Brennan et al compared the suppressive function of expanded allo-specific Treg versus polyclonal Treg in immunocompetent hosts. In their approach, nTreg were initially isolated from a MACS-purified $CD4^+$ population followed by FACS-sorting for $CD4^+CD25^+CD62L^{hi}$ from either TCR transgenic specific for MHC Class II $I\text{-}A^d$ (called 4C) or wild-type (WT) C57BL/6, both on the $H2^b$ background. nTreg were then expanded with anti-CD3/CD28 antibody-conjugated beads and IL-2 for 12-15 days *in vitro*. Expanded allospecific or polyclonal Treg were given to C57BL/6 recipients one day prior to the transplant of a heterotopic heart graft. $5x10^6$ or $30x10^6$ expanded allospecific Treg (>90% $Foxp3^+$) were able to prolong the survival of a BALB/c F1 (BALBc x C57BL/6) graft with a MST of 20 days compared to 10 days in untreated mice. However, allospecific Treg were unable to control the rejection of a BALB/c allograft at $5x10^6$ (MST=10 days). Furthermore, expanded polyclonal Treg (>90% $Foxp3^+$) had no effect on the protection of a BALB/c F1 heart graft (MST =10 days). These data demonstrated that Treg therapy alone was unable to confer long-term tolerance.

Taken together, these studies showed that alloreactive Treg may be generated *ex vivo* by various methods and there was strong evidence to suggest that Treg may be harnessed as therapeutic agents to suppress alloreactivity. However, the application of this approach in immunocompetent recipients has remained uncertain and further investigations are necessary.

1.4.6 Current development of Treg clinical trials in transplantation

Clinical trials of using Treg to attenuate immune responses are progressing rapidly in the field of transplantation as well as autoimmune disorders. At the time of writing this thesis, a number of clinical trials demonstrated great potentials of translating Treg from bench-to-beside medicine[430]. The first in man clinical trial was carried out in the setting of GVHD post Haematopoetic stem cell transplant (HSCT) in Poland. Trzonkowski et al demonstrated that donor polyclonal expanded Treg were safe with no major events reported post administration of Treg therapy[431]. More interestingly, they showed that Treg therapy showed significant improvement in chronic GVHD but they worked only transiently in acute GVHD. Several trials have started since then in Belgium, Germany, Italy, Portugal and the US to investigate Treg therapy in the prophylaxis and treatment of GVHD in HSCT[432].

In solid organ transplantation, a joint European and US collaboration, multi-centre consortium of the study of autologous Treg therapy in renal transplantation started in 2011 – the ONE study[433]. The ONE study includes 4 trials carried out in European centres investigating autologous polyclonal expanded nTreg, tolerogenic DC and regulatory macrophages; and 2 trials in the US investigating donor alloantigen reactive (DAR) Treg generated with donor B cells or PBMC with the common aim to assess the safety profile of regulatory cell therapy in the

management of living donor renal transplant recipients in conjuction with standard immunosuppressive regimens[434,435]. The TRACT (Trial of Treg Adoptive Cell transfer) trial is a phase I trial based in Chicago which has been completed recently[436]. It was designed to look at the safety profile of polyclonal expanded Treg in living donor renal transplant. One cadveat in the design of this trial is that all recipients were given alemtuzumab as induction plus standard maintenance immunosuppressants and they were given Treg therapy 60 days post transplant. Preliminary data indicated that there were no adverse events reported in all 9 patients recruited[434]. The TASK trial was set up to test for the therapeutic effect of Treg therapy in subclinical renal allograft inflammation by reviewing the histological changes in protocol biopsy based on positive results in their preliminary study[434].

Liver transplantation poses an interesting situation for the role of Treg therapy in drug minimization in that it is well established that 10% liver allografts would undergo spontaneous operational tolerance 2 to 6 years after transplantation[437]. Todo et al recently completed a clinical trial using autologous Treg stimulated with modulated irradiated donor PBMC in living donor liver transplantation. They reported 7 out of 10 recipients were able to achieve complete withdrawal of immunosuppressive drugs 16-33 months after transplantation without signs of rejection compared to 15% spontaneous tolerance in 2 years[438,439]. Donor-alloantigen-reactive regulatory t cells (DAR Treg) in liver transplantation – the deLTa Trial based in San Francisco has been designed to recruite patients investigating the use of autologous donor alloantigen-reactive Treg at 3 cell dose tiers for the induction of tolerance in liver transplant[434]. Two similar clinical trials with the study aim of assessing the efficacy of polyclonal expanded Treg in gradual withdrawl of immunosuppression in liver transplant patients based in London and Naning[434]. Lastly, the AMTEMIS trial is designed to look at the

plausibility of using Treg in extending the rate of spontaneous tolerance in liver transplant recipients with stable graft function 2-6 years post transplant[434].

1.5 Thesis Aims and Objectives

The aims of this thesis are:

- To validate and optimize our mouse Treg generation protocol ***(Chapter 3)***
- To test if *in vitro* generated Treg could prolong allograft survival in the presence of a low dose costimulation blockade ***(Chapter 3)***
- To explore the best Treg dosing strategies ***(Chapter 3)***
- To investigate the suppressive mechanisms mediated by Treg and to compare those with nTreg ***(Chapter 4)***
- To develop a robust mouse Treg expansion protocol ***(Chapter 5)***
- To compare the suppressive function between iTreg and nTreg *in vivo* ***(Chapter 5)***
- To assess heart allograft function following Treg therapy using non-invasive magnetic resonance imaging ***(Chapter 6)***

Chapter 2 Materials and Methods

2.1 Experimental mice

Experimental mice were bred and housed in vented cages provided with food and water in specific pathogen-free, temperature-controlled (22°C) facilities at the Biomedical Services Unit, University of Oxford, The John Radcliff Hospital, Oxford. Experimental mice were used in accordance to the Home Office regulations under the Scientific Act 1986.

GFP/Foxp3 KI CBA mice were bred from cross-breeding wild-type (WT) CBA and GFP/Foxp3 C57BL/6 mice (carried out by A.Bushell). CBA x GFP/Foxp3 C57BL/6 F1 were backcrossed with CBA for at least 10 generations to minimize heterogeneity of the transgenic GFP/Foxp3 CBA mice. Colonies were screened for the expression of GFP and Foxp3 by flow cytometry. The exclusion of $H2^b$ phenotype in the littlemates was screened by using monoclonal antibodies against $H2^b$ by flow cytometry. Reciprocal skin transplants were carried out between WT CBA and screened GFP/Foxp3 KI CBA mice to ensure functional compatibility *in vivo*.

Animal welfare was monitored regularly throughout the procedures using designated animal welfare score sheets. Any mice showing signs of distress which attained pre-defined welfare scores would be sacrificed immediately. At the end of each experiment, animals were sacrificed by approved Schedule 1 procedures followed by cervical dislocation.

Table 2.1.1. MHC *H2* Haplotypes of experimental mice used in this thesis

Strain	Abbrev.	Haplotype	Class Ia	Class II				Class III	Class Ia		Class Ib		
			K	*Ab*	*Aa*	*Eb*	*Ea*	*S*	*D*	*L*	*Qa-2*	*T18*	*Qa-1*
Inbred mice													
CBA.Ca	CBA	***k***	*k*	*k*	*k*	*k*	*k*	*k*	*k*	-	*b*	*b*	*b*
C57BL/6	B6	***b***	*b*	*b*	*b*	*b*	-	*b*	*b*	-	*a*	*b*	*b*
BALB/c	BALB/c	***d***	*d*	*d*	*d*	*d*	*d*	*d*	*d*	*d*	*a*	*c*	*b*
T and B cell deficient mice													
CBA RAG$^{-/-}$	CBA RAG	***k***	*k*	*k*	*k*	*k*	*k*	*k*	*K*	-	*b*	*b*	*b*
GFP reporter mice													
C57BL/6 GFP/Foxp3	B6 GFP	***b***	*b*	*b*	*b*	*b*	-	*b*	*b*	-	*a*	*b*	*b*
CBA GFP/Foxp3 KI	CBA GFP	***k***	*k*	*k*	*k*	*k*	*k*	*k*	*k*	-	*b*	*b*	*b*
Others													
CAMPATH-1	CP-1	***k***	*k*	*k*	*k*	*k*	*k*	*k*	*k*	-	*b*	*b*	*b*

2.2 Experimental surgical procedures

2.2.1 Anaesthesia, analgesics and recovery from anaesthesia

Mice undergoing major surgical procedures were given general anaesthesia. This was delivered by subcutaneous administration of a 200µl mixture of 100µg/ml Domitor® (medetomidine hydrochloride, Pfizer Pharmaceuticals, UK) and 8µg/ml Ketaset® (ketamine hydrochloride, Fort Dodge Animal Health Ltd, UK), combined with a long acting analgesic 200ul of 10µg/ml Vetergesic® (buprenorphine hydrochloride, Reckitt Benckinser, UK) and 120µl of 250µg/ml Metacam® (meloxicam, Boehringer Ingelheim, Germany), unless otherwise stated. Upon completion of surgery, mice were reversed using subcutaneous injection of 300µl of 100µg/ml Antisedan® (atipamezol hydrochloride, Pfizer Pharmaceuticals, UK) and 500µl sterile normal saline, and placed in a temperature-controlled (26°C) cabinet until full recovery, before returned to normal housing facilities. Metacam (120µl of 250µg/ml) was given post-operatively if necessary.

2.2.2 Skin transplantation

2.2.2.1 Donor mice

Donor mice were sacrificed by exposure to a rising concentration of CO_2, followed by cervical dislocation by approved Schedule 1 procedures. Full thickness tail skin grafts were harvested and prepared into 1cm^2-sized grafts.

2.2.2.2 Recipient mice

Recipient mice were given general anesthesia and analgesia as above ***(Chapter 2.2.1)***. Anaesthetized mice were shaved over the left thoraco-abdominal area by a clipper, and laid on the right lateral position. Skin was disinfected with Hibiscrub® (chlorhexidine gluconate 4% w/v; Mölnlycke Health Care Ltd, UK) and an incision was made. By taking the whole layer of skin, 1cm^2 of skin was removed to accommodate the donor skin graft. Donor grafts were transposed to the recipient and secured by applying methylated flexible colloidion glue B.P. (William Ransom & Son, UK) to the skin edges. An iodine-containing dry dressing (Inadine®, Johnson and Johnson, UK) was placed over the wound and secured by placing a bandage which consisted of multiple layers of adhesive autoclave tape circumferentially around the trunk of the recipients. Recipients were then reversed as stated above ***(Chapter 2.2.1)***.

Bandages were removed under general anaesthesia 7 days post-transplantation. Mice were recovered from anaesthesia as mentioned above ***(Chapter 2.2.1)***. Grafts were assessed daily for signs of rejection macroscopically. Rejection was defined as complete destruction of donor skin graft tissue.

2.2.3 Second skin graft transplantation

For the determination of the persistence of functional Treg *in vivo*, a second skin allograft of the same donor strain was transplanted 100 days after the first transplantation. Donor skin grafts were harvested and prepared as above. Donor skin grafts were transposed to the right thoraco-abdominal area of anaesthetized recipient mice and secured using methylated flexible colloidion glue as mentioned in ***Chapter 2.2.2.2***. Iodinated dressings and bandages were applied and

recipients were reversed for full recovery. After 7 days, bandages and dressings were removed under anaesthesia for gross examination of both new and old grafts. Complete destruction of donor skin graft tissue indicated rejection.

2.2.4 Heterotopic heart transplantation

Heterotopic heart transplant procedure was carried out using aseptic technique with sterile materials and autoclaved microsurgical instruments (B Braun, UK), under binocular operating microscope (Carl Zeiss, Germany). The average operating duration was approximately 60 minutes with an average cold and warm ischemia time of 10 minutes and 30 minutes, respectively. Technical errors were less than 5%.

2.2.4.1 Donor mice

Donor mice were given a non-reversible overdose of general anaesthesia (500µl of Domitor®/Ketaset® mixture, subcutaneously). Skin was disinfected with Hibiscrub® and an extended mid-line laparotomy incision was performed. Bowel loops were retracted to expose the inferior vena cava (IVC). 0.5 to 1.0ml venous blood was withdrawn from the IVC and replaced by 1ml of cold (4°C) heparinized saline (5000 units/ml; CP Pharmaceuticals, UK) to cool the donor heart. Bilateral thoracotomies were performed to expose the mediastinal structures. IVC, azygos vein, and superior vena cava were sequentially ligated with 7/0 braided silk sutures (Pearsalls Ltd, UK) and transected. Ascending aorta and pulmonary artery (PA) were dissected and transected proximal to their divisions. All pulmonary veins were ligated using a single loop

of 7/0 braided silk suture at the base of the heart. The heart graft was removed from the thoracic cavity and stored in ice-cold saline on ice bath (4°C).

In order to minimize cold ischaemia time, preparation of donor heart graft was usually carried out after the dissection of the abdominal aorta and IVC of the recipient ready for implantation.

2.2.4.2 Recipient mice

Recipient mice were given general anaesthesia and analgesics as described above ***(Chapter 2.2.1)***. The ventral abdominal wall was shaved using a clipper. In the supine position, the skin was disinfected with Hibiscrub® and a midline laparotomy incision was made from pubis symphysis to xiphisternum. A self-retaining retractor was placed, bowel loops and sigmoid colon were dissected, retracted superiorly and covered with sterile drapes (Buster drapes, Oxford University Veterinary Services). Abdominal aorta and IVC were dissected off surrounding retroperitoneal structures for adequate exposure. Lumbar veins were ligated with 7/0 braided silk sutures when necessary. A proximal vessel clamp (Downs surgical Ltd, UK) was applied to occlude the abdominal aorta and IVC below the origins of the renal arteries/veins and a distal clamp was applied above the bifurcation of the aorta/IVC.

An aortotomy was performed using the tip of a 30G needle and the incision was extended to approximate the aperture of the donor heart ascending aorta using Vanna microscissors (B Braun Medical Ltd, UK). An end-to-side anastomosis of the donor ascending aorta and the recipient's abdominal aorta was performed using 10/0 synthetic monofilament suture (Bear Medic Corp, Japan). Two stay sutures were anchored at the 12 and 6 o'clock position, respectively, followed by two continuous sutures starting from 12 to 6 o'clock and 6 to 12

o'clock position, in a clockwise direction sequentially to complete the aorto-aorta end-to-side anastomosis.

A venotomy was performed using the tip of a 30G needle 2-3mm inferior to the aorto-aorta anastomosis and the incision was extended to approximate the aperture of the donor heart PA. An end-to-side anastomosis of the donor PA and the recipient's IVC was performed using 10/0 sutures. Two stay sutures were anchored at the 12 o'clock and 6'o'clock position. Starting at the 6 o'clock position, a continuous suture was placed towards the 12 o'clock position in a counter-clockwise direction. The heart graft was flipped over to the right. The suture was then passed through the space between the donor aorta and PA for the completion of the continuous suture placed from 12 to 6 o'clock position. The end-to-side anastomosis between the donor PA and IVC was completed.

Small pieces of Spongostan® (Johnsons & Johnsons, UK) were placed around each anastomotic site for haemostatic purposes. The distal clamp was released, followed by the proximal clamp. Haemostasis was secured. As the heart graft was perfused, it began to contract within 30 seconds. Bowel loops were re-positioned into the abdominal cavity and the abdominal wall was closed in two layers using continuous absorbable 4/0 Vicryl® sutures (Johnson & Johnson, UK). Recipient mice were reversed and placed in recovery as mentioned above ***(Chapter 2.2.1)***.

The conventional method of assessing heart graft survival was carried out by regular bi-manual abdominal palpation and a palpation score (PS) was assigned according to the strength of the pulsation produced by the heterotopic heart graft (0-4): 0= no pulsation; 1= definitive but very weak impulses; 2= weak but regular impulses; 3=strong but sub-optimal pulsation; 4= forceful impulses. Rejection of heart graft was determined by the complete cessation of pulsation and

confirmed under direct vision by laparotomy. Animals were then sacrificed using approved Schedule 1 procedures at the end of the experiment.

2.3 Experimental non-surgical procedures

2.3.1 Administration of pharmacological reagents

Pharmacological reagents were injected subcutaneously (s.c.), intraperitoneally (i.p.) or intravenously (i.v.) without anaesthesia.

2.3.2 Adoptive cell transfer

Cell suspensions in phosphate buffered saline (PBS) up to 200µl were administered i.v. into lateral tail vein without anaesthesia.

2.3.3 Blood sampling

Under general analgesia ***(Chapter 2.2.1)***, distal tail was excised and peripheral blood samples (up to 20µl) were collected in eppendorf tubes containing 50µl of heparinized saline.

2.3.4 *In vivo* generation of CD44^{hi} memory T cells

Polyclonal CBA memory T cells were generated *in vivo* by challenging CBA mice with 1x10^6 B6 splenocytes. CBA mice were rested for at least 50 days to allow alloantigen clearance and the generation of quiescent polyclonal memory T cells. Spleen and mesenteric lymph nodes were then harvested. Animals were then sacrificed by approved Schedule 1 procedures. A single cell expansion was prepared as described above and the expression of CD4 and CD44 were examined by flow cytometry. The CD4$^+$CD44^{hi} population was isolated by FACS ARIA sorter (see below).

2.4 *In vivo* Magnetic Resonance Imaging

Recipients of heterotopic heart transplantation underwent *in vivo* Magnetic Resonance imaging (MRI) post-transplantation for the assessment of graft outcome ***(Chapter 6)***. In agreement with the University Veterinary Surgeon-in-Charge and the Named Animal Care and Welfare Officer, heart transplant recipients were monitored regularly and allowed for full recovery for 2 weeks prior to the first *in vivo* MRI. Mice were then transferred from the Biomedical Services Unit at the John Radcliff Hospital to the temporary housing facilities at the Department of Physiology, Anatomy and Genetics in between MRI.

Mice were anaesthetized with isoflurane (2-4 units in oxygen at a flow rate of 2ml/min) and placed in a cradle in supine position. Two electrocardiogram (ECG) electrode probes were attached subcutaneously in the ventral abdominal wall adjacent to the palpable heterotopic heart graft. ECG tracing was examined to ensure that electrical activities were derived from the heterotopic heart graft and not the recipient's native heart. A respiratory trigger wire loop was

secured on the ventral chest wall for the continuous monitoring of respiration during MRI. ECG and respiratory trigger levels were adjusted according to the cardiac cycle of the graft prior scanning. The cradle was then placed into the vertical-bore 500MHz, 11.7 Tesla MR System attached to a Bruker console. Scouting images of low resolution (128x128 pixels) were obtained for localization and 3-dimensional orientation of the heterotopic heart graft to optimize subsequent true short-axis images acquisition. True high resolution (256x256 pixels) Cine-MR images were acquired in 4-10 contiguous slices in the short-axis orientation including the base and the apex of the heart graft. At the end of the procedure, the cradle was elevated with the recipient removed from the cradle and placed in a temperature-controlled chamber for full recovery. Following an overnight rest, mice were then transferred and housed at the Oxford University Biomedical Services at South Park Road until the end of the experiment.

Data were retrieved and analyzed using ImageJ® software (version 1.44p, National Institutes of Health, USA). Cardiovascular functional parameters of the heterotopic heart graft were derived as follows: Using a 10 pixels/mm scale, the end-diastolic (EDV) and end-systolic volumes (ESV) of the right ventricle were derived from the compounded endocardial luminal volumes of each slice of the MR images (1mm in thickness) at the end-diastolic and end-systolic phase of the cardiac cycle. Subsequently, stroke volumes (SV=EDV-ESV) (µl), ejection fraction [EF= (EDV-ESV)/EDV)] (%), cardiac output (CO=SVxHR) (ml/min) of the right ventricle were calculated as shown. Heart rate was recorded using the ECG tracing. In contrast to the working heart model, the parameters of the unloaded left heart in our heterotopic heart model would be irrelevant.

Video images were reconstructed using all Cine-MR slices in GIF and avi formats.

2.5 Organ/tissue harvest and histopathology examination

2.5.1 Spleen, lymph nodes

Mice were given a non-reversible overdose of anaesthestics subcutaneously (500ul Domitor®/Ketaset® mixture at the concentration mentioned in ***Chapter 2.2.1***). In supine position an extended laparotomy incision was made. The mesenteric lymph nodes, axillary lymph nodes and the spleen were identified and harvested. Lymphoid tissues were stored in complete media and kept on ice for further use.

2.5.2 Heart graft harvesting in heterotopic heart transplant recipients

Mice were given a non-reversible overdose of anaesthestics subcutaneously (500ul Domitor®/Ketaset® mixture at the concentration mentioned in ***Chapter 2.2.1***). In supine position an extended laparotomy incision was made. The heterotopic heart graft was identified and dissected from surrounding adherent tissues carefully. The graft was removed from the recipient by transecting across the donor pulmonary artery and aorta. The graft was then washed in PBS and submerged in OCT media (Tissue-Tek, Netherlands) in a 1.5ml eppendorf tube and flash frozen in liquid nitrogen immediately, prior to being stored at -80°C until required.

2.5.3 Skin graft harvesting in skin transplant recipients

Mice were given a non-reversible overdose anaesthestics subcutaneously (500ul Domitor®/Ketaset® mixture at the concentration mentioned in ***Chapter 2.2.1***). An incision was made around the skin graft in the lateral position. The skin graft was harvested, submerged in OCT media in a 1.5ml eppendorf tube and flash frozen in liquid nitrogen immediately, prior to being stored at -80°C until required.

2.5.4 Histopathology

2.5.4.1 Tissue frozen sections preparation

Frozen heart graft blocks (***Chapter 2.5.2***) were thawed and removed from eppendorf tubes and mounted onto metallic sample stubs. Frozen blocks were then allowed to equilibrate in cryostat chamber temperature (-20°C to -25°C) for 30 minutes. 8-10µm sections were cut from the frozen blocks using a cryostat microtome (Bright Instruments, UK). Sections were mounted on PTFE-coated multispot microscope slides and allowed to dry overnight. Sections were finally fixed in 100% acetone the next day and store at -80°C until further use.

2.5.4.2 Haematoxylin and Eosin staining protocol

Frozen section slides were placed in designated rack submerged in formalin (10% v/v in water) for 10 minutes and then washed with water thrice. Sections were stained with haematoxylin (VWR, UK) for 20 seconds and washed with water thrice. Sections were then stained with eosin (VWR, UK) for 10 seconds and washed with water thrice. Sections were dehydrated sequentially

with 70%, 90% and 100% ethanol for 1 minute followed by clearing with xylene twice (10 seconds each). Sections were finally allowed to dry for 10 minutes and were mounted using DPX (VWR, UK) and cover slips.

2.5.4.3 Elastin Van Gieson staining protocol

Frozen section slides were placed in designated rack submerged in formalin (10% v/v in water) for 10 minutes and then washed with water thrice. Sections were stained with Miller Elastin (VWR, UK) for 10 minutes and washed with water thrice and dH_2O once. Sections were then stained with Van Gieson (VWR, UK) for 1 minute and washed with water thrice. Sections were dehydrated sequentially with 70%, 90% and 100% ethanol for 1 minute followed by clearing with xylene twice (10 seconds each). Sections were finally allowed to dry for 10 minutes and were mounted using DPX (VWR, UK) and cover slips.

2.5.4.4 Immunohistochemistry protocol

Frozen section slides were placed in designated rack submerged in ice cold 100% acetone for 15 minutes. Slides were allowed to dry for 5 minutes and rehydrated with PBS for 10 minutes. Tissue sections were incubated with 0.3% hydrogen peroxide in PBS for 2 minutes at room temperature within a humidified chamber. Slides were then washed thrice with PBS. 10% BSA (in PBS) was added to sections to block non-specific binding and slides were incubated for 30 minutes at room temperature and then washed thrice with PBS. Sections were then washed with PBS thrice. 1 drop of Avidin (Ventor Laboratories, USA) block was applied to sections and

incubated for 15 minutes followed by washing the sections thrice with PBS. 1 drop of Biotin block (Vector Laboratories, USA) was applied and incubated for 15 minutes followed by washing the sections thrice with PBS. Primary biotinylated antibody against mouse CD3 (1 in 100), CD8 (1 in 100) and Foxp3 (1 in 50) (eBiosciences, UK) were added per section and incubated for 1 hour at room temperature. Sections were washed thrice with PBS. Vectastain elite ABC solution (Vector Laboratories, USA) was applied and incubated for 45 minutes at room temperature in the humidified chamber. Sections were washed thrice with PBS. Diamniobenzidine (DAB; Sigma-Aldrich, UK) solution was applied to sections and incubated for 5 minutes for the development of brown-black staining which correlated to the peroxidase activity. DAB reaction was stopped by placing sections under running water. Sections were counterstained with Gills haematoxylin (VWR, UK) for 20 seconds, rinsed in running water and then dehydrated sequentially with 70%, 90% and 100% ethanol for 1 minute each, followed by clearing with xylene twice (10 seconds each). Sections were finally allowed to dry for 10 minutes and were mounted using DPX and cover slips. Enumeration of $CD3^+$, $CD8^+$ and $Foxp3^+$ cells were done manually at original magnification x400 in 3 separate sections defined by a graticule, the sum of cell counts from 5 high power fileds in each 3 sections were recorded and compared to unstained controls.

2.6 Reagents

2.6.1 Monoclonal antibodies

Conjugated and unconjugated monoclonal antibodies of various specificites were purchased from commercial suppliers ***(Table 2.6.1)***. Working concentrations between 1/50 and 1/400 were defined after initial titration experiments using splenocytes obtained from naïve animals.

Table 2.6.1. Monoclonal antibodies used in this thesis

Antibody	Conjugate	Host	Ig Class	Clone	Supplier
CD3e	PE-Cy7	Hamster	IgG	145-2C11	eBioscience, UK
CD4	PerCP, APC, PB	Rat	IgG2a	RM4-5	eBioscience, UK
CD8	PE, APC	Rat	IgG2b	YTS169.4	eBioscience, UK
CD11b	PE	Rat	IgG2b	M1/70.15	eBioscience, UK
CD11c	PB	Hamster	IgG	N418	eBioscience, UK
CD16/CD32 (Fc Block)	unconjugated	Rat	IgG2b, κ	2.4G2	BD Biosciences, UK
CD25	PE	Rat	IgG1, λ	PC61.5	eBioscience, UK
CD39	PE	Rat	IgG2b, κ	24DMS1	eBioscience, UK
CD40	PE	Rat	IgG2a, κ	1C10	eBioscience, UK
CD44	PE	Rat	IgG2b	IM7.8.1	eBioscience, UK
CD62L	PE	Rat	IgG2a, κ	MEL-14	eBioscience, UK
CD69	PE	Hamster	IgG	H1.2F3	eBioscience, UK
CD73	PE	Rat	IgG1	TY/11.8	eBioscience, UK
CD80	PE	Rat	IgG2a	RMMP-1	eBioscience, UK
CD86	PE	Rat	IgG2a, κ	GL1	eBioscience, UK
CD103	PE	Hamster	IgG	2E7	eBioscience, UK
CD122	PE	Rat	IgG2a,κ	5H4	eBioscience, UK
CTLA-4	PE	Hamster	IgG	UC10-4F10-11	eBioscience, UK

Table 2.6.1. Monoclonal antibodies used in this thesis

Antibody	Conjugate	Host	Ig Class	Clone	Supplier
FasL	PE	Hamster	IgG	MFL3	eBioscience, UK
Foxp3	APC	Rat	IgG2a,κ	FJK-16s	eBioscience, UK
GITR	PE	Rat	IgG2b, κ	DTA-1	eBioscience, UK
GR-1	APC	Rat	IgG2b, κ	RB6-8C5	eBioscience, UK
Helios	APC	Hamster	IgG	22F6	eBioscience, UK
Human CD52	Biotin	Recombinant	IgG1	REA164	Miltenyi Biotec, UK
Human CD52	PE	Rat	IgG2b	YTH34.5	eBioscience, UK
IL-10	PE	Rat	IgG2b, κ	JES5-16E3	eBioscience, UK
LAG-3	PE	Rat	IgG1, κ	C9B7W	eBioscience, UK
MHC class II	PE	Rat	IgG2b, κ	M5/114.15.2	eBioscience, UK
Perforin	PE	Rat	IgG2a	eBioOMAK-D	eBioscience, UK
TCR-β	FITC, PE	Hamster	IgG	H57-597	eBioscience, UK
TIM-3	PE	Rat	IgG1, κ	8B.2C12	eBioscience, UK

2.6.2 Monoclonal antibody from culturing hybridomas

YTS3.1, YTS177, YTS 169, TIB20, RA38B2, M70, 4F10, 1B1.2 hybridomas were grown as spent tissue culture supernatants in complete media (by G.Plant). Cultures were allowed to grow to exhaustion which was defined by less than 90% viability. The supernatant was centrifuged at 2000 rpm for 5 minutes, before being stored at 4°C until purification. Precipitation was carried out by adding ammonium sulphate 29.5% w/v (Sigma, UK) slowly into supernatant. The mixture was stirred and left overnight at 4°C. Ultra-centrifugation of the mixture was carried out at 10000 rpm for 20 minutes and the supernatant was discarded. Pellet was resuspended in Buffer A (11.9g sodium dihydrogen orthophosphate and 5g sodium azide per litre of dH_2O). Protein solution was dialyzed in Buffer A for at least 3 times over the next few days. The solution was centrifuged at 10000 rpm for 20 minutes and then filtered through a 22µm microfilter. Using a Fast Protein Liquid Chromatography machine, the solution was then loaded onto a Hitrap-Protein G column (VWR, UK) and washed through with Buffer B (0.2M glycine buffered at pH 2.3). 2ml eluted fractions were collected and examined for optical density using a standard spectrometer for the calculation of the amount of protein yielded. (Total protein in mg/ml = optical density at 280nm/1.4). The fractions were then pooled and dialyzed into PBS and stored. Endotoxin levels were tested using the QCL-1000 kit (Lonza, UK), as appropriate.

2.6.3 Cytokines and growth factors

Mouse IL-2, IL-7, IL-15; mouse GM-CSF, human TGF-β1 and mouse IFN-γ were purchased from Peprotech EC, UK. Stock solutions were reconstituted in sterile RPMI containing 2% fetal calf serum and stored at -80°C.

2.6.4 Pharmacological agents

Rapamycin was purchased from Calbiochem, EMD Bioscience, USA.

Cilostamide was purchased from Enzo Lifescience, UK. Lyophilized form of cilostamide was reconstituted with DMSO to a form a working stock solution with a final concentration of 20mM at stored at -20°C.

Abatacept (CTLA-4 Ig) (Orencia®) was purchased from Bristol Myers Squibb, USA. Working abatacept drug solution was made at a concentration at 100ug/ml by dissolving lyopholysed form of the drug in sterile PBS and stored at -20°C.

Alemtuzumab (CAMPATH-1H) was a kind gift from the Oxford Transplant Centre, UK. Working alemtuzumab drug solution was made at a concentration at 1mg/ml with sterile PBS and store -20°C.

2.6.5 Con A supernatant production

Lewis rat spleen was harvested and homogenized into a single cell suspension ($2x10^6$ cells/ml), which was resuspended in complete media containing concanavalin A (2.5µg/ml; Sigma-Aldrich, UK) and cultured for 48 hours. Supernatant was harvested by centrifuge at 400 x g for 10 minutes at 4°C. 400mg of α-methyl mannoside (Sigma-Aldrich, UK) was added to each 20ml of supernatant and the mixture was stored at -20C°. A few days later, the mixture was then thawed at 37°C and passed through a 22µm microfilter and 'Con A sup' aliquots were prepared and stored at -20°C.

2.7 Cell culture, isolation and purification

2.7.1 Cell culture

Cells were incubated at 37°C, 5% CO_2, in complete culture media unless otherwise stated. Complete media were composed of 450ml RPMI (Roswell Park Memorial Institute)-1640 medium (PAA Laboratories, Austria or Sigma-Aldrich, UK), 50ml heat-inactivated (56°C x 30mins) Fetal calf serum (PAA Laboratories, Austria), 2mM L-glutamine (PAA, Laboratories, Austria), 0.5mM 2-mercaptoethanol (Sigma-Aldrich, UK), 100units/ml penicillin (Sigma-Aldrich, UK) and 100units/ml streptomycin (Sigma-Aldrich, UK). PBS (Oxoid Ltd, UK)

Centrifuge: spin at 1500 rpm, 4°C for 5 minutes unless otherwise stated.

Non-sterile soluble reagents were allowed to pass through 22µm microfilter (Millipore Ltd, UK) to maintain sterility.

2.7.2 Single cell preparation

Spleens were removed aseptically and a single cell suspension was generated by mechanical segregation through a sterile 70µm nylon cell strainer (BD Biosciences, UK). Cell suspension was washed in PBS/2% FCS buffer and centrifuged at 1500 rpm for 5 minutes. Erythrocytes were removed from cell suspension by hypotonic cell lysis for 4-5 minutes using Pharmlyse buffer (BD Biosciences, UK) at room temperature. Cells were resuspended in PBS/2% FCS buffer until further use.

2.7.3 $CD4^+$ T cells enrichment protocol

A single cell suspension (at approximately $2x10^8$ cells/ml) was resuspended in 1ml PBS/2% FCS containing a cocktail of antibodies at a final concentration of 10µg/ml: 60µL TIB120 (1mg/ml) (anti-MHC class II), 60µl RA38B2 (1mg/ml) (anti-B cell), 60 µl YTS 169 (500µg/ml) (anti-CD8), 10µl M1/70 (500µg/ml) (anti-macrophages) and 50µl Dynal® depletion antibody cocktail (Invitrogen, Norway), and it was incubated at 4°C for 20 minutes. Cells were washed once and resuspended at approximately $1x10^8$/ml in PBS (without FCS). Sheep anti-rat coated Dynabeads® (Invitrogen, Norway) were added at a ratio of one bead per cell and incubated on a rotating device at 4°C for 20 minutes. $CD4^+$ cells (unlabelled) were isolated by negative selection using a Dynal® magnet (Invitrogen, UK). Cell count was performed and resuspended in PBS/2% FCS prior to further use.

2.7.4 $CD4^+CD25^+$ and $CD4^+CD25^-$ cell isolation protocol

Enriched $CD4^+$ cells were washed, resuspended in 900µl PBS/2%FCS, labeled with 5µl anti-CD25 PE antibody (eBioscience, UK) and incubated on ice for 20 minutes. Cells were then washed, resuspended in 900µl PBS/2%FCS and incubated with 50µl anti-PE microbeads (Miltenyi Biotec, UK) at 4°C for 20 minutes. Cells were washed and resuspended in 500µl PBS/2% FCS before being loaded into a MACS column (Miltenyi Biotec, UK). The $CD4^+CD25^-$ T cell population was first isolated by negative selection and collected as the unbound population. The bound $CD4^+CD25^+$ T cell population was then eluted according to the manufacturer's protocol.

2.7.5 Bone marrow cell isolation

Bone marrow (BM) cells were harvested from the femora and tibiae of C57BL/6 mice and perfused in RPMI. A single cell suspension was prepared and erythrocytes were separated following osmotic lysis using filtered ultrapure water. Cells were filtered and resuspended in 1ml PBS/2% FCS prior to further use.

2.7.6 Modulated BM-APC generation

BM cells were resuspended in PBS containing the following rat-anti-mouse antibodies: TIB120 (10µg), RA32B2 (10µg), YTS 169 (10 µg), YTS 3.1(10 µg), which were specific for MHC class II, B220, CD8 and CD4, respectively. The cell mixture was incubated on ice for 20 minutes. Cells were washed and resuspended in 4ml PBS. 500µl of paramagnetic beads coated with sheep-anti-rat immunoglobulin (Dynal® beads, Invitrogen, UK) was added and incubated at 4°C for 20 minutes on a rotating device. Unlabeled granulocyte progenitors were negatively selected by applying a magnet to the cell suspension. Cells were washed, resuspended in complete media containing GM-CSF (2ng/ml) and TGF-β (2ng/ml) at $1x10^6$ cells/ml, and cultured at 1ml/well in a 24-well flat-bottom plate (Corning, USA) for a total of 6 days. 500µl of supernatant was removed from each well and replaced with fresh complete media containing GM-CSF (2ng/ml) and TGF-β (2ng/ml) on day 2 and 4. After 6 days, BM-APC were harvested, washed and used as 24-well BM-APC when necessary.

In certain experiments, BM-APC were generated in a similar way, but were cultured in 10cm petridishes in complete media containing GM-CSF (2ng/ml) and TGF-β (2ng/ml) in a final volume of 10ml. 5ml of supernatant was removed and replaced with fresh complete media containing

GM-CSF (2ng/ml) and TGF-β (2ng/ml). On day 6, cells were harvested, washed and used as Pet BM-APC.

In some experiments, BM-APC were generated with a graded concentration of GM-CSF (2-20ng/ml) with or without TGF-β (2ng/ml).

2.7.7 Mature BM-DC generation

BM cells were isolated as described above ***(Chapter 2.7.5)*** and resuspended at $1x10^6$/ml and cultured in 10cm petridishes in complete medium containing GM-CSF (20ng/ml) in a final volume of 10ml for 6 days. On day 2 and 4, 5 ml of supernatant was removed and replaced with an equal volume of complete media containing GM-CSF (20ng/ml). Matured with LPS or Poly:IC overnight and then harvested.

2.7.8 $CD11c^+$ and $CD11c^-$ BM-APC isolation

BM-APC were resuspended in 500µl PBS/2%FCS incubated with 5µl anti-CD11c-PE antibody (Miltenyi Biotec, UK) on ice for 20 minutes. Cells were washed once and incubated with anti-PE microbeads at 4°C for 20 minutes. Cells were then washed once and resuspended in 500µl PBS/2% FCS prior to being loaded into MACS column. $CD11c^-$ BM-APC were collected as the unbound population by negative selection. The bound $CD11c^+$ population was then eluted and collected by positive selection.

2.8 *In vitro* alloantigen-driven Treg generation protocols

2.8.1 IFN-γ conditioning Treg generation protocol

WT CBA or GFP/Foxp3 KI CBA or CP-1 ($H2^k$) $CD4^+$ T cells were positively selected by MACS as follows. A single cell suspension was isolated from spleens as described in ***Chapter 2.7.2***. Cells were counted and resuspended at in PBS/2% FCS at $1x10^8$ cells/ml. 10µl MACS rat anti-mouse CD4 antibody conjugated microbeads (Miltenyi Biotec, UK) were added to cell suspension and incubated at 4°C for 20 minutes. Cells were then washed once and resuspended in PBS/2% FCS (up to $2x10^8$/ml) prior to be applied into a MACS MS/LS column (Miltenyi Biotec, UK). Unbound $CD4^-$ and bounded $CD4^+$ T cells were eluted and collected separately, in accordance to manufacturer's instructions.

MACS-isolated $CD4^+$ T cells ($H2^k$) were stimulated with two successive rounds of allogeneic modulated B6 BM-APC ($H2^b$) in the presence of exogenous IFN-γ for a total of 14 days. Modulated B6 BM-APC were generated from B6 BM cells incubated with GM-CSF (2ng/ml) and TGF-β (2ng/ml) for 6 days, as described in ***Chapter 2.7.6***. On day 0, $5x10^5$ $CD4^+$ T cells were stimulated with $5x10^4$ freshly-harvested BM-APC (10:1 $CD4^+$ T cells :BM-APC ratio) in a final volume of 2ml per well on a 24-well flat-bottom plate containing IFN-γ (5ng/ml). On day 7, 1ml of supernatant was removed from each well and it was replaced by an equal volume of complete medium containing $5x10^4$ freshly-harvested BM-APC and IFN-γ (5ng/ml). After 14 days, the resultant population was harvested, washed and counted prior to further use.

As seen in ***Chapter 3.2.3***, the optimization experiments indicated an increased number of allogeneic BM-APC ($1.5x10^5$; thus 3xBM-APC) in both rounds of stimulation resulted in a higher

Foxp3 enrichment and cell yield, which formed the revised standard IFN-γ conditioning protocol unless otherwise stated.

2.8.2 TGF-β/IL-2 Treg generation protocol

MACS-isolated $CD4^+$ T cells ($H2^k$) were stimulated with two successive rounds of allogeneic modulated B6 BM-APC ($H2^b$) in the presence of exogenous TGF-β and IL-2 for a total of 14 days. Modulated B6 BM-APC were generated from B6 BM cells incubated with GM-CSF (2ng/ml) and TGF-β (2ng/ml) for 6 days, as described in ***Chapter 2.7.6***. On day 0, $5x10^5$ $CD4^+$ T cells were stimulated with $1.5x10^5$ freshly-harvested BM-APC (10:3 $CD4^+$ T cells :BM-APC ratio) in a final volume of 2ml per well in a 24-well flat-bottom plate containing TGF-β (2ng/ml) and IL-2 (20U/ml). On day 7, 1ml of supernatant was removed from each well and it was replaced by an equal volume of complete medium containing $1.5x10^5$ freshly-harvested BM-APC and TGF-β (2ng/ml) and IL-2 (20U/ml). After 14 days, the resultant population was harvested, washed and counted prior to further use.

2.8.3 Cliostamide Treg generation protocol

MACS-isolated $CD4^+$ T cells ($H2^k$) were stimulated with two successive rounds of allogeneic modulated B6 BM-APC ($H2^b$) in the presence of cliostamide (a phosphodiesterase inhibitor (PDEi)) for a total of 14 days. Modulated B6 BM-APC were generated from B6 BM cells incubated with GM-CSF (2ng/ml) and TGF-β (2ng/ml) for 6 days, as described in ***Chapter 2.7.6***. On day 0, $5x10^5$ $CD4^+$ T cells were stimulated with $1.5x10^5$ freshly-harvested BM-APC (10:3 $CD4^+$

T cells :BM-APC ratio) in a final volume of 2ml per well in a 24-well flat-bottom plate containing cliostamide (10µM). On day 7, 1ml of supernatant was removed from each well and it was replaced by an equal volume of complete medium containing $1.5x10^5$ freshly-harvested BM-APC and cliostamide (10µM). After 14 days, the resultant population was harvested, washed and counted prior to further use.

2.9 Cryopreservation of leukocytes

2.9.1 Freezing media for BM-APC

BM-APC or BM-DC were resuspended in 250µl freezing media containing voluven, DMSO and FCS (adopted protocol from S. Preston and K. English from our Department) and cryopreserved in liquid nitrogen.

2.9.2 Freezing media for lymphocytes

T cells or Treg were resuspended in freezing media containing RPMI (45%) and azide free DMSO (10%) (adopted protocol from J. Hester from our Department) and cryopreserved in liquid nitrogen.

2.10 *In vitro* Treg expansion protocol

2.10.1 Anti-CD3/CD28 bead-based protocol

2.10.1.1 Invitrogen® protocol

Dynabeads® mouse T-Activator CD3/CD28 beads (Invitrogen, Norway) were uniform 4.5µm superparamagnetic polymer beads coated with an optimized mixture of anti-CD3 and anti-CD28 monoclonal antibodies. A desired volume of anti-CD3/CD28 beads (stock concentration $4x10^7$ beads/ml) was transferred into an eppendorf tube. Anti-CD3/CD28 beads were washed with 1ml of PBS/2% FCS. Supernatant was removed by placing the eppendorf on a magnet and anti-CD3/CD28 beads were removed and resuspended in complete media prior to use. Isolated T cell populations were resuspended in complete media containing a graded concentration of IL-2 (0-1000U/ml). Anti-CD3/CD28 beads were added to the cultures at a graded bead-to-cell ratios (1:2 to 4:1) to make up a total of volume of 200µl per well in a round-bottom 96-well plate. Cultures were examined regularly and split in IL-2-containing culture media, if necessary. Expanded T cells were harvested on day 7, unless otherwise stated.

2.10.1.2 Miltenyi® protocol

CD3/CD28 MACSiBead™ particles were pre-loaded with anti-CD3 and anti-CD28 antibodies. A desired volume of anti-CD3/CD28 beads (stock concentration $6x10^7$/ml) was washed with 5-10x volume of complete media and centrifuged at 300xg for 5 minutes. Supernatant was removed and anti-CD3/CD28 beads were resuspended in complete media to a concentration of $6x10^6$ beads/ml. Isolated T cell populations were resuspended in complete media containing a graded concentration of IL-2 (0-1000U/ml). Anti-CD3/CD28 beads were added to the culture at a 3:1 bead-to-cell ratio to make up a total of volume of 200ul per well in a round-bottom 96-well

plate. Cultures were examined regularly and split in IL-2-containing culture media, if necessary. Expanded T cells were harvested on day 7, unless otherwise stated.

2.10.2 APC-based protocol

mBM-DC were prepared as described above (***Chapter 2.7.7***). Isolated T cell populations were resuspended in IL-2-containing complete media (graded IL-2 concentration at 0-1000U/ml). mBM-DC were added to T cell suspensions at a graded T cell to mBM-DC ratio. Cells were harvested on day 7 unless otherwise stated.

2.10.3 Plate-bound antiCD-3/CD28 antibody-based protocol

Anti-CD3/CD28 antibody solution was prepared by reconstituting purified functional grade anti-CD3 antibody (145.2C11; eBioscience, UK) and anti-CD28 antibody (37.51; eBioscience, UK) in 0.1M borate buffer (pH adjusted to 8.5). 60mmx15mm polystyrene non-tissue culture-treated bacteriological petridishes (BD Biosciences, UK) were coated with 2ml of anti-CD3/CD28 antibody solution and were kept overnight at room temperature. Petridishes were washed with PBS three times and treated with 10% bovine serum albumin (BSA) for 1 hour. Anti-CD3/CD28 antibody-coated petridishes were then washed with complete media three times and ready for use.

Isolated T cell populations were resuspended in IL-2 containing complete media to a final volume of 5/ml and transferred to anti-CD3/CD28 antibody-coated petridishes. 2.5ml of supernatant was removed and replaced with an equal volume of IL-2 containing complete media

every 2-3 days, if necessary. Expanded T cells were harvested on day 5 in the established protocol, unless otherwise stated.

2.11 *In vitro* Treg activation

Isolated T cell populations were resuspended in IL-2 (50U/ml) containing complete media to a final volume of 5ml. Cells suspensions were dispensed to anti-CD3/CD28 antibody-coated petridishes ***(Chapter 2.10.3)*** and incubated at 37°C up to 24 hours. Activated T cells were examined for the expression of a variety of T cell activation markers by flow cytometry.

2.12 Cell labeling with CFSE, PKH26, eFluor 670 dyes

2.12.1 CFSE fluorescent dye

CFSE fluorescent dye was purchased from eBioscience, UK. CFSE has a peak excitation of 494nm and its emission could be detected with FACS filter used for FITC. Lyophilized formed of CFSE was reconstituted to a stock solution (10mM) with 90µl DMSO and stored at -20°C according to the manufacturer's instructions. A single cell suspension was prepared at 2x final concentration and washed with PBS thrice at room temperature to remove excessive FCS. 10µM CFSE dye solution was prepared with PBS at room temperature and added to 2x single cell suspension (thus a 1:1 ratio). Cells were incubated at room temperature for 10 minutes in the dark. Staining was terminated by adding 5x volumes of cold complete media and incubating on ice for 5 minutes. Cells were washed thrice with complete media and ready for use.

2.12.2 PKH26 fluorescent dye

PKH26 fluorescent cell linker kits were purchased from Sigma-Aldrich, UK. PKH26 has a peak excitation of 551nm and its emission could be detected with FACS filter used for PE. A single cell suspension was prepared and washed with PBS at room temperature to remove excessive FCS. 2x single cell suspension was prepared by adding 1ml of Diluent C to cell pellet. 2x dye solution was prepared immediately by adding 4µl of PKH26 ethanolic dye solution to 1 ml of Diluent C. 2x dye solution was added to 2x single cell suspension and incubated at room temperature for 5 minutes. Staining was terminated by adding an equal volume of complete media and incubating for 1 minute. Cells were washed thrice with complete media and ready for use.

2.12.3 eFluor 670 cell proliferation dye

eFluor 670 cell proliferation dye was purchased from eBioscience, UK. eFluor 670 has a peak excitation of 647nm and its emission could be detected with FACS filter used for APC. Lyophilized formed of eFluor 670 was reconstituted to a stock solution (5mM) with 126µl DMSO and stored at -20°C according to the manufacturer's instructions. A single cell suspension was prepared at 2x final concentration and washed with PBS thrice at room temperature to remove excessive FCS. 10µM eFluor 670 solution was prepared with PBS at room temperature and added to 2x single cell suspension. Cells were incubated at 37°C for 10 minutes in the dark. Staining was terminated by adding 5x volumes of cold complete media and incubating on ice for 5 minutes. Cells were washed thrice with complete media and ready for use.

2.13 *In vitro* Treg suppression assay

2.13.1 Beads as stimulators

A defined number of CBA splenocytes or isolated $CD4^+CD25^-$ T cells were used as responders, which were labelled with eFluor 670 fluorescent dye before being added to the stimulators in a round-bottom 96-well plate. Anti-CD3/CD28 antibody-conjugated beads were used as stimulators at a defined Responders to Stimulators ratio. The suppressive function of Treg was deduced from their effect on the proliferation of responders as a function of eFluor 670 dye dilution *in vitro*, in the presence of a defined number of $CD4^+CD25^+$ nTreg. Cells were harvested for the examination by flow cytometry over a period of 1-7 days.

2.13.2 Allogeneic BM-APC as stimulators

A defined number of CBA $CD4^+CD25^-$ T cells were used as responders which were labelled with eFluor 670 fluorescent dye before being added to stimulators in a round-bottom 96-well plate. Irradiated (3000 rad) allogneneic (B6) BM-APC were used as stimulators at a defined Responders to Stimulators ratio. The suppressive function of $CD4^+CD25^+$ nTreg was deduced from their effect on the proliferation of responders as a function of eFluor 670 dye dilution, in the presence of a defined number of $CD4^+CD25^+$ nTreg. After 4-5 days, cells were harvested and examined by flow cytometry. B6 BM-APC driven by GM-CSF, BM-APC driven by GM-CSF plus poly:IC, and BM-APC driven by GM-CSF plus LPS were tested as stimulators for the *in vitro* suppression assay. $5x10^4$ eFluor 670 stained CBA $CD4^+CD25^-$ T cells were incubated with $1x10^4$ BM-APC, $1x10^4$ BM-APC (poly:IC) or $1x10^4$ BM-APC (LPS) over 7 days. Unstimulated responders served as controls in

each group. The proliferation profiles of the responder population were analyzed using flow cytometry.

2.13.3 Proliferation index calculations

Fluorescence-labelled naïve T cells proliferate in response to polyclonal or allogeneic stimulation *in vitro*. Cells were harvested and analysed using flow cytometry. Cell numbers of each division cycle were enumerated using the division history of the fluorescent dye signals ***(Figure 4.2.3.2)***. Undivided and the first 4 divisions were included. The ***number of precursor responders*** (cells) and the ***proliferative indices*** were calculated using the formulae listed below:

$$\textit{Number of precursor responders} = \frac{[u]}{1} + \frac{[div^1]}{2} + \frac{[div^2]}{4} + \frac{[div^3]}{8} + \frac{[div^4]}{16}$$

$$\textit{Proliferation Index} = \frac{\frac{[div^1]}{2} + \frac{[div^2]}{4} + \frac{[div^3]}{8} + \frac{[div^4]}{16}}{\textit{Number of precursor responders}}$$

[u] = number of undivided responders

[div^1] = number of responders in 1st division

[div^2] = number of responders in 2nd division

[div^3] = number of responders in 3rd division

[div^4] = number of responders in 4th division

2.14 Flow cytometry

2.14.1 Cell surface staining

A single cell suspension was prepared and resuspended in FACS buffer- PBS with 2% FCS and 0.02% sodium azide (Sigma-Aldrich, UK). Cells were incubated with Fc receptor block (BD Biosciences, UK) for 15 minutes at room temperature to reduce non-specific binding of monoclonal antibody binding to Fc receptors. Cells were then added with appropriate monoclonal antibodies (at pre-defined concentrations) at 4°C for 30 minutes in the dark. 7AAD (7-amino-actinomycin D, BD Biosciences, UK) was included as part of the surface staining for the assessment of cell viability, where appropriate. Cells were then washed with FACS buffer. A repeat incubation process with a second reagent such as a streptavidin-conjugated fluorochrome for primary biotinylated antibodies was performed, when necessary. Cells were then resuspended in 200µl of FACS buffer prior to acquisition by flow cytometer (FACS Sort, FACS Canto or FACS ARIA cell sorter, BD Biosciences, USA). Cell surface expression was analyzed using Cellquest (BD Biosciences, USA) or FACS Diva (BD Biosciences, USA) softwares.

2.14.2 Intracellular staining (Foxp3, Helios, CTLA-4)

Surface molecules were stained as above ***(Chapter 2.14.1)*** and washed with FACS buffer. Cells were fixed by the addition of 500µl of freshly prepared fixation/permeabilisation buffer (eBioscience, UK) and incubated at 4°C for 2-18 hours in the dark. Cells were then washed with FACS buffer once followed by washing with 2ml of permeabilisation buffer (eBioscience, UK). Cells were then incubated with Fc block at 4°C for 20 minutes in the dark. Without washing,

Foxp3, Helios or CTLA-4 antibodies were added and incubated at 4°C for 30 minutes in the dark. Cells were washed with permeabilisation buffer, then washed with FACS buffer and resuspended in 200µl of FACS buffer before being examined by flow cytometry.

2.14.3 Intracellular cytokine signaling (IL-10)

Isolated T cell populations were resuspended at $1x10^5$ in 200µl complete media containing a protein transport inhibitor and T cell mitogens: (3µl/ml of Golgi Stop, BD Biosciences, UK; 100ng/ml Phorbol 12-myristate 13-acetate (PMA), Sigma-Aldrich, UK; and 1µg/ml ionomycin, Sigma-Aldrich UK), in 96-well round bottom plate for 5 hours. Cells were then washed with FACS buffer. Surface staining was performed, followed by intracellular staining for IL-10 in a similar way as described above ***(Chapter 2.14.2)***. Cells were then washed with FACS buffer and examined for the intracellular expression of IL-10 by flow cytometry.

2.14.4 Cell enumeration with counting beads

Unconjugated polymer beads (Calibrite beads, BD Biosciences, UK) were added at a pre-defined concentration to each specimen. Typically $1x10^5$ beads were added. Thus, the absolute number of cells was calculated by using the following formula: absolute cell number = number of cells acquired / number of beads acquired x $1x10^5$ beads added per tube.

2.14.5 FACS cell sorting

Single cell suspension was prepared as above, with or without enrichment for a $CD4^+$ population. Cells were stained for the surface expression of CD25 using PE-conjugated anti-CD25 antibody (eBioscience, UK) at 4°C for 30 minutes in the dark. Cells were then washed with PBS/ 2% FCS and resuspended to a final concentration of $2x10^7$/ml for flow sorting using FACS ARIA sorter (BD Biosciences, USA). $CD4^+CD25^+$ and $CD4^+CD25^-$ T cell populations were sorted and collected separately in PBS / 2% FCS. In specific experiments, cells were prepared similarly and sorted for $CD4^+GFP^+$ or $CD4^-GFP^-$ T cell populations. $CD4^+CD44^{hi}$ memory T cells generated *in vivo* ***(Chapter 2.3.4)*** were sorted based on the expression of the surface expression of CD44, and the $CD44^{hi}$ sub-population was isolated. Doubly-sorted Treg was done by acquiring and sorting the same population twice.

2.15 Statistical analysis

All statistical analysis was performed using computer software Graphad version 5. Power calculation with an aim to have an accuracny of >80% using the formula denoting the two means and signal/noise ratio using the conventional formula $\delta=|\mu 1-\mu 2|/\sigma$. Sample size is determined from a normogram according to the calculated standardized effect size. Adequate sample size of experiments was determined based on power calculation with a confidence interval of 95%, where appropriate. For *in vivo* transplant experiments, the calculated sample size was modulated and kept to the minimum number of animal used (typically $n\geq 3$) in accordance to the Scientific Act 1986. Unpaired Student *t* tests were used for nominal statistical comparisons. Data were presented as mean$\pm$ 1 standard deviation (S.D.), unless otherwise stated. Statistical comparisons between graft survivals were carried out using log-rank tests. *p* values <0.05 denoted statistical significance.

Chapter 3 *In vitro* generated Regulatory T cells prolonged allograft survival in immunocompetent recipients

3.1 Introduction

There is strong evidence in the literature to suggest that $CD4^+CD25^+$ Treg prepared *in vitro* could attenuate alloresponses *in vivo* in various transplant models using immunodeficient hosts. Adoptive transfer transplant models offer an excellent tool for investigators to establish the proof-of-concept protocols. As outlined in ***Chapter 1.4***, the seminal studies that involved the use of immunodeficient mice demonstrated suppressive capability of Treg in controlling GVHD[423]. They also provide a unique platform for the evaluation of employing Treg in the prevention of GVHD in clinical trials. However, it is often difficult to extrapolate these results from highly constrained adoptive transfer models to recipients with an intact immune repertoire. The observations from these experiments were also confounded by the effect of homeostatic proliferation on both the infused Treg and effector T cells when the cells are transferred to immunodeficient hosts.

A limited number of studies have shown that Treg therapy might have the potential to control allograft rejection in immunocompetent hosts in heart transplant models[425]. The use of T cell depletion strategies although less clinically relevant, has been used to create a window of opportunity to demonstrate suppressive function of Treg[428,429].

In our group, G. Feng developed a novel *in vitro* Treg enrichment protocol using exogenous IFN-γ that enriched for Foxp3$^+$ alloreactive Treg. These cells effectively suppressed allograft rejection mediated by co-transferred naïve CD4$^+$CD25$^-$ T cells in immunodeficient hosts of a full MHC-mismatched skin transplant model[256]. To take this work forward we hypothesized that these cells were capable of controlling allograft rejection in immunocompetent recipients.

The aim of this chapter is to validate and optimize the IFN-γ conditioning protocol for the generation of regulatory T cells (IFN-γ Treg) and to test if these cells could control allograft rejection in immunocompetent recipients using an experimental heart transplant model.

3.2 Results

3.2.1 The IFN-γ conditioning protocol is a robust system that enriches for a dominant CD4$^+$Foxp3$^+$ alloantigen-experienced Treg population

G. Feng initially described the IFN-γ enrichment protocol using B10 (haplotype H2^b) bone marrow-derived APC (BM-APC) to stimulate CBA.Ca (CBA; haplotype H2^k) splenic CD4$^+$ T cells in the presence of IFN-γ at a defined concentration *in vitro*. In our experiments, we employed a similar full MHC-mismatched strain combination: C57BL/6 (B6; haplotype H2^b) as donors and CBA (haplotype H2^k) as recipients. 5x10^5 CBA CD4$^+$ T cells were stimulated with 2 successive rounds of 5x10^4 B6 BM-APC at 7-day intervals in the presence of IFN-γ (5ng/ml) *in vitro* for 14 days ***(see Chapter 2.8.1 and Figure 3.2.1.1.i)***.

CBA $CD4^+$ T cells were isolated from splenocytes by positive selection with a purity ≥ 95% ***(Figure 3.2.1.1.iia)***. The expression Foxp3 by naive $CD4^+$ T cells prior to the IFN-γ conditioning was 6.5% ***(Figure 3.2.1.1.iib)***. After two-rounds of alloantigen stimulation with B6 BM-APC, all cells were retrieved and reassessed for their expression of Foxp3. The resultant $CD4^+$ T cell population, called 'IFN- γ Treg' was enriched for a dominant $Foxp3^+$ phenotype from on average 6-8% to 40-60% (n=13). A representative dot plot showed an enrichment of 53.8% $Foxp3^+$ within the dual-coloured stained $CD4^+$TCR-β^+ population ***(Figure 3.2.1.1.iiia)***. Cell viability was confirmed by trypan blue staining under light microscopy. On average, less than 5% of cells were stained positive for trypan blue at the time of harvesting (*data not shown*). In addition, IFN-γ Treg were assessed for their expression of 7AAD, a marker for cells prone to apoptosis. A representative dot plot illustrates that <10% of $Foxp3^+$ cells were $7AAD^+$ ***(Figure 3.2.1.1.iiib)***.

Figure 3.2.1.1. IFN-γ conditioning protocol enriched for a Foxp3⁺ dominant population *in vitro*

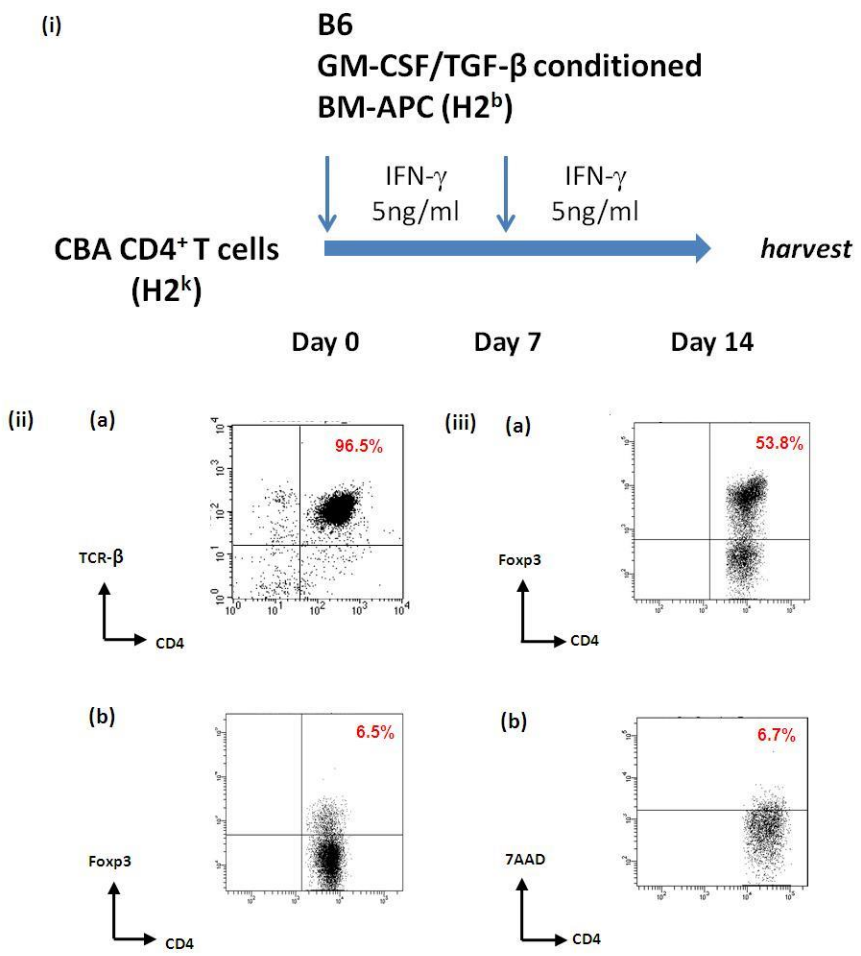

Figure 3.2.1.1. IFN-γ conditioning protocol enriched for a dominant Foxp3⁺ population *in vitro*. (i) A flow chart showing the experimental set up of the IFN-γ conditioning protocol. MACS-selected naive CBA ($H2^k$ haplotype) $CD4^+$ T cells were stimulated with two successive rounds of freshly-harvested B6 ($H2^b$ haplotype) BM-APC on day 0 and day 7 *in vitro*. BM-APC were pre-conditioned with GM-CSF (2ng/ml) and TGF-β (2ng/ml) for 6 days *in vitro*. BM-APC were then harvested, washed and resuspended in culture media in the presence of IFN-γ at 5ng/ml before adding to the $CD4^+$ T cell suspension as described in ***Chapter 2.8.1***. **(iia)** Representative FACS dot plots show that $CD4^+$ T cells isolation by MACS yielded a purity in excess of 96%. **(iib)** 6.5% of naive CBA $CD4^+$ T cells expressed the intracellular transcription factor Foxp3. **(iiia)** The proportion of $Foxp3^+$ population within the resultant $CD4^+$ T cells pool increased to 53.8% after the stimulation by allogeneic BM-APC in the presence of IFN-γ for 14 days. **(iiib)** Cell viability of the resultant $CD4^+$ population following IFN-γ conditioning protocol was determined by surface staining of 7AAD. A representative dot plot shows that 6.7% of the gated $CD4^+Foxp3^+$ cells were $7AAD^+$. Data above are representative of at least 2 independent experiments.

3.2.2 IFN-γ Treg prevented skin graft rejection in an adoptive transfer model

The next question was whether these IFN-γ Treg function *in vivo*. We investigated the suppressive function of IFN-γ Treg using a well-established full-thickness skin transplant model. This skin transplant model involves adoptive transfer of a defined number of naïve $CD4^+CD25^-$ T cells, which mediate skin allograft rejection in immunodeficient mice ***(Figure 3.2.2.1.i)***. Naïve $CD4^+CD25^-$ T cells were negatively selected from splenocytes, which excludes the majority of $CD25^+$ and $Foxp3^+$ Treg, leaving a typical purity of 99% $CD25^-$ and 98% $Foxp3^-$ as shown in ***Figure 3.2.2.1.ii***. IFN-γ Treg were generated *in vitro* and their phenotypic features were analyzed before being administered to immunodeficient recipients. Gated on the $CD4^+TCR^+$ population, 82% and 62% of IFN-γ Treg expressed CD25 and Foxp3, respectively. CBA $RAG^{-/-}$ (recombination activating gene knock-out) mice were reconstituted with $1x10^5$ $CD4^+CD25^-$ naïve T cells as an effector T cell population and these cells rejected B6 skin allografts acutely with a MST of 18.5 days (n=6) ***(Figure 3.2.2.2.i)***. Skin allografts undergoing acute rejection showed generalized necrosis leading to prompt complete rejection ***(Figure 3.2.2.2.i)***. On the other hand, CBA $RAG^{-/-}$ mice reconstituted with the same effector population together with $2x10^5$ IFN-γ Treg accepted their allografts long-term beyond 100 days (n=6) ***(Figure 3.2.2.2.i & iib)***. This graft protective effect delivered by IFN-γ Treg persisted well beyond 100 days post-transplant as shown by the pristine macroscopic features of the skin allografts ***(Figure 3.2.2.2.iib)***.

Figure 3.2.2.1. Functional assessment of IFN-γ Treg using an adoptive transfer model

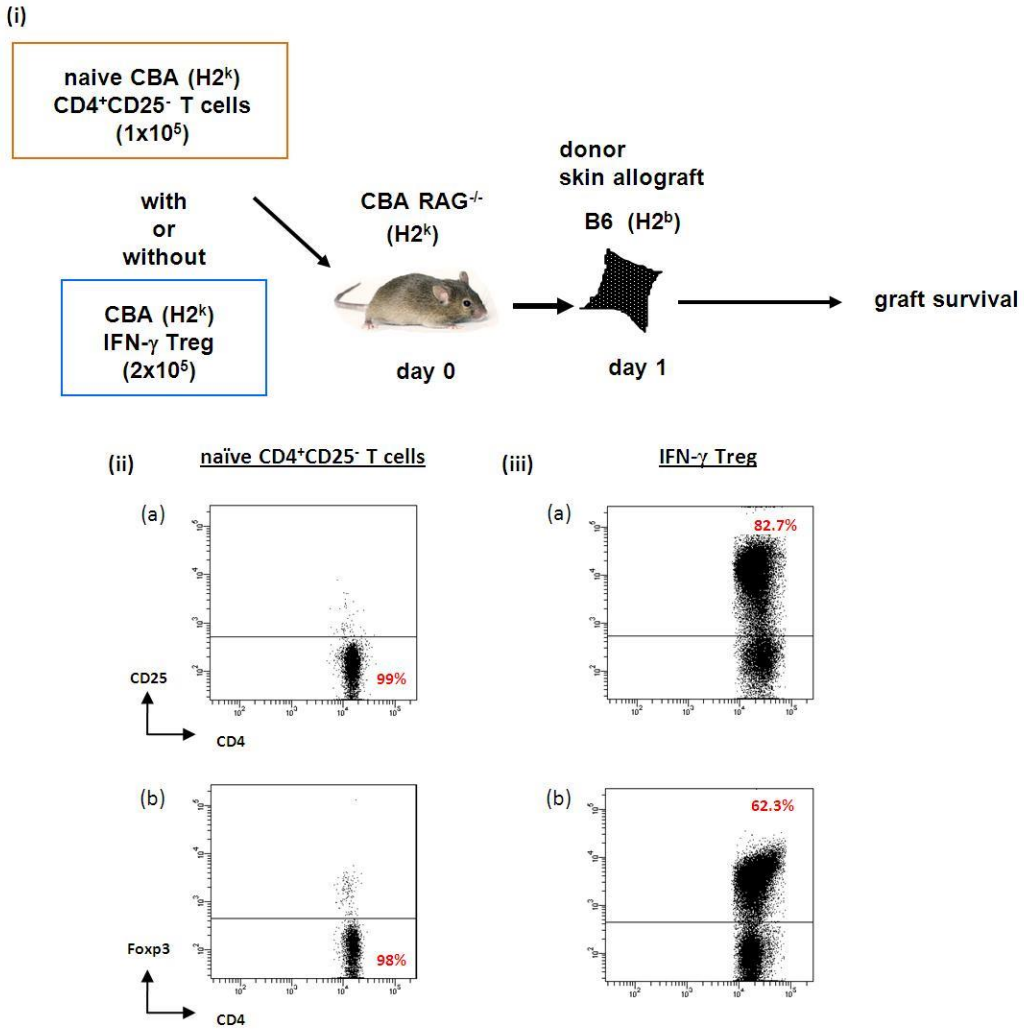

Figure 3.2.2.1. Functional assessment of IFN-γ Treg using an adoptive transfer model. (i) Schematic diagram of the skin transplant adoptive transfer model set up. CBA RAG$^{-/-}$ mice were reconstituted with 1x10^5 naïve CBA CD4$^+$CD25$^-$ T cells one day prior to the transplant of a full MHC -mismatched B6 skin allograft, with or without co-transferred 2x10^5 IFN-γ Treg. **(iia-b)** Naïve CD4$^+$CD25$^-$T cells were evaluated for their expression of CD25 and Foxp3 by flow cytometry. 1% and 2% of the negatively-selected CD4$^+$CD25$^-$ population expressed CD25 and Foxp3, respectively. **(iii)** A high proportion of alloantigen-driven IFN-γ Treg expressed CD25 (82.7%) and Foxp3 (62.3%) confirming their typical regulatory phenotype. Data above are representative of at least 2 independent experiments.

Figure 3.2.2.2. IFN-γ Treg prevented skin allograft rejection in an adoptive transfer model

(i)

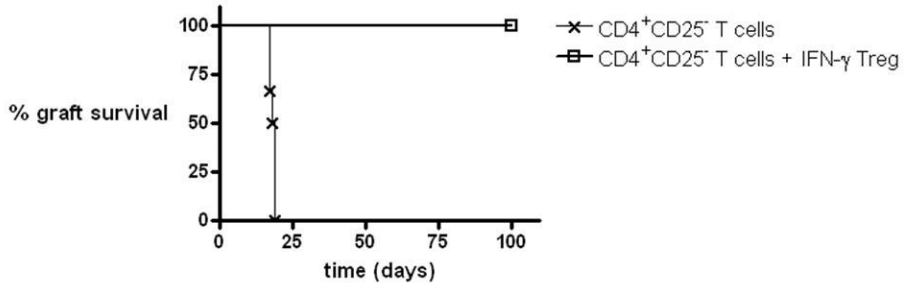

Group	n	graft survival (days)	MST (days)	p-value
$CD4^+CD25^-$ T cells	6	17,17,18,19,19,19	18.5	$p = 0.0010$
$CD4^+CD25^-$ T cells + IFN-γ Treg	6	>100,>100,>100,>100,>100,>100	>100	

(ii)

(a)



skin allograft rejected on day 18 with macroscopic features of tissue inflammation and necrosis

(b)



skin allograft accepted as seen with pristine, healthy tissue on day 100

Figure 3.2.2.2. IFN-γ Treg prevented skin allograft rejection in an adoptive transfer model. (i) Kaplan-Meier survival curves show that when CBA $RAG^{-/-}$ mice reconstituted with $1x10^5$ $CD4^+CD25^-$ T cells alone, skin allografts were rejected acutely with a median survival time (MST) of 18.5 days (17-19 days; n=6). In contrast, in the presence of co-transferred $2x10^5$ IFN-γ Treg , all skin allografts were accepted long-term with a MST >100 days (all >100 days; n=6; p=0.001). **(ii)** Representative photographs illustrate the macroscopic changes of skin allografts in these groups. **(a)** Acute rejection mediated by $CD4^+CD25^-$ T cells caused generalised inflammation and necrosis leading to complete rejection on day 18 **(b)**. IFN-γ Treg prevented skin allograft rejection long-term and these allografts retained pristine and healthy macroscopic features on day 100 post-transplant. Log rank test was used for statistical comparisons (p<0.05 denotes statistically significant).

3.2.3 Optimization of IFN-γ conditioning protocol

While the IFN-γ conditioning protocol could be replicated, we encountered inconsistent Foxp3 enrichment in the resultant population, which could range from 10% to 70%. But, more importantly, it was also complicated by a persistent low cell yield. The limited cell numbers generated could potentially make it impossible to test the suppressive function of IFN-γ Treg in immunocompetent transplant recipients. We therefore investigated optimizing the protocol with the objective of improving cell yields while retaining the suppressive capacity of the resulting population.

The IFN-γ conditioning protocol exploits the use of repeat alloantigen stimulation, which results in alloreactive Treg proliferation, whereas the action of IFN-γ in culture was responsible in shaping the T cell repertoire by inducing activation-induced cell death of non-Treg. Hence, we hypothesized that an increased concentration of IFN-γ would not lead to an increase overall cell yield. Indeed, in preliminary experiments G. Feng had previously shown that increasing the concentration of IFN-γ to 10-50ng/ml (i.e. a 2 to 10-fold increase from the original protocol) led to detrimental Foxp3 enrichment[256,440]. We therefore hypothesized that an increased amount of alloantigen delivered in culture could potentially enhance cell yield. With reference to various publications, reports and personal communications, we aimed to optimize the IFN-γ conditioning protocol by enhancing alloantigen stimulation using various methods to maximize the yield of $Foxp3^+$ population as follows.

3.2.3.1 Enhancing alloantigen stimulation in the culture system

G. Feng developed the original IFN-γ conditioning protocol with an initial aim to polarize the differentiation of whole $CD4^+$ T cells between Th1 and Th2 cells. The original protocol used a 10:1 $CD4^+$ T cells: BM-APC ratio ($5x10^5$ $CD4^+$ T cells : $5x10^4$ BM-APC cells/well), which was based on the culture system widely used in many mixed lymphocyte reaction (MLR) experiments[256]. To test our hypothesis that the low cell yield was due to a sub-optimal antigenic stimulation delivered by BM-APC, we first investigated the effect of increasing the number of BM-APC present in the culture, while keeping the rest of the culture conditions constant.

As previously reported by G. Feng, the first round of alloantigen stimulation in the IFN-γ conditioning protocol was thought to be linked to the repertoire shaping of the $CD4^+$ T cells, while the second round of the protocol was thought to be important for the proliferative phase of alloantigen-stimulated Treg[440]. A pilot study showed that additional BM-APC (up to 4x the original input number) solely in the second round of alloantigen stimulation led to an increased $Foxp3^+$ composition by 10-15% (range 20.9-37.7%) ***(Figure 3.2.3.1.1.i)***. More interestingly, this was accompanied by an improvement of cell yield by 1.6-2.8 fold ***(Figure 3.2.3.1.1.ii)***.

Figure 3.2.3.1.1. Increasing alloantigen stimulation at the second round led to an improvement of Foxp3⁺ T cell enrichment and overall cell yield of the IFN-γ conditioning protocol

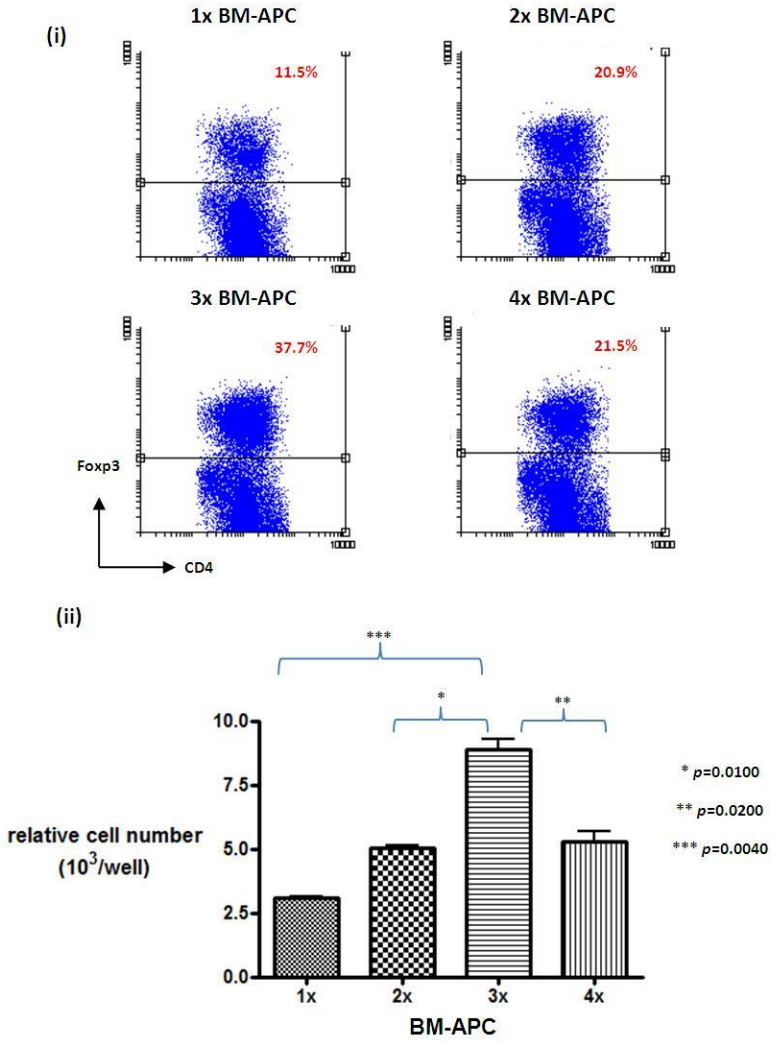

Figure 3.2.3.1.1. Increasing alloantigen stimulation at the second round led to an improvement of Foxp3⁺ T cell enrichment and overall cell yield of the IFN-γ conditioning protocol. An increased number of BM-APC in the second round of alloantigen stimulation alone resulted in an increased Foxp3⁺ T cell enrichment as well as an improved cell yield. **(i)** Representative FACS dot plots show the expression of Foxp3 in the CD4⁺ population of the resultant IFN-γ Treg governed by different amount of alloantigen stimulation: 11.5% (1x original set up; i.e. $5x10^4$ BM-APC), 20.9% (2x), 37.7% (3x), and 21.5% (4x). **(ii)** The absolute number of Foxp3⁺ cells retrievable from the IFN-γ protocol was highest in the 3x group ($8.5x10^3$) compared to the others: 1x ($3.0x10^3$); 2x ($5.1x10^3$); and 4x ($5.3x10^3$ cells/well). Relative cell numbers were enumerated by flow cytometry using counting beads as described in ***Chapter 2.14.4***. Bar charts illustrates the mean relative cell number per well ± 1 S.D. (standard deviation) of 3 samples. The unpaired student's t-tests were used for statistical comparisons ($p<0.05$ denotes statistically significant).

Changing both first and second round of BM-APC stimulation by increasing the number of BM-APC led to an increased number of resultant IFN-γ Treg, while the level of Foxp3 enrichment was preserved. An increased number of BM-APC at both round of stimulation increased the percentages of $Foxp3^+$ cells significantly at 3x BM-APC (44.3%; *p*=0.0431), but not at 2x BM-APC (39.8%), and 4x BM-APC group (43.2%), as compared to the original protocol, i.e. 1x BM-APC (32.9%) ***(Figure 3.2.3.1.2.i)***. There were significantly higher numbers of $Foxp3^+$ cells when the number of BM-APC was increased from 1x (53.8 $x10^3$) to 2x (121.1 $x10^3$), 3x (143.6 $x10^3$) and 4x (125.6 $x10^3$), respectively. There was at least a 2-3 fold increase in the cell yield when the number of BM-APC was increased to 2 to 4 times the number present in the original set up. In fact, it appeared to be detrimental to Foxp3 yield by adding excessive BM-APC (4x BM-APC in ***Figure 3.2.3.1.2.ii***). Although we saw no statiscially significant in the number of Treg cell yield between the 2x and 3x BM-APC group, we chose the 3x BM-APC protocol based on the consistently higher enrichment rate ***(Figure 3.2.3.1.2.i)***. Moreover, the batch-to-batch enrichment inconsistency was eliminated by employing the 3x BM-APC protocol in subsequent repeat experiments (*data not shown*). Hence, the 3x BM-APC protocol was adapted for the rest of the project unless otherwise stated.

Figure 3.2.3.1.2. Increasing alloantigen stimulation in both rounds led to an improvement of Foxp3$^+$ T cell enrichment and overall cell yield of the IFN-γ conditioning protocol

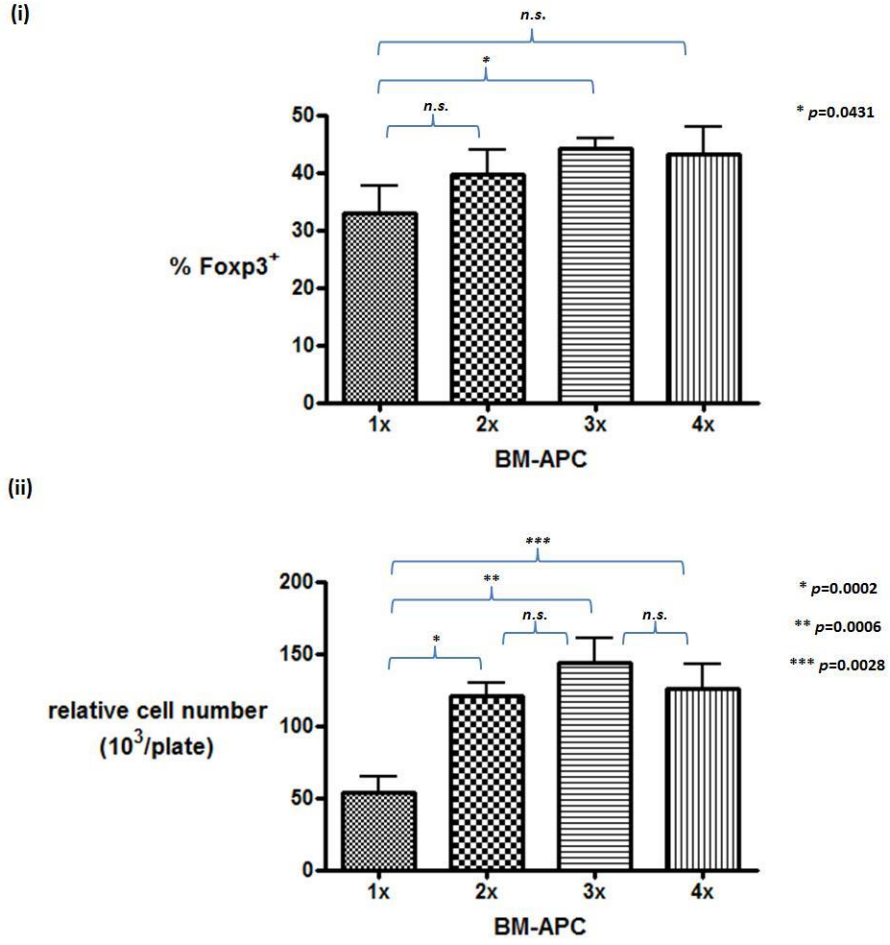

Figure 3.2.3.1.2. Increasing alloantigen stimulation in both rounds led to an improvement of Foxp3$^+$ T cell enrichment and overall cell yield of the IFN-γ conditioning protocol. CBA CD4$^+$ T cells were incubated with titrated numbers of freshly-harvested BM-APC for two successive rounds as follows: 1xBM-APC - the original protocol using $5x10^4$, 2xBM-APC ($1x10^5$), 3xBM-APC ($1.5x10^5$) and to 4xBM-APC ($2x10^5$ cells /well), in the presence of IFN-γ at 5 ng/ml. **(i)** There were no significant differences in the proportion of the Foxp3$^+$CD25$^+$ population in the resultant IFN-γ Treg among all groups, except that between 1x BM-APC (32.9%) and 3xBM-APC (44.3%) (p=0.0431). **(ii)** More importantly, all groups have a significantly higher cell yield compared to the 1xBM-APC ($53.8x10^3$ cells/24-well plate). The 3xBM-APC group had the highest mean number of cells ($143.6x10^3$ cells/24-well plate), though not significantly different from the 2xBM-APC ($121.1x10^3$ cells/24-well plate) or 4xBM-APC group ($125.6x10^3$ cells/24-well plate). Data are representative of mean % Foxp3$^+$ T cells and mean relative cell number of 3 individual samples. The unpaired student's t-tests were used to compare the differences among each group (p<0.05 denotes statistically significant).

3.2.3.2 Increasing the overall cell density in the IFN-γ conditioning protocol did not improve quality or the quantity of the output Treg population

The original IFN-γ conditioning protocol was developed based on the methodology of a mixed-lymphocyte reaction (MLR) cultured in a flat-bottom 24-well tissue culture plate. Each well was given $5x10^5$ $CD4^+$ T cells plus $1.5x10^5$ allogeneic BM-APC in 2ml of media. Interval examination under light microscopy revealed that these cells resided on small spatial areas in the periphery of the wells leaving >95% of the space unoccupied. With reference to T cell expansion protocols published by manufacturers for mouse Treg expansion, cells were resuspended at $1x10^6$ cells/ml/cm^2, thus $2x10^6$/2ml/well of a 24-well plate[441]. Similarly, mouse MLR protocols also employed a density of $1x10^6$/ml[442]. We reasoned that the sub-optimal cell density in our cultures might be responsible for the persistent low cell yield because of the lack of physico-chemical interaction between the $CD4^+$ T cells and BM-APC. We therefore hypothesized that increasing the overall cell density in each well would improve cell yield.

Cultures of different overall cell densities were set up in the presence of a constant IFN-γ concentration (5ng/ml) in 2ml/well in a 24-well plate as follows: the original cell density ($5x10^5$ $CD4^+$ T cells: $1.5x10^5$ BM-APC cells/well); 2x cell density ($1x10^6$ $CD4^+$ T cells: $3x10^5$ cells/well); 6x cell density ($3x10^6$ $CD4^+$ T cells: $9x10^5$ BM-APC cells/well). Doubling the overall cell density (2x) did not improve enrichment of $Foxp3^+$ cells (15.9%) compared to the original methodology (28.3%; n=3; *p*=0.0527) ***(Figure 3.2.3.2.1.i)***. Moreover, in terms of absolute cell numbers, doubling the cell density had no impact on the cell yield of $Foxp3^+$ cells ($9.4x10^3$ cells/well) when compared to the original set up conditions ($14.x10^3$ cells/well, n=3; *p*=0.0796) ***(Figure 3.2.3.2.1.ii)***. Limited observations indicated that a further increase in the cell density in each

well by 6-folds resulted in an increased cell yield ($18x10^3$ cells/well); however it was accompanied with a reduced percentage of $Foxp3^+$ cells (20.2%) ***(Figure 3.2.3.2.1.i & ii)***. More importantly, the proportion of the $Foxp3^+CD62L^+$ population was higher in cultures using the original set up (24.6%) compared to 2x (10.6%) or 6x (16.0%) the cell density. The $CD62L^+$ phenotype has been reported to be positively correlated to Treg function. These data suggest that increasing the cell density in this culture system had no real advantage to achieve a better yield output, but that it could be detrimental to Foxp3 enrichment.

Figure 3.2.3.2.1. Increased cell density of the IFN-γ conditioning protocol did not improve Foxp3 enrichment and cell yield

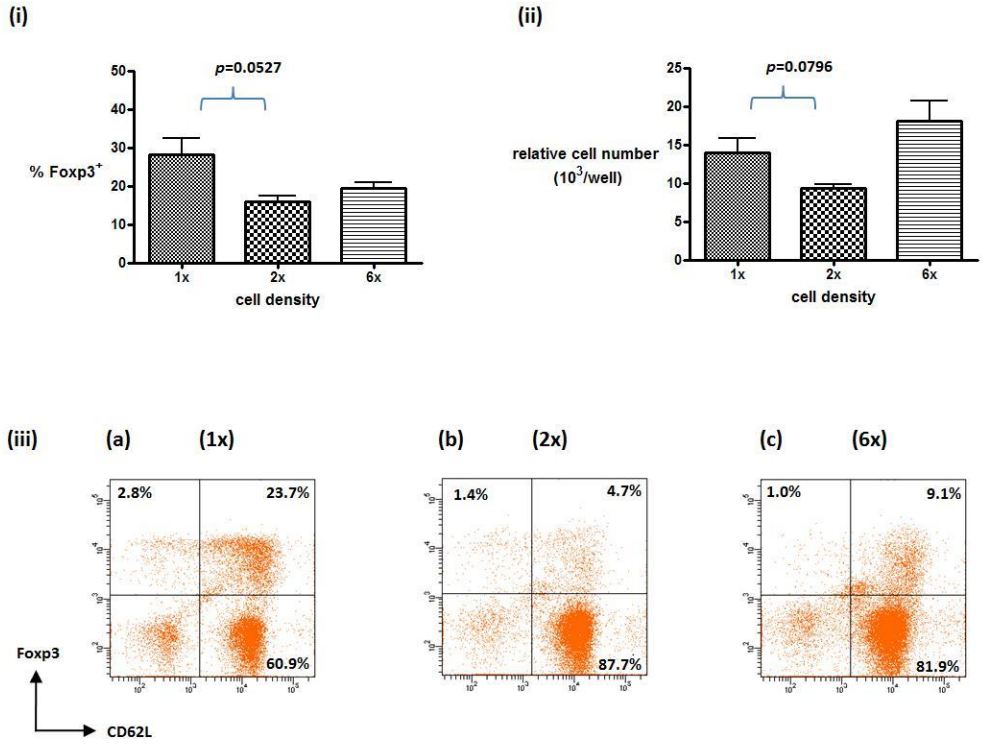

Figure 3.2.3.2.1. Increased cell density of the IFN-γ conditioning protocol did not improve Foxp3 enrichment and cell yield. The amount of both $CD4^+$ T cells and BM-APC were increased by 2x or 6 x in each well in a 24-well tissue culture plate in an attempt to increase the cell yield and Foxp3 enrichment by means of enhancing stochastic cellular interaction between $CD4^+$ T cells and BM-APC. **(i)** Increased cellular density to twice as much as the input cell number per well in the 24-well tissue culture plate led to an average reduction of Foxp3 enrichment from 28.3% to 15.9%. (n=3, p=0.0527) **(ii)** Similarly, the absolute cell number per well was reduced from $14.0x10^3$ to $9.4x10^3$ (n=3, p=0.0796) as determined by intracellular Foxp3 staining and enumerated by flow cytometry using counting beads. **(iii)** Representative FACS dot plots indicate that IFN-γ Treg generated under the original condition (1x) comprised of a higher proportion of $Foxp3^+CD62L^+$ (24.6%) population compared to the conditions with 2x (10.6%) or 6x (16.0%) cell density **(iiib & iiic)**. Bar charts illustrate the mean % Foxp3 and relative cell number per well ± 1 S.D. of 2-3 samples. The unpaired student's t-tests were used for statistical comparisons (p<0.05 denotes statistically significant).

3.2.3.3 Phenotypic features of BM-APC affected by incubation in a 24-well plate versus a petridish

We then looked at the possibility of manipulating the maturity status of the modulated BM-APC used in this IFN-γ conditioning protocol in an attempt to enhance antigenic stimulation, which might ultimately lead to an increased cell yield by promoting proliferation of alloreactive Treg. The salient phenotypic features of BM-APC could be an important factor in governing the differentiation or proliferation of $CD4^+$ T cells. In addition to growth factors and other known chemical stimulants, the physico-chemical interactions between bone marrow cells and the *in vitro* apparatus could affect the maturity status of BM-APC, and hence the outcome of the IFN-γ conditioning protocol. Our IFN-γ protocol used 24-well tissue culture plates with the intent that non-adherent immature BM-APC could be easily harvested, while mature and well differentiated BM-APC were adherent strongly to the bottom of the plates. On the other hand, with reference to Ralph Steinmann's seminal paper, which was commonly cited for the generation of conventional mouse mature BM-DC[443], petridishes were used instead of 24-well plates. We hypothesized that BM-APC generated using petridishes could give rise to a more mature BM-APC phenotype, which could then deliver a stronger antigenic signal for T cell proliferation compared to immature APC. Our intention was that while all alloreactive T cells would undergo proliferation, the $Foxp3^-$ population would preferentially be subject to activation-induced cell death (AICD) in the presence of exogenous IFN-γ, which would then lead to an improved $Foxp3^+$ cell yield.

BM-APC were cultured with GM-CSF (2ng/ml) and TGF-β (2ng/ml) in either flat-bottom 24-well tissue culture plates, or 10cm petridishes. The phenotypic features of BM-APC were evaluated at the time of harvest by flow cytometry analysis before being added to $CD4^+$ T cells at each

round of stimulation. The proportion and number of $Foxp3^+$ cells in the resultant IFN-γ Treg generated by two different types of BM-APC was compared.

Dot plots illustrate the differences in the expression of a number of key costimulation and MHC class II molecules on BM-APC generated using 24-well plates (24w-BM-APC) or petridishes (Pet-BM-APC) in ***Figure 3.2.3.3.1.i***. CD11c is a phenotypic marker commonly used to differentiate functional mature BM-DC from immature BM-DC. Within the $CD11c^+$ population, the proportion of 24w-BM-APC expressing CD40 was similar to Pet-BM-APC (2.9% versus 2.3%). However, the proportion of 24w-BM-APC expressing CD80 (13.7% versus 8.8%), CD86 (14.8% versus 8.9%) and MHC class II (10.0% versus 5.1%) was higher when compared to Pet-BM-APC, respectively. The higher proportion of $CD80^+$ $CD86^+$ MHC class II^+ within the $CD11c^+$ population of 24w-BM-APC might contribute to a higher Foxp3 enrichment efficiency (51.1% versus 22.2%; n=3; *p*=0.0059) and a higher cell yield (35.8 $x10^3$ versus 23.1 $x10^3$ cells/ plate; n=3; *p*=0.0014), when compared to the Pet-BM-APC group ***(Figure 3.2.3.3.1.iii)***. More interestingly, we observed that there was a higher percentage of $CD62L^+$ population in the 24w-BM-APC IFN-γ Treg group compared to the Pet-BM-APC IFN-γ Treg group ***(Figure 3.2.3.3.1.ii)***.

We then tested if these differences translated into their suppressive function *in vivo*. CBA $RAG^{-/-}$ mice were reconstituted with $1x10^5$ naïve $CD4^+CD25^-$ T cells with or without co-transfer of $1x10^5$ IFN-γ Treg (either '24-well BM-APC IFN-γ Treg' or 'Pet BM-APC IFN-γ Treg') one day before the transplant of a B6 skin allograft ***(Figure 3.2.3.3.2.i)***. Despite the differences seen in their Foxp3 and CD62L expression, there were no differences between 24-well BM-APC IFN-γ Treg and Pet BM-APC IFN-γ Treg in their abilities to deter rejection mediated by $CD4^+CD25^-$ T cells in the adoptive transfer model with a MST of 76.5 days (n=6) versus 82.5 days (n=6; *p*=0.9842), respectively (***Figure 3.2.3.3.2.ii***).

Figure 3.2.3.3.1. 24-well BM-APC were superior to Petridish BM-APC in generating Foxp3⁺ IFN-γ Treg

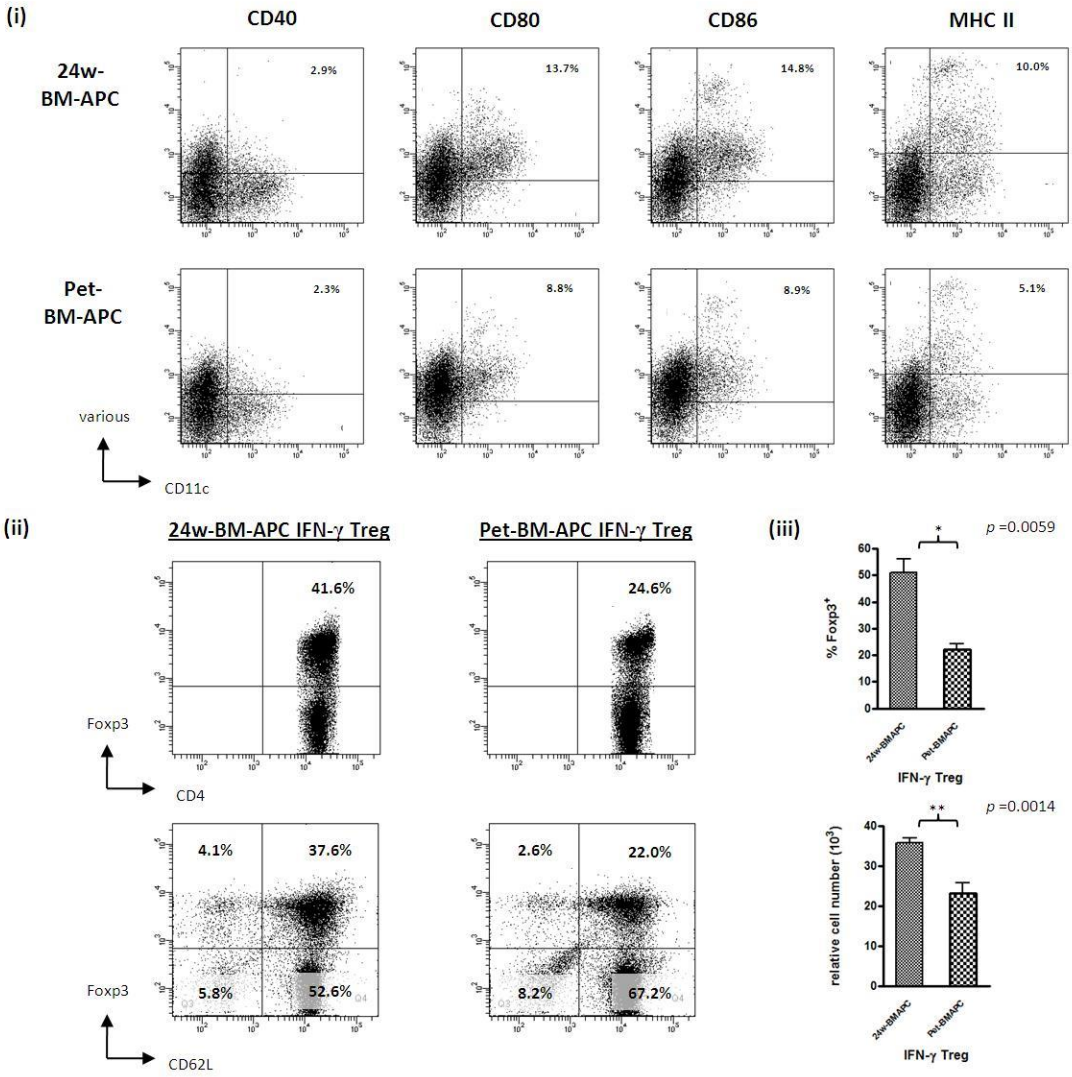

Figure 3.2.3.3.1. 24-well BM-APC were superior to Petridish BM-APC in generating Foxp3⁺ IFN-γ Treg. **(i)** At the time of harvest, aliquots from each group of BM-APC were examined for the expression of accessory molecules by flow cytometry. Dot plots show 24w-BM-APC expressed higher levels of CD80 (13.7 versus 8.8%), CD86 (14.8 versus 8.9%) and MHC class II (10.0 versus 5.1%) within the CD11c⁺ population compared to Pet-BM-APC. There was no difference in the expression of CD40. The resultant IFN-γ Treg populations were examined for the expression of Foxp3 prior to *in vivo* studies. **(ii)** Representative dot plots show an enrichment of Foxp3 to 41.6% and 24.6% in the 24w-BM-APC and Pet-BM-APC group, respectively. 24-well BM-APC IFN-γ Treg contained a higher percentage of Foxp3⁺CD62L⁺ population compared to Petridish BM-APC IFN-γ Treg (37.6% versus 22.0%). **(iii)** The 24w-BM-APC protocol led to a significant higher Foxp3 enrichment yield compared to the Pet-BM-APC protocol (representative data from 3 independent experiments). The unpaired student t-tests were used for statistical comparisons ($p<0.05$ denotes statistically significant).

Figure 3.2.3.3.2. No functional difference between 24w-BM-APC IFN-γ Treg and Pet-BM-APC IFN-γ Treg *in vivo*.

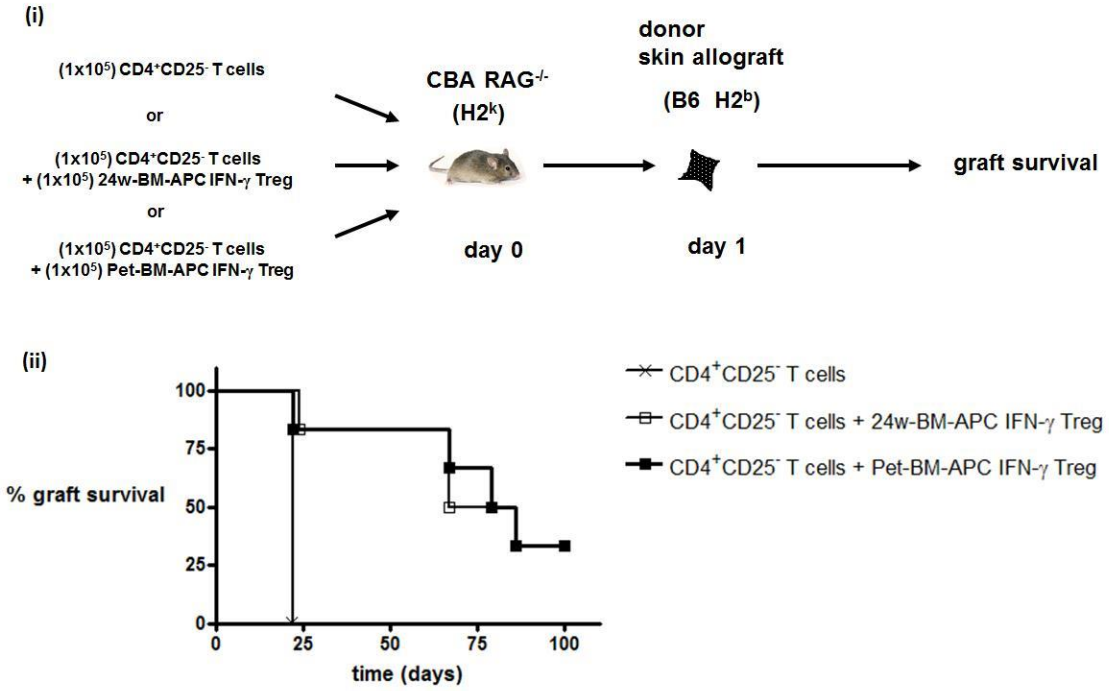

Group	n	graft survival (days)	MST (days)	p-value
CD4⁺CD25⁻ T cells	3	22,22,22	22	
CD4⁺CD25⁻ T cells + 24w-BM-APC IFN-γ Treg	6	24,67,67,86,>100,>100	76.5	*p = 0.9842*
CD4⁺CD25⁻ T cells + Pet-BM-APC IFN-γ Treg	6	22,67,79,86,>100,>100	82.5	

Figure 3.2.3.3.2. No functional difference between 24w-BM-APC IFN-γ Treg and Pet-BM-APC IFN-γ Treg *in vivo*. **(i)** The suppressive function of 24w-BM-APC IFN-γ Treg and Pet-BM-APC IFN-γ Treg was assessed using the adoptive transfer skin allograft model. CBA RAG$^{-/-}$ mice were reconstituted with 1x10^5 naive CD4$^+$CD25$^-$ T cells with either 1x10^5 **24w-BM-APC IFN-γ Treg** or 1x10^5 **Pet-BM-APC IFN-γ Treg** one day prior to the transplant of a B6 skin allograft. **(ii)** Naive CD4$^+$CD25$^-$ T cells rejected skin allografts acutely in all three mice with a MST of 22 days. On the other hand, both 24w-BM-APC IFN-γ Treg and Pet-BM-APC IFN-γ Treg prolonged allograft survival significantly with a MST of 76.5 (n=6) and 82.5 days (n=6), respectively. However, there was no significant difference between these two groups (p=0.9842). Log rank tests were used for statistical comparisons (p<0.05 denotes statistically significant).

3.2.3.4 Differentiation status of allogeneic BM-APC altered by GM-CSF and TGF-β

Bone marrow cells proliferated and matured to various degrees in response to different concentrations of GM-CSF *in vitro*. Previously, G. Feng showed that while immature BM-APC cultured in GM-CSF (2ng/ml) and TGF-β (2ng/ml) could enrich for $Foxp3^+$ T cells using the IFN-γ protocol, BM-APC driven solely by GM-CSF (2ng/ml) was unable to do so[440]. We therefore searched for the optimal maturity status of BM-APC for Foxp3 enrichment by increasing the concentration of GM-CSF in BM-APC cultures, while keeping the concentration of TGF-β constant at 2ng/ml. Our hypothesis was that an increased concentration of GM-CSF in BM-APC culture would increase the frequency of cells expressing high levels of CD80, CD86 and MHC class II to deliver an optimal antigenic stimulation for $CD4^+$ T cell proliferation, which would then enhance IFN-γ Treg cell yield.

Modulated BM-APC were generated from B6 bone marrow cells stimulated with TGF-β (2ng/ml) in a gradient of GM-CSF (2 to 20 ng/ml). Mature BM-APC were generated from B6 bone marrow cells stimulated with GM-CSF (20ng/ml) alone and were used as control. The expression of costimulation and MHC class II molecules was assessed at the time of harvest by flow cytometry. BM-APC differentiated into a more mature phenotype and upregulated their expression of CD40 (2.0% to 49.8%), CD80 (2.2% to 65.2%), CD86 (1.6% to 37.3%) and MHC class II (3.7% to 61.8%) within the $CD11c^+$ population when the concentration of GM-CSF was increased from 2 to 20ng/ml, in the presence of TGF-β (2ng/ml) ***(Figure 3.2.3.4.1)***. In contrast, mature BM-APC generated with GM-CSF alone expressed high levels of CD40 (61.9%), CD80 (72.9%), CD86 (25.3%) and MHC class II (67.6%) ***(Figure 3.2.3.4.1)***.

Figure 3.2.3.4.1. BM-APC generated at a gradient concentration of GM-CSF showed different accessory molecule expression profiles reflecting their maturation status

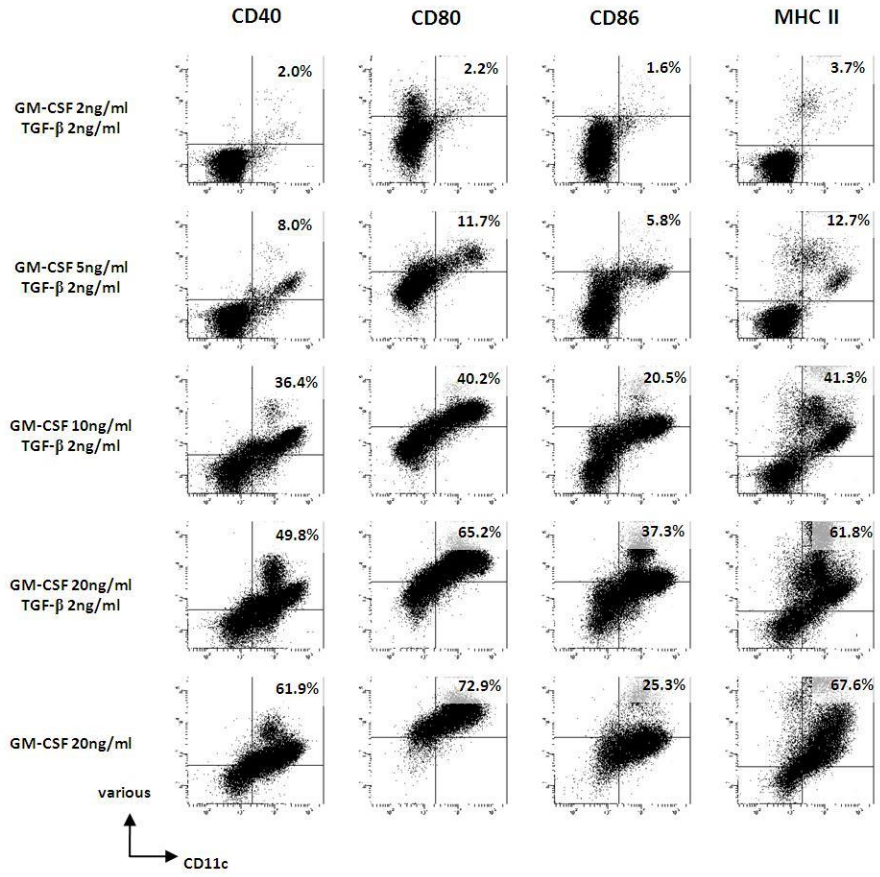

Figure 3.2.3.4.1. BM-APC generated at a gradient concentration of GM-CSF showed different accessory molecule expression profiles reflecting their maturation status. BM-APC were generated from B6 bone marrow cells cultured in GM-CSF 2ng/ml + TGF-β 2ng/ml; GM-CSF 5ng/ml + TGF-β 2ng/ml; GM-CSF 10ng/ml + TGF-β 2ng/ml; GM-CSF 20ng/ml + TGF-β 2ng/ml ; or GM-CSF 20ng/ml alone, for 6 days. Their surface expression of several costimulatory molecules and MHC class II molecules were examined by flow cytometry. Dot plots show upregulation of the expression of several costimulatory molecules and MHC class II within $CD11c^+$ population (right upper quadrant): CD40 increased from 2.0 to 49.8%, CD80 increased from 2.2 to 65.2%, CD86 increased from 1.6% to 37.3% and MHC class II increased from 3.7% to 61.8%. Mature BM-APC generated with GM-CSF alone expressed high levels of CD40 (61,9%), CD80 (72.9%), CD86 (25.3%) and MHC class II (67.6%). Data above are representative of at least 3 independent experiments.

These modulated BM-APC and mature BM-APC were used as allogeneic stimulators in the IFN-γ protocol and the resultant proportion ***(Figure 3.2.3.4.2.i)*** and number of $Foxp3^+$ cells ***(Figure 3.2.3.4.2.ii)*** was analyzed by flow cytometry. Using BM-APC generated under the original conditions (i.e. GM-CSF 2ng/ml and TGF-β 2ng/ml), the IFN-γ protocol produced an enriched Foxp3 population (27.4±9.8%). Interestingly, using BM-APC generated with an increased concentration of GM-CSF (5ng/ml), while keeping TGF-β at 2ng/ml, it resulted in a significant improvement of Foxp3 enrichment to 37.8±12.9%. When the concentration of GM-CSF was increased to 10ng/ml, the rate of Foxp3 enrichment was enhanced further to 44.8±13.8%. However, a further increase in the GM-CSF concentration to 20ng/ml did not show any additional improvement of Fox3 enrichment (34.5±12.8%). On the other hand, as we expected, the IFN-γ protocol using mature BM-APC led to the lowest rate of Foxp3 enrichment (19.8±9.5%), compared to all other modulated BM-APC groups. Similarly, modulated BM-APC generated with GM-CSF at 10ng/ml and TGF-β at 2ng/ml (G10T2 BM-APC) gave rise to the highest yield of $Foxp3^+$ cells (66.8±33.5 $x10^3$ cells) compared to that of GM-CSF at 2ng/ml (10.7±4.1 $x10^3$ cells), 5ng/ml (28.7±10.6 $x10^3$ cells) and 20ng/ml (36.1±20.9 $x10^3$ cells) and mature BM-APC (23.8±7.6 $x10^3$ cells), respectively.

Based on the results above, we generated IFN-γ Treg using G10T2 BM-APC and tested their suppressive function *in vivo* ***(Figure 3.2.3.4.3.i)***. CBA $RAG^{-/-}$ mice were reconstituted with $1x10^5$ naïve $CD4^+CD25^-$ T cells with or without 'G10T2 IFN-γ Treg' one day before the transplant of a B6 skin allograft. G10T2 IFN-γ Treg were able to delay skin allograft rejection long-term mediated by $CD4^+CD25^-$ T cells with a MST >100 days (n=6) (***Figure 3.2.3.4.3.ii***). However, 2 out of 6 allografts were rejected on day 95 when compared to G2T2 IFN-γ Treg where all allografts were accepted well beyond 100 days (historical control, see ***Figure 3.2.2.2.2.i***) when the same cell number was delivered. However, these differences could be explained by the unexpected

differences observed between the two control groups. The contemporary control group in the G10T2 experiment had a MST of 13 days compared to 18.5 days in the historical control. The disparity between these control groups might be explained by different age group of CBA $RAG^{-/-}$ mice being used, while the small variation between the purity of $CD4^{+}CD25^{-}$ T cells could also be as a result of using CBA mice of disparate age groups. As a result, the apparent reduced suppressive function of G10T2 IFN-γ Treg in this experiment might be artificially discounted. Thus, G10T2 IFN-γ Treg might have a similar suppressive ability compared to G2T2 IFN-γ Treg. Further cell titration experiments by increasing the number of $CD4^{+}CD25^{-}$ T cells in each group could reveal the real differences.

Figure 3.2.3.4.2. BM-APC cultured in optimal conditions improved Foxp3 enrichment and cell yield

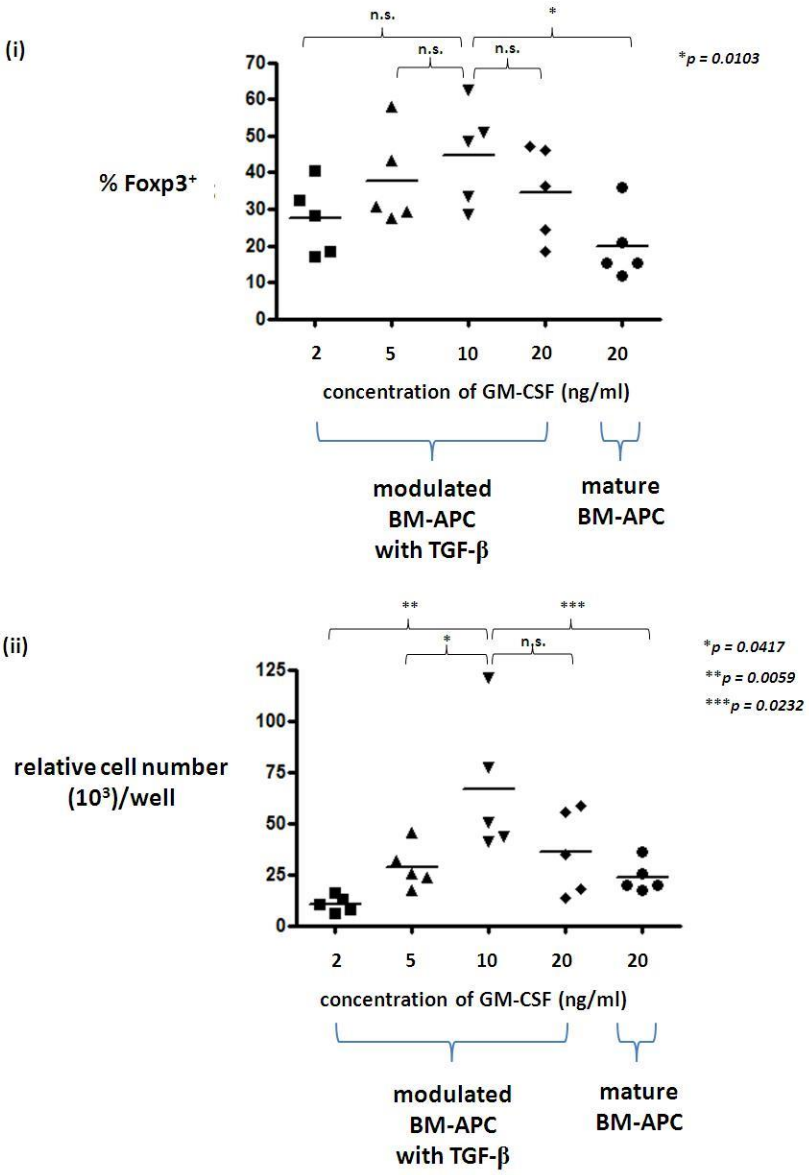

Figure 3.2.3.4.2. BM-APC cultured in optimal conditions improved Foxp3 enrichment and cell yield. Modulated BM-APC were generated by culturing donor BM cells in TGF-β (2ng/ml) and various concentration of GM-CSF (2-20ng/ml). Mature BM-APC were generated by culturing donor BM cells in GM-CSF alone (20ng/ml), as described in ***Chapter 2.7.6***. BM-APC generated in 10ng/ml GM-CSF and TGF-β (2ng/ml) appeared to be the optimal choice to achieve optimal Foxp3 enrichment **(i),** as well as cell yield **(ii)**.

Figure 3.2.3.4.3. G10T2 IFN-γ Treg prolonged skin allograft survival long-term in the adoptive transfer model

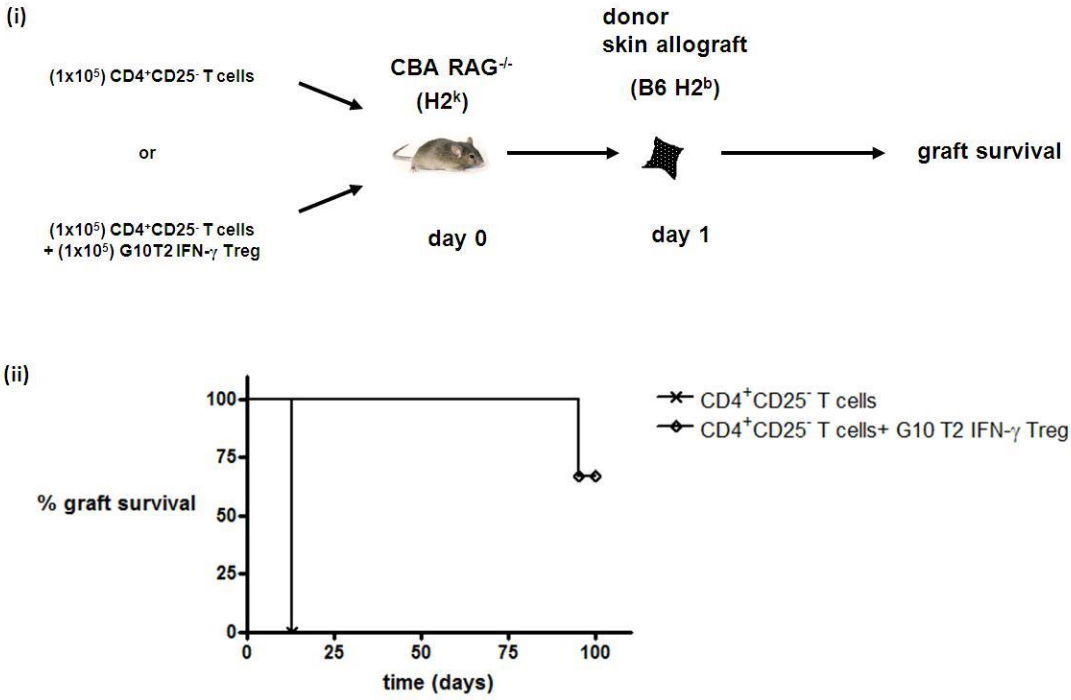

Group	n	graft survival (days)	MST (days)	p-value
$CD4^+CD25^-$ T cells	6	13,13,13,13,13,13	13	
$CD4^+CD25^-$ T cells + G10T2 IFN-γ Treg	6	95,95,>100,>100, >100, >100	>100	p=0.0009

Figure 3.2.3.4.3. G10T2 IFN-γ Treg prolonged skin allograft survival long-term in the adoptive transfer model. (i) CBA $RAG^{-/-}$ mice were reconstituted with $1x10^5$ $CD4^+CD25^-$ naive T cells with or without $1x10^5$ G10T2 IFN-γ Treg (IFN-γ Treg generated with BM-APC stimulated with GM-CSF and TGF-β at 10ng/ml and 2ng/ml, respectively. **(ii)** Mice reconstituted with $CD4^+CD25^-$ T cells alone rejected their skin grafts with a MST of 13 days (n=6). Those mice reconstituted with $CD4^+CD25^-$ T cells together with G10T2 IFN-γ Treg accepted their skin allografts long-term with a MST of >100 days (95-100 days; n=6). Log rank tests were used for statistical comparisons (p<0.0.5 denotes statistically significant).

3.2.3.5 Frozen BM-APC could be utilized as a single batch to reduce variation of IFN-γ protocol conversion rate

Besides the problem of a low yield output, we also encountered some variations of Foxp3 enrichment in batches of IFN-γ Treg generated at different times. We postulated that different batches of BM-APC could be one of the reasons contributing to this heterogenicity. Therefore, we considered the possibility of using a single batch of cryopreserved BM-APC in an attempt to conserve protocol consistency. In addition, the use of cryopreserved BM-APC as 'off-the shelf' alloantigen stimulators could give a real advantage in logistical terms if this strategy were translated into a permissive clinical protocol in the future.

BM-APC were generated from B6 bone marrow cells in GM-CSF and TGF-β as described above. At the time of harvest, 1x 10^7 BM-APC were resuspended in 250μl freezing media and stored in liquid nitrogen. After thawing, the average recovery rates of these cells were well above 80% and trypan blue staining confirmed viability exceeded 90% in all batches. The phenotypic features of BM-APC were assessed by flow cytometry before and after cryopreservation ***(Figure 3.2.3.5.1.i)***. There were no significant differences in the phenotypic profiles between freshly-harvested BM-APC and cryopreserved BM-APC, except for the expression of CD86 as follows: CD40 (4.7% versus 3.5%), CD80 (1.7% versus 5.6%), CD86 (2.0% versus 2.5%) and MHC class II (11.1% versus 13.3%). More importantly, IFN-γ conditioning protocol using cryopreserved BM-APC could maintain a satisfactory Foxp3 enrichment compared to that using freshly-harvested BM-APC ***(Figure 3.2.3.5.1.ii)***. In fact, the percentage of Foxp3 enrichment was higher in IFN-γ Treg generated with cryopreserved BM-APC (81.3%) than freshly-harvested BM-APC (72.7%). Moreover, the proportion of the $CD62L^+$ subset in the resultant $Foxp3^+$ population was higher in those generated with cryopreserved BM-APC (66.7%), compared to freshly-harvested BM-APC

(57.3%) ***(Figure 3.2.3.5.1.iib)***. These results suggest that the cryopreservation process might upregulate the expression of CD80, CD86 and MHC class II by BM-APC thereby enhancing the enrichment of Foxp3$^+$ IFN-γ Treg *in vitro*.

Foxp3 enrichment efficiency was compared between 5 batches of IFN-γ Treg generated from a single batch of BM-APC and 18 consecutive batches of IFN-γ Treg generated from different freshly-harvested BM-APC ***(Figure 3.2.3.5.2)***. IFN-γ Treg generated from the single batch of BM-APC had a mean Foxp3$^+$ population of 32.0% (20.9-44.0%; standard error 3.917%) with a coefficient of variation of 27.4%. On the other hand, IFN-γ Treg generated from different batches of freshly-harvested BM-APC had a mean Foxp3$^+$ population of 28.8% (0.8-72.5%; standard error 3.986% with a coefficient of variation of 58.7%. However, student F-test comparing the variances between these two groups showed that these variances were not significantly different (p=0.1056) suggesting that using a single batch cryopreserved BM-APC did not improve reproducibility of the IFN-γ conditioning protocol for the generation of Foxp3$^+$ Treg.

Figure 3.2.3.5.1. Cryopreserved BM-APC were compatible to freshly-harvested BM-APC for the generation of IFN-γ Treg

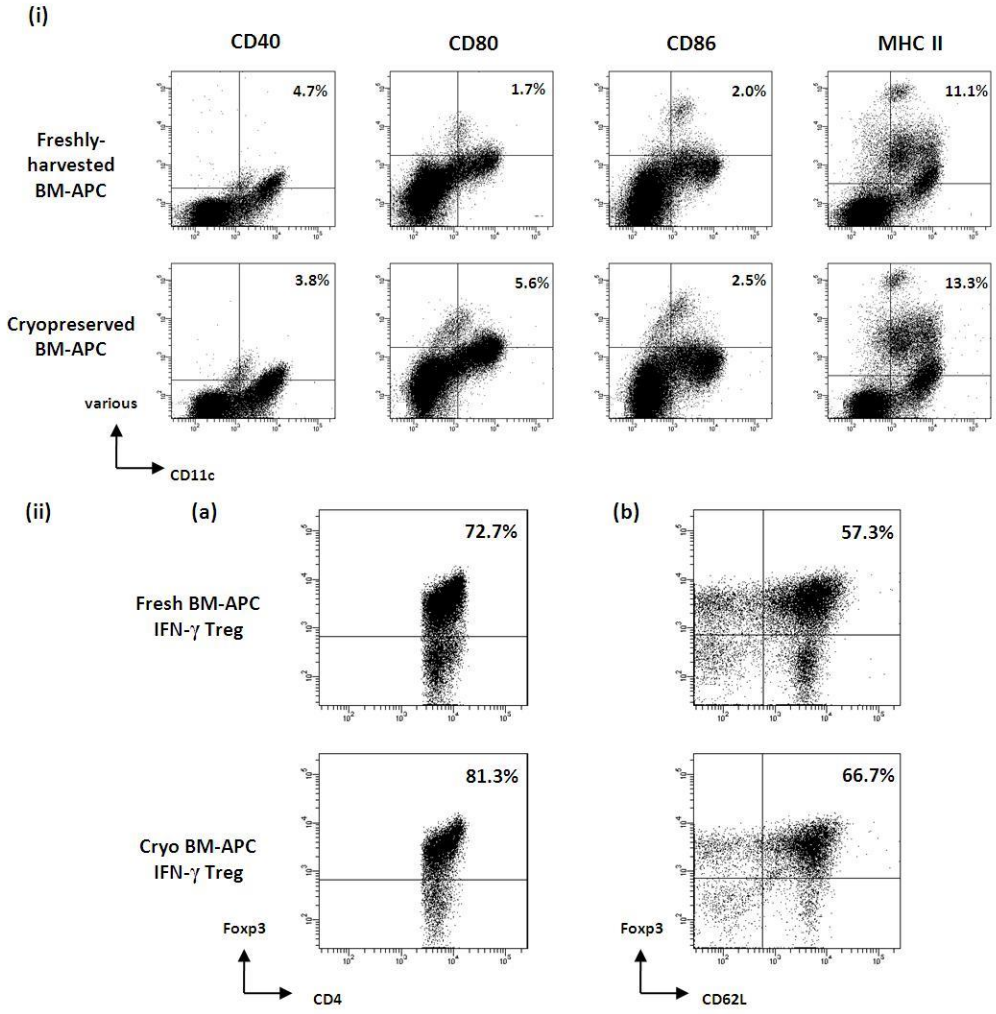

Figure 3.2.3.5.1. Cryopreserved BM-APC were compatible to freshly-harvested BM-APC for the generation of IFN-γ Treg. **(i)** Representative dot plots show that phenotypic characteristics of cryopreserved BM-APC were not significantly different from that of freshly-harvested BM-APC cultured under the same conditions (GM-CSF 2ng/ml and TGF-β 2ng/ml), except for the expression of CD80 (5.6% versus 1.7%) and MHC Class II (13.3% versus 11.1%). **(ii)** IFN-γ conditioning protocol employing cryopreserved BM-APC led to a higher Foxp3 enrichment compared to freshly-harvested BM-APC (66.7% versus 57.3%). Data above are representative of at least 3 independent experiments.

Figure 3.2.3.5.2. A single batch of cryopreserved BM-APC did not improve the reproducibility of the IFN-γ conditioning protocol

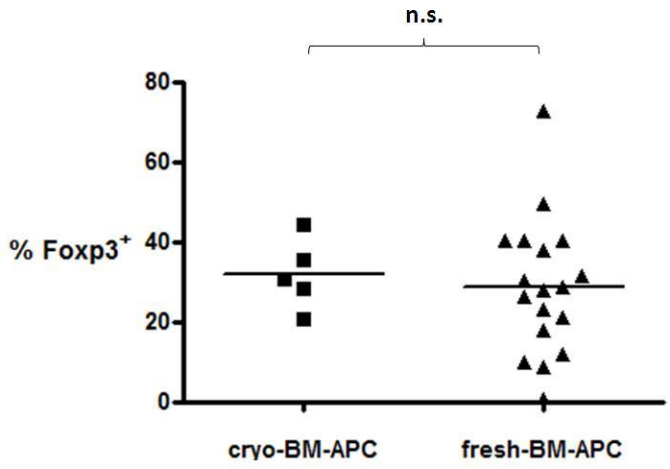

Figure 3.2.3.5.2. A single batch of cryopreserved BM-APC did not improve the reproducibility of the IFN-γ conditioning protocol. Foxp3 enrichment efficiency of the IFN-γ protocols using a single batch of cryopreserved BM-APC as stimulators was compared with freshly-harvested BM-APC. IFN-γ Treg obtained from 5 independent experiments using a single batch of cryopreserved BM-APC were compared with samples obtained from the immediate past 18 independent experiments using different freshly-harvested BM-APC. IFN-γ Treg generated from the single batch of BM-APC had a mean Foxp3$^+$ population of 32.0% (20.9-44.0%; standard error 3.917%; coefficient of variation 27.4%. IFN-γ Treg generated from different batches of freshly-harvested BM-APC had a mean Foxp3$^+$ population of 28.8% (0.8-72.5%); standard error 3.986%; coefficient of variation 58.7%. Using F-test for the comparison of variance between each group revealed that these variances were not statistically differently from each other (p=0.1056). These data suggest that using a single batch of cryopreserved BM-APC did not have a significant impact on the reproducibility of the IFN-γ protocol in terms of Foxp3 enrichment.

Next, we looked at the efficiency of Foxp3 enrichment of the IFN-γ protocol using a single source of $CD4^+$ precursors. Three different batches of cryopreserved BM-APC were compared to freshly harvested BM-APC in their abilities to enrich for $Foxp3^+$ cells. $5x10^5$ $CD4^+$ precursors were stimulated with either $5x10^4$ (1x) or $1.5x10^5$ (3x) freshly-harvested BM-APC or cryopreserved BM-APC batch A, B or C ***(Figure 3.2.3.5.3.i)***. When the optimal number (3x) of BM-APC were added ***(as shown in Figure 3.2.3.1.2)***, all three batches of cryopreserved BM-APC could maintain the production of a high proportion of $Foxp3^+$ cells with a mean of 57.2% (54.8-60.2%), which was compatible to the freshly harvested BM-APC counterpart (65.5%). While using fewer freshly-harvested BM-APC could lead to a high Foxp3 enrichment efficiency (41.3%), this level of Foxp3 enrichment could not be achieved when the number of cryopreserved BM-APC was reduced from 3x to 1x (original protocol), with a mean of 12.3% (7.8-15.8%). These data affirm that an optimal number of BM-APC in culture could consistently enhance Foxp3 enrichment and reduce the variance of this protocol. However, the reproducibility of the IFN-γ protocol appeared to be affected by different sources of CD4 precursors rather than batches of BM-APC employed. The variable Foxp3 enrichment might be inevitable in our model and it would therefore be essential to perform a quality check prior to *in vivo* studies.

On the other hand, the relative cell number of $Foxp3^+$ cells generated using 3x cryopreserved BM-APC was only approximately one-third of that using 3x freshly-harvested BM-APC with an average of 5.0 $x10^3$ (3.2-7.6 $x10^3$) cells/well versus 14.6 $x10^3$ cells/well ***(Figure 3.2.3.5.3.ii)***. The difference in cell yield was wider when 1x cryopreserved BM-APC and 1x freshly-harvested BM-APC were used 0.39 $x10^3$ (0.20-0.59 $x10^3$ cells/well) versus 2.72 $x10^3$ cells/well ***(Figure 3.2.3.5.3.ii)***. These findings suggest that a significant compromise on cell yield would have to be anticipated if cryopreserved BM-APC were used for the IFN-γ conditioning protocol.

Figure 3.2.3.5.3. IFN-γ conditioning protocol using cryopreserved BM-APC led to a compatible Foxp3 enrichment but not cell yield when compared to freshly-harvested BM-APC

(i)

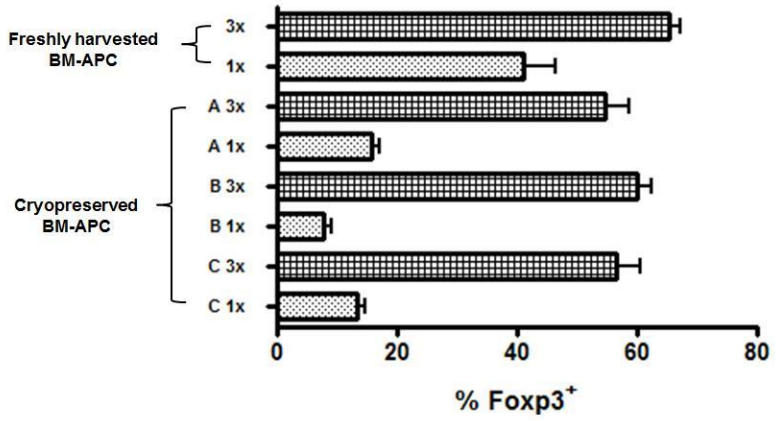

(ii)

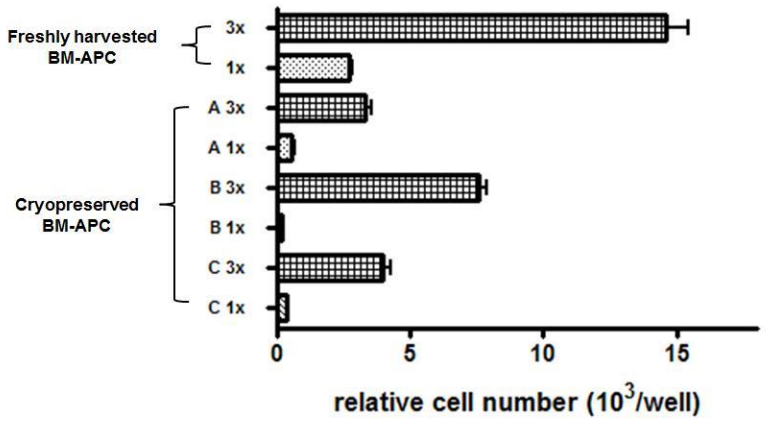

Figure 3.2.3.5.3. IFN-γ conditioning protocol using cryopreserved BM-APC led to a compatible Foxp3 enrichment but not cell yield when compared to freshly-harvested BM-APC. (i) CBA $CD4^+$ T cells were stimulated with either freshly harvested BM-APC (fresh) or cryopreserved BM-APC (batch A, B, and C); at either 10:1 or 10: 3 ratio in the presence of IFN-γ for a total of 14 days. A reliable Foxp3 enrichment was observed when either freshly-harvested BM-APC or cryopreserved BM-APC were used at the 10:3 $CD4^+$ T cells:BM-APC ratio. **(ii)** However, the absolute number of $Foxp3^+$ Treg generated by the IFN-γ conditioning protocol was clearly higher when freshly harvested BM-APC were used compared to that of cryopreserved BM-APC. Data above represent 3 samples from each group with error bars showing 1 S.D. from the mean values.

When we made a direct comparison between the functional properties of IFN-γ Treg generated using either freshly-harvested BM-APC or cryopreserved BM-APC *in vivo*, there were no differences in their abilities to control allograft rejection. CBA $RAG^{-/-}$ mice were reconstituted with $1x10^5$ naïve $CD4^+CD25^-$ T cells with or without $1x10^5$ IFN-γ Treg generated with either freshly-harvested BM-APC – 'fresh BM-APC IFN-γ Treg' or cryopreserved BM-APC – 'cryo BM-APC IFN-γ Treg', one day before the transplant of a B6 skin allograft ***(Figure 3.2.3.5.4.i)***. Both fresh BM-APC IFN-γ Treg (n=5) and cryo IFN-γ Treg (n=5) prevented allograft rejection mediated by the $CD4^+CD25^-$ T cells with a MST beyond 100 days, compared to $CD4^+CD25^-$ T cells alone (MST= 17 days; n=5) ***(Figure 3.2.3.5.4.ii)***. However, the functional differences between these two groups might be made more revealing by either titrating number of $CD4^+CD25^-$ T cells up (thus, $2x10^5$, $4x10^5$ cells per recipient); or titrating the number of each of the IFN-γ Treg prepation down (from $1x10^5$ to $5x10^4$ and $2.5x10^4$ cells per recipient).

Figure 3.2.3.5.4. IFN-γ Treg generated with cryopreserved BM-APC were compatible to freshly-harvested BM-APC in the control of allograft rejection in the adoptive transfer model

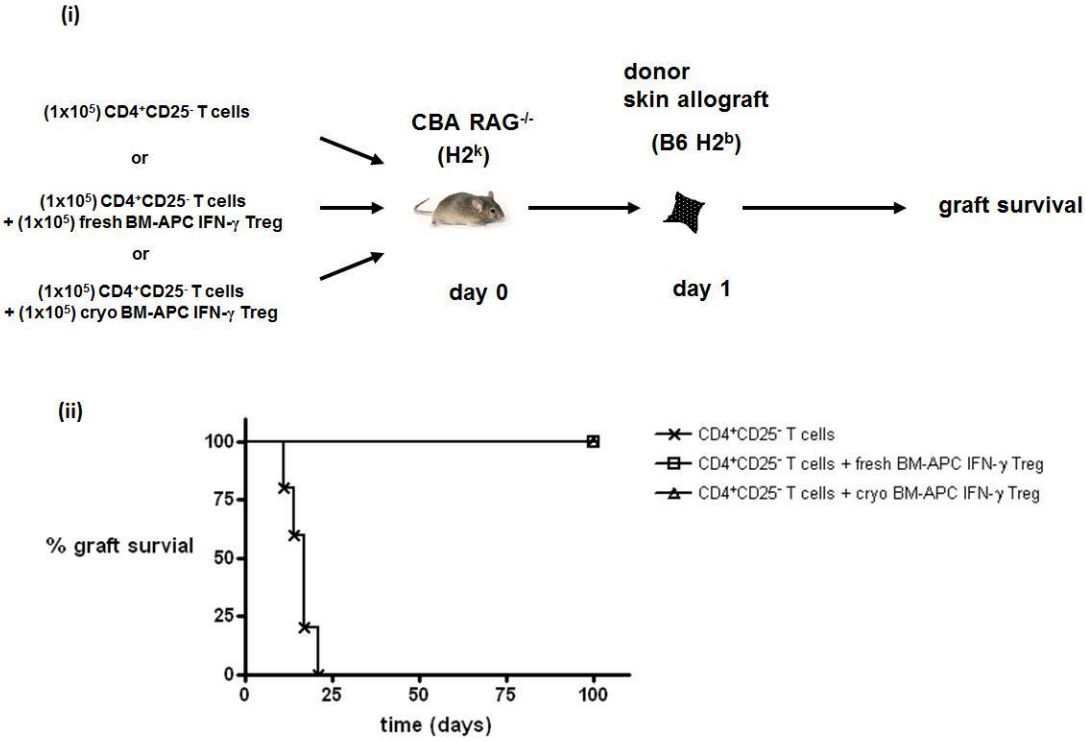

Group	n	graft survival (days)	MST (days)	p-value
$CD4^+CD25^-$ T cells	5	11,14,17,17,21	17	
$CD4^+CD25^-$ T cells + fresh BM-APC IFN-γ Treg	5	>100,>100,>100>100,>100	>100	*n.d.*
$CD4^+CD25^-$ T cells + cryo BM-APC IFN-γ Treg	5	>100,>100,>100,>100,>100	>100	

Figure 3.2.3.5.4. IFN-γ Treg generated with cryopreserved BM-APC were compatible to freshly-harvested BM-APC in the control of allograft rejection in the adoptive transfer model. (i) CBA $RAG^{-/-}$ mice were reconstituted with $1x10^5$ naive $CD4^+CD25^-$ T cells with or without $1x10^5$ fresh BM-APC IFN-γ Treg or cryo BM-APC IFN-γ Treg one day before the transplant of a B6 skin allograft. **(ii)** $CD4^+CD25^-$ T cells rejected skin allografts acutely with MST of 17 days (n=5). IFN-γ Treg generated with fresh BM-APC or cryopreserved BM-APC prevented skin allograft rejection long-term with a MST of >100 days (n=5) and >100 days (n=5); there was no difference (n.d.) between these two groups. Log rank tests were used for statistical comparisons ($p<0.05$ denotes statistically significant).

3.2.3.6 CD11c$^+$ BM-APC were not essential for the enrichment for Foxp3$^+$ IFN-γ Treg

CD11c$^+$ BM-DC or splenic DC have been used to expand CD4$^+$CD25$^+$ T cells under certain conditions *in vitro*[443-445]. In the majority of the published protocols, BM-DC were cultured in GM-CSF with or without additional LPS or poly I:C to generate a bonafide BM-DC, which were then subjected to positive selection for CD11c through a MACS column. We hypothesized that the CD11c$^+$ sub-population of BM-APC might confer a superior Foxp3 enrichment and cell yield compared to whole BM-APC or CD11c$^-$ counterparts in our IFN-γ protocol.

BM-APC were generated from B6 bone marrow cells cultured in GM-CSF and TGF-β for 6 days. CD11c$^+$ and CD11c$^-$ fractions were collected separately after whole BM-APC were subjected to CD11c positive selection via MACS. In ***Figure 3.2.3.6.1.i***, dot plots show the expression of CD11c and GR-1 on BM-APC before and after CD11c selection. The majority of whole BM-APC were CD11c$^-$GR-1$^+$, only 19.7% expressed CD11c (11.6% CD11c$^+$GR-1$^-$, 8.1% CD11c$^+$GR-1$^+$) ***(Figure 3.2.3.6.1.ia)***. MACS-selected CD11c$^+$ BM-APC consisted of a 97.3% purity (70.2% CD11c$^+$GR-1$^-$, 27.1% CD11c$^+$GR-1$^+$) ***(Figure 3.2.3.6.1.ib)***.

CD4$^+$ precursors were stimulated with: whole BM-APC, CD11c$^+$ BM-APC or CD11c$^-$ BM-APC in two successive rounds in the presence of exogenous IFN-γ. The percentage and number of Foxp3$^+$ cells in cultures were analyzed over each 7-day intervals ***(Figure 3.2.3.6.1.ii)***. On day 0, the culture contained between 9.5-11.0% Foxp3$^+$ cells among all groups. On day 7, after the first round of BM-APC stimulation, the proportion of Foxp3$^+$ dropped from 11.0% to 5.1%, 9.5% to 3.1% and 11.0% to 5.0% when whole, CD11c$^+$ and CD11c$^-$ BM-APC were used, respectively. At the time of harvest (day 14), the Foxp3 enrichment was more profound in the CD11c$^+$ BM-APC

group (41.5%) compared to their $CD11c^-$ counterpart (10.7%) and whole BM-APC (13.1%). The relative number of $Foxp3^+$ cells was assessed over time. At time 0, the initial cultures consisted of 39.8-61.4 $x10^3$ $Foxp3^+$ cells/well. On day 7, the number of $Foxp3^+$ cells dropped from 55.6 to 16 $x10^3$ cells/well, 39.8 to 11.9 $x10^3$ cells/well, 61.4 to 21.2 $x10^3$ cells/well, when whole BM-APC, $CD11c^+$ and $CD11c^-$ BM-APC were used, respectively. The reduction of cell number on day 7 in these cultures was anticipated because of the initial shaping of an alloreactive T cell repertoire. At the time of harvest (day 14), the number of retrievable $Foxp3^+$ cells was equally high in the $CD11c^+$ (31.9 $x10^3$ cells/well) and $CD11c^-$ (31.3 $x10^3$) BM-APC group, compared to a lower yield when whole BM-APC were used (24.1 $x10^3$ cells/well) ***(Figure 3.2.3.6.iii)***.

Taken together, we have identified the potential use of G10/T2 BM-APC and $CD11c^+$ BM-APC as allogeneic stimulators in our IFN-γ conditioning protocol for the enrichment of a dominant $Foxp3^+$ T cells. However, none of the above protocol modifications could really demonstrate a significant impact on the cell yield beyond a 2-fold increase. While we were in the midst of searching for an expansion protocol for IFN-γ Treg, we developed a mouse transplant model that incorporated a sub-optimal costimulation blockade protocol, which could possibly create a window of opportunity for a relatively small number of IFN-γ Treg to elicit their suppressive function in immunocompetent hosts.

Figure 3.2.3.6.1. CD11c$^+$ BM-APC enhanced Foxp3 enrichment but not cell yield

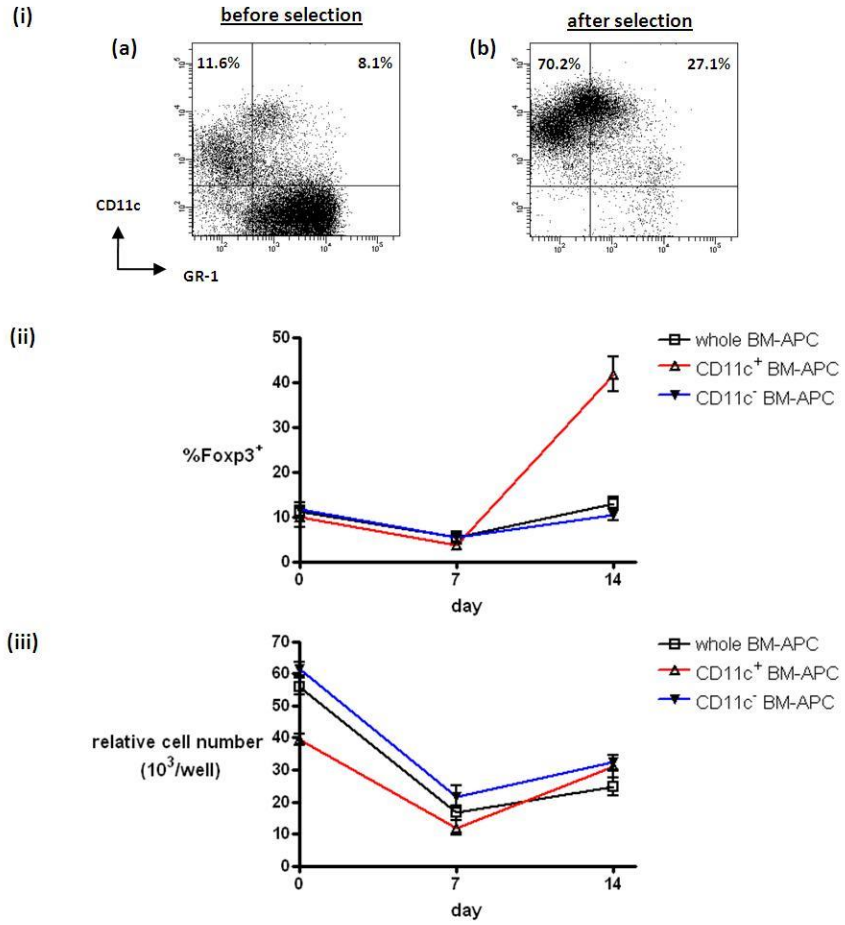

Figure 3.2.3.6.1. CD11c$^+$ BM-APC enhanced Foxp3 enrichment but not cell yield. (ia) Dot plot shows CD11c expression prior to MACS selection. A total of 19.7% of BM-APC expressed CD11c (11.6% CD11c$^+$GR-1- and 8.1% CD11c$^+$GR-1$^+$). **(ib)** After positive selection the overall purity for CD11c population was 97.3% (90.1% CD11c$^+$GR-1$^-$ and 27.2% CD11c$^+$GR-1$^+$). Whole, CD11c$^+$ or CD11c$^-$ BM-APC fractions were used to generate IFN-γ Treg as described in ***Chapter 2.8.1.*** The percentage and number of Foxp3$^+$ cells in respective culture conditions were analyzed over time. **(ii)** At time 0, the culture contained between 9.5-11.0% Foxp3$^+$ among all groups. On day 7, this proportion of Foxp3$^+$ cells dropped to a trough level between 3.1-5.1% among all groups. However, at the time of harvest on day 14, the Foxp3 enrichment was significantly higher in the CD11c$^+$ BM-APC group (41.5%) compared to the whole BM-APC (13.1%) and CD11c$^-$ BM-APC group (10.7%). **(iii)** The relative number of Foxp3$^+$ cells was assessed over time. At time 0, the culture contained between 39.8 to 61.4 x10^3 Foxp3$^+$ cells/well. This number dropped to a trough level between 11.9-21.2 x10^3 Foxp3$^+$ cells/well on day 7. At the time of harvest on day 14, there was no significant difference in the number of Foxp3$^+$ cells between the CD11c$^+$ BM-APC group (31.9x10^3) and the CD11c$^-$ BM-APC groups (31.3x10^3), which were both higher than the whole BM-APC (24.1x10^3) group. Data above represent means of 3 replicates with error bars showing 1 S.D. from the mean values.

3.2.4 Rationale of using adjunctive immunosuppressive therapy in immunocompetent recipients

We believe that Treg therapy is unlikely to be a stand-alone treatment modality in solid organ transplantation, at least when it is being rolled out at the initial phase. It is also unlikely to replace the mainstay of treatment-conventional immunosuppressive drugs, but we believe that it can play a role as an adjunct therapy that aims to minimize adverse effects secondary to pan-immunosuppression. In addition, despite the fact that successful expansion protocols for human Treg have been reported, there is still lack of a precise Treg-specific maker to delineate 'true Treg' against activated T cells. As a result, unless we have a limitless supply of 'true Treg', Treg therapy would require some form of support from a carefully designed immunosuppressive regimen. Furthermore, according to our previous unpublished data (R. Francis and R. Devlin, personal communications) with regard to the use of $CD4^+CD25^+$ nTreg in a mouse skin transplant model, the number of Treg required to show any demonstrable immunosuppressive responses in intact animals was in the excess of $1x10^7$. Taking all of these considerations into account we therefore aimed to develop an adjunct immunosuppressive regimen that would not only allow for a window of opportunity for IFN-γ Treg to exert their suppressive effect, but a potential synergism in preventing allograft rejection in the heterotopic heart transplant model.

Abatacept was deliberately selected for the purpose of this study because of its translational potentials in clinical medicine. Abatacept is the first generation CTLA-4Ig that belongs to the costimulation blockade family. It is a fusion protein of the extracellular domain of the CTLA-4 molecule conjugated with a human Fc portion of the immunoglobulin IgG1. Its CTLA-4 moiety preferentially binds to CD80 and CD86 expressed by APC, preventing their interaction with CD28 on T cells because of its higher affinity for CD80 and CD86. In turn, the lack of signal through

CD28 on allo-specific T cells would lead to anergy and/or apoptosis and hence a dampened response. It is a licensed medication that has been marketed as Orencia® for the treatment of refractive rheumatic arthritis not responding to first-line treatment. A newer CTLA-4Ig analogue-belatacept (Nulojix®) has already been approved by the FDA in renal transplantation and entered Phase III clinical trial[80], which has established the role costimulation blockade agents in clinical transplantation. Abatacept was deliberately chosen for this study because of these unique mechanisms of action to avoid a direct effect on alloreactive Treg in our model. It has been reported that current immunosuppressive drugs have detrimental effects on both conventional T cells and Treg, for example: calcineurin inhibitors such as cyclosporine and tacrolimus. On the other hand, a number of papers have demonstrated that rapamycin (sirolimus) are favourable to Treg. This might appear as the candidate of choice; however, the direct suppressive effect of Treg might not be easily dissected away from the confounded effect of rapamycin on Treg[444].

Wild-type (WT) CBA mice were transplanted heterotopically with a B6 heart allograft with or without abatacept. Abatacept was given intravenously (i.v.) at 25μg per dose per mouse, (which was pre-defined by the preliminary work done by A. Bushell in our group) on day 0, 1; day 0, 1, 5; day 0, 1, 8; and day 0,1,8,9 ***(Figure 3.2.4.1)***. When no treatment was given, CBA mice rejected B6 heart allografts acutely with a MST of 7.5 days (n=10). CBA mice treated with the 2-dose abatacept regimen (day 0, 1) also rejected their grafts acutely with a MST of 8.5 days (n=6). Mice treated with the 3-dose regimen (day 0, 1, 5) accepted their grafts for a longer period of time with a MST of 51 days (n=5). A modified 3-dose regimen (day 0, 1, 8) also led to the prolongation of graft survival with a MST of 24.5 days (n=8). The 4-dose regimen (day 0, 1, 8 and 9) prolonged graft survival with a MST of 39 days (n=9). The three- or four-dose regimen (day 0, 1 and 8, or day 0, 1, 8 and 9) both prolonged of allograft survival beyond 20 days, however, results from

these groups were considered poorly reproducible as some of the mice rejected their grafts even before the last designated dose of abatacept on day 8 or day 9 (denoted by * in ***Figure 3.2.4.1***). These data suggest that the timing of the third dose was crucial to achieve a more consistent outcome and hence the third dose was brought forward to day 5 in an attempt to circumvent such inconsistency. Indeed, the day 0, 1 and 5 regimen provided more consistent results, which were subsequently affirmed by repeat observations. Therefore, the sub-optimal abatacept protocol was established at a dose of i.v. 25µg given on day 0, 1 and 5 with respect to the day of transplant, unless otherwise stated. The most suitable control for this set of experiments should include a drug vehicle only group, thus PBS alone (in which CTLA-4Ig was dissolved (see pharmacological agents in ***Chapter 2.6.4***); or a commercially available human IgG1 protein without the CTLA-4 domain. In the absence of these sets of control, we acknowledge that the interpretation of the pure effect of CTLA-4Ig on graft survival and the effect between CTLA4-Ig and infused Treg would be limited.

Figure 3.2.4.1. Titration of an adjunct peri-operative costimulation blockade regimen in a heart transplant model

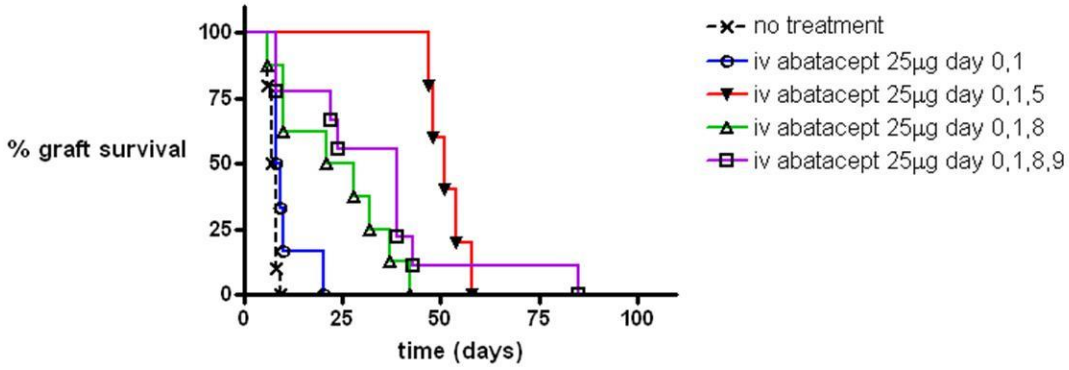

group	n	graft survival	MST	p-value
no treatment	10	6,6,7,7,7,8,8,8,8,9	7.5	p = 0.0005
i.v. abatacept 25µg day 0,1	6	8,8,8,9,10,20	8.5	p = 0.0011
i.v. abatacept 25µg day 0,1,5	5	47,48,51,54,58	51	
i.v. abatacept 25µg day 0,1,8	8	6*,10,10,21,28,32,37,42	24.5	
i.v. abatacept 25µg day 0,1,8,9	9	8*,8*,22,24,39,39,39,43,85	39	

Figure 3.2.4.1. Titration of an adjunct peri-operative costimulation blockade regimen in a heart transplant model. CBA recipients were transplanted with a B6 heart allograft heterotopically, with or without sub-optimal doses of abatacept 25µg administered intravenously on day 0, 1, day 0, 1, 5, day 0, 1, 8, or day 0, 1, 8, 9. CBA mice rejected their heart allografts acutely with a MST of 7.5 days (n=10), if no treatment was given. Mice treated with the 2-dose regimen on day 0 and 1 also rejected their grafts acutely with a MST of 8.5 days (n=6). Mice treated with the 3-dose regimen on day 0, 1, 5 had delayed allograft rejection with a MST of 51 days (47-58 days; n=5). Another 3-dose regimen (day 0, 1, 8) led to the prolongation of graft survival with a MST of 24.5 days (n=8). The 4-dose regimen (day 0, 1, 8, 9) prolonged graft survival with a MST of 39 days (n=9). Allografts were rejected before the last designated dose of abatacept in the respective experimental groups (*). Log rank tests were used for statistical comparisons ($p<0.05$ denotes statistically significant).

3.2.5 Treg therapy in combination with a sub-optimal abatacept regimen prevented heart allograft rejection in immunocompetent mice

Among other transplant models, we have chosen to test the regulatory function of IFN-γ Treg in WT CBA recipients using the heterotopic heart transplant model for the following reasons: firstly it was anticipated that by using a wild-type skin allograft model much larger cell numbers would be required. Therefore, given only a finite number of Treg was practically available, the heart model was chosen because of the differential susceptibility to rejection between skin and heart allografts[446]. Secondly, a vascularized allograft is a closer model to that of clinical organ transplantation. Thirdly, a heterotopic heart allograft model has the advantage that it provides a functional readout that could be stratified[447]. Other models have also been tested, such as the pancreatic islet model[256] and the abdominal aortic interpositional graft model[448]. The former would require frequent invasive blood sampling to determine serum glucose level and the latter would require an autopsy assessment of the intimal proliferation of the interpositioned aortic graft.

We tested the regulatory function of IFN-γ Treg in WT CBA mice in conjunction with a sub-optimal abatacept protocol using the heterotopic heart transplant model ***(Figure 3.2.5.1.i)***. A single dose of $2x10^6$ IFN-γ Treg was given to CBA mice intravenously one day prior to the transplant of a B6 heart allograft. Recipients were given 25μg abatacept intravenously on day 0, 1, and 5. Graft outcome in this group of mice was compared to mice which received no treatment, abatacept alone or IFN-γ Treg alone. Untreated CBA mice rejected their allografts acutely with a MST of 7.5 days (n=10). In the absence of abatacept, $2x10^6$ IFN-γ Treg had a modest effect on graft survival with a MST of 15.5 days (n=2). The abatacept protocol prolonged graft survival to a MST of 51 days (n=5). In clear contrast, the addition of IFN-γ Treg

to the abatacept protocol led to a striking improvement of graft outcome with the majority of heart allografts survived beyond 100 days (7 out of 9). [CBA isografts were accepted long-term without any manipulation (MST >100; n=6) repeated in at least two sets, *data not shown*)]

Figure 3.2.5.1. The combination of IFN-γ Treg and sub-optimal abatacept prevented allograft rejection long-term in immunocompetent recipients

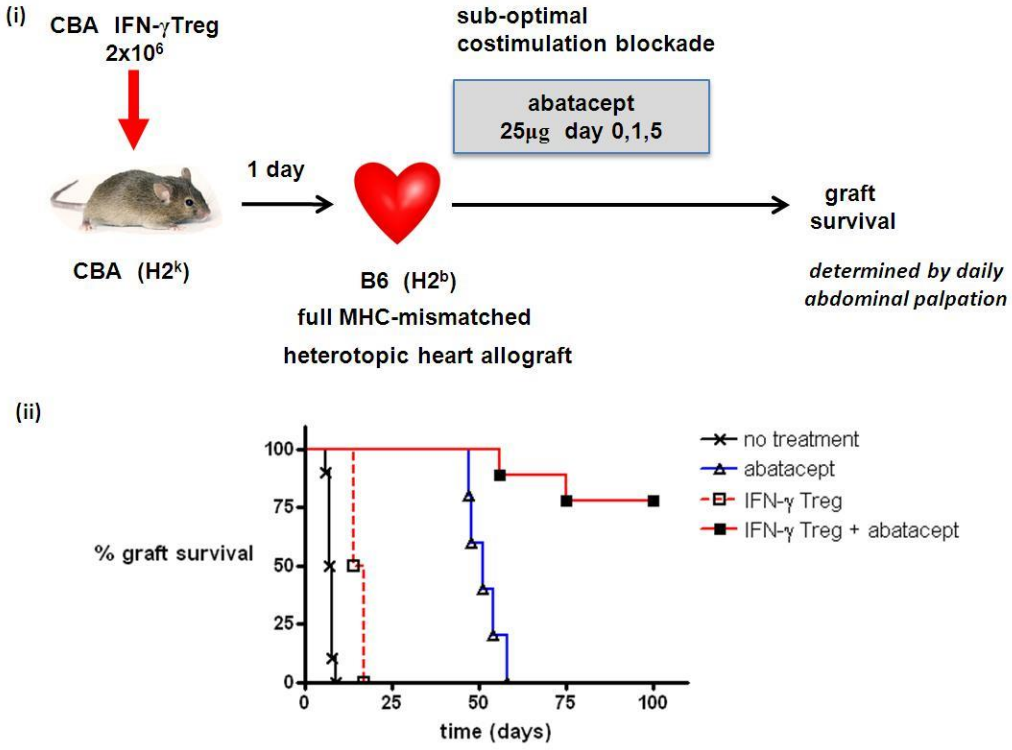

Group	n	graft survival (days)	MST (days)	p-value
no treatment	10	6,7,7,7,7,8,8,8,8,9	7.5	
abatacept	5	47,48,51,54,58	51	*p = 0.013*
IFN-γ Treg	2	14,17	15.5	*p = 0.0002*
abatacept + IFN-γ Treg	9	56,75,>100,>100>100,>100,>100,>100,>100	>100	*p = 0.0004*

Figure 3.2.5.1. The combination of IFN-γ Treg and sub-optimal abatacept prevented allograft rejection long-term in immunocompetent recipients. (i) A schematic diagram illustrates the experimental set up of this heart transplant model. **(ii)** CBA mice rejected heart allografts acutely without any treatment (MST=7.5 days, n=10). A sub-optimal abatacept regimen (25μg day 0, 1 and 5) prolonged graft survival with a MST of 51 days (n=5). A single dose of $2x10^6$ IFN-γ Treg given one day before the transplant led to a modest prolongation of graft survival with a MST of 15.5 days (n=2). The combination of abatacept plus IFN-γ Treg ($2x10^6$) led to significant prolongation of graft survival with a MST>100 days (n=9; p=0.0002). Log rank tests were used for statistical comparisons (p<0.05 denotes statistically significant).

A direct comparison of the suppressive effect of allograft rejection in the adoptive transfer skin transplant model and the heart transplant model was performed. At the time of harvest IFN-γ Treg were assessed for the expression of Foxp3 by flow cytometry. For the adoptive transfer model, CBA $RAG^{-/-}$ mice were reconstituted with $1x10^5$ naïve $CD4^+CD25^-$ T cells with or without $1x10^5$ IFN-γ Treg one day before transplant of a B6 skin allograft ***(***see *fresh BM-APC IFN-γ Treg group* in ***Figure 3.2.3.5.4)***. $CD4^+CD25^-$ T cells rejected skin allografts acutely with a MST of 17 days (n=5). IFN-γ Treg prevented allograft rejection mediated by co-transferred $CD4^+CD25^-$ T cells long-term (MST>100 days; n=6) ***(Figure 3.2.3.5.4.ii)***. The same batch of IFN-γ Treg ($5x10^5$) were given to WT CBA recipient 3 days before the transplant of a heterotopic B6 heart graft, together with the abatacept protocol (day 0, 1 and 5) ***(Figure 3.2.5.2.i)***. The abatacept protocol prolonged allograft survival with a MST of 51 days (n=5). On the other hand, in the presence of abatacept IFN-γ Treg extended all allograft survival beyond 100 days (n=4) ***(Figure 3.2.5.2.ii)***. These data confirm that the immunosuppressive effects of IFN-γ Treg in the heart graft model mirrors to that in the adoptive transfer skin graft model and vice versa.

Figure 3.2.5.2. Simultaneous validation of the suppressive effect of IFN-γ Treg cell therapy in two experimental transplant models – heterotopic heart graft model

(i)

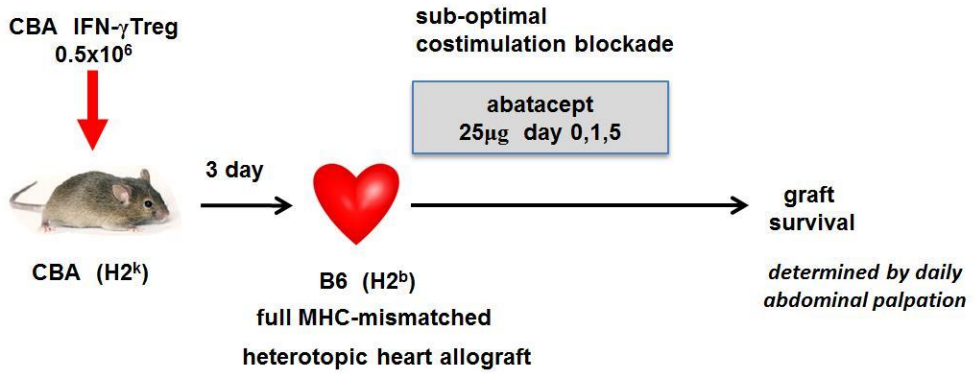

(ii)

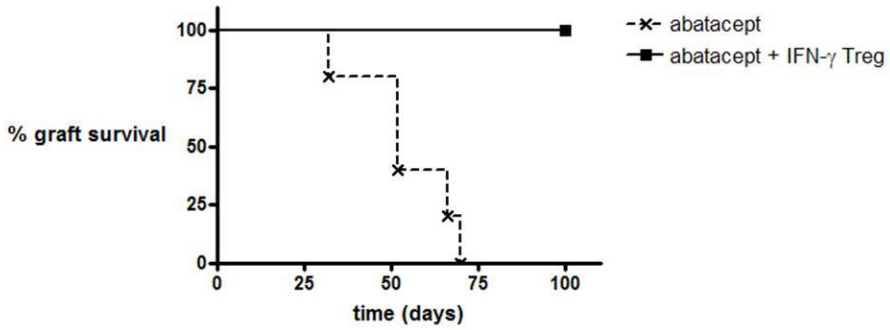

Group	n	graft survival (days)	MST (days)	p-value
abatacept	5	32,52,52,66,70	51	p = 0.0046
abatacept+ IFN-γ Treg	4	>100, >100, >100, >100	>100	

Figure 3.2.5.2. Simultaneous validation of suppressive function of IFN-γ Treg in the adoptive transfer skin graft model and heterotopic heart graft model. (i) Schematic diagram shows the heterotopic heart graft model set up. $5x10^5$ IFN-γ Treg were given to CBA mice 3 days before the transplant of a B6 heart allograft heterotopically. On day 0,1 and 5, these mice were also given abatacept (25μg per dose, intravenously). The effect of IFN-γ Treg on graft survival was compared between mice receiving IFN-γ Treg plus abatacept or abatacept alone. **(ii)** CBA recipients received abatacept alone rejected their grafts with a MST of 51 days (n=5). In contrast, all recipients accepted their heart allografts beyond 100 days (n=4; p=0.0046). Log rank test was used for statistical comparisons (p<0.05 denotes statistically significant).

3.2.6 IFN- γ Treg dosing strategies

3.2.6.1 Graft protection manifested in a dose-dependent manner

We have demonstrated that *in vitro* generated IFN-γ Treg could extend allograft survival long-term in immunocompetent recipients receiving a sub-optimal costimulation blockade regimen. The initial dose estimation was calculated based on the presumed precursor frequency of alloreactive T effector cells in an individual recipient and the data we obtained from the adoptive transfer experiments using the skin graft model ***(Chapter 3.2.2, Figure 3.2.2.1&2)***. However, the limited number of IFN-γ Treg that we could generate often raises the following question: what is the minimum number of cells would be required for a successful Treg therapy to control an immune response against an allograft relative to an intact mouse with a normal immune repertoire? There are always concerns about the potential adverse effects of by-stander immuosuppression introduced by Treg cell therapy, especially if their immunosuppressive effects on allograft can be long-lasting. Therefore, using more suppressor cells might not necessary be the best solution. The manifestation of autoimmune disease is also a credible concern as a result of the potential for contamination of any Treg preparation by activated conventional T cells reactive against self-antigens in the culture mix. We would argue that an ideal Treg therapy would be a single short induction with possible subsequent top-up dosing for break-through rejection episodes.

For these studies our aim was to evaluate possible strategies to provide the best delivery of IFN-γ Treg for the control of alloresponses against an allograft in immunocompetent recipients using our transplant models. Firstly, using the adoptive transfer model, we demonstrated that IFN-γ Treg controlled rejection was mediated by the co-transferred $CD4^+CD25^-$ naïve T cells in a dose-

dependent manner ***(Figure 3.2.6.1.1.i)***. At a high Treg : $CD4^+CD25^-$ T cell ratio (2:1), IFN-γ Treg prevented skin graft rejection long-term (MST >100 days; n=3) ***(Figure 3.2.6.1.1.ii)***. IFN-γ Treg could only control rejection long-term if they were delivered at a 1:1 ratio (MST > 100 days; n=3) and not lower than a 1:2 ratio (MST=34 days; n=3). Moreover, at a given dose ($1x10^5$ IFN-γ Treg that contained 72.5% $Foxp3^+$ T cells), IFN-γ Treg did not induce allograft rejection in their own right suggesting that the potential alloreactive $Foxp3^-$ T effectors in the cell mixture were controlled by the $Foxp3^+$ cohort when delivered *in vivo*.

Figure 3.2.6.1.1. IFN-γ Treg therapy prolonged skin allograft survival in the adoptive transfer model in a dose-dependent manner

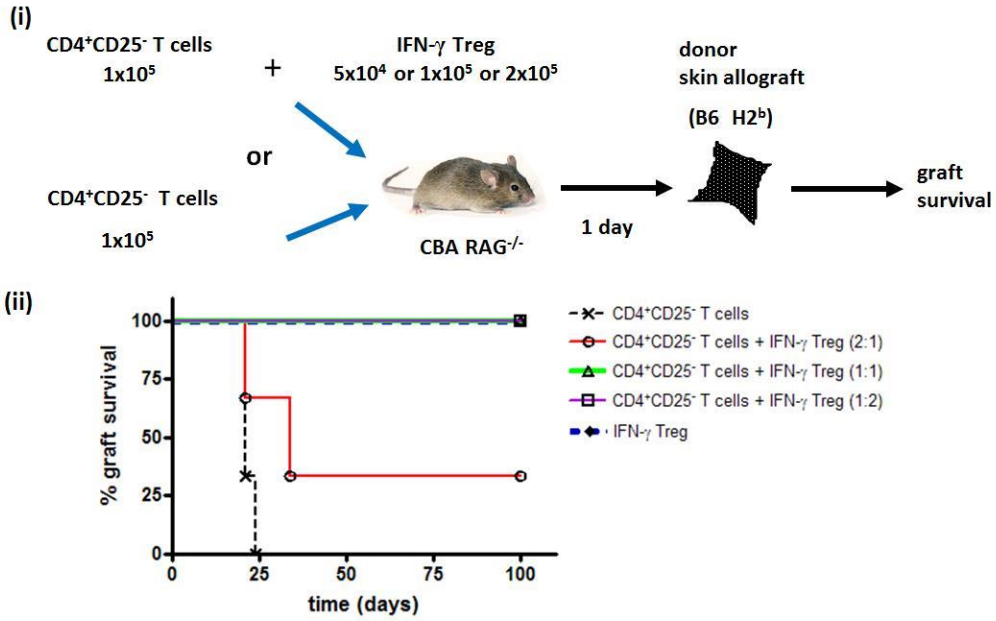

Group	n	graft survival (days)	MST (days)	p-value
$CD4^+CD25^-$ T cells	3	21,21,24	21	$p = 0.1547$
$CD4^+CD25^-$ T cells + IFN-γ Treg (2:1)	3	21,34,>100	34	$p = 0.0224$
$CD4^+CD25^-$ T cells + IFN-γ Treg (1:1)	3	>100,>100,>100	>100	
$CD4^+CD25^-$ T cells + IFN-γ Treg (1:2)	3	>100,>100,>100	>100	
IFN-γ Treg	3	>100,>100>100	>100	

Figure 3.2.6.1.1. IFN-γ Treg therapy prolonged skin allograft survival in the adoptive transfer model in a dose-dependent manner. **(i)** IFN-γ Treg were generated by the IFN-γ protocol as described above ***(Chapter 2.8.1.)***. CBA $RAG^{-/-}$ mice were reconstituted with $1x10^5$ naïve $CD4^+CD25^-$ T cells with or without the co-transfer of IFN-γ Treg at various ratios one day before the transplant of a B6 skin allograft. **(ii)** Naïve $CD4^+CD25^-$ T cells rejected all skin allografts acutely with a MST of 21 days (n=3). At the ratio of 2:1 ($CD4^+CD25^-$ T cells: IFN-γ Treg), IFN-γ Treg led to partial protection of graft survival with a MST of 34 days, with one graft accepted long-term (n=3). When an equal (1:1 ratio) or a higher number (1:2) of IFN-γ Treg was delivered, all allografts were accepted long-term (both MST>100 days; n=3 per group). These data suggest that IFN-γ Treg control allograft rejection in a dose-dependent manner in the adoptive transfer model. Log-rank tests were used for statistical comparisons ($p<0.05$ denotes statistically significant)

We then tested the ability of IFN-γ Treg for the control of allograft rejection in the presence of the adjunct sub-optimal abatacept protocol in WT CBA mice using a Treg cell dose between $5x10^5$ and $4x10^6$ cells per recipient ***(Figure 3.2.6.1.2.i)***. $5x10^5$, $1x10^6$, $2x10^6$ and $4x10^6$ IFN-γ Treg given one day prior to the transplant of a full MHC-mismatched B6 heterotopic heart allograft led to the prolongation of allograft survival with a MST of 64 days (n=7), >100 days (n=4), >100 days (n=9) and >100 days (n=3), respectively, when compared to mice treated with abatacept alone (MST =48 days, n=4) ***(Figure 3.2.6.1.2.ii)***.

While IFN-γ Treg given at $1x10^6$ per recipient on day-1 could lead to long-term graft survival, a divided dose of $5x10^5$ cells given on day-1 and day-3 did not lead to superior graft outcome with a MST of 46 days (n=5) ***(Figure 3.2.6.1.3)***. More interestingly, the graft outcome using a divided dose was not statistically different from those received a single dose of $5x10^5$ given on either day-1 (MST=64, n=7) or day-3 (MST>100, n=3) ***(Figure 3.2.6.1.3.ii)***. Collectively, these data suggest that both cell number and frequency are important factors in determining graft outcome when Treg are used as a cellular therapy *in vivo*.

Figure 3.2.6.1.2. IFN-γ Treg therapy prevented heart allograft rejection in immunocompetent recipients in a dose-dependent manner

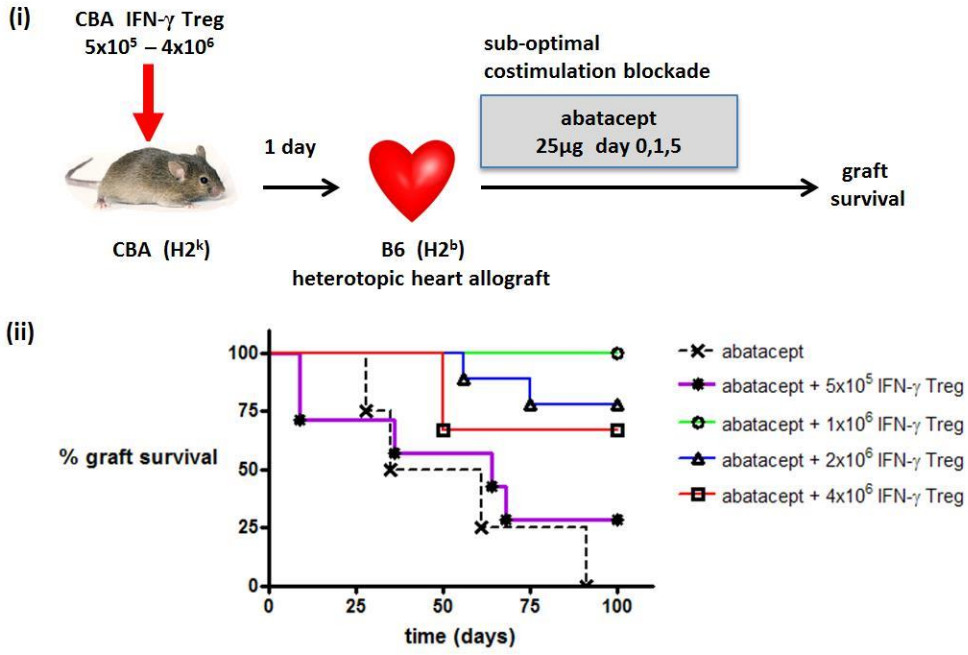

Group	n	graft survival (days)	MST (days)	p-value
abatacept	4	28,35,61,91	48	p = 0.4451
abatacept + IFN-γ Treg 5x10⁵	7	9,9,36,64,68,>100,>100	64	
abatacept + IFN-γ Treg 1x10⁶	4	>100,>100,>100,>100	>100	p = 0.0067
abatacept + IFN-γ Treg 2x10⁶	9	56, 75,>100,>100>100,>100,>100,>100,>100	>100	
abatacept + IFN-γ Treg 4x10⁶	3	>100,>100>100	>100	

Figure 3.2.6.1.2 IFN-γ Treg therapy prevented heart allograft rejection in immunocompetent recipients in a dose-dependent manner. (i) IFN-γ Treg were generated by the IFN-γ protocol as described above ***(Chapter 2.8.1.)***. CBA mice were transplanted with a B6 heart allograft heterotopically and received abatacept i.v. 25µg on day 0, 1 and 5, with or without IFN-γ Treg one day before the transplant (day -1). **(ii)** Sub-optimal abatacept treatment prolonged heart allograft survival with a MST of 48 days (n=4). When 5x10⁵ IFN-γ Treg were delivered, graft survival did not improve significantly compared to the abatacept only control with a MST of 64 days (n=7), while 2 grafts survived long-term >100 days. When the cell dose was increased to 1x10⁶, all mice accepted their allografts long-term (MST > 100 days; n=4). A further increase in the cell dose to 2x10⁶ (n=9) or 4x10⁶ (n=3), most allografts were accepted long-term with a MST >100 days. These data suggest that the addition of IFN-γ Treg to abatacept in this heart transplant model led to further prolongation of graft survival in a dose-dependent manner. Log rank tests were used for statistical comparisons. (p<0.05 denotes statistically significant)

Figure 3.2.6.1.3. Multiple dosing of IFN-γ Treg therapy did not improve graft outcome

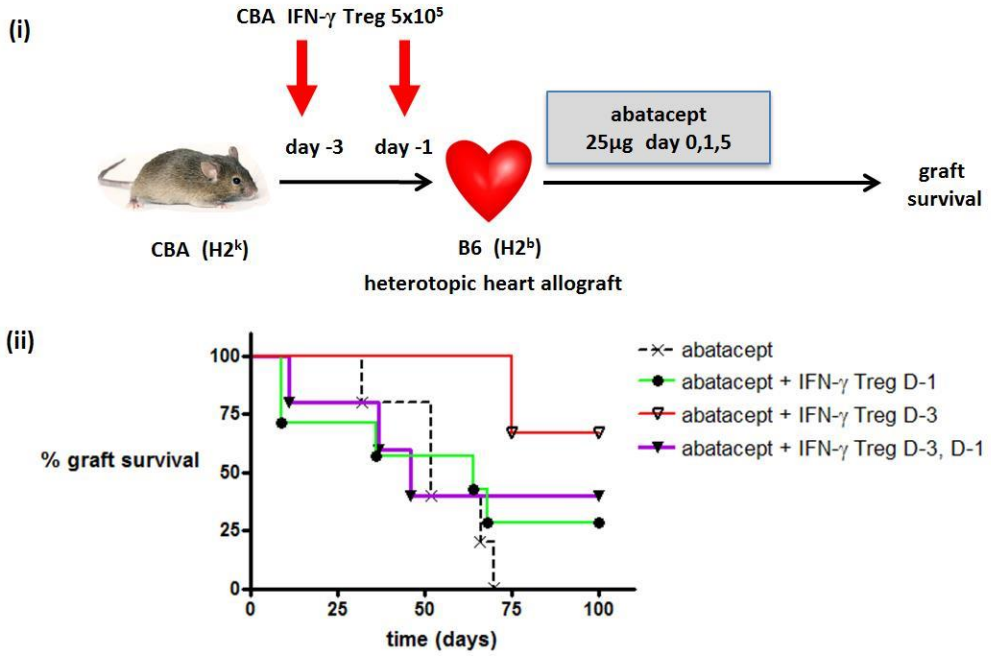

Group	n	graft survival (days)	MST (days)	p-value
abatacept	5	32,52,52,66,70	52	
abatacept + IFN-γ Treg 5x10⁵ day-3	3	75,>100,>100	>100	*p = 0.3587*
abatacept + IFN-γ Treg 5x10⁵ day-1	7	9,9,36,64,68,>100,>100	64	*p = 0.7495*
abatacept + IFN-γ Treg 5x10⁵ day-1,-3	5	11,37,46,>100,>100	46	

Figure 3.2.6.1.3. Multiple dosing of IFN-γ Treg therapy did not improve graft outcome.
(i) IFN-γ Treg were generated by the IFN-γ protocol as described above ***(Chapter 2.8.1.)***. CBA mice were transplanted with a B6 heart allograft heterotopically and received i.v. abatacept 25µg on day 0, 1 and 5. 5x10^5 IFN-γ Treg were given 3 days before (D-3), 1 day before (D-1) or both 1 and 3 days before the transplantation (D-1,D-3). **(ii)** Sub-optimal abatacept treatment prolonged heart allograft survival with a MST of 52 days (n=5). When 5x10^5 IFN-γ Treg were delivered 3 days (D-3) before the heart transplant, graft survival was significantly prolonged with a MST >100 days (n=3). When 5x10^5 IFN-γ Treg were delivered 1 day before the heart transplant (D-1), graft rejection was partially prevented with a MST of 64 days (n=7). A two-dose IFN-γ Treg treatment given pre-operatively showed no significant difference in graft outcome with a MST of 46 days (n=5), when compared to IFN-γ Treg given on either D-3 or D-1 as a single-dose therapy. These data suggest that multiple doses of IFN-γ Treg given pre-operatively did not result in an improved graft outcome when compared to a single-dose regimen. Log rank tests were used for statistical comparisons. (p<0.05 denotes statistically significant)

3.2.6.2 Timing of IFN-γ Treg delivery critically affected graft outcome

Most induction and desensitization protocols are designed to work most effectively when delivered before transplantation because it is generally thought that it would be impossible to reverse an overwhelming alloresponses after engraftment. Similarly, Treg delivery in various transplant models tested in our laboratory was also by and large based on a single-dose regimen one day before the transplant. However, we hypothesized that IFN-γ Treg are sufficiently equipped following alloantigen stimulation for 14 days *in vitro* and the presence of a powerful immunosuppressive drug- abatacept, they might be able to control rejection even when being delivered post-transplantation.

CBA mice were given either $5x10^5$ or $1x10^6$ IFN-γ Treg 3 days before, 1 day before or 3 days after the transplant of a B6 heart allograft in addition to the sub-optimal abatacept protocol ***(Figure 3.2.6.2.1.i)***. When $5x10^5$ IFN-γ Treg were given before the transplant on day-3 or day-1, we saw prolongation of allograft survival with a MST of >100 days (n=3) and 64 days (n=7), respectively ***(Figure 3.2.6.2.1.ii)***. In clear contrast, $5x10^5$ IFN-γ Treg given on day+3 showed no graft protective effects (MST=17.5 days; n=4) compared to abatacept alone (MST=52 days; n=5) ***(Figure 3.2.6.2.1.ii)***. More interestingly, the rejection kinetics also appeared to be aggravated when IFN-γ Treg were delivered post-transplantation when compared to the abatacept control group.

Figure 3.2.6.2.1. Timing of IFN-γ Treg delivery was critical in determining graft outcome

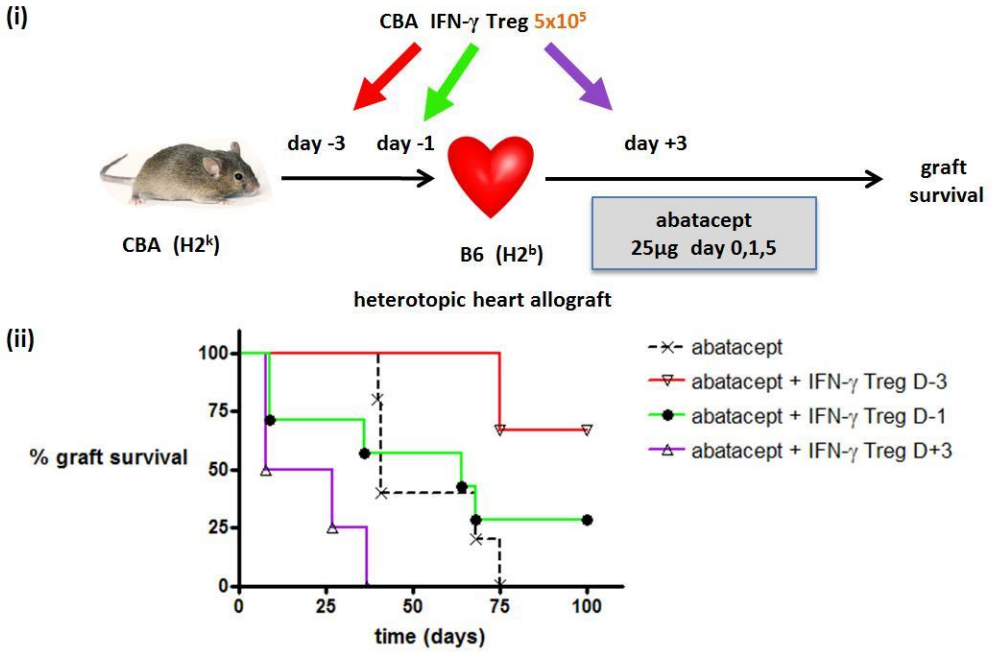

Group	n	graft survival (days)	MST (days)	p-value
abatacept	5	40,41,41,68,75	41	p = 0.0284
abatacept + IFN-γ Treg 5x10⁵ day-3	3	75,>100,>100	>100	p = 0.0158
abatacept + IFN-γ Treg 5x10⁵ day-1	7	9,9,36,64,68,>100,>100	64	p = 0.049
abatacept + IFN-γ Treg 5x10⁵ day+3	4	8,8,27,37	17.5	

Figure 3.2.6.2.1. Timing of IFN-γ Treg delivery was critical in determining graft outcome. IFN-γ Treg were generated by the IFN-γ conditioning protocol as described above ***(Chapter 2.8.1.)***. CBA mice were transplanted with a B6 heart allograft heterotopically and received i.v. abatacept 25µg on day 0,1 and 5. 5x10^5 IFN-γ Treg were given 3 days before (D-3), 1 day before (D-1) or 3 days after (D+3) the transplantation. Sub-optimal abatacept treatment prolonged heart allograft survival with a MST of 41 days (n=5). When 5x10^5 IFN-γ Treg were delivered 3 days before (D-3) the heart transplant, it led to significant prolongation of graft survival with a MST >100 days (n=3). When 5x10^5 IFN-γ Treg were given 1 day before the heart transplant, graft survival was not significantly different from the abatacept control group with a MST of 64 days (n=7) and 41 days (n=5), respectively. When 5x10^6 IFN-γ Treg were delivered after the heart transplant on day 3 (D+3), all the grafts were rejected with a MST of 17.5 days (n=4) in a faster tempo when compared to IFN-γ Treg delivered on D-1 or D-3. The graft rejection kinetics was more profound than the abatacept control group. These data suggest that the timing of IFN-γ Treg delivery was critical in determining graft outcome. Log rank tests were used for statistical comparisons. (p<0.05 denotes statistically significant)

Doubling the dose of IFN-γ Treg to $1x10^6$ did not result in improved graft prolongation. $1x10^6$ IFN-γ Treg given pre-operatively, either 1 day or 3 days prior to the transplant, led to significant prolongation of allograft survival (MST>100 days, n=4; MST>100 days, n=4), compared to those mice receiving abatacept alone (MST=52 days; n=5) ***(Figure 3.2.6.2.2.)***. On the other hand, IFN-γ Treg ($1x10^6$) were not able to extend graft survival when they were given 3 days after transplant (MST of 42 days (n=6)).

As we lowered the doses of abatacept to 10μg or 20μg on day 0, 1 and 5, there were modest prolongation of graft survival with a MST of 10 days (n=3) and 17 days (n=3) compared to historical controls of mice which received no treatment (MST=7.5 days, n=10) ***(Figure 3.2.6.2.3.)***. The addition of IFN-γ Treg at $5x10^5$ on day+3 to the 10μg or 20μg abatacept protocol showed no significant difference in their graft outcome (MST=10 days, n=3 ; MST =10 days, n=3) compared to the respective abatacept control groups ***(Figure 3.2.6.2.3.)***. These data suggest that the timing of Treg delivery appeared optimal when given pre-operatively in this model. The failure of IFN-γ Treg to exert any suppressive effect when delivered post-operatively could possibly due to: 1) the interaction between CTLA-4 Ig and infused Treg *in vivo*[449]; and 2) insufficient time for Treg to home to the relevant secondary lymphoid tissue or graft.

Figure 3.2.6.2.2. Timing of IFN-γ Treg delivery was the rate-limiting factor to determine graft outcome irrespective of cell dose

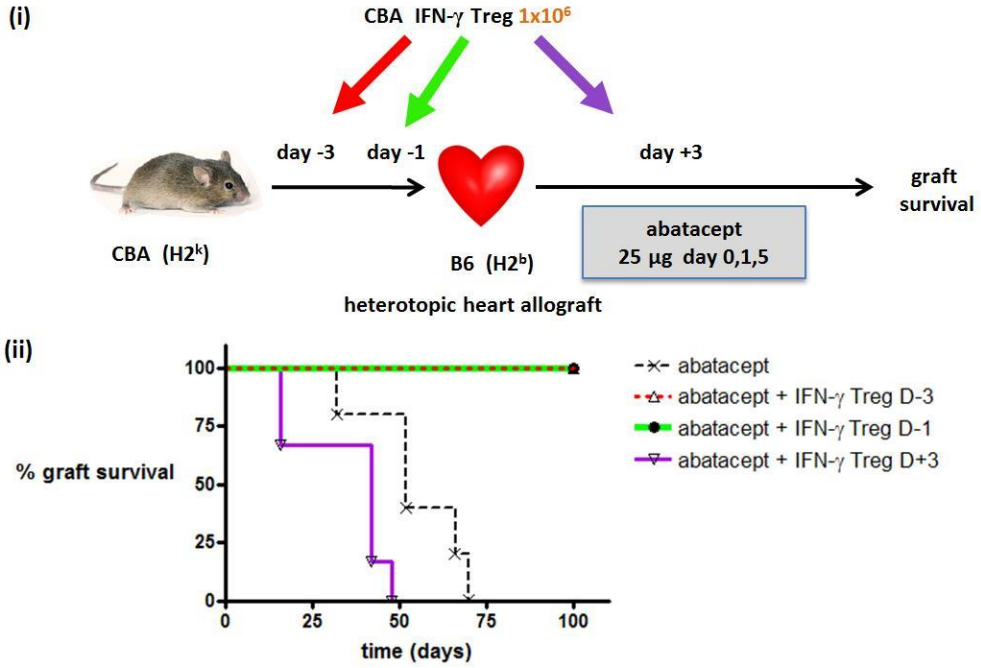

Group	n	graft survival (days)	MST (days)	p-value
abatacept	5	32,52,52,66,70	52	
abatacept + IFN-γ Treg 1x10⁶ day-3	4	>100,>100,>100,>100	>100	*p = 0.0003*
abatacept + IFN-γ Treg 1x10⁶ day-1	4	>100,>100>100,>100	>100	*p = 0.0046*
abatacept + IFN-γ Treg 1x10⁶ day+3	6	16,16,42,42,42,48	42	*p = 0.019*

Figure 3.2.6.2.2. Timing of IFN-γ Treg delivery was the rate-limiting factor to determine graft outcome irrespective of cell dose. (i) IFN-γ Treg were generated by the IFN-γ conditioning protocol described above ***(Chapter 2.8.1.)***. CBA mice were transplanted with a B6 heart allograft heterotopically and received i.v. abatacept 25µg on day 0, 1 and 5. 1x10⁶ IFN-γ Treg were given 3 days before (D-3), 1 day before (D-1) or 3 days after (D+3) the transplantation. **(ii)** Sub-optimal abatacept treatment prolonged heart allograft survival with a MST of 52 days (n=5). When 1x10⁶ IFN-γ Treg were delivered 3 days or 1 day before the heart transplant, graft survival was significantly prolonged with a MST of >100 days (n=4 per group). When 1x10⁶ IFN-γ Treg were delivered after the heart transplant on day 3 (D+3), all the grafts were rejected with a MST of 42 days (n=6). The rejection kinetics was more profound compared to the abatacept control group. These data ascertain that post-transplant IFN-γ Treg delivery could not offer any graft protection benefits, while pre-transplant IFN-γ Treg delivery led to a significant improvement of graft outcome, irrespective of the cell dose (see also ***Figure 3.2.6.2.1.***). Log rank tests were used for statistical comparisons. ($p<0.05$ denotes statistically significant)

Figure 3.2.6.2.3. Post-transplant IFN-γ Treg therapy was unable to control allograft rejection irrespective of the dose of costimulation blockade agent

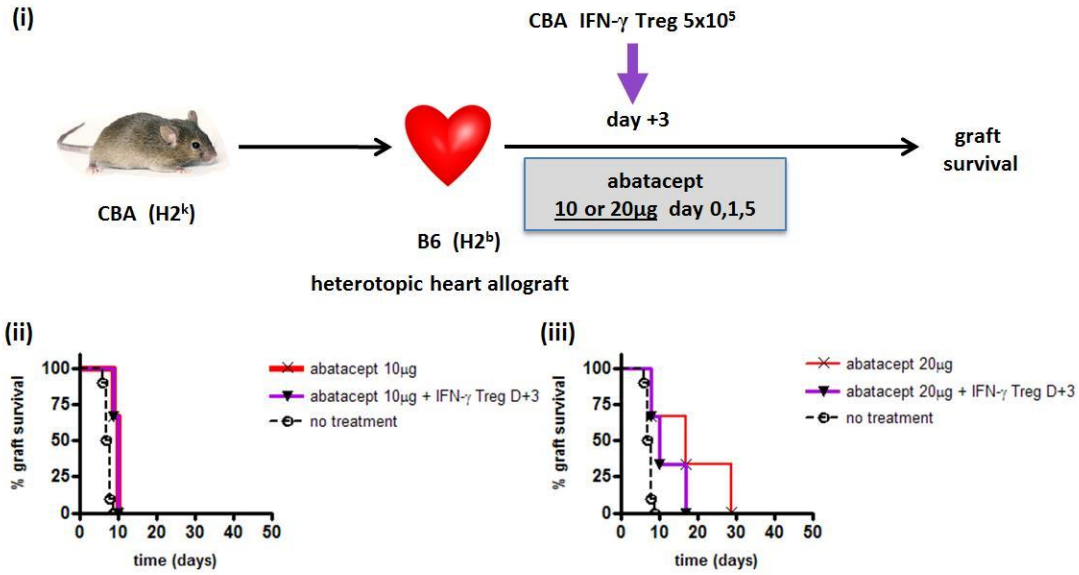

Group	n	graft survival (days)	MST (days)	p-value
abatacept 10µg	3	9,10,10	10	*p = 0.0085*
abatacept 10µg + IFN-γ Treg 5x10⁵ day+3	3	9,10,10	10	*p = 0.0085*
abatacept 20µg	3	8,17,29	17	*p = 0.0212*
abatacept 20µg + IFN-γ Treg 5x10⁵ day+3	3	8,10,17	10	*p = 0.3722*
no treatment (historical control)	10	6,7,7,7,7,8,8,8,8,9	7.5	*p = 0.0212*

Figure 3.2.6.2.3. Post-transplant IFN-γ Treg therapy was unable to control allograft rejection irrespective of the dose of costimulation blockade agent. (i) IFN-γ Treg were generated by the IFN-γ protocol as described above ***(Chapter 2.8.1.)***. CBA mice were transplanted with a B6 heart allograft heterotopically and received i.v. abatacept either 10 or 25µg on day 0, 1 and 5, with or without 5x10^5 IFN-γ Treg on day 3 post-transplantation (D+3). **(ii)** i.v. abatacept 10µg given on day 0, 1, and 5 led to a modest improvement of graft outcome with a MST of 10 days (n=3) compared to historical control of untreated mice (MST=7.5 days; n=10). 5x10^5 IFN-γ Treg had no impact on graft survival in mice treated with the abatacept 10µg protocol (MST= 10 days, n=3). **(iii)** i.v. abatacept 20µg given on day 0, 1, and 5 led to delayed graft rejection with a MST of 17 days (n=3). 5x10^5 IFN-γ Treg had no significant impact on graft survival in mice treated with the abatacept 20µg protocol (MST 10 days; n=3). Log rank tests were used for statistical comparisons. (p<0.05 denotes statistically significant)

3.2.7 Comparison between IFN-γ Treg and adaptive Treg generated by other established protocols

Adaptive Treg could be induced either *in vivo* or *in vitro*. Our group has previously described the induction of $CD4^+CD25^+$ adaptive Treg by exposing recipients to donor-specific blood transfusion prior to an implant of the allograft. $CD4^+CD25^+$ Treg isolated from these tolerized animals were able to regulate skin graft rejection mediated by $CD4^+CD25^-$ effectors in the adoptive transfer models[450]. On the other hand, adaptive Treg could be induced *in vitro*. Total $CD4^+$ splenocytes could be enriched for a higher proportion of alloantigen-experienced Treg population by the IFN-γ protocol as shown above[256]. Our group previously showed that adaptive Treg generation was nitric oxide dependent. Cilostamide, a PDEi (phosphodiesterase inhibitor) was shown to render enrichment of $Foxp3^+$ Treg by promoting Treg proliferation[451]. The proportion of $Foxp3^+$ Treg generated by this cilostamide protocol was compatible to that of the IFN-γ protocol ***(Figure 3.2.7.1.ii)***. However, the viability or the expansion potential of these cells was very restricted making it impossible to proceed for further experiments (*data not shown*).

Alternatively, Zheng et al[425] showed that adaptive Treg could be generated by stimulating $CD4^+$ precursors using allogeneic BM-APC in the presence of TGF-β and IL-2 *in vitro*. Adaptive Treg generated by the TGF-β/IL-2 protocol could lead to the prolongation of heart allograft survival long-term. We were able to replicate this protocol and generate adaptive Treg using this TGF-β/IL-2 protocol with minor modifications ***(Figure 3.2.7.1.iii)***. These cells expressed high levels of Foxp3 after 2 weeks of stimulation compared to Treg generated by the IFN-γ protocol (19.7% versus 20.1%). Typically, the TGF-β/IL-2 protocol could generate as high as 20% of the starting input number, compared to the IFN-γ protocol (5%) (*data not shown*).

Figure 3.2.7.1. Comparison amongst different alloantigen-driven *in vitro* conditioning protocols for the enrichment of CD4⁺Foxp3⁺ Treg

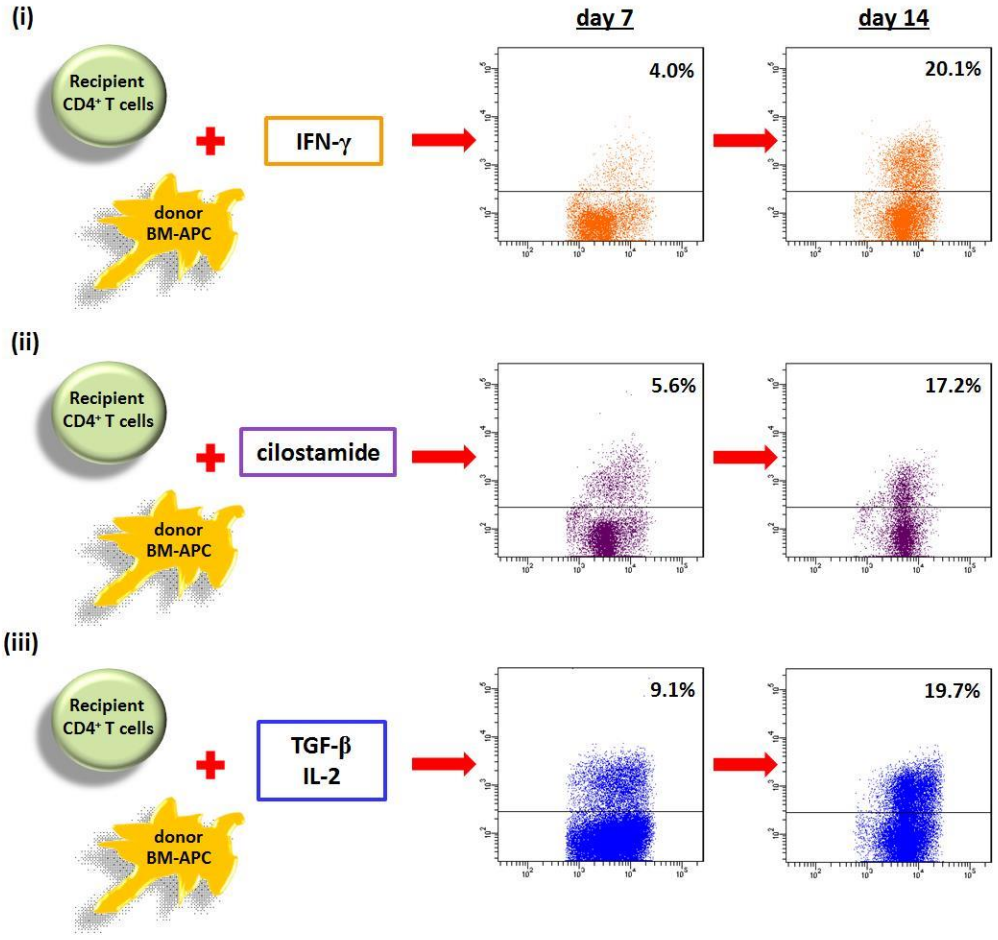

Figure 3.2.7.1. Comparison amongst different alloantigen-driven *in vitro* conditioning protocols for the enrichment of CD4⁺ Foxp3⁺ Treg. Recipient CD4⁺ T cells were stimulated with two successive rounds of alloantigen in the form of donor BM-APC, in the presence of **(i)** IFN-γ, **(ii)** cilostamide, or **(iii)** TGF-β + IL-2 for 14 days. After the first round of alloantigen stimulation, none of the conditioning protocols showed significant Foxp3 enrichment. However, after 2 rounds of alloantigen stimulation in a total of 14 days, the IFN-γ, and cilostamide, and TGF-β/IL-2 conditioning protocol showed improvement in the enrichment of Foxp3⁺ Treg: 20.1%, 17.2% and 19.7% Foxp3⁺ Treg, respectively. Data above represent at least 2 independent experiments.

When we compared the suppressive function of TGF-β/IL-2 Treg with IFN-γ Treg *in vivo*, we noted that at the same cell dose TGF-β/IL-2 Treg could also prevent skin allograft rejection long-term using the adoptive transfer skin allograft model (MST>90 days n=8); similar to that of IFN-γ Treg (at a 1:1 Treg: $CD4^+CD25^-$ T cells ratio) ***(Figure 3.2.7.2)***. On the other hand, IFN-γ Treg appeared to be superior to TGF-β/IL-2 Treg in the control of allograft rejection in immunocompetent recipients ***(Figure 3.2.7.3)***. In the presence of a sub-optimal abatacept treatment, $1x10^6$ TGF-β/IL-2 Treg could not prolong heart allograft survival with a MST of 40 days (n=3), compared to abatacept control (MST=52 days; n=5); whereas $1x10^6$ of IFN-γ Treg could prolong allograft rejection long-term (MST>100; n=4). Similarly, $2x10^6$ TGF-β/IL-2 Treg delayed allograft rejection with MST of 74.5 days (n=2), while the same number of IFN-γ Treg prevented allograft rejection long-term (MST>100 days; n=3). The role of IFN-γ in the elimination of alloreactive effector T cells by means of AICD could explain the superior suppressive function of IFN-γ Treg over TGF-β/IL-2 Treg on a cell-to-cell basis, given their Foxp3 expression was similar ***(Figure 3.2.7.1.)***.

Figure 3.2.7.2. IFN-γ Treg and TGF-β/IL-2 Treg were equally effective in controlling allograft rejection n the adoptive transfer skin transplant model

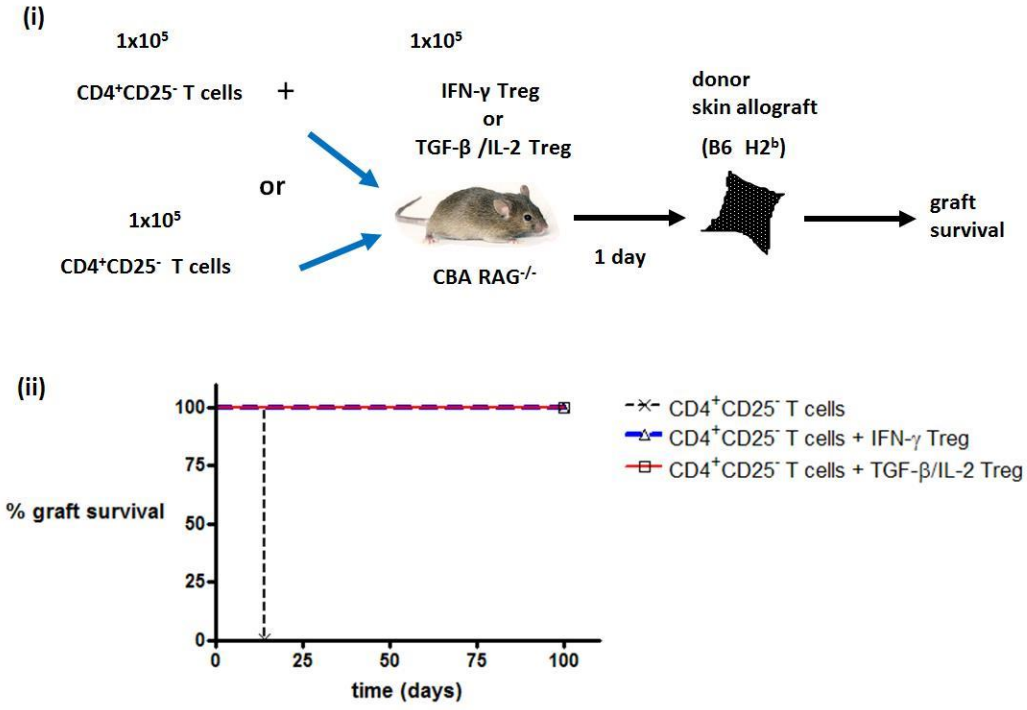

Group	n	graft survival (days)	MST (days)	p-value
CD4⁺CD25⁻ T cells	3	14,14,14	14	
CD4⁺CD25⁻ T cells + IFN-γ Treg	7	>100,>100,>100,>100,>100,>100,>100	>100	
CD4⁺CD25⁻ T cells + TGF-β/IL-2 Treg	7	>100,>100,>100,>100,>100,>100,>100	>100	*p = 0.0027*

Figure 3.2.7.2. IFN-γ Treg and TGF-β/IL-2 Treg were equally effective in controlling allograft rejection in the adoptive transfer skin transplant model. (i) Schematic diagram illustrates the experimental set up. CBA RAG$^{-/-}$ mice were reconstituted with 1x10^5 naive CD4$^+$CD25$^-$ T cells with or without 1x10^5 IFN-γ Treg or TGF-β/IL-2 Treg one day before the transplant of a B6 skin allograft. **(ii)** CBA RAG$^{-/-}$ mice reconstituted with CD4$^+$CD25$^-$ T cells rejected their skin allografts acutely with a MST of 14 days (n=3). IFN-γ Treg prevented skin allograft rejection mediated by CD4$^+$CD25$^-$ T cells long-term (MST>100 days; n=7). TGF-β/IL-2 Treg were equally effective in the prevention of allograft rejection mediated by CD4$^+$CD25$^-$ T cells in this adoptive transfer transplant model (MST>100 days; n=7). Log rank tests were used for statistical comparisons (p<0.05 denotes statistically significant).

Figure 3.2.7.3. IFN-γ Treg were superior to TGF-β/IL-2 Treg in controlling allograft rejection in immunocompetent heart transplant recipients

(i)

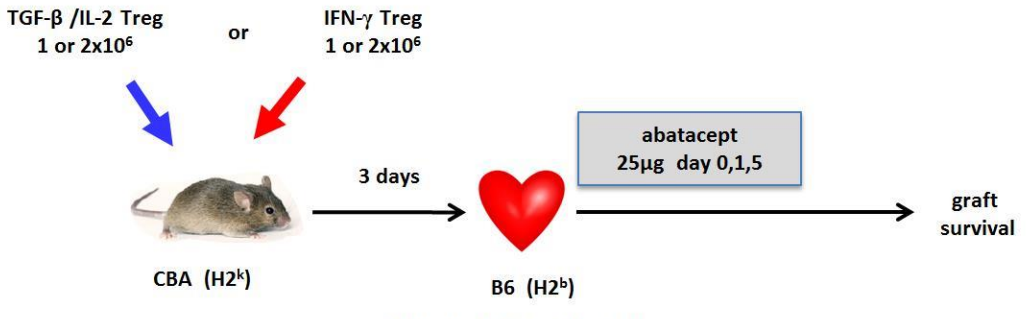

(ii)

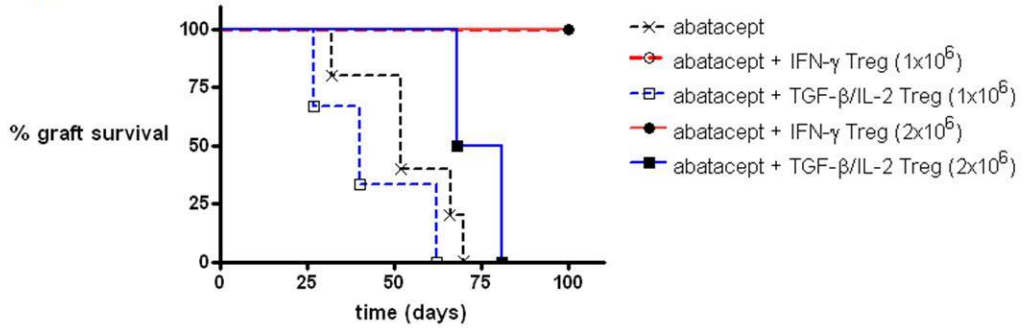

Group	n	graft survival (days)	MST (days)	p-value
abatacept	5	32,52,52,66,70	52	
abatacept + IFN-γ Treg (1x10⁶)	4	>100,>100,>100,>100	>100	
abatacept + TGF-β/IL-2 Treg (1x10⁶)	3	27,40,62	40	*p = 0.2298*
abatacept + IFN-γ Treg (2x10⁶)	3	>100,>100,>100	>100	
abatacept + TGF-β/IL-2 Treg (2x10⁶)	2	68,81	74.5	*p = 0.1527*

Figure 3.2.7.3. IFN-γ Treg were superior to TGF-β/IL-2 Treg in controlling allograft rejection in immunocompetent heart transplant recipients. (i) Schematic diagram illustrates the experimental set up. A sub-optimal abatacept treatment (i.v. 25µg day 0,1, and 5) was given to CBA mice with or without 1x10⁶ or 2x10⁶ IFN-γ Treg or TGF-β/IL-2 Treg, 3 day before the transplant of a B6 heart allograft. **(ii)** The sub-optimal abatacept protocol prolonged allograft survival with a MST of 52 days (n=5). 1x10⁶ or 2x10⁶ IFN-γ Treg prevented heart allograft rejection long-term (MST>100 days, n=4 and MST>100 days, n=3, respectively). 1x10⁶ TGF-β/IL-2 Treg were unable to control allograft rejection with a MST of 40 days (n=3). 2x10⁶ TGF-β/IL-2 Treg were able to delay allograft rejection with a MST of 74.5 days (n=2). These data indicate that IFN-γ Treg were superior to TGF-β/IL-2 Treg in the control of allograft rejection in immunocompetent recipients at the same cell dose. Log rank tests were used for statistical comparisons ($p<0.05$ denotes statistically significant).

3.3 Discussion

Our data have provided evidence which support the possibility of harnessing *in vitro* generated Treg to control alloresponses in solid organ transplantation. Stemming from previous work from our laboratory, we have shown that $CD4^+$ T cells stimulated with allogeneic BM-APC in the presence of exogenous IFN-γ were enriched for a $Foxp3^+$ population. The suppressive function of these conditioned T cells -'IFN-γ Treg', was clearly demonstrated when reconstituted together with naïve $CD4^+CD25^-$ T cells in immunodeficient mice using the skin allograft model ***(Figure 3.2.2.2.)***.

The adoptive transfer skin transplant model offers a robust and reliable method to assess the function of *in vitro* generated Treg. It is often used as the first step for the initial proof-of-principle experiments. With this tightly controlled system, it also serves as an invaluable tool to interrogate the mechanisms of action of Treg *in vivo*. There are a few limitations to this approach. The translational potential of this model to clinical studies is limited due to the confounded effect of homeostatic proliferation of reconstituted T cells in immunodeficient environment. In addition, transplant patients are rarely immunosuppressed to such an extent by current treatment modalities, unlike when total body irradiation was used. Therefore, in order to best mimic the clinical scenario we elected to test the suppressive function of *in vitro* generated IFN-γ Treg in a transplant model that uses immunocompetent recipients. We chose not to use the immunocompetent mouse skin graft model for a number of reasons. Firstly, according to our experience the number of Treg required to elicit any convincing suppressive effect in a skin allograft model is in the region of $10\text{-}20x10^6$ cells per mouse (R. Francis and R. Devlin in our laboratory, personal communication). Given the intrinsic anergic feature and scarcity of Treg, unless we have unlimited supply of Treg this would be technically impossible.

On the other hand, the number of Treg required to control rejection in immunocompetent recipients of a heterotopic heart graft model is conceivably lower than that of the skin graft model because of the differential susceptibility to rejection in different organs as we previously reported[446]. Second, the heterotopic heart transplant model, although technically more demanding than the skin transplant model, a fully vascularized heart graft better mimics solid organ transplantation. Thirdly, the heart graft model also provides a functional readout for comparisons, whereas the skin graft model generally provides a qualitative readout.

There are many different *in vitro* Treg generation protocols that have been published in the literature. These could be classified in terms of the Treg precursors, stimulators and the special culture conditions they utilized. The majority of protocols involved the use of a purified $CD4^+CD25^+$ nTreg precursors with an aim to achieve the highest purity in mind. Polyclonal or allogeneic stimulators in the form of anti-CD3/CD28 beads and allogeneic APC were used to generate polyclonally-expanded/activated nTreg and alloreactive/allospecific Treg, respectively. IL-2 was included in the protocols to boost Treg proliferation and survival[452,453]. TGF-β was also included in some protocols with an aim to generate Treg preferentially[423,454]. We showed that the IFN-γ conditioning protocol could enrich for a similar Treg population when compared directly with the TGF-β/IL-2 protocol ***(Figure 3.2.7.1)***. But more importantly, we demonstrated that IFN-γ Treg were superior to TGF-β/IL-2 Treg in the control of allograft rejection in immunocompetent recipients in the heart transplant model on a cell-to-cell basis ***(Figure 3.2.7.3)***. We think that the functional differences between these two Treg populations might be explained by the unique action of IFN-γ in shaping the IFN-γ Treg repertoire *in vitro*.

The main advantage of our *in vitro* IFN-γ Treg generation protocol compared to others is the avoidance of performing any stringent cell sorting or isolation processes. Exogenous IFN-γ

employed in our culture system serves as a 'chemical cell sorter', which preferentially induces AICD in the non-Treg population amongst the $CD4^+$ precursors upon repeatedly stimulated with immature BM-APC *in vitro*[256,440]. By separating the Treg and non-Treg population by using flow cytometry sorted WT $CD4^+CD25^-$ and CP-1 $CD4^+CD25^+$ T cells as precursors, we have previously shown that our IFN-γ conditioning protocol led to the expansion of nTreg and conversion of non-Treg precursors to $Foxp3^+$ Treg[256]. In addition, we showed that the action of immature BM-APC conditioned by TGF-β led to a reduction of IL-6 production which favoured Treg generation[440]. Furthermore, the production of endogenous TGF-β by BM-APC was responsible for the enrichment of $Foxp3^+$ cohort as neutralizing anti-TGF-β antibody abolished Treg enrichment in this protocol[440]. This ultimately resulted in an enriched Treg population from an initial 6-8% polyclonal $Foxp3^+$ population to a final IFN-γ Treg product, which consists of an average 40-60% $Foxp3^+$ alloreactive Treg population ***(Figure 3.2.1.1)***. In addition, a BM-APC removal step was not necessary in our protocol as we found >90% were TCR-β^+ or $CD3^+$ in the final product (*data not shown*).

According to the data available in the literature[425,426] and the experience from our laboratory, it was anticipated that the number of IFN-γ Treg required to control alloresponses in an immunocompetent recipient of the heart graft model might be in the region of 1 to $10x10^6$ cells even in the presence of an adjunct immunosuppressive treatment. Hence, we attempted to optimize the cell yield of the IFN-γ conditioning protocol. The physico-chemical properties of *in vitro* cultures are important factors to determine the outcome of Treg yield. Although an overall increase in the cell density in our culture system did not enhance cell yield, the antigen dose[455,456] and the maturity status of APC[457-459] could have an impact on the expansion of Treg *in vitro*. An optimal alloantigen dose was found in our protocol, with a 3-fold increase in the number of BM APC present in the culture led to an increased cell yield of IFN-γ Treg with a

stable Foxp3 enrichment ***(Figure 3.2.3.1.2)***. This was then adopted as the standard protocol for the rest of the project.

We also aimed to fine tune the maturity status of BM-APC by culturing BM-APC in different plates and by the titration of the concentration of APC growth factors. Subtle differences in the phenotypic characteristics of BM-APC could be detected, such as the expression of CD80 and CD86. However, it is often difficult to quantify their action and translate it to the final outcome. Unfortunately, there was no dramatic increase in the cell yield, possibly due to the primary action of exogenous IFN-γ-mediated AICD. Besides, there were no real differences in their suppressive function *in vivo* using the adoptive transfer skin graft model ***(Figure 3.2.3.3.2, Figure 3.2.3.4.3 and Figure 3.2.3.5.4)***.

More importantly, we have demonstrated that IFN-γ Treg could control the rejection of a full MHC-mismatched (major and minor histocompatibilty antigens) heart transplant in the presence of a sub-optimal costimulation blockade treatment. A single-dose IFN-γ Treg could prevent allograft rejection long-term in immunocompetent heart transplant recipients in conjunction with a sub-optimal abatacept. The choice of costimulation blocking agent abatacept was based on its clinical translation potentials. Current immunosuppressive strategies are moving away from the use of CNI, which have been known to have a negative effect on IL-2-dependent Treg survival[460,461]. Rapamycin is an alternative maintenance immunosuppressive drug which has been shown to augment Treg proliferation and survival[461,462], but also possesses a lower incidence of *de novo* skin cancers in renal transplant patients after switching from a CNI-based to a rapamycin-based therapy[463]. Although recent evidence have emerged that costimulation blockade might be detrimental to Treg, we believe that the impact on alloantigen-driven, activated Treg in our study was minimal. It has been suggested that Treg require CD28

stimulation for peripheral development and expansion *in vivo* and the administration of CTLA-4Ig dampened Treg-mediated regulation by limiting the availability for CD28-dependent activation[464], however, we think that this requirement might not be necessary for IFN-γ Treg which had been activated by alloantigens *in vitro* in that sense. We hypothesized that the influence of abatacept was maximal to naïve Treg, but not pre-activated Treg by alloantigens. We will discuss this in more details in ***Chapter 5.2.5.***, when we compared and contrasted the suppressive function between nTreg and IFN-γ Treg in the presence of a sub-optimal abatacept effect. Although we have previously demonstrated allospecificty using the same IFN-γ Treg protocol published elsewhere[256] and there was an apparent difference between mice treated with alloantigen-experienced T cell therapy plus abatacept compared to abatacept alone, we acknowledge the data above should be interpreted with limitation without a third party control such as the use of BALB/c grafts in order to demonstrate true alloreactivity. This could be achieved firstly by substituting B6 with BALB/c grafts in the adoptive transfer skin graft model above using the same B6-driven IFN-γ Treg to exclude non-specific suppression. Second, in order to affirm allospecific control, we could test the suppressive function of IFN-γ Treg driven by BALB/c BM-APC using the exact Treg generation protocol. The findings from these adoptive transfer models should be supplemented with testing the suppressive function of B6-driven and BALB/c-driven IFN-γ Treg in a separate set of BALB/c to CBA heart transplant experiments together with titration of abatacept controls using the BALB/c to CBA strain combination.

Various titration experiments reported in this chapter indicated that graft outcome depends on the delivery of an adequate number of Treg in relation to the precursor frequency of alloreactive effector T cells *in vivo*. Graft outcome was directly proportional to the number of IFN-γ Treg administered in our transplant models ***(Figure 3.2.6.1. & 3.2.6.2.)***. While expansion of IFN-γ Treg was very limited as shown in ***Chapter 5.2.1***, expansion of freshly-isolated $CD4^+CD25^+$

nTreg was possible using the plate-bound anti-CD3/CD28 antibody protocol ***(Chapter 5.2.4)***. In contrast, large numbers of human Treg could be obtained from efficient expansion protocols because of the inherent different expansion potential between mouse and human Treg. However, the lack of a unique surface marker for human Treg has made it difficult to isolate a homogenous population of potent Treg. A combination of surrogate surface markers has been used in the early stage of clinical studies such as selective $CD127^{lo}$ sub-population of human $CD4^{+}CD25^{hi}$ expanded Treg.

Our data showed that the timing of Treg delivery in the heart transplant model appeared to be critical in determining graft outcome. This might be explained in part by: 1) the homing properties of Treg, 2) the effect of CTLA-4Ig on Treg and 3) the combination of both. Our data suggest that Treg given after transplant surgery had negligible impact on graft survival, whilst Treg delivered prior to the transplant significantly prolonged graft survival. Other studies have demonstrated that post-transplant multi-dose Treg therapy could enhance graft survival in the background of certain immunosuppressive protocols. In our model, we believe that alloantigen-driven IFN-γ Treg when delivered 3 days prior to transplant allowed them to home to the secondary lymphoid tissues and to take residence within the allograft.

In conclusion, we have demonstrated that the IFN-γ conditioning protocol was a robust protocol to generate functional Treg. We propose that in synergy with a sub-optimal dose of costimulation blockade-abatacept, the translational potentials of alloantigen-driven Treg in solid organ transplantation should not be overlooked, despite the emerging development of nTreg-based therapy in preliminary clinical studies.

Chapter 4 Suppression of allograft rejection by *in vitro* generated Treg - Mechanisms of action

4.1 Introduction

$CD4^+CD25^+$ nTreg were amongst other regulatory cells that have been studied extensively in the last few decades. Subsequently, the master gene for Treg lineage development and function-Foxp3 was identified in 2003[259-261]. Until recently, the phenotypic and genetic features of nTreg have been further characterized; however, their precise mechanisms of action remain inconclusive. Several reviews in the literature summarized these proposed mechanisms of nTreg[347,465-467] and a brief account is summarized in ***Chapter 1.3.2.7***.

The role of CTLA-4 pathway in the mechanisms of Treg suppression remains controversial[468]. However, with the latest insight into CTLA-4-mediated trans-endocytosis of CD80/CD86 molecules[393], it would be interesting to examine the requirement of CTLA-4 for the suppression of allograft rejection mediated by *in vitro* generated alloantigen-reactive Treg using our established transplant models.

IL-10 was identified as one of the immunosuppressive cytokines secreted by a subpopulation of T cells. $CD4^+CD45RB^{lo}$ T cells controlled the effector function of the $CD45RB^{hi}$ population in an adoptive transfer colitis model via the action of IL-10[379]. In addition, Tr1 cells were also shown to mediate their suppressive action principally through the secretion of IL-10[262]. We investigated if alloantigen-reactive Treg suppress allograft rejection in a similar manner via the IL-10-IL-10R pathway.

We previously encountered significant difficulties in designing a robust *in vitro* suppression assay to evaluate the function of mouse Treg. We aimed to revisit the possibility of developing this assay with the availability of GFP/Foxp3 reporter in CBA mice, new mouse T cells/Treg compatible cell proliferation fluorescent dyes and a new multichannel flow cytometer.

One pertinent question we would like to ask was the fate of Treg after being infused *in vivo*. Did these cells persist indefinitely? What was the functional significance of these cells in the maintenance of long-term allograft acceptance? Could these cells mediate suppression via the process of infectious tolerance[304]? We employed a specific Treg depletion strategy to evaluate the function of exogenous Treg in recipients who have accepted allografts long-term.

Furthermore, it has been shown that nTreg were not effective in controlling memory responses *in vivo*[192]. Using $CD4^{+}CD44^{hi}$ T cells as an adoptive transferred memory cell population which was generated against donor alloantigens, we investigated if alloreactive IFN-γ Treg could attenuate memory responses against allograft in sensitized recipients.

The aim of this chapter is to evaluate these possible mechanisms of action that IFN-γ Treg utilize in order to exert their suppressive function in comparison with $CD4^{+}CD25^{+}$ nTreg.

4.2 Results

4.2.1 IFN-γ Treg mediated suppression of alloresponses through CTLA-4

Our group previously demonstrated in an adoptive transfer model that anti-CTLA-4 antibody abrogated the graft protective effect of $CD4^+CD25^+$ Treg induced by the YTS 177/DST protocol[450]. We therefore hypothesized that CTLA-4 would contribute to the mechanisms of suppression by IFN-γ Treg.

We first examined the expression of CTLA-4 on IFN-γ Treg as compared to nTreg by flow cytometry. Capturing of the surface expression of CTLA-4 on nTreg or IFN-γ Treg was unsuccessful possibly due to rapid endocytosis of this molecule[469] ***(Figure 4.2.1.1.i-ii)***. Instead, the surrogate intracellular CTLA-4 expression was evaluated. In the naive CBA $CD4^+$ T cell population, 4.5% co-expressed Foxp3 and CTLA-4 ***(Figure 4.2.1.1.iii)***. In clear contrast, 9.2% of IFN-γ Treg co-expressed Foxp3 and CTLA-4, which possibly correlated with the activation status of these cells after being repeatedly stimulated by allogeneic BM-APC *in vitro* ***(Figure 4.2.1.1.iii)***.

Figure 4.2.1.1. CTLA-4 expression on IFN-γ Treg

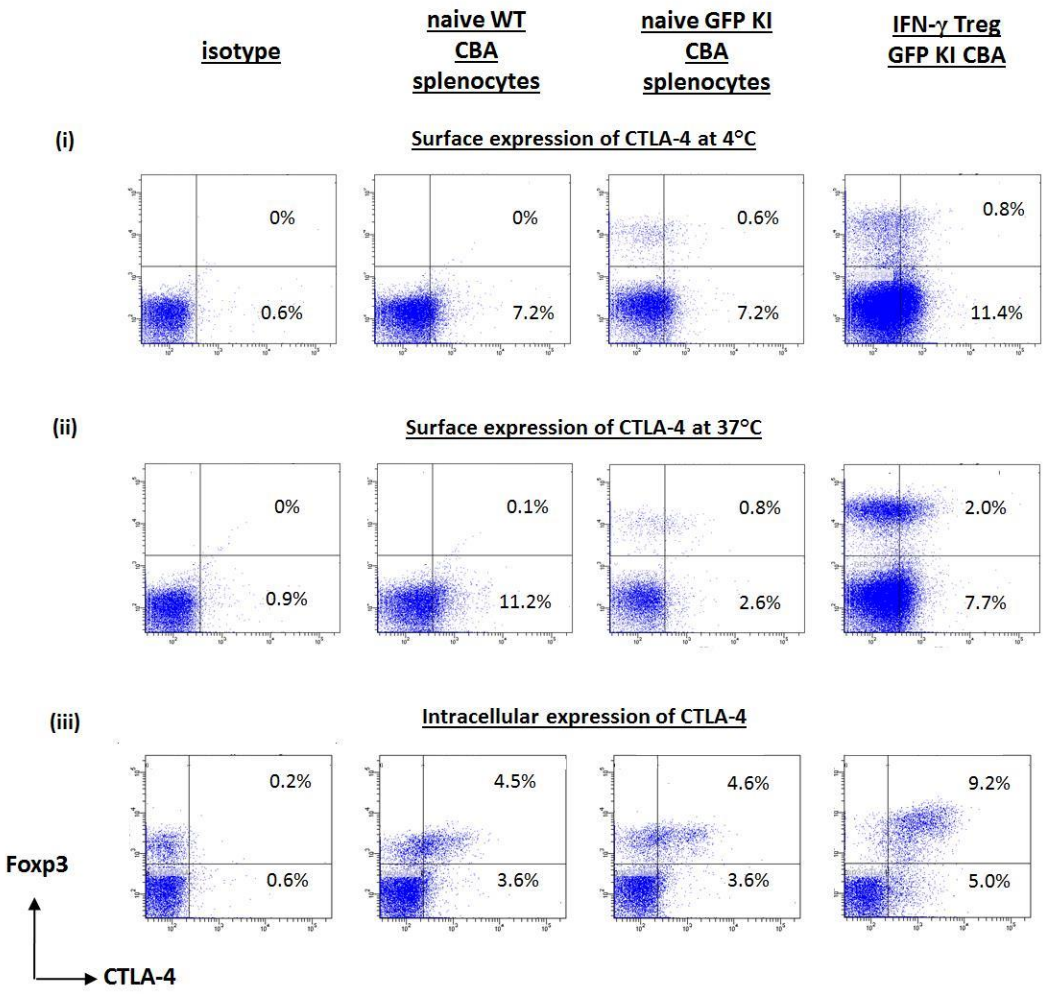

Figure 4.2.1.1. CTLA-4 expression on IFN-γ Treg. FACS dot plots show the surface and intracellular expression of CTLA-4 on gated $CD4^+$ T cells obtained from naïve WT CBA splenocytes, naïve GFP/Foxp3 KI CBA splenocytes and IFN-γ Treg generated from GFP/Foxp3 KI CBA splenocytes. **(i)** At 4°C, there was no demonstrable level of surface CTLA-4 in the gated $CD4^+$ $Foxp3^+$ T cell populations in each group (<1%). **(ii)** At 37°C, the expression of surface CTLA-4 remained indeterminate. These results were consistent with the notion of the difficulty in capturing the cell surface expression of CTLA-4 due to rapid endocytosis of this molecule. **(iii)** When cells were permeablized and stained for the expression of intracellular CTLA-4, the percentage of cells expressing CTLA-4 in the gated $CD4^+Foxp3^+$ T cells obtained from WT CBA splenocytes, GFP/Foxp3 KI CBA splenocytes and IFN-γ Treg were 4.5%, 4.6% and 9.2%, respectively .

Next, the critical role of CTLA-4 in IFN-γ Treg function was assessed *in vivo*. We hypothesized that an anti-CTLA-4 antibody treatment will abolish IFN-γ Treg function in the skin allograft adoptive transfer model ***(Figure 4.2.1.2.i-ii)***. CBA $RAG^{-/-}$ mice were reconstituted with naive $CD4^+CD25^-$ T cells with or without IFN-γ Treg, with or without anti-CTLA-4 antibody (4F10) or an isotype antibody. CBA $RAG^{-/-}$ mice reconstituted with $1x10^5$ naïve CBA $CD4^+CD25^-$ T cells rejected their B6 skin allografts acutely with a MST of 13 days (n=6). Graft rejection mediated by $CD4^+CD25^-$ effectors was delayed in the presence of anti-CTLA-4 antibody (4F10) with a MST of 22 days (n=6). This paradoxical effect might be explained in two-folds. This naïve $CD4^+CD25^-$ population contains a small (typically 2 %) but non-negligible number of $Foxp3^+$ T cells ***(***see ***Figure 3.2.2.1.ii.b)*** due to imperfect negative *in vitro* selection process by MACS. At the initially stage of homeostatic proliferation, these $CD25^+$ nTreg underwent more extensive proliferation compared to the naive $CD25^-$ non-Treg counterpart *in vivo*. Their phenotype could also change into their function into a more memory phenotype which could lead to delayed rejection. However, all allografts were ultimately rejected once the homeostatic proliferation of non-Treg catched up in time. Mice reconstituted with $CD4^+CD25^-$ T cells, but co-transferred with an equal number of IFN-γ Treg ($1x10^5$) accepted their allografts long-term (MST>100days; n=6). The addition of 4F10 reversed the graft protective effect of co-transferred IFN-γ Treg, which led to rejection of all allografts with MST of 15 days (n=6). In contrast, an isotype anti-hamster Ig had no impact on IFN-γ Treg suppressive function, in which most of the grafts were accepted long-term (MST>100 days; n=6). Similar to IFN-γ Treg, $1x10^5$ $CD4^+CD25^+$ nTreg prevented allograft rejection mediated by the same effector population long-term with a MST >70 days (n=3). The addition of 4F10 abrogated nTreg suppressive function rendering a MST of 13 days (n=4). These data collectively suggests that CTLA-4 is critical for the suppressive function of both IFN-γ Treg and nTreg.

Figure 4.2.1.2. IFN-γ Treg mediated suppressive function via CTLA-4 *in vivo*

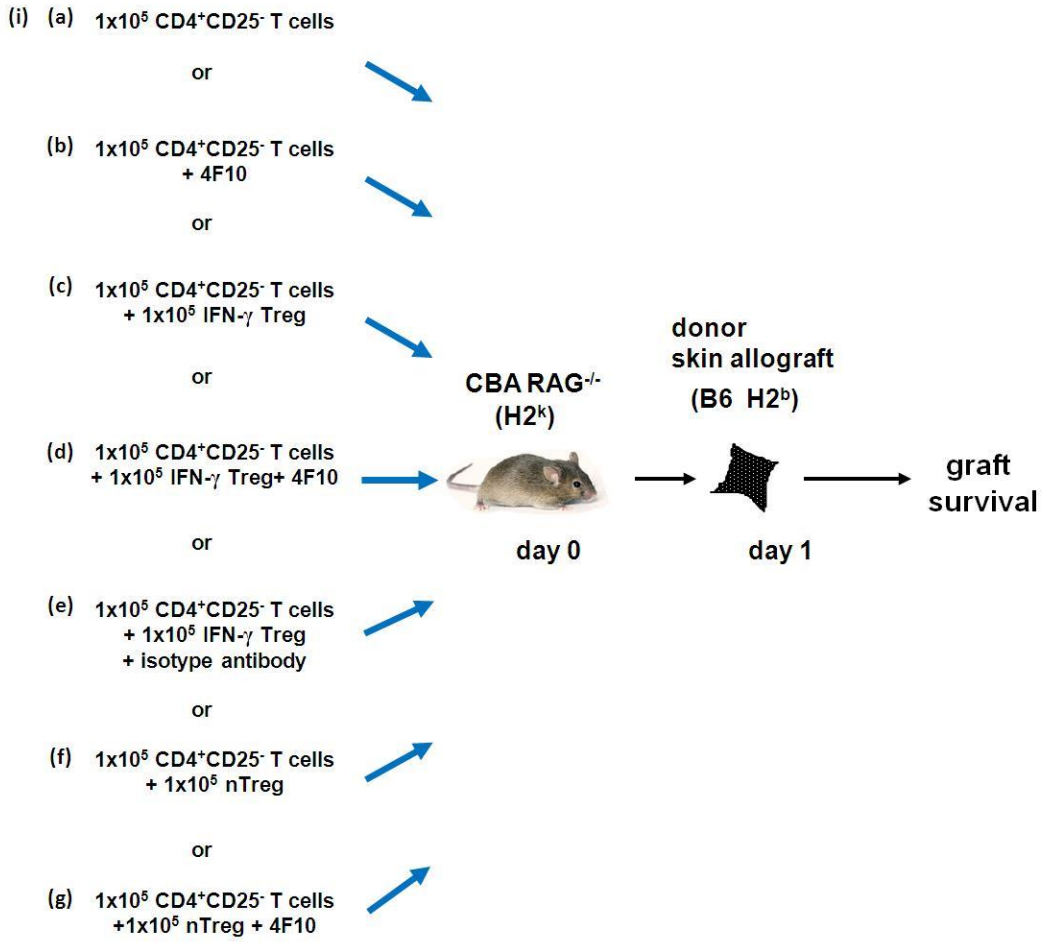

Figure 4.2.1.2.i. IFN-γ Treg mediated suppressive function via CTLA-4 *in vivo*. The role of CTLA-4 in IFN-γ Treg suppressive function was examined using the adoptive transfer skin transplant model. CBA RAG$^{-/-}$ mice were reconstituted with 1x10^5 CD4$^+$CD25$^-$ T cells with or without 1x10^5 IFN-γ Treg or 1x10^5 CD4$^+$CD25$^+$ nTreg one day before the transplant of a B6 skin allograft. In some groups of mice an anti-CTLA-4 antibody (4F10) or an isotype antibody (anti-hamster Ig) was administered. The impact of anti-CTLA-4 antibody on IFN-γ Treg or nTreg function was determined by the differential graft outcome compared to the controls.

Figure 4.2.1.2. IFN-γ Treg mediated suppressive function via CTLA-4 *in vivo*

(ii)

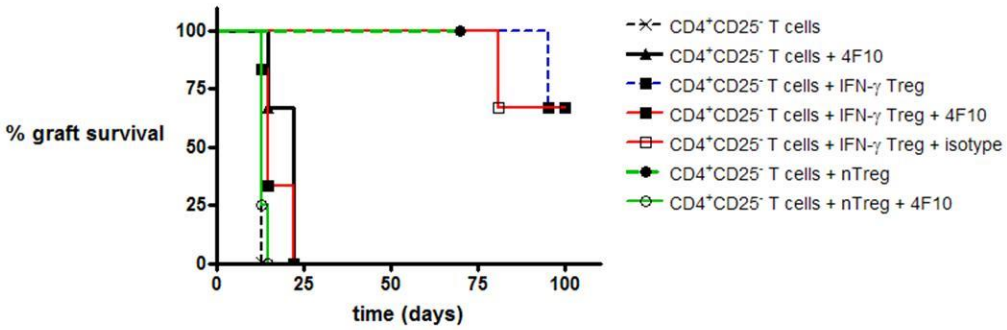

Group	n	graft survival (days)	MST (days)	p-value
$CD4^+CD25^-$ T cells	6	13,13,13,13,13,13	13	*p = 0.0009*
$CD4^+CD25^-$ T cells + 4F10	6	15,15,22,22,22,22	22	
$CD4^+CD25^-$ T cells + IFN-γ Treg	6	95,95,>100,>100,>100,>100	>100	*p = 0.0008*
$CD4^+CD25^-$ T cells + IFN-γ Treg + 4F10	6	13,15,15,15,22,22	15	
$CD4^+CD25^-$ T cells + IFN-γ Treg + isotype	6	81,81,>100,>100,>100,>100	>100	
$CD4^+CD25^-$ T cells + nTreg	3	>70,>70,>70	>70	*p = 0.0134*
$CD4^+CD25^-$ T cells + nTreg + 4F10	4	13,13,13,15	13	

Figure 4.2.1.2.ii. IFN-γ Treg mediated suppressive function via CTLA-4 *in vivo*. CBA $RAG^{-/-}$ mice reconstituted with $1x10^5$ naïve CBA $CD4^+CD25^-$ T cells rejected their B6 skin allografts acutely with a MST of 13 days (n=6). Anti-CTLA-4 antibody (4F10) delayed allograft rejection mediated by $CD4^+CD25^-$ T cells with a MST of 22 days (n=6). Mice reconstituted with $CD4^+CD25^-$ T cells, but co-transferred with an equal number of IFN-γ Treg ($1x10^5$) accepted their allografts long-term (MST>100days; n=6). The addition of 4F10 reversed the graft protective effect of co-transferred IFN-γ Treg, which led to acute rejection of all allografts with MST of 15 days (n=6). In contrast, an isotype anti-hamster Ig had no impact on IFN-γ Treg function, in which most of the grafts were accepted long-term (MST>100 days; n=6). $1x10^5$ $CD4^+CD25^+$ nTreg prevented allograft rejection mediated by the same effector population long-term with a MST >70 days (n=3). The addition of 4F10 abrogated nTreg suppressive function leading to a MST of 13 days (n=4). These data suggest that IFN-γ Treg and $CD4^+CD25^+$ nTreg both mediated their suppressive function via CTLA-4. Log rank tests were used for statistical comparisons. ($p<0.05$ denotes statistically significant)

4.2.2 IFN-γ Treg mediated suppressive function was partially dependent on the IL-10-IL-10R pathway

We previously showed that $CD4^+CD25^+$ Treg induced by the YTS 177/DST protocol elicit their suppressive function via IL-10[450]. We hypothesized that IFN-γ Treg mediated immunosuppression via the secretion of IL-10 similar to that of other regulatory T cells.

We attempted to detect the intracellular IL-10 expression in IFN-γ Treg. IFN-γ Treg were generated with GFP/Foxp3 KI CBA $CD4^+$ precursors- called 'GFP IFN-γ Treg'. Freshly-harvested GFP IFN-γ Treg were restimulated with PMA/ionomycin *in vitro*. Their intracellular IL-10 expression was compared with that of re-stimulated splenocytes from GFP/Foxp3 KI CBA mice ***(Figure 4.2.2.1)***. Only a small proportion of cells expressed IL-10: 1.8% and 0.9% $CD4^+$ T cells from GFP/Foxp3 KI CBA splenocytes and GFP IFN-γ Treg expressed IL-10, respectively ***(Figure 4.2.2.1.i)***. Looking at GFP^+CD4^+ T cells subpopulation in GFP KI CBA splenocytes and GFP IFN-γ Treg, the proportion of cells expressing IL-10 were 5.7% and 3.1%, respectively ***(Figure 4.2.2.1.ii)***. It appeared that a very small number of GFP^+ T cells express intracellular IL-10 upon re-stimulation *in vitro*.

Figure 4.2.2.1. IFN-γ Treg expressed low level of intracellular IL-10

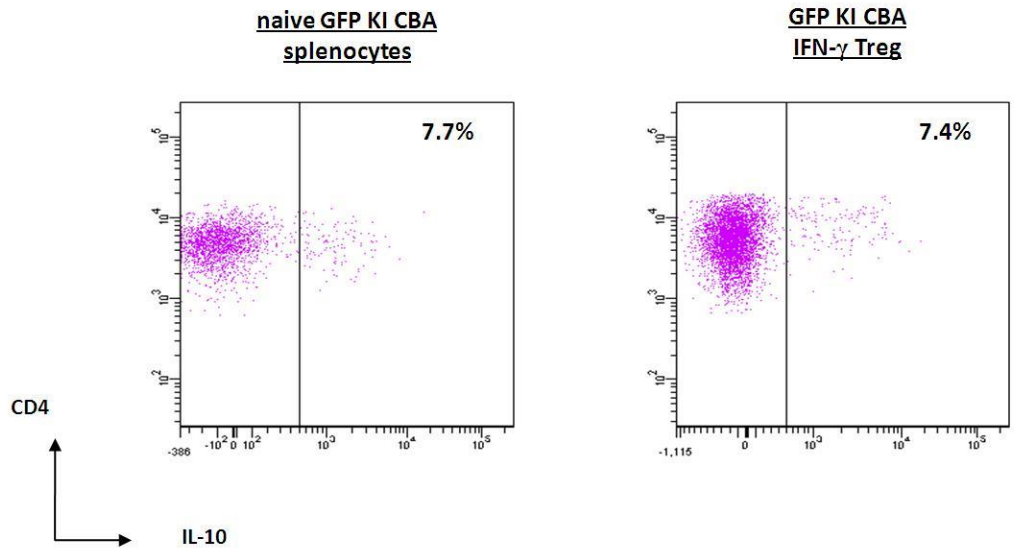

Figure 4.2.2.1. IFN-γ Treg expressed low level of intracellular IL-10. IFN-γ Treg were generated with GFP/Foxp3 KI CBA $CD4^+$ precursors (GFP IFN-γ Treg). Freshly-harvested IFN-γ Treg were restimulated with PMA/ionomycin *in vitro*. Their intracellular IL-10 expression was compared with restimulated splenocytes from GFP/Foxp3 KI CBA mice. 7.7% and 7.4% of GFP^+CD4^+ T cells from GFP/Foxp3 KI CBA splenocytes and GFP IFN-γ Treg expressed IL-10, respectively.

Next, we investigated the role of IL-10-IL-10R pathway in IFN-γ Treg suppressive function *in vivo* ***(Figure 4.2.2.2.i-ii)***. We hypothesized that IFN-γ Treg exerted their immunosuppressive effects that was dependent on IL-10 signaling. We showed that an anti-IL-10R antibody (1B1.2) partially reversed the immunosuppressive effect of IFN-γ Treg in an adoptive transfer skin transplant model. CBA $RAG^{-/-}$ mice were reconstituted with naïve $1x10^5$ CBA $CD4^+CD25^-$ T cells one day prior to the transplant of a B6 skin allograft. These mice rejected their B6 skin grafts acutely with a MST of 13 days (n=6). 1B1.2 alone had very limited impact on graft outcome (MST=13 day; n=6.). IFN-γ Treg prevented graft rejection long-term in majority of recipients (MST>100 days; n=3). On the other hand, the graft protection effect of IFN-γ Treg was partially reversed by the addition of 1B1.2, which resulted in a MST of 41 days (n=5), but this was not affected by the addition of an isotype antibody (anti-rat Ig) (MST=97 days; n=5). Interestingly, while $CD4^+CD25^+$ nTreg prevented skin graft rejection long-term with a MST of >100 days (n=5), 1B1.2 had no effect on the graft protective effect provided by nTreg (MST >100 days (n=5). These data suggest that IFN-γ Treg mediated suppression was partially dependent on the IL-10-IL-10R pathway. This is consistent with our previous data obtained from the DST-induced Treg model, in which Treg mediated suppression was also partially reversed by the administration of 1B1.2 antibody. More interestingly, it appeared that freshly-isolated nTreg controlled allograft rejection independent of the IL-10-IL-10R pathway.

Figure 4.2.2.2. IFN-γ Treg mediated suppression partially dependent on the IL-10-IL-10R pathway *in vivo*

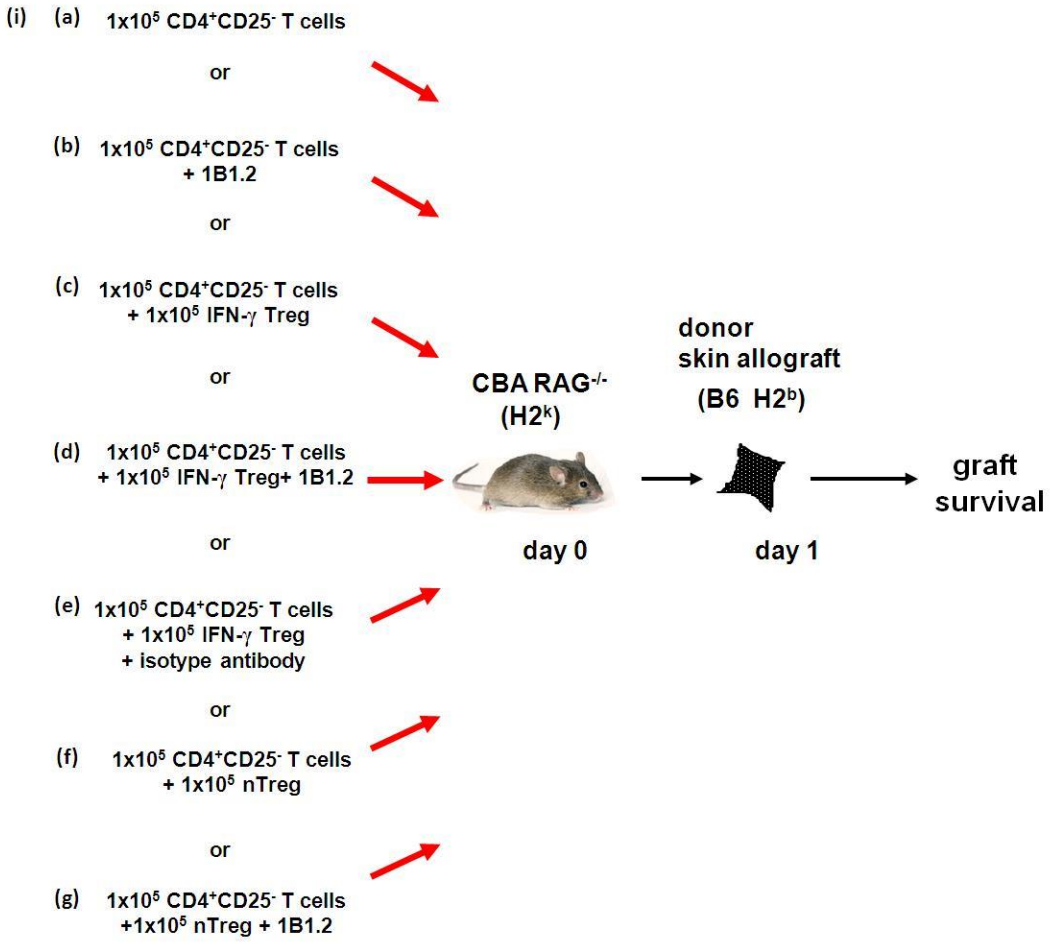

Figure 4.2.2.2.i. IFN-γ Treg mediated suppression partially dependent on the IL-10-IL-10R pathway *in vivo*. The role of IL-10-IL-10R pathway in IFN-γ Treg function was examined *in vivo*. CBA RAG$^{-/-}$ mice were reconstituted with 1x10^5 CD4$^+$CD25$^-$ T cells with or without 1x10^5 IFN-γ Treg or 1x10^5 CD4$^+$CD25$^+$ nTreg one day before the transplant of a B6 skin allograft. In order to ascertain if the prevention of IL-10 signalling through the IL-10R could abrogate the suppressive effects of IFN-γ Treg or nTreg, certain groups of mice were given either an anti-IL-10R antibody (1B1.2) or an isotype antibody (anti-rat Ig).

Figure 4.2.2.2. IFN-γ Treg mediated suppression partially dependent on the IL-10-IL-10R pathway *in vivo*

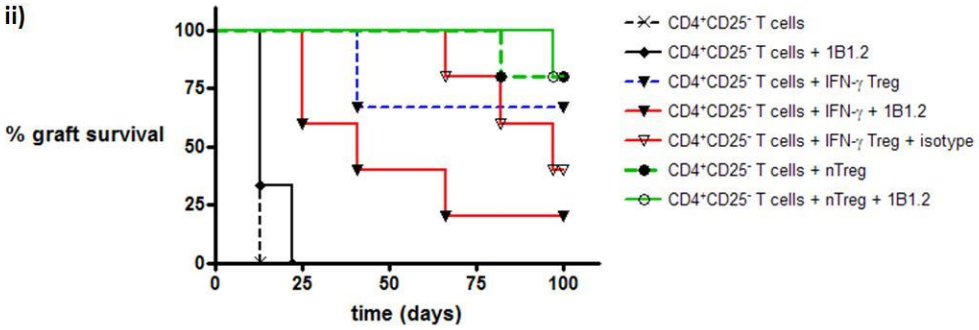

Group	n	graft survival (days)	MST (days)	p-value
$CD4^+CD25^-$ T cells	6	13,13,13,13,13,13	13	
$CD4^+CD25^-$ T cells + 1B1.2	6	13, 13,13,13,22,22	13	
$CD4^+CD25^-$ T cells + IFN-γ Treg	3	41,>100,>100	>100	*p = 0.2229*
$CD4^+CD25^-$ T cells + IFN-γ Treg + 1B1.2	5	25,25,41,66,>100	41	*p = 0.1701*
$CD4^+CD25^-$ T cells + IFN-γ Treg + isotype	5	66,82,97,>100,>100	97	
$CD4^+CD25^-$ T cells + nTreg	5	82, >100,>100, >100, >100	>100	
$CD4^+CD25^-$ T cells + nTreg + 1B1.2	5	97, >100, >100, >100, >100	>100	

Figure 4.2.2.2.ii. IFN-γ Treg mediated suppression partially dependent on the IL-10-IL-10R pathway *in vivo*. CBA $RAG^{-/-}$ mice reconstituted with $CD4^+CD25^-$ T cells rejected their grafts acutely with a MST of 13 days (n=6). Anti-IL-10R antibody (1B1.2) alone had no significant impact on the rejection mediated by $CD4^+CD25^-$ T cells. IFN-γ Treg prolonged allograft survival long-term with a MST >100 days (n=3). When 1B1.2 was given to CBA $RAG^{-/-}$ mice reconstituted with $CD4^+CD25^-$ T cells plus IFN-γ Treg, 1B1.2 partially reversed the graft protective effect of IFN-γ Treg leading to a shortened MST of 41 days (n=5), however, the difference in graft survival in these group was not statistically significant (p=0.2229). An isotype antibody (anti-rat Ig) did not show any significant impact on IFN-γ Treg function as most of the grafts survived long-term with a MST of 97 days. Similarly, 1B1.2 had no significant impact on the suppressive function of $CD4^+CD25^+$ nTreg. CBA $RAG^{-/-}$ mice reconstituted with $CD4^+CD25^-$ T cells and nTreg accepted their skin allografts long-term (MST>100 days; n=5). Mice that reconstituted with $CD4^+CD25^-$ T cells plus $CD4^+CD25^+$ nTreg were given 1B1.2 and their grafts survived long-term (>100 days; n=5). Log rank tests were used for statistical comparisons. (p<0.05 denotes statistically significant)

4.2.3 IFN-γ Treg suppressed the proliferation of alloreactive effector T cells *in vitro*

A number of studies demonstrated that an *in vitro* proliferation assay could be used as a tool for a quality control to assess the suppressive function of Treg. These studies usually involved stimulators, responders incorporated with a suitable readout, and the regulatory cell population of interest. A soluble or conjugated antibody-based system, or irradiated allogeneic APC were commonly used stimulators. Responders were usually in the form of splenocytes or a specific effector T cell population such as $CD45RB^{hi}$, or $CD4^{+}CD25^{-}$ T cells, which were either labelled with a proliferative dye, ^{3}H thymidine or BrdU. We have elected to use a fluorescent proliferative dye instead of ^{3-}H thymidine or BrdU, in which we could identify the Treg population in the cell mixture by flow cytometry.

The basic experimental set up is illustrated in ***Figure 4.2.3.1***. CBA splenocytes or purified $CD4^{+}CD25^{-}$ T cells were labelled with eFluor 670 before being stimulated with anti-CD3/CD28 antibody-conjugated beads or allogeneic (B6) APC, with or without the addition of Treg. All cells were recovered and the gated $CD4^{+}$TCR-β^{+} or $CD4^{+}CD3^{+}$ population was examined for eFluor 670 dilution history by flow cytometry at a given time point.

Initial studies revealed that $CD4^{+}$ T cells responded rapidly to the polyclonal stimulus and started to divide from day 2. $CD8^{+}$ T cells also responded and started to divide from day 2 onwards, however their division profile was less profound compared to $CD4^{+}$ T cells. A small number of $CD4^{-}$TCR-β^{-} cells also responded and divided from day 4. By day 7, only a small number of $eFluor^{+}CD4^{+}$ T cells remained in culture. At the same time, the optimal concentration of eFluor 670 was determined by a serial titration experiments (1-10μM).

$CD4^+CD25^-$ T cells responded to the polyclonal stimulus rapidly from day 2 onwards when they were stimulated with anti-CD3/CD28 beads at a 1:1 ratio. Further titration experiments confirmed the optimal conditions for a bead-based *in vitro* suppression assay would include a starting population of $5x10^4$ to $1x10^5$ responders, an eFluor 670 dye staining protocol at 5µM to avoid potential toxicity, and an analysis of the division history by flow cytometry no further than day 5.

Figure 4.2.3.1. Anti-CD3/CD28 bead-based *in vitro* suppression assay

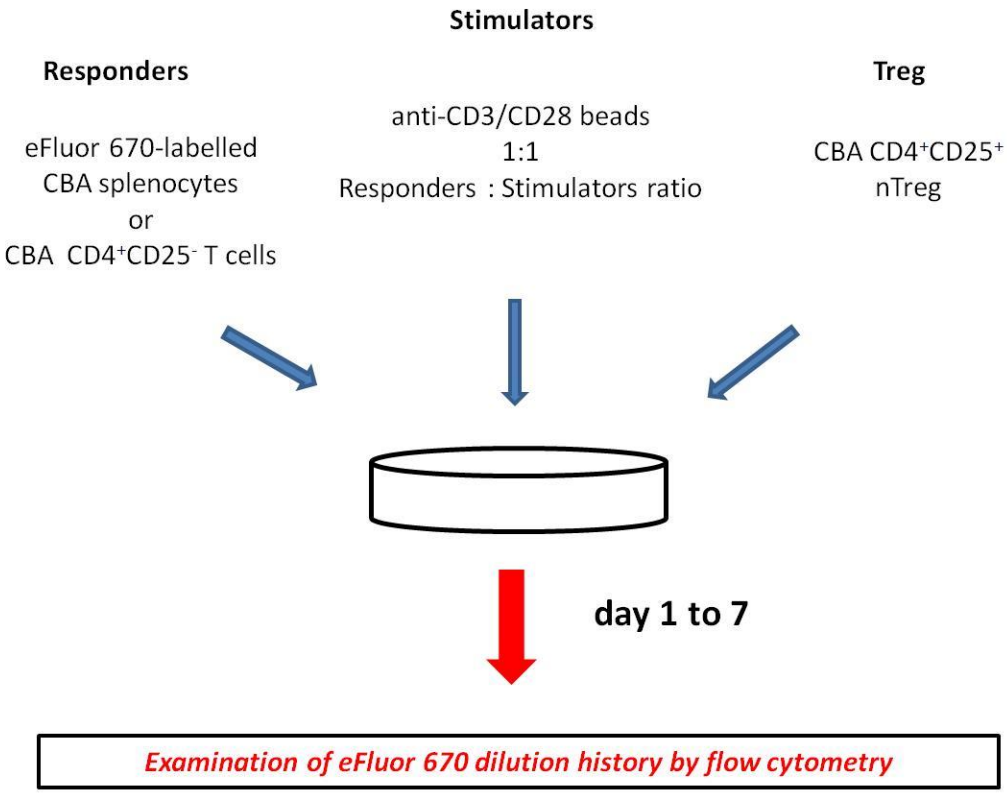

Figure 4.2.3.1. Anti-CD3/CD28 bead-based *in vitro* suppression assay. A defined number of CBA splenocytes or isolated $CD4^+CD25^-$ T cells were used as responders which were labelled with eFluor 670 fluorescent dye before being added to the stimulators in round-bottom 96-well plates. Anti-CD3/CD28 antibody-conjugated beads were used as stimulators at a defined 1:1 Responders : Stimulators ratio. The suppressive function of Treg was deduced from their effect on the proliferation of responders as a function of eFluor 670 dye dilution *in vitro*, in the presence of a defined number of $CD4^+CD25^+$ nTreg. Cells were harvested and examinede by flow cytometry over a period of 1-7 days.

We first used this anti-CD3/CD28 bead-based assay to assess for the suppressive function of $CD4^+CD25^+$ nTreg ***(Figure 4.2.3.2)***. In the control arm of the experiment, dot plot shows the dominant $CD4^+TCR\text{-}\beta^+$ T cells in recovered cells. When these cells were examined for the dilution profile of eFluor 670, there were 6 distinct peaks to suggest that $CD4^+CD25^-$ T cells responded rapidly to polyclonal stimulation provided by anti-CD3/CD28 beads. In clear contrast, in the presence of $CD4^+CD25^+$ nTreg at a 1:1 Treg: Responders ratio, a small peak (*) noted on the far right of the histogram denoted an undivided population and a dampened peaks of dividing cells suggesting that eFluor-stained cells proliferated less vigorously in the presence of nTreg. In ***Figure 4.2.3.3***, we demonstrated that the suppression of polyclonally-stimulated $CD4^+CD25^-$ T cells by $CD4^+CD25^+$ nTreg was dose-dependent, with at least a 1:1 nTreg: $CD4^+CD25^-$ T cells ratio showing effective suppression compared to the Responders+Stimulators controls in 3 independent experiments. However, the main caveat of these initial assays was that although the only $CD4^+CD25^-$ T cells were stained with eFluor 670 dye, we could not gate out the nTreg within the $eFluor^-$ population. The number of responders in the undivided cycle and in each of the first 4 successive division cycles were individually enumerated ***(Figure 4.2.3.2.ii)***. Proliferation indices (PI) were then calculated as shown in ***Chapter 2.13.3***.

Figure 4.2.3.2. $CD4^+CD25^+$ nTreg suppressed proliferation of polyclonally-stimulated $CD4^+CD25^-$ T cells *in vitro*

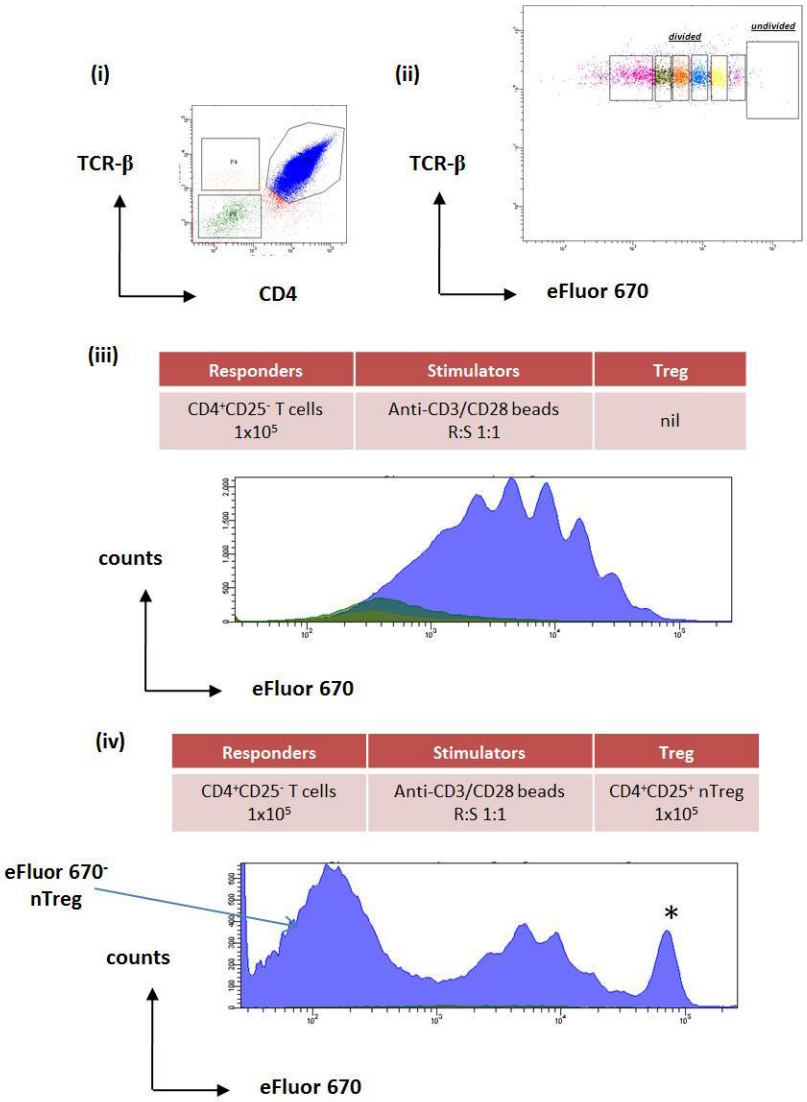

Figure 4.2.3.2. $CD4^+CD25^+$ nTreg suppressed proliferation of polyclonally-stimulated $CD4^+CD25^-$ T cells *in vitro*. **(i)** Dot plot shows the predominant $CD4^+$ T cells in culture after 4 days of incubation. **(ii)** Division history of eFluor 670-labelled $CD4^+CD25^-$ T cells is illustrated in the representative dot plot. **(iii)** Representative histogram demonstrates the initial $CD4^+CD25^-$ population proliferated vigorously in response to anti-CD3/CD28 beads in the absence of Treg. **(iv)** In the presence of $CD4^+CD25^+$ nTreg at a 1:1 Treg: Responders ratio, the proliferative response of $CD4^+CD25^-$ responder cells was attenuated by nTreg as noted by the presence of a clear undivided population (*) and a reduced number of proliferated daughter cells. A large eFluor 670^- population denotes the co-cultured nTreg.

Figure 4.2.3.3. $CD4^+CD25^+$ nTreg suppressed proliferation of polyclonally-stimulated $CD4^+CD25^-$ T cells in a dose-dependent manner *in vitro*

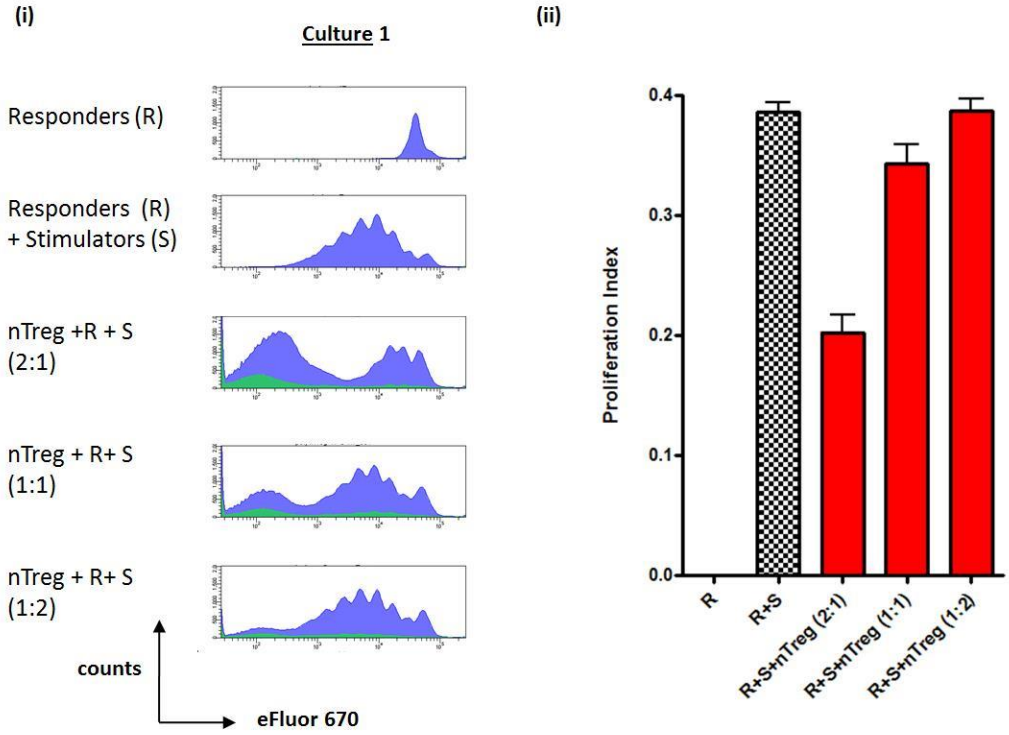

Figure 4.2.3.3. $CD4^+CD25^+$ nTreg suppressed proliferation of polyclonally-stimulated $CD4^+CD25^-$ T cells in a dose-dependent manner *in vitro*. $1x10^5$ $CD4^+CD25^-$ responders were co-cultured with anti-CD3/CD28 beads at a 1:1 ratio with or without $CD4^+CD25^+$ nTreg (GFP/Foxp3 KI CBA) at various (Treg : Responders) ratios for 4 days. **(i)** Histograms obtained from flow cytometry analyses of a representative culture illustrating that $CD4^+CD25^+$ nTreg attenuated the proliferation of $CD4^+CD25^-$ responders in a dose-dependent-manner. These data suggest that a 1:1 nTreg : Responders ratio was required for nTreg to elicit a demonstrable suppressive effect in this *in vitro* setting. The co-cultured nTreg is denoted by the gated population GFP^+ (green) in the histograms. (ii) Bar chart indicates proliferation indices of each culture conditions with respect to positive control (R+S). Negligible proliferation seen in un-stimulated cells (R). Error bars represents 1 S.D. from the mean value in each group.

Next, we investigated the use of alloantigen as stimulators for $CD4^+CD25^-$ T cells in this *in vitro* suppression assay, which was essentially an MLR for our *in vivo* model ***(Figure 4.2.3.4)***. We used B6 bone marrow cells to generate BM-DC driven by GM-CSF (20ng/ml) over 6 days. BM-DC were irradiated before adding into the culture. We individually tested the use of BM cells, BM-DC driven by GM-CSF and poly:IC and BM-DC driven by GM-CSF and LPS in our system. Un-modulated BM cells were not able to elicit any profound stimulatory effects on $CD4^+CD25^-$ T cells (*data not shown*). The number of allogeneic BM-DC required for producing adequate stimulation was pre-determined by titration experiments using between 10:1 and 1:1 Responders: Stimulators ratio. We found that BM-DC driven by GM-CSF alone were satisfactory to serve as stimulators ***(Figure 4.2.3.5)***. BM-DC driven by GM-CSF then matured with either poly:IC or LPS offered no advantages for the readouts as compared to BM-DC driven by GM-CSF alone. The proliferation profiles of $CD4^+CD25^-$ T cells stimulated by allo-BM-DC were different from those using anti-CD3/CD28 beads. Firstly, only alloreactive T cells responded and proliferated leaving a significant number of undivided cells. Second, the proliferation kinetics were slower in this allo-stimulated system compared to that of the bead-stimulated systems, but it appeared that all the alloreactive cells responded at the same time as shown by the single peak started to emerge from day 4 in the proliferative phase of the histograms. Beyond day 6, a significant number of cells underwent further clonal expansion as shown by appearance of a large eFluor 670^- population.

Figure 4.2.3.4. Alloantigen-based *in vitro* suppression assay

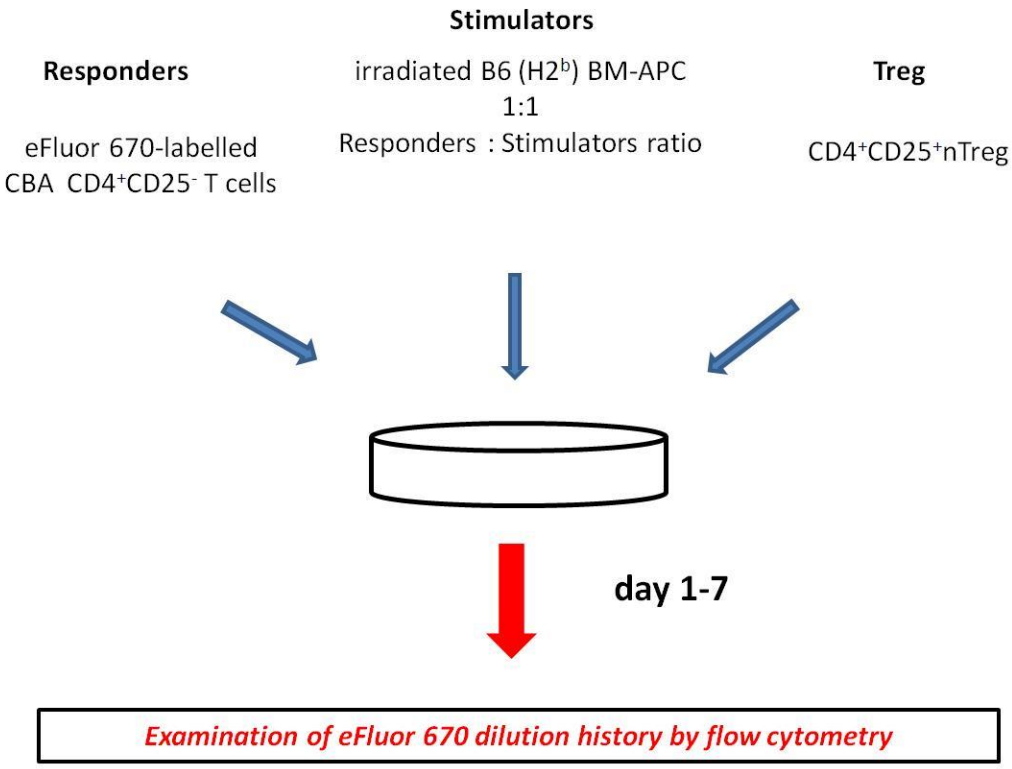

Figure 4.2.3.4. Alloantigen-based *in vitro* suppression assay. A defined number of CBA $CD4^+CD25^-$ T cells were used as responders which were labelled with eFluor 670 fluorescent dye before being added to stimulators in round-bottom 96-well plates. Irradiated allogeneic (B6) BM-APC were used as stimulators at a defined 1:1 Responders : Stimulators ratio. The suppressive function of $CD4^+CD25^+$ nTreg was deduced from their effect on the proliferation of responders as a function of eFluor 670 dye dilution, in the presence of a defined number of $CD4^+CD25^+$ nTreg. Cells were harvested and examined by flow cytometry.

Figure 4.2.3.5. $CD4^+CD25^-$ T cells stimulated by allogeneic BM-APC *in vitro*

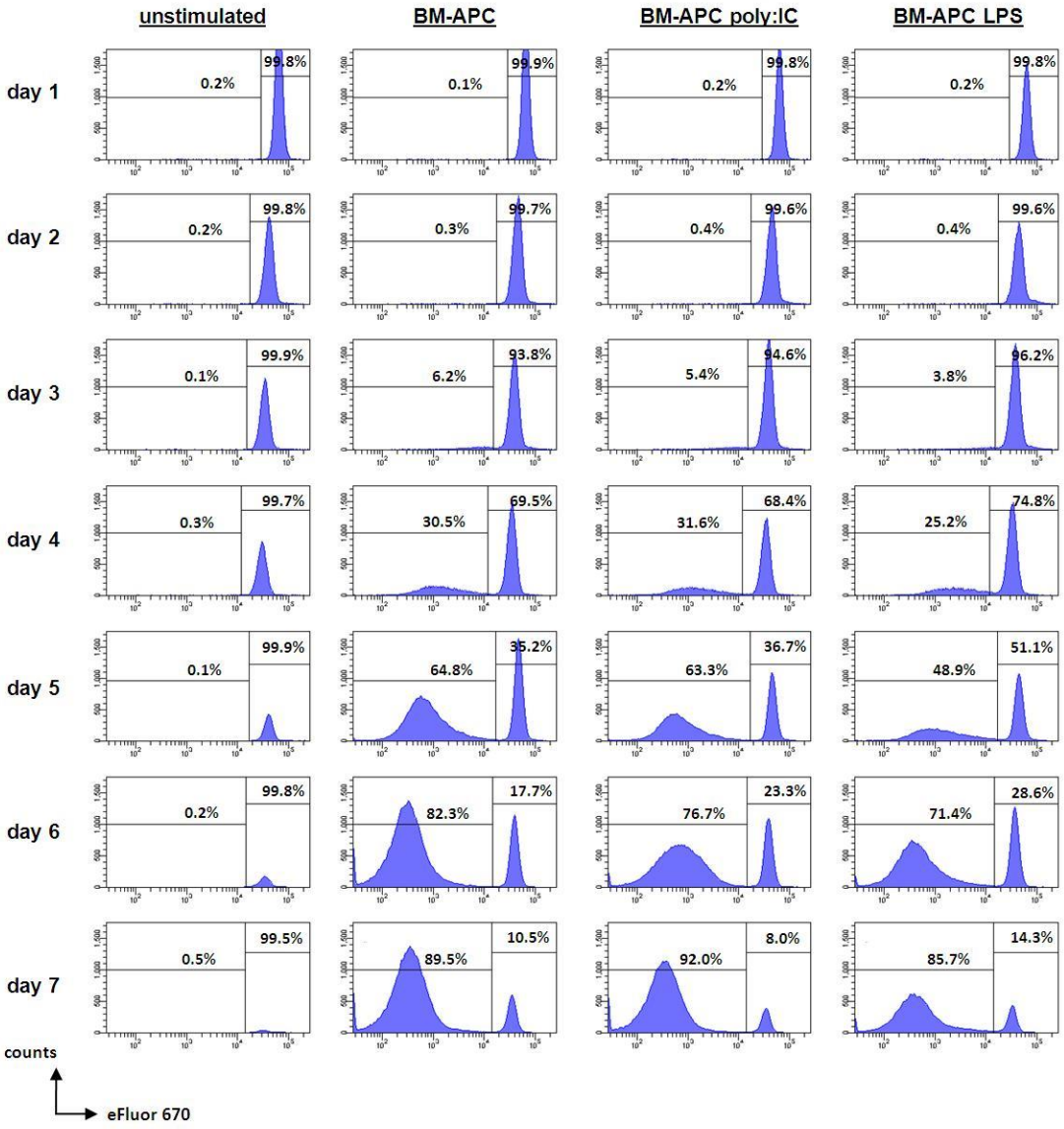

Figure 4.2.3.5. $CD4^+CD25^-$ T cells stimulated by allogeneic BM-APC *in vitro*. B6 BM-APC driven by GM-CSF, BM-APC driven by GM-CSF plus poly:IC, and BM-APC driven by GM-CSF plus LPS were tested as stimulators for the *in vitro* suppression assay. $5x10^4$ eFluor 670 stained CBA $CD4^+CD25^-$ T cells were incubated with $1x10^4$ BM-APC, BM-APC (poly:IC) and BM-APC (LPS) over 7 days, respectively. Un-stimulated responders served as controls in each group demonstrating that unstimulated T cells undergo apoptosis. The proliferation profiles of the responder population were analyzed using flow cytometry. Histograms show the undivided and divided populations in each condition with illustrated percentages. Alloreactive T cells proliferated in response to BM-APC, BM-APC (poly:IC) and BM-APC (LPS) with the optimal readout obtained on day 5.

We then validated this alloantigen-based *in vitro* suppression assay using $CD4^+CD25^+$ nTreg. nTreg obtained from GFP/Foxp3 KI CBA mice were expanded with anti-CD3/CD28 plate-bound antibody *in vitro*, which yielded a dominant 97.9% $Foxp3^+$ Treg population. We tested their suppressive function for the control of $CD4^+CD25^-$ T cells proliferation stimulated by allogeneic BM-DC or anti-CD3/CD28 beads ***(Figure 4.2.3.6.i)***. $5x10^4$ expanded nTreg (GFP^+) ***(Figure 4.2.3.6.ii.a)*** were added to $5x10^4$ eFluor 670-labelled CBA $CD4^+CD25^-$ T cells which were stimulated by $5x10^4$ B6 BM-DC or $5x10^4$ anti-CD3/CD28 beads. Cells were harvested on day 4 for polyclonally-stimulated and day 5 for allogeneic-stimulated assays, respectively. $CD4^+CD25^-$ T cells proliferated in response to allogeneic BM-DC leaving a 59.6% undivided population. In the presence of expanded nTreg, the proliferation was attenuated leaving 89.6% undivided ***(Figure 4.2.3.6.ii.b)***. However, it would not be possible to define the divided population clearly, unless the Treg populations (GFP^+) were gated and removed. The suppressive effect was demonstrated with a mean proliferative index (PI) of 0.077 versus 0.022, in the R+S and the R+S+nTreg group, respectively (p=0.0004) ***(Figure 4.2.3.6.iii.a, left panel)***. This was compared and contrasted with assays using anti-CD3/CD28 beads as stimulators. Aforementioned, all $CD4^+CD25^-$ T cells responded vigorously and divided leaving a very small undivided population (0.7%) in response to the polyclonal stimuli provided by the beads. On the other hand, the proliferation of eFluor-labelled $CD4^+CD25^-$ T cells was hampered by the presence of an equal number of expanded nTreg, which resulted in an undivided population of 22.6% ***(Figure 4.2.3.6.ii.b)***. The suppressive effect was demonstrated with a mean PI of 0.57 versus 0.43, in the R+S and the R+S+nTreg group, respectively (p<0.0001) ***(Figure 4.2.3.6.iii.a, right panel)***.

Figure 4.2.3.6.i. Comparing alloantigen-based versus bead-based *in vitro* suppression assays

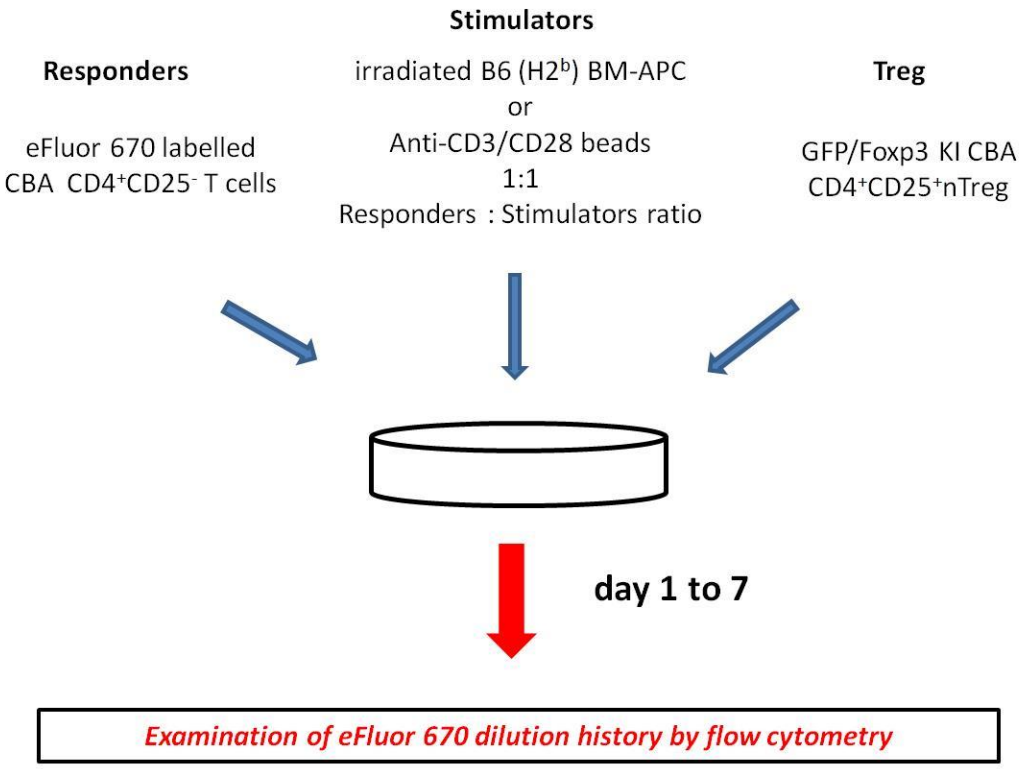

Figure 4.2.3.6.i. Comparing alloantigen-based versus bead-based *in vitro* suppression assays. A defined number of CBA $CD4^+CD25^-$ T cells were used as responders which were labelled with eFluor 670 fluorescent dye before being added to the stimulators in round-bottom 96-well plates. Either irradiated allogeneic (B6) BM-APC or anti-CD3/CD28 antibody conjugated beads were used as stimulators at a defined ratio, typically a 1:1 Responders : Stimulators ratio. The suppressive function of nTreg was then deduced from their effect on the proliferation of responders as a function of eFluor 670 dye dilution history, in the presence of a defined number of Treg. Cells were harvested for the examination by flow cytometry.

Figure 4.2.3.6.ii. Expanded nTreg suppressed proliferation of CD4$^+$CD25$^-$ T cells driven by polyclonal or allogeneic stimuli *in vitro*

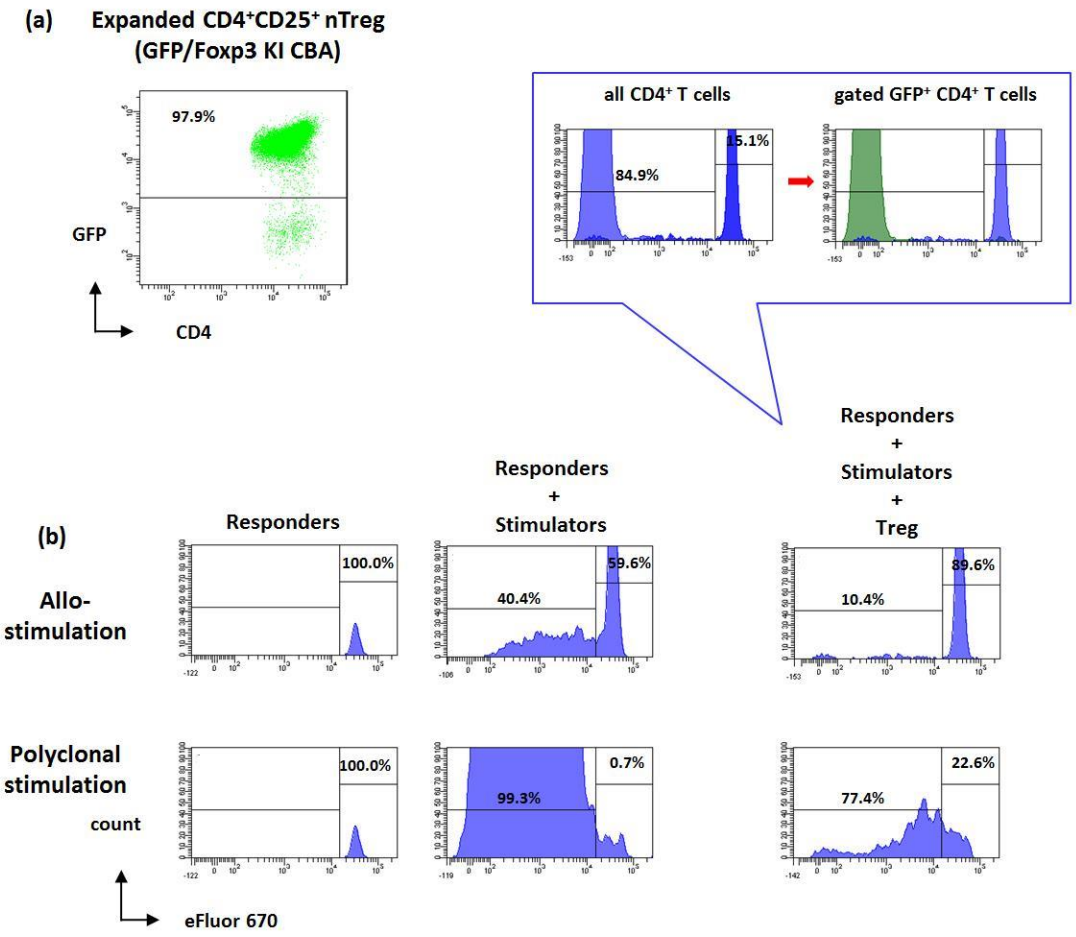

Figure 4.2.3.6.ii. Expanded nTreg suppressed proliferation of CD4$^+$CD25$^-$ T cells driven by polyclonal or allogeneic stimuli *in vitro*. **(a)** CD4$^+$CD25$^+$ nTreg were isolated from GFP/Foxp3 KI CBA mice and expanded *in vitro* using plate-bound anti-CD3/CD28 antibody and IL-2 (see ***Chapter 2.10.3*** for plate-bound nTreg expansion protocol). Expanded nTreg consisted of a purity of 97.9% CD4$^+$GFP$^+$ (Foxp3$^+$) T cells as confirmed by flow cytometry analysis. **(b)** *In vitro* suppression assays using eFluor 670 fluorescent dye dilution as readouts: Expanded nTreg controlled the proliferation of both allo- or polyclonal stimulated CD4$^+$CD25$^-$ responders *in vitro*. In the presence of expanded nTreg, there was a simultaneous increase in the proportion of the undivided population (89.6% from 59.6%) and a decrease in the divided population (10.4% from 40.4%) of the responders in the allo-stimulation assay. In the polyclonal stimulation assays, there was an increase in the proportion of the undivided population (22.6% from 0.7%) and a decease in the divided population (77.4% from 99.3%). GFP$^+$ nTreg were gated out and removed from the eFluor$^-$ 670 population to facilitate the calculation of the divided responder population.

We also validated this assay using expanded nTreg with another fluorescent dye which produced similar results. PKH26 red fluorescent dye staining protocol was optimized prior to its use in this assay ***(Figure 4.2.3.6.ii.c)***. $5x10^4$ CBA $CD4^+CD25^-$ T cells were labelled with 2μM PKH26. $5x10^4$ B6 BM-DC or $5x10^4$ anti-CD3/CD28 beads were added in the culture as simulators. PKH26-labelled $CD4^+CD25^-$ T cells responded to allogeneic BM-DC stimulation resulting in an undivided population of 54.9%. In the presence of nTreg, the proliferation was attenuated leaving 87.2% undivided. The suppressive effect was shown with a mean PI of 0.13 versus 0.04 in the R+S and the R+S+nTreg group, respectively (p<0.0001) ***(Figure 4.2.3.6.iii.b, left panel)***. Similarly, $CD4^+CD25^-$ T cells responded vigorously to polyclonal stimulation leaving a 2.6% undivided population ***(Figure 4.2.3.6.ii.c)***. Expanded nTreg attuated the proliferation of PKH26-labelled $CD4^+CD25^-$ T cells resulted in a 44.1% undivided population. This suppressive effect was shown by the mean PI of 0.44 versus 0.29 in the R+S and the R+S+nTreg group, respectively (p=0.0001) ***(Figure 4.2.3.6.iii.b, right panel)***. Of note, there was no evidence of further expansion of nTreg in culture by examining the GFP^+ population in culture over a total 7 days in either the allo- or polyclonally-stimulated systems *(data not shown)*.

Figure 4.2.3.6.ii. PKH26 was a permissible alternative proliferation dye used in the bead- or alloantigen-based *in vitro* suppression assays

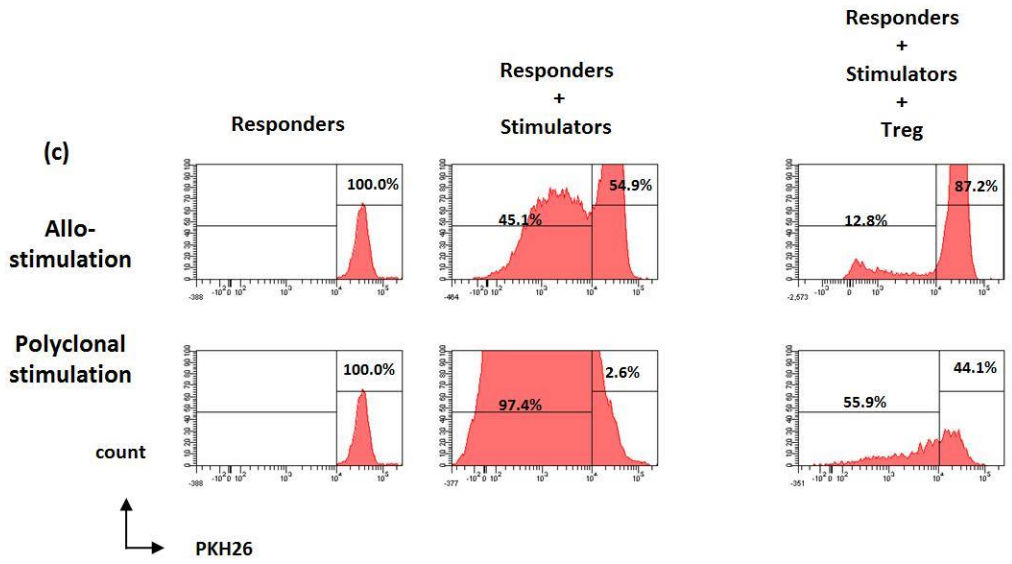

Figure 4.2.3.6.ii. PKH26 was a permissible alternative proliferation dye used in the bead- or alloantigen-based *in vitro* suppression assays. An alternative fluorescent dye was used to test for its applicability in these *in vitro* suppression assays. **(c)** *in vitro* suppression assays using PKH26 fluorescent dye dilution as readouts: Expanded nTreg controlled the proliferation of both allo- or polyclonal stimulated $CD4^{+}CD25^{-}$ responders *in vitro*. In the presence of expanded nTreg, there was a simultaneous increase in the proportion of the undivided population (87.2% from 55.9%) and a decrease in the divided population (12.8% from 45.1%) of the responders in the allo-stimulation assay. In the polyclonal stimulation assays, there was an increase in the proportion of the undivided population (44.1% from 2.6%) and a decease in the divided population (55.9% from 97.4%). GFP^{+} nTreg were gated out using the gating strategy shown for the calculation of the true divided responder population. Data above represent at 2 independent experiments.

Figure 4.2.3.6.iii. Expanded nTreg suppressed proliferation of CD4$^+$CD25$^-$ T cells driven by allogeneic or polyclonal stimuli *in vitro*

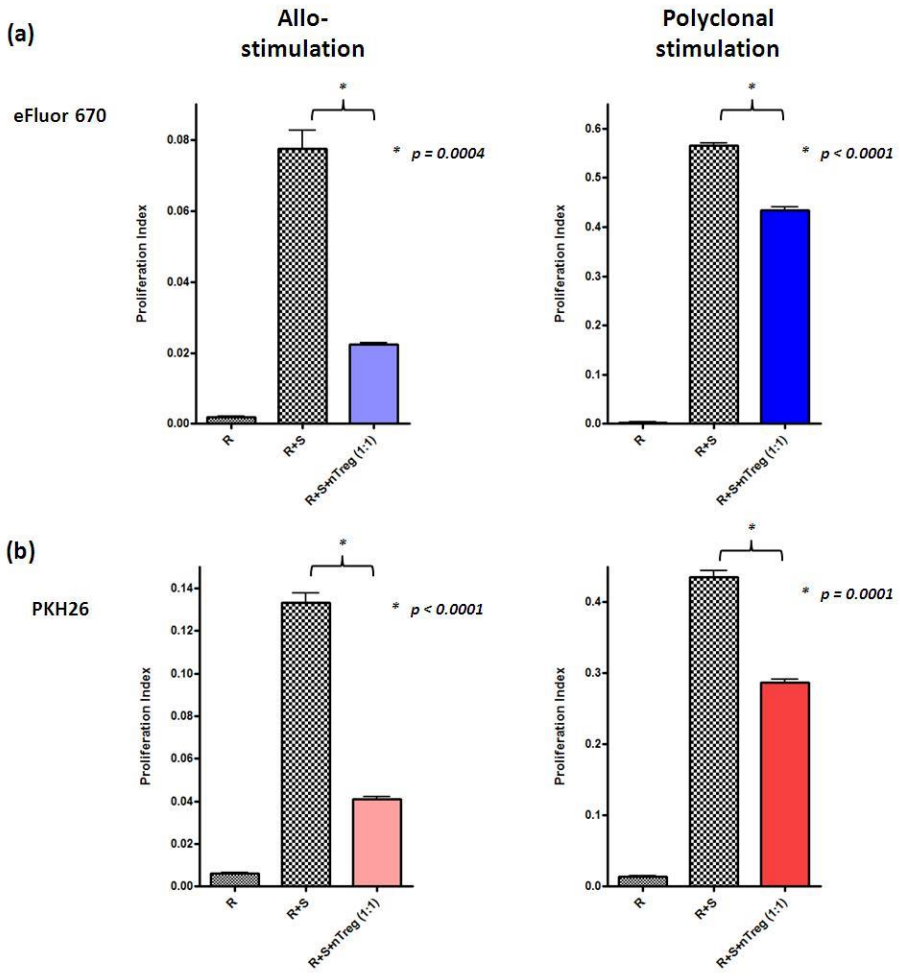

Figure 4.2.3.6.iii. Expanded nTreg suppressed proliferation of CD4$^+$CD25$^-$ T cells driven by allogeneic or polyclonal stimuli *in vitro*. (a) *In vitro* suppression assays using ***eFluor 670*** fluorescent dye dilution as readouts: Expanded nTreg controlled the proliferation of both allogeneic or polyclonally-stimulated CD4$^+$CD25$^-$ responders *in vitro* at a 1:1 nTreg to responders ratio. Bar charts show the calculated proliferation indices (PI) from each group with reference to the positive control (R+S). In the presence of expanded nTreg, the mean PI for eFluor 670-labelled responders decreased from 0.077 to 0.022 in the allogeneic-stimulated (p=0.0004) and 0.57 to 0.43 (p<0.0001) in the polyclonally-stimulated group, respectively. **(b)** We also tested the use of ***PKH26*** in the same experiment demonstrating that expanded nTreg controlled the proliferation of responders resulting in a decrease of the mean PI from 0.13 to 0.04 (p<0.0001) and 0.44 to 0.29 (p=0.0001) in the allogeneic- and polyclonally-stimulated group, respectively. PI were calculated as described in ***Chapter 2.13.3***. Data above represent means of 3 replicates with error bars showing 1 S.D. from the mean values. Student's t-tests were used for statistical comparisons. (p<0.05 denotes statistically significant)

In order to test the suppressive function of IFN-γ Treg in this assay, we opted to use a combination of eFluor 670 and PKH26 fluorescent dyes to stain two different populations, as well as using GFP/Foxp3 KI CD4 precursors for the generation of IFN-γ Treg ***(Figure 4.2.3.7)***. IFN-γ Treg were harvested and examined for their Foxp3 and GFP expression prior to the study. The IFN-γ conditioning protocol led to an enriched $Foxp3^+$ population up to 35.6%. Amongst the 35.6% $Foxp3^+$ $CD4^+$ T cells, 12.8% and 22.8% were GFP^- and GFP^+, respectively. In order to track all cells from the Treg group including the GFP^-Foxp3^+, as well as the GFP^-Foxp3^- population, IFN-γ Treg were labelled with eFluor670. On the other hand, CBA $CD4^+CD25^-$ T cell responders were labelled with PKH26. $5x10^4$ PKH26-labelled $CD4^+CD25^-$ T cell responders were stimulated with $5x10^4$ irradiated B6 BM-DC driven by GM-CSF. Titrated number of eFluor 670-labelled IFN-γ Treg were added to the culture mix with a range of Treg: Responder ratio from 2:1 to 1:32. The fluorescent dye dilution profiles were examined by flow cytometry after 5 days. A gating strategy was used such that all GFP^+ and eFluor 670^+ cells were excluded from the $PKH26^-$ population leaving the surrogate $PKH26^+$ divided population ***(Figure 4.2.3.8)***. The number of PKH26-labelled $CD4^+CD25^-$ T cells responding to alloantigen stimulation was 17.6 $x10^3$ cells (R+S). Addition of IFN-γ Treg at a 2:1 ratio led to 50% reduction in proliferation of responding $CD4^+CD25^-$ T cells (8.8 $x10^3$ cells, p=0.0007). As the number of IFN-γ Treg was reduced in the culture, the number of divided PKH-labelled responders increased and reached a similar level to that of the control when the ratio of Treg : Responders was 1:1 and beyond and paradoxically a significant increased in number when the ratio was beyond 1:4 ($38.2x10^3$ cells; p=0.011) ***(Figure 4.2.3.8.i)***. Similarly, the proliferative indices was significantly reduced when the ratio of Treg : Responders was 2:1 compared to the R+S control (PI=0.031 versus PI=0.054; p=0.0019). Paradoxically, the proliferation of PKH26-labelled cells was significantly increased when the ratio of Treg: Responders was beyond 1:4 (PI=0.09; p=0.001) ***(Figure 4.2.3.8.ii)***. These data suggest

that IFN-γ Treg were only able to control the proliferation of naïve $CD4^+CD25^-$ T cells *in vitro* at a ratio of at at least 2:1. The paradoxically enhanced proliferative profile of the naïve $CD4^+CD25^-$ responders beyond the control in which the ratio of Treg : Responder was less than 1:4 was an unexpected finding. It might be explained by provison of cytokines released from the non-Treg cohort within the IFN-γ Treg population upon reactivation *in vitro*.

Figure 4.2.3.7. The development of an *in vitro* suppression assay to assess IFN-γ Treg function

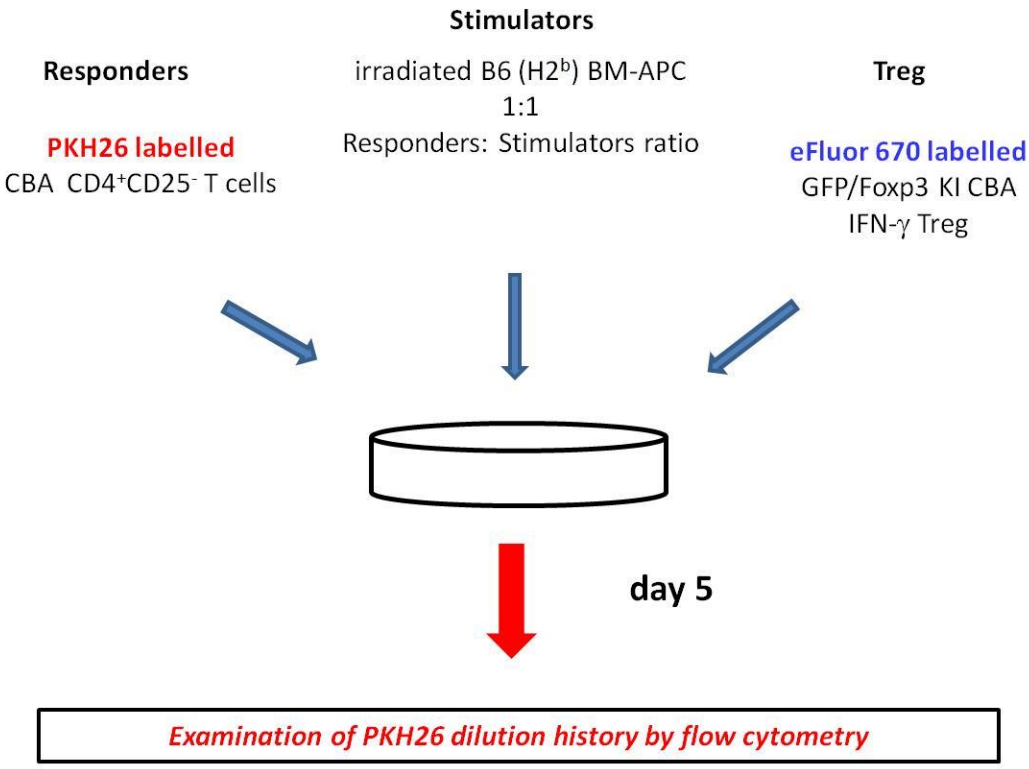

Figure 4.2.3.7. The development of an *in vitro* suppression assay to assess IFN-γ Treg function. A defined number of CBA $CD4^+CD25^-$ T cells were used as responders which were labelled with PKH26 fluorescent dye before being added to the stimulators in round-bottom 96-well plates. Irradiated allogeneic (B6) BM-APC were used as stimulators at a 1:1 Responders : Stimulators ratio. The suppressive function of IFN-γ Treg was then deduced from their effect on the proliferation of responders as a function of PKH26 dye dilution of the eFluor 670^-GFP^- population, in the presence of a defined number of IFN-γ Treg. After 5 days, cells were harvested and examined by flow cytometry.

Figure 4.2.3.8. IFN-γ Treg controlled proliferation of alloantigen-stimulated CD4⁺CD25⁻ T cells in a dose-dependent manner *in vitro*

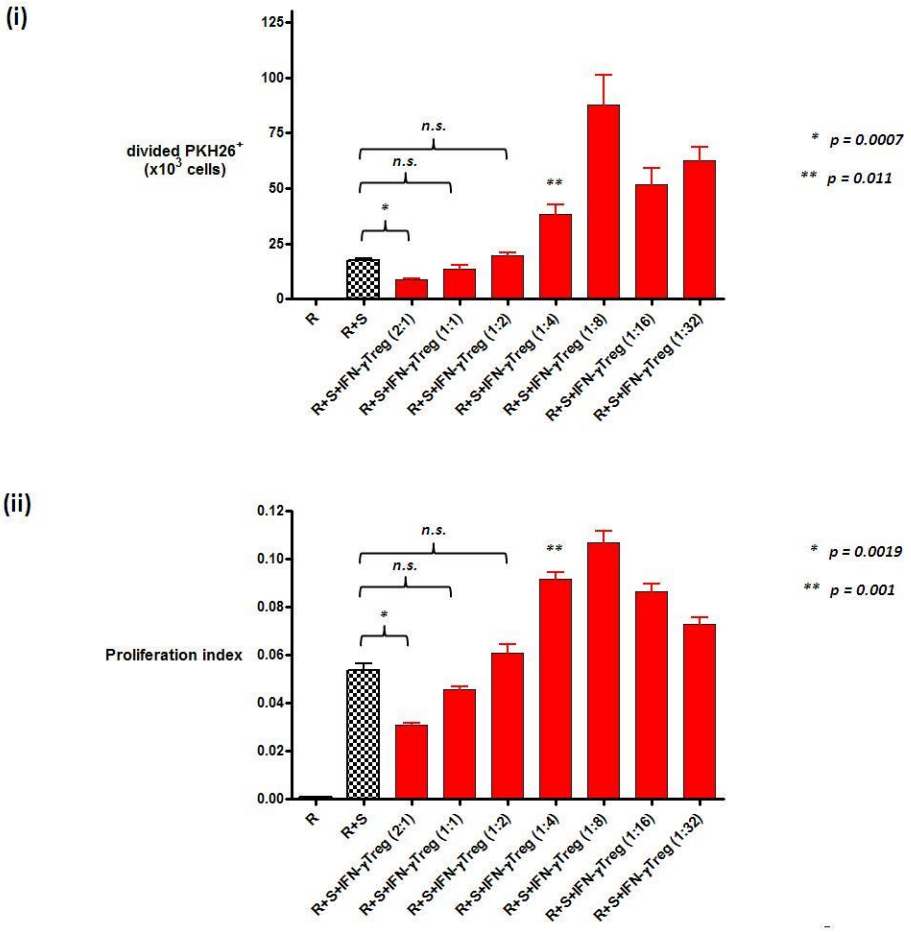

Figure 4.2.3.8. IFN-γ Treg controlled proliferation of alloantigen-stimulated CD4⁺CD25⁻ T cells in a dose-dependent manner *in vitro*. PKH26-labelled CD4⁺CD25⁻ T cell responders were stimulated with B6 BM-APC *in vitro* for 5 days with or without a graded number of eFluor 670-labelled IFN-γ Treg that were generated from GFP/Foxp3 KI CBA splenocytes. The percentages and number of cells in the divided population (efluor 670⁻ GFP⁻) from each condition was compared to that of the Responders + Stimulators control (R+S). **(i)** In the presence of IFN-γ Treg at a 2:1 ratio, there was significant suppression of the proliferation of the responders when compared to the control (8.8 versus 17.6 x10^3 cells; p=0.0007). The number of divided cells were paradoxically greater than the control at low Treg: Responder ratios possibly due to the presence of the Foxp3⁻ cohort within the IFN-γ Treg population which was previously stimulated with alloantigen. (ii) Similarly, the proliferation indices (PI) were significantly lower when the Treg : Responder ratio was 2:1 compared to the control (PI=0.031 versus 0.054; p=0.0019). PI were calculated as described in ***Chapter 2.13.3***. Data above represent replicates of 3 in each condition with error bars showing 1 S.D. from the mean values. Student's t-tests were used for statistical comparisons. ($p<0.05$ denotes statistically significant)

4.2.4 Persistence of infused IFN-γ Treg was essential to maintain dominant suppression via infectious tolerance

We hypothesized that recipients receiving Treg therapy have an altered Treg composition, which contributed to long-term acceptance of allografts ***(Chapter 3.2.5, Figure 3.2.5.1)***. We anticipated that there could be a higher percentage and/or number of $Foxp3^+$ T cells in tolerant animals compared to naive mice, especially in the draining lymphoid tissues. Therefore, we gave CBA $RAG^{-/-}$ mice $1x10^5$ naive $CD4^+CD25^-$ T cells and $1x10^5$ IFN-γ Treg one day before the transplant of a B6 skin allograft, in which we knew that this protocol controlled allograft rejection in this model (cross ref). All recipients accepted their allografts long-term and their lymphoid tissues were harvested on day 100 at steady state. Flow cytometry analysis showed that the mean proportion of $Foxp3^+$ T cells were 11.6% and 10.3% in the draining lymph nodes (dLN) and contra-lateral lymph nodes (cLN), respectively ***(Figure 4.2.4.1)***. The relative number of $Foxp3^+$ T cells was higher in the dLN ($27.0x10^3$) compared to the cLN ($13.2x10^3$), respectively; however these differences did not reach statistical significance. The $Foxp3^+$ population could be derived from clonal expansion of IFN-γ Treg or they could be derived from the conversion of $CD4^+CD25^-$ T cells *in vivo*. The findings observed above could also be explained by homeostatic proliferation of adoptively transferred T cells since the percentage of Treg in these recipients approximate to naive mice (8-10% $Foxp3^+$). Additional experiments that could demonstrate the conversion of $CD25^-$ to $Foxp3^+$ T cells would be able to explain this phenomenon. For instance, we could use congenic labelled CBA effector cells with additional unlabelled GFP^+ cells used in this model. However, the influence of homeostatic proliferation on the number of Treg could not be neglected.

Figure 4.2.4.1. Proportion and number of Treg remained similar in the draining versus contralateral lymph nodes in tolerized skin allograft recipients

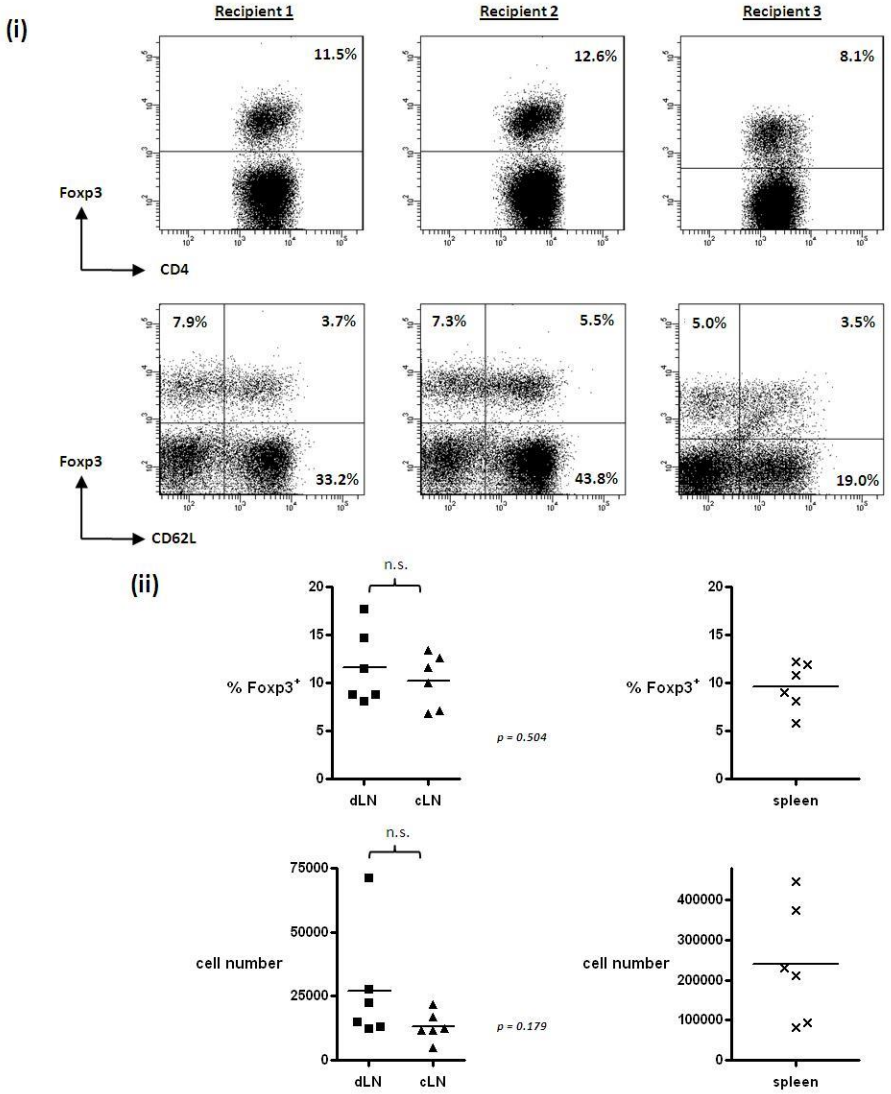

Figure 4.2.4.1. Proportion and number of Treg remained similar in the draining versus contralateral lymph nodes in tolerized skin allograft recipients. CBA RAG$^{-/-}$ mice received 1x10^5 CD4$^+$CD25$^-$ T cells and 1x10^5 IFN-γ Treg one day before the transplant of a B6 skin allograft. All recipients accepted their grafts long-term and their lymphoid tissues were harvested on day 100. **(i)** Splenic T cells obtained from 3 tolerant mice after 100 days. Dot plots indicate that up to 12.6% of total splenic CD4$^+$ population express Foxp3. However, only a small proportion co-express Foxp3 and CD62L (3-6%). **(ii)** Percentage and number of Foxp3$^+$ T cells in the draining lymph nodes (dLN), contra-lateral lymph nodes (cLN) and the spleen obtained from tolerized recipients are shown. The mean percentage and the mean number of Foxp3$^+$ T cells were not statistically different between dLN and cLN (n=6 per group; p= 0.504 and p= 0.179 respectively). Unpaired t tests were used for statistical comparisons. (p<0.05 denotes statistically significant)

On the other hand, immunocompetent CBA mice which accepted B6 heart grafts long-term following the combination of a sub-optimal regimen of abatacept and IFN-γ Treg treatment possessed a slightly higher proportion of $Foxp3^+$ T cells in the spleen on day 100 compared to their naive state ***(Figure 4.2.4.2)***. The average percentages of $Foxp3^+$ T cells in the spleen in those received $5x10^5$, $2x10^6$ and $4x10^6$ IFN-γ Treg were 11.8%, 10.0%, 11.5%, respectively. Whether such a disparity of the proportion of $Foxp3^+$ T cells between naive and tolerant states correlates with their immunosuppressive function remains difficult to dissect. It was impossible to determine how many donor alloantigen-reactive Treg were present within such population, although our laboratory recently described a new bioimaging technique to visualize the immune synapse between polyclonal T cells and allogeneic APC, which might provide an *in vitro* platform for the quantification of alloreactivity[470,471]. With an indirect inference, we then opted to investigate if the function of infused Treg persists in these tolerized animals and if the tolerant state of these allografts could be reversed by additional effector T cells, with or without a new alloantigen challenge.

Figure 4.2.4.2. Treg therapy increased the frequency of Foxp3$^+$ T cells in tolerized immunocompetent recipients compared to their naïve states

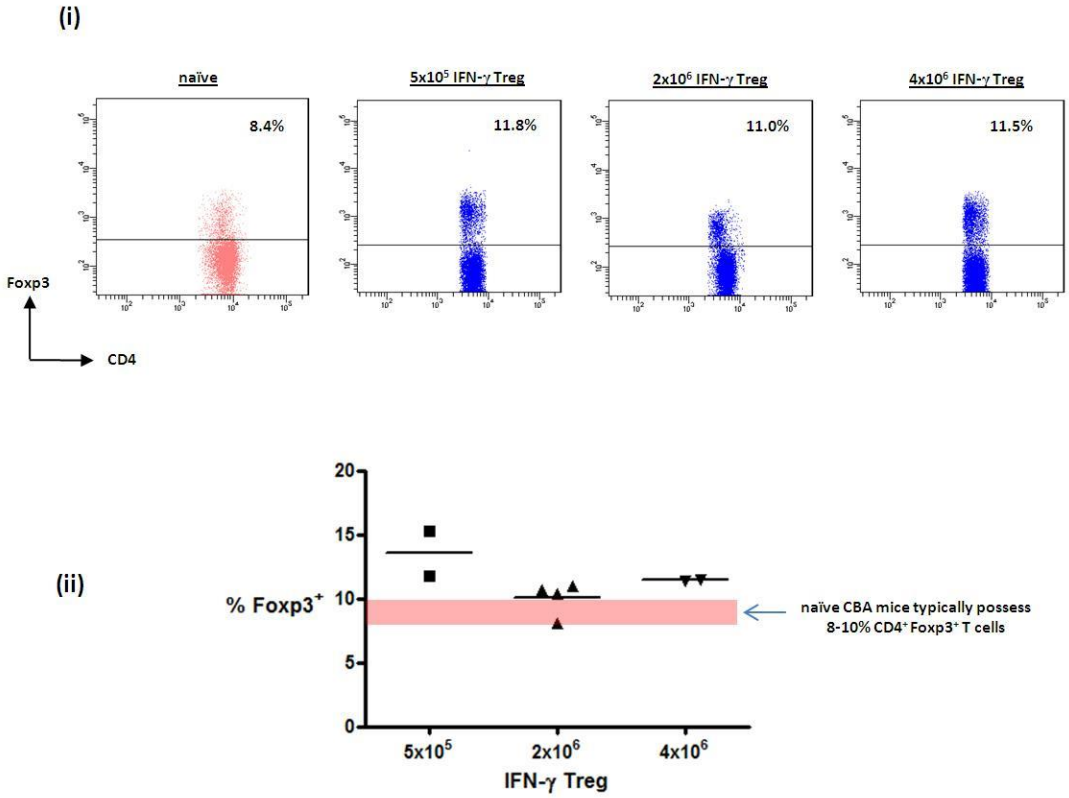

Figure 4.2.4.2. Treg therapy increased the frequency of Foxp3$^+$ T cells in tolerized immunocompetent recipients compared to their naïve states. CBA mice received 5x10^5, 2x10^6 or 4x10^6 IFN-γ Treg one day before the transplant of a B6 heart allograft in addition to abatacept (i.v. 25μg on day 0, 1 and 5). All recipients accepted their allografts long-term and their spleens were harvested on day 100. **(i)** Representative dot plots show the expression of Foxp3 on splenic T cells obtained from: tolerized mice receiving 5x10^5 (11.8%) , 2x10^6 (11.0%) and 4x10^6 (11.5%) IFN-γ Treg compared to splenic T cells from naïve CBA mice (8.4%). **(ii)** The mean percentage of Foxp3$^+$ T cells in the spleen of tolerant mice appeared to be slightly elevated compared to a naïve mice when they were given 5x10^5 (13.6%; n=2), 2x10^6 (10.0%; n=4) and 4x10^6 (11.45%; n=2) IFN-γ Treg.

We examined the functional aspect of endogenous Treg in tolerant animals using a pilot experiment. We asked if accepted allografts would be rejected if they were re-challenged in reconstituted recipients. A second skin graft of the same strain combination (B6 to CBA) was transplanted in these recipients prior to the infusion of new effectors to serve as an internal control to demonstrate that these recipients were able to reject allografts of the same strain when tolerance was broken in the form of a recall challenge. As shown in ***Figure 4.2.4.3.i***, a group of CBA $RAG^{-/-}$ mice reconstituted with $1x10^5$ naïve $CD4^+CD25^-$ T cells and $2x10^5$ IFN-γ Treg that accepted their B6 skin allografts long-term (100 days) were recruited in this study. This group of mice with long-term graft survival (LTS) was split into 2 groups: 1) ***LTS (WT IFN-γ Treg) Group 1*** were given $1x10^5$ $CD4^+GFP^-$ T cells (obtained from GFP/Foxp3 KI CBA splenocytes) as an effector population; 2) ***LTS (WT IFN-γ Treg) Group 2*** were given $1x10^5$ $CD4^+GFP^-$ T cells as well as a new second B6 skin allograft on the contralateral flank. The introduction of $CD4^+GFP^-$ T cells had no effect on the old skin allografts and these grafts remained accepted for >40 days, n=3 ***(Figure 4.2.4.3.ii)***. These findings were not suprising as the introduction of a relative small number of naïve $CD4^+CD25^-$ T cells in these reconstituted recipients might not have any significant impact on graft outcome. In the presence of both new effectors and a new skin allograft, 3 out of 4 old skin allografts remained unchanged >40 days except one which was rejected acutely (20 days) ***(Figure 4.2.4.3.ii)***. When a second alloantigen challenge was deliverered in the form of a skin graft, a break of tolerance was seen in 1 out of 4 recipients leading to the acute loss of the old graft which was previously accepted long-term. However, given the small sample size in these groups, repeat experiments would be necessary to affirm these observations. On the other hand, all second skin allografts were rejected acutely with a MST of 10 days ***(Figure 4.2.4.3.ii)***. Rejection of all second skin allografts ascertain that these long-term recipients were fully immunocompetent to reject tissues obtained from the same

donor strain. The accelerated rejection tempo of the second skin allografts (MST =10 days) in these reconstituted recipients were similar to that of wide-type CBA mice rejecting a B6 skin allografts *(data not shown)*. These observations could be explained by a recall response in the form of a second challenge and endogenous Treg might not be able to suppress a recall response. However, the data above in this set of experiments were not able to show why the majority of the old allografts remained intact. One of the possible reasons could be that of the infused IFN-γ Treg could only maintain local control in the tolerant allograft, but not a recall response by means of a second skin allograft which delivered additional donor APC via the direct pathway. It might also be explained by the presence of tissue-resident alloreactive Treg. We attempted to assess the phenotype and the number of graft-infiltrating cells in these recipients. However, we were not able to accurately identify these cells *(data not shown)*. This speculation would require validation. A possible solution to that would be the use of a labelled cells or the use of congenic marker that could be tracked using *in vivo* imaging across a longitudinal study.

Figure 4.2.4.3. Infused IFN-γ Treg maintained long-term local control of tolerized allograft upon secondary challenge

(i)

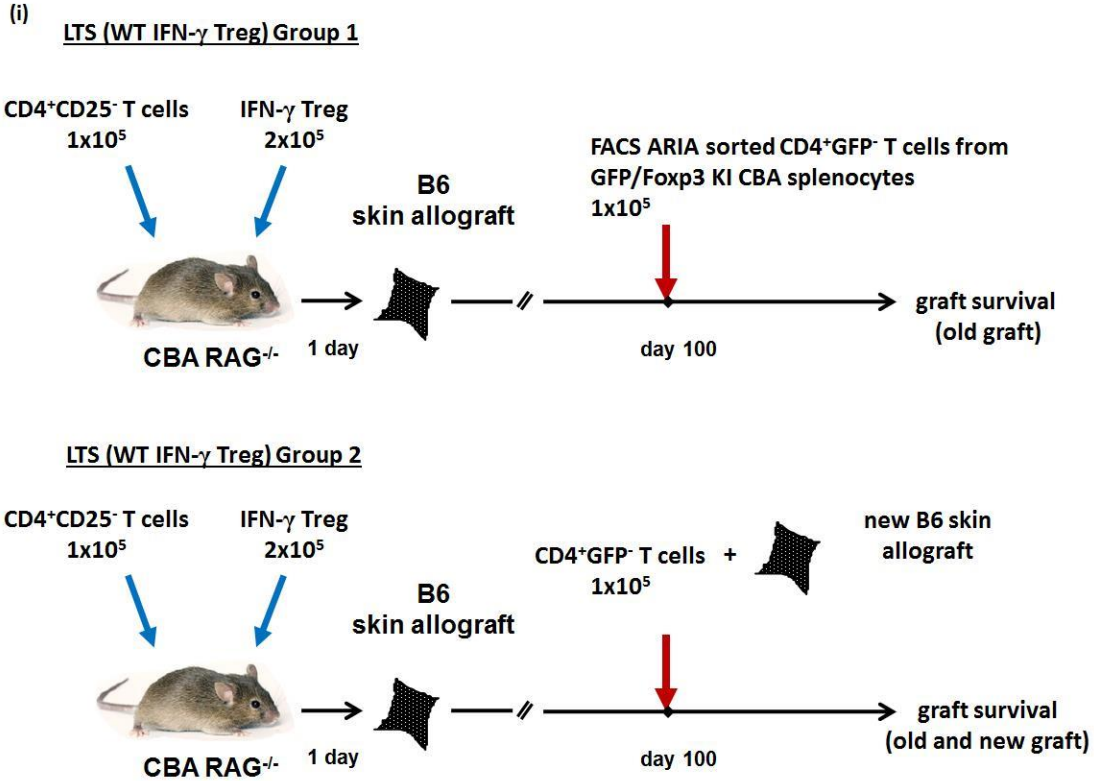

Figure 4.2.4.3.i Infused IFN-γ Treg maintained long-term local control of tolerized allograft upon secondary challenge. Schematic diagram illustrates the experimental set up. Two groups of CBA RAG$^{-/-}$ mice were reconstituted with 1x10^5 naïve CD4$^+$CD25$^-$ T cells and 2x10^5 IFN-γ Treg one day before the transplant of a B6 skin allograft. All skin allografts were accepted long-term, compatible with historical data when 2x10^5 IFN-γ Treg were co-transferred with 1x10^5 CD4$^+$CD25$^-$ effectors (see ***Chapter 3.2.2***). On day 100, this group of mice were split into two groups: 1) **LTS (WT IFN-γ Treg) Group 1** mice received new effectors (1x10^5 naïve CD4$^+$GFP$^-$ T cells isolated from GFP/Foxp3 KI CBA splenocytes by FACS sorting); 2) **LTS (WT IFN-γ Treg) Group 2** mice received new effectors plus a new B6 skin allograft transplanted on the contralateral flank. Graft survival of the 'old graft' in **LTS (WT IFN-γ Treg) group 1** and 'old graft 'and 'new graft' in LTS **(WT IFN-γ Treg) Group 2** were monitored over time.

Figure 4.2.4.3. Infused IFN-γ Treg maintained long-term local control of tolerized allograft upon secondary challenge

(ii)

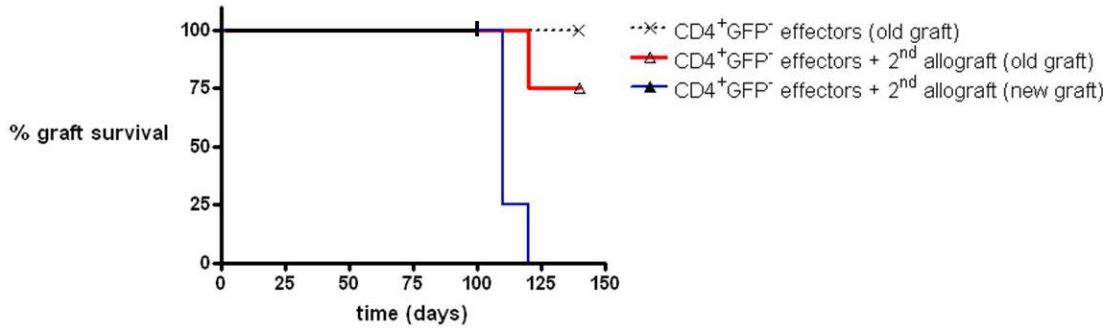

Group	n	graft survival (days)	MST (days)	p-value
LTS (WT IFN-γ Treg) Group 1 + $CD4^+GFP^-$ effectors (old graft)	3	>140, >140, >140	>140	*p = 0.3865*
LTS (WT IFN-γ Treg) Group 2 + $CD4^+GFP^-$ effectors + 2nd graft (old graft)	4	120, >140, >140, >140	>140	
LTS (WT IFN-γ Treg) Group 2 + $CD4^+GFP^-$ effectors + 2nd graft (new graft)	4	10,10,10,20	10	

Figure 4.2.4.3. (ii) Infused IFN-γ Treg maintained long-term local control of tolerized allograft upon secondary challenge. All old skin allografts in **LTS (WT IFN-γ Treg) Group 1** mice that received a new set of effectors ($1x10^5$ $CD4^+GFP^-$) alone remained unchanged for at least another 40 days (n=3). In the **LTS (WT IFN-γ Treg) Group 2** mice that received a new set of effectors as well as a new B6 allograft, there were no changes in the majority of the old grafts (MST >140 days; n=4), but all new allografts transplanted on day 100 were rejected acutely with a MST of 10 days (10-20 days; n=4). These pilot data suggest that the tolerant state enabled the local control against rejection of the old allografts upon new challenge. However, it was not able to suppress a recall response against newly transplanted allografts. Log rank tests were used for statistical comparisons. ($p<0.05$ denotes statistically significant)

We then hypothesized that tolerance was chiefly maintained by the persistence of infused Treg. Thus, tolerance would be broken if infused Treg were subsequently depleted *in vivo*. In the absence of a congenic marker in the recipient mouse strain that we used, we exploited the use of CP-1 mice of the same $H2^k$ allele as CBA mice, but constitutively expressed human CD52 (hCD52) on all leukocytes ***(Figure 4.2.4.4.i)***. IFN-γ Treg generated with CP-1 $CD4^+$precursors could then be depleted selectively using anti-hCD52 antibody (alemtuzumab –CAMPATH-1H) *in vivo*. The end-products of the IFN-γ conditioning protocol using CP-1 $CD4^+$ precursors were consistent to produce a highly-enriched $Foxp3^+$ T cells population (62.3%) ***(Figure 4.2.4.4.ii)***. A titrated regimen of alemtuzumab for complete lymphodepletion in CP-1 mice was previously determined (*data not shown*). A single dose of 100μg alemtuzumab given intra-peritoneally was sufficient for complete depletion ***(Figure 4.2.4.5)***.

Figure 4.2.4.4. Exploiting hCD52-expressing CP-1 CD4⁺ T cells to generate IFN-γ Treg

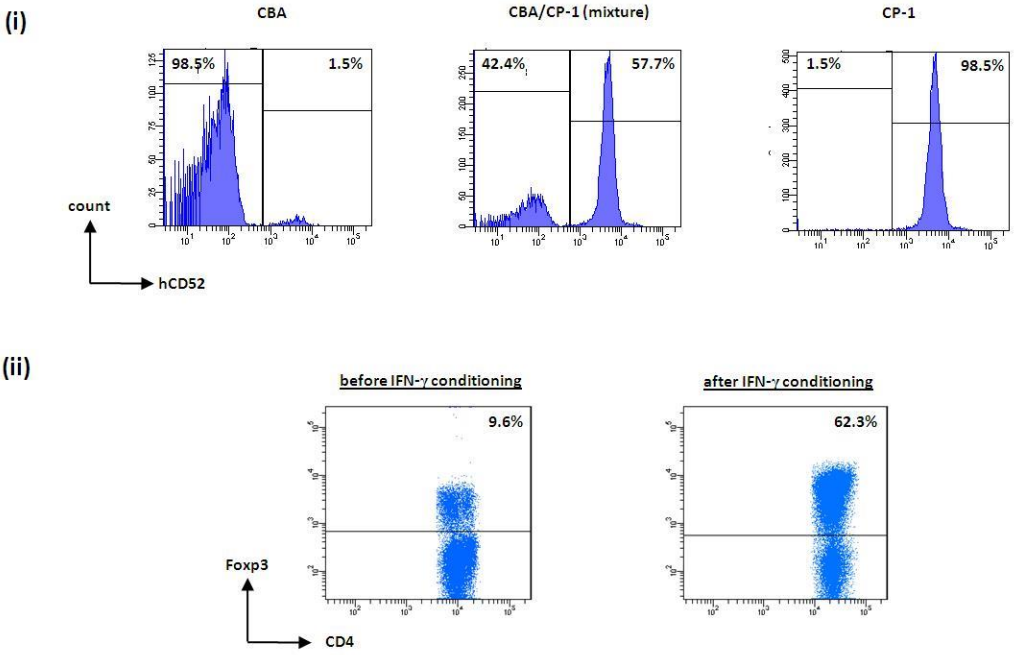

Figure 4.2.4.4. Exploiting hCD52-expressing CP-1 CD4⁺ T cells to generate IFN-γ Treg.
(i) The expression of hCD52 was tested using splenocytes from CBA ($H2^k$) and CP-1 ($H2^k$). CBA splenocytes do not express hCD52. In a mixture of CBA and CP-1 splenocytes a separate $hCD52^+$ and $hCD52^-$ population was demonstrated. CP-1 mice constitutively express hCD52 on all their leukocytes (gated on $CD4^+TCR\text{-}\beta^+$ T cells). **(ii)** The expression of Foxp3 on CP-1 $CD4^+$ T cells was compared to that of CBA $CD4^+$ T cells after allogeneic APC stimulation and IFN-γ conditioning for 14 days *in vitro*. CP-1 $CD4^+$ T cells were isolated by MACS and stimulated with 2 rounds of B6 BM-APC in the presence of IFN-γ, for the generation of CP-1 IFN-γ Treg. Representative dot plots show the initial Foxp3 expression on CP-1 $CD4^+$ precursors (9.6%) and the resultant Foxp3 enrichment (62.3%). These data were compatible with the Foxp3 expression on resultant IFN-γ Treg generated with CBA $CD4^+$ precursors ***(Chapter 3.2.1.)***.

Figure 4.2.4.5. Depletion of hCD52⁺ lymphocytes *in vivo* using alemtuzumab

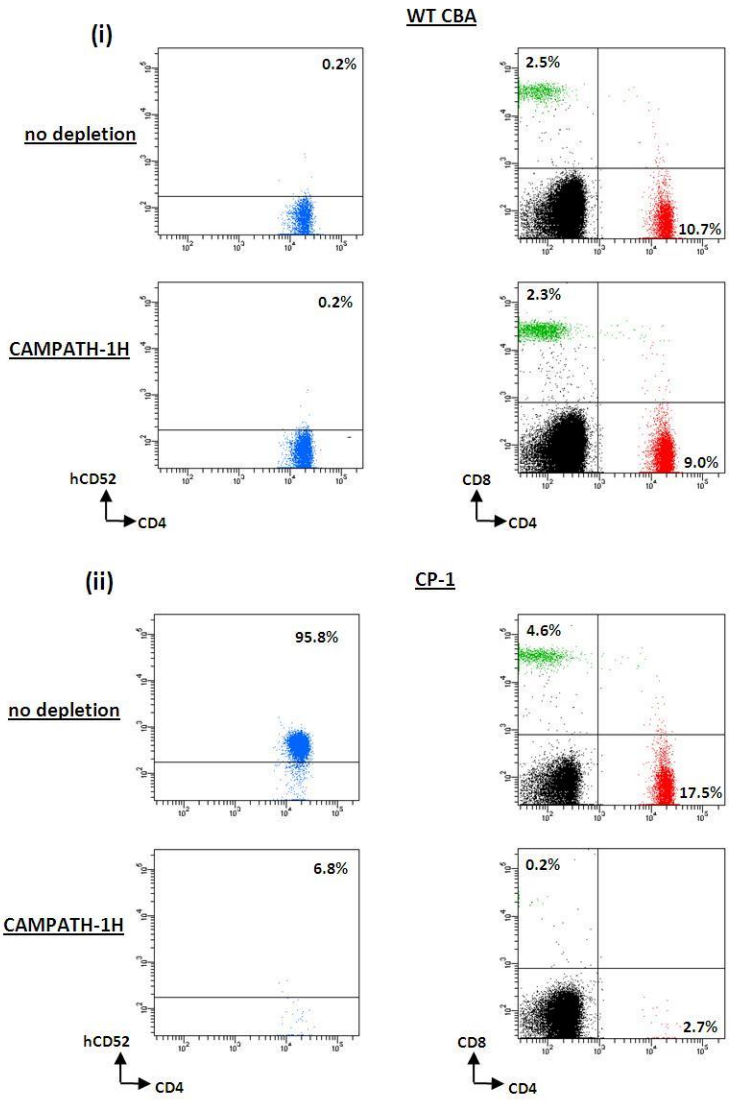

Figure 4.2.4.5. Depletion of hCD52⁺ lymphocytes *in vivo* using alemtuzumab. WT CBA or CP-1 mice were given a single dose of i.p. 100μg alemtuzumab (CAMPATH-1H) and their spleens were harvested the following day. **(i)** The presence of splenic $CD4^+$ (red) and $CD8^+$ (green) T cells in WT CBA mice with or without CAMPATH-1H treatment. CAMPATH-1H had no depleting effect on WT CBA lymphocytes. **(ii)** CAMPATH-1H significantly depleted both $CD4^+$ and $CD8^+$ T cells in CP-1 mice.

We tested the impact of depleting IFN-γ Treg in recipient mice with long-term surviving allografts induced by IFN-γ Treg therapy. IFN-γ Treg generated from CP-1 $CD4^+$ T cell precursors (called CP-1 IFN-γ Treg) were given to WT CBA mice 3 days prior to the transplant of a heterotopic B6 heart allograft, together with a pre-defined sub-optimal regimen of abatacept ***(Figure 4.2.4.6.i)***. We chose the day-3 Treg delivery protocol because we found that this was the best protocol to demonstrate long-term graft survival. Historical control experiments indicated that IFN-γ Treg could lead to long-term graft survival in WT CBA recipients when given at $5x10^5$ as a single dose on day-3, together with abatacept ***(see Chapter 3.2.6.2.)***. Recipients of heart allograft which were tolerized and accepted their grafts long-term would then be given a single dose of alemtuzumab (100μg intra-peritoneally) for the depletion of exogenous CP-1 IFN-γ Treg. The results indicated that all 4 mice that received $5x10^5$ CP-1 IFN-γ Treg and the sub-optimal abatacept regimen had accepted their heart allografts beyond 100 days. Administration of alemtuzumab had no effect on further graft outcome. These allografts continued to survive for at least another 60 days suggesting that persistence of exogenous Treg might not solely be responsible for graft tolerance, at least in this model ***(Figure 4.2.4.6.ii)***.

Figure 4.2.4.6. Depletion of exogenous IFN-γ Treg had no effect on tolerized heart allografts *in vivo*

(i)

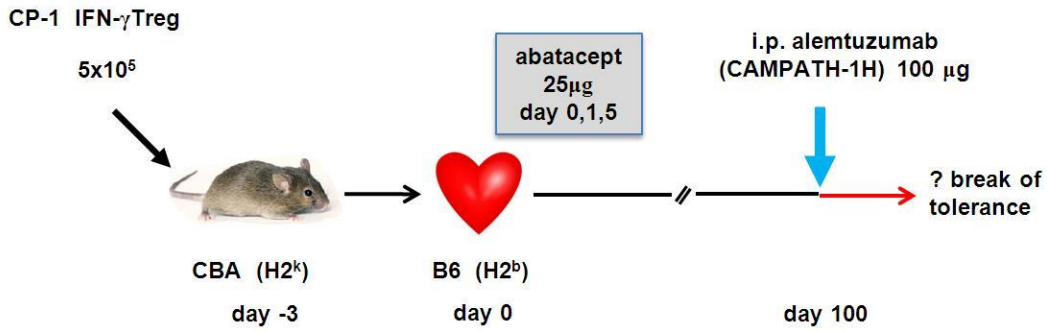

(ii)

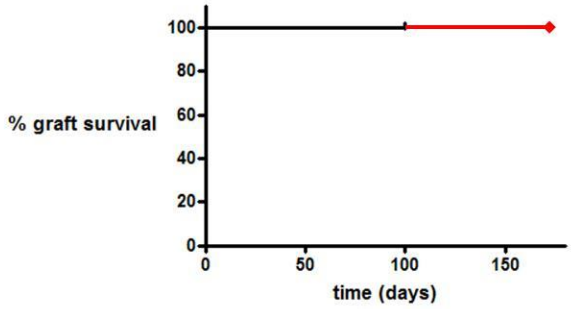

Group	n	graft survival (days)	MST (days)
LTS (5x10⁵ CP-1 IFN-γ Treg D-3 + abatacept)	4	>160,>160>160>160	>160

Figure 4.2.4.6. Depletion of exogenous IFN-γ Treg had no effect on tolerized heart allografts *in vivo*.
(i) CP-1 IFN-γ Treg were generated *in vitro* using CP-1 $CD4^+$ precursors as described above ***(Chapter 2.8.1)***. CBA mice were given $5x10^5$ CP-1 IFN-γ Treg 3 days before the transplant of a B6 heterotopic heart allograft. All recipients also received a sub-optimal dose of abatacept (i.v. 25μg day 0,1,and 5). After 100 days, mice which accepted allograft long-term received 100μg alemtuzumab (CAMPATH-1H) intra-peritoneally (i.p.) for the depletion of infused IFN-γ Treg. **(ii)** All 4 mice received CP-1 IFN-γ Treg and abatacept accepted their heart allografts >100 days. Following the single dose of alemtuzumab (CAMPATH-1H), all mice continued to accept their heart allografts which survived for at least another 60 days. These data suggest that the depletion of infused Treg after tolerance has been established long-term had no effect on subsequent heart graft outcome in this model. The maintenance of graft acceptance could perhaps be explained by infectious tolerance.

To consolidate these findings, we also tested this depletion approach using the adoptive transfer skin allograft model using the same batch of ***CP-1 IFN-γ Treg*** used in the heart model above to determine if this phenomen is model specific. In addition, we also tested if these recipients could reject the tolerized graft when new alloantigen challenge is delivered in the form of a second skin allogrft of the same strain combination, in addition to depletion using alemtuzumab. The graft outcome of these mice was compared with a group of tolerized mice in the exact same setting, which were initially tolerized with ***WT CD4$^+$CD25$^+$ nTreg*** instead and used as the contemporary control for alemtuzumab depletion.

CBA RAG$^{-/-}$ mice were given 1x10^5 CD4$^+$CD25$^-$ T cells with or without either 1x10^5 ***WT CD4$^+$CD25$^+$ nTreg***, or 1x10^5 **CP-1 IFN-γ Treg** one day prior to the transplanted with a B6 skin allograft. Those accepted their skin allografts long-term (>100 days) would be recruited in this study and received further manipulation in the following 4 groups: ***LTS (nTreg)*** and ***LTS (nTreg) with new effectors*** would receive a second B6 skin graft on the contra-lateral side and one dose of i.p. 100μg alemtuzumab, with or without 1x10^5 naive CD4$^+$CD25$^-$ new effectors as designated ***(Figure 4.2.4.7.i)***; ***LTS (CP-1 IFN-γ Treg)*** and ***LTS (CP-1 IFN-γ Treg) with new effectors*** would receive a second B6 skin graft on the contra-lateral side and one dose of i.p. 100μg alemtuzumab with or without 1x10^5 naive CD4$^+$CD25$^-$ new effectors as designated ***(Figure 4.2.4.7.ii)***.

Figure 4.2.4.7.i. Alemtuzumab had no effect on WT nTreg-induced skin allograft tolerance

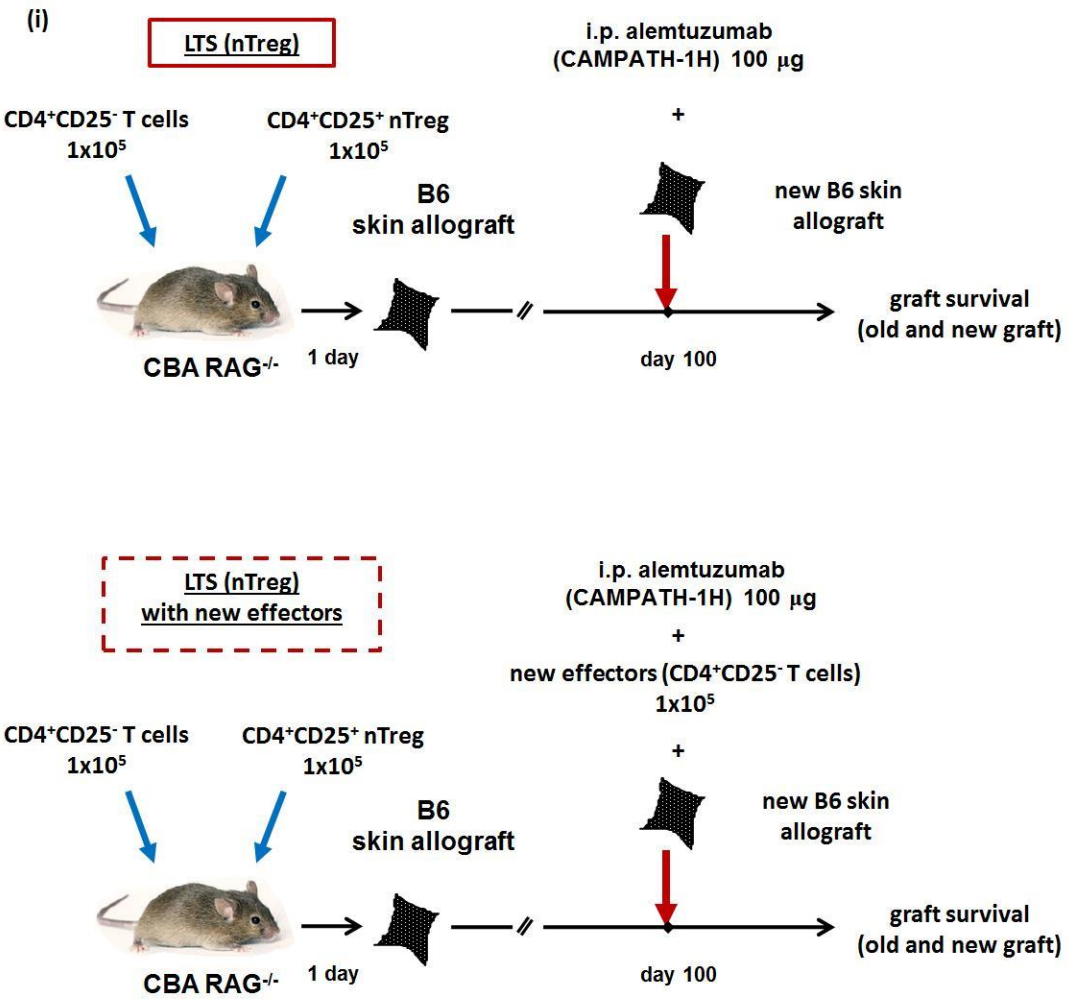

Figure 4.2.4.7.i. Alemtuzumab had no effect on WT nTreg-induced skin allograft tolerance. Schematic diagram illustrates the experimental set up. Two groups of CBA RAG$^{-/-}$ mice were reconstituted with 1x10^5 naïve CD4$^+$CD25$^-$ T cells and 1x10^5 CD4$^+$D25$^+$ nTreg one day before the transplant of a B6 skin graft. All skin allografts were accepted long-term, compatible with historical data when 1x10^5 CD4$^+$CD25$^+$ nTreg were co-transferred with 1x10^5 CD4$^+$CD25$^-$ effectors. On day 100, **LTS (nTreg)** mice received a single dose of i.p. 100µg alemtuzumab (CAMPATH-1H) and a transplant of a new B6 skin allograft on the contra-lateral flank. **LTS (nTreg) with new effectors** mice received the same dose of alemtuzumab (CAMPATH-1H), a new set of new effectors (1x10^5 CD4$^+$CD25$^-$ T cells) and a transplant of a new B6 skin allograft on the contralateral flank. Graft survival of the 'old graft' and 'new graft' in each group was monitored over time.

Figure 4.2.4.7.ii. Depletion of exogenous IFN-γ Treg in tolerized recipients partially reversed tolerance in the skin allograft model

(ii)

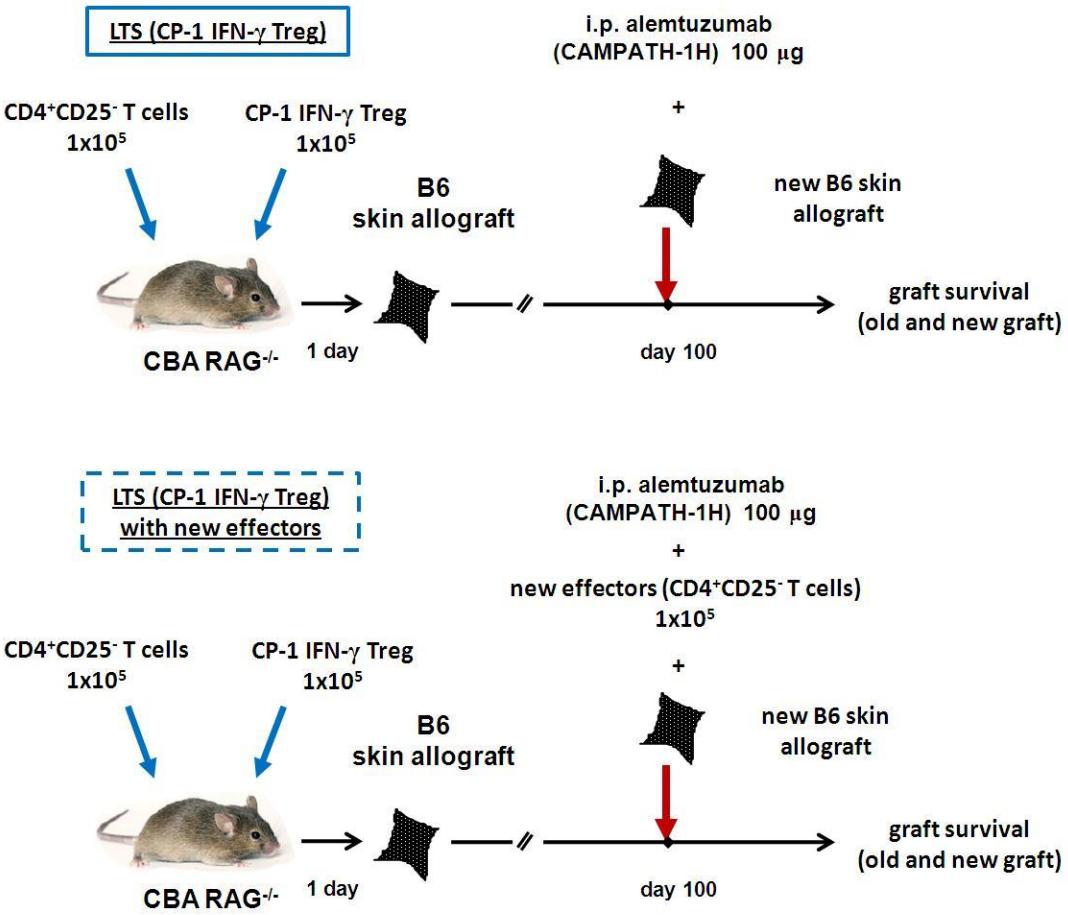

Figure 4.2.4.7.ii. Depletion of exogenous IFN-γ Treg in tolerized recipients partially reversed tolerance in the skin allograft model. Schematic diagram illustrates the experimental set up. Two groups of CBA RAG$^{-/-}$ mice were reconstituted with 1x10^5 naïve CD4$^+$CD25$^-$ T cells and 1x10^5 CP-1 IFN-γ Treg one day before the transplant of a B6 skin graft. All skin allografts were accepted long-term, compatible with historical data when 1x10^5 IFN-γ Treg were co-transferred with 1x10^5 CD4$^+$CD25$^-$ effectors. On day 100, **LTS (CP-1 IFN-γ Treg)** mice received a single dose of alemtuzumab (CAMPATH-1H) for the depletion of CP-1 IFN-γ Treg and a transplant of a new B6 skin graft on the contralateral flank. **LTS (CP-1 IFN-γ Treg) with new effectors** mice received a dose of alemtuzumab (CAMPATH-1H), a new set of new effectors (1x10^5 CD4$^+$CD25$^-$ T cells) and a transplant of a new B6 skin graft on the contra-lateral flank. Graft survival of the 'old graft' and 'new graft' in each group was monitored over time.

In mice which were initially treated with ***WT CD4^{+}CD25^{+} nTreg***, all the old grafts remained unchanged and survived for another 100 days regardless of the presence or absence of new effectors (n=3 per group) ***(Figure 4.2.4.7.iii)***. Alemtuzumab had no apparent effect in these groups. In contrast, the impact of alemtuzumab on graft tolerance was demonstrated in the LTS group in which mice were initially tolerized with ***CP-1 IFN-γ Treg (LTS CP-1 IFN-γ Treg)***. The majority (2 out of 3) of the old grafts were rejected with a MST of 72 days (n=3) suggesting that long-term survival of the old allografts might be partially reversed upon depletion of ***CP-1 IFN-γ Treg*** *in vivo*, although it did not reach statistically significance when compared to the ***LTS (nTreg)*** group (p=0.1161). In the presence of additional effectors, thus in the ***LTS (CP-1 IFN-γ Treg) with new effectors*** group, the break of tolerance was more apparent as demonstrated by a faster rejection tempo with a MST of 41 days (n=3), which was statistically different from that of ***LTS (nTreg) with new effectors*** group (MST >100 days, n=3; p=0.0246) ***(Figure 4.2.4.7.iii)***.

In clear contrast, all new allografts were rejected acutely at a similar tempo in all groups regardless of the presence or absence of new effectors with a MST of 16 days (n=3 per group) ***(Figure 4.2.4.7.iv)***.

Figure 4.2.4.7.iii. Depletion of exogenous IFN-γ Treg in tolerized recipients partially reversed tolerance in the skin allograft model

(iii)

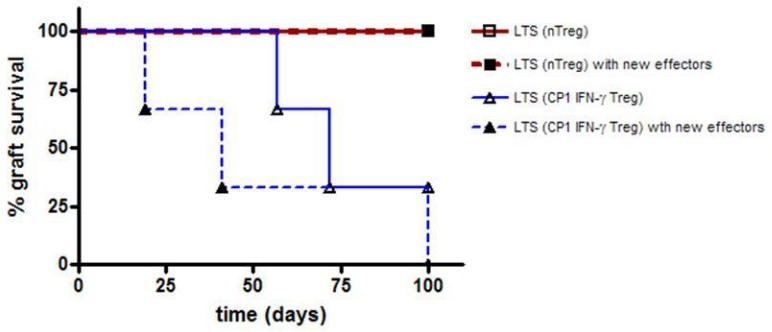

Group	n	graft survival (days)	MST (days)	p-value
LTS (nTreg)	3	>100,>100,>100	>100	
LTS (nTreg) with new effectors	3	>100,>100,>100	>100	*p = 0.1161*
LTS (CP-1 IFN-γ Treg)	3	57,72,>100	72	*p = 0.0246*
LTS (CP-1 IFN-γ Treg) with new effectors	3	19,41,100	41	

Figure 4.2.4.7.iii. Depletion of exogenous IFN-γ Treg in tolerized recipients partially reversed tolerance in the skin allograft model. No change of the graft status in the **LTS (nTreg)** & **LTS (nTreg) with new effectors** regardless the presence or absence of new effectors. All of these grafts were accepted >100 days. (n=3 per group). After depletion of previously infused CP-1 IFN-γ Treg using a single dose of alemtuzumab (CAMPATH-1H): in the **LTS (CP-1 IFN-γ Treg)** group, there was a partial loss of tolerance of the first grafts with a MST of 72 days (n=3). With limited numbers in the sample group, it did not reach statistical significance (p=0.1161), when compared to **LTS (nTreg)** group. In the **LTS (CP-1 IFN-γ Treg) with new effectors** group, in which new effectors were given in addition to a second skin graft, there was also partial loss of tolerance with a MST of 41 days (n=3), which was statistically different from the **LTS (nTreg) with new effectors** group; p=0.0246). These data suggest that infused IFN-γ Treg persisted and the depletion of these cells led to the rejection of previously tolerant skin allografts. Log rank tests were used for statistical comparisons. (p<0.05 denotes statistically significant)

Figure 4.2.4.7.iv. Alemtuzumab had no effect on WT nTreg-induced skin allograft tolerance

(iv)

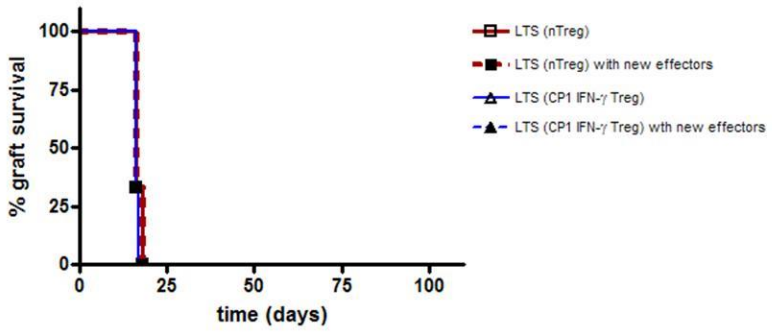

Group	n	graft survival (days)	MST (days)	p-value
LTS (nTreg)	3	16,16,18	16	
LTS (nTreg) with new effectors	3	16,16,18	16	*n.d.*
LTS (CP-1 IFN-γ Treg)	3	16,16,17	16	*n.d.*
LTS (CP-1 IFN-γ Treg) with new effectors	3	16,16,17	16	

Figure 4.2.4.7.iv. Alemtuzumab had no effect on WT nTreg-induced skin allograft tolerance. (ii) All of the second implanted skin grafts from each group were rejected acutely with a MST of 16 days (n=3 per group). The addition of new effectors did not change the tempo of the rejection kinetics. Combined with the data observed above ***Figure 4.2.4.7.iii***, the depletion of infused Treg in tolerized recipients led to a partial break of tolerance, however, this could not control a recall response as seen with acute rejection of all second skin grafts. Log rank tests were used for statistical comparisons. ($p<0.05$ denotes statistically significant)

We acknowledge that the numbers per experimental group were too small to deliver a statistically sound conclusion. Repeat experiment with larger groups might reveal the true findings with more statistical power. However, given the extended housing requirement for these LTS and secondary surgical procedures in these mice, experimental groups were kept as minimal, thus 3 per group. Nevertheless, there was an apparent change in the state of tolerance when these mice were re-challanged and when exogenous IFN-γ Treg were deliberately targetted and depleted. The graft protective mechanism was partially reversed and we spectulate that the persistence of IFN-γ Treg could be in part responsible for the maintenance of long-term graft survival in this model.

Selective depletion of adoptive transferred Treg in long-term graft survival recipients led to a partial reversal of graft acceptance in the presence or absence of new effectors suggesting that the persistence of Treg was an important consideration for the maintenance of long-term graft survival. On the other hand, some of the allografts remained accepted suggesting that the survival of these allografts could result from infectious tolerance[472]. According to our own and others' observations, we understand that infectious tolerance using various induction protocols could take approximately 4-6 weeks from the initial engraftment. We therefore wanted to investigate if Treg therapy would induce infectious tolerance at an earlier time-point than it was anticipated in our heart transplant model.

We generated IFN-γ Treg using $CD4^+$ precursors from GFP/Foxp3 KI CBA splenocytes, so that we could exclude exogenous Treg (GFP^+) by cell sorting subsequently. Two different GFP IFN-γ Treg populations were used. ***GFP IFN-γ Treg (A)*** (mixed of male and female mice) and ***GFP IFN-γ Treg (B)*** (solely male mice) were generated from splenocytes of either a mixed of male and female GFP mice, or solely male mice, respectively ***(Figure 4.2.4.8)***. Both preparations showed high Foxp3 enrichment in which ***GFP IFN-γ Treg (A)*** and ***GFP IFN-γ (B)*** had 35.5% and 44.3% $Foxp3^+$ cells, respectively. However, about half of the $Foxp3^+$ cells were GFP^- in ***GFP IFN-γ Treg (A)*** (12.8% GFP^- versus 22.7% GFP^+) because of the mixture of male and female GFP/Foxp3 KI CBA mice. The expression of GFP/Foxp3 was X-linked and thus the random inhibition of the expression of GFP/Foxp3 in female mice led to approximately 50% reduction of $Foxp3^+$ cells expressing GFP. On the other hand, almost all $Foxp3^+$ T cells express GFP in male GFP/Foxp3 KI mice (1.6% GFP^- versus 42.7% GFP^+).

Figure 4.2.4.8. IFN-γ Treg conferred long-term immunosuppression via infectious tolerance

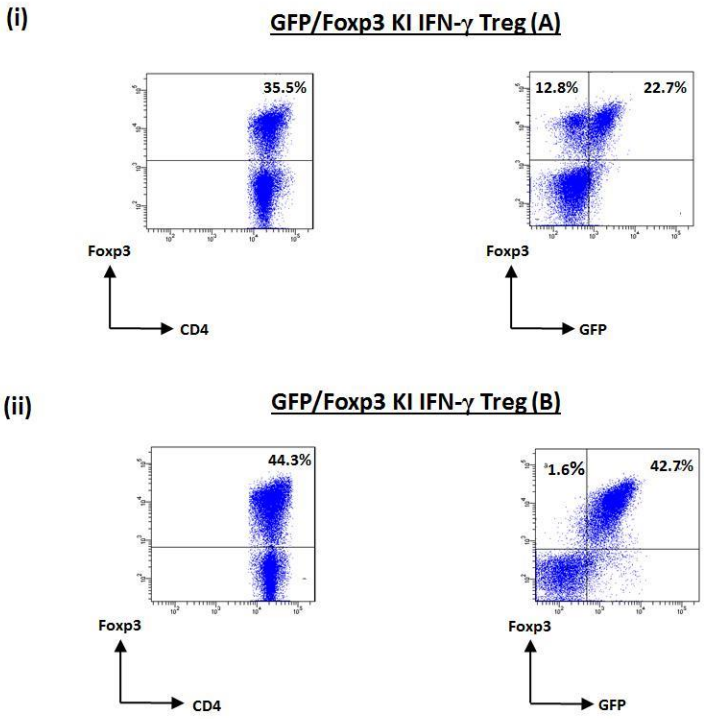

Figure 4.2.4.8. IFN-γ Treg conferred long-term immunosuppression via infectious tolerance. IFN-γ Treg were generated *in vitro* as described above using the IFN-γ conditioning protocol by stimulating $CD4^+$ precursors with allogeneic B6 BM-APC ***(Chapter 2.8.1)***. **(i)** ***GFP/Foxp3 KI IFN-γ Treg (A)*** were generated using male and female GFP/Foxp3 KI CBA $CD4^+$ precursors. Dot plots indicate that approximately 50% of $Foxp3^+$ $CD4^+$ T cells in the resultant IFN-γ Treg population were GFP^-. **(ii)** ***GFP/Foxp3 KI IFN-γ Treg (B)*** were generated using only male GFP/Foxp3 KI CBA $CD4^+$ precursors. Dot plots indicate that almost all $Foxp3^+$ $CD4^+$ T cells in the resultant IFN-γ Treg population express GFP. The difference above could be explained by the random inactivation of the X-linked Foxp3 gene in female GFP/Foxp3 KI mice.

We took a defined $CD4^+$ population from tolerized CBA mice following IFN-γ Treg therapy plus abatacept. IFN-γ Treg were generated with GFP/Foxp3 KI CBA mice. These cells were then flow sorted based on the expression of GFP, serve as a surrogate marker of Foxp3 and hence eliminating infused $Foxp3^+$ Treg. These sorted $CD4^+$ T cells were then adoptively transferred to secondary transplant recipients ***(Figure 4.2.4.9.i)***. Our hypothesis was that adoptive transfer of the $CD4^+$ population devoid of infused Treg from tolerized recipient to a second recipient would render the latter to accept allografts of the same strain as a result of infectious tolerance. 'GFP IFN-γ Treg' were generated using $CD4^+$ precursors from GFP/Foxp3 KI CBA mice driven by B6 BM-APC. WT CBA mice were given GFP IFN-γ Treg 3 days prior to the implant of a B6 heterotopic heart graft in the presence of a sub-optimal abatacept treatment. The day-3 protocol was used here because we knew that this gave the best graft outcome ***(see Chapter 3.2.6.2.)***. A separate group of mice received the abatacept treatment protocol alone, which served as a control. Spleens from each group of heart transplant recipients were harvested 2 weeks post-transplant, which is earlier than 4-8 weeks of which infectious tolerance has been proposed to occur. $CD4^+$ cells were pooled from mice within each group (***abatacept*** or ***abatacept + GFP IFN-γ Treg-A*** or ***abatacept + GFP IFN-γ Treg-B***), which were then sorted by flow cytometer to separate the $CD4^+GFP^+$ from the $CD4^+GFP^-$ population. These sorted $CD4^+GFP^-$ cells were adoptively transferred to CBA $RAG^{-/-}$ mice (at either $1x10^5$ or $5x10^5$ per mouse) receiving B6 skin allografts a day later. Rejection kinetics were compared between these $CD4^+$ GFP^- T cells obtained from recipients treated with abatacept alone or with abatacept plus IFN-γ Treg.

Figure 4.2.4.9. Induction of infectious tolerance by Treg therapy did not occur at the early time point post-transplant

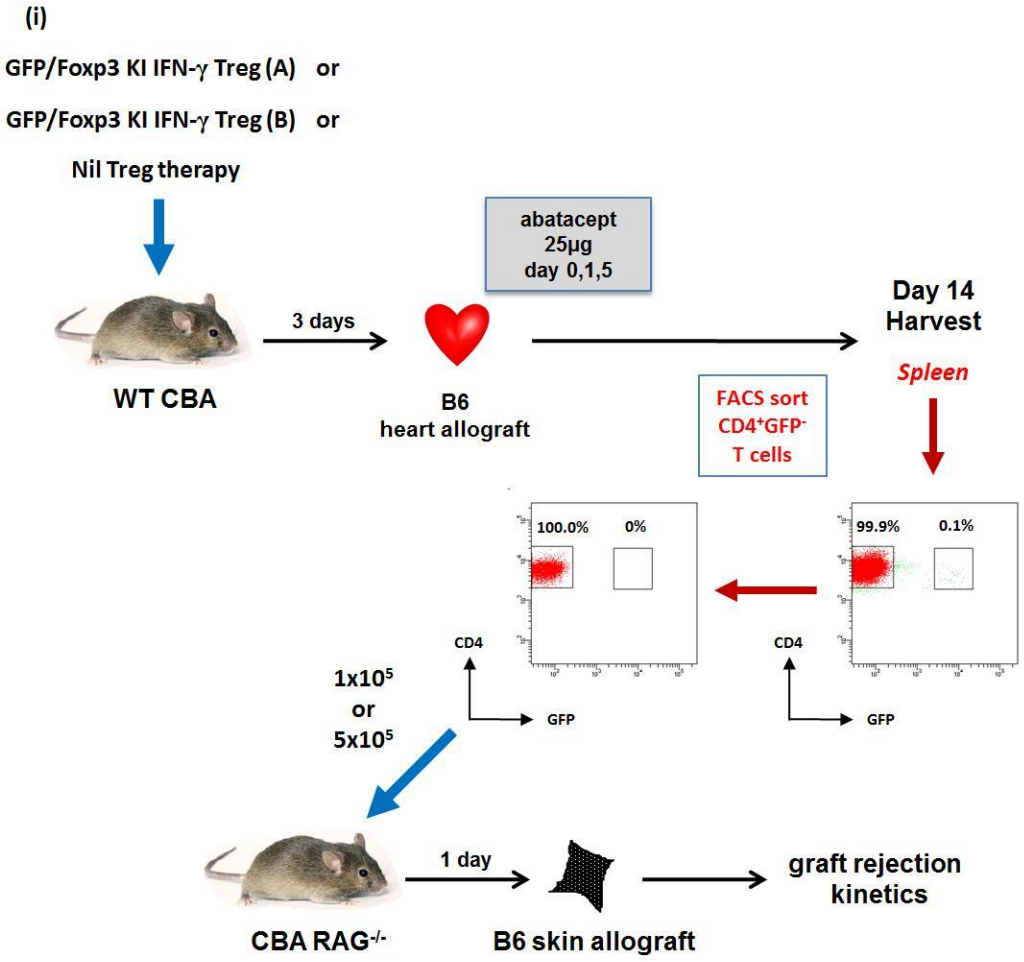

Figure 4.2.4.9. Induction of infectious tolerance by Treg therapy did not occur at the early time point post-transplant. (i) Schematic diagram illustrates the experimental set up. ***GFP/Foxp3 KI CBA IFN-γ Treg (A)*** or ***GFP/Foxp3 KI CBA IFN-γ Treg (B) (see Figure 4.2.4.8)*** were given to WT CBA mice 3 days prior to the transplant of a heterotopic B6 heart allograft. On day 0, 1 and 5, these recipients were given i.v. 25µg abatacept. A separate group of mice were used as control which underwent heterotopic heart transplant and received the abatacept regimen without IFN-γ Treg therapy. On day 14, spleens from each group of mice were pooled separately and were subjected to flow cytometry to remove any $CD4^+GFP^+$ components. Sorted $CD4^+$ GFP^- T cells were then adoptively transferred to CBA $RAG^{-/-}$ mice at a dose of $1x10^5$ or $5x10^5$ per mouse one day before the transplant of a B6 skin allograft. The skin graft rejection kinetics were compared and contrasted with historical data obtained from experiments using naïve $CD4^+CD25^-$ T cells as effectors in the same adoptive transfer model.

Compared to a historical control ***(Figure 3.2.2.2.i)*** using a $CD4^+CD25^-$ population in the skin graft model, $1x10^5$ $CD4^+$ GFP^- cells from mice treated with abatacept alone prolonged graft survival modestly with a MST of 27.5 days (n=4) versus 18.5 days ***(Figure 4.2.4.9.ii)***. On the other hand, when the cell number was increased to $5x10^5$ cells per mouse, all of the skin grafts rejected at a faster tempo with a MST of 14 days (n=4) ***(Figure 4.2.4.9.iii)***. $CD4^+GFP^-$ T cells from recipients treated with abatacept plus **GFP IFN-γ Treg-A**, which consisted of a small proportion of GFP^- $Foxp3^+$ cells, led to prolongation of graft survival with a MST of 48.5 days (n=4) compared to 27.5 days (n=4) when treated with abatacept alone ***(Figure 4.2.4.9.ii)***. Similarly, when the cell number was increased to $5x10^5$ cells per mouse, it led to long-term graft survival in 50% of the recipients with a MST of 61 days (n=4) ***(Figure 4.2.4.9.iii)***. In contrast, $CD4^+GFP^-$ T cells from recipients treated with abatacept plus **GFP IFN-γ Treg-B**, consisting of a negligible number of GFP^-Foxp3^+ T cells rejected all their allografts acutely. $1x10^5$ $CD4^+GFP^-$ T cells and $5x10^5$ $CD4^+GFP^-$ T cells from this group rejected all skin allografts in CBA $RAG^{-/-}$ mice acutely with the same MST of 15 days (n=8 per group) ***(Figure 4.2.4.9.ii & iii)***.

Collectively, the data above suggest that $CD4^+$ T cells obtained from recipients treated with a sub-optimal costimulation blockade regimen could prolong allograft survival upon adoptive transfer in a dose-dependent manner. The data from the ***abatacept + GFP IFN-γ Treg (A)*** group indicated that the transfer of $CD4^+$ Treg, could lead to a more profound graft protection compared to the ***abatacept*** group suggesting that adoptive transfer of a small population of $Foxp3^+$ T derived from recipient cells treated with Treg could confer tolerance. A $CD4^+$ population that was devoid of all exogenous Treg ($CD4^+GFP^+$ cells were excluded by cell sorting-***abatacept + GFP IFN-γ Treg (B)*** group) rejected skin allografts acutely suggesting that infectious tolerance, or linked suppression did not take place following the initial engraftment (14 days).

Figure 4.2.4.9. Induction of infectious tolerance by Treg therapy did not occur at an early time point post-transplant

(ii)

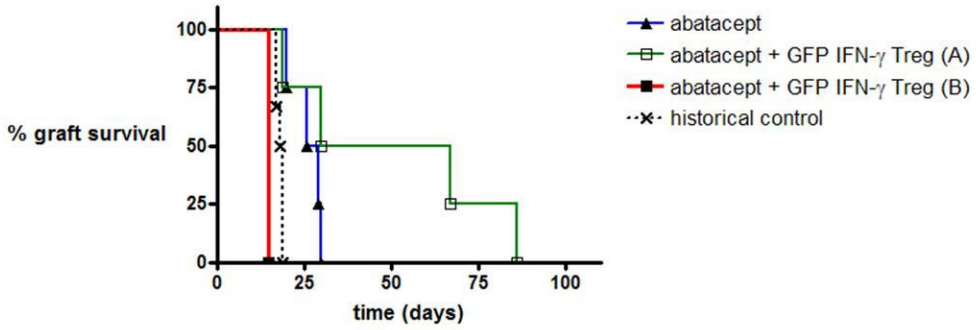

adoptively transferred 1x10^5 CD4$^+$GFP$^-$ T cells	n	graft survival (days)	MST (days)	p-value
abatacept	4	20,26,29,30	27.5	
abatacept + GFP IFN-γ Treg (A)	4	19,30,67,86	48.5	
abatacept + GFP IFN-γ Treg (B)	8	15,15,15,15,15,15,15,15	15	*p = 0.0009*
historical control (1x10^5 CD4$^+$CD25$^-$ T cells)	6	17,17,18,19,19,19	18.5	

Figure 4.2.4.9. Induction of infectious tolerance by Treg therapy did not occur at an early time point post-transplant. (ii) Robust historical controls indicate that 1x10^5 naïve CD4$^+$CD25$^-$ T cells reject B6 skin allografts with a MST of 18.5 days in CBA RAG$^{-/-}$ mice (n=6). CBA RAG$^{-/-}$ mice reconstituted with CD4$^+$GFP$^-$ T cells obtained from CBA recipients that were treated with abatacept alone rejected their skin allografts in a slower tempo with a MST of 27.5 days (n=4) compared to historical control. CBA RAG$^{-/-}$ mice that received CD4$^+$GFP$^-$ T cells obtained from WT CBA recipients treated with abatacept plus **GFP IFN-γ Treg (A)** (containing Foxp3$^+$GFP$^-$ cells) rejected their skin allografts in a delayed fashion with a MST of 48.5 days (n=4). On the other hand, CBA RAG$^{-/-}$ mice that received CD4$^+$GFP$^-$ T cells obtained from WT CBA recipients treated with abatacept plus **GFP IFN-γ Treg (B)** (GFP was expressed exclusively on Foxp3$^+$ subset) rejected their skin allografts acutely with a MST of 15 days (n=8). When the GFP$^+$ Treg were removed from the adoptive transfer effector population, the remaining GFP$^-$ population were not able to control graft rejection in secondary adoptive cell transfer suggesting that infectious tolerance has not taken place as early as 14 days post-transplant. Log rank tests were used for statistical comparisons. (p<0.05 denotes statistically significant)

Figure 4.2.4.9. Induction of infectious tolerance by Treg therapy did not occur at an early time point post-transplant

(iii)

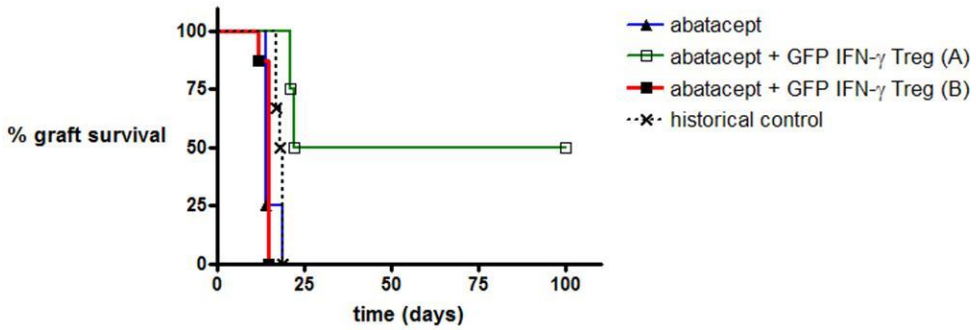

adoptively transferred 5x10^5 CD4$^+$GFP$^-$ T cells	n	graft survival (days)	MST (days)	p-value
abatacept	4	14,14,14,19	14	
abatacept + GFP IFN-γ Treg (A)	4	21,22,>100,>100	61	*p = 0.002*
abatacept + GFP IFN-γ Treg (B)	8	12,15,15,15,15,15,15,15	15	
historical control (1x10^5 CD4$^+$CD25$^-$ T cells)	6	17,17,18,19,19,19	18.5	

Figure 4.2.4.9. Induction of infectious tolerance by Treg therapy did not occur at an early time point post-transplant. (iii) Graft outcome was similar when the number of adoptive transferred CD4$^+$GFP$^-$ T cells was increased from 1x10^5 to 5x10^5. CD4$^+$GFP$^-$ T cells, which were obtained from recipients previously treated with abatacept, abatacept plus ***GFP IFN-γ Treg (A)*** or abatacept plus ***GFP IFN-γ Treg (B)*** were adoptively transferred to CBA RAG$^{-/-}$ mice one day before the transplant of a B6 skin allograft. CD4$^+$GFP$^-$ T cells obtained from recipients treated with abatacept plus ***GFP IFN-γ Treg (A)*** led to a partial graft protection response with a MST of 61 days (n=4) The partial graft protection effect was possibly due to the carry over of infused Treg from the ***GFP IFN-γ Treg (A)*** group. On the other hand, all skin allografts were rejected acutely when infused Treg population were removed from the adoptive cell transfer cohort (***GFP IFN-γ Treg (B)***), suggesting that infectious tolerance did not take place as early as day 14. Log rank tests were used for statistical comparisons. ($p<0.05$ denotes statistically significant)

4.2.5 Treg therapy was less effective in controlling memory responses *in vivo*

IFN-γ Treg were generated *in vitro* by stimulation with alloantigens in the presence of exogenous IFN-γ. We hypothesized that these alloreactive Treg might be able to attenuate memory responses in sensitized hosts. IFN-γ Treg were tested for their ability to control allograft rejection mediated by a selected population of effector memory T cells in an adoptive transfer model. CD44 expression has been documented as an activation marker of both CD4 and CD8 T cells. T cells expressing high level of CD44, i.e. $CD44^{hi}$, has been described as a marker for memory T cells. Our group has previously used this selected population in adoptive transfer studies to demonstrate the suppressive function of Treg against $CD4^{+}CD44^{hi}$ effector T cells[473]. Purified $CD4^{+}CD44^{hi}$ T cells were used as a deliberately designed memory population in the following experiment. $CD4^{+}CD44^{hi}$ T cells were induced *in vivo* by challenging CBA hosts with B6 blood transfusion over a minimum of 40 days. Splenocytes from sensitized CBA mice were then harvested and $CD4^{+}CD44^{hi}$ T cells selected by FACS Aria sorting ***(Chapter 2.3.4)***. The surface expression of CD44 in naïve $CD4^{+}CD25^{-}$ T cells (8.7% $CD44^{hi}$) and these *in vivo* generated memory $CD4^{+}CD44^{hi}$ T cells (99.5% $CD44^{hi}$) were assessed by flow cytometry ***(Figure 4.2.5.1)***.

$1x10^{5}$ $CD4^{+}CD44^{hi}$ T cells were adoptively transferred to CBA $RAG^{-/-}$ mice one day before the implant of a B6 skin allograft. The rejection kinetics was compared to that of contemporary and historical controls ***(Figure 4.2.5.2)***. $1x10^{5}$ naive CBA $CD4^{+}CD25^{-}$ T cells rejected B6 skin allografts acutely with a MST of 16 days (n=3). $CD4^{+}CD44^{hi}$ effector memory T cells rejected B6 skin allografts acutely with MST of 15 days (n=3). However, while at the 2:1 Treg:effector ratio, IFN-γ Treg were able to control naïve $CD4^{+}CD25^{-}$ T cells-mediated skin allograft rejection long-term (MST>100 days, historical control), they were unable to prevent rejection mediated by

$CD4^+CD44^{hi}$ effector memory T cells, with a MST of 42 days (n=3; *p*=0.0246) ***(Figure 4.2.5.2)***. Similarly, while *in vitro* expanded $CD4^+CD25^+$ nTreg were able to control rejection mediated by naïve $CD4^+CD25^-$ T cells (MST >100 days, historical control), they were not able to control memory T cells responses and these skin grafts were rejected with a MST of 31 days (n=5; *p*=0.0042) ***(Figure 4.2.5.2)***.

We also tested if IFN-γ Treg have the ability to prevent allograft rejection in previously sensitized immunocompetent hosts ***(Figure 4.2.5.3)***. CBA mice were transplanted with a B6 skin allograft. All skin grafts were rejected acutely with a MST of 13 days (n=6). These mice were then re-challenged with a B6 heart allograft 6 weeks later. They were given the sub-optimal abatacept protocol, with or without day-3 IFN-γ Treg treatment ($1x10^6$ cells per mouse, 3 days prior to heart transplant). Mice received abatacept without IFN-γ Treg treatment rejected the B6 heart allografts acutely with a MST of 5 days (n=3) ***(Figure 4.2.5.3)***. Interestingly, mice treated with abatacept and IFN-γ Treg also rejected their heart allografts acutely with a MST of 5 days (n=3). Comparing to historical controls with naive mice transplanted with a heterotopic heart graft without any Treg treatment, sensitized mice rejected their grafts much more vigorously even in the presence of a sub-optimal abatacept treatment (MST= 5 days versus 52 days). Even in the presence of the IFN-γ Treg, all mice rejected acutely (MST= 5 days versus >100 days). Collectively, these data indicate that at this given cell dose of IFN-γ Treg were unable to control vigorous immunological memory responses in pre-sensitized recipients, even in with the presence of a low dose costimulation blockade.

Figure 4.2.5.1. Expression of CD44 on adoptively transferred effector T cell populations in the skin allograft model

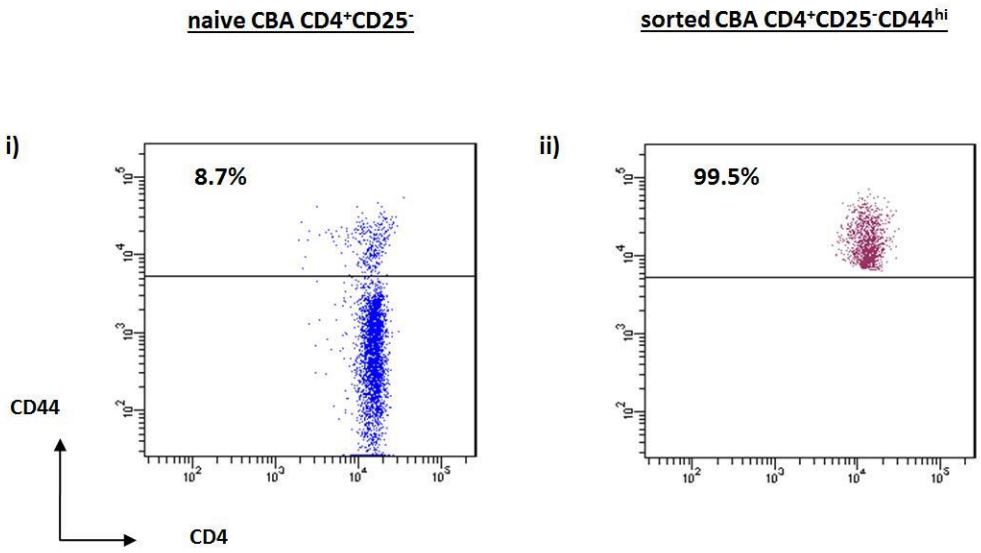

Figure 4.2.5.1. Expression of CD44 on adoptively transferred effector T cell populations. (i) CBA $CD4^+$ T cells were depleted from $CD25^+$ T cells by MACS to yield >90% $CD4^+CD25^-$ T cells as described in ***Chapter 2.7.4***. The expression of CD44 within this $CD25^-$ population was determined by flow cytometry. 8.7% of this naïve $CD4^+CD25^-$ T cell population expressed high levels of CD44 ($CD44^{hi}$), which was used as $CD4^+CD25^-$ T cells as the effector population in the allogeneic skin allograft model (as shown in Figure 4.x.x.x). (ii) Memory T cells against B6 alloantigen were generated *in vivo* by challenging CBA mice with B6 splenocytes as described in ***Chapter 2.3.4***. $CD4^+CD25^-$ T cells were isolated as above ***(Chapter 2.7.4)***, and sorted for $CD44^{hi}$ by FACS ARIA yielding purity of 99.5% $CD4^+CD44^{hi}$ T cells, which were used as a memory T cell population in the allogeneic skin allograft model (as shown in ***Figure 4.2.5.2***).

Figure 4.2.5.2. IFN-γ Treg were less efficient in controlling a memory response *in vivo* at a defined dosage

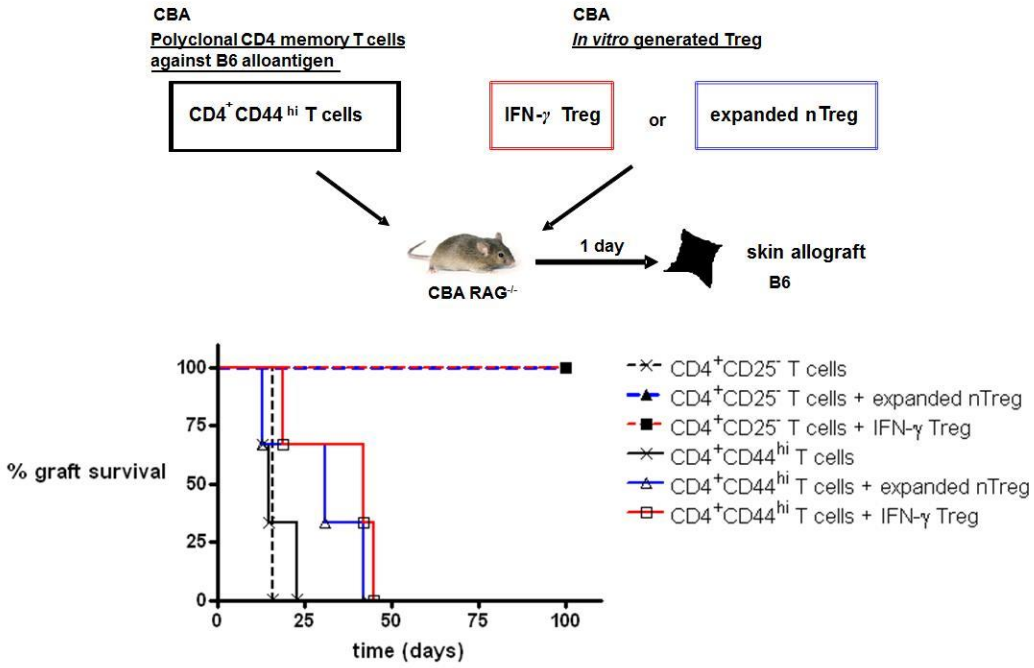

Group	N	graft survival (days)	MST (days)	p-value
$CD4^+CD25^-$ T cells	3	16,16,16	16	
$CD4^+CD25^-$ T cells + expanded nTreg	5	>100,>100,>100,>100,>100	>100	
$CD4^+CD25^-$ T cells + IFN-γ Treg	3	>100,>100,>100	>100	
$CD4^+CD44^{hi}$ T cells	3	13,15,23	15	*p = 0.0042*
$CD4^+CD44^{hi}$ T cells + expanded nTreg	3	13,41,42	31	
$CD4^+CD44^{hi}$ T cells + IFN-γ Treg	3	19,42,45	42	*p = 0.0246*

Figure 4.2.5.2. IFN-γ Treg were less efficient in controlling a memory response *in vivo* at a defined dosage. $CD4^+CD44^{hi}$ T cells were used as a memory effector T cell population. B6 allografts were rejected acutely by both naïve $CD4^+CD25^-$ T cells as well as $CD4^+CD44^{hi}$ memory effectors with a MST of 16 days (n=3) and 15 days (n=3), respectively. *In vitro* expanded $CD4^+CD25^+$ nTreg prevented allograft rejection long-term (MST>100 days) when given at a 2:1 Treg : naïve $CD4^+CD25^-$ T cells ratio (n=5). However, these cells could not control a memory response elicited by $CD4^+CD44^{hi}$ memory effectors with a MST of 31 days (n=3) at the same ratio. Likewise, IFN-γ Treg were able to prevent allograft rejection mediated by $CD4^+CD25^-$ T cells long-term (MST >100 days) when given at a 2:1 Treg : effectors ratio (n=3). In clear contrast, they could not control rejection mediated by $CD4^+CD44^{hi}$ effector memory population with MST of 42 days (n=3) at the same ratio. Log rank tests were used for statistical comparisons. (p<0.05 denoted statistically significant).

Figure 4.2.5.3. At a given dose, IFN-γ Treg were incapable of controlling allograft rejection in pre-sensitized immunocompetent recipients

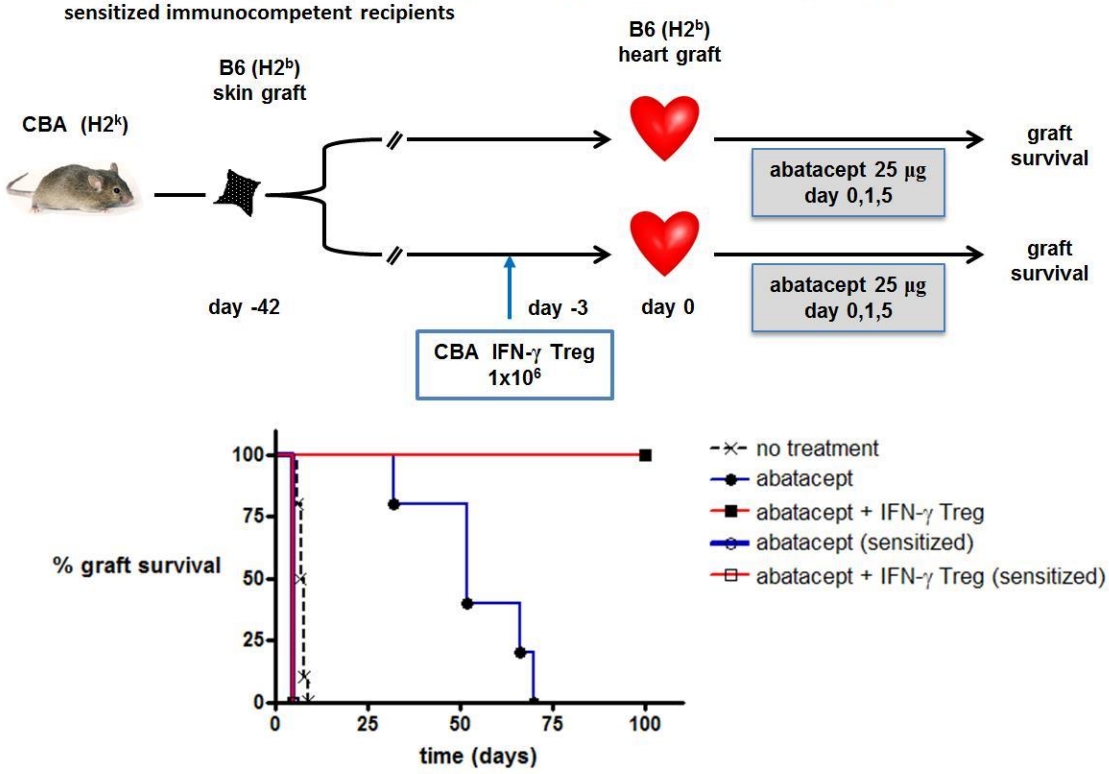

Group	N	graft survival (days)	MST (days)	p-value
no treatment (naïve)	10	6,6,7,7,7,8,8,8,8,9	7.5	
abatacept (naïve)	5	32,52,52,66,70	52	
abatacept + IFN-γ Treg (1x10^6) (naïve)	4	>100,>100,>100,>100	>100	*p = 0.0082*
abatacept (sensitized)	3	5,5,5	5	*p = 0.0143*
abatacept + IFN-γ Treg (1x10^6) (sensitized)	3	5,5,5	5	

Figure 4.2.5.3. At a given dose, IFN-γ Treg were incapable of controlling allograft rejection in pre-sensitized immunocompetent recipients. Immunological memory was induced by transplanting a B6 skin allograft to immunocompetent CBA mice. These mice rejected their skin allografts acutely with a MST of 13 days (data not shown). Six weeks later some mice received 1x10^6 IFN-γ Treg three days prior to a transplant of a B6 heterotopic heart allograft with abatacept. Another group of mice received abatacept alone. B6 heart allografts were rejected at a faster tempo in sensitized mice compared to naïve mice receiving abatacept treatment alone (MST=5 days, n=3 versus 52 days, n=5). IFN-γ Treg were able to control allograft rejection in the presence of abatacept in naïve mice but not sensitized mice (MST >100 days ; n=4) versus 5 days; n=3). Log rank tests were used for statistical comparisons. (p<0.05 denoted statistically significant)

4.3 Discussion

The intriguing biology of CTLA-4 has puzzled scientists for many years. Undoubtedly, CTLA-4 is a major immune regulatory molecule; however its mechanisms of action have remained unresolved. New insights recently have shown that T cells bearing CTLA-4 could capture B7 molecules (CD80/CD86) from adjacent cells in the form of trans-endocytosis[393]. The rapid turnover of CTLA-4 between the cell surface and cytosol explained the difficulty to demonstrate the cell surface expression of CTLA-4. The intracellular expression of CTLA-4 has become more widely accepted. We have demonstrated the role of CTLA-4 in the function of IFN-γ Treg *in vivo*. In the presence of anti-CTLA-4 antibody, IFN-γ Treg were unable to prevent allograft rejection *in vivo* ***(Figure 4.2.1.2)***, similar to nTreg and consistent with our previous findings[450].

The recent development of immune checkpoint therapy in the treatment of metastatic cancers has brought the resurgence of the interest of the CTLA-4 pathway. Another interesting negative immune checkpoint molecule of interest is PD-1. Both PD-1 and its ligand PD-L1 were shown to be implicated in transplant tolerance[399,474-476]. Given there is major redundancy in the complex costimulation cascade; it would be interesting to see the combination effect of the CTLA-4Ig and the stimulation of PD-1 or PD-L1 on the efficacy of Treg in the control of alloresponses in the context of transplantation. Targetting both costimulatory (CD40L) and coinhibitory (PD1) pathways was shown to be effective in prolonging islet allograft survivals *in vivo*[477]. In addition, the combination of CTLA-4Ig and anti-BTLA were shown to be synergistic to promote islet allograft acceptance[478].

IL-10 has been suggested to be a major suppressive cytokines for Treg function. We were unable to show that restimulated nTreg or IFN-γ Treg expressed IL-10. This is in line with the observation that Treg normally do not express high levels of IL-10. In addition, it has been shown

that IL-10-expressing Treg could only be detected at high levels in those obtained from inflammatory tissues. On the other hand, our *in vivo* data suggest that the IL-10-IL-10R pathway was only partially responsible for IFN-γ Treg suppression ***(Figure 4.2.2.2.ii)*** as compared to an exclusive effect as seen with CTLA-4 blockade ***(Figure 4.2.1.2.ii)***. These results were compatible with our previous published reports which showed that *in vivo* alloantigen-driven $CD4^+CD45RB^{lo}$ and $CD4^+CD25^+$ Treg suppress the rejection mediated by co-transferred effector T cells in a similar skin transplant model[450,479]. On the other hand, our data indicated that neutralization with anti-IL-10R antibody did not abrogate suppression mediated by freshly-isolated $CD4^+CD25^+$ nTreg suggesting that nTreg controlled skin allograft rejection in an IL-10-independent manner ***(Figure 4.2.2.2.ii)***. Freshly-isolated $CD4^+CD25^+$ nTreg from our experiments expressed high levels of CD25 (95%) and Foxp3 (>95%), as compared to $Foxp3^-$ Tr1 cells, which have been described to mediate their suppressive function primarily via IL-10 and TGF-β[480,481]. Furthermore, a recent report by Yao et al showed that Tr1 but not $Foxp3^+$ Treg mediated suppression via IL-10[482].

The demonstration of the suppressed proliferation of effector T cells *in vitro* by Treg is a valuable tool for the functional validation of Treg[483,484]. Using a similar set up as that for an MLR, many researchers have used ^{3}H-thymidine incorporation assays to generate the proliferation indices as co-cultured responders divide *in vitro* upon stimulation. Because of the sensitivity of these DNA-incorporation assays a lower number of cells are generally required. However, besides the inconvenience of using radioisotopes in these assays, it has also become clear that while one cannot separate the Treg and effector T cell populations as cell contact is required for Treg function, the radioactivity readout could not be excluded from the Treg population present. In fact, Treg proliferated in the presence of allogeneic or polyclonal stimuli, which would skew the end results (M. Karim D.Phil. Thesis and R. Francis D.Phil. Thesis,

University of Oxford). Flow cytometry-based cell proliferation assays using a cell proliferative dye are now being used more commonly[485]. These cell proliferation dyes serve as a unique tool to investigate the proliferation profile of each cell population in culture. We demonstrated that, by using two separate cell dyes (in the absence of a cogenic marker in our strain combination used) we could confirm the suppression of the effector population *in vitro* by the dilution of the labelled dye and simultaneously study the activity of Treg. More interestingly, we found that at low IFN-γ Treg numbers, the $Foxp3^-$ cohort would drive the proliferation of responders at an exponential rate. These data suggest that the $Foxp3^+$ cohort could control the $Foxp3^-$ cohort within the IFN-γ Treg preparation, but also control the responders *in vitro*. Although it has been argued that results obtained from *in vitro* suppression assay might not conform to Treg function *in vivo*, these assays have remained an important tool to ensure quality control of freshly-prepared Treg prior to administration to patients.

Our initial hypothesis was that the combination of exogenous Treg and abatacept was more efficient in the induction of infectious tolerance compared to the use of anti-CD4/CD8 antibody[472]. Although we found that infectious tolerance did not develop 2 weeks post-transplant, we demonstrated that infectious tolerance occurred in mice that accepted their heart allografts long-term (100 days post-transplant). On week 2, adoptive transfer of $CD4^+$ T cells devoid of infused Treg in recipients treated with abatacept with IFN-γ Treg into secondary skin transplant recipients did not prevent allograft rejection ***(Figure 4.2.4.9)***. On the other hand, adoptive transfer of $CD4^+$ T cells containing a small percentage of infused Treg could delay rejection ***(Figure 4.2.4.9)***. The depletion of infused IFN-γ Treg that express hCD52 using alemtuzumab (anti-hCD52 antibody) in recipients which accepted their heart allograft long-term (>100 days) following abatacept plus IFN-γ Treg therapy did not trigger rejection and allografts remained accepted for another 100 days ***(Figure 4.2.4.6)***. These data were consistent with the

observations in which infectious tolerance was induced by anti-CD4/CD8 antibody in a mouse skin transplant model[472] and by DST in a rat liver transplant model[486], whereby approximately 30 days and 60 days were required for the development of infectious tolerance, respectively.

To our surprise tolerance was not broken when infused Treg were depleted in the heart transplant model. We reasoned that this could be due to differences in susceptibility to tolerance between different organs or tissues. It had been suggested that the mode of alloantigen delivery and the number of alloantigen present could be important factors to consider.

When the same batch of IFN-γ Treg that express hCD52 were depleted in tolerant skin transplant recipients, we observed partial reversal of tolerance as some of the old skin allografts were rejected ***(Figure 4.2.4.7.iii)***. Those reconstituted with WT CBA nTreg which did not express hCD52, thus exogenous Treg were not depleted, tolerance of old allografts sustained suggesting that the persistence of infused Treg was required for the development and maintenance of infectious tolerance ***(Figure 4.2.4.7.iii)***.

Depletion of infused Treg had no effect on the outcome of a fresh second skin allograft of the same strain, suggesting that infectious tolerance was not able to control a secondary response, regardless of the presence or absence of newly introduced naïve $CD4^{+}CD25^{-}$ T cells ***(Figure 4.2.4.7.iv)***. Using the same cell dose, alloantigen-driven Treg were unable to control memory T cell responses mediated by a $CD4^{+}CD44^{hi}$ effector T cell population in the adoptive transfer skin allograft model ***(Figure 4.2.5.1)*** and a secondary response to a skin allograft in immunocompetent recipients of the heart transplant model ***(Figure 4.2.5.2)***, respectively. Recall responses are important issues to be considered given a wide variety of intervention in clinical

medicine. Blood transfusion, infection, graft failure and second transplant are main causes of the development of memory T cells in transplant recipients.

In conclusion, we have demonstrated that *in vitro* generated Treg mediate their suppressive function via mechanisms shared by other Treg populations. Further insights into the CTLA-4 mechanisms and tissue resident Treg are important features to be explored in future work.

Chapter 5 Expansion of regulatory T cells

5.1 Introduction

The paucity of Treg as well as their inherent anergy features had led many groups to attempt to develop protocols to efficiently expand Treg *in vitro*. Taylor et al were amongst the first group to test the expansion potential of $CD4^+CD25^+$ T cells *in vitro*[423]. In this study, $CD4^+CD25^+$ T cells could be expanded using plate-bound anti-CD3 antibody or allogeneic APC that led a 12-fold and 1-2 fold expansion, respectively. More importantly, these cells could attenuate GVHD *in vivo*. Tang et al[487] employed the technology of using polymer beads conjugated with ant-CD3 and anti-CD28 antibody to expand Treg and they reported that expansion of flow cytometer sorted $CD4^+CD25^+CD62L^+$ T cells using anti-CD3 and anti-CD28-coupled beads plus high-dose of IL-2 led to a significant yield of 200-fold $CD4^+CD25^+$ T cells after 12 days. These expanded Treg demonstrated suppressive function *in vitro* and reversed the onset of diabetes in NOD mice[339].

Other groups have attempted to expand Treg using APC as a natural source of costimulatory signals. Battaglia et al[488] showed that mouse $CD4^+CD25^+$ nTreg could be expanded using APC-pulsed with transgenic TCR-cognate antigen, or a combination of anti-CD3 and CD28 antibody, in the presence of rapamycin. They showed that nTreg expanded with rapamycin possessed suppressive function in a pancreatic islet transplant model. Tarbell et al[489] showed that DC pulsed with autoantigen could expand transgenic $CD4^+CD25^+$ T cells bearing the TCR specific to the cognate autoantigen up to 10-fold in 5 days *in vitro*. Subsequently, the same group reported that they could expand $CD4^+CD25^+$ T cells with allogeneic DC that led to the suppression of

GVHD[443]. Nishimura et al[490] also reported the use of allogeneic DC that could expand $CD4^+CD25^+$ T cells in the presence of IL-2 *in vitro* for 5 days, which led to a 2-fold increase. These expanded Treg controlled allograft rejection in an adoptive skin transplant model.

Syngeneic APC were also found to be effective in expanding Treg *in vitro*. Golshayan et al[491] found that the use of syngeneic DC pulsed with alloantigenic peptide to expand $CD4^+CD25^+$ T cells that could control allo-specific skin graft rejection in an adoptive transfer model. Anlun et al[492] showed that expanded $CD4^+CD25^+$ T cells by syngeneic DC pulsed with donor splenocytes could suppress the proliferation of $CD25^-$ T cells and control allograft rejection in conjunction with a combination of induction and maintenance immunosuppressive therapy *in vivo*. More recently, modulated APC represents a new avenue for the expansion of $CD4^+CD25^+$ nTreg, in the presence of certain Treg-favourable cytokines such as IL-33 and vitamins such as retinoic acid[493-495].

A number of methods have been reported to expand Treg in animal models. In contrast, expansion protocols of human $CD4^+CD25^+$ nTreg have been shown to be more promising and these methods were able to generate an even greater number of Treg *in vitro*. Levings et al[496] were first to demonstrate that human $CD4^+CD25^+$ nTreg could be expanded using a combination of anti-CD3 antibody, allogeneic feeder cells and IL-2 with a yield of 20 to 30-fold increase after 2 weeks. Hoffmann et al[424] first showed that human flow cytometer-sorted $CD4^+CD25^{hi}$ T cells could be expanded in a large scale up to 40000-fold expansion using artificial APC plus anti-CD3 and anti-CD28 antibody, in the presence of IL-2 after 3 weeks of culture. Godfrey et al[453] demonstrated that MACS-isolated $CD4^+CD25^+$ T cells could be expanded using anti-CD3/CD28 antibody-coated beads, feeder cells plus IL-2 leading to > 90-fold expansion after 3 weeks of culture. These expanded $CD4^+CD25^+$ Treg could attenuate allogeneic MLR cultures

effectively. Earle et al[497] found that anti-CD3/CD28 bead-expanded human $CD4^+CD25^+$ Treg could effectively suppress allo-stimulated PBMC cultures. Peters et al[498] used a combination of alloantigenic and polyclonal stimuli to model a two-cycle human nTreg expansion, which led to a 100-fold expansion. The same group later developed a GMP-compatible protocol that would allow expanded Treg to be translated into clinical medicine[499]. In our laboratory, we successfully developed a protocol to expand human $CD4^+CD25^{hi}$ $CD127^{lo}$ nTreg which suppress alloresponses *in vitro* and in humanized transplant models[500-502].

In this chapter, we aimed to develop a protocol to expand IFN-γ Treg in sufficient quantities for the purpose of evaluating their characteristics and functions in subsequent experiments. We also revisited the potential of using $CD4^+CD25^+$ nTreg, and compared freshly-isolated, expanded nTreg and activated nTreg as an alternative to alloantigen-driven Treg in their suppressive properties *in vivo*.

5.2 Results

5.2.1 Expansion of IFN-γ Treg

5.2.1.1 Expanding IFN-γ Treg with anti-CD3/28 antibody-conjugated beads

The number of IFN-γ Treg that could be generated by the IFN-γ conditioning protocol remained very limited ***(Chapter 3.2.3 – Optimization of IFN-γ conditioning protocol)***. On average, only a maximum of 10% of the initial input $CD4^+$ T cells was retrievable after 14 days of culture. From the titration experiments we noted that a minimum of $5x10^5$ - $1x10^6$ IFN-γ Treg would be

required to elicit a demonstrable response in a single recipient in the heart transplant model in the presence of a sub-optimal abatacept regimen ***(Chapter 3.2.5; Figure 3.2.5.1)***. Therefore, we began searching for a protocol to expand IFN-γ Treg *in vitro*. The theoretical approach was first to exploit the IFN-γ conditioning protocol which enables the shaping of a T cell repertoire from a polyclonal to an alloantigen-specific population in the presence of modulated BM-APC and the induction of preferential AICD in the non-Treg (Foxp3$^-$) population ***(Figure 5.2.1.1.1)***. Second, by using a polyclonal stimulus that would break the inherent anergy properties of Foxp3$^+$ Treg, we hoped to preferentially expand Treg followed by further AICD in the non-Treg population, which had been shown to be pro-apoptotic previously[440]. A commercially available T cell expansion kit consists of magnetic Dynabeads® (Invitrogen, Norway) conjugated with a defined concentration of anti-CD3 and anti-CD28 antibody on their surface that provide T cell activation signals to CD3/TCR complex and CD28, simultaneously. These reagents have been shown to be able to expand mouse Treg[503-505] ***(Figure 5.2.1.1.2)***. We hypothesized that IFN-γ Treg would respond to this polyclonal activation and continue to proliferate and expand in large numbers in the presence of high-dose exogenous IL-2 *in vitro*.

Figure 5.2.1.1.1. Expansion of IFN-γ Treg using anti-CD3/CD28 antibody-conjugated beads and IL-2 *in vitro*

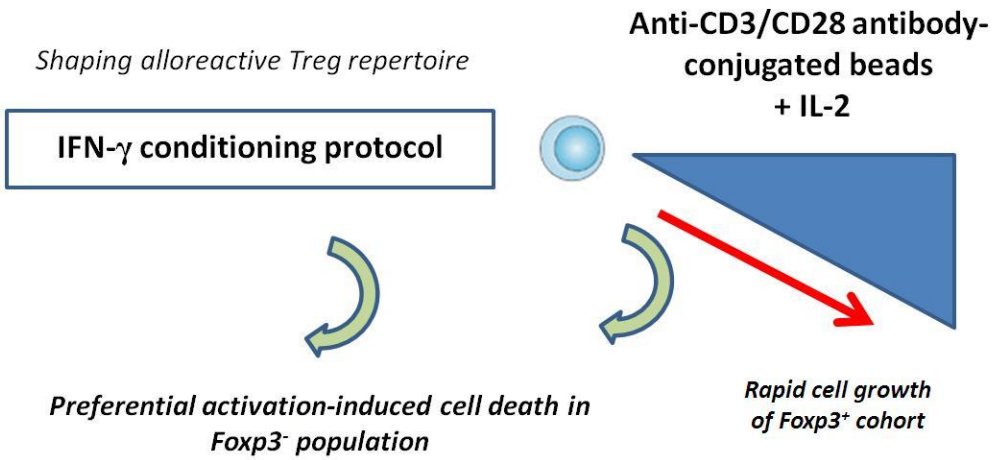

Figure 5.2.1.1.1. Expansion of IFN-γ Treg using anti-CD3/CD28 antibody-conjugated beads and IL-2 *in vitro*. One of the commonly used T cell expansion protocols described in the literature involves the use of anti-CD3/CD28 beads plus exogenous IL-2. The principle of this protocol incorporates the original IFN-γ conditioning protocol that entails shaping of a $CD4^+$ T cell repertoire by selecting alloreactive $Foxp3^+$ Treg. The $Foxp3^-$ cohort is thought to be pro-apoptotic and preferentially undergo AICD under the influence of IFN-γ. Therefore, by incubating IFN-γ Treg with anti-CD3/CD28 antibody and IL-2, we hypothesized that the healthy $Foxp3^+$ cohort would continue to expand secondary to a strong polyclonal stimulus, while the $Foxp3^-$ cohort would undergo apoptosis instead.

Figure 5.2.1.1.2. Principles of polyclonal activation of IFN-γ Treg using anti-CD3/CD28 antibody-conjugated beads and exogenous IL-2 *in vitro*

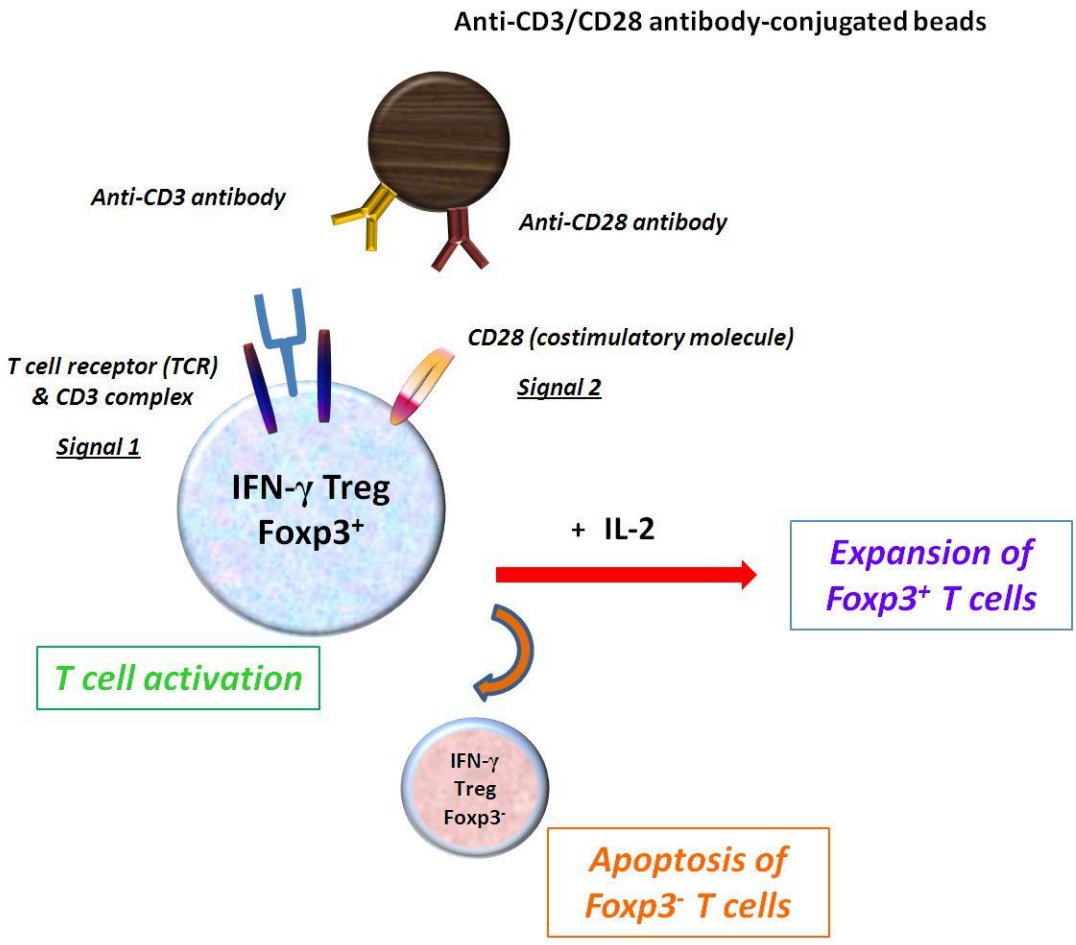

Figure 5.2.1.1.2 Principles of polyclonal activation of IFN-γ Treg using anti-CD3/CD28 antibody-conjugated beads and exogenous IL-2 *in vitro*. IFN-γ Treg are stimulated with anti-CD3/CD28 antibody-conjugated beads (anti-CD3/CD28 beads) via two signals at the immunological synapse. Positive signal through TCR/CD3 complex triggers initial T cell activation. A second signal is delivered via the costimulatory molecule CD28, which leads to full T cell activation and begin to proliferate. In the presence of a defined concentration of T cell growth factor such as interleukin-2 (IL-2), the division of daughter cells is propagated resulting in the expansion of $Foxp3^+$ T cells. Upon stimulation, $Foxp3^-$ T cells undergo apoptosis via AICD. We hypothesize that the combination of these mechanisms would result in a net increase in the $Foxp3^+$ Treg population.

IFN-γ Treg were enriched for a 48.0% Foxp3^{+} population from CD4^{+} precursors using the IFN-γ conditioning protocol for 2 weeks ***(Figure 5.2.1.1.3.i)***. 2x10^{4} freshly-harvested IFN-γ Treg were incubated with or without anti-CD3/CD28 beads (1:1 bead:cell ratio) in the presence of a graded concentration of IL-2 (0-1000 U/ml) for 7 days. On day 4, IFN-γ Treg responded to the stimulation provided by anti-CD3/CD28 beads and formed clusters as seen under light microscopy ***(Figure 5.2.1.1.3.iia)***. The size of cell clusters was directly proportional to the concentration of exogenous IL-2. At the time of harvest, a small number of IFN-γ Treg survived in IL-2 containing cultures in the absence of anti-CD3/CD28 bead stimulation. IFN-γ Treg stimulated with anti-CD3/CD28 beads plus IL-2 continued to expand in large numbers ***(Figure 5.2.1.1.3.iib)***. In the absence of anti-CD3/CD28 stimulation, a 1.5-fold expansion was seen at the highest IL-2 concentration (1000U/ml) ***(Figure 5.2.1.1.4.i)***. As suggested by the time-line observations above, IFN-γ Treg expanded in large numbers in response to anti-CD3/CD28 beads with a yield generated greater than the input population (up to a 50-fold expansion) directly proportional to the concentration of IL-2 added into the culture ***(Figure 5.2.1.1.4.ii)***.

Figure 5.2.1.1.3. IFN-γ Treg responded to the polyclonal stimuli and expanded *in vitro*

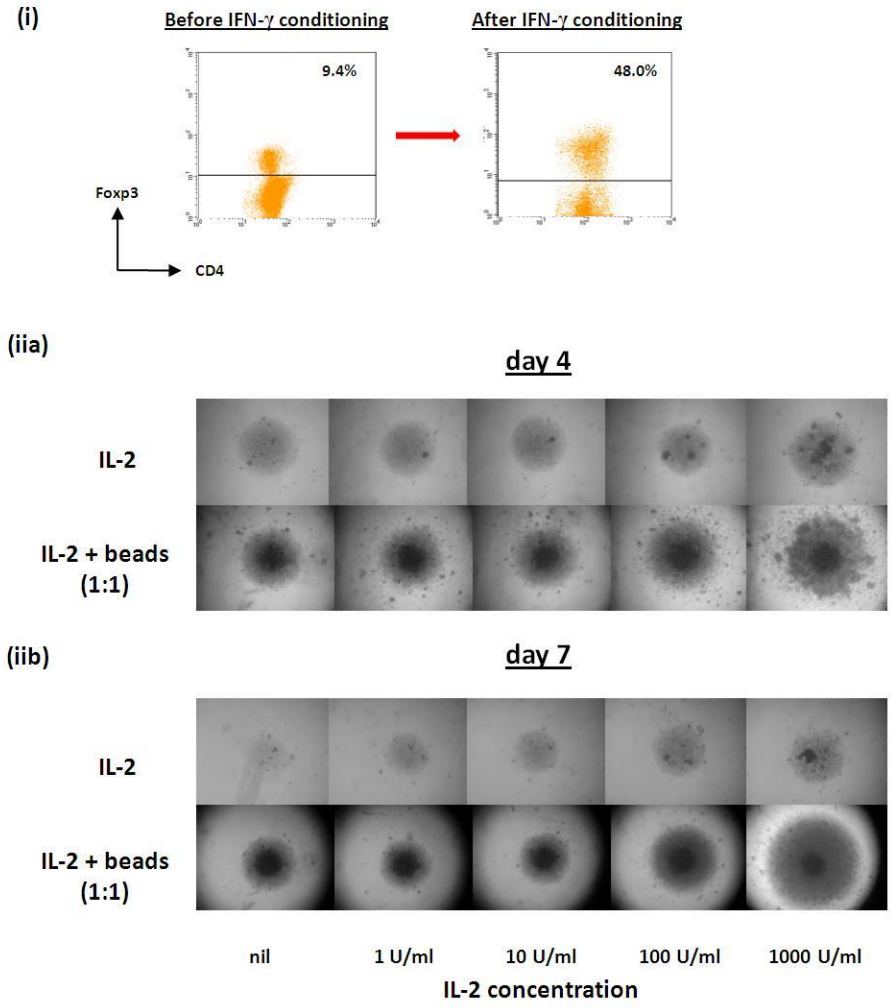

Figure 5.2.1.1.3 IFN-γ Treg responded to the polyclonal stimuli and expanded *in vitro*. (i) Dot plots illustrate that the percentage of Foxp3$^+$ population before and after IFN-γ conditioning. IFN-γ Treg generated from CBA CD4$^+$ precursors showed an enriched Foxp3$^+$ population from 9.4% to 48.0% prior to expansion. **(ii)** When these cells were harvested and subjected to *in vitro* stimulation using IL-2 or IL-2 plus anti-CD3/CD28 beads (at a 1:1 bead to cell ratio), clusters of proliferating IFN-γ Treg were detected in cultures under light microscopy on day 4 **(iia)** and 7 **(iib)**. Minimal IFN-γ Treg proliferation was observed in culture condition with IL-2 alone, whereas IFN-γ Treg proliferated in response to anti-CD3/CD28 bead-driven stimulation. The magnitude of proliferation was directly proportional to the IL-2 concentration. Data above represent results obtained from 2 independent experiments.

Figure 5.2.1.1.4. Expansion of IFN-γ Treg using anti-CD3/CD28 beads and IL-2

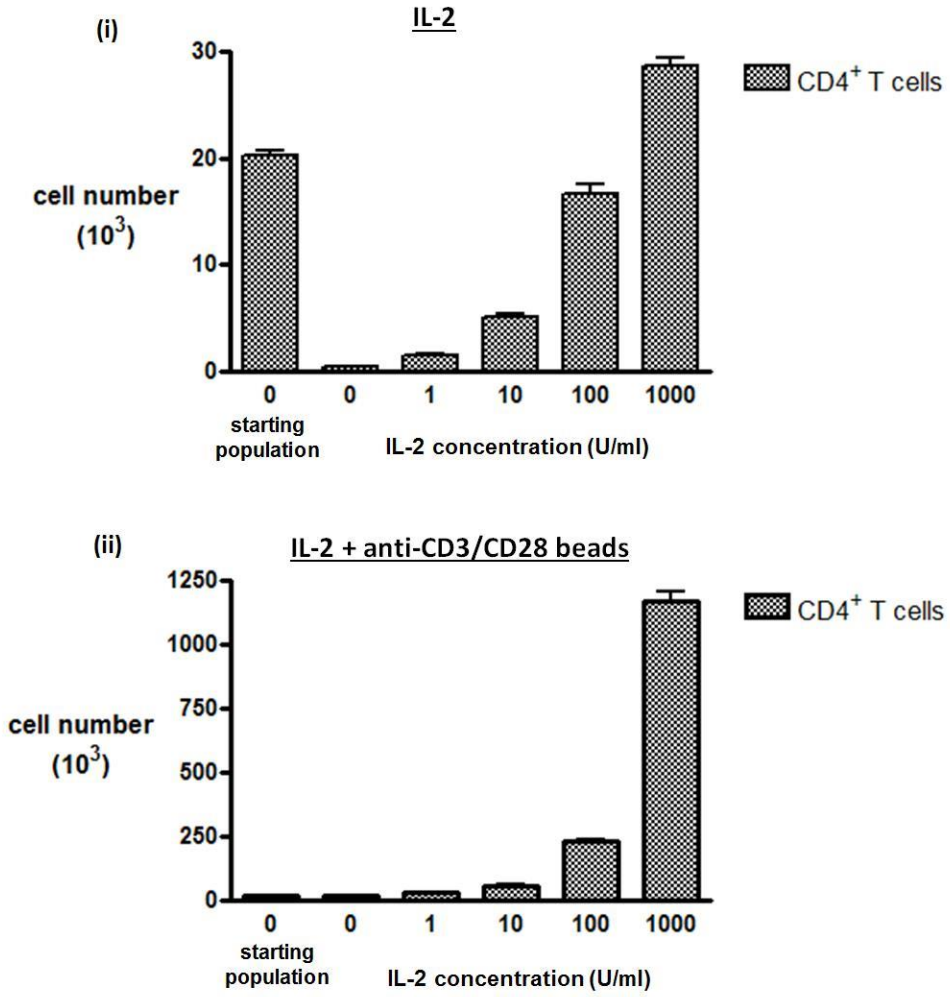

Figure 5.2.1.1.4. Expansion of IFN-γ Treg using anti-CD3/CD28 beads and IL-2. $1x10^5$ freshly- harvested IFN-γ Treg were incubated with various concentrations of IL-2 (0-1000U/ml) in the presence or absence of anti-CD3/CD28 beads (at a 1:1 bead : cell ratio) *in vitro* for 7 days. At the time of harvest, the number of $CD4^+$ T cells was enumerated by flow cytometry using counting beads. **(i)** A high-dose of exogenous IL-2 (minimum of 100 U/ml) provided sufficient growth factors to maintain survival of a small number of IFN-γ Treg without expansion. **(ii)** IFN-γ Treg expanded in response to the polyclonal activation provided by anti-CD3/CD28 beads in the presence of a high-dose IL-2 (>100 U/ml). These data indicate that IFN-γ Treg expanded using this protocol with an increase in the total number of cells (2 to 10-fold). Data above represent means of 3 replicates with error bars showing 1 S.D. from the mean values.

However, when we examined the phenotypic profiles of these expanded cells by flow cytometry analysis the results were disappointing. As shown in ***Figure 5.2.1.1.5.i***, IFN-γ Treg incubated with IL-2 alone resulted in the survival of a dominant, but a very small number of $Foxp3^+$ T cells up to the IL-2 concentration reaching 100U/ml. At 1000U/ml, we observed a resurgence of $Foxp3^-$ cohort in the culture. On the other hand, in the presence of anti-CD3/CD28 stimulation, the dominance of a $Foxp3^+$ population was sustained at low IL-2 concentrations (0-10U/ml). At a higher IL-2 concentration, a predominant $Foxp3^-$ population was observed ***(Figure 5.2.1.1.5.ii)***. The proportion of $Foxp3^+$ T cells present in the expanded population was preserved at a low concentration of IL-2 ***(Figure 5.2.1.1.6.i)***. When the cells were enumerated under each culture condition, we found that the number of cells recoverable was directly proportional to the concentration of IL-2, however, this was achieved in the expense of an exponential outgrowth of the $Foxp3^-$ cohort ***(Figure 5.2.1.1.6.ii)***.

Figure 5.2.1.1.5. Expansion of the Foxp3$^-$ cohort within the IFN-γ Treg population via the action of anti-CD3/CD28 beads and IL-2 *in vitro*

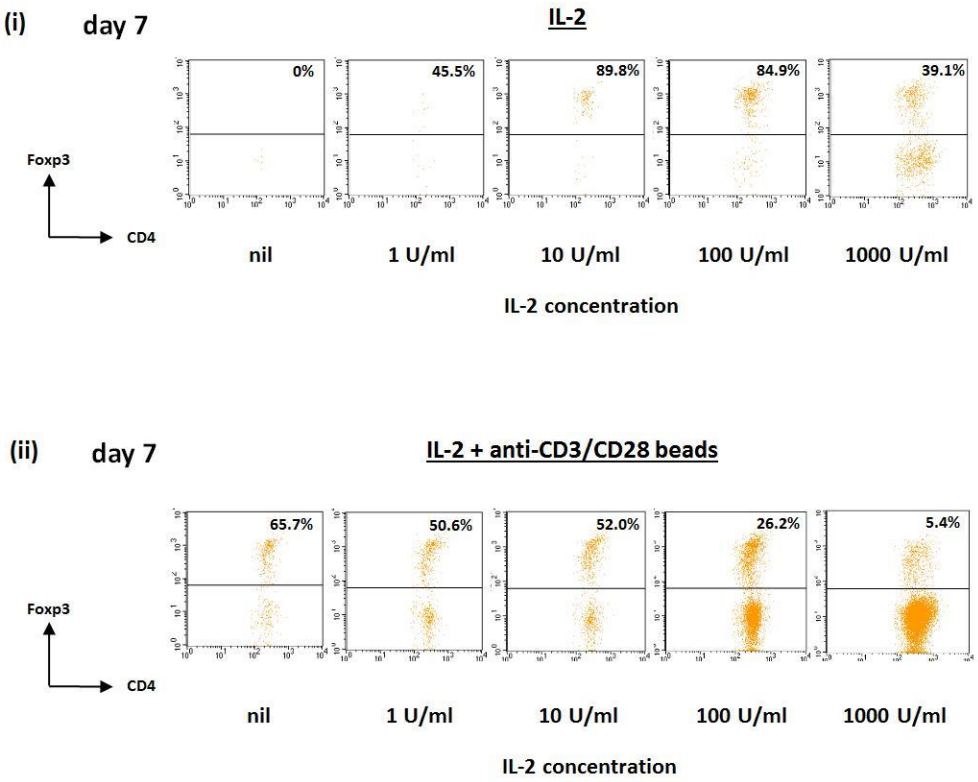

Figure 5.2.1.1.5. Expansion of the Foxp3$^-$ cohort within the IFN-γ Treg population via the action of anti-CD3/CD28 beads and IL-2 *in vitro*. Representative dot plots illustrate the Foxp3 expression on CD4$^+$ T cells in the resultant IFN-γ Treg population after stimulated with IL-2 or IL-2 plus anti-CD3/CD28 beads *in vitro* for 7 days. **(i)** Without anti-CD3/CD28 beads, a small number of CD4$^+$ Foxp3$^+$ T cells sustained in the presence of IL-2 at a concentration between 10 to 100 U/ml. However, at a higher IL-2 concentration (i.e. 1000 U/ml) both Foxp3$^+$ and Foxp3$^-$ T cells sustained but the culture was dominated by the Foxp3$^-$ cohort. **(ii)** In the presence of anti-CD3/CD28 beads, Foxp3$^+$ T cells dominated in the culture at low IL-2 concentrations. The Foxp3$^-$ cohort was dominated in the resultant population when the concentration of IL-2 was elevated ≥100 U/ml. Data above represent results obtained from 3 independent experiments.

Figure 5.2.1.1.6. Expansion of IFN-γ Treg using anti-CD3/CD28 beads and IL-2 resulted in an outgrowth of the Foxp3⁻ cohort

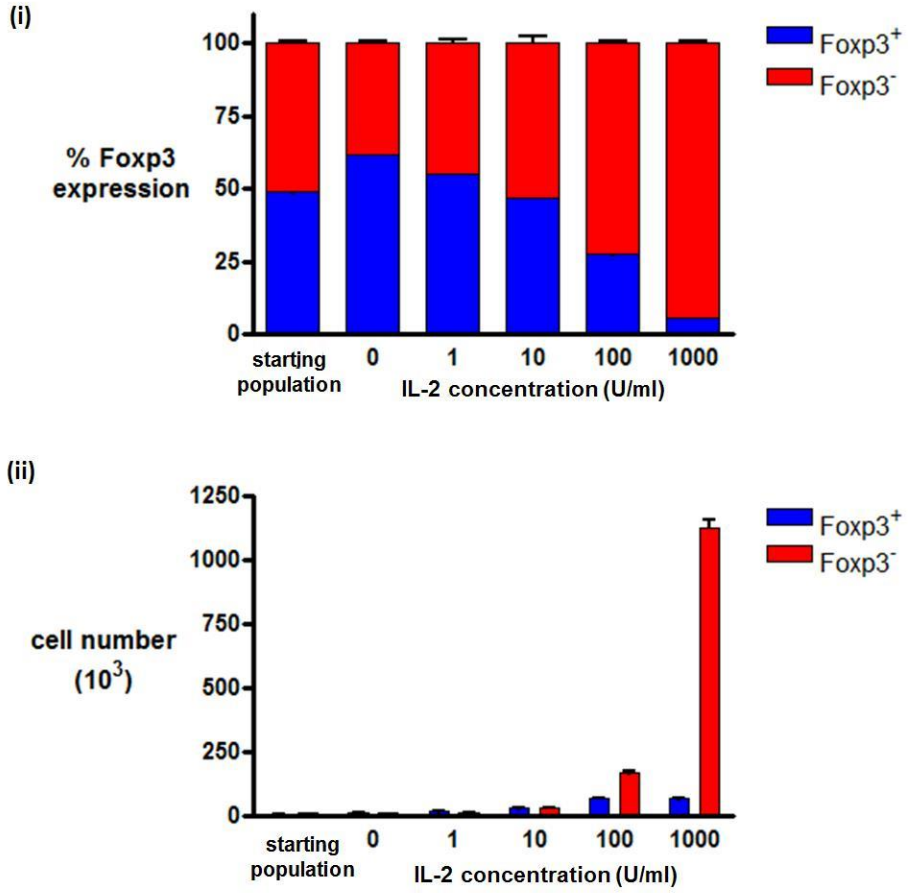

Figure 5.2.1.1.6. Expansion of IFN-γ Treg using anti-CD3/CD28 beads and IL-2 resulted in an outgrowth of the Foxp3⁻ cohort. (i) Bar charts represent the distribution of Foxp3⁺ and Foxp3⁻ population in culture after 7 days of expansion in percentages. At low IL-2 concentrations (1-10 U/ml) the proportion of Foxp3⁺ sustained at the levels similar to the starting population. The proportion of Foxp3⁺ cohort dropped by >50% when the IL-2 concentration exceeded 100 U/ml. **(ii)** Prominent IFN-γ Treg expansion occurred at IL-2 concentration exceeding 100 U/ml, however, this was accompanied by an outgrowth of Foxp3⁻ cohort in cultures. While there was dramatic expansion of the Foxp3⁻ cohort, there was no real expansion of the Foxp3⁺ cohort. Cell numbers were calculated based on flow cytometry analysis using counting beads. Data above represent means of 3 replicates with error bars showing 1 S.D. from the mean values.

According to the observations above, an optimal dose of exogenous IL-2 appeared to be in the range of 100U/ml in order to obtain a reasonable $Foxp3^+$ T cell expansion without an overwhelming outgrowth of $Foxp3^-$ T cells. An extended period of stimulation with anti-CD3/CD28 beads with IL-2 up to 14 days led to a further reduction of the proportion and absolute number of the $Foxp3^+$ population *(data not shown)*. We then attempted to manipulate this *in vitro* expansion protocol by increasing the bead:cell ratio from 1:1 to 2:1 and 4:1 for the expansion of IFN-γ Treg in a graded IL-2 concentration (0-1000U/ml) for 7 days. $1x10^4$ freshly-harvested IFN-γ Treg contained a 48.0% $Foxp3^+$ population on day 0 as determined by flow cytometry analysis. When the bead:cell ratio was increased from 1:1 to 2:1 and 4:1, the proportion of $Foxp3^+$ IFN-γ Treg decreased to a lower level than the starting population, inversely proportional to the IL-2 concentration ***(Figure 5.2.1.1.7.i, ii & iii)***. Using the optimal IL-2 concentration (100U/ml), the proportion of the $Foxp3^+$ cohort was inversely proportional to the number of beads added ***(Figure 5.2.1.1.7.iv)***. The dominance of $Foxp3^-$ cohorts under these culture conditions is illustrated in ***Figure 5.2.1.1.8***. Overall T cell growth was seen with a 1:1 bead to cell ratio with a dominant $Foxp3^-$ cohort at high IL-2 concentration (1000U/ml) ***(Figure 5.2.1.1.8.i)***. At a higher bead: cell ratios (2:1 or 4:1), there was no improvement in the number of recoverable cells, but a sustained dominant $Foxp3^-$ cohort in culture ***(Figure 5.2.1.1.8.ii & iii)***. At the optimal IL-2 concentration (100U/ml), additional anti-CD3/CD28 beads did not reverse the outgrowth of the $Foxp3^-$ cohorts ***(Figure 5.2.1.1.8.iv)***. We also titrated down the bead:cell ratio against a graded IL-2 concentration and observed a similar situation where there was definitive T cell expansion, but a dominant $Foxp3^-$ cohort persisted ***(Figure 5.2.1.1.9.i & ii)***. In short, the initial attempts to expand IFN-γ Treg using the anti-CD3/CD28 bead protocol did not achieve a preferential expansion of $Foxp3^+$ IFN-γ Treg.

With the notion that IFN-γ could potentially induce AICD preferentially in the $Foxp3^-$ population, we attempted to incorporate exogenous IFN-γ in the anti-CD3/CD28 bead expansion protocol. $2x10^4$ freshly-harvested IFN-γ Treg with a starting $Foxp3^+$ population of 28.8% were expanded with ant-CD3/CD28 beads (1:1 ratio) in the presence of a graded concentration of IL-2 (0-1000U/ml), with or without exogenous IFN-γ (5ng/ml) for 7 days. The $Foxp3^+$ and $Foxp3^-$ cohorts were enumerated in each culture condition by flow cytometry analysis. In the absence of anti-CD3/CD28 bead stimulation, exogenous IFN-γ had no impact on the persistence of the outgrowth of the $Foxp3^-$ cohort ***(Figure 5.2.1.1.10.i)***. When IFN-γ Treg were restimulated with anti-CD3/CD28 beads plus IL-2 in the presence of exogenous IFN-γ, we continued to detect an outgrowth of the $Foxp3^-$ cohort ***(Figure 5.2.1.1.10.ii)***.

Figure 5.2.1.1.7. Increasing the number of anti-CD3/CD28 beads failed to improve the expansion of the Foxp3$^+$ cohort of IFN-γ Treg

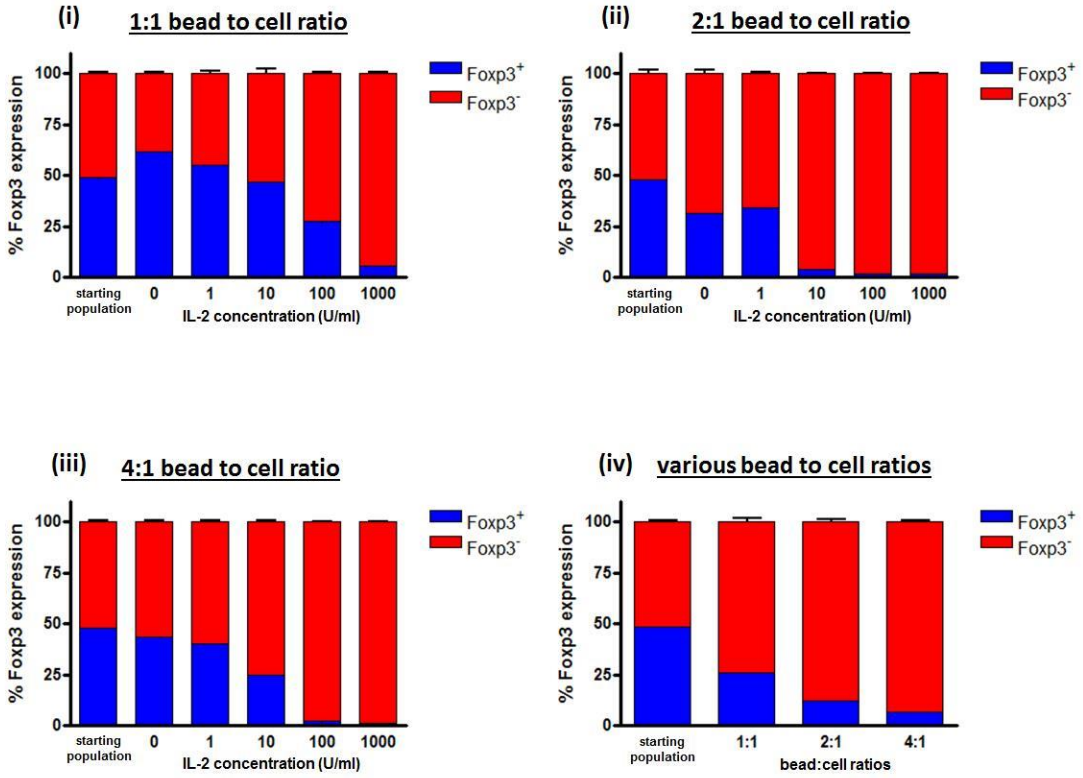

Figure 5.2.1.1.7. Increasing the number of anti-CD3/CD28 beads failed to improve the expansion of the Foxp3$^+$ cohort of IFN-γ Treg. Bar charts show the proportion of the Foxp3$^+$ and Foxp3$^-$ cohorts in the resultant IFN-γ Treg population after being stimulated with anti-CD3/CD28 beads at **(i)** 1:1 bead to cell ratio; **(ii)** 2:1 bead to cell ratio; and **(iii)** 4:1 bead to cell ratio at various concentrations of IL-2 for 7 days. Additional anti-CD3/CD28 beads did not favour a higher proportion of Foxp3$^+$ Treg within the expanded IFN-γ Treg population. **(iv)** A direct comparison between culture conditions using anti-CD3/CD28 beads at a 1:1, 2:1 and 4:1 bead to cell ratio indicated that an increased number of polyclonal stimulation led to a dominant Foxp3$^-$ cohort in the expanded IFN-γ Treg population when a high dose of IL-2 was used (100 U/ml). Data above represent means of 3 replicates with error bars showing 1 S.D. from the mean values.

Figure 5.2.1.1.8. Significant outgrowth of the Foxp3⁻ cohort of IFN-γ Treg persisted when the number of anti-CD3/CD28 beads was increased at a high IL-2 concentration

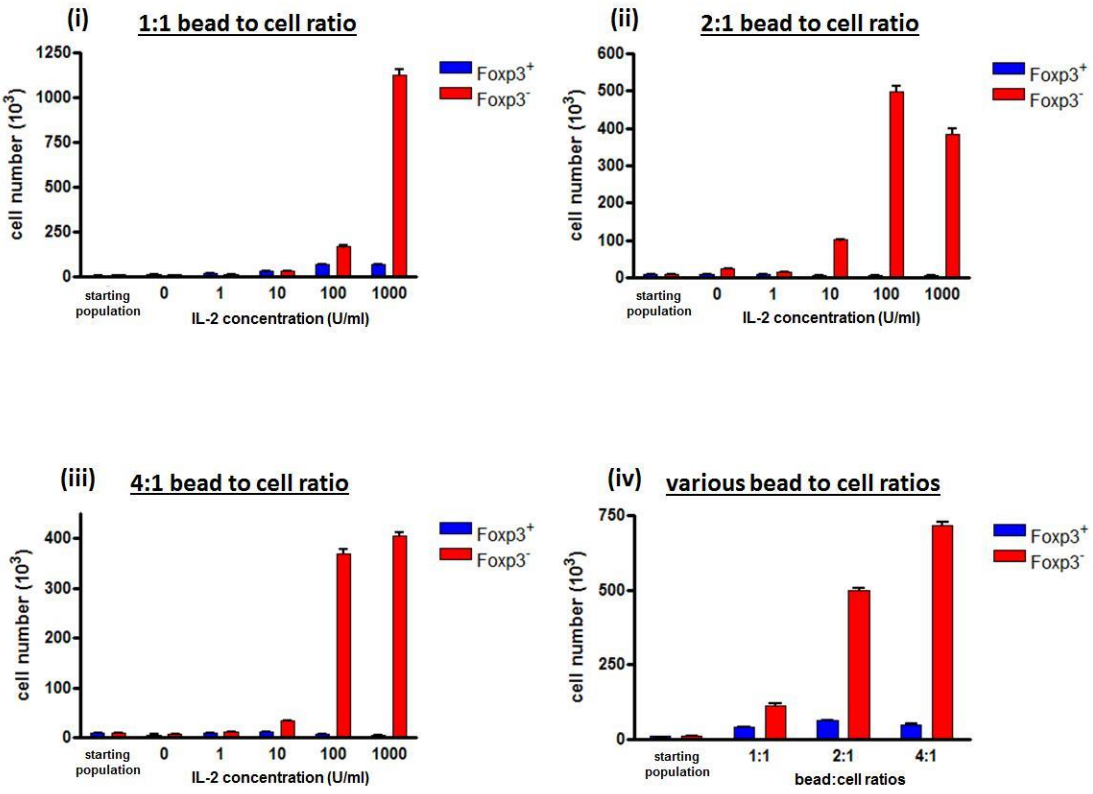

Figure 5.2.1.1.8. Significant outgrowth of the Foxp3⁻ cohort of IFN-γ Treg persisted when the number of anti-CD3/CD28 beads was increased at a high IL-2 concentration. The number of Foxp3⁺ and Foxp3⁻ T cells were enumerated in the resultant IFN-γ Treg population after being expanded with anti-CD3/CD28 beads at **(i)** 1:1 bead to cell ratio; **(ii)** 2:1 bead to cell ratio; and **(iii)** 4:1 bead to cell ratio at various concentrations of IL-2 for 7 days. At high IL-2 concentrations (>100 U/ml), anti-CD3/CD28 bead stimulation at 1:1, 2:1 or 4:1 bead to cell ratio led to an exponential outgrowth of the Foxp3⁻ cohorts. At low IL-2 concentrations (10 U/ml), no expansion of the Foxp3⁺ or Foxp3⁻ cohorts was observed. **(iv)** At the optimal IL-2 concentration (100 U/ml), an increased number of anti-CD3/CD28 beads enhanced the proliferation of Foxp3⁻ cohort but not the Foxp3⁺ cohort. Data above represent means of 3 replicates with error bars showing 1 S.D. from the mean values.

Figure 5.2.1.1.9. Reducing the number of anti-CD3/CD28 beads worsened the output of expanded IFN-γ Treg

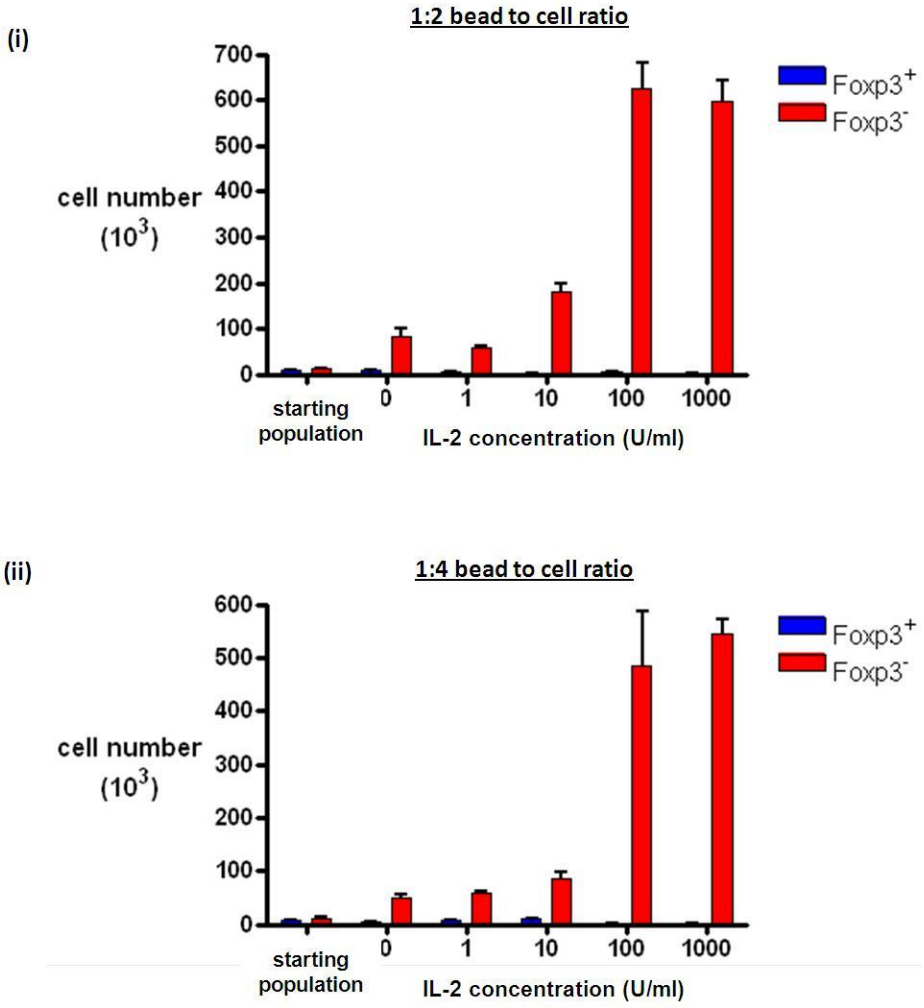

Figure 5.2.1.1.9. Reducing the number of anti-CD3/CD28 beads worsened the output of expanded IFN-γ Treg. $2x10^4$ IFN-γ Treg (40.4% $Foxp3^+$ as determined by flow cytometry analysis) were stimulated with $1x10^4$ or $5x10^3$ anti-CD3/CD28 beads in the presence of a graded concentration of IL-2 (0-1000 U/ml) for 7 days. Further titration of bead to cell ratio to 1:2 **(i)** or 1:4 **(ii)** against a range of IL-2 concentrations revealed that the $Foxp3^+$ cohort failed to expand, whereas the $Foxp3^-$ cohort expanded efficiently under the same culture conditions. Data above represent means of 3 replicates with error bars showing 1 S.D. from the mean values.

Figure 5.2.1.1.10. Exogenous IFN-γ in the anti-CD3/CD28 bead expansion protocol failed to remove the outgrowth of the Foxp3⁻ cohort of IFN-γ Treg

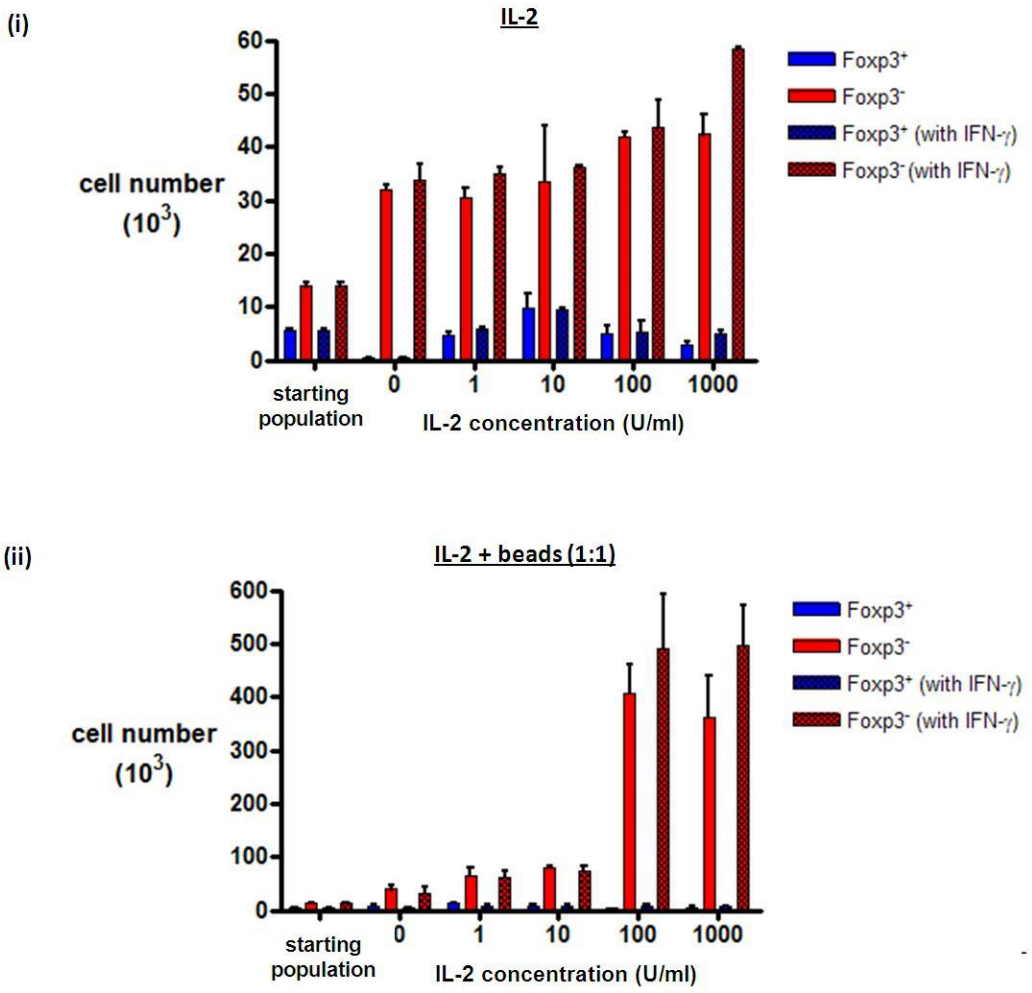

Figure 5.2.1.1.10. Exogenous IFN-γ in the anti-CD3/CD28 bead expansion protocol failed to remove the outgrowth of the Foxp3⁻ cohort of IFN-γ Treg. With the notion that IFN-γ has the ability to induce AICD *in vitro*, we investigated if the addition of exogenous IFN-γ could alter the composition of the expanded product. **(i)** IFN-γ Treg were generated as described above and then incubated with IL-2 for 7 days in the presence or absence of IFN-γ (5ng/ml). The addition of IFN-γ could not induce preferential selection of Foxp3⁺ cohort after 7 days of expansion. **(ii)** When IFN-γ Treg were stimulated with anti-CD3/CD28 beads in the presence of IL-2, the addition of IFN-γ showed no impact on the expansion of Foxp3⁺ population. The outgrowth of Foxp3⁻ cohort could not be prevented by the addition of exogenous IFN-γ *in vitro*. Data above represent means of 3 replicates with error bars showing 1 S.D. from the mean values.

5.2.1.2 Expansion of IFN-γ Treg using allogeneic mature BM-DC

With reference to separate reports by Yamazaki et al[443] and Liu et al[506] that allogeneic mature bone marrow-derived DC (mBM-DC) were superior to splenic $CD11c^+$ DC or syngeneic DC for the expansion of nTreg *in vitro*, we next attempted to expand IFN-γ Treg with allogeneic mBM-DC in the presence of exogenous IL-2. Similar to a traditional MLR, we aimed to expand IFN-γ Treg with allogeneic APC, which we hypothesized might provide a more physiological milieu of costimulation interaction for optimal Treg expansion. In theory, the pro-apoptotic $Foxp3^-$ cohort in the resultant population of IFN-γ Treg would undergo activation-induced cell death, which would then lead to a preferential expansion of $Foxp3^+$ IFN-γ Treg ***(Figure 5.2.1.2.1)***.

B6 mBM-DC were generated by culturing bone marrow cells with GM-CSF (20ng/ml) with or without IL-4 (10ng/ml) for 6 days and matured overnight using LPS (50ng/ml) as described in ***Chapter 2.7.7***[507]. $2x10^4$ Freshly-harvested CBA IFN-γ Treg (40.4% $Foxp3^+$ as determined by flow cytometry analysis) were then co-cultured with allogeneic B6 mBM-DC (previously cultured with or without IL-4 in addition to GM-CSF) at a 1:1 ratio plus a graded concentration of exogenous IL-2 (0-1000U/ml) for 7 days ***(Figure 5.2.1.2.2)***. Cultures using mBM-DC cultured without IL-4 as stimuli appeared to lead to a lower number of cells being recovered compared to that of mBM-DC cultured in IL-4 (2 to 10-fold difference in overall cell yield). More specifically, there was no expansion of the $Foxp3^+$ cohort compared to the input population, but the outgrowth of the $Foxp3^-$ cohort persisted when IFN-γ Treg were stimulated with mBM-DC cultured without IL-4 ***(Figure 5.2.1.2.2.i)***. Similarly, IFN-γ Treg stimulated with mBM-DC cultured with IL-4 also showed no expansion of the $Foxp3^+$ cohort in all culture conditions, but a more profound outgrowth of the $Foxp3^-$ cohort (20-fold expansion), which was directly proportional to the IL-2 concentration ***(Figure 5.2.1.2.2.ii)***.

Figure 5.2.1.2.1. Expansion of IFN-γ Treg using allogeneic mature BM-DC and IL-2 *in vitro*

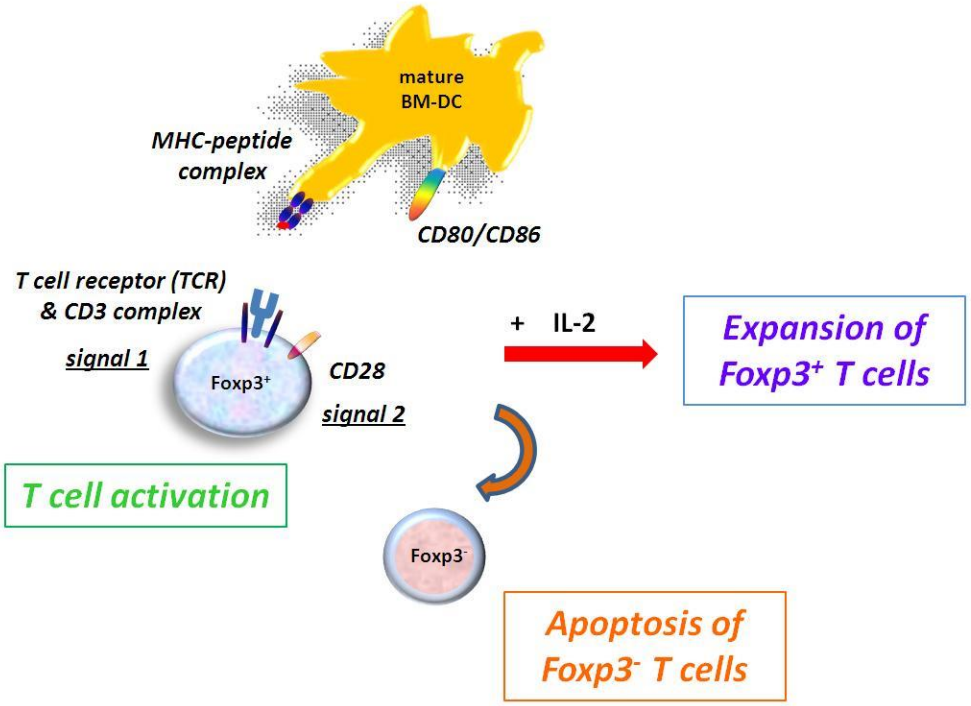

Figure 5.2.1.2.1. Expansion of IFN-γ Treg *in vitro* using allogeneic mature BM-DC and IL-2 *in vitro*. Mixed lymphocyte reactions (MLRs) could lead to profound T cell proliferation and expansion. Mature bone marrow-derived dendritic cells (mBM-DC) were generated from B6 bone marrow cells cultured in GM-CSF (20ng/ml) for 6 days then matured with LPS (20ng/ml) overnight using the conventional BM-DC generation protocol as described in ***Chapter 2.7.7***. CBA IFN-γ Treg were stimulated with allogeneic B6 mBM-DC, which could provide the alloantigenic stimulation, as well as a near physiological profile of costimulatory signals for full T cell activation. In the presence of exogenous IL-2, activated T cells proliferated. Our hypothesis was that in the absence of exogenous IFN-γ, the $Foxp3^+$ cohort in freshly-isolated IFN-γ Treg which had already been activated with alloantigens *in vitro* for 14 days would then respond and expand in the presence of new alloantigen challenge and IL-2; while the pro-apoptotic $Foxp3^-$ cohort would undergo AICD and apoptosis.

Figure 5.2.1.2.2. Outgrowth of the Foxp3$^-$ cohort IFN-γ Treg persisted when expanded using allogeneic mBM-DC and IL-2 *in vitro*

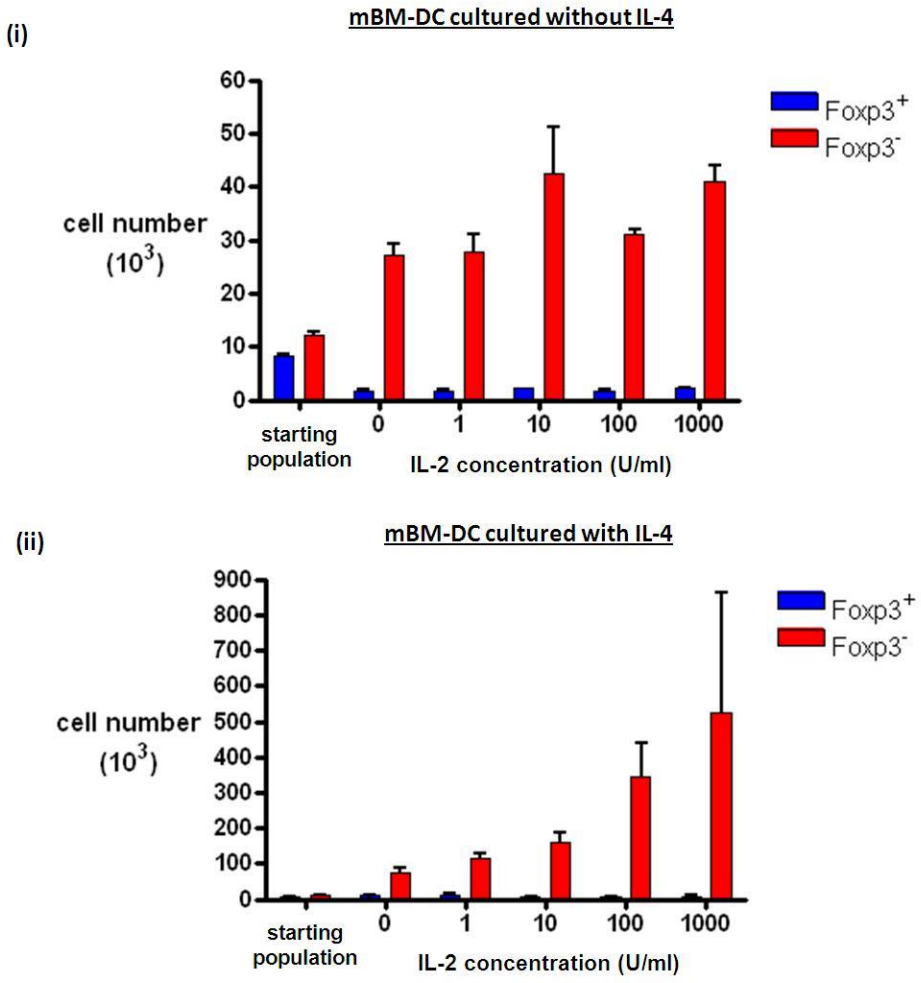

Figure 5.2.1.2.2. Outgrowth of the Foxp3$^-$ cohort IFN-γ Treg persisted when expanded using allogeneic mBM-DC and IL-2 *in vitro*. Mature bone marrow-derived DC (mBM-DC) were prepared with or without IL-4 as described in ***Chapter 2.7.7***. 2x10^4 IFN-γ Treg were stimulated with B6 allogeneic mBM-DC (at a 1:1 mBM-DC to IFN-γ Treg ratio) and various concentrations of IL-2 (0-1000 U/ml) for 7 days *in vitro*. **(i)** The proportion and the number of the Foxp3$^+$ population was reduced compared to the initial starting population regardless the concentration of IL-2 in cultures when IFN-γ Treg were stimulated with allogeneic mBM-DC generated without IL-4. **(ii)** The Foxp3$^-$ cohort of IFN-γ Treg expanded and outgrew the Foxp3$^+$ counterparts, which was directly proportional to the concentration of IL-2 in cultures; whereas the Foxp3$^+$ cohort did not expand in response to the stimulation provided by allogeneic mBM-DC generated with IL-4. Data above represent means of 3 replicates with error bars showing 1 S.D. from the mean values.

Titration of the mBM-DC:IFN-γ Treg ratio had no impact on the expansion of $Foxp3^+$ cohort ***(Figure 5.2.1.2.3)***. $2x10^4$ IFN-γ Treg were expanded with mBM-DC at various mBM-DC:IFN-γ Treg ratios (1:1, 2:1 and 4:1), in the presence of IL-2 at 100U/ml, or at a 2:1 mBM-DC:IFN-γ Treg ratio plus IL-2 at 2000U/ml. IFN-γ Treg stimulated with an increasing number of mBM-DC cultured without IL-4 resulted in an increasing outgrowth of the $Foxp3^-$ cohort (up to a 3-fold expansion) without any demonstrable expansion of the $Foxp3^+$ cohort ***(Figure 5.2.1.2.3.i)***. A higher mBM-DC: IFN-γ Treg ratio (2:1) plus a higher concentration of IL-2 (2000U/ml) had no impact on the expansion of $Foxp3^+$ Treg either. IFN-γ Treg stimulated with an increased number of mBM-DC cultured in IL-4 also led to a dominant $Foxp3^-$ cohort in the resultant population. However, the highest magnitude of the outgrowth of the $Foxp3^-$ cohort was observed when IFN-γ Treg were stimulated at the 1:1 mBM-DC: IFN-γ Treg ratio ***(Figure 5.2.1.2.3.ii)***. Collectively, after several attempts we were yet to develop a successful Treg expansion protocol using either an anti-CD3/CD28 bead-based or an alloantigen-based system.

Figure 5.2.1.2.3. Increasing the number of allogeneic mature BM-DC did not reverse the outgrowth of the Foxp3$^-$ cohort of IFN-γ Treg

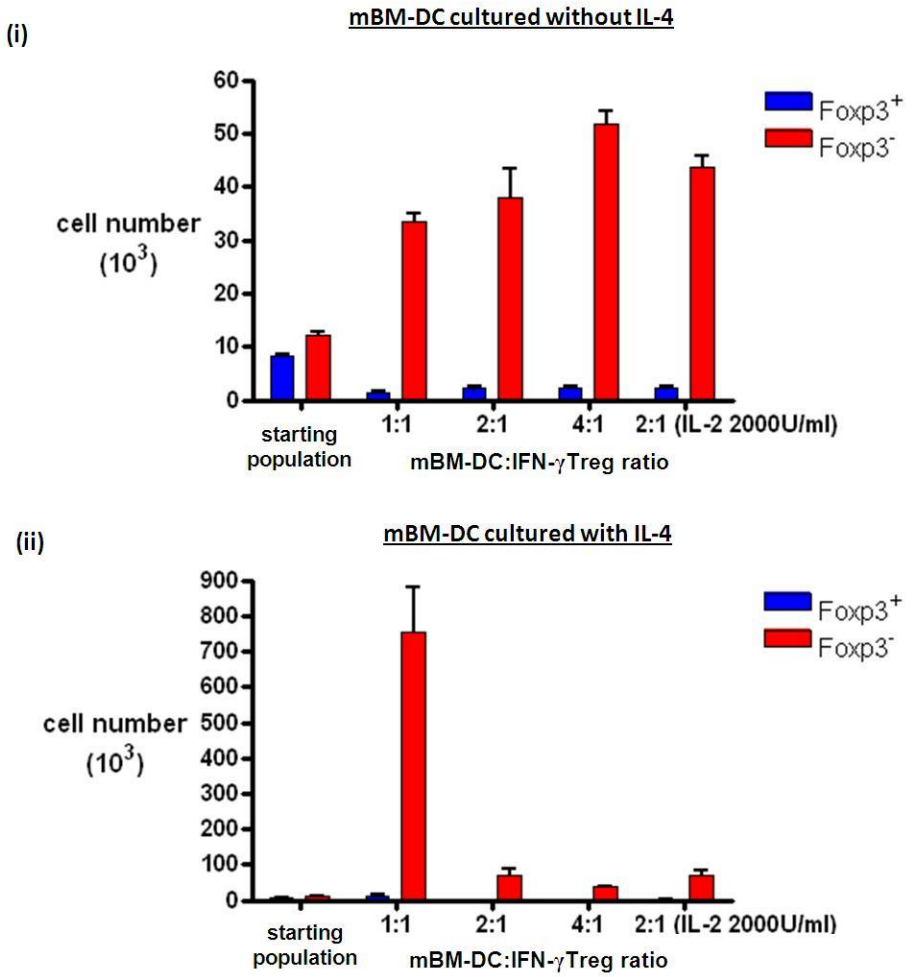

Figure 5.2.1.2.3. Increasing the number of allogeneic mature BM-DC did not reverse the outgrowth of the Foxp3$^-$ cohort of IFN-γ Treg. Allogeneic mature bone marrow-derived DC (mBM-DC) were prepared with or without IL-4 as described in ***Chapter 2.7.7***. IFN-γ Treg were stimulated with mBM-DC (at a 1:1, 2:1 or 4:1 mBM-DC to IFN-γ Treg ratio) in the presence of IL-2 (100 U/ml), or at 2:1 ratio with IL-2 at 2000 U/ml. **(i)** mBM-DC generated without IL-4 led to an expansion of the Foxp3$^-$ cohort of IFN-γ Treg up to a 5-fold increase, which was directly proportional to the ratio of mBM-DC to IFN-γ Treg. On the other hand, there was no expansion of the Foxp3$^+$ cohort. **(ii)** mBM-DC generated with IL-4 led to a more efficient expansion of the Foxp3$^-$ cohort when delivered at a 1:1 mBM-DC:IFN-γ Treg ratio. However, there was no expansion of the Foxp3$^+$ cohort. Data above represent means of 3 replicates with error bars showing 1 S.D. from the mean values.

5.2.1.3 Expansion of IFN-γ Treg using other potential T cell proliferation stimuli

We next turned to investigate the addition of established T cell growth factor such as Concanavalin A supernatant (ConA sup) to incorporate into the anti-CD3/CD28 bead system. ConA sup was traditionally used as supplementary culture medium for the maintenance of T cell clones and was subsequently found to contain a milieu of T cell growth factors including IL-2[508-510]. ConA sup was prepared from rat splenocytes according to established protocol as described in ***Chapter 2.6.5***[511]. $2x10^4$ freshly-harvested IFN-γ Treg (28.8% $Foxp3^+$ as determined by flow cytometry analysis) were cultured in a graded concentration of ConA sup, with or without anti-CD3/CD28 beads (1:1 ratio), in the presence or absence of exogenous IFN-γ (5ng/ml) ***(Figure 5.2.1.3.1)***. In the absence of anti-CD3/CD28 stimulation, ConA supernatant alone had no impact on the growth of IFN-γ Treg. In addition, exogenous IFN-γ with anti-CD3/CD28 beads plus Con A supernatant yielded similar results where the cultures were dominated by a $Foxp3^-$ population (>95%) ***(Figure 5.2.1.3.1.i)***. When IFN-γ Treg were stimulated with anti-CD3/CD28 beads in the presence of ConA sup, a larger number of cells were recovered directly proportional to the concentration of ConA sup (up to a 2-fold increase). However, these cultures were again dominated by a $Foxp3^-$ cohort (>90%). The addition of exogenous IFN-γ could not reverse the outgrowth of non-Treg in these cultures ***(Figure 5.2.1.3.1.ii)***.

Figure 5.2.1.3.1. The Foxp3$^+$ cohort of IFN-γ Treg responded modestly to the stimulation provided by a combination of anti-CD3/CD28 beads and ConA supernatant

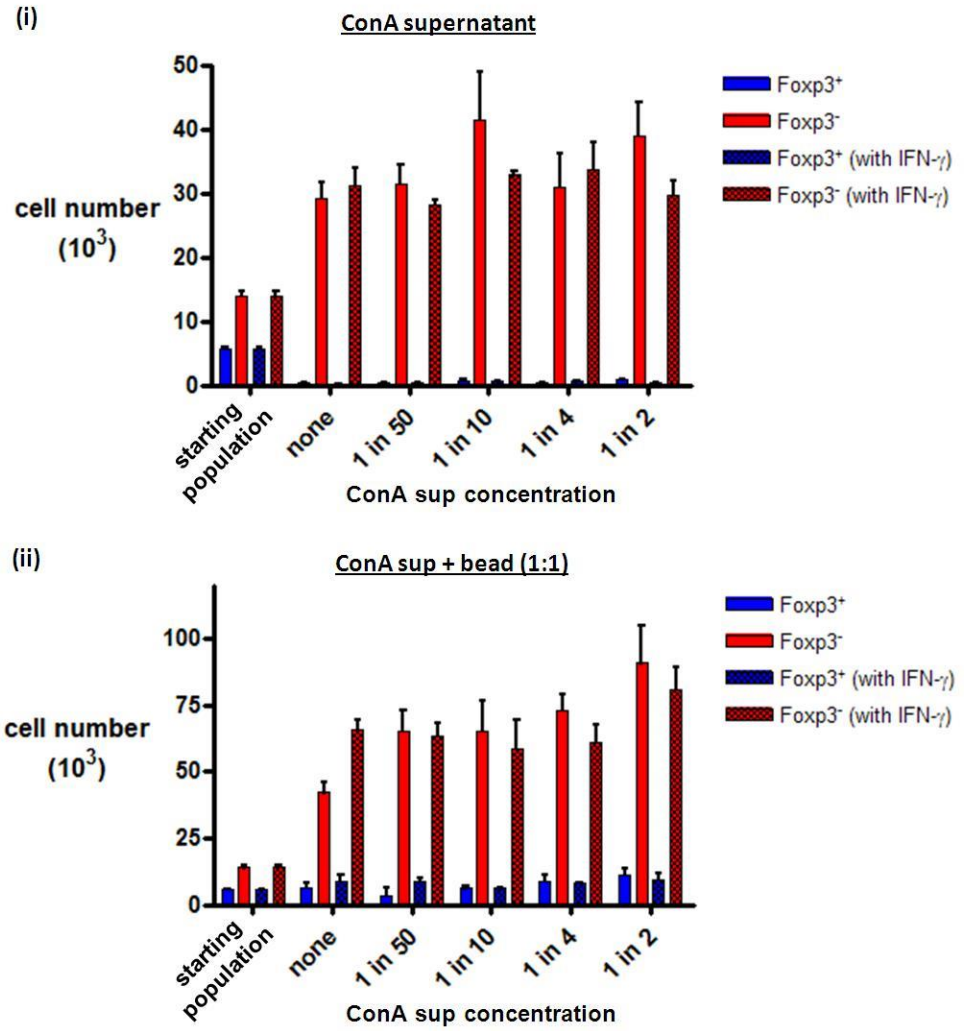

Figure 5.2.1.3.1. The Foxp3$^+$ cohort of IFN-γ Treg responded modestly to the stimulation provided by a combination of anti-CD3/CD28 beads and ConA supernatant. (i) ConA supernatant was prepared as described in ***Chapter 2.6.5***. 2x10^4 IFN-γ Treg (28.8% Foxp3$^+$ as determined by flow cytometry analysis) were incubated with ConA supernatant with or without anti-CD3/CD28 beads at a 1:1 bead to cell ratio. The Foxp3$^+$ cohort of IFN-γ Treg did not expand in response to ConA supernatant. On the other hand, the Foxp3$^-$ cohort expanded with a 2-fold increase. The addition of IFN-γ (5 ng/ml) had no effect on the T cell growth. **(ii)** In the presence of anti-CD3/CD28 stimulation, the Foxp3$^-$ cohort expanded directly proportional to the concentration of ConA supernatant. On the other hand, the Foxp3$^+$ cohort only expanded modestly in response to anti-CD3/CD28 stimulation at high concentration of ConA supernatant. The addition of IFN-γ did not lead to preferential AICD of the Foxp3$^-$ cohort. Data above represent means of 3 replicates with error bars showing 1 S.D. from the mean values.

As opposed to the replacement of T cell growth factors, we aimed to investigate the potential of expanding IFN-γ Treg with traditional mouse T cell mitogens such as concanavalin A (ConA)[512] in place of anti-CD3/CD28 beads. $2x10^4$ freshly-harvested IFN-γ Treg (28.8% $Foxp3^+$ as determined by flow cytometry analysis) were expanded with ConA (0-50ng/ml), with or without exogenous IFN-γ (5ng/ml). As shown in ***Figure 5.2.1.3.2***, IFN-γ Treg responded to the mitogenic stimulation provided by ConA with an expansion up to a 1.5-fold increase of the overall cell number. However, these cultures were again dominated by the $Foxp3^-$ cohort (>95%). The addition of exogenous IFN-γ did not reverse the dominance of the $Foxp3^-$ cohort, but appeared to enhance to the proliferation of $Foxp3^-$ cells at low concentration of ConA (1-10ng/ml), compared to cultures without exogenous IFN-γ.

Figure 5.2.1.3.2. Expansion of IFN-γ Treg using Concanavalin A mitogens

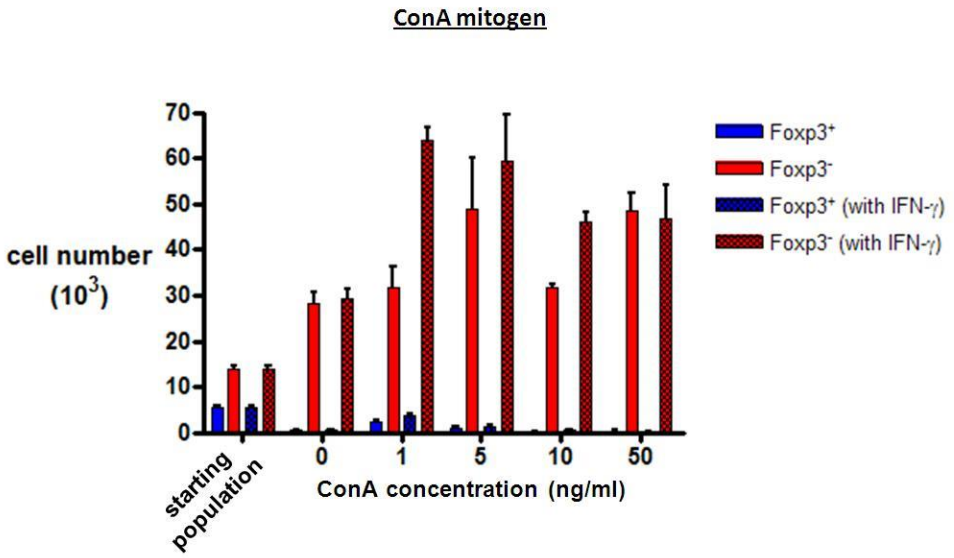

Figure 5.2.1.3.2 Expansion of IFN-γ Treg using Concanavalin A mitogens. $2x10^4$ IFN-γ Treg were stimulated with Concanavalin A (ConA) mitogen at a concentration between 0-50 ng/ml, in the presence or absence of exogenous IFN-γ (5 ng/ml) for 7 days. In the absence of exogenous IFN-γ, the $Foxp3^-$ cohort of IFN-γ Treg responded to the stimulus provided by ConA and expanded up to a 1.5-fold increase. To our surprise, exogenous IFN-γ appeared to enhance the expansion of the $Foxp3^-$ cohort in some instances. There was no expansion of the $Foxp3^+$ cohort regardless the concentrations of ConA mitogens tested. Exogenous IFN-γ did not lead to preferential AICD of the $Foxp3^-$ cohort when IFN-γ Treg were stimulated by ConA mitogens. Data above represent means of 3 replicates with error bars showing 1 S.D. from the mean values.

5.2.1.4 Expansion of cryopreserved IFN-γ Treg with anti-CD3/CD28 beads plus rapamycin

Cryopreservation and the thawing process might trigger pro-apoptotic cells to die. We exploited this theoretical phenomenon to test if we could expand cryopreserved IFN-γ Treg which contained a significant proportion of pro-apoptotic $Foxp3^-$ non-Treg in the resultant population after IFN-γ conditioning. In addition, we added a graded concentration of rapamycin to drive the culture environment to be favourable to Foxp3 enrichment as rapamycin has been shown to facilitate the expansion of $CD4^+CD25^+Foxp3^+$ Treg preferentially *in vitro*[488].

Freshly-harvested IFN-γ Treg contained a high $Foxp3^+$ population (80.1% $Foxp3^+$) as determined by flow cytometry analysis prior to the cryopreservation processes ***(Figure 5.2.1.4.1.i)***. Cryopreserved and thawed IFN-γ Treg retained the enrichment of Foxp3-expressing cells as shown in ***Figure 5.2.1.4.1.ii***. The Foxp3 expression of thawed IFN-γ Treg was re-checked prior to the expansion process and compared to that of an isotype control (84.9% versus 1.0%). On this occasion, in order to mimic the protocol as described by Battaglia et al[488], we increased the initial input number to $1x10^5$, the bead:cell ratio to 3:1, and the IL-2 concentration to 2000U/ml.

Figure 5.2.1.4.1. Expansion of cryopreserved IFN-γ Treg using anti-CD3/CD28 beads and IL-2

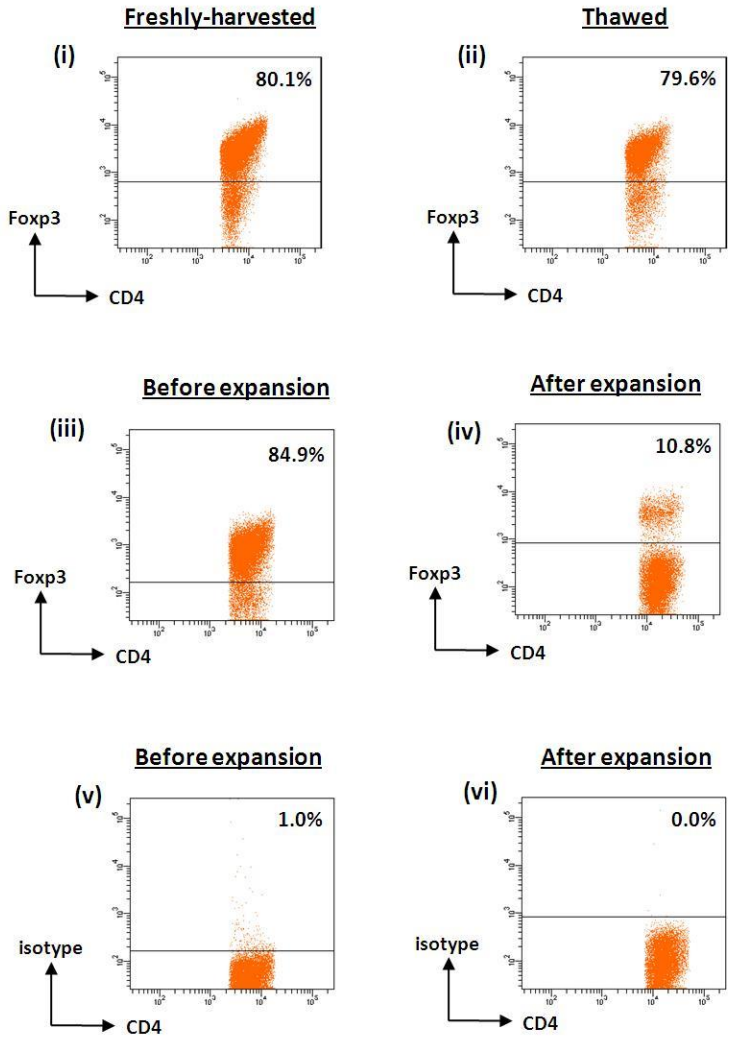

Figure 5.2.1.4.1 Expansion of cryopreserved IFN-γ Treg using anti-CD3/CD28 beads and IL-2. The Foxp3 expression on **(i)** freshly-harvested and **(ii)** cryopreserved IFN-γ Treg was examined using flow cytometry. Cryopreserved IFN-γ Treg were stimulated with anti-CD3/CD28 beads (at 1:1 bead to cell ratio) in the presence of a high dose IL-2 (2000 U/ml) for 7 days. A significant reduction of Foxp3 expression in cryopreserved IFN-γ Treg was observed following expansion using anti-CD3/CD28 beads and IL-2 from 84.9% **(iii)** to 10.8% **(iv)**, compared to isotype controls **(v & vi)**. Data above represent results obtained from at least 2 independent experiments.

Despite having a very high Foxp3$^+$ starting population, the expanded cryopreserved IFN-γ Treg population contained a predominant Foxp3$^-$ cohort (>95%) after 7 days, in the absence of rapamycin. Addition of rapamycin did not favour the expansion of Foxp3$^+$ cohort in response to anti-CD3/CD28 stimulation plus high dose IL-2 ***(Figure 5.2.1.4.2.i)***. However, in contrast to the results of the expansion of freshly-harvested IFN-γ Treg in this section, the outgrowth of the Foxp3$^-$ cohort was clearly less profound ***(Figure 5.2.1.4.2.ii)***, suggesting that cryopreservation and the thawing processes might have altered the expansion potential of both Foxp3$^+$ and Foxp3$^-$ cohorts in cryopreserved IFN-γ Treg. In comparison with the expansion of CD4$^+$CD25$^+$ nTreg using rapamycin *in vitro* reported by others, Battaglia et al reported that using transgenic DC11.1 CD4$^+$ T cells stimulated with APC and ovalbumin in the presence of rapamycin led to a 5-fold increase in cell number after 1 week and up to 20-fold after 3 weeks of incubation[488]. Our results showed that the number of the Foxp3$^-$ cohort increased regardless the presence or absence of rapamycin consistent with their findings that rapamycin did not affect activation induced cell death (AICD) in the expanded CD4$^+$ population *in vitro*. Also consistent with their observation was that polyclonal activation of a highly purified CD25$^+$ population led to an outgrowth of activated effector T cells rather than Treg. These expanded cells appeared to lose their suppressive function *in vitro*, however, they did not assess further should these cells lose their intracellular expression of Foxp3. When CD25$^+$ T cells were depleted from their cultures, there was no Foxp3 enrichment. On th other hand, when an unsorted CD4$^+$ T cells were used as the starting population, there was a significant increase in the expression of Foxp3 mRNA in this population up to 3-fold compared to those without rapamycin. Above all, we acknowledge that our 7-day culture period might not be satisfactory as their group only achieved preferential expansion after 3 weeks of incubation.

Figure 5.2.1.4.2. Cryopreserved IFN-γ Treg failed to expand using anti-CD3/CD28 beads plus rapamycin

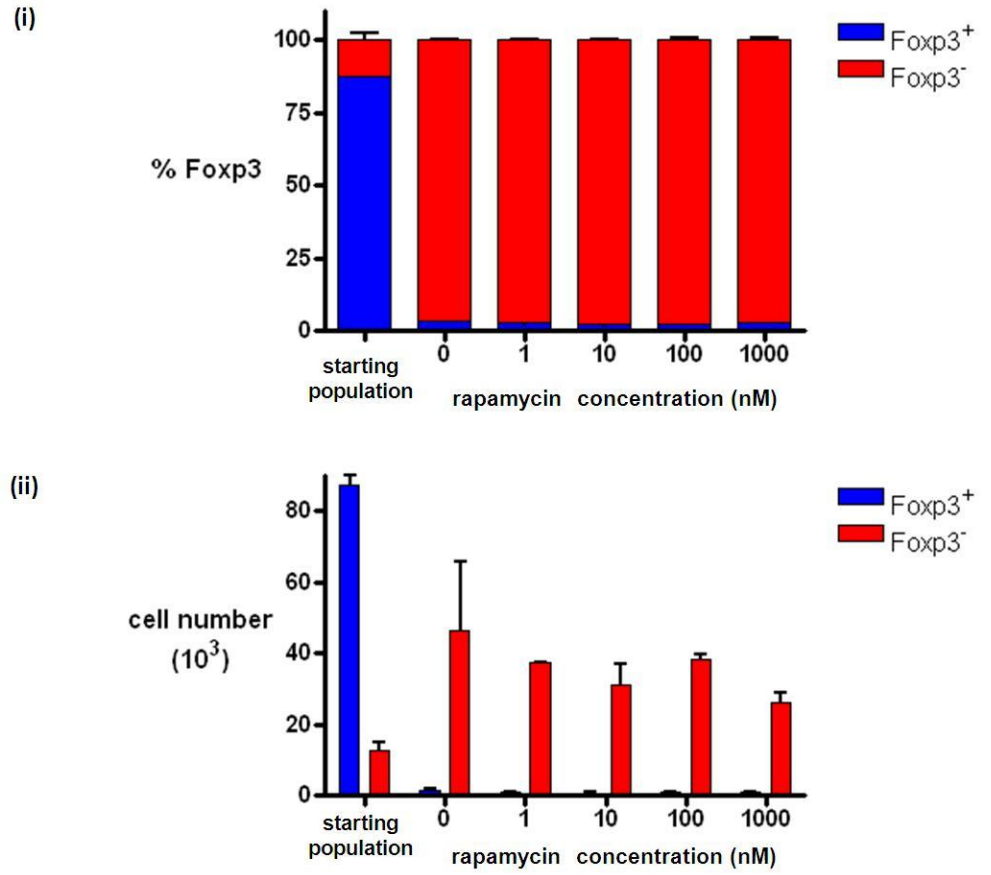

Figure 5.2.1.4.2. Cryopreserved IFN-γ Treg failed to expand using anti-CD3/CD28 beads plus rapamycin. $1x10^5$ cryopreserved IFN-γ Treg were stimulated with anti-CD3/CD28 beads (3:1 ratio) plus IL-2 (2000 U/ml), in the presence of a graded concentration of rapamycin (0-1000 nM) for 7 days. The resultant population was assessed for the expression of Foxp3 and the cell number was enumerated using flow cytometry. **(i)** Despite a high Foxp3 enrichment in the initial preparation approaching almost 90%, cryopreserved IFN-γ Treg failed to expand in response to anti-CD3/CD28 bead stimulation in the presence of a high-dose IL-2. On the other hand, the resultant population was dominated by a $Foxp3^-$ cohort in excess of 95%. Addition of rapamycin in these cultures had no effect on the preferential expansion of $Foxp3^+$ cohorts regardless of the concentration used. **(ii)** In comparison with the results of the expansion of freshly-harvested IFN-γ Treg shown in this section, cryopreservation appeared to alter the expansion potential of both $Foxp3^+$ and $Foxp3^-$ cohorts. We did not observe an overwhelming outgrowth of the $Foxp3^-$ cohort even in the presence of a high-dose IL-2. However, the addition of rapamycin did not favour the expansion of cryopreserved $Foxp3^+$ Treg. Data above represent means of 2 independent experiments with error bars showing 1 S.D. from the mean values.

5.2.1.5 Expansion of cryopreserved IFN-γ Treg with mature BM-DC

Given IFN-γ Treg were initially generated with modulated allogeneic BM-APC, we hypothesized that the Foxp3$^+$ cohort within the cryopreserved IFN-γ Treg population could be re-expanded selectively with the same alloantigen challenge plus IL-2 *in vitro*, instead of the pro-apoptotic Foxp3$^-$ cohort which would undergo activation-induced cell death. To interrogate the potential detrimental effects secondary to different kinds of freezing media, freshly-harvested IFN-γ were resuspended in complete freezing media (45% RPMI, 45% FCS and 10% DMSO) or FCS + 10% DMSO or RMPI + 10% DMSO. These cells were then stored at -80°C overnight in a rate-controlled freezing apparatus and subsequently stored in liquid nitrogen. Cryopreserved IFN-γ Treg stored in various types of media were then thawed, washed and their Foxp3 expression was determined by flow cytometry analysis prior to expansion. The proportion of Foxp3$^+$ cells increased in thawed IFN-γ Treg frozen in complete media, FCS + 10% DMSO and RPMI + 10% DMSO from 30.7% to 43.8%, 23.4% to 39.3% and 23.5% to 37.9%, respectively ***(Figure 5.2.1.5.1.i-iii)***. This proportionate increase in the Foxp3$^+$ cohort could possibly be explained by the natural selection process of the more resilient Foxp3$^+$ cohort combined with cell death of the pro-apoptotic Foxp3$^-$ cohort after the cryopreservation and thawing processes.

Figure 5.2.1.5.1. Expansion of cryopreserved IFN-γ Treg using allogeneic mature BM-DC *in vitro*

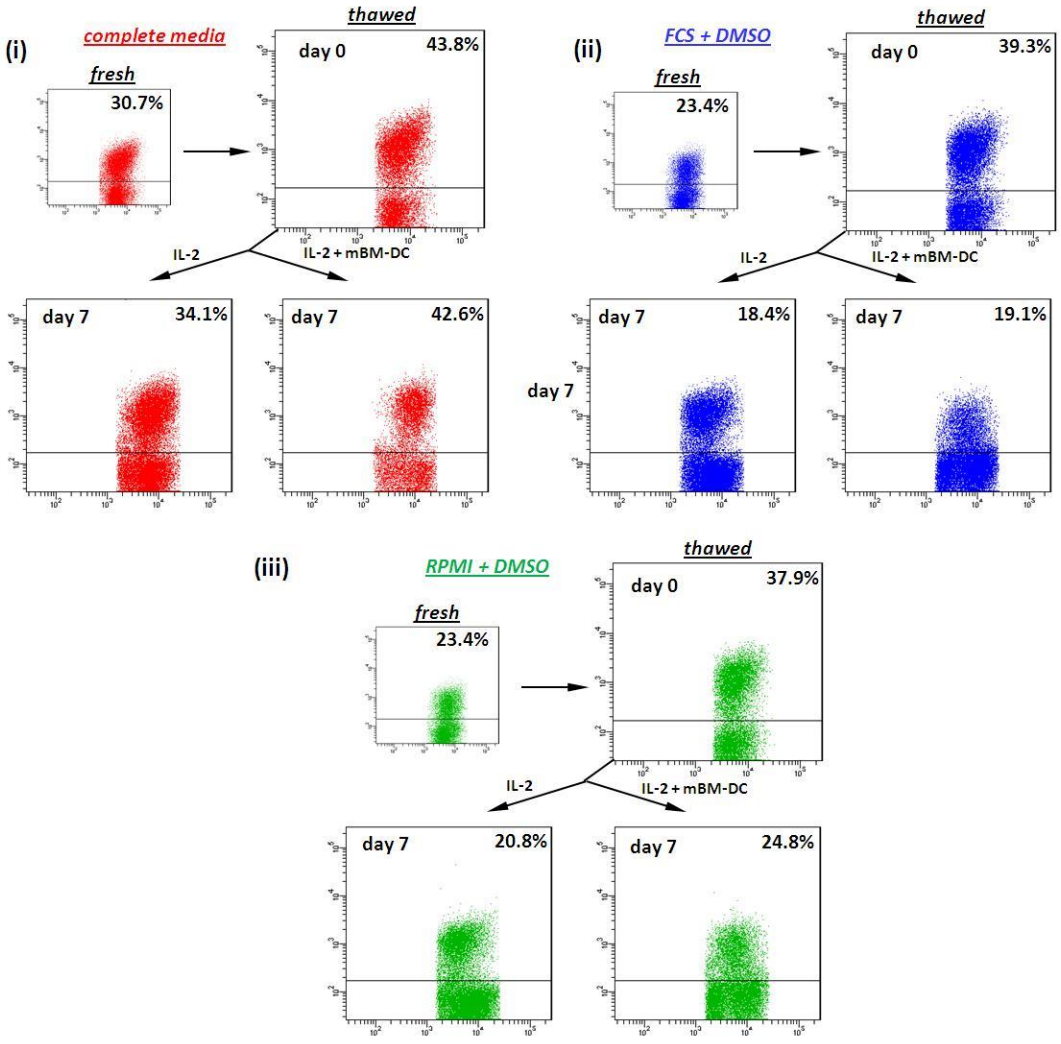

Figure 5.2.1.5.1. Expansion of cryopreserved IFN-γ Treg using allogeneic mature BM-DC *in vitro*. Foxp3 expression of freshly-harvested IFN-γ Treg was determined by flow cytometry before and after cryopreservation. IFN-γ Treg were cryopreserved in **(i)** complete freezing media (45% FCS, 45% RPMI 10% DMSO) or **(ii)** FCS + 10% DMSO or **(iii)** RPMI + 10% DMSO. Subsequently, thawed IFN-γ Treg were incubated with IL-2 (100 U/ml), in the presence or absence of B6 mature BM-DC (mBM-DC) for 7 days. Allogeneic mBM-DC were generated from B6 bone marrow cells incubated with GM-CSF (20 ng/ml) for 6 days and then matured with LPS (20 ng/ml) overnight using the protocol described in ***Chapter 2.7.7***. IFN-γ Treg cryopreserved in complete freezing media, FCS + DMSO and RPMI + DMSO retained their Foxp3 expression after cryopreservation and thawing. However, the percentage of Foxp3-expressing cells decreased after expansion with IL-2 or IL-2 plus allogeneic mBM-DC. Data above represent results obtained from 3 replicates.

Cryopreserved and thawed IFN-γ Treg were then incubated in IL-2 (100U/ml) with or without mature BM-DC (at 1:1 ratio) for 7 days. Mature BM-DC (mBM-DC) were generated using the protocol described in ***Chapter 2.7.7***[507]. The proportion of $Foxp3^+$ cells in the expanded IFN-γ Treg cryopreserved in complete freezing media decreased by 40% when incubated with IL-2 alone but it was sustained when incubated with IL-2 plus mBM-DC ***(Figure 5.2.1.5.2.i)***. On the other hand, the proportion of $Foxp3^+$ cells in the other two cryopreserved IFN-γ Treg preparations decreased up to 50% following expansion with IL-2 or IL-2 plus mBM-DC ***(Figure 5.2.1.5.2.i)***. There was no significant expansion of the $Foxp3^+$ cohort in all 3 preparations regardless of the culture conditions ***(Figure 5.2.1.5.2.ii)***. The $Foxp3^-$ cohort expanded when incubated in IL-2 alone in all three preparations. But interestingly, the number of the $Foxp3^-$ cohort of IFN-γ Treg cryopreserved in complete freezing media decreased following expansion with IL-2 plus mBM-DC, while this population appeared to sustain or expand in IFN-γ Treg preparation cryopreserved in FCS or RPMI-based media ***(Figure 5.2.1.5.2.ii)***. Collectively, these data suggest that $Foxp3^+$ IFN-γ Treg could be sustained *in vitro* under an optimal antigenic stimulation provided by allogeneic mBM-DC in the presence of sufficient T cell growth factor. However, the difficulty in the selective expansion of the $Foxp3^+$ cohort has remained unresolved and *in vitro* expansion of IFN-γ Treg is generally overshadowed by the outgrowth of the $Foxp3^-$ cohort instead.

Figure 5.2.1.5.2. The Foxp3⁺ cohort of IFN-γ Treg cryopreserved in different freezing media failed to expand using allogeneic mBM-DC and IL-2 *in vitro*

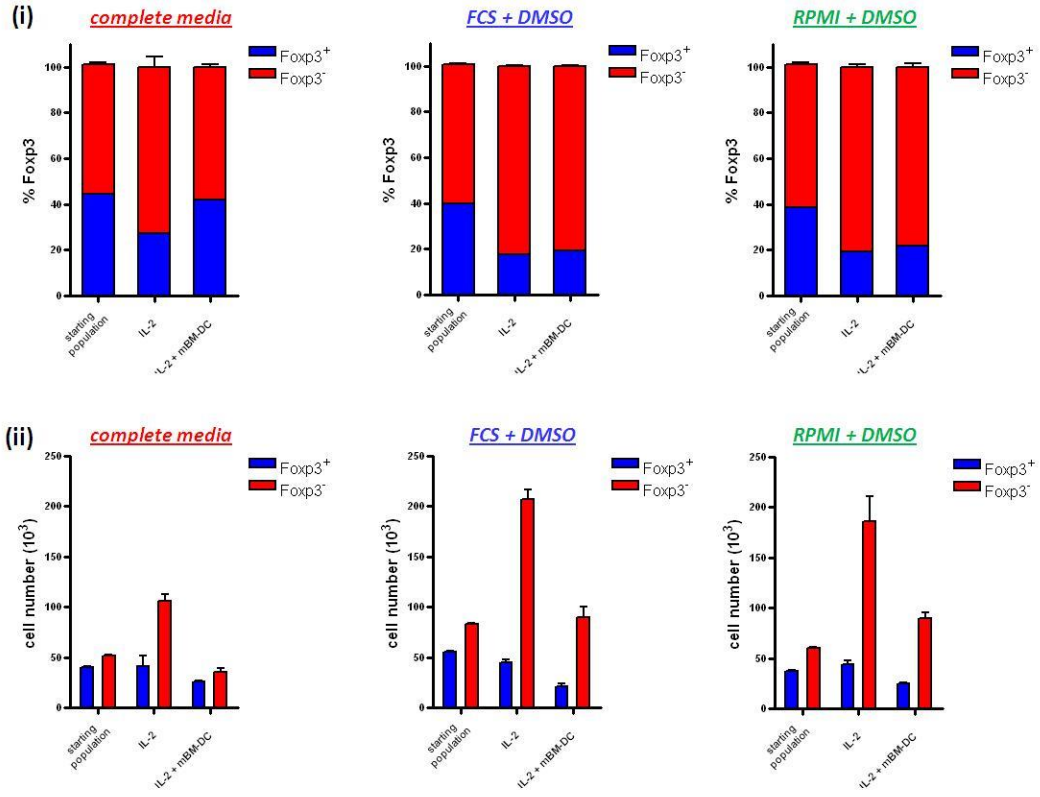

Figure 5.2.1.5.2. The Foxp3⁺ cohort of IFN-γ Treg cryopreserved in different freezing media failed to expand using allogeneic mBM-DC and IL-2 *in vitro*. IFN-γ Treg were resuspended in complete freezing media, (45% FCS, 45% RPMI and 10% DMSO), 90% FCS +10% DMSO or 90% RPMI+10% DMSO and frozen towards -80°C in a freezing rate-controlled apparatus overnight, then were stored in liquid nitrogen prior to be expanded using IL-2 with or without mBM-DC for 7 days. **(i)** Initial freezing and thawing processes did not significantly alter the Foxp3 expression on the Foxp3⁺ cohort of IFN-γ Treg, regardless the type of freezing media used. In the absence of antigenic stimulation, all 3 preparations were unable to retain a comparable proportion of Foxp3⁺ cohort when incubated with IL-2 (100 U/ml) alone. IFN-γ Treg cryopreserved in complete freezing media retained a higher proportion of their Foxp3⁺ cohort when compared to FCS and RPMI, upon stimulated by mBM-DC plus IL-2. **(ii)** The Foxp3⁺ cohorts of cryopreserved IFN-γ Treg prepared in all three freezing media did not expand after incubated with IL-2, in the presence or absence of mBM-DC. The Foxp3⁻ cohorts on the other hand expanded to a greater extent when incubated with IL-2 alone compared to IL-2 plus mBM-DC. Data above represent means of 3 replicates with error bars showing 1 S.D. from the mean values.

5.2.1.6 Ultra-purification of Foxp3$^+$ IFN-γ Treg

Potential contamination of activated T effector cells in the Treg preparation is of considerable concerns for the development of novel immunomodulating therapeutics after serious cytokine storm incident occurred during the clinical trial involving anti-CD28 antibody TGN1412[513,514]. This is particularly relevant to IFN-γ Treg as they consist of a significant proportion of activated Foxp3$^-$ cells (20-80%), which had been repeatedly stimulated by alloantigens *in vitro*. Foxp3 has remained the most reliable marker for the identification of T cells with regulatory function in mice. The IFN-γ protocol would be deemed unsatisfactory if the enriched Foxp3 population was less than 10%, compared to the starting population (8-10%). We aimed to interrogate the potential deleterious effects of the Foxp3$^-$ cohort within the IFN-γ Treg cell mixture *in vivo*.

CBA RAG$^{-/-}$ mice were reconstituted with naïve 1x10^5 CD4$^+$CD25$^-$ T cells with or without IFN-γ Treg that were enriched for a ***high*** or ***low*** proportion of Foxp3$^+$ T cells using the IFN-γ conditioning protocol, one day before the transplant of a B6 skin allograft ***(Figure 5.2.1.6.1.i)***. CD4$^+$CD25$^-$ T cells rejected skin allografts acutely with a MST of 20 days (n=3). IFN-γ Treg that were enriched for a ***high*** proportion of Foxp3$^+$ T cells (72.5% Foxp3$^+$) prevented allograft rejection when the precursor frequency of CD4$^+$CD25$^-$ T cells were lower than (1:2) or the same (1:1) as the number of IFN-γ Treg administered (MST>100 days, n=3; MST >100 days; n=3, respectively). At a higher precursor frequency of CD4$^+$CD25$^-$ T cells, a 2:1 ratio, IFN-γ Treg were unable to suppress rejection (MST=34 days, n=3) as compared to the control ***(Figure 5.2.1.6.1.ii)***.

In clear contrast, IFN-γ Treg that comprised of a ***low*** percentage of $Foxp3^+$ T cells (8.8%) were unable to prevent acute rejection of allograft despite being delivered at a high ratio against co-transferred naïve $CD4^+CD25^-$ T cells leading to graft survival with a MST 18-20 days (n=3 per group) ***(Figure 5.2.1.6.1.iii)***. Moreover, IFN-γ Treg with a ***low*** but not *a* ***high*** level of Foxp3 enrichment could cause acute skin graft rejection in their own rights ***(Figure 5.2.1.6.1.iii versus 5.2.1.6.1.ii; blue dashed lines)***. These data suggest that the $Foxp3^-$ cohort within the resultant IFN-γ Treg population that was exposed to alloantigen stimulation *in vitro* might have the potential to react against the allograft if the number of $Foxp3^+$ cohort was low in the IFN-γ Treg preparation.

Figure 5.2.1.6.1. Degree of Foxp3 enrichment within the resultant IFN-γ Treg population correlated with their suppressive function *in vivo*

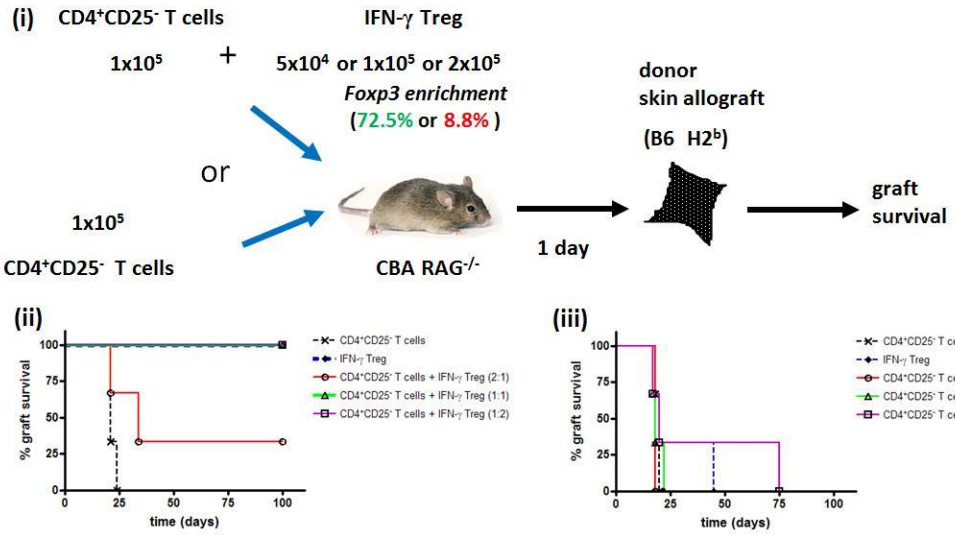

Group	n	graft survival (days)	MST (days)	p-value
IFN-γ Treg with ***high*** Foxp3 enrichment rate				
$CD4^+CD25^-$ T cells	3	21,21,24	21	
IFN-γ Treg	3	>100,>100,>100	>100	
$CD4^+CD25^-$ T cells + IFN-γ Treg (2:1)	3	21,34,>100	34	*p=0.1547*
$CD4^+CD25^-$ T cells + IFN-γ Treg (1:1)	3	>100,>100,>100	>100	*p=0.0224*
$CD4^+CD25^-$ T cells + IFN-γ Treg (1:2)	3	>100,>100,>100	>100	

Group	n	graft survival (days)	MST (days)	p-value
IFN-γ Treg with ***low*** Foxp3 enrichment rate				
$CD4^+CD25^-$ T cells	3	18,20,20	20	
IFN-γ Treg	3	18,18,45	18	
$CD4^+CD25^-$ T cells + IFN-γ Treg (2:1)	2	18,18	18	
$CD4^+CD25^-$ T cells + IFN-γ Treg (1:1)	3	17,18,22	18	
$CD4^+CD25^-$ T cells + IFN-γ Treg (1:2)	3	17,20,75	20	

Figure 5.2.1.6.1. Degree of Foxp3 enrichment within the resultant IFN-γ Treg population correlated with their suppressive function in *vivo*. (i) CBA $RAG^{-/-}$ mice were reconstituted with $1x10^5$ naïve $CD4^+CD25^-$ T cells with or without IFN-γ Treg that were enriched for a ***high*** (*72.5%*) or a ***low*** (*8.8%*) proportion of a $Foxp3^+$ population one day prior to the transplant of a B6 skin allograft. **(ii)** IFN-γ Treg with a ***high*** Foxp3 enrichment controlled the rejection mediated by naïve $CD4^+CD25^-$ T cells in a dose-dependent manner as shown in ***Figure 3.2.6.1.1***. **(iii)** IFN-γ Treg with a ***low*** Foxp3 enrichment were unable to control allograft rejection mediated by $CD4^+CD25^-$ T cells irrespective of the cell dose given, with a MST=18-20 days similar to the control group. Furthermore, $1x10^5$ IFN-γ Treg with a ***low*** Foxp3 enrichment rejected skin allografts acutely with a MST of 18 days (n=3), while $1x10^5$ IFN-γ Treg with a ***high*** Foxp3 enrichment led to long-term skin allograft acceptance **(ii versus iii)**. These data suggest that the $Foxp3^-$ cohort could elicit an alloresponse against allograft on their own right, while $Foxp3^+$ cohort could control the potential alloresponses mediated by the $Foxp3^-$ cohort within the IFN-γ Treg population. Log rank tests were used for statistical comparisons. ($p<0.05$ denotes statistically significant)

Although, the main advantage of the IFN-γ conditioning protocol was that it could generate competent suppressive cells without the need of further cell sorting, we also investigated if further selection of the $Foxp3^+$ population would enhance the suppressive function. In addition, we also explored the possibility that if the $Foxp3^-$ cohort could elicit an alloreactive response against allograft *in vivo*.

IFN-γ Treg were generated with $CD4^+$ precursors obtained from GFP/Foxp3 KI CBA splenocytes. The resultant IFN-γ Treg population contained a 22.5% GFP^+ sub-population and was used as an unsorted population, or sorted GFP^+ (purity 96.3%) or a sorted-GFP^- (purity 99.8%) population using flow cytometer *(data not shown)*. Their suppressive function was compared using the adoptive transfer skin allograft model ***(Figure 5.2.1.6.2.i)***. CBA $RAG^{-/-}$ mice were reconstituted with $1x10^5$ $CD4^+CD25^-$ T cells with unsorted IFN-γ Treg or, GFP^+ IFN-γ Treg, or GFP^- IFN-γ Treg one day prior to the transplant of a B6 skin allograft. $CD4^+CD25^-$ T cells rejected skin allografts acutely with a MST of 21 days (n=3). $2x10^5$ unsorted IFN-γ Treg prevented allograft rejection long-term (>100 days) in 3 out of 4 recipients. $1x10^5$ sorted GFP^+ IFN-γ Treg controlled rejection in 50% of recipients with a MST of 59.5 days (n=4). $1x10^5$ sorted GFP^- IFN-γ Treg could not control the rejection mediated by $CD4^+CD25^-$ T cells with a MST of 16 days (n=6) ***(Figure 5.2.1.6.2.ii)***. More interestingly, $1x10^5$ sorted GFP^- IFN-γ Treg rejected skin allografts acutely with a tempo similar to that of the $CD4^+CD25^-$ T cells control (MST=16 days, n=6) ***(Figure 5.2.1.6.2.ii)***.

Figure 5.2.1.6.2. Foxp3$^-$ cohort of IFN-γ Treg had the potential to reject allografts *in vivo*

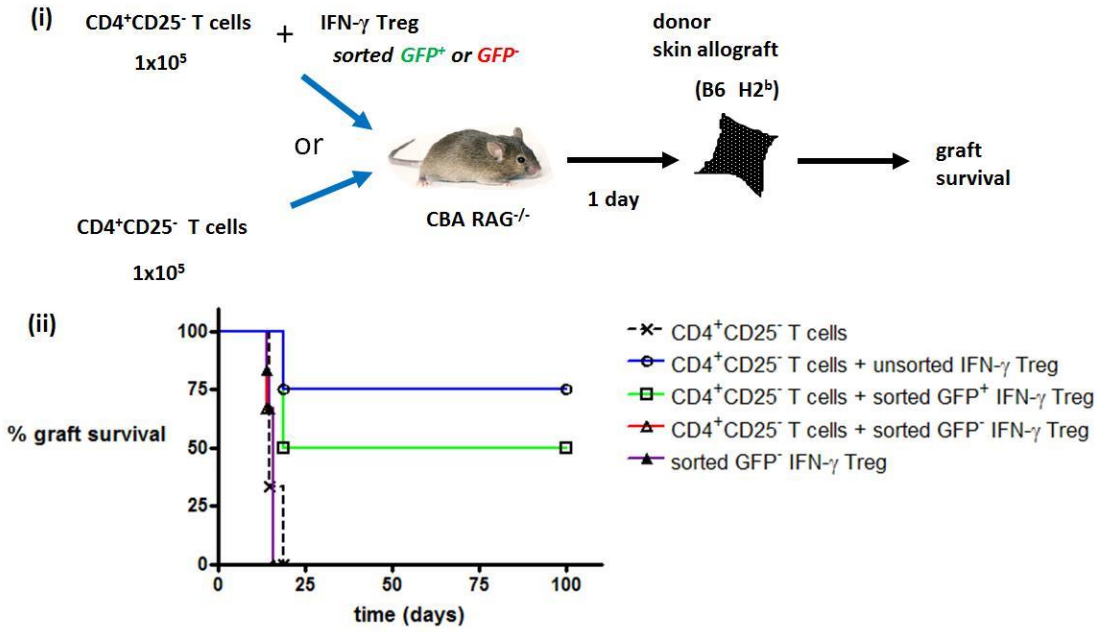

Group	n	graft survival (days)	MST (days)	p-value
CD4$^+$CD25$^-$ T cells	3	15,15,19	21	
CD4$^+$CD25$^-$ T cells + unsorted IFN-γ Treg (2x10^5)	4	19,>100>100>100	>100	
CD4$^+$CD25$^-$ T cells + sorted GFP$^+$ IFN-γ Treg (1x10^5)	4	19,19,>100,>100	59.5	*p = 0.0051*
CD4$^+$CD25$^-$ T cells + sorted GFP$^-$ IFN-γ Treg (1x10^5)	6	14,14,16,16,16,16	16	
sorted GFP$^-$ IFN-γ Treg (1x10^5)	6	14,15,16,16,16,16	16	

Figure 5.2.1.6.2. Foxp3$^-$ cohort of IFN-γ Treg had the potential to reject allografts *in vivo*. (i) CBA RAG$^{-/-}$ mice were reconstituted with naïve CD4$^+$CD25$^-$ T cells with or without co-transfer of: 2x10^5 unsorted IFN-γ Treg or 1x10^5 sorted GFP$^+$ IFN-γ Treg or 1x10^5 GFP$^-$ IFN-γ Treg one day before the transplant of a B6 skin allograft. A separate group of CBA RAG$^{-/-}$ mice received sorted GFP$^-$ IFN-γ Treg without CD4$^+$CD25$^-$ T cells prior to skin transplantation. **(ii)** CD4$^+$CD25$^-$ T cells rejected skin allografts with a MST of 21 days (n=3). Unsorted IFN-γ Treg prevented allograft rejection long-term in 3 our of 4 recipients (MST>100 days). Sorted GFP$^+$ IFN-γ Treg prevented allograft rejection in 50% of recipients (MST=59.5 days; n=4). Sorted GFP$^-$ IFN-γ Treg were not able to prevent rejection with a tempo similar to rejection mediated by naïve CD4$^+$CD25$^-$ cells alone (MST= 16 days; n=6). Sorted GFP$^-$ IFN-γ Treg rejected skin allografts acutely with a MST of 16 days (n=6). These data suggest that further sorting for the GFP$^+$ cohort of IFN-γ Treg did not enhance the suppressive potency of Treg therapy against skin allograft rejection in this adoptive transfer model. The Foxp3$^-$ cohort appeared to possess potential alloreactivity against allografts. Log rank tests were used for statistical comparisons. (p<0.05 denotes statistically significant)

Unsorted IFN-γ Treg contained $2x10^5$ x 22.5%= $4.4x10^4$ GFP^+ Treg, which were able control $1x10^5$ $CD4^+CD25^-$ T cells. On the other hand, sorted-GFP^+ IFN-γ Treg contained $1x10^5$ x 96.3%= $9.6x10^4$ GFP^+ Treg, which had double the number of GFP^+ Treg but were only 50% as effective as unsorted-IFN-γ Treg for the control of rejection mediated by $1x10^5$ $CD4^+CD25^-$ T cells. These data suggest that on a cell-to-cell basis, sorted $Foxp3^+$ IFN-γ Treg did not confer superior suppressive function compared to unsorted IFN-γ Treg, possibly due to the additional strain when the cells passed through the sorting processes. More importantly, the $Foxp3^-$ cohort did not exacerbate rejection of $CD4^+CD25^-$ T cells, but have the potential to react to allografts and mediate acute rejection in their own right. Thus, further sorting for $Foxp3^+$ cohort to produce ultra-purified IFN-γ Treg offered no real advantages when delivered at the optimal dose.

5.2.1.7 Cryopreserved IFN-γ Treg retained Foxp3 expression and suppressive function *in vivo*

In view of persistent low cell yield and logistic issues, we explored the possibility of banking cryopreserved IFN-γ Treg. A few reports have suggested that cryopreservation could lead to reduced cell recovery, viability and suppressive function of human Treg, depending on the freezing media used[499,515-517]. However, the impact of cryopreservation on mouse Treg has not been fully elucidated. We hypothesized that hostile freezing and thawing processes could alter the phenotypic features and suppressive function of IFN-γ Treg.

IFN-γ Treg were generated using the IFN-γ conditioning protocol as described above that yielded a Foxp3 enrichment of 42.7% in the resultant population ***(Figure 5.2.1.7.1.i, left panel)***. These cells were then cryopreserved in freezing media containing 45% RPMI, 45% FCS and 10% DMSO at -80°C overnight in an automated rate-controlled (1°C per minute) freezing apparatus then stored in liquid nitrogen thereafter. Cryopreserved IFN-γ Treg were thawed and examined for their phenotypic expression by flow cytometry. Cryopreserved IFN-γ Treg retained their Foxp3 expression (43.8%) as shown in ***Figure 5.2.1.7.1.i, right panel***. However, the proportion of IFN-γ Treg co-expressed Foxp3 and CD62L was reduced from 37.0% to 23.3% following cryopreservation and thawing ***(Figure 5.2.1.7.1.ii left versus right panel)***.

By gating the $Foxp3^+$ and $Foxp3^-$ cohorts separately, we observed that the proportion of cells expressing CD62L decreased in both $Foxp3^+$ and $Foxp3^-$ population, from 86.6% to 51.0% and 82.3% to 54.4%, respectively ***(Figure 5.2.1.7.1.iii)***. The reduction of CD62L expression in both $Foxp3^+$ and $Foxp3^-$ cohorts in cryopreserved IFN-γ Treg might have significant impact on their homing characteristics and function as recently reported by Florek et al[518]. On the other hand, the presence of a negligible number of $7AAD^+$ cells ***(Figure 5.2.1.7.1.iv)*** suggested that the cryopreservation and thawing process had little impact on the viability of mouse T cells, which was supported by trypan blue staining under light microscopy that showed ≥95% cell viability *(data not shown)*.

Figure 5.2.1.7.1. IFN-γ Treg retained a high level of Foxp3 expression and cell viability after cryopreservation

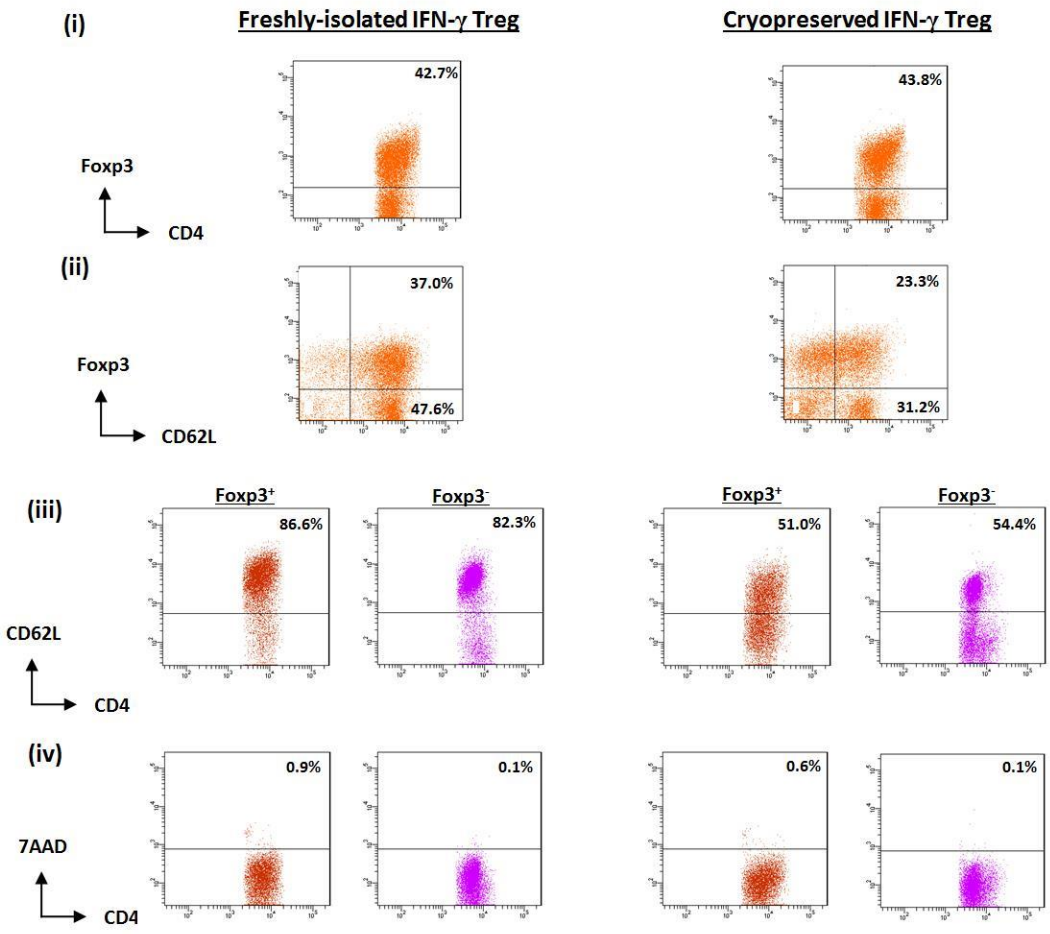

Figure 5.2.1.7.1. IFN-γ Treg retained a high level of Foxp3 expression and cell viability after cryopreservation. IFN-γ Treg were generated using CBA $CD4^+$ precursors using the IFN-γ conditioning protocol as described in ***Chapter 2.8.1***. Freshly-harvested IFN-γ Treg contained 42.7% $Foxp3^+$ T cells as shown by flow cytometry analysis. These cells were resuspended in freezing medium containing 45% RPMI, 45% FCS and 10% DMSO, stored at -80°C overnight, and then stored in liquid nitrogen. **(i)** Following the cryopreservation and thawing processes, IFN-γ Treg retained a high proportion of $Foxp3^+$ T cells (43.8%). **(ii)** The proportion of the $Foxp3^+CD62L^+$ subset reduced from 37.0% to 23.3% after cryopreservation and thawing. **(iii)** By gating the $Foxp3^+$ and $Foxp3^-$ populations separately, the proportion of $CD62L^+$ population decreased from 86.6% to 51.0% and 82.3% to 54.4%, respectively. **(iv)** Cryopreservation and thawing did not increase cell death as shown by the limited proportion of $7AAD^+$ cells, which was affirmed by trypan blue staining under light microscopy. Data above represent at least 3 independent experiments.

We compared the suppressive function of freshly-harvested IFN-γ Treg and cryopreserved IFN-γ Treg *in vivo* using the adoptive transfer skin allograft model ***(Figure 5.2.1.7.2.i)***. CBA RAG-/- mice were reconstituted with $1x10^5$ $CD4^+CD25^-$ T cells with or without a graded number ($5x10^4$ to $2x10^5$) of either freshly-harvested IFN-γ Treg or cryopreserved IFN-γ Treg one day prior to the transplant of a B6 skin allograft. Similar to freshly-harvested IFN-γ Treg ***(Figure 5.2.1.7.2.ii)***, cryopreserved IFN-γ Treg controlled skin allograft rejection mediated by $CD4^+CD25^-$ T cells when given at a high ratio compared to the precursor frequency of $CD4^+CD25^-$ T cells (1:2 or 1:1 $CD4^+CD25^-$ T cells: IFN-γ Treg; MST= 100 days; n=3 per group) ***(Figure 5.2.1.7.2.iii)***. When cryopreserved IFN-γ Treg were outnumbered by $CD4^+CD25^-$ T cells at a 2:1 $CD4^+CD25^-$ T cells to IFN-γ Treg ratio, they failed to suppress allograft rejection with a MST of a 26 days (n=3), similar to freshly-harvested IFN-γ Treg (MST=34 days; n=3), and mice adoptively transferred with $CD4^+CD25^-$ T cells alone (MST=21 days, n=3; MST=18 days, n=3 in each contemporary control groups)***(Figure 5.2.1.7.2.ii & Figure 5.2.1.7.2.iii)***. These data suggest that cryopreservation and the thawing process had no impact on the suppressive function of IFN-γ Treg in the adoptive transfer skin allograft model.

Figure 5.2.1.7.2. Cryopreserved IFN-γ Treg controlled allograft rejection as effectively as freshly-harvested IFN-γ Treg in the adoptive transfer skin transplant model

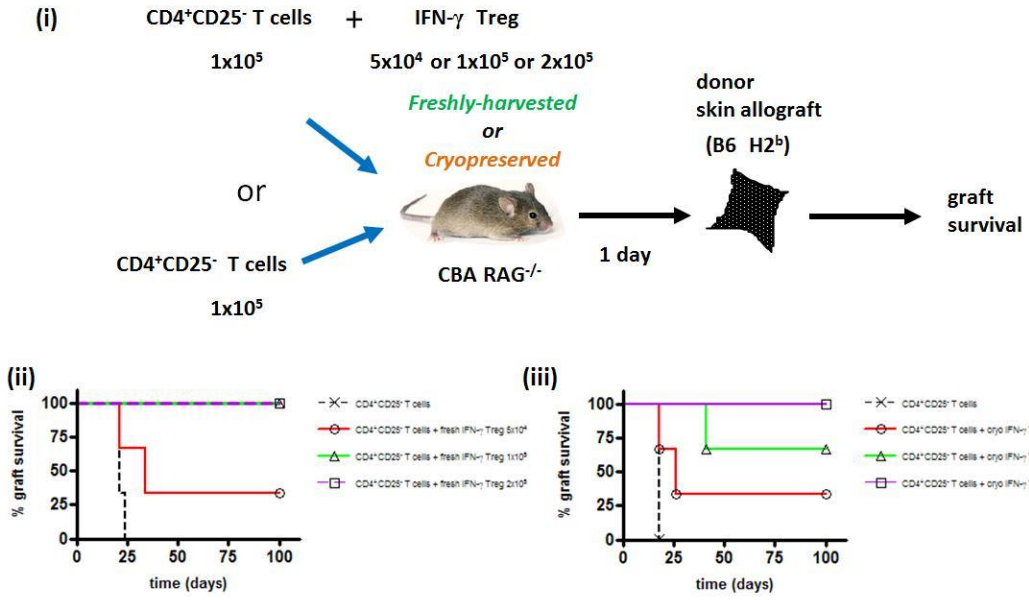

Group	n	graft survival (days)	MST (days)	p-value
Freshly-harvested IFN-γ Treg				
CD4+CD25- T cells	3	21,21,24	21	p=0.1547
CD4+CD25- T cells + IFN-γ Treg (2:1)	3	21,34,>100	34	p=0.0224
CD4+CD25- T cells + IFN-γ Treg (1:1)	3	>100,>100,>100	>100	
CD4+CD25- T cells + IFN-γ Treg (1:2)	3	>100,>100,>100	>100	

Group	n	graft survival (days)	MST (days)	p-value
Cryopreserved IFN-γ Treg				
CD4+CD25- T cells	3	18,18,18	18	p=0.1138
CD4+CD25- T cells + IFN-γ Treg (2:1)	3	18,26,>100	26	p=0.0253
CD4+CD25- T cells + IFN-γ Treg (1:1)	3	41,>100,>100	>100	
CD4+CD25- T cells + IFN-γ Treg (1:2)	3	>100,>100,>100	>100	

Figure 5.2.1.7.2. Cryopreserved IFN-γ Treg controlled allograft rejection as effectively as IFN-γ Treg in the adoptive transfer skin transplant model. (i) Harvested IFN-γ Treg were split into two groups: 1) Freshly-harvested IFN-γ Treg were adoptively transferred to CBA RAG$^{-/-}$ mice with naïve CD4^{+}CD25^{-} T cells in various doses one day before the transplant of a B6 skin allograft; 2) IFN-γ Treg were cryopreserved and stored for one week in liquid nitrogen, prior to being thawed and adoptively transferred to CBA RAG$^{-/-}$ mice using the same skin transplant model. **(ii)** ***Freshly-harvested IFN-γ Treg*** controlled rejection mediated by co-transferred CD4^{+}CD25^{-} T cells in a dose-dependent manner as previously shown in ***Figure 3.2.6.1.1***. **(iii)** ***Cryopreserved IFN-γ Treg*** were also able to prevent allograft rejection mediated by co-transferred CD4^{+}CD25^{-} T cells in a dose-dependent manner. Despite the differences in the expression of CD62L and Foxp3 between these two population following the cryopreservation (86.6% versus 51.0%; ***Figure 5.2.1.7.1***), there was no significant differences in their suppressive function *in vivo*. Log rank tests were used for statistical comparisons. (p<0.05 denotes statistically significant)

Furthermore, we tested the suppressive function between freshly-harvested IFN-γ Treg and cryopreserved IFN-γ Treg in immunocompetent recipients of a heterotopic heart transplant in the presence of a sub-optimal abatacept protocol ***(Chapter 3.2.4)***. CBA mice were given $5x10^5$ of either freshly-harvested or cryopreserved IFN-γ Treg 3 days before the transplant of a B6 heart allograft in the presence of a sub-optimal abatacept protocol (i.v. 25 μg day 0, 1 and 5) ***(Figure 5.2.1.7.3.i)***. Freshly-harvested IFN-γ Treg controlled allograft rejection with a MST >100 days (n=3), when compared to mice receiving abatacept alone (MST= 63 days, n=6). In clear contrast, cryopreserved IFN-γ Treg were not able to prevent allograft rejection in the majority of the recipients (MST of 63 days (n=5)), similar to mice which received abatacept alone. ***(Figure 5.2.1.7.3.ii)***.

Collectively, these data suggest that cryopreservation did not have any impact on the function of IFN-γ Treg in the adoptive transfer model. This might be due to the fact that cryopreservation had limited effect on the homeostatic proliferation of Treg *in vivo*. On the other hand, the impaired suppressive function observed in immunocompetent recipients could possibly result from: 1) altered CD62L expression which is responsible for efficient homing to secondary lymphoid tissue; 2) the activation status of Treg following the freezing and thawing processes.

Figure 5.2.1.7.3. At a given cell dose, cryopreserved IFN-γ Treg were inferior to freshly-harvested IFN-γ Treg in their capability of controlling allograft rejection in immunocompetent recipients

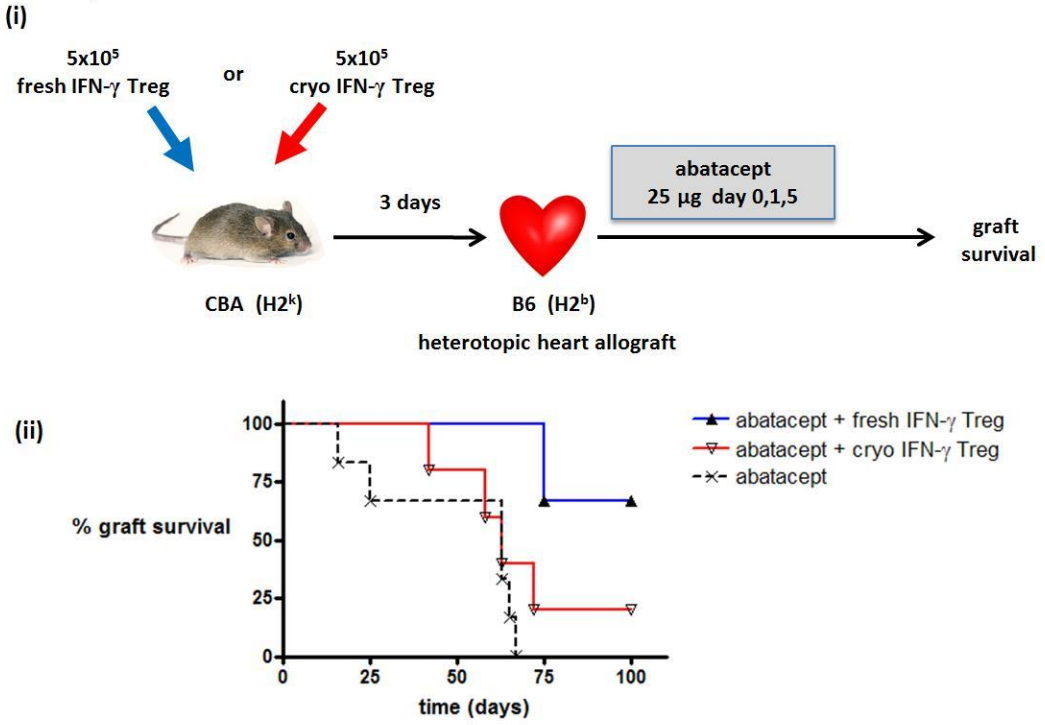

Group	n	graft survival (days)	MST (days)	p-value
abatacept	6	16,25,63,63,65,67	63	*p = 0.0103*
abatacept + fresh IFN-γ Treg	3	75,>100,>100	>100	
abatacept + cryo IFN-γ Treg	5	42,58,63,72,>100	63	*p = 0.2958*

Figure 5.2.1.7.3. At a given cell dose, cryopreserved IFN-γ Treg were inferior to freshly-harvested IFN-γ Treg in their capability of controlling allograft rejection in immunocompetent recipients. (i). IFN-γ Treg were generated by the IFN-γ protocol as described above ***(Chapter 2.8.1)***. CBA mice were given i.v. abatacept 25µg on day 0, 1, and 5, with or without $5x10^5$ freshly-harvested IFN-γ Treg or cryopreserved IFN-γ Treg 3 days before the transplant of a heterotopic B6 heart allograft. **(ii)** Abatacept delayed allograft rejection with a MST of 63 days (n=6). $5x10^5$ freshly-harvested IFN-γ Treg prolonged graft survival long-term (MST>100 days; n=3), in the presence of abatacept. $5x10^5$ cryopreserved IFN-γ Treg were not able to prolong graft survival in the same fashion as freshly-harvested IFN-γ Treg (MST=63 days, n=5). These data suggest that, although the cryopreservation processes did not affect Foxp3 expression on IFN-γ Treg and these cells controlled graft rejection in the adoptive transfer skin graft model ***(Figure 5.2.1.7.2)***. The cryopreservation processes had a negative impact on the suppressive function of IFN-γ Treg in immunocompetent heart transplant recipients, which could be related to the reduced expression of CD62L ***(Figure 5.2.1.7.1)***. Log rank tests were used for statistical comparisons. ($p<0.05$ denotes statistically significant)

5.2.2 Revisiting $CD4^+CD25^+$ nTreg

While there was great difficulty in selectively expanding $Foxp3^+$ IFN-γ Treg *in vitro*, we decided to turn to examine naturally-occurring $CD4^+CD25^+$ Treg (nTreg) as it has been well-documented in the literature that they could be expanded in large numbers *in vitro*.

5.2.2.1 Freshly-isolated $CD4^+CD25^+$ nTreg

$CD4^+CD25^+$ nTreg could be isolated using magnetic-activated (MACS) or flow cytometry (FACS) cell sorting devices that typically yield a purity of >90% $CD4^+CD25^+$ nTreg using standard cell isolation protocols as described in ***Chapter 2.7.4***. Freshly-isolated nTreg enriched by MACS or FACS ARIA sorting (based on the expression of CD25) were able to prevent skin allograft rejection in the adoptive transfer model. CBA $RAG^{-/-}$ mice were reconstituted with either $1x10^5$ or $4x10^5$ naïve $CD4^+CD25^-$ T cells with or without $1x10^5$ $CD4^+CD25^+$ freshly-isolated nTreg one day before the transplant of a full MHC-mismatched B6 skin allograft ***(Figure 5.2.2.1.1.i)***. All skin allografts were rejected acutely with a MST of 17 days (n=5) and 12 days (n=5), when $1x10^5$ or $4x10^5$ $CD4^+CD25^-$ T cells were given alone, respectively ***(Figure 5.2.2.1.1.ii)***. At a 1:1 ratio, $1x10^5$ freshly-isolated $CD4^+CD25^+$ nTreg were able to prevent graft rejection long-term (MST>100 days, n=6). In clear contrast, $1x10^5$ freshly-isolated nTreg could only partially control rejection mediated by a larger effector population ($4x10^5$) with a MST of 12 days (n=6). Their suppressive function was directly compared with freshly-isolated IFN-γ Treg (37.2% $Foxp3^+$ as determined by flow cytometry analysis). $1x10^5$ freshly-isolated IFN-γ Treg controlled the rejection mediated by $1x10^5$ $CD4^+CD25^-$ T cells long-term (MST>100days, n=6). $1x10^5$ IFN-γ Treg could only partially control rejection mediated by $4x10^5$ $CD4^+CD25^-$ T cells with a MST 65 days (n=6), which was not

statistically different from nTreg. These data suggest that both nTreg and IFN-γ Treg exhibit their suppressive function in a dose-dependent manner in the adoptive transfer skin graft model. However, IFN-γ Treg appeared to be more potent than nTreg on a cell-to-cell basis as the former contained approximately $4x10^4$ $Foxp3^+$ T cells (37.2% of $1x10^5$ cells) whereas the latter contained $9x10^4$ $Foxp3^+$ T cells (90% of $1x10^5$ cells) based on flow cytometry analysis. The differences in their potency could be explained by the fact that IFN-γ Treg were enriched for an alloreactive Treg population following stimulation with alloantigens *in vitro*; whereas polyclonal freshly-isolated nTreg only contained approximately 10% of alloreactive Treg with the assumption that precursor frequency of alloreactive T cells in a polyclonal $CD4^+$ T cell population is estimated to be around 10%[519]. Nevertheless, their suppressive function could also be confounded by their differential ability to undergo homeostatic proliferation *in vivo.*

Figure 5.2.2.1.1. Freshly-isolated CD4⁺CD25⁺ nTreg control allograft rejection in a dose-dependent manner in an adoptive transfer skin transplant model

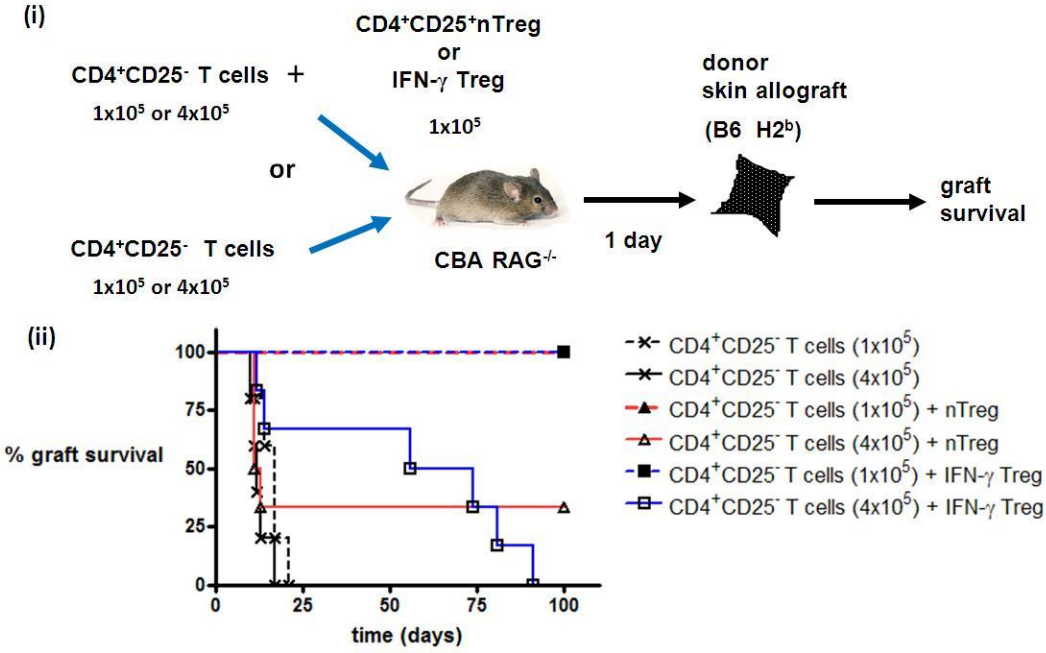

Group	n	graft survival (days)	MST (days)	p-value
CD4⁺CD25⁻ T cells (1x10⁵)	5	11,14,17,17,21	17	
CD4⁺CD25⁻ T cells (4x10⁵)	5	10,11,12,13,17	12	
CD4⁺CD25⁻ T cells (1x10⁵) + nTreg	6	>100,>100>100,>100,>100,>100	>100	*p = 0.0008*
CD4⁺CD25⁻ T cells (4x10⁵) + nTreg	6	11,11,11,13,>100,>100	12	*p = 0.3171*
CD4⁺CD25⁻ T cells (1x10⁵) + IFN-γ Treg	6	>100,>100>100,>100,>100,>100	>100	
CD4⁺CD25⁻ T cells (4x10⁵) + IFN-γ Treg	6	12,14,56,74,81,91	65	*p = 0.7909*

Figure 5.2.2.1.1. Freshly-isolated CD4⁺CD25⁺ nTreg control allograft rejection in a dose-dependent manner in an adoptive transfer skin transplant model. CD4⁺CD25⁺ nTreg were isolated from CBA splenocytes using MACS to yield a purity >90% Foxp3⁺ population. IFN-γ Treg were generated using the IFN-γ conditioning protocol (37.2% Foxp3⁺), as described in ***Chapter 2.8.1***. **(i)** CBA RAG⁻/⁻ mice were reconstituted with naïve 1x10⁵ or 4x10⁵ CD4⁺CD25⁻ T cells with or without co-transfer of 1x10⁵ CD4⁺CD25⁺ nTreg or IFN-γ Treg one day before the transplant of a B6 skin allograft. **(ii)** 1x10⁵ or 4 x10⁵ naïve CD4⁺CD25⁻ T cells rejected skin allografts acutely with a MST of 17 days (n=5) and 12 days (n=5), respectively. Freshly-isolated 1x10⁵ CD4⁺CD25⁺ nTreg controlled rejection mediated by CD4⁺CD25⁻ T cells long-term (MST>100 days; n=6) at a 1:1 nTreg:CD4⁺CD25⁻ T cell ratio, but they could only partially control rejection at a 1:4 ratio (MST=12 days; n=6). These graft protective effects were not statistically different from that provided by IFN-γ Treg at the same cell dose. Log rank tests were used for statistical comparisons. ($p<0.05$ denotes statistically significant)

We then tested the suppressive function of freshly-isolated $CD4^+CD25^+$ nTreg in immunocompetent recipients using our heterotopic heart transplant model. $2x10^6$ Freshly-isolated CBA nTreg selected by MACS based on the expression of CD25 (with a purity of >90%) were given to WT CBA recipients one day prior to the transplant of a B6 heart allograft in the presence of the sub-optimal abatacept treatment (i.v. 25μg day 0, 1 and 5) ***(Figure 5.2.2.1.2.i)***. The abatacept protocol led to delayed graft rejection with a MST of 63 days (n=6) ***(Figure 5.2.2.1.2.ii)***. $2x10^6$ freshly-isolated nTreg was not able to prolong heart allograft survival in the presence of the abatacept protocol with a MST of 22 days (n=5; *p*=0.0143), which was significantly shorter than abatacept control ***(Figure 5.2.2.1.2.ii)***. On the other hand, $2x10^6$ IFN-γ Treg were able to control allograft rejection long-term in this model (MST>100 days, n=9; *p*=0.0001) ***(Figure 5.2.2.1.2.ii)***.

To our surprise, the rejection kinetics appeared to be aggravated in mice treated with nTreg plus abatacept compared to those treated with abatacept alone. We reasoned that the accelerated rejection kinetics could be due to the competitive binding to the limited available CD80/CD86 on donor passenger leukocytes via the direct pathway shortly after transplantation. The CTLA-4 domain on abatacept has a higher affinity to CD80/CD86 than the natural lignad CD28 on T cells, which is critical for the initial priming and activation of resting nTreg after being administered. In addition, nTreg constitutively express CTLA-4 and mediate suppression via CTLA-4 as shown from our previous findings in ***Chapter 4.2.1*** and others[450] that blocking the CTLA-4 abrogated the suppressive function of nTreg. As a result, due to the shortfall in the available CD80/CD86 binding sites, infused nTreg could not be primed or activated fully for their suppressive function. At the same time, abatacept failed to exert its optimal immunosuppressive effect via costimulation blockade due to the limited occupancy of CD80/CD86 binding sites, ultimately leading to the apparent accelerated graft rejection seen in ***Figure 5.2.2.1.2***.

Figure 5.2.2.1.2. Freshly-isolated CD4⁺CD25⁺ nTreg were unable to control allograft rejection in immunocompetent heart transplant recipients

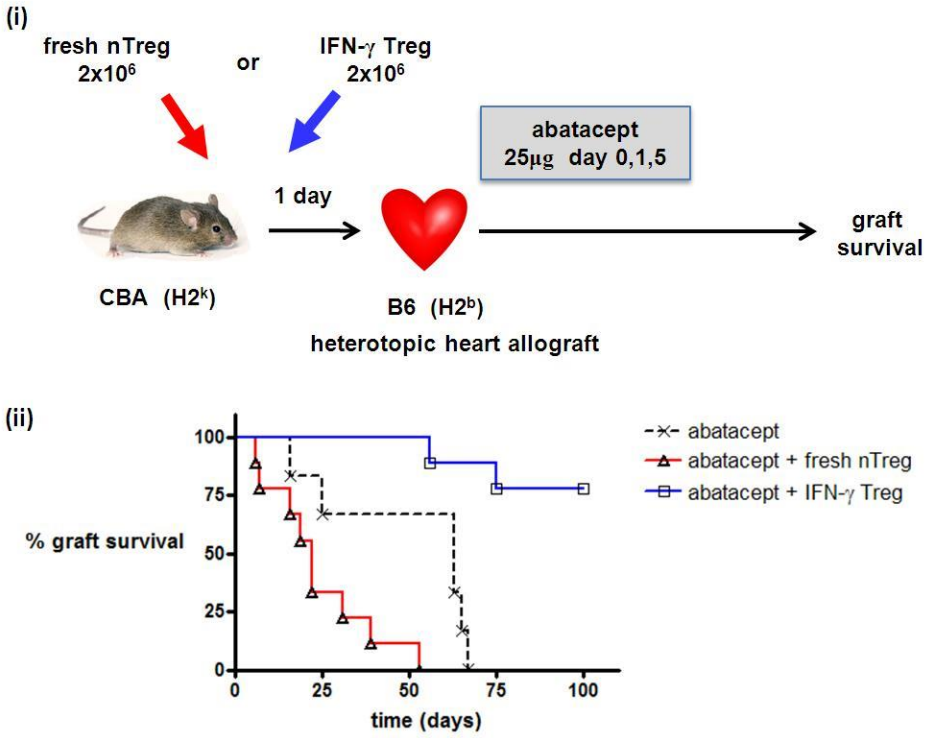

Group	n	graft survival (days)	MST (days)	p-value
abatacept	6	16,25,63,63,65,67	63	
abatacept + fresh nTreg	9	6,7,16,19,22,22,31,39,53	22	*p = 0.0143*
abatacept + IFN-γ Treg	9	56,75,>100,>100>100,>100,>100,>100,>100	>100	*p = 0.0001*

Figure 5.2.2.1.2. Freshly-isolated CD4⁺CD25⁺ nTreg were unable to control allograft rejection in immunocompetent heart transplant recipients. CD4⁺CD25⁺ nTreg were isolated from CBA splenocytes using MACS to yield a purity >90% Foxp3⁺ population. IFN-γ Treg were generated by the IFN-γ conditioning protocol (40.2% Foxp3⁺) as descrbied in ***Chapter 2.8.1***. **(i)** CBA mice were given 2x10⁶ freshly-isolated CD4⁺CD25⁺ nTreg or 2x10⁶ IFN-γ Treg one day before the transplant of a B6 heterotopic heart allograft plus the sub-optimal abatacept regimen (i.v. 25μg day 0,1 and 5). Mice in the control group received abatacept alone. **(ii)** The sub-optimal abatacept regimen prolonged allograft survival with a MST of 63 days (n=6). 2x10⁶ freshly-isolated nTreg were not able to control allograft rejection with a MST of 22 days (n=9). At the same cell dose, IFN-γ Treg led long-term graft survival in the majority of recipients (MST>100 days; n=9). Log rank tests were used for statistical comparisons ($p<0.05$ denotes statistically significant).

The difference in graft outcome seen between mice treated with the same cell number of IFN-γ Treg and nTreg could merely be attributed by the apparent lower precursor frequency of alloreactive Treg in the nTreg preparation compared to alloantigen-driven IFN-γ Treg. Devoid of the need for activation, we believe that IFN-γ Treg and abatacept appeared to work syneregistically in the control of graft rejection in the same model. Nevertheless, we could not exclude the possible direct detrimental effect of abatacept on thymic-derived nTreg *in vivo* as it has been reported recently[449].

5.2.2.2 Expansion of nTreg using anti-CD3/CD28 antibody-conjugated beads

In order to ascertain that a low precursor frequency was the chief factor for the inferior graft outcome we observed with nTreg in the heterotopic heart model, we would need to acquire a much larger number of $CD4^+CD25^+$ nTreg to pursue further experiments. Unless we have access to an unlimited number of nTreg, an expansion protocol for $CD4^+CD25^+$ nTreg is warranted. Using the commercially available Treg expansion kits, freshly-isolated nTreg were expanded with anti-CD3/CD28 antibody-conjugated beads plus IL-2 *in vitro* for 7 days. The resultant T cell mixture was then examined using flow cytometry analysis ***(Figure 5.2.2.2.1)***. nTreg could be isolated using MACS or FACS ARIA that provide a pure population of $CD4^+CD25^+$ nTreg or GFP^+ nTreg using $CD4^+$ precursors from GFP/Foxp3 KI splenocytes, which invariably lead to a yield of >90% $CD4^+CD25^+Foxp3^+$ nTreg. We first tested the expansion protocol using B6 splenocytes as the source of $CD4^+$ precursors as most documented expansion protocols, including the anti-CD3/CD28 bead manufacturer's protocol, were based on this mouse strain (*personal communication*).

As shown in ***Figure 5.2.2.2.2***, $1x10^4$ MACS-isolated B6 $CD4^+CD25^+$ T cells and $CD4^+CD25^-$ T cells population were incubated separately with anti-CD3/CD28 beads (1:1 bead:cell ratio) and a graded concentration of IL-2 (0-1000U/ml). After 7 days, cell cultures were evaluated for the proportion and absolute number of $Foxp3^+$ T cells by flow cytometry analysis. The proportion of $Foxp3^+$ cells within the '$CD4^+CD25^+$' population reduced from 91.1% to 25% when stimulated with anti-CD3/CD28 beads without IL-2 ***(Figure 5.2.2.2.2.i)***. Although a low-dose IL-2 (1-10U/ml) in culture appeared to support the proportion of $Foxp3^+$ cohort, the number of $Foxp3^+$ cells in these culture conditions was smaller than the starting population. At higher concentration of IL-

2, there was a dominant Foxp3$^-$ cohort (>75%) ***(Figure 5.2.2.2.2.ii)***. There was a significant change is the Foxp3$^+$/Foxp3$^-$ composition in the expanded 'CD4$^+$CD25$^-$'cultures directly proportional to the concentration of IL-2 as the Foxp3$^-$ cohort expanded exponentially (up to a 40-fold expansion) ***(Figure 5.2.2.2.2.iii & iv)***. Nevertheless, the Foxp3$^+$ cohort within the 'CD4$^+$CD25$^-$' cultures at high IL-2 concentration did comparatively expand in the shadow of this outgrowth of Foxp3$^-$ cohort up to a 4-fold increase. Similar to the findings reported in the previous section regarding the expansion of IFN-γ Treg, we encountered the main issue of the contamination of non-Treg in the expanded population.

Figure 5.2.2.2.1. Expansion of nTreg using anti-CD3/CD28 antibody conjugated beads and IL-2 *in vitro*

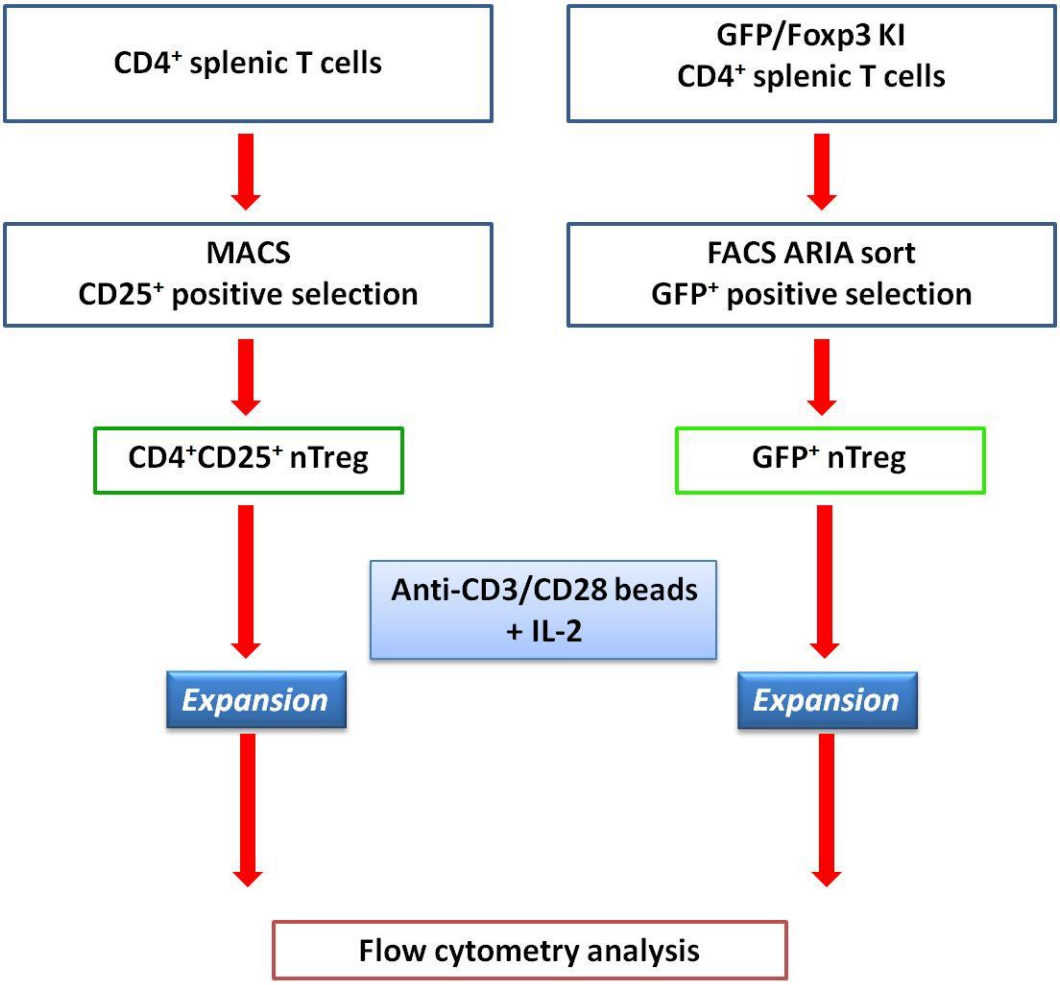

Figure 5.2.2.2.1 Expansion of nTreg using anti-CD3/CD28 antibody conjugated beads and IL-2 *in vitro*. nTreg were isolated as follows: $CD4^+CD25^+$ nTreg were positively selected using MACS that typically yielded 80-90% $CD4^+CD25^+Foxp3^+$ nTreg. Alternatively, GFP^+ nTreg were sorted from GFP/Foxp3 KI splenocytes, which typically yielded a purity of 90-95% GFP^+ nTreg. These cells were then stimulated with anti-CD3/CD28 beads (at different bead to cell ratios), in the presence of IL-2 (at various concentrations) for 7 days *in vitro*. Foxp3 expression on the resultant nTreg population was examined by flow cytometry.

Figure 5.2.2.2.2. Expansion of nTreg versus non-Treg with anti-CD3/CD28 beads and IL-2 *in vitro*

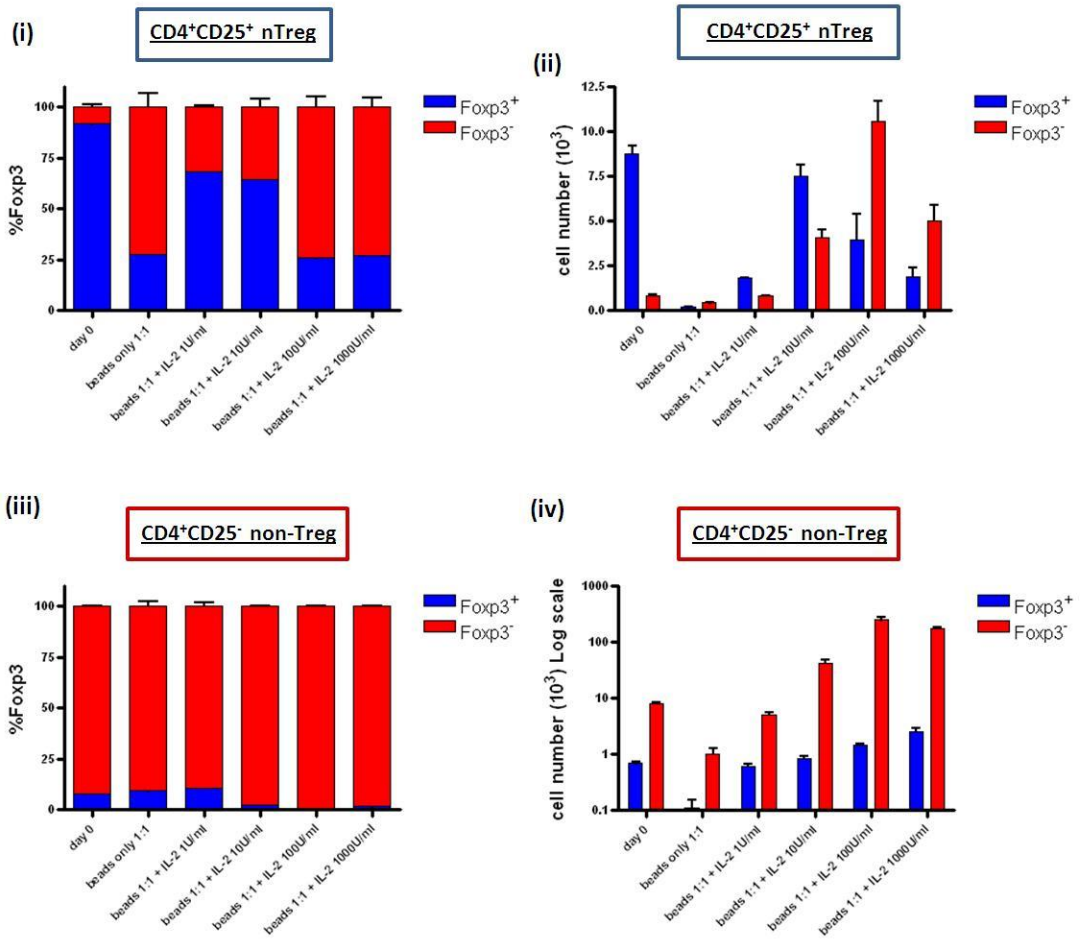

Figure 5.2.2.2.2. Expansion of nTreg versus non-Treg with anti-CD3/CD28 beads and IL-2 *in vitro*. MACS-isolated B6 $CD4^+CD25^+$ nTreg ($1x10^4$) with a purity of 91.1% $Foxp3^+$ nTreg were expanded using anti-CD3/CD28 beads (at a 1:1 bead to cell ratio), in the presence or absence of IL-2 (0-1000 U/ml) for 7 days. Their $CD4^+CD25^-$ non-Treg counterparts (>90% $Foxp3^-$) were expanded in the same way serving as controls. The proportion and the number of $Foxp3^+$ and $Foxp3^-$ cells in the resultant populations in each culture condition were determined by flow cytometry. **(i)** $CD4^+CD25^+$ nTreg retained a high level of Foxp3 expression when stimulated with anti-CD3/CD28 beads with a low IL-2 concentration (1-10 U/ml). **(ii)** However, while the proportion of $Foxp3^+$ population could be maintained at certain concentrations of IL-2, the number of $Foxp3^+$ cells remained low compared to the initial input, suggesting that expansion of nTreg was limited. At high IL-2 concentration (≥100 U/ml), there was an overgrowth of the $Foxp3^-$ cohort. **(iii)** $CD4^+CD25^-$ non-Treg responded to the polyclonal stimulus provided by anti-CD3/CD28 beads and IL-2. The proportion of $Foxp3^-$ cohort in these cultures increased directly proportional to the IL-2 concentration. **(iv)** While the $Foxp3^-$ cohort expanded efficiently in Log-scales, the $Foxp3^+$ cohort expanded modestly up to a 4-fold increase comparing to the input number. Data above represent means of 3 replicates with error bars showing 1 S.D. from the mean values.

5.2.2.3 nTreg expansion incorporated with other 'Treg-favourable' soluble growth factors

It is known that common γ-chain$^{-/-}$ mice lack Treg and that common γ-chain cytokines are believed to be essential for Treg development[520-525]. Vang et al[522] showed that IL-7 and IL-15 could compensate for the absence of the major Treg growth factor IL-2 for the development of Treg. Based on the reports published in the literature we tested whether IL-2 in combination with IL-7[524] and IL-15[246] would facilitate the expansion of nTreg *in vitro* using the anti-CD3/CD28 bead protocol described above ***(Chapter 5.2.1.1)***.

1x10^4 B6 CD4$^+$CD25$^+$ nTreg (isolated by MACS with a purity 91.1%) or CD4$^+$CD25$^-$ non-Treg were stimulated with anti-CD3/CD28 beads (1:1 bead: cell ratio) in the presence of IL-2 (100U/ml) and a graded concentration of IL-7 (0-200ng/ml) for 7 days. The proportion of Foxp3$^+$ cells in the expanded CD4$^+$CD25$^+$ nTreg population remained constant regardless of the addition of IL-7 to the cultures ***(Figure 5.2.2.3.1.i)***. Similarly, the number of the Foxp3$^+$ or Foxp3$^-$ cohorts in the expanded CD4$^+$CD25$^+$ nTreg was unchanged in cultures with addition IL-7 ***(Figure 5.2.2.3.1.ii)***. The proportion and the number of Foxp3$^+$ cells in the expanded CD4$^+$CD25$^-$ non-Treg were not significantly different in the presence or absence of additional IL-7. Similarly, IL-7 had no impact on the expansion of the Foxp3$^-$ cohorts under these culture conditions ***(Figure 5.2.2.3.1.iii & iv)***.

Figure 5.2.2.3.1. Expansion of nTreg versus non-Treg with anti-CD3/CD28 beads plus IL-2 and IL-7

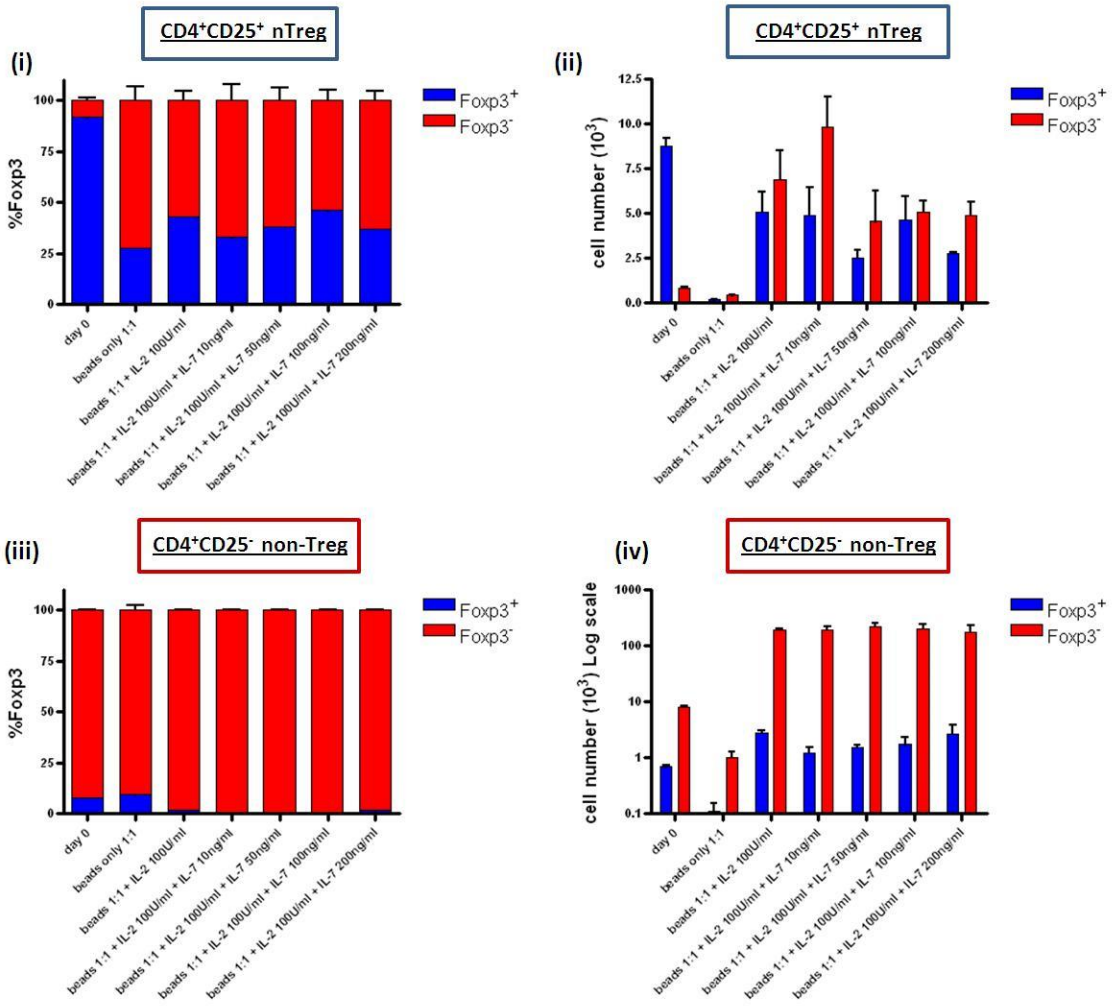

Figure 5.2.2.3.1. Expansion of nTreg versus non-Treg with anti-CD3/CD28 beads plus IL-2 and IL-7. MACS-isolated B6 $CD4^+CD25^+$ nTreg ($1x10^4$) with a purity of 91.1% were expanded using anti-CD3/CD28 beads (at a 1:1 bead to cell ratio), in the presence of IL-2 (100 U/ml), with or without the addition of IL-7 (0-200 ng/ml) for 7 days. $CD4^+CD25^-$ non-Treg were expanded in the same way as controls. The proportion and number of $Foxp3^+$ and $Foxp3^-$ cohorts in the resultant population in each experimental condition were determined by flow cytometry. **(i)** The addition of IL-7 was not able to reverse the dominant proportion of $Foxp3^-$ cohort in the resultant population. **(ii)** The $Foxp3^+$ cohort did not expand, suggesting that the addition of IL-7 could not induce a preferential expansion of $Foxp3^+$ nTreg *in vitro*. **(iii) & (iv)** When $CD4^+CD25^-$ non-Treg were used as the starting population, IL-7 had no impact on the expansion of the $Foxp3^-$ cohorts. Data above represent means of 3 replicates with error bars showing 1 S.D. from the mean values.

To evaluate the impact of IL-15 on the expansion of nTreg, $1x10^4$ MACS-isolated $CD4^+CD25^+$ nTreg or $CD4^+CD25^-$ non-Treg were stimulated with anti-CD3/CD28 beads (1:1 bead: cell ratio) in the presence of IL-2 (100U/ml) and a graded concentration of IL-15 (0-200ng/ml) for 7 days. The proportion of $Foxp3^+$ cells in the expanded $CD4^+CD25^+$ nTreg was not altered by the addition of IL-15 ***(Figure 5.2.2.3.2.i)***. Additional IL-15 was not beneficial for the expansion of the $Foxp3^+$ cohort. At high concentrations (200ng/ml), it appeared to be detrimental to the expansion of $Foxp3^+$ nTreg ***(Figure 5.2.2.3.2.ii)***. The addition of IL-15 did no alter the proportion of the $Foxp3^+$ and $Foxp3^-$ cohort in expanded $CD4^+CD25^-$ non-Treg ***(Figure 5.2.2.3.2.iii)***. At the optimal concentration (100ng/ml), IL-15 showed a marginal benefit on the expansion of the $Foxp3^+$ cohort in the background of an outgrowth of the $Foxp3^-$ cohort ***(Figure 5.2.2.3.2.iv)***.

Figure 5.2.2.3.2. Expansion of nTreg versus non-Treg with anti-CD3/CD28 beads plus IL-2 and IL-15

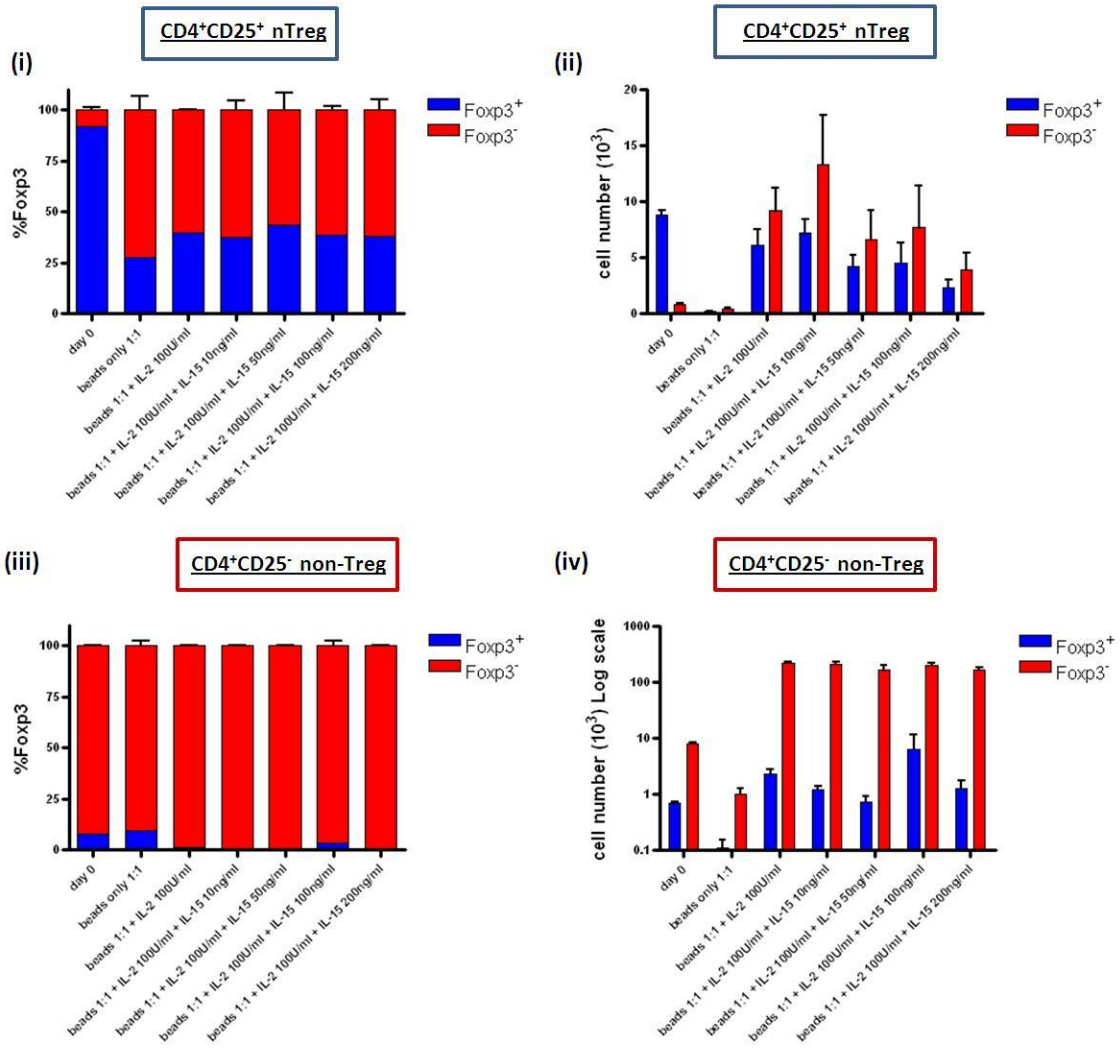

Figure 5.2.2.3.2. Expansion of nTreg versus non-Treg with anti-CD3/CD28 beads plus IL-2 and IL-15. MACS-isolated B6 CD4$^+$CD25$^+$ nTreg (1x10^4) with a purity of 91.1% Foxp3$^+$ nTreg were expanded using anti-CD3/CD28 beads (at a 1:1 bead to cell ratio), in the presence of IL-2 (100 U/ml), with or without the addition of IL-15 (0-200 ng/ml) for 7 days. The proportion and number of the Foxp3$^+$ and Foxp3$^-$ cohorts in the resultant population in each experimental condition were determined by flow cytometry. **(i)** The addition of IL-15 was not able to reverse the dominance of the Foxp3$^-$ cohort in the resultant population. **(ii)** There was an outgrowth of the Foxp3$^-$ cohort indicating that IL-15 could not induce a preferential expansion of the Foxp3$^+$ cohort *in vitro*. **(iii) & (iv)** When CD4$^+$CD25$^-$ non-Treg were used as the starting population, the addition of IL-15 had no impact on the proportion of Foxp3$^+$ and Foxp3$^-$ cohort significantly, but appeared to have a marginal effect on promoting the expansion of the Foxp3$^+$ cohort at 100 ng/ml. IL-15 had no impact on the expansion of the Foxp3$^-$ cohort. Data above represent means of 3 replicates with error bars showing 1 S.D. from the mean values.

Finally, we tested the combination of IL-2, IL-7 and IL-15 in the same cultures for the expansion of nTreg. $1x10^4$ MACS-isolated $CD4^+CD25^+$ nTreg or $CD4^+CD25^-$ non-Treg were stimulated with anti-CD3/CD28 beads (1:1 or 2:1 bead:cell ratio), in the presence of IL-2 (100U/ml) in combination with either IL-7 (200ng/ml) or IL-15 (200ng/ml) or both for 7 days. The combination of IL-2, IL-7 and IL-15 did not gear the culture towards a higher proportion of the $Foxp3^+$ cohort in the expanded $CD4^+CD25^+$ nTreg population ***(Figure 5.2.2.3.3.i)***. The combination of IL-2, IL-7 and IL-15 led to a lower expansion of the $Foxp3^+$ cohort than the addition of a high-dose IL-7 or IL-15 alone to the IL-2 containing cultures ***(Figure 5.2.2.3.3.ii)***. Nevertheless, these cultures were contaminated with a high proportion of a $Foxp3^-$ cohort. Doubling the number of anti-CD3/CD28 beads could lead to a higher expansion rate of the $Foxp3^+$ cohort, but upon a background outgrowth of $Foxp3^-$ cohort. Using $CD4^+CD25^-$ non-Treg as the starting population, the combination of IL-2, IL-7 and IL-15 had no effect on the expansion of the $Foxp3^+$ or $Foxp3^-$ cohort compared to the addition of a high-dose IL-7 or IL-15 to the IL-2 containing cultures. Collectively, these data suggest that the addition of IL-7 and IL-15 could not produce a more selective $Foxp3^+$ Treg anti-CD3/CD28 bead-based expansion protocol.

Figure 5.2.2.3.3. Expansion of nTreg versus non-Treg with anti-CD3/CD28 beads plus IL-2, IL-7 and IL-15

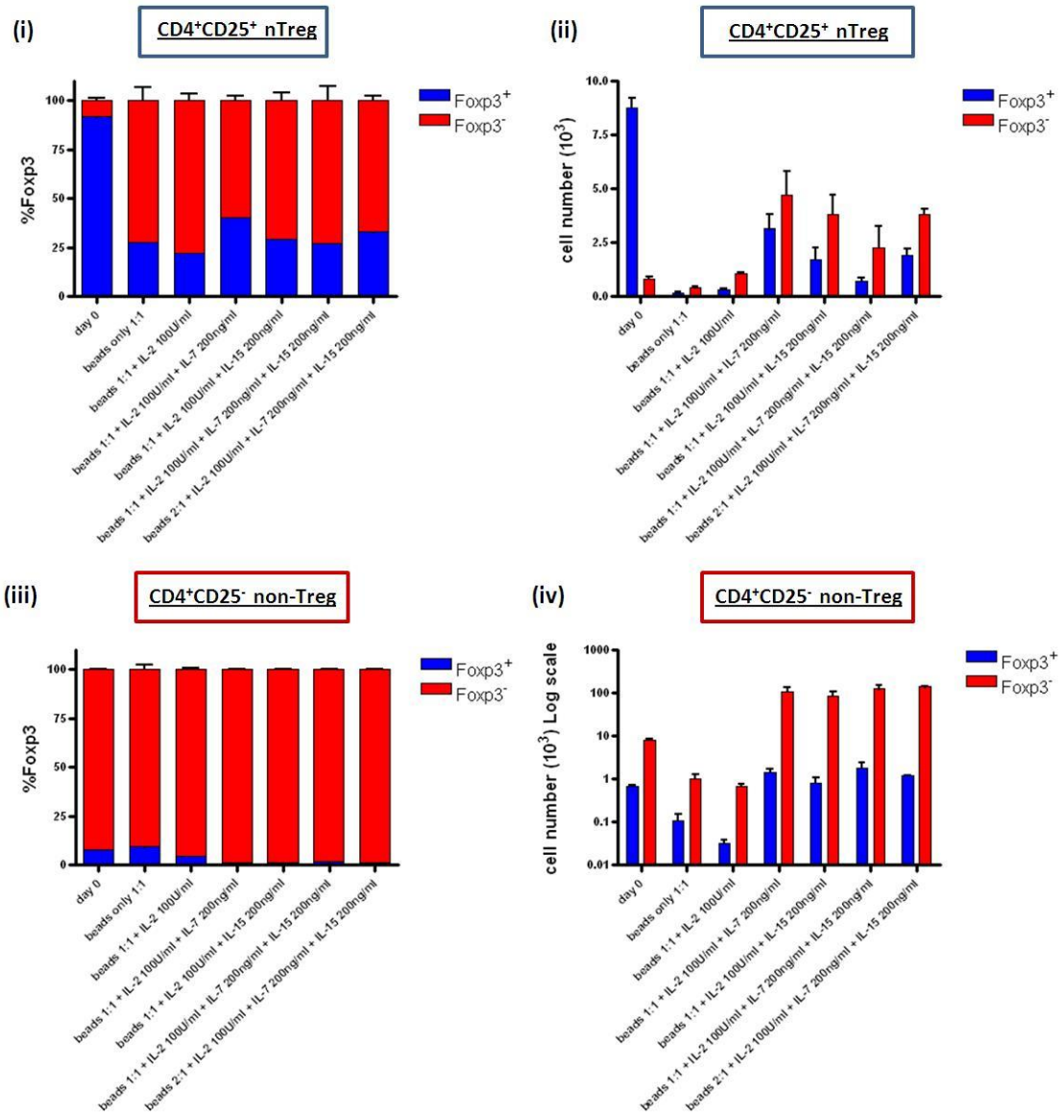

Figure 5.2.2.3.3. Expansion of nTreg versus non-Treg with anti-CD3/CD28 beads plus IL-2, IL-7 and IL-15. MACS-isolated B6 $CD4^+CD25^+$ nTreg ($1x10^4$) were expanded using anti-CD3/CD28 beads at a 1:1 or 2:1 ratio, in the presence of IL-2 (100 U/ml) with or without IL-7 (200 ng/ml) or IL-15 (200 ng/ml) for 7 days. $CD4^+CD25^-$ non-Treg were expanded in the same way as controls. **(i) & (ii)** When using nTreg as the input population, the addition of IL-7 and IL-15 were not able to reverse the outgrowth of the $Foxp3^-$ cohorts. **(iii) & (iv)** The addition of IL-7 and IL-15 preserved the efficient expansion of non-Treg, but they could not induce a preferential expansion of the $Foxp3^+$ cohorts. Data above represent means of 3 replicates with error bars showing 1 S.D. from the mean values.

5.2.2.4 Expansion of MACS-isolated versus FACS-sorted nTreg

According to the experiments reported above, the resultant expanded T cell population was almost always dominated by a $Foxp3^-$ cohort even though we started with an input $Foxp3^+$ population in excess of 90%. We hypothesized that we could possibly minimize the overgrowth of the dominant $Foxp3^-$ cohort in the expanded population by improving the initial selection process to eliminate the presence of the $Foxp3^-$ cohort as much as possible. In this section, our objective was to compare the expansion potential of MACS-isolated versus FACS ARIA-sorted nTreg based on the expression of CD25 in WT mice or GFP in GFP/Foxp3 KI mice using two different commercially available Treg expansion kits which have been shown to have the capability to expand mouse Treg up to 4 to 10-folds expansion.

Using GFP/Foxp3 KI CBA splenocytes as the common nTreg source, following a CD4 enrichment protocol using a negative selection process as described in ***Chapter 2.7.3***, we isolated nTreg using the MACS or FACS ARIA technique which yielded a purity of 66.2% and 95.1% $CD4^+GFP^+$ nTreg, respectively ***(Figure 5.2.2.4.1.i & ii)***. The percentage of GFP^+ in the MACS-isolated nTreg population was unexpectedly low (~50% of expected) due to the random inhibition of the heterozygous expression of the X-linked Foxp3 genes in female GFP/Foxp3 KI CBA mice, while using all male GFP/Foxp3 KI CBA mice all $Foxp3^+$ cells would be GFP^+. MACS-isolated nTreg or ARIA-sorted nTreg were then stimulated with either Invitrogen® anti-CD3/CD28 beads (at a 1:1 bead:cell ratio) or Miltenyi® anti-CD3/CD28 beads (at 3:1 bead:cell ratio), in the presence of a graded concentration of IL-2 (0-2000U/ml) for 7 days, according to the manufacturer's recommendations[441,503] ***(Figure 5.2.2.4.1.iiia & b)***. The proportion and absolute number of GFP^+ cells were then determined by flow cytometry analysis.

Figure 5.2.2.4.1. Expansion of MACS-isolated CD4$^+$CD25$^+$ nTreg versus FACS ARIA-sorted CD4$^+$GFP$^+$ nTreg with two different commercially available Treg expansion anti-CD3/CD28 bead-based protocols *in vitro*

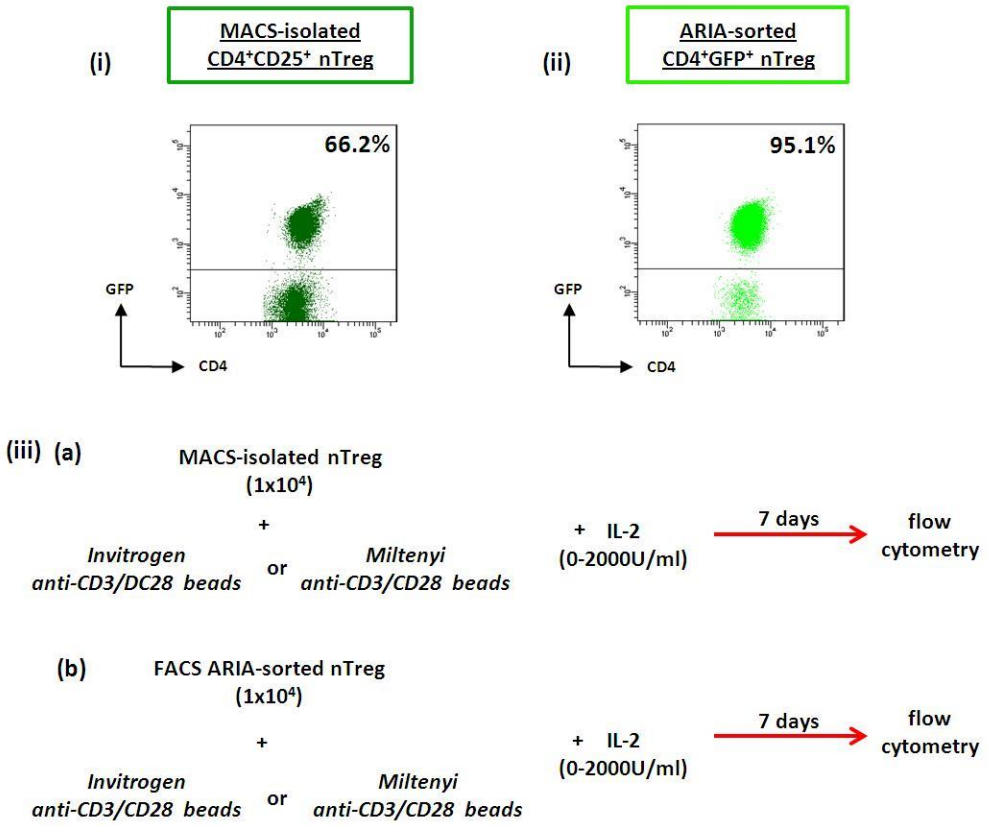

Figure 5.2.2.4.1. Expansion of MACS-isolated CD4$^+$CD25$^+$ nTreg versus FACS ARIA-sorted CD4$^+$GFP$^+$ nTreg with two different commercially available Treg expansion anti-CD3/CD28 bead-based protocols *in vitro*. GFP/Foxp3 KI CBA nTreg were isolated using MACS based on the expression of CD4 and CD25. **(i)** FACS dot plot shows that MACS-isolated nTreg had a purity of 66.2% GFP$^+$ nTreg. The low purity of GFP$^+$ nTreg was anticipated because of the use of female GFP/Foxp3 KI CBA mice, in which up to 50% Foxp3$^+$ cells did not co-express GFP due to X-chromosome inactivation. **(ii)** GFP/Foxp3 KI CBA CD4$^+$GFP$^+$ nTreg were sorted by FACS ARIA sorter, which yielded a purity of 95.1% GFP$^+$CD4$^+$ nTreg. MACS-isolated or FACS ARIA-sorted nTreg were expanded using either ***Invitrogen***® anti-CD3/CD28 beads (at a 1:1 bead to cell ratio) or ***Miltenyi***® anti-CD3/CD28 beads (at a 3:1 bead to cell ratio), in the presence of various concentrations of IL-2 (0-2000U/ml) for 7 days. The proportion and relative number of the CD4$^+$GFP$^+$ and CD4$^+$GFP$^-$ cohorts in the expanded T cell populations were examined using flow cytometry.

Using the Invitrogen® protocol, expanded MACS-isolated $CD4^+CD25^+$ nTreg maintained a high proportion of the GFP^+ cohort matching that of the input population when stimulated with anti-CD3/CD28 beads plus IL-2 ***(Figure 5.2.2.4.2.i)***. Similarly, expanded ARIA-sorted $CD4^+GFP^+$ nTreg also maintained a high proportion of the GFP^+ cohort, except when nTreg were stimulated with anti-CD3/CD28 beads without IL-2 ***(Figure 5.2.2.4.2.ii)***. However, when the cells were enumerated, we noticed that although we eliminated the outgrowth of GFP^- cohorts, no real expansion of the GFP^+ cohort actually occurred irrespective of the concentration of IL-2 in both MACS-isolated nTreg ***(Figure 5.2.2.4.2.iii)*** or ARIA-sorted nTreg ***(Figure 5.2.2.4.2.iv)***, when compared to the initial population.

Using the Miltenyi® protocol, expanded MACS-isolated $CD4^+CD25^+$ nTreg maintained a high proportion of the GFP^+ cohort compared to the starting population ***(Figure 5.2.2.4.3.i)***. Expanded ARIA-sorted $CD4^+GFP^+$ nTreg also maintained a high proportion of the GFP^+ cohort if stimulated with anti-CD3/CD28 beads plus IL-2 ***(Figure 5.2.2.4.3.ii)***. However, there was no statistically significant expansion of the GFP^+ cohort when compared to the starting population in both MACS-isolated nTreg and ARIA-sorted nTreg group ***(Figure 5.2.2.4.3.iii & iv)***.

Although neither protocol could provide a reliable expansion of nTreg, the data above indicate that a higher purity of nTreg in the starting population could minimize the potential contamination by non-Treg in the expanded population.

Figure 5.2.2.4.2. Expansion of MACS-isolated versus FACS ARIA-sorted nTreg with *Invitrogen*® anti-CD3/CD28 beads and IL-2

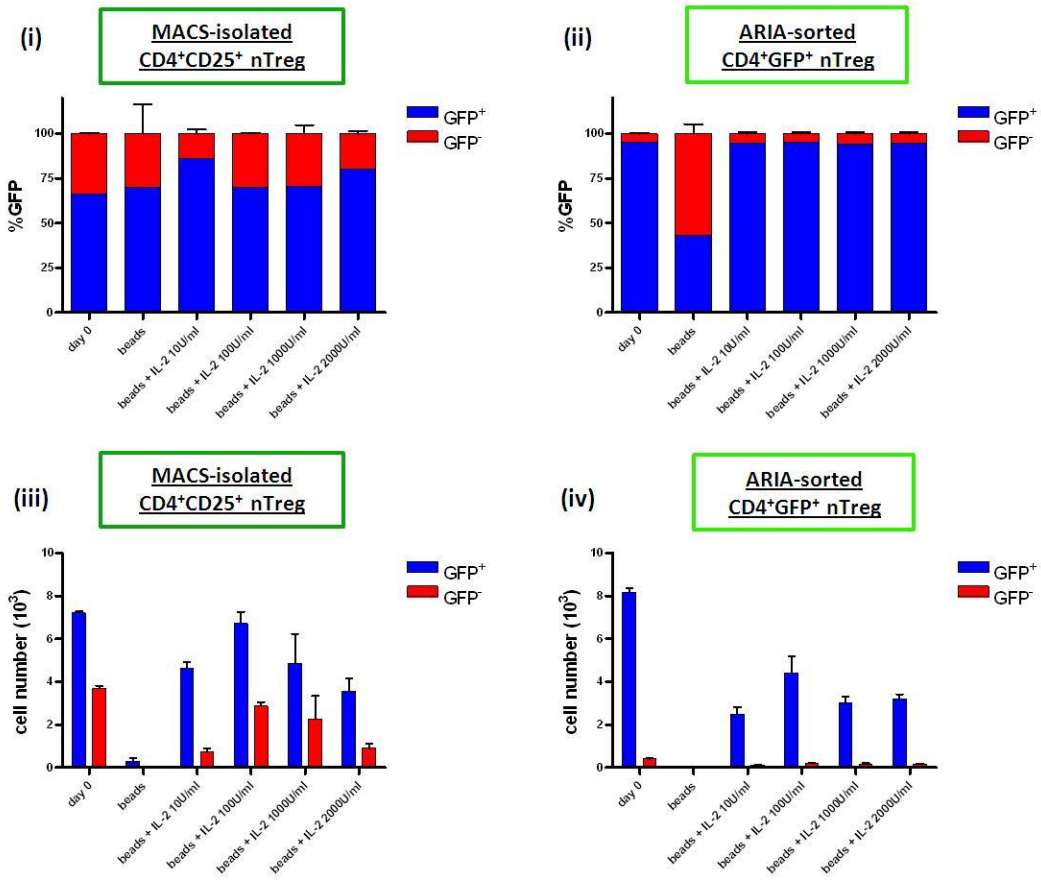

Figure 5.2.2.4.2. Expansion of MACS-isolated CD4⁺CD25⁺ nTreg versus FACS ARIA-sorted CD4⁺GFP⁺ nTreg using the *Invitrogen*® anti-CD3/CD28 bead-based protocol *in vitro*. (i) Using the ***Invitrogen***® protocol, MACS-isolated nTreg could maintain the initial proportion of GFP⁺ expression after 7 days of expansion regardless of the concentration of IL-2. **(ii)** Similarly, FACS ARIA-sorted nTreg also sustained their initial proportion of GFP⁺ cohort, except when cells were stimulated without supplementary IL-2. **(iii)** In terms of relative cell number, MACS-isolated nTreg stimulated with beads and IL-2 led to the a resultant population similar to that of the initial input, with a significant contaminant of a GFP⁻ cohort. **(iv)** FACS ARIA-sorted nTreg remained a dominant GFP⁺ population. However, the yield achieved was only approximately 50% of the initial input under optimal culture conditions. These data suggest that expanded nTreg using the bead-based protocol could be devoid of a significant contaminant of GFP⁻ non-Treg cohort in the resultant population, possibly due to a higher purity of the starting population provided by flow cytometry cell sorter. Data above represent means of 3 replicates with error bars showing 1 S.D. from the mean values.

Figure 5.2.2.4.3. Expansion of MACS-isolated versus FACS ARIA-sorted nTreg with *Miltenyi*® anti-CD3/CD28 beads and IL-2

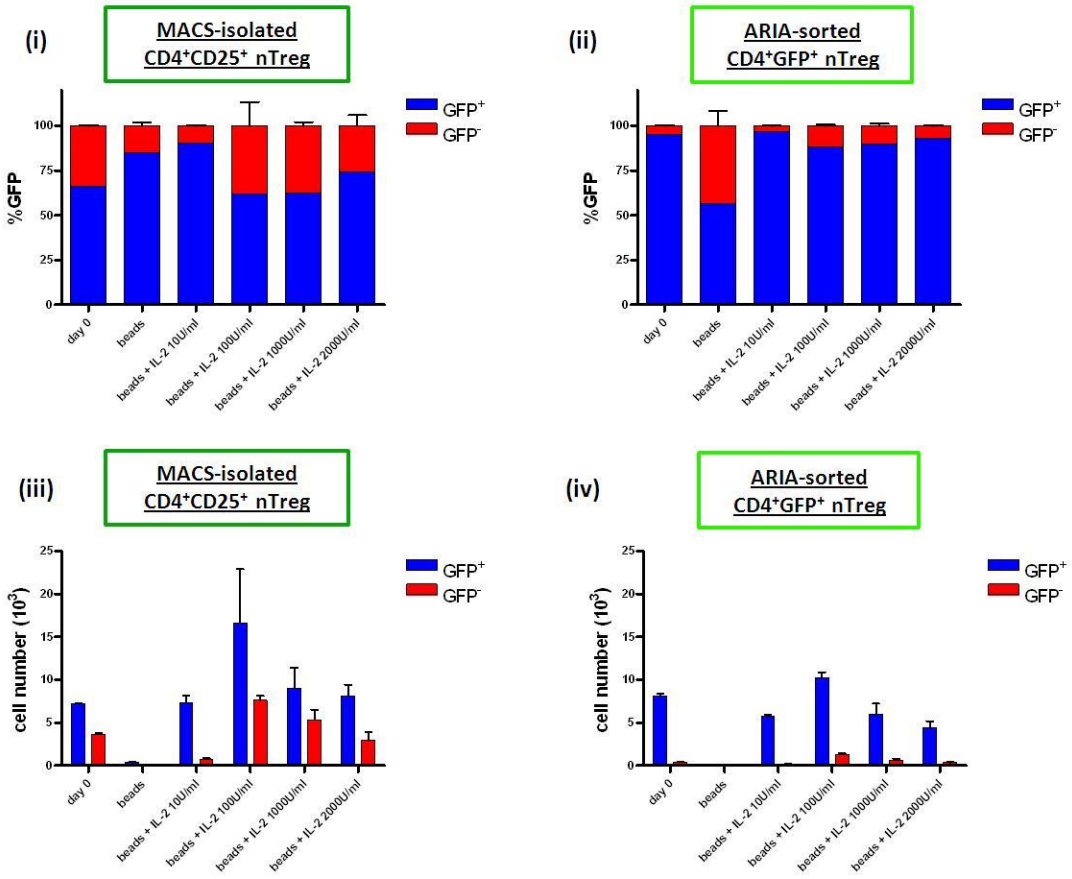

Figure 5.2.2.4.3. Expansion of MACS-isolated CD4⁺CD25⁺ nTreg versus FACS ARIA-sorted CD4⁺GFP⁺ nTreg using the *Miltenyi*® anti-CD3/CD28 bead-based protocol *in vitro*. **(i)** Using the ***Miltenyi***® protocol, MACS-isolated nTreg maintained the initial proportion of GFP⁺ expression after 7 days of expansion. **(ii)** FACS ARIA-sorted nTreg also sustained a similar proportion of GFP⁺ cohort compared to the initial population, except when cells were stimulated without supplementary IL-2. **(iii)** MACS-isolated nTreg stimulated with beads and IL-2 led to a resultant population with cell count similar to that of the initial input, but with a significant contaminant of a GFP⁻ cohort. **(iv)** FACS ARIA-sorted nTreg remained a dominant GFP⁺ population with a post-expansion cell yield compatible to the initial input number under optimal culture conditions. These data further affirm that in order to avoid contaminant with a non-Treg population after expansion, a highly purified nTreg input population is a pre-requisite using these bead-based Treg expansion protocols. Data above represent means of 3 replicates with error bars showing 1 S.D. from the mean values.

5.2.2.5 Expansion of doubly-sorted nTreg

Deducing from the results above that an initial purity of GFP^+/$Foxp3^+$population might be a pre-requisite to avoid significant contamination by a large non-Treg population in the final expanded nTreg mixture, we employed a double-sorting strategy to achieve the highest possible input purity of nTreg based on CD25 or GFP.

GFP/Foxp3 KI CBA splenocytes contained 9.1% $CD4^+GFP^+$ nTreg. These cells were then enriched for a $CD4^+$ population by a negative selection process before being subjected to the first round of flow sorting. The purity of $CD4^+GFP^+$ nTreg improved from 93.6% to 98.7% after two successive rounds of flow sorting, respectively ***(Figure 5.2.2.5.1.i)***. $1x10^5$ doubly-sorted $CD4^+GFP^+$ nTreg were expanded with Invitrogen® anti-CD3/CD28 beads (1:1 bead:cell ratio) plus IL-2 (2000U/ml) for 7 days. This set of experiment used a much higher starting population compared to other experiments in this Chapter ($1x10^5$ cells/well versus $1x10^4$ cells/well in previous experiments), because we were able to acquire a much larger number of GFP/Foxp3 KI CBA mice for splenocyte harvest on this particular occasion to optimize the culture conditions provided by the expander bead manufacturer *(personal communication)*.

Cells were split on day 4 and replenished with IL-2-containing medium. Cells were harvested on day 7 for the examination of their proportion and number of $CD4^+GFP^+$ nTreg by flow cytometry. After expansion, the purity of expanded nTreg maintained at 96.9% $CD4^+GFP^+$ ***(Figure 5.2.2.5.1.ii)***. Compared to the starting population there was a small increase of the GFP^- cohort from 1.8 to 3.1% ***(Figure 5.2.2.5.2.i)***. On this occasion, we saw a significant expansion of the GFP^+ cohort after between day 0 and 7 with, with an average of a 3.7-fold increase ***(Figure 5.2.2.5.2.ii & iii)***. Of note, although the number of GFP^- cohort was relatively small, there was a significant expansion of an average of 6.5-fold increase from day 0 suggesting that the GFP^-

cohort could still potentially present as a significant outgrowth if being cultured for a longer period of time.

Although a significant expansion was observed, a 4-fold increase was not comparable to those reported by various authors and the manufacturers (at least a 10-fold increase by day 7). To eliminate an inherent strain issue, we then elected to use nTreg from BALB/c mice which have been shown to be successfully expanded *in vitro*. $1x10^5$ doubly-sorted BALB/c $CD4^+CD25^+$ nTreg (purity of 99.7% $CD4^+CD25^+$) were expanded using the Invitrogen® or Miltenyi® protocol plus IL-2 (2000U/ml) initially for 7 days. We also investigated if we could obtain a higher yield of nTreg by extending these cultures up to 3 weeks, but at the same time to explore if an outgrowth of the $Foxp3^-$ cohort would catch up.

Figure 5.2.2.5.1. Expansion of doubly-sorted nTreg with anti-CD3/CD28 beads and IL-2

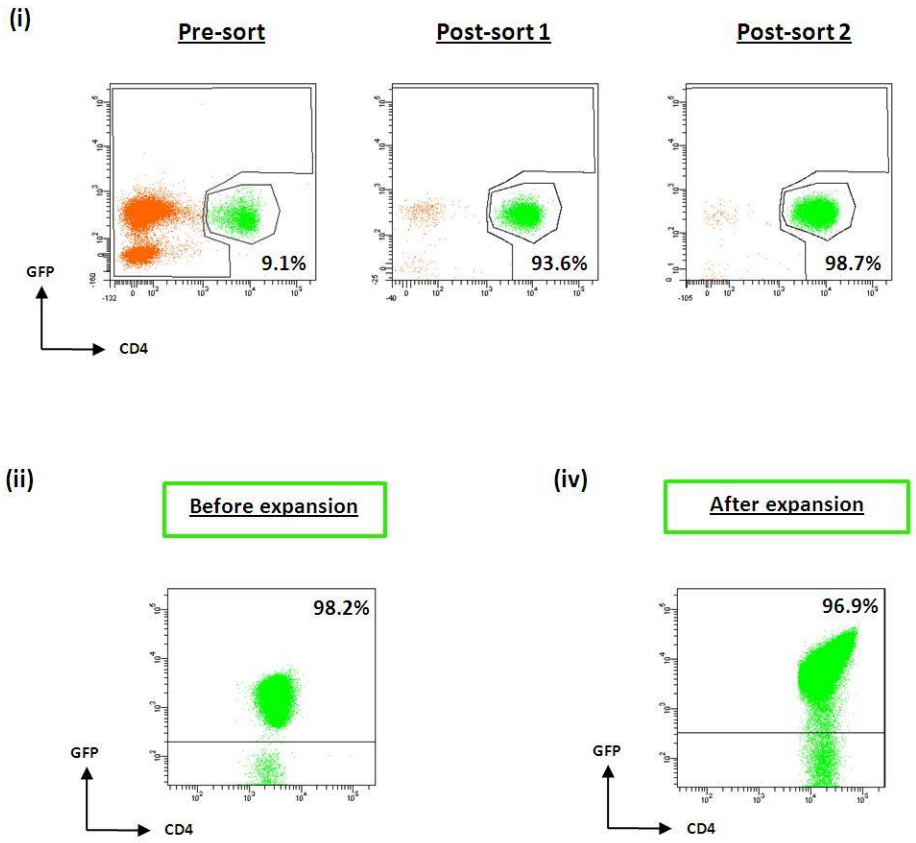

Figure 5.2.2.5.1. Expansion of doubly-sorted GFP⁺ nTreg with anti-CD3/CD28 bead-based protocol *in vitro*. GFP/Foxp3 KI CBA splenocytes were sorted for CD4⁺GFP⁺ nTreg using FACS ARIA sorter from an initial 9.1% population **(i)**. The efficiency of flow cytometry sorting is demonstrated above showing that the purity of GFP⁺ nTreg improved from 93.6 % to 98.7% after two successive sorting procedures. **(ii)** Doubly-sorted GFP⁺ nTreg with a starting purity of 98.2% were expanded using anti-CD3/CD28 beads plus an optimal IL-2 concentration that led to a final product that was consisted of 96.9% GFP⁺ nTreg after 7 days.

Figure 5.2.2.5.2. Expansion of doubly-sorted nTreg with anti-CD3/CD28 beads and IL-2

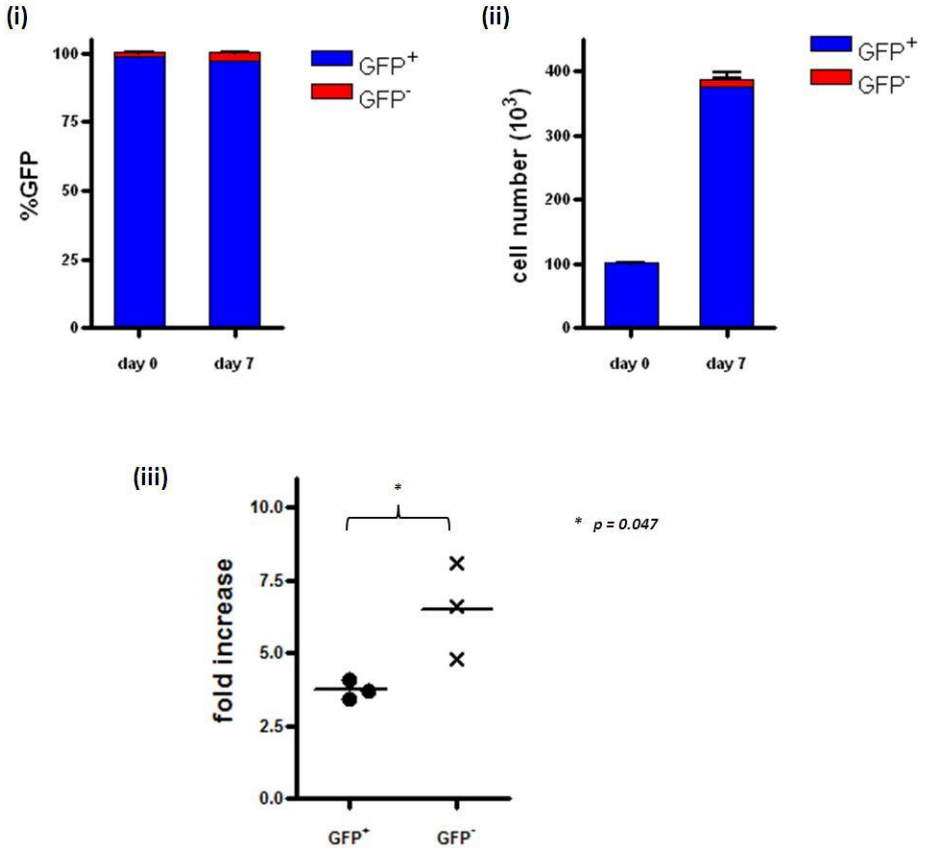

Figure 5.2.2.5.2. Expansion of doubly-sorted GFP⁺ nTreg with anti-CD3/CD28 bead-based protocol *in vitro*. The resultant population of the expanded doubly-sorted GFP⁺ nTreg was assessed by flow cytometry. **(i)** After 7 days, the proportion of GFP⁺ nTreg sustained at 96.9% compared to the input population (98.2%). **(ii)** The expansion of a highly-purified GFP⁺ nTreg population generated a dominant GFP⁺ final product with approximately a 4-fold increase. **(iii)** Examination of the expanded sub-populations indicated that the GFP⁺ cohort proliferated and expanded with a mean of 3.7-fold increase. However, the GFP⁻ cohort also expanded in a greater magnitude with a mean of 6.5-fold increase. These data suggest that the expansion of a highly-purified nTreg population using the bead-based protocol could result in a 4-fold increase in yield, but a contaminating non-Treg population would still remain in the resultant cell mixture. Data above represent means of 3 replicates with error bars showing 1 S.D. from the mean values. Student's t-tests were used for statistical comparisons. (p<0.05 denotes statistically significant)

Using the Invitrogen® protocol, the percentage of the Foxp3$^+$ cohort was maintained at >97.5% at week 1, then dropped to 44.5% at week 2 and reached a plateau at 48.6% at week 3. Similarly, using the Miltenyi® protocol the percentage of the Foxp3$^+$ cohort was initially maintained at a high level (99.2%; week one), but it dropped to 41.6% and 36.7% at week 2 and 3, respectively ***(Figure 5.2.2.5.3.i)***. Conversely, the percentages of the Foxp3$^-$ cohorts in the expanded nTreg population using both protocols increased dramatically from week 2 and was sustained at week 3 ***(Figure 5.2.2.5.3.ii)***. More importantly, while there was only a modest expansion of the Foxp3$^+$ cohort using the Invitrogen® protocol at week 1 (1.3-fold), the number of the Foxp3$^+$ cohort increased significantly from week 1 to week 2 (2.2-fold) and reached a plateau at week 3 (overall 3-fold increase) ***(Figure 5.2.2.5.3.iii)***. On the other hand, using the Miltenyi® protocol, the expansion of the Foxp3$^+$ cohort did not start until after week 1, peaked at week 2 (2.9-fold) then declined at week 3 (overall 1.2-fold) ***(Figure 5.2.2.5.3.iii)***. On the contrary, while there was no outgrowth of the Foxp3$^-$ cohort seen at week 1 in both preparations, there was an exponential expansion of the Foxp3$^-$ cohorts in both preparations at week 2 (>2000-fold), which declined at week 3 (1300 to 2000-fold expansion) ***(Figure 5.2.2.5.3.iv)***.

Collectively, these data suggest that Foxp3$^+$ nTreg could be expanded in small numbers in our hands (3-fold expansion) using the anti-CD3/CD28 bead protocols, which was not by-and-large mouse strain-dependent. Contamination by a large non-Treg population could be minimized by using a highly purified Foxp3$^+$ input population by cell sorting and harvesting expanded cells within 1 week at the expense of a modest yield. Extended cultures allowed a small Foxp3$^-$ cohort to overgrow and overshadow the expansion of the Foxp3$^+$ cohort. The overall cell yield began to decline after week 3 which was suggestive of cell exhaustion in culture.

Figure 5.2.2.5.3. Extended expansion of doubly-sorted CD25⁺ nTreg with two different protocols using anti-CD3/CD28 beads and IL-2

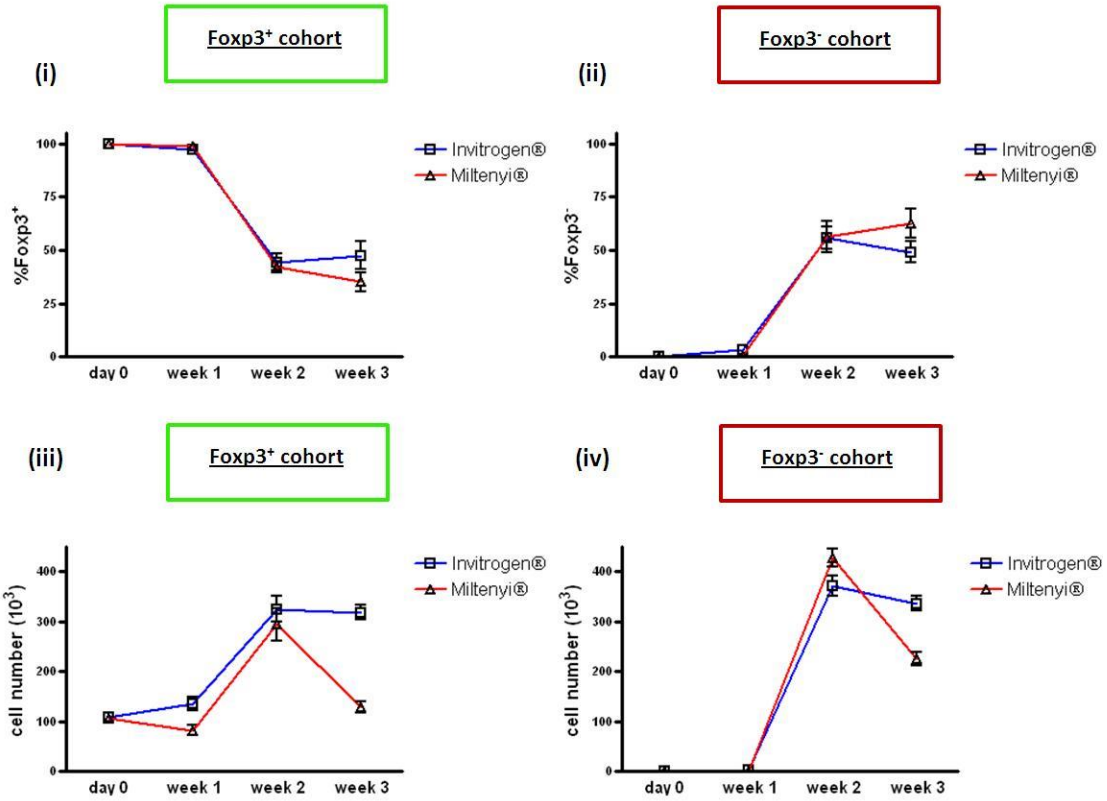

Figure 5.2.2.5.3. Extended expansion of doubly-sorted CD4⁺CD25⁺ nTreg with two different anti-CD3/CD28 bead-based protocols *in vitro*. BALB/c nTreg were isolated by doubly-sorting for CD4⁺CD25⁺ T cells. These cells were expanded using the Invitrogen® or the Miltenyi® anti-CD3/CD28 beads plus exogenous IL-2 under optimal culture conditions with interval cell splitting and replenishment of IL-2-containing media up to 3 weeks. **(i) & (ii)** On day 0, the starting population consisted of a 99.7% purity of CD4⁺Foxp3⁺ nTreg and a very small Foxp3⁻ non-Treg population (<0.3%). After 1 week of expansion with either protocol, it resulted in a highly-sustainable Foxp3⁺ cohort. However, the percentages of the Foxp3⁺ cohort dropped significantly beyond week 2 and the cultures were dominated by a Foxp3⁻ cohort in either group (>50%). **(iii) & (iv)** Although there was a 2-3 fold increase in the Foxp3⁺ cohort, there was an exponential increase in the number of the Foxp3⁻ cohort from week 1 to week 2. Collectively, these data suggest that expanding highly-purified nTreg over a short period of time (up to 1 week) could lead to a modest level of Foxp3⁺ nTreg expansion. However, continual expansion of nTreg would ultimately lead to an extensive contaminant of Foxp3⁻ non-Treg using the bead-based Treg expansion protocols.

5.2.3 Treg expanded efficiently using a plate-bound anti-CD3/28 antibody protocol

Although it appeared seemingly impossible to expand mouse nTreg without the contamination of a significant number of Foxp3$^-$ T cells, the Foxp3$^+$ population responded to the polyclonal stimuli and expanded up to 4-fold in our hands ***(Chapter 5.2.2; Figure 5.2.2.5.2)***. In fact, further discussion with the manufacturers of the anti-CD3/CD28 beads revealed that an 8 to 10-fold expansion of mouse Treg was actually fairly optimistic according to their own data *(Invitrogen and Miltenyi Biotec unpublished data personal communication)*.

We then returned to investigate the use of soluble or immobilized anti-CD3/anti-CD28 antibody which formed the prototype of the current anti-CD3/CD28 bead protocol. Hoffmann et al were first to demonstrate that immobilized anti-CD3 antibody plus soluble anti-CD28 antibody could break the anergy status of human CD4$^+$CD25$^+$ T cells and they were able to expand CD4$^+$CD25$^+$ T cells 20 to 200-fold after 7 days *in vitro*[424]. Fantini et al[526] described an *in vitro* Treg expansion protocol, which entailed converting flow cytometer-sorted CD4$^+$CD25$^-$ conventional T cells (0.76% Foxp3$^+$) into a dominant Treg population using the combination of plate-bound anti-CD3 antibody, soluble anti-CD28 antibody and TGF-β. The end product consisted of an equal number of cells, but with an enrichment of 66.4% Foxp3$^+$ Treg that suppressed the proliferation of CD4$^+$CD25$^-$ T cells *in vitro*. nTreg are anergic upon stimulation via the TCR alone. Hunig et al developed a super agonistic anti-CD28 anti-body which bypasses the TCR signal and IL-2 requirement and it was shown to be able to preferentially induce nTreg proliferation *in vitro[527,528]* and *in vivo[529]*. Moreover, super agonistic anti-CD28 antibody induced nTreg proliferation and alleviation in a mouse colitis model[530].

In the midst of our continued search for possible solutions to expand mouse Treg, we came across a report by Singh et al[531] that described a novel mechanism in which Treg were resistant to activation-induced apoptosis following the stimulation of plate-bound anti-CD3 and anti-CD28 antibody. A direct comparison was made between a plate-bound anti-CD3/CD28 antibody-based versus an anti-CD3/CD28 antibody-conjugated bead-based protocol, which showed that the former restricted the growth of non-Treg in response to anti-CD3/CD28 stimulation, whereas the latter led to profound non-Treg expansion *in vitro*. Such differences were explained by their differential expression of Fas/FasL and p53 upon stimulation with plate-bound anti-CD3/CD28 antibody versus anti-CD3/CD28 beads using knock-out animals. More importantly, it was CD28-dependent. As a result, a non-classical form of AICD occurred with non-Treg, but Treg expanded significantly and outgrew the non-Treg cohort in expanded T cell cultures using an unsorted population. Therefore, this plate-bound anti-CD3/CD28 antibody Treg expansion protocol represented a feasible tool to selectively expand $Foxp3^+$ mouse Treg in large scale (40-fold) *in vitro*.

We therefore adopted Singh's protocol with minor modifications (*personal communication with authors*) and attempted to expand $CD4^+CD25^+$ nTreg *in vitro*. Plastic petridishes were pre-coated with a high concentration of purified anti-CD3 (5μg/ml) and anti-CD28 (5μg/ml) in borate buffer overnight at 4°C as described in ***Chapter 2.9.3***. Petridishes were then washed with copious amount of complete medium before plating with isolated T cell population with IL-2-containing medium (50U/ml) ***(Figure 5.2.3.1.i)***. $5x10^5$ MACS-isolated $CD4^+CD25^+$ nTreg (68.9% GFP^+) or $CD4^+CD25^-$ non-Treg (2.9% GFP^+) from GFP/Foxp3 KI CBA splenocytes were cultured with plate-bound anti-CD3/CD28 antibody plus IL-2 for 2 weeks. Cultures were monitored regularly and replenished with fresh IL-2-containing medium every 2-3 days. Cells were then harvested at week 1 and week 2 for the examination of their Foxp3 expression and their cell number was enumerated ***(Figure 5.2.3.1.ii)***. At week 1, the proportion of the GFP^+ cohort in expanded $CD4^+CD25^+$ nTreg increased to from 68.9% to 92.7%; whereas the GFP^+ cohort in expanded $CD4^+CD25^-$ non-Treg also increased from 2.9% to 8.0%. At week 2, the proportion of the GFP^+ cohort in expanded $CD4^+CD25^+$ nTreg sustained at 96.9%; whereas the GFP^+ cohort in expanded $CD4^+CD25^-$ non-Treg increased to 11.1%. Unlike the bead-based protocols we have tested above ***(Chapter 5.2.2.2)***, expanding nTreg using this plate-bound anti-CD3/CD28 antibody protocol did not lead to an outgrowth of the non-Treg population, even in extended cultures up to 2 weeks.

Figure 5.2.3.1. Expansion of CD4$^+$CD25$^+$ nTreg using plate-bound anti-CD3/CD28 antibody Treg expansion protocol

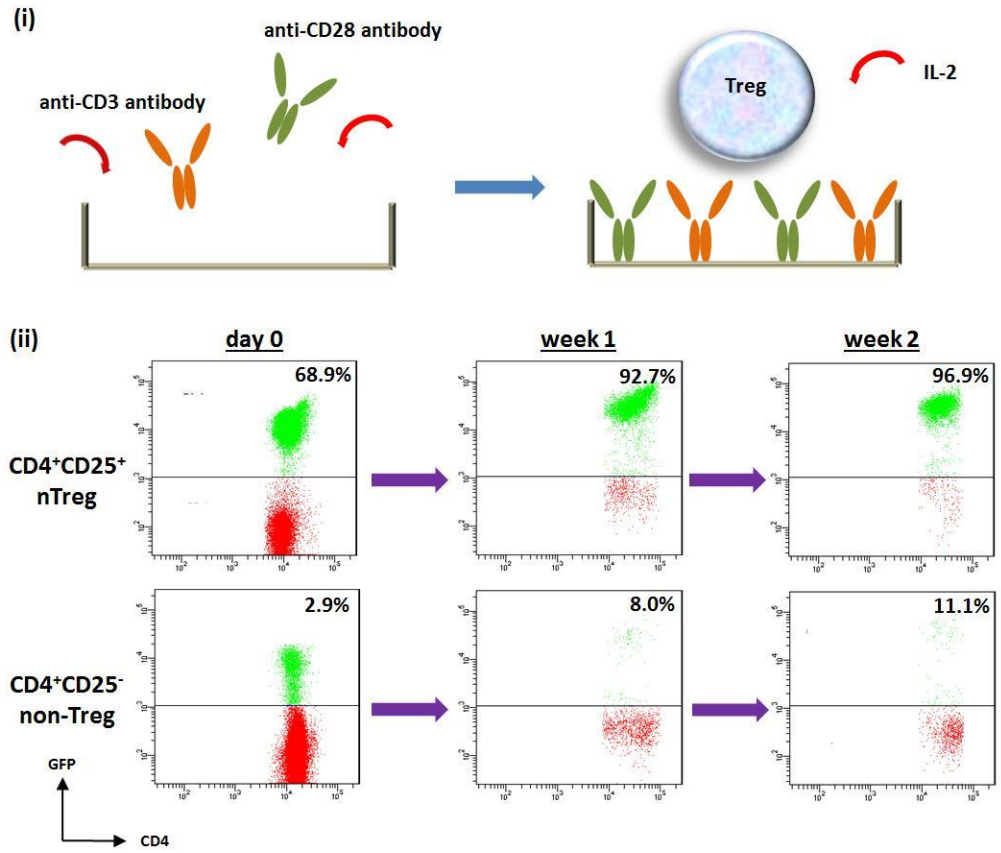

Figure 5.2.3.1. Expansion of Treg using plate-bound anti-CD3 and anti-CD28 antibody *in vitro*. (i) Adopting the Treg expansion protocol by Singh et al [457], we employed plate-bound anti-CD3 and anti-CD28 antibody plus IL-2 to expand Treg. Petridishes were pre-coated with purified anti-CD3 and anti-CD28 antibody at 5μg/ml in borate buffer overnight at 4°C as described in ***Chapter 2.10.3***. Isolated Treg population was resuspended at 1x10^5 cells/ml in complete culture media containing IL-2 (50U/ml) in petridishes after borate buffer was washed away copiously with PBS/media. Cultures were examined at regular intervals. Cells were split into new antibody-coated petridishes with replenishment of IL-2-containing media where appropriate. The final product of this expansion protocol was examined for the expression of GFP or Foxp3 by flow cytometry after a given period of time. **(ii)** MACS-isolated CD4$^+$CD25$^+$ nTreg or CD4$^+$CD25$^-$ non-Treg were expanded using this plate-bound anti-CD3/CD28 protocol. FACS dot plots illustrate the Foxp3 expression of nTreg and non-Treg on day 0 (68.9% versus 2.9%), at week 1 (92.7% versus 8.0%) and week 2 (96.9% versus 11.1%) following expansion, respectively. Unlike the bead-based protocol mentioned in the previous sections in ***Chapter 5.2***, these data suggest that this plate-bound anti-CD3/CD28 antibody protocol was able to preferentially expand Foxp3$^+$ nTreg , even in the presence of a sub-optimal purity in the starting population. Data above represent at least 3 independent experiments.

Aliquots were taken from the cultures and the GFP^+ and GFP^- cohorts enumerated from day 0 to 10 ***(Figure 5.2.3.2.i)***. Both GFP^+ and GFP^- cohorts decreased sharply following plating and began to increase in number beyond the input number from day 5. The rate of expansion was highest on day 6 but declined thereafter. In comparison with the GFP^+ cohort, the number of the GFP^- cohort remained largely unchanged. More importantly, given the massive AICD induced with this system, we examined the expression 7AAD in the whole population. We found that the number of $7AAD^+$ cells remained low until day 7 but then increased substantially ***(Figure 5.2.3.2.ii)***. By looking at the number of GFP^+7AAD^+ cells, it was noted that, although it constituted a small number, the number of GFP^+7AAD^+ cells (non-viable Treg) increased sharply after day 5 and peaked on day 7***(Figure 5.2.3.2.iii)***. On the other hand, the number of GFP^-7AAD^- cells (contaminated viable non-Treg through expansion) began to increase after day 4 and peaked at day 6 ***(Figure 5.2.3.2.iv)***.

According to the report from Singh et al[531], massive AICD occurred using this protocol and we examined cell death in cultures over time. The initial MACS selection led to a significant amount of cell death as represented by a distinct $CD4^+7AAD^+$ population ***(Figure 5.2.3.3.i)***. The proportion of $CD4^+7AAD^+$ cells increased dramatically from week 1 onwards. An overlaying dot plot of lymphocyte gate illustrates that the majority of cells expressing 7AAD belonged to the GFP^- cohort, on the other hand, the GFP^+ cohort remained $7AAD^-$ from week 1 to week 2 ***(Figure 5.2.3.3.i)***. Up to 15% of MACS-isolated nTreg coexpressed 7AAD and the pro-apoptotic marker Annexin V and 6.6% were $7AAD^-$Annexin V^+, prior to expansion. At week 1, the majority of the expanded cells were $7AAD^-$Annexin V^-, with a small proportion being $7AAD^+$Annexin V^- (3.0%). By week 2, the proportion of $7AAD^+$ increased to 9.2% ***(Figure 5.2.3.3.ii)***.

Figure 5.2.3.2. AICD of T cells as a result of the plate-bound anti-CD3/CD28 antibody Treg expansion protocol

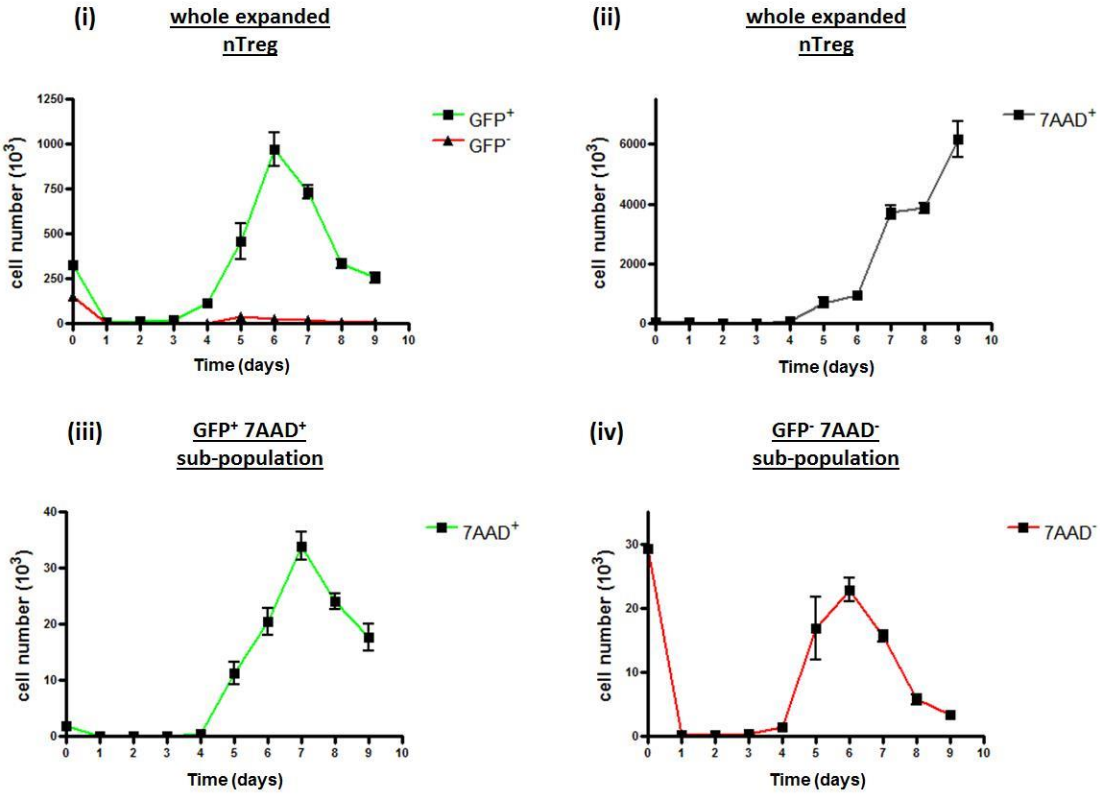

Figure 5.2.3.2. AICD of T cells as a result of the plate-bound anti-CD3 and anti-CD28 antibody-based Treg expansion protocol. (i) The majority of T cells underwent AICD during the first 3 days of culture, however, efficient GFP$^+$ nTreg expansion occurred after day 4 (peak at day 6) with a minimal number of non-Treg expansion suggesting that the plate-bound anti-CD3/CD28 antibody expansion protocol led to preferential proliferation of the Foxp3$^+$ subset but not the Foxp3$^-$ counterpart. **(ii)** The number of the 7AAD$^+$ population increased dramatically from day 6, which coincides with the time-frame where rapid nTreg proliferation occurred. Rapid cell turnover leading to a significant amount of cell death as seen by the continual increase of the 7AAD$^+$ population approaching week 2 of expansion. **(iii)** Although the number of 7AAD$^+$ within the GFP$^+$/Foxp3$^+$ sub-population was relatively small compared to the overall cell yield, this proportion began to rise after day 4. **(iv)** The number of live GFP$^-$/Foxp3$^-$ subset began to rise after day 4. Collectively, this plate-bound anti-CD3/CD28 antibody expansion protocol was able to offer a preferential expansion of GFP$^+$/ Foxp3$^+$ nTreg. However, in order to minimize the contaminant of non-Treg and cell debris, it appeared that expanded nTreg should be harvested by day 5 post-expansion. Data above represent means of 3 replicates with error bars showing 1 S.D. from the mean values.

Figure 5.2.3.3. Quality of expanded of nTreg using plate-bound anti-CD3/CD28 antibody-based protocol

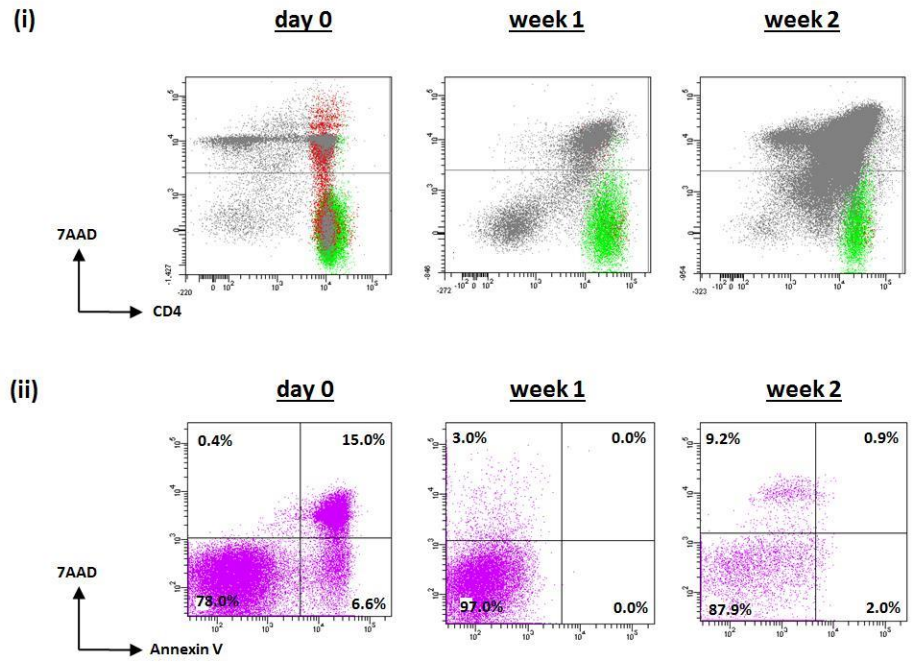

Figure 5.2.3.3. Quality of expanded nTreg using the plate-bound anti-CD3 and anti-CD28 antibody-based protocol. (i) Overlaying FACS dot plots illustrates the distribution of GFP^+ (green) , GFP^- (red) sub-population and cell debris (grey) in the MACS-isolated $CD4^+CD25^+$ nTreg. Significant cell death occurred following isolation processes through MACS column with the majority of cells expressing 7AAD belonging to the GFP^- sub-group as opposed to the GFP^+ counterparts, which are predominantly $7AAD^-$ on day 0. One week after expansion, the GFP^+ subset remained $7AAD^-$ while the culture consisted of a significant GFP^-7AAD^+ population as well as cell debris following extensive proliferation and AICD. By week 2, the presence of cell debris appeared overwhelming. **(ii)** $CD4^+CD25^+$ nTreg were assessed for the expression of pro-apoptotic marker Annexin V. A significant proportion of $7AAD^+$ and Annexin V^+ subset (15%) was present in the freshly-isolated nTreg population possibly as a result of the harsh isolation processes. However, after being expanded for 1 week only a small proportion of nTreg expressed 7AAD (3.0%) and none expressed Annexin V, suggesting that AICD in the $Foxp3^+$ population was minimal using this plate-bound anti-CD3/CD28 antibody Treg expansion protocol. Furthermore, the diminished cell number after 2 week of expansion suggesting that a high level of cell exhaustion and cell death occurred after extended expansion.

In another experiment, MACS-isolated $CD4^+CD25^+$ nTreg (with a purity of 55.8% GFP^+) from GFP/Foxp3 KI CBA splenocytes were pre-labelled with the eFluor 670 fluorescent dye prior to the stimulation with plate-bound anti-CD3/CD28 antibody/IL-2 to study for their proliferation during the first 5 days of incubation ***(Figure 5.2.3.4.i)***. On day 3, the proportion of the GFP^+ cohort increased from 55.8% to 81.5%. By gating the GFP^+ and GFP^- cohorts separately, we saw that both populations had divided extensively (63.8% and 78.2%, respectively) ***(Figure 5.2.3.4.ii)***. On day 5, almost all of the cells had divided and lost their eFluor 670 signals. However, the resultant expanded nTreg consisted of a high proportion of GFP^+ cohort (72.6%). Taking these data together, nTreg were shown to proliferate and expand in response to plate-bound anti-CD3/CD28 antibody plus IL-2 and we have chosen to harvest expanded nTreg on day 5 in which a reasonable yield could be achieved with the lowest number of GFP^+7AAD^+ and GFP^-7AAD^- cells were found.

Figure 5.2.3.4. Proliferation of nTreg in response to plate-bound anti-CD3/CD28 antibody stimulation

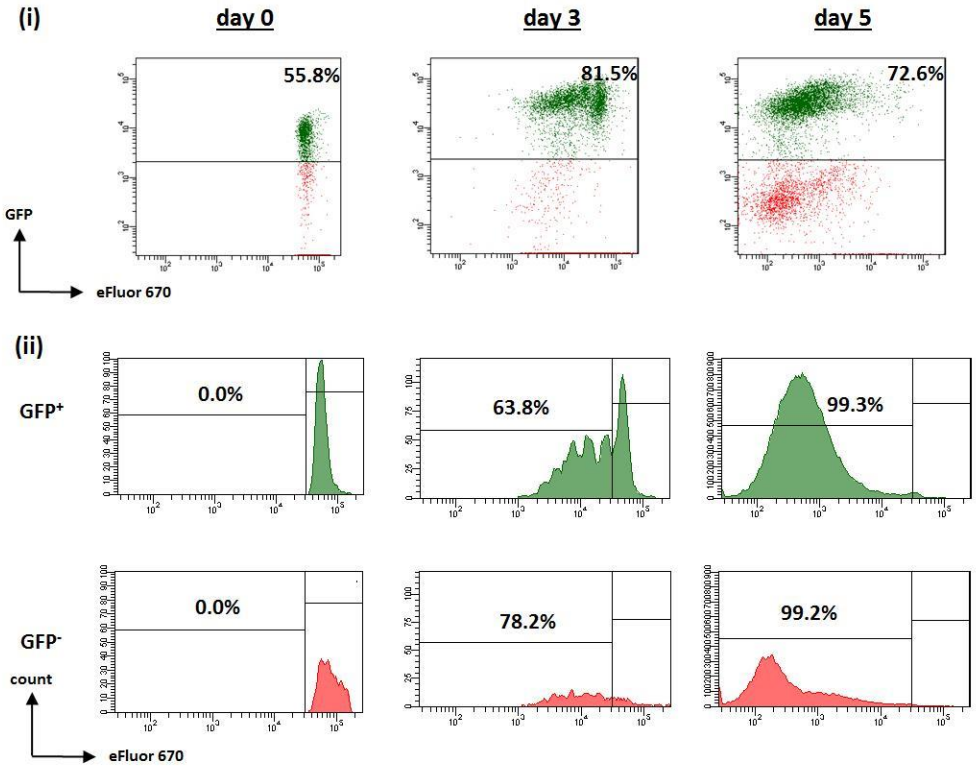

Figure 5.2.3.4. Proliferation of nTreg in response to plate-bound anti-CD3/CD28 antibody stimulation. GFP/Foxp3 KI CBA $CD4^+CD25^+$ nTreg were selected by MACS. These cells were then labelled with eFluor 670 fluorescent dye before they were incubated with plate-bound anti-CD3/CD28 antibody and IL-2 *in vitro*. Cells were examined for eFluor 670 dilution profile on day 0, 3 and 5 by flow cytometry. **(i)** FACS dot plots show the expression of GFP and eFluor 670 on these cells on day 0, 3 and 5. There was no overgrowth of GFP^- cells as the proportion of GFP^+ cells sustained from 55.8% to 72.6% after 5 days of incubation. **(ii)** GFP^+ and GFP^- sub-population proliferation profiles are illustrated by eFluor 670-labelled cells. Top panel illustrates the gated GFP^+ sub-population cell division profile as denoted by the dilution of eFluor 670 from day 0 to 5. The majority of cells divided on day 3 – 63.8%, and almost all cells divided by day 5 (99.3%). Bottom panel illustrates the division profile of the gated GFP^- sub-population suggesting that these cells also underwent proliferation, although their numbers were proportionally lower than their GFP^+ counterparts. These data reinforce the notion that this plate-bound anti-CD3/CD28 antibody Treg expansion protocol enabled preferential proliferation of $Foxp3^+$ Treg as opposed to $Foxp3^-$ non-Treg within the same culture.

We attempted to expand IFN-γ Treg using this plate-bound anti-CD3/CD28 protocol and compared with $CD4^+CD25^+$ nTreg. IFN-γ Treg were generated from $CD4^+$ precursors obtained from GFP/Foxp3 KI CBA splenocytes using the IFN-γ conditioning protocol as described in ***Chapter 2.8.1***. Freshly-harvested IFN-γ Treg (37.5% $Foxp3^+$) were incubated with plate-bound anti-CD3/CD28 antibody in the presence IL-2 (50U/ml) for 5 days. MACS-isolated $CD4^+CD25^+$ nTreg (91.1% $Foxp3^+$) were expanded in the same way. The proportion of the $Foxp3^+$ cohort in the expanded IFN-γ Treg increased from 37.5% to 39.0%, whereas the proportion of $Foxp3^+$ cells in the expanded nTreg decreased from 91.1% to 83.5% after 5 days of incubation ***(Figure 5.2.3.5.i)***. However, enumeration of the resultant population revealed that IFN-γ expanded by a 4.2-fold increase accompanied by a dominant $Foxp3^-$ cohort; whereas $CD4^+CD25^+$ nTreg expanded more efficiently by a 13.0-fold increase ***(Figure 5.2.3.5.ii)***.

We then attempted to expand the cryopreserved IFN-γ Treg predicting that the $Foxp3^-$ cohort would undergo rapid AICD upon thawing and re-stimulation or expansion *in vitro*. Cryopreserved IFN-γ Treg were expanded using the plate-bound anti-CD3/CD28 antibody protocol for 2 rounds (10 days in total). Cryopreserved $CD4^+CD25^+$ nTreg and cryopreserved expanded nTreg were cultured in the same way for comparison. The proportion of the $Foxp3^+$ cohorts in cryopreserved IFN-γ Treg, cryopreserved $CD4^+CD25^+$ nTreg and cryopreserved nTreg were reduced from 72.9% to 65.2% to 18.3%, 96.0% to 95.7% to 54.4% and 93.5% to 58.5% to 48.5%, from day 0, 5 and 10, respectively ***(Figure 5.2.3.6.i)***. Upon enumeration of the resultant population, the number of $Foxp3^+$ cohorts in cryo IFN-γ Treg, cryo $CD4^+CD25^+$ nTreg and cryo expanded nTreg increased by 2.0-fold, 1.9-fold and 3.8-fold from day 0 to 5, respectively. Extended expansion for another 5 days led to a decrease in the number of $Foxp3^+$ cohorts in all groups ***(Figure 5.2.3.6.ii)***. On the other hand, after the first round of expansion the $Foxp3^-$ cohorts increased by 2.9-fold and 2.1-fold in cryo IFN-γ Treg and cryo $CD4^+CD25^+$ nTreg, respectively, but more strikingly with a 38.1-

fold increase in the cryo expanded nTreg group. Another round of expansion led to a further increase of 2.3-fold and 7.0-fold in the IFN-γ Treg and cryo $CD4^+CD25^+$ nTreg, respectively, but on the other hand to a reduction of 80% in the cryo expanded nTreg group ***(Figure 5.2.3.6.ii)***.

These data indicate that while the plate-bound anti-CD3/CD28 antibody protocol could preferentially expand the $Foxp3^+$ cohort in cryopreserved $CD4^+CD25^+$ nTreg after one round of stimulation, it led to a significant increase in the number of the $Foxp3^-$ cohort in cryopreserved IFN-γ Treg and cryo expanded nTreg.

Figure 5.2.3.5. The plate-bound anti-CD3/CD28 antibody protocol failed to preferentially expand freshly-harvested Foxp3$^+$ IFN-γ Treg as opposed to nTreg

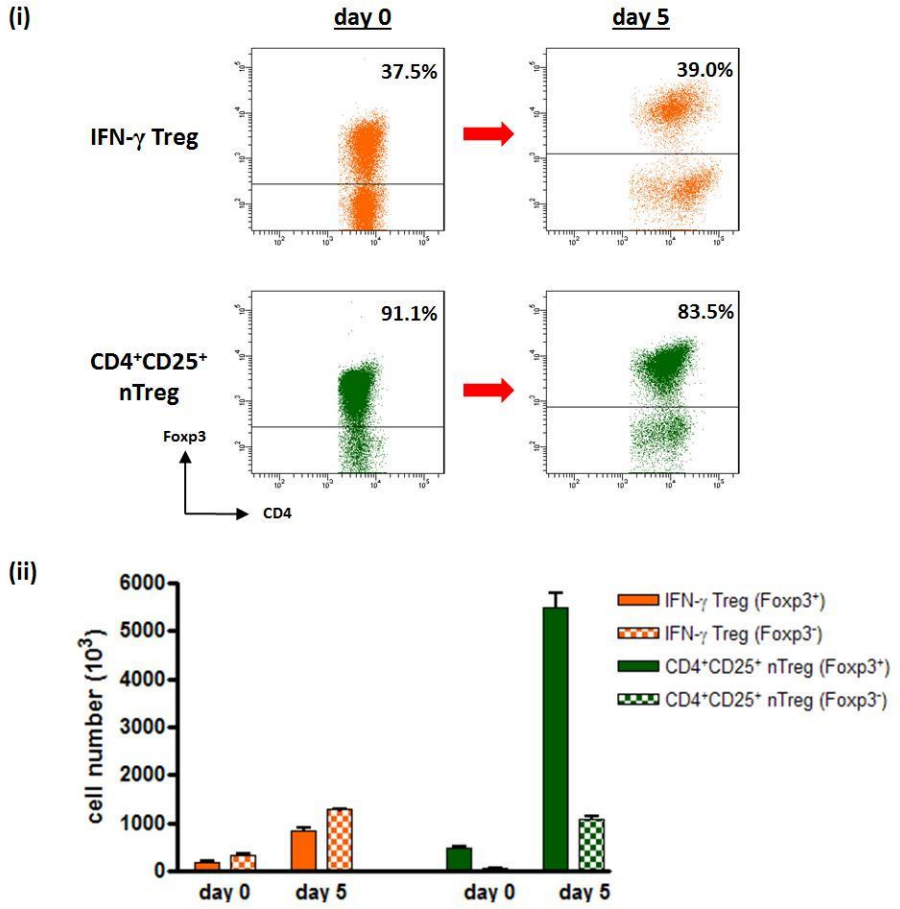

Figure 5.2.3.5. The plate-bound anti-CD3/CD28 antibody protocol failed to preferentially expand freshly-harvested Foxp3$^+$ IFN-γ Treg as opposed to nTreg. (i) Freshly-harvested IFN-γ Treg were expanded using the plate-bound anti-CD3/CD28 antibody protocol ***(Chapter 2.10.3)*** for 5 days *in vitro*. The resultant population retained a similar Foxp3 enrichment (39.0%) compared to the starting population (37.5%). MACS-isolated CD4$^+$CD25$^+$ nTreg (with an initial purity 91.1% Foxp3$^+$) were expanded in the same way, which yielded a Foxp3$^+$ population with a purity of 83.5%. **(ii)** There was a 4.4-fold and 11.9-fold increase in the number of Foxp3$^+$ subsets in IFN-γ Treg and nTreg, respectively. The Foxp3$^-$ subset also expanded and remained a dominant population in IFN-γ Treg. The Foxp3$^+$ subset expanded efficiently (13.3-fold increase) and remained a dominant population in nTreg after 5-day expansion. These data suggest that the plate-bound anti-CD3/CD28 antibody protocol was unable to preferentially expand freshly-harvested Foxp3$^+$ IFN-γ Treg, when compared to CD4$^+$CD25$^+$ nTreg *in vitro*. Data above represent means of 3 replicates with error bars showing 1 S.D. from the mean values.

Figure 5.2.3.6. The plate-bound anti-CD3/CD28 antibody protocol was able to expand cryopreserved nTreg but not IFN-γ Treg or expanded nTreg

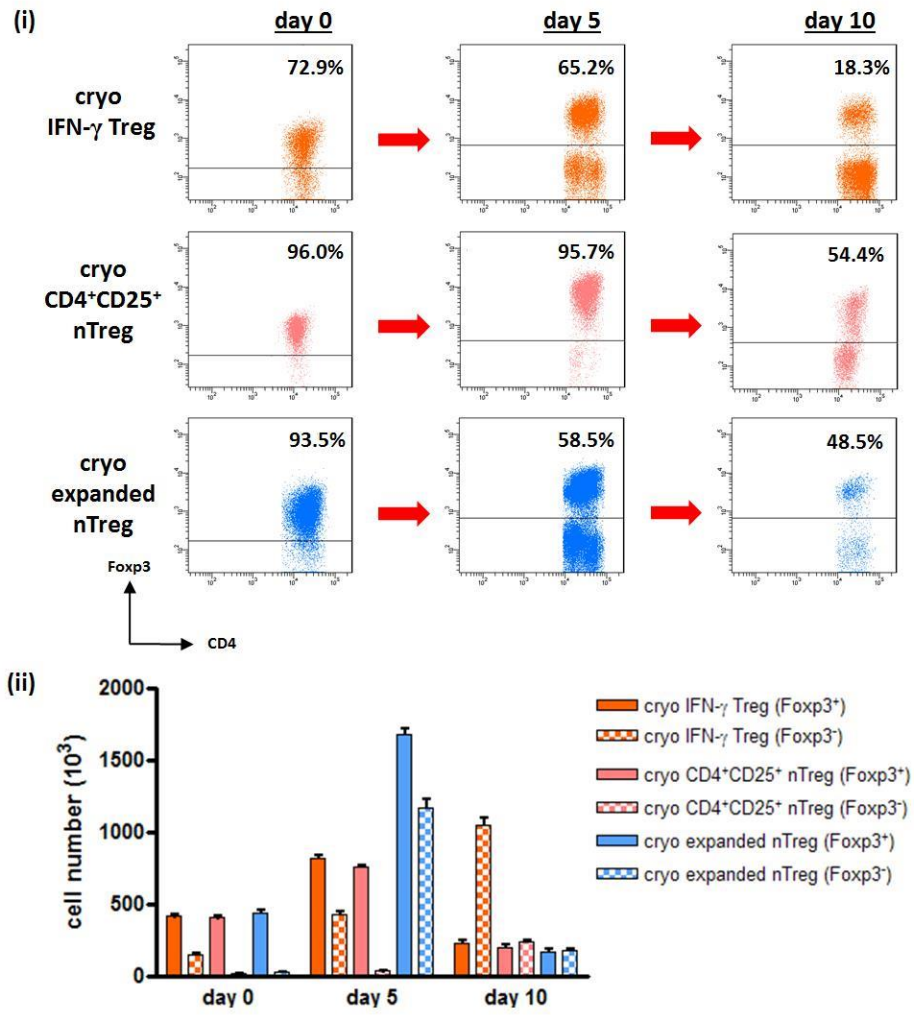

Figure 5.2.3.6. The plate-bound anti-CD3/CD28 antibody protocol was able to expand cryopreserved nTreg but not IFN-γ Treg or expanded nTreg. (i) Cryopreserved IFN-γ Treg, cryopreserved $CD4^+CD25^+$ nTreg and cryopreserved expanded nTreg were expanded using the plate-bound anti-CD3/CD28 antibody protocol for 5 days ***(Chapter 2.10.3)***. The resultant population of expanded cryopreserved IFN-γ Treg or $CD4^+CD25^+$ nTreg retained a high level of Foxp3 expression, whereas the Foxp3 expression dropped by 30% in expanded nTreg on day 5. All groups lost the majority of the $Foxp3^+$ cohorts after the second round of expansion by day 10. **(ii)** After 5 days of incubation, the number of the $Foxp3^+$ cohorts and the $Foxp3^-$ cohorts in cryopreserved IFN-γ Treg, $CD4^+CD25^+$ nTreg and expanded nTreg increased by 2.0, 1.9 and 3.8-fold; and 2.9, 2.1, and 38.1-fold, respectively. Prolonged expansion (up to 10 days) failed to expand the $Foxp3^+$ cohorts in all groups. The $Foxp3^-$ cohorts in IFN-γ Treg, $CD4^+CD25^+$ nTreg continued to increase by 2.3 and 7.0-fold, respectively. The number of the $Foxp3^-$ cohorts in expanded nTreg declined by 80% from day 5 to day 10. Data above represent means of 3 replicates with error bars showing 1 S.D. from the mean values.

5.2.4 Suppressive function of expanded nTreg *in vivo*

The suppressive function of expanded $CD4^+CD25^+$ nTreg was evaluated using our adoptive skin transplant model. MACS-isolated CBA $CD4^+CD25^+$ nTreg were expanded using the plate-bound anti-CD3/CD28 antibody protocol for 5 days as described above ***(Chapter 2.10.3)***. CBA $RAG^{-/-}$ mice were reconstituted with $1x10^5$ naïve $CD4^+CD25^-$ T cells with or without a graded number ($2.5x10^4$ to $2x10^5$) of expanded nTreg (with a purity of 94.5% $Foxp3^+$) one day before the transplant of a B6 skin allograft ***(Figure 5.2.4.1.i)***. At a high precursor frequency of naïve $CD4^+CD25^-$ T cells versus expanded nTreg (4:1), expanded nTreg could not prevent allograft rejection resulting in a MST of 16 days (n=5). More interestingly, the rejection kinetics appeared to be more aggressive than the control group (MST =20 days, n=3). When the number of adoptive transferred expanded nTreg matched (1:1) or exceeded the number of co-transferred $CD4^+CD25^-$ T cells (1:2), expanded nTreg led to long-term graft survival (MST >100 days; n=4-5 per group) ***(Figure 5.2.4.1.ii)***.

These data indicated that expanded nTreg, like freshly-isolated nTreg and IFN-γ Treg, were able to control allograft rejection in this adoptive transfer model in a dose-dependent manner reinforcing the fact that precursor frequency of Treg could be an important factor to consider for successful regulation *in vivo*. However, in the absence of adequate control, the expanded non-Treg population, although in small numbers could lead to an aggravated alloresponse in this model.

Figure 5.2.4.1. Expanded CD4⁺CD25⁺ nTreg controlled allograft rejection in the adoptive transfer skin transplant model in a dose-dependent manner

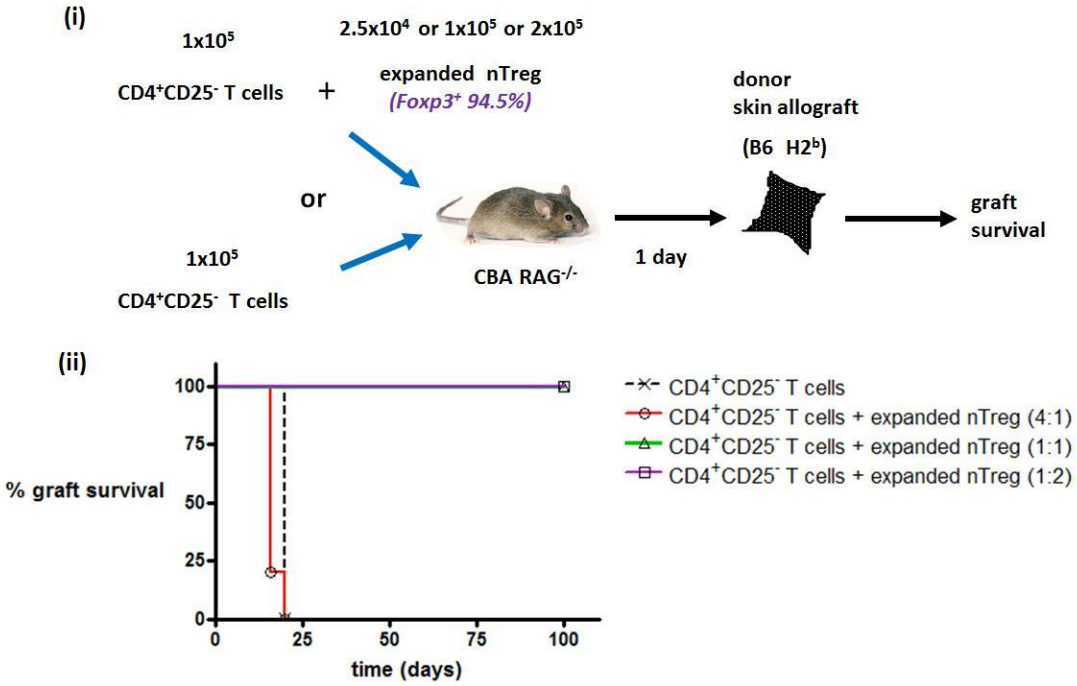

Group	n	graft survival (days)	MST (days)	p-value
CD4⁺CD25⁻ T cells	3	20,20,20	20	*p = 0.0404*
CD4⁺CD25⁻ T cells + expanded nTreg (4:1)	5	16,16,16,16,20	16	
CD4⁺CD25⁻ T cells + expanded nTreg (1:1)	4	>100,>100,>100,>100	>100	*p = 0.0035*
CD4⁺CD25⁻ T cells + expanded nTreg (1:2)	5	>100,>100,>100,>100,>100	>100	

Figure 5.2.4.1. Expanded CD4⁺CD25⁺ nTreg controlled allograft rejection in the adoptive transfer skin transplant model in a dose-dependent manner. (i) CBA CD4⁺CD25⁺ nTreg were expanded using the plate-bound anti-CD3/CD28 antibody protocol and yielded a purity of 94.5% Foxp3⁺ expanded nTreg after 5 days. CBA RAG⁻/⁻ mice were reconstituted with $1x10^5$ naïve CD4⁺CD25⁻ T cells with or without co-transfer of $2.5x10^4$, $1x10^5$ or $2x10^5$ expanded nTreg one day before the transplant of a B6 skin allograft. **(ii)** Naïve CD4⁺CD25⁻ T cells rejected skin allografts acutely with a MST of 20 days (n=3). Expanded nTreg could not control allograft rejection in this adoptive transfer model when the ratio between CD4⁺CD25⁻ T cells and expanded nTreg exceeded 4:1. Expanded nTreg could control allograft rejection long-term if they were delivered at least a 1:1 ratio (MST>100 days, 4-5 per group). Log rank tests were used for statistical comparisons. ($p<0.05$ denotes statistically significant)

Inferred from the data presented above, we proposed that expanded nTreg could also prolong allograft survival in immunocompetent mice, in the presence of the sub-optimal abatacept treatment ***(Figure 5.2.4.2)***. MACS-isolated CBA $CD4^+CD25^+$ nTreg were expanded using the plate-bound anti-CD3/CD28 protocol for 5 days, which yielded a purity of 94.8% $Foxp3^+$ expanded nTreg. $2x10^6$ expanded nTreg given to three groups of CBA recipients which received a B6 heart allograft 1 day, 3 days or 7 days before the transplant of a heterotopic B6 heart allograft in the presence of the sub-optimal abatacept treatment (i.v. 25μg day 0, 1 and 5). Sub-optimal abatacept treatment led to the prolongation of allograft survival with a MST of 52 days (n=5). The delivery of expanded nTreg 7 days prior to the transplant was ineffective in prolonging allograft survival, but it also appeared to cause an aggravated allograft rejection rate with a MST of 37 days (n=3) compared to the abatacept only control group. Expanded nTreg given 3 days or 1 day prior to the transplant had no significant impact on graft survival compared to the control group which led to a MST of 50 days (n=5) and 40 days (n=5), respectively. Nevertheless, these data suggest that expanded nTreg could not prevent allograft rejection in immunocompetent recipients receiving a sub-optimal abatacept protocol when given at the same cell dose as IFN-γ Treg, despite consisting of more than twice the number of the $Foxp3^+$ cohort, whereby the latter could lead to long-term graft survival ***(see Chapter 3.2.5)***.

Figure 5.2.4.2. Expanded CD4⁺CD25⁺ nTreg were unable to control allograft rejection in immunocompetent heterotopic heart allograft recipients

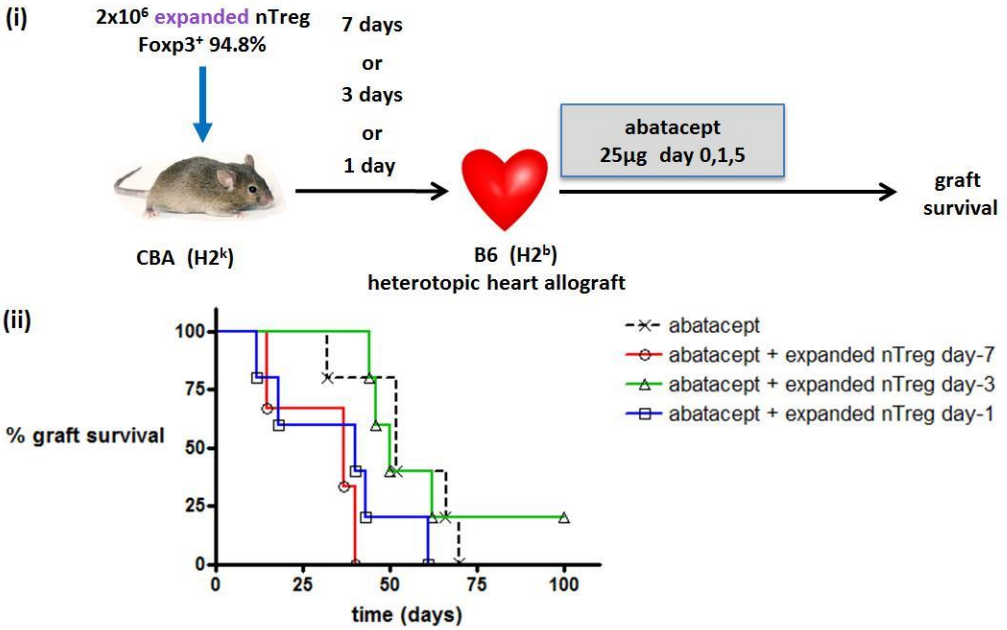

Group	n	graft survival (days)	MST (days)	p-value
abatacept	5	32,52,52,60,70	52	p = 0.0462
abatacept + expanded nTreg day-7	3	15,37,40	37	
abatacept + expanded nTreg day-3	5	44,46,50,62,>100	50	p = 0.9912
abatacept + expanded nTreg day-1	5	12,18,40,43,61	40	p = 0.0899

Figure 5.2.4.2. Expanded nTreg were unable to control allograft rejection in immunocompetent recipients of heterotopic heart allograft. (i) CBA CD4⁺CD25⁺ nTreg were expanded using the plate-bound anti-CD3/CD28 antibody protocol which yielded a purity of 94.8% Foxp3⁺ expanded nTreg as confirmed by flow cytometry analysis. 2x10⁶ expanded nTreg were given to CBA mice 7 days, 3 days or 1 day prior to the transplant of a B6 heterotopic heart allograft together with a sub-optimal abatacept protocol (i.v. 25µg day 0,1 and 5). **(ii)** Allografts in mice received the sub-optimal abatacept treatment alone had a MST of 52 days (n=5). When expanded nTreg were given on day -7, the allograft rejection kinetics was aggravated significantly with a MST of 37 compared to abatacept alone. When expanded nTreg were delivered on day-3 or day-1, there was no difference in the graft outcome compared to abatacept treatment alone, with a MST of 50 days and 40 days, respectively (n=5 per group). These data suggest that expanded nTreg were unable to control allograft rejection in the presence of a sub-optimal abatacept protocol in immunocompetent recipients, unlike IFN-γ Treg ***(see Figure 5.2.1.1.2.)*** Log rank tests were used for statistical comparisons. (p<0.05 denotes statistically significant)

5.2.5 Activation alone could fully equip nTreg to function *in vivo*

Traditionally, it has been widely accepted that activation of resting nTreg is required for their full function. Although it has been demonstrated by Szymczak-Workman et al[336] that Treg were able to suppress independent of an antigen-specific TCR activation signal *in vitro*, Thornton et al[243,532] and Takahashi et al[244] found that polyclonal activation of TCR using anti-CD3 antibody plus exogenous IL-2 was required to break the anergized state of nTreg in order for them to exert their suppression in an antigen non-specific manner *in vitro*. Moreover, polyclonally-activated nTreg were shown to possess comparable suppressive function to antigen-specific Treg in a delayed type hypersensitivity model[533]. Various strategies have been employed to induce, activate or expand nTreg *in vivo[534]*; however, a direct comparison of the functional aspects of freshly-isolated versus activated nTreg in the transplant setting has not been fully elucidated.

K. Milward and J. Hester from our group have shown that a brief activation of human nTreg using anti-CD3/CD28 beads conferred an equivalent suppressive function compared to expanded nTreg in a humanized skin transplant model *(K. Milward and J. Hester unpublished observations, personal communication)*. Data presented in the previous section ***(Chapter 5.2.5)*** imply that at a given cell dose freshly-isolated or expanded nTreg might not be equipped sufficiently to exert their suppressive function in recipients with an intact immune repertoire. We hypothesized that a short activation process might be able to render nTreg fully equipped to elicit their suppressive function *in vivo*.

A range of common T cell activation markers have been linked to the identification of functional Treg[535]. We first examined the kinetics of the expression of CD25, CD44, CD62L CD69 CD103, CD122 and CD152 on *in vitro* activated nTreg.

nTreg were isolated from GFP/Foxp3 KI CBA splenocytes by flow cytometry, which yielded a purity of >95% GFP^+CD4^+ nTreg. GFP^+ nTreg were then activated *in vitro* by incubating with plate-bound anti-CD3 and anti-CD28 antibody in the presence or absence of IL-2 (50U/ml). Cells without polyclonal activation/IL-2 were used as controls. Aliquots of cell suspensions were taken at time 0,1,2,4,8,16 hours post-stimulation and their phenotypic markers were evaluated by flow cytometry analysis ***(Figure 5.2.5.1)***.

Figure 5.2.5.1 Changes of phenotypic profiles in activated nTreg over a short period of time *in vitro*

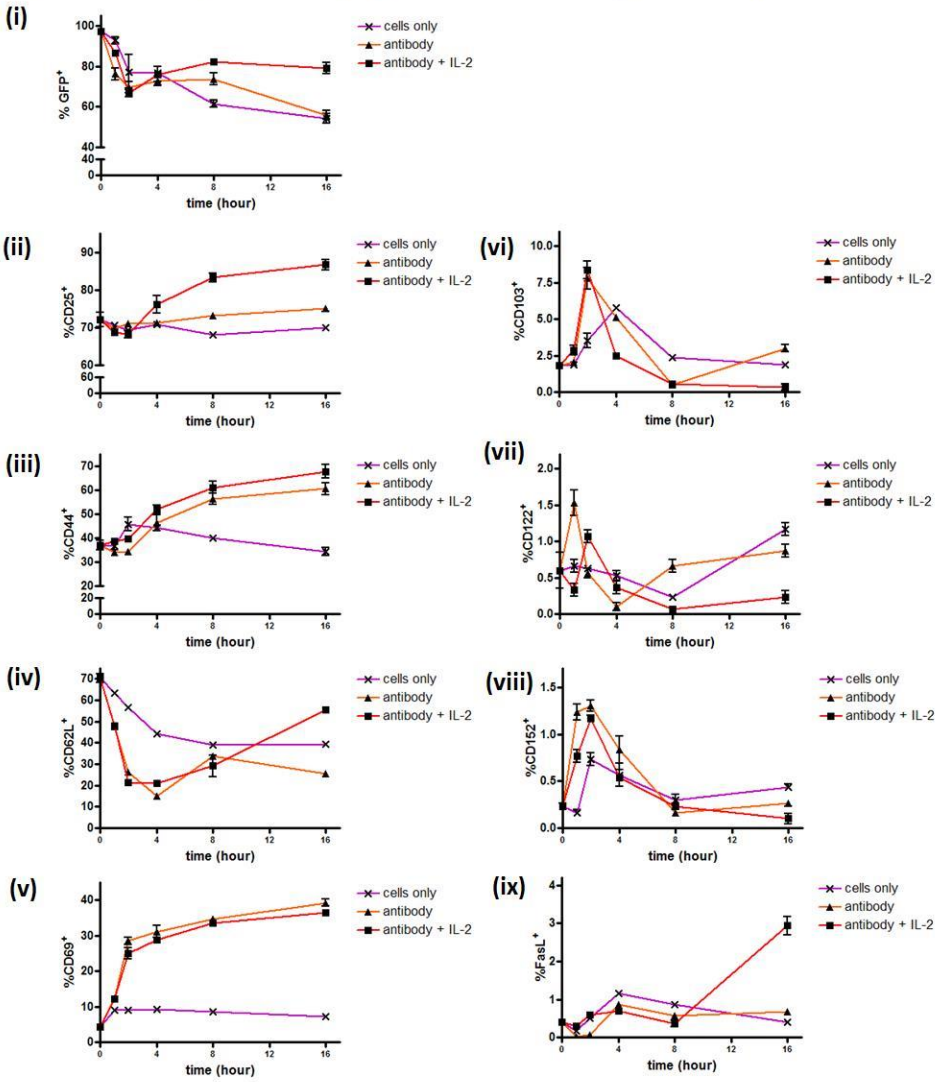

Figure 5.2.5.1. Changes of phenotypic profiles in activated nTreg over a short period of time *in vitro*. Flow cytometer sorted GFP⁺ nTreg were activated using plate-bound anti-CD3/CD28 antibody, with or without IL-2, up to 16 hours *in vitro*. Cells incubated without anti-CD3/CD28 antibody activation and IL-2 were used as controls. Expression of GFP/Foxp3, as well as other phenotypic markers such as CD25, CD44, CD62L, CD69, CD103, CD122, CD152 and FasL were analyzed at time 0, 1, 2, 4, 8, 16 hours by flow cytometry. While there was a brief down-regulation of GFP shortly after nTreg being incubated *in vitro*, this returned to a peak level by 8 hours. The activation marker-CD69 was up-regulated within 1-2 hours and peaked at 8 hours. Similarly, CD25 was up-regulated after 2 hours. CD62L was also up-regulated from 4 hours onwards. Data above represent means of 3 replicates with error bars showing 1 S.D. from the mean values.

The percentage of GFP^+ ($Foxp3^+$) nTreg decreased sharply during the first 2 hours of culture and continued to fall in un-stimulated cells or cells treated with anti-CD3/CD28 antibody alone. On the other hand, the percentage of GFP^+ nTreg rebounded to a plateau, approximately 80%, after 8 hours of stimulation with anti-CD3/CD28 antibody plus IL-2 ***(Figure 5.2.5.1.i)***.

CD25 (IL-2 α chain) was initially found to be an identification marker for mouse Treg, however, up-regulation of CD25 was also thought to be involved in depriving conventional T cells from IL-2. The percentage of $CD25^+$ nTreg decreased abruptly in the first 2 hours post-plating and remained at 70% in un-stimulated cells or cells treated with anti-CD3/CD28 antibody alone. However, in the presence of exogenous IL-2, activated nTreg further up-regulate their CD25 expression, which continued to increase to >80% after 8 hours ***(Figure 5.2.5.1.ii)***.

CD44 is commonly used to define an antigen experienced/memory T cell sub-population. However, reports illustrated that CD44 expression was also correlated with the potency of activated nTreg[536,537]. The percentage of $CD44^+$ nTreg decreased modestly during the first 1 hour in all conditions. Un-stimulated cells upregulated their expression of CD44 at 2 hours, which declined thereafter. In contrast, nTreg activated with anti-CD3/CD28 antibody with or without IL-2 upregulated their CD44 expression after 2 hours and sustained a high level thereafter ***(Figure 5.2.5.1.iii)***.

CD62L (L-selectin) has been correlated with a potent subset of nTreg[501] as well as IFN-γ Treg[256] as described above. The percentage of $CD62L^+$ nTreg decreased steadily when cells were un-stimulated. On the other hand, the percentage of $CD62L^+$ nTreg activated with anti-CD3/CD28 antibody without IL-2 decreased abruptly in the first 4 hours, transiently increased at 8 hours and declined steadily subsequently. nTreg activated with anti-CD3/CD28 antibody plus

IL-2 upregulated their expression of CD62L after the initial trough level for the first 4 hours ***(Figure 5.2.5.1.iv)***.

CD69 (VEA-very early activation antigen), is rapidly induced on activated T cells. Unlike other markers mentioned, which were expressed in a significant number of resting nTreg, the percentage of $CD69^+$ nTreg increased dramatically upon 1 hour of activation with or without IL-2 and sustained throughout the course of study. On the other hand, unstimulated cells maintained a background level of CD69 ***(Figure 5.2.5.1.v)***.

We included the study of the expression of CD103 (integrin αEβ7) and CD122 (IL-2β chain) which were known not to be related to T cell activation. The expression of both CD103 and CD122 on activated nTreg with or without IL-2 was not significantly different from un-stimulated cells ***(Figure 5.2.5.1.vi & vii)***.

Surface expression of CD152 (CTLA-4) was not readily detectable on resting or activated nTreg ***(Figure 5.2.5.1.viii)***, in contrast to the intracellular expression of CTLA-4 ***(see Figure 4.2.1.1.)***.

FasL (CD95L) is associated with AICD and apoptosis of T cells. The expression of FasL in un-stimulated or activated nTreg was largely unchanged during the first 8 hours of incubation. However, we observed a rapid increase, albeit a small percentage (<4%), in nTreg activated with anti-CD3/CD28 antibody plus IL-2 implying that nTreg could undergo activation-induced cell death in extended activation ***(Figure 5.2.5.1.ix)***. Taken together, based on these results, we elected to harvest functional competent activated nTreg between 4-8 hours for subsequent experiments, given the optimal expression of CD25, CD44, CD62L and CD69.

Next, we compared and contrasted the phenotypic characteristics of different Treg and non-Treg preparations. Important lineage and functional markers: Foxp3, Helios, CD25 and CTLA-4 were examined as follows ***(Figure 5.2.5.2.i & ii)***. The forkhead transcription factor-Foxp3[259-261] has remained the most reliable lineage marker for Treg in mouse unlike human T cells, which up-regulate Foxp3 expression upon activation[538-540]. Recently, another transcription factor-Helios has been linked to the identification of the origin of $Foxp3^+$ Treg[311,314,541]. However, it has remained debatable whether activated T cells could also express Helios[318,319]. Here, we showed that the expression of Helios correlated with the expression of Foxp3 on nTreg ***(Figure 5.2.5.2.1)***. Activation or expansion did not lead to the loss of Helios expression on nTreg. On the other hand, activated or expanded non-Treg did not express high levels of Foxp3 or Helios. Interestingly, only 29.4% of IFN-γ Treg expressed Helios as compared to 46.6% $Foxp3^+$ suggesting that IFN-γ Treg consisted of a mixture of Treg lineage derived from the thymus and the periphery.

As mentioned previously ***(Chapter 5.2.5.1)***, CD25 is upregulated in both Treg and non-Treg upon activation. Only freshly-isolated, activated and expanded nTreg expressed a high level of CD25 (69.5%, 88.4% and 100.0%, respectively). Activated and expanded non-Treg also expressed a high level of CD25 (86.1% and 99.8%, respectively), but not resting non-Treg (3.4%). Alloantigen-driven IFN-γ Treg consisted of a 45.6% $CD25^+$ cohort suggestive of their activation status.

As opposed to surface expression of CTLA-4 (CD152), we found that freshly-isolated and activated nTreg expressed a high level of intracellular CTLA-4 (45.5% and 58.4%, respectively) ***(Chapter 4.2.1)***. On the other hand, the intracellular expression of CTLA-4 was not elevated in resting or activated non-Treg (3.2% and 8.0%, respectively). However, expansion using anti-CD3/CD28 antibody for 5 days led to comprehensive up-regulation of CTLA-4 in both expanded nTreg (99.5%) and non-Treg (98.9%). IFN-γ Treg also expressed a high level of intracellular CTLA-4, which has been shown to be responsible for their suppressive function in ***(Figure 4.2.1.1 and 4.2.1.2)***.

Figure 5.2.5.2.i Lineage and functional phenotypic profiles of various nTreg preparations compared to IFN-γ Treg

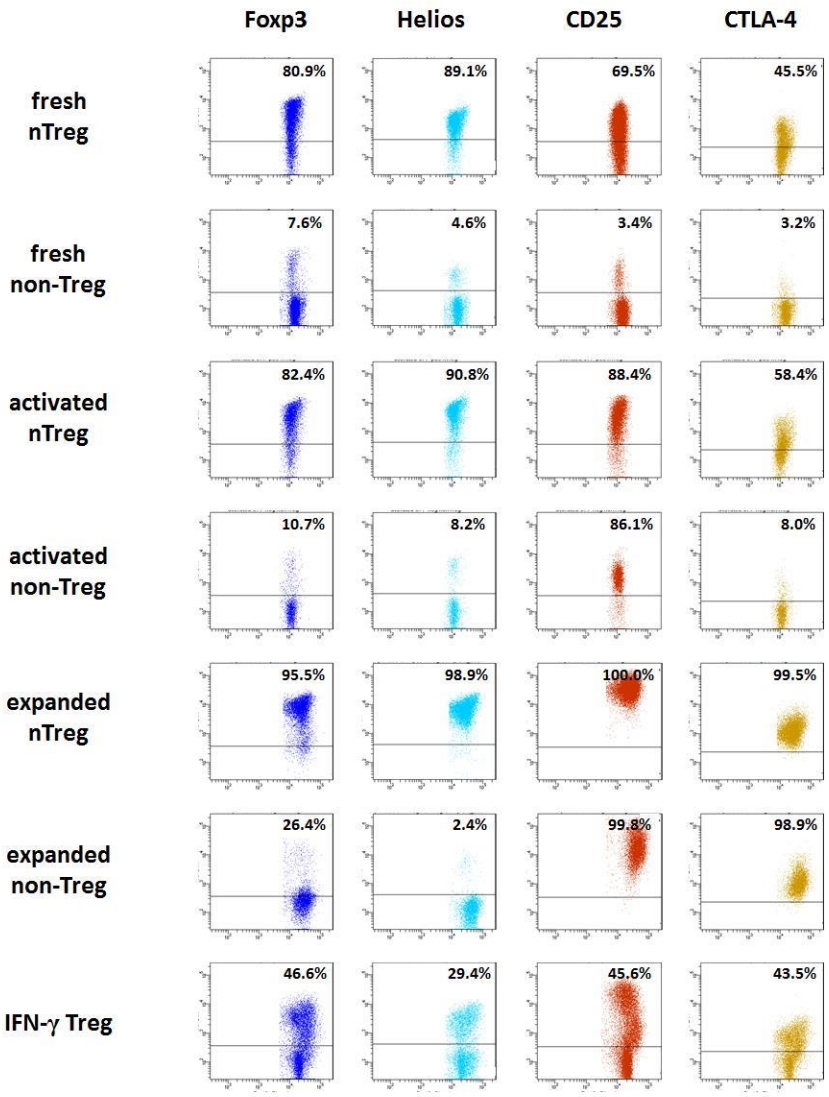

Figure 5.2.5.2.i. Lineage and functional phenotypic profiles of various Treg preparations compared to IFN-γ Treg. The expression of Foxp3, Helios, CD25 and CTLA-4 were compared and contrasted amongst freshly-harvested nTreg and non-Treg; activated nTreg and non-Treg; expanded nTreg and non-Treg; as well as IFN-γ Treg. Data above are representative of 3 replicates.

Figure 5.2.5.2.ii. Lineage and functional phenotypic profiles of various nTreg preparations compared to IFN-γ Treg

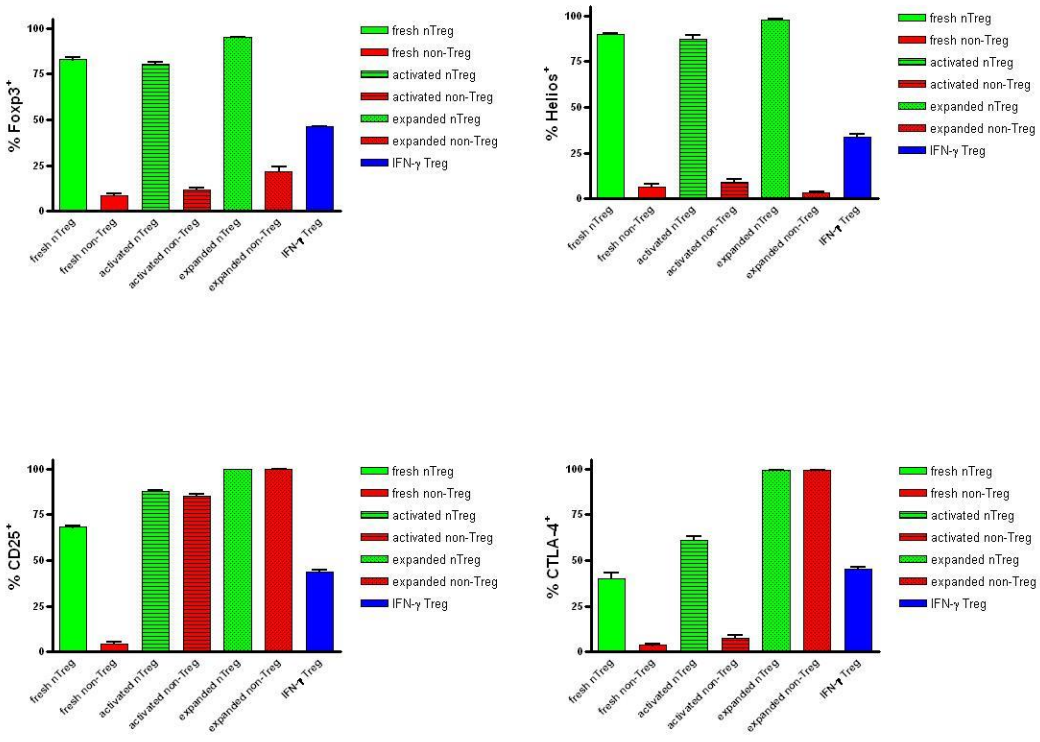

Figure 5.2.5.2.ii. Phenotypic profiles of various Treg preparations. The expression of Foxp3, Helios, CD25 and CTLA-4 were compared and contrasted amongst freshly-harvested nTreg and non-Treg; activated nTreg and non-Treg; expanded nTreg and non-Treg; as well as IFN-γ Treg. Data above represent the means of 3 replicates with error bars showing 1 S.D. from the mean values.

We have also investigated some of the recently recognized surface makers which have been implicated in Treg function such as CD39, CD73, TIM-3 and LAG-3 ***(Figure 5.2.5.3.i & ii)***.

CD39 and CD73 are membrane enzymatic proteins that are often examined together as a 'purinergic system', which is responsible for the metabolism of ATP to adenosine. Although they are not found exclusively on Treg, CD39/CD73 has been linked to the functional identity of a subset of Treg[383,542-545]. Activation with anti-CD3/CD28 antibody decreased the expression of CD39 on nTreg by 42%, but it modestly increased the expression of CD39 on non-Treg from 11.6% to 14.1%. However, expanded nTreg and non-Treg expressed a much higher level of CD39 (96.7% and 98.6% respectively). IFN-γ Treg also expressed a high level of CD39 (52.1%). Activation alone did not change the expression of CD73 on nTreg or non-Treg significantly. However, expansion induced a high level of CD73 expression on both nTreg (87.9%) and non-Treg (71.9%). IFN-γ Treg expressed a significant level of CD73 (56.9%), similar to CD39.

TIM-3 belongs to the T cell Immunoglobulin and Mucin domain family, which has been linked to the suppressive function of Treg[546,547]. However, we observed a small percentage of resting nTreg and non-Treg expressed TIM-3 (6.5% and 0.3%, respectively). Activation led to a small decrease in the percentage of TIM-3$^+$ nTreg but it led to >30-fold increase in non-Treg. Similarly, expanded nTreg and non-Treg expressed a higher level of TIM-3 (11.1% and 76.6%, respectively). IFN-γ Treg expressed a similar level of TIM-3 (12.1%) to expanded nTreg.

Lymphocyte-activated gene-3 (LAG-3) is a CD4 co-receptor homolog that binds to the MHC class II molecule and it was proposed that Treg could employ this mechanism to inhibit the action of DC[369]. It has also been shown to correlate with the suppressive function of Treg that Treg function was lost when LAG-3 was depleted by an anti-LAG-3 antibody *in vitro* and *in vivo*[548]. However, LAG-3 was also a target for depleting activated conventional T cells that led to attenuated alloresponses[549]. Activation alone did not lead to the up-regulation of LAG-3 in nTreg or non-Treg. In contrast, expanded Treg expressed a high level of LAG-3 (from <1% to 36.4%), and almost all expanded non-Treg expressed LAG-3 (98.7%). Interestingly, LAG-3^+ cells only contributed to 10.6% of IFN-γ Treg.

Figure 5.2.5.3.i. Expression of recently recognized Treg surface markers in various nTreg preparations compared to IFN-γ Treg

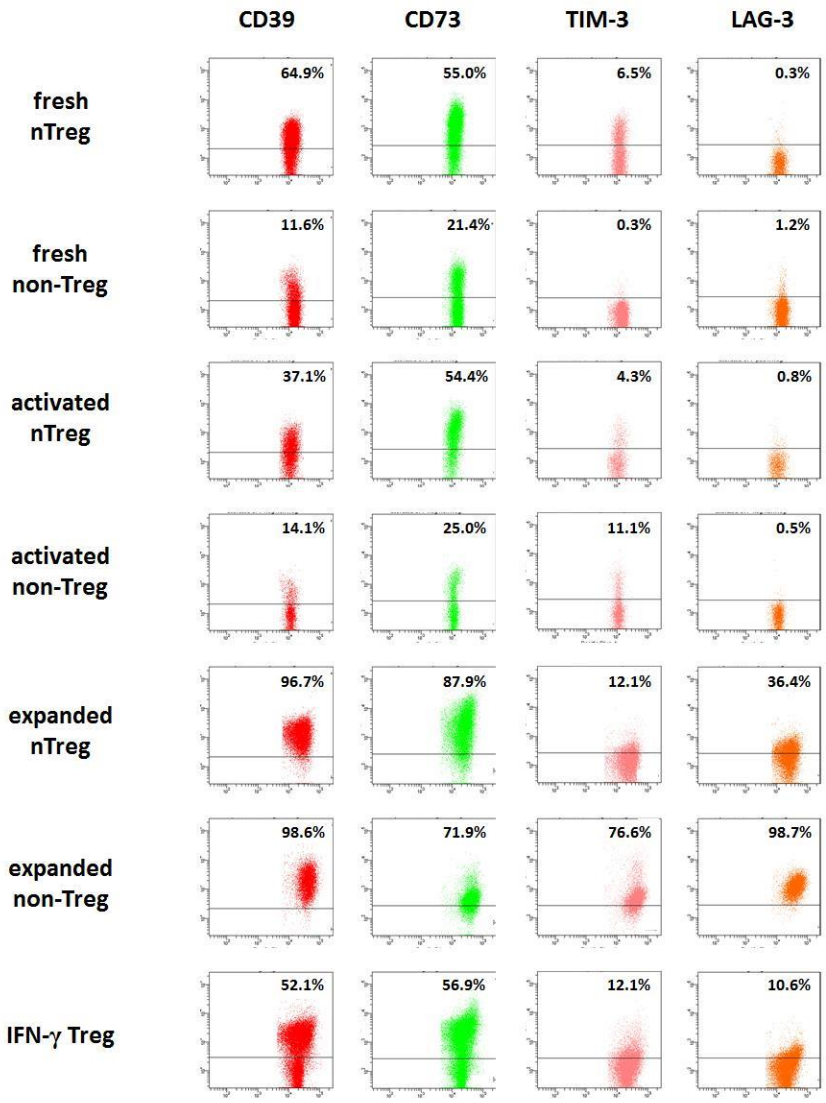

Figure 5.2.5.3.i. Expression of recently recognized Treg surface markers in various Treg preparations compared to IFN-γ Treg. The expression of CD39, CD73, TIM-3 and LAG-3 were compared and contrasted amongst freshly-harvested nTreg and non-Treg; activated nTreg and non-Treg; expanded nTreg and non-Treg; as well as IFN-γ Treg.

Figure 5.2.5.3.ii. Expression of recently recognized Treg surface markers in various nTreg preparations compared to IFN-γ Treg

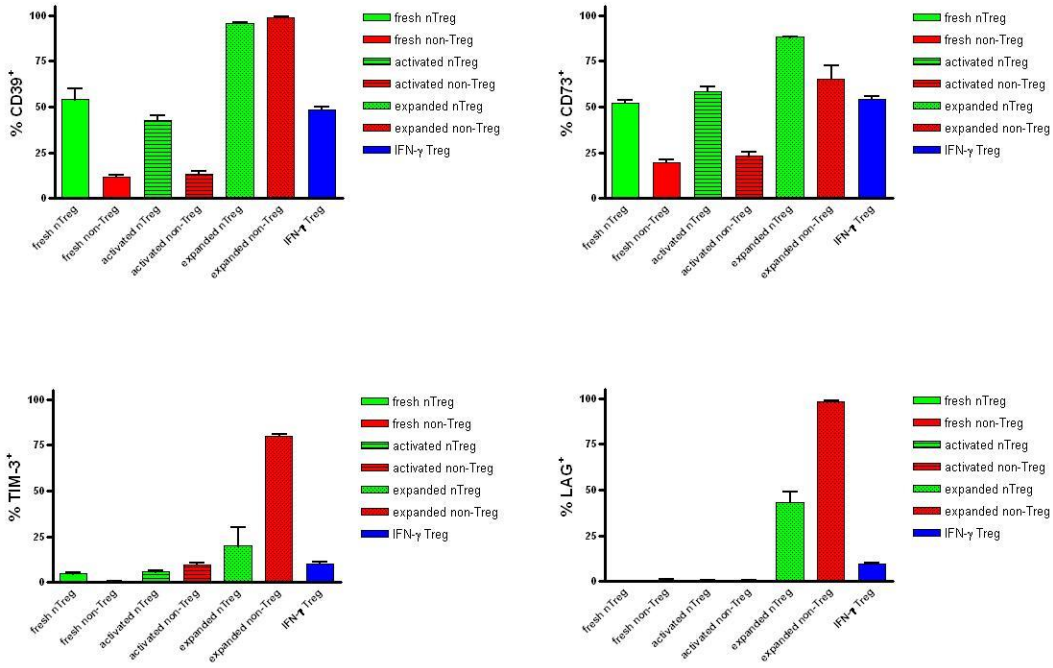

Figure 5.2.5.3.ii. Expression of recently recognized Treg surface markers in various Treg preparations compared to IFN-γ Treg. The expression of CD39, CD73, TIM-3 and LAG-3 were compared and contrasted amongst freshly-harvested nTreg and non-Treg; activated nTreg and non-Treg; expanded nTreg and non-Treg; as well as IFN-γ Treg. Data above represent the means of 3 replicates with error bars showing 1 S.D. from the mean values.

We subsequently examined the expression of GITR, FasL, Perforin and CD103 on various Treg preparations ***(Figure 5.2.5.4.i & ii)***. Glucorticoid-induced tumour necrosis factor receptor family-related gene (GITR) has been found to be predominantly expressed by Treg[550]. We and others have demonstrated that signalling through GITR on Treg would abrogate their suppressive function *in vitro* and *in vivo*[253,254]. We found that a predominant population of freshly-isolated nTreg expressed GITR (71.6%) but not resting non-Treg (5.7%). Activation using plate-bound anti-CD3/CD28 antibody led to a further up-regulation of GITR on nTreg (95.2% $GITR^+$), but also non-Treg (19.6%). All expanded Treg and non-Treg expressed GITR, whereas 61.7% $GITR^+$ cells were found in IFN-γ Treg.

Another TNF protein superfamily- FasL (CD95) has been shown to be expressed by activated T cells. We found that resting nTreg and non-Treg expressed very low levels of FasL (0.1% and 0.4%, respectively), however, FasL expression was modestly upregulated after activation in Treg (0.4%) and non-Treg (3.5%), but to a greater extent following expansion in nTreg and non-Treg (3.6% and 66.1%, respectively). A small proportion of IFN-γ Treg express FasL (6.1%). The Perforin pathway has also been demonstrated to be implicated in the suppression function of Treg[375,551,552]. Resting nTreg or non-Treg contained a negligible number of $perforin^+$ cells (<0.4%). On the other hand, perforin was upregulated in expanded nTreg and non-Treg (4.4% and 58.2%, respectively). IFN-γ Treg expressed a low level of perforin (5.4%).

A subset of Treg (up to 30%) expresses CD103 constitutively. As previously shown in ***Figure 5.2.5.1.vi***, the expression of CD103 was not correlated with the activation status of Treg. We observed that the expression CD103 decreased in nTreg following activation (from 8.7% to 3.9%), but it increased dramatically after expansion (21.5%). On the other hand, non-Treg expressed low level of CD103 at rest (1.2%) and after activation (1.2%), but increased dramatically following expansion (70.3%). Following activation, a low percentage of resting or activated nTreg and non-Treg expressed CD103. In contrast, 13.2% of IFN-γ Treg expressed CD103.

Figure 5.2.5.4.i. Expression of functional Treg markers in various nTreg preparations compared to IFN-γ Treg

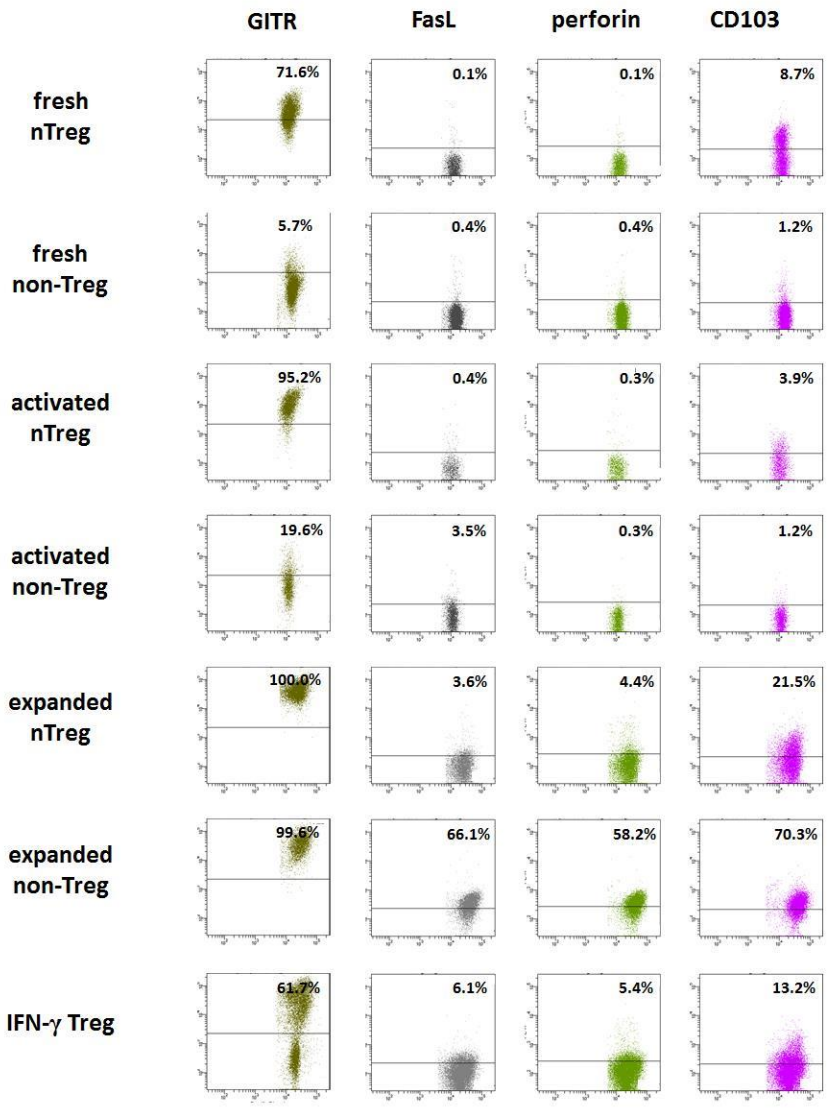

Figure 5.2.5.4.i. Expression of functional Treg markers in various Treg preparations compared to IFN-γ Treg. The expression GITR, FasL, perforin and CD103 were compared and contrasted amongst freshly-harvested nTreg and non-Treg; activated nTreg and non-Treg; expanded nTreg and non-Treg; as well as IFN-γ Treg.

Figure 5.2.5.4.ii. Expression of functional Treg markers in various nTreg preparations compared to IFN-γ Treg

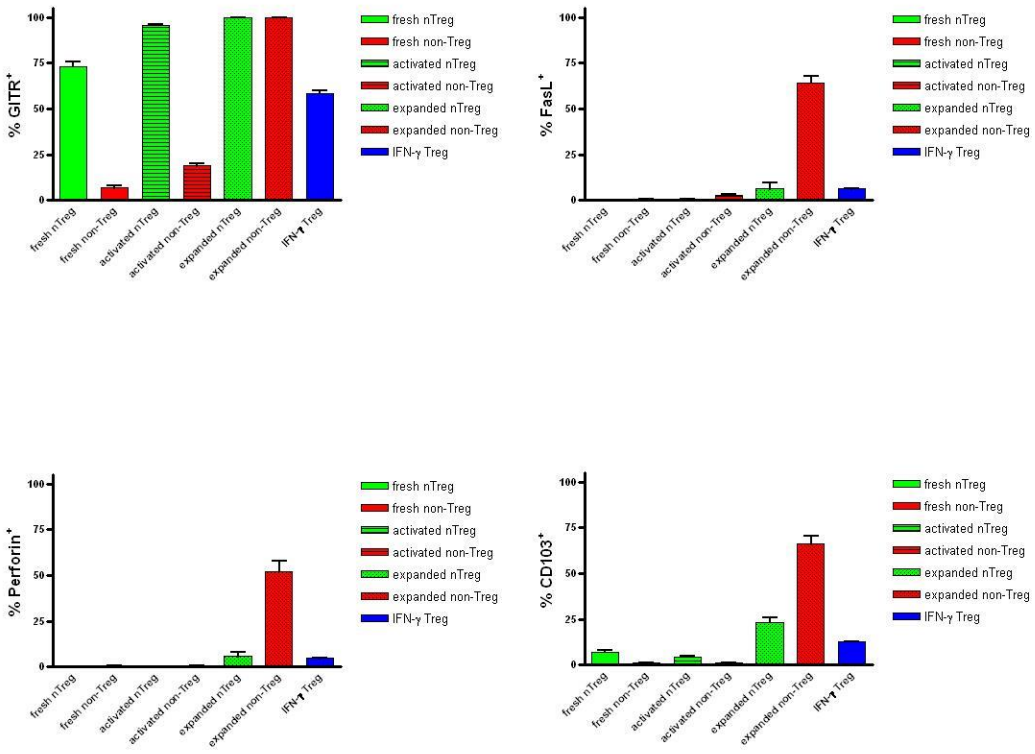

Figure 5.2.5.4.ii. Expression of functional Treg markers in various Treg preparations compared to IFN-γ Treg. The expression GITR, FasL, perforin and CD103 were compared and contrasted amongst freshly-harvested nTreg and non-Treg; activated nTreg and non-Treg; expanded nTreg and non-Treg; as well as IFN-γ Treg. Data above represent the means of 3 replicates with error bars showing 1 S.D. from the mean values.

Having characterized the phenotype of freshly-isolated nTreg, activated nTreg and expanded nTreg we compared their suppressive function *in vivo* using the heterotopic heart transplant model. Freshly-isolated $CD4^+CD25^+$ nTreg were obtained from CBA mice using MACS isolation which yielded a purity of ≥90% $Foxp3^+$. $CD4^+CD25^+$ nTreg were activated using plate-bound ant-CD3/CD28 antibody plus IL-2 (50U/ml) and harvested after 4-8 hours. Expanded $CD4^+CD25^+$ nTreg were obtained by culturing $CD4^+CD25^+$ nTreg using plate-bound anti-CD3/CD28 antibody plus IL-2 (50U/ml) for 5 days. CBA mice were given $2x10^6$ freshly-isolated, activated or expanded nTreg one day before the transplant of a B6 heart allograft, together with the sub-optimal abatacept treatment (i.v. 25μg day 0,1 and 5) ***(Figure 5.2.5.5.i)***.

Mice receiving no treatment rejected their allografts acutely with a MST of 7.5 days (n=10). A sub-optimal abatacept protocol extended graft survival with a MST of 63 days (n=6). Freshly-isolated nTreg were not only unable to extend graft survival, but aggravated the rejection kinetics (MST=22 days, n=9). All mice receiving activated nTreg accepted their allografts long-term (MST>100 days, n=2 - limited to 2 recipients because of unexpected low cell yield). Expanded nTreg had no impact of graft outcome with a MST indifferent from the abatacept control (MST=40 days n=5). All recipients that received $2x10^6$ activated nTreg accepted their graft long-term beyond 100 days (n=5), compared to abatacept control (MST=52 days; n=5) ***(Figure 5.2.5.5.ii)***.

Figure 5.2.5.5. Activated CD4⁺CD25⁺ nTreg controlled allograft rejection long-term in immunocompetent heterotopic heart transplant recipients

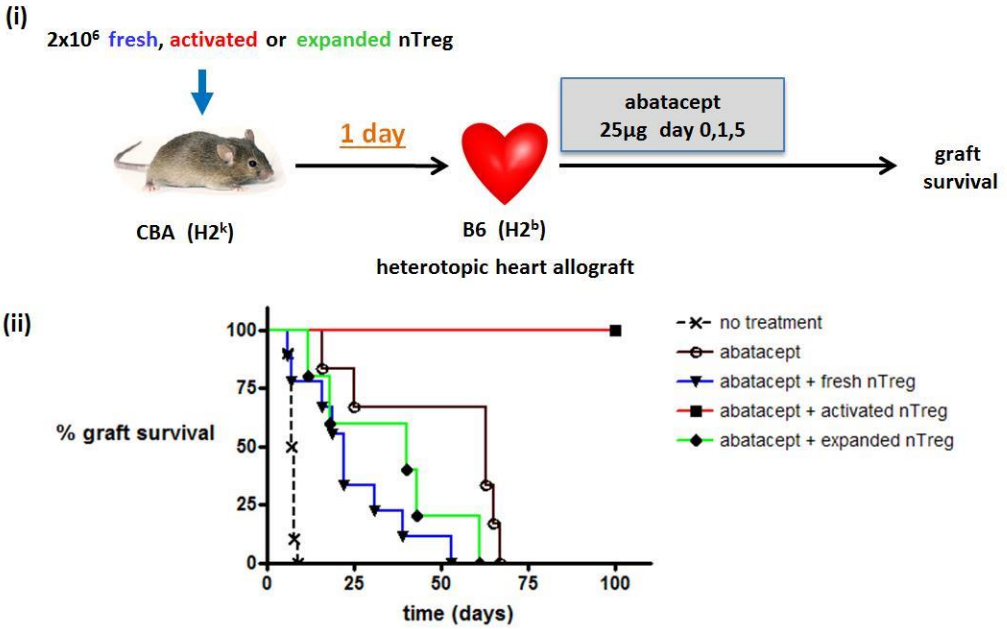

Group	n	graft survival (days)	MST (days)	p-value
no treatment	10	6,7,7,7,7,8,8,8,8,9	7.5	
abatacept	6	16,25,63,63,65,67	63	
abatacept + fresh nTreg	9	6,7,16,19,22,22,31,39,53	22	*p = 0.0143*
abatacept + activated nTreg	2	>100,>100	>100	*p = 0.0319*
abatacept + expanded nTreg	5	12,18,40,43,61	40	*p = 0.0613*

Figure 5.2.5.5. Activated CD4⁺CD25⁺ nTreg controlled allograft rejection long-term in immunocompetent heterotopic heart transplant recipients. (i) CD4⁺CD25⁺ nTreg were isolated from CBA splenocytes using MACS or FACS ARIA sorter to yield a purity of >94% Foxp3⁺ nTreg. Expanded nTreg were generated from nTreg precursors using plate-bound anti-CD3/CD28 antibody plus IL-2 (250U/ml) for 5 days. Activated nTreg were generated by incubating nTreg using plate-bound anti-CD3/CD28 antibody for 4-8 hours plus IL-2. 2x10⁶ ***freshly-isolated***, ***activated*** or ***expanded nTreg*** were given to CBA mice *one* day before the transplant of a B6 heterotopic heart allograft with a sub-optimal abatacept regimen. **(ii)** Mice received no treatment rejected their allografts acutely with a MST of 7.5 days (n=10). A sub-optimal abatacept regimen prolonged allograft survival with a MST of 63 days (n=6). In the presence of the abatacept regimen, neither freshly-isolated, nor expanded nTreg could extend graft survival with a MST of 22 days (n=9) and 40 days (n=5), respectively. In clear contrast, activated nTreg in combination with the abatacept regimen led to long-term allograft survival (MST>100 days; n=2). Log rank tests were used for statistical comparisons. ($p<0.05$ denotes statistically significant)

At the same cell dose, freshly-isolated or expanded nTreg could not prolong graft survival, whereas activated nTreg appeared to be effectively controlling graft survival long-term. This might be explained by the differences in the phenotypic profiles of these cell types in this chapter ***(see Figure 5.2.5.2-4)***. Although all Treg populations express high levels of intracellular Foxp3, Helios and CTLA-4, the significant high expression of CD39/73, LAG-3, and CD103 were negatively correlated with their function in vivo. Activated nTreg expressed high levels of Treg lineage markers and low levels of LAG-3 and CD103. Expanded nTreg, however, expressed high levels of LAG-3 and CD103. The abatacept effect on graft survival appeared to be reduced or abolished when nTreg or expanded nTreg were delivered in our heart transplant model might be attributed by the phenotypic differences amongst these Treg preparations. However, as discussed previously in ***Chapter 5.2.2.1 and 5.2.4*** that the activation status of each Treg preparations and their requirement for competitive binding of CTLA-4 and B7 molecules with abatacept *in vivo* could also play a a critical role in governing the ultimate graft outcome when these two therapeutic modalities were combined.

To further support these observations, we tested if activated nTreg could control allograft rejection when delivered 3 days prior to the transplant as this appeared to be the optimal timing for Treg delivery. Activated nTreg and expanded nTreg were generated as described above by incubating MACS-isolated $CD4^+CD25^+$ nTreg using plate-bound anti-CD3/CD28 antibody and IL-2 (50U/ml) for 4-8 hours and 5 days, respectively. IFN-γ Treg were generated using the IFN-γ conditioning protocol as described in ***Chapter 2.8.1***. CBA mice were given $2x10^6$ activated nTreg, expanded nTreg or IFN-γ Treg 3 days before the transplant of a heterotopic B6 heart allograft and subsequently received a sub-optimal abatacept regimen (i.v. 25μg day 0, 1 and 5) Mice that received abatacept treatment alone were used as controls ***(Figure 5.2.5.6.i)***.

Sub-optimal abatacept regimen prolonged allograft survival with a MST of 52 days (n=5). Expanded nTreg had no impact on graft survival when compared to abatacept only control (MST=50day, n=5). IFN-γ Treg led to significant improvement of graft outcome with 4 out of 6 recipients accepted their allografts long-term (MST>100 days, n=6). Strikingly, activated nTreg given on day -3 led to long-term graft survival in all recipients (MST>100 days, n=6). Collectively, these data suggest that activated nTreg generated as a result of short activation process, although comprising of theoretically fewer alloreactive Treg compared to alloantigen-driven IFN-γ Treg at the same cell dose, possessed a superior suppressive function compared to expanded or alloantigen-experienced IFN-γ Treg. We propose that the activation characteristics of Treg preparations could either act in synergy or antagonism with concurrent use of conventional immunosuppressive agents, which warrat further studies[553].

Figure 5.2.5.6. Activated nTreg controlled allograft rejection long-term in immunocompetent heterotopic heart transplant recipients

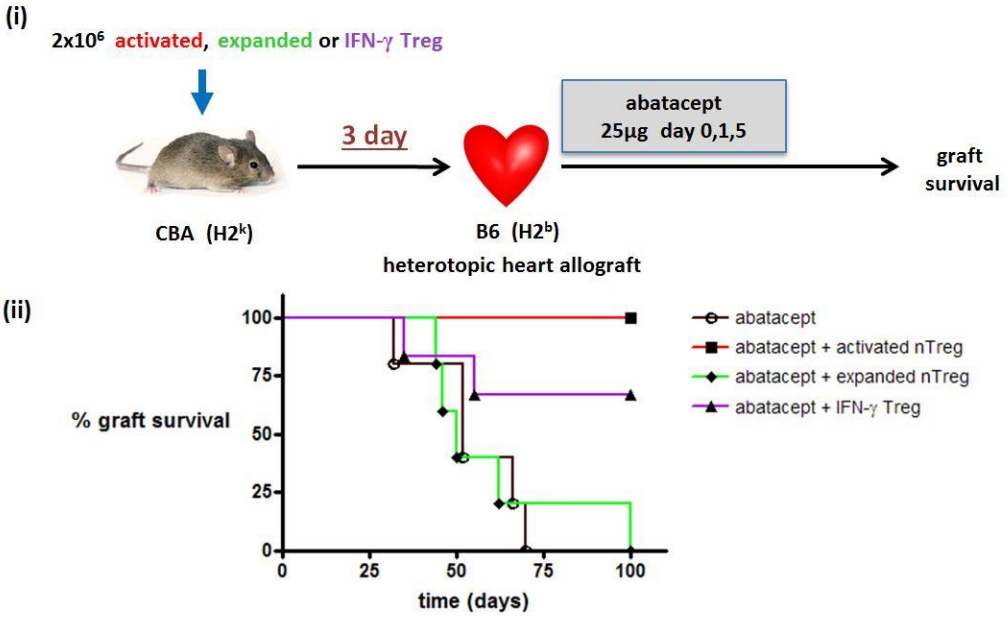

Group	n	graft survival (days)	MST (days)	p-value
abatacept	5	32,52,52,66,70	52	
abatacept + activated nTreg	6	>100,>100,>100,>100,>100,>100	>100	*p = 0.0007*
abatacept + expanded nTreg	5	44,46,50,62,>100	50	*p = 0.9912*
abatacept + IFN-γ Treg	6	35,55,100,>100,>100,>100	>100	*p = 0.047*

Figure 5.2.5.6. Activated CD4⁺CD25⁺ nTreg controlled allograft rejection long-term in immunocompetent heterotopic heart transplant recipients. (i) CD4⁺CD25⁺ nTreg were isolated from CBA splenocytes using MACS to yield a purity of >94% Foxp3⁺ nTreg. Activated nTreg were generated by incubating nTreg using plate-bound anti-CD3/CD28 antibody plus IL-2 (50U/ml) for 4-8 hours. Expanded nTreg were generated from nTreg precursors using the plate-bound anti-CD3/CD28 antibody plus IL-2 (50U/ml) for 5 days. 2x10⁶ ***activated nTreg***, ***expanded nTreg*** or ***IFN-γ Treg*** were given to CBA mice *3* days before the transplant of a B6 heterotopic heart allograft, in the presence of the sub-optimal abatacept protocol (i.v. 25µg day 0, 1 and 5). Mice received abatacept alone were used as controls. **(ii)** A sub-optimal abatacept regimen prolonged allograft survival with a MST of 52 days (n=5). Expanded nTreg had no impact on graft survival, when compared to abatacept control (MST=50 days, n=5). IFN-γ Treg led to a significant improvement in graft survival with 4 out of 6 recipients accepted their allografts long-term (MST >100 days, n=6). In the presence of the abatacept regimen, activated nTreg led to long-term graft survival in all recipients (MST>100 days; n=6). Log rank tests were used for statistical comparisons. ($p<0.05$ denotes statistically significant)

5.3 Discussion

The scarcity and anergic status of Treg have been the chief limiting factors for Treg-based research. In rodent Treg at least, their proliferative potential is different from that of human Treg. A more stringent *in vitro* protocol is required to facilitate the expansion of mouse Treg to enable extensive characterization and comparison of different protocols before translation. In principle, the anergic status could be broken by delivering a stimulating signal to Treg via their TCR and costimulatory molecules in the presence of exogenous IL-2. The precise reason for our initial failure to expand mouse IFN-γ Treg was unknown. However, we postulated that it could be due to the terminal differentiation of the $Foxp3^+$ cohort upon repeated stimulation with alloantigens *in vitro*. On the other hand, the presence of a predominant $Foxp3^-$ population following expansion using anti-CD3/CD28 beads or mBM-DC plus high-dose IL-2 suggested that the non-Treg population in the IFN-γ Treg mixture was still reactive upon further challenge. Moreover, as we saw in ***Chapter 5.2.1.6*** that the flow sorted GFP^- ($Foxp3^-$) cohort of the IFN-γ Treg was able to reject skin allografts in its own right upon adoptive transfer. We concluded that the $Foxp3^+$ cohort was able to control the $Foxp3^-$ cohort when unsorted IFN-γ Treg were delivered to control allograft rejection *in vivo*.

The heterogeneous Treg population yielded from the IFN-γ conditioning protocol raises the question if the $Foxp3^-$ cohort were detrimental to graft survival in their own right. We have shown that when given together with the $Foxp3^+$ cohort, at a given cell dose, they control allograft rejection long-term ***(Figure 3.2.6.1.2)***. When we separate the $Foxp3^+$ and $Foxp3^-$ cohorts, we found that when given at an equal cell dose, the former but not the latter could prevent allograft rejection ***(Figure 5.2.1.6.2)***. But interestingly, they did not cause accelerated rejection kinetics. Because of the cell yield issue and the failure to identify a reiable expansion

protocol for IFN-γ Treg, we did not pursue the use of ultrapurified IFN-γ Treg in the lymphorepleted heart transplant model.

From a practical point of view, Treg would likely be generated and stored prior to be used in transplant patients. However, cryopreservation processes could change the phenotypic and functional properties of Treg. Whether this is due to the expression of surface molecules or the viability of cells is unknown, however, it is possible that both contribute to the end results. Our data indicated that cryopreservation of mouse Treg preparation was feasible and the recovery of cells exceeded 90%. However, the freeze-and-thaw processes might be detrimental to the quality of Treg, which could be an important consideration for clinical translation. Peters et al showed that viable human Treg were retrievable following cryopreservation, but might require reactivation prior to use[499]. This was supported by work done by Hippen et al where restimulation of cryopreserved nTreg maintained adequate suppressive function[554]. Elkord et al showed that the number of Treg in cryopreserved PBMC was significantly reduced by 40% following cryopreservation by means of the average $Foxp3^+$ population[515]. On the other hand, Hemelen et al reasoned that the reduction of Treg frequency was due to the media used as their own study did not reveal any significant reduction of Treg[517]. Several methods could be used to minimize the negative impact of cryopreservation of Treg. Optimal DMSO concentration (<20%) should be used. The addition of buffered saline or media to FCS and DMSO appeared to improve cell recovery and minimize the negative effects on Treg[555].

Weinberg et al initially reported that following cryopreservation of PBMC there was a significant decrease in the frequency of $CD4^+CD62L^+$ T cells that could affect their homing properties[556]. Hattori et al showed that this loss of surface CD62L on T cells by shedding resulted from the activation of matrix metalloproteinases by DMSO present in the freezing media[557]. Our data

indicated that the cryopreservation of mouse IFN-γ Treg led to a reduction of the expression of CD62L ***(Figure 5.2.1.7.1)***. *In vivo*, we observed that cryopreserved Treg were less potent than freshly-harvested Treg ***(Figure 5.2.1.7.3)***. These results were in line with the observations by Taylor et al[558] and Ermann et al[255] that the $CD4^+CD25^+CD62L^+$ Treg were the critical Treg subset that were responsible for the protection against GVHD *in vivo*.

In contrast, nTreg could proliferate in response to the plate-bound antibody plus IL-2. However, we noticed that rapid cell turn over resulted in massive cell death and apoptosis. The physic-chemical properties of the *in vitro* expansion protocol could explain this situation. Signals through CD28 could trigger an alternative AICD pathway which favoured the apoptosis of non-Treg; these observations could be important for future research.

We have interrogated various methods to expand mouse Treg *in vitro*. We found that the Treg expansion kit using anti-CD3/CD28 antibody coated beads led to an overgrowth of the non-Treg cohort. On the other hand, the plate-bound anti-body-based protocol was robust and was able to preferentially expand $Foxp3^+$ Treg.

Despite the fact that mouse and human Treg behave differently, rodent models remain an invaluable tool for the study of more intricate mechanisms. Therefore, the development of an efficient Treg expansion protocol is still warranted, especially when we are still searching for a unique marker for the identification of true potent Treg. To identify Treg we are currently using a combination of Foxp3 plus other surrogate markers which indirectly indicate Treg lineage. Activation alone could be an important aspect and an alternative to expansion of Treg. One way forward is to identify such pathway to selectively activate $Foxp3^+$ Treg to enhance their suppressive potency and to identify a surrogate marker to reflect their potency.

The phenotypic markers of Treg continue to be a conundrum in Treg research. Thus far we are still lacking a Treg specific cell surface marker in both rodent and human Treg. An alternative approach is to use a combination of surface markers; however, studies have shown that non-Treg also share the expression of these combinations of these surface molecules. In this chapter we report our findings from studying an array of surface and intracellular markers that have been reported to be expressed by Treg. We confirmed that: 1) Foxp3 expression in mouse nTreg was relatively stable, despite a short activation process or repeated expansion *in vitro*. 2) The expression of Helios on nTreg was closely related to the expression of Foxp3. Polyclonal activation of nTreg led to a modest shift of the expression of Helios suggesting that activation could also lead to upregulation of Helios, which was consistent with the data published by others. On the other hand, we found that Helios was expressed almost exclusively on the Treg preparations but not non-Treg. 3) CD25 expression was upregulated in activated and expanded Treg as well as non-Treg. 4) Intracellular CTLA-4 expression was upregulated in activated nTreg but not activated non-Treg. On the other hand, following polyclonal expansion, CTLA-4 expression was upregulated in both Treg and non-Treg. 5) The expression of CD39/CD73, TIM-3 and LAG-3 was not upregulated in activated nTreg compared to resting Treg, but upregulated following expansion *in vitro*. More interestingly, expanded non-Treg could also upregulate all these markers suggesting that the expression of these molecules was shared between Treg and non-Treg. 6) Our Treg preparations expressed high levels of GITR compared to non-Treg. However, expanded non-Treg also significantly upregulated their expression of GITR. 7) The Treg population we prepared did not express high levels of FasL or perforin. On the other hand, these molecules were upregulated in expanded non-Treg population. 8) The expression of CD103 was higher in Treg compared to non-Treg. However, expansion of non-Treg expressed high levels of CD103. Overall, as far as the surface markers we have tested, we could not identify a unique

profile that mirrored the suppressive function of these Treg preparations *in vivo*. However, future work might include the combination of positive selection for $GITR^+$ and negative selection for $LAG\text{-}3^-$ Treg based on their behavior we tested *in vivo* ***(Chapter 5.2.6)***.

Amongst the activation marker panel we tested, we found that the expression of CD69 was upregulated sharply following polyclonal activation *in vitro* and sustained for at least 16 hours. When these activated nTreg were tested in the heterotopic heart transplant model, to our surprise, they were able to prevent allograft rejection long-term. In contrast, freshly-isolated or expanded nTreg could not prevent allograft rejection in the same setting. We think that a short activation process was able to equip nTreg to function as competent alloantigen-driven Treg *in vivo* on a cell-to-cell basis.

The comparison between the use of polyclonal nTreg and allospecific Treg in the context of cell therapy in transplantation has remained controversial. On one hand, allospecific or alloreactive Treg were shown to be more potent than polyclonal nTreg on a cell-to-cell basis. Our data shown above suggest that while in the presence of a sub-optimal abatacept treatment, IFN-γ Treg prevented heart allograft rejection long-term ***(Figure 3.2.5.1),*** but freshly-isolated nTreg or expanded nTreg were not able to control allograft rejection at the same cell number ***(Figure 5.2.5.5-6)***. Furthermore, the tempo of allograft rejection was significantly faster than abatacept control suggesting that abatacept might be detrimental to nTreg function, or vice versa. One could argue that the number of alloreactive Treg within the freshly-isolated nTreg could be 1/10 of those in IFN-γ Treg based on the assumption of 10% of the precursors frequency of alloreactive T cells. The counter argument to that was that activated nTreg were able to confer long-term graft protection at the same setting, suggesting that the activation status of Treg could be more important than allospecificity as it has been shown that when nTreg were

activated, they could mediate suppression in antigen-independent manner via bystander suppression.

The effect of CTLA-4Ig on Treg may also explain the differences seen in the graft outcome using nTreg versus alloreactive IFN-γ Treg or activated nTreg. As shown in ***Figure 5.2.5.5***, shortened graft survival was seen in mice treated with nTreg or expanded nTreg in the presence of abatacept, but not activated nTreg. We reasoned such differences could be due to the different effect of CTLA-4Ig on nTreg of different activation status. Both naïve and nTreg were shown to be detrimental in the abatacept protocol, whereas activated nTreg (up to 6 hours of anti-CD3/CD28 antibody) were spared. The competitive binding of CD28 and/or CTLA-4 on nTreg or expanded nTreg to B7 (CD80/CD86) on APC could offer an explanation of such differences. Freshly isolated nTreg require activation and proliferation *in vivo* via bnding of CD28 and B7. This could compete with a suboptimal dose of CTLA-4Ig administered and rendering rejection at a faster tempo when compared to abatacept alone. On the othe hand, expanded nTreg express very high level of CTLA-4 ***(Figure 5.2.5.2)***, which can either act as competitive binding to B7, but the capturing of B7 molecules via transendocytosis could lead to a reduction of available of B7 binding site.

It had been reported from the initial Phase III Belatacept clinical trial that an increased incidence of acute rejection occurred in the high-dose arm of belatacept treatment in renal transplant patients[77,82]. Controversial findings have emerged that CTLA-4Ig has a negative impact on Treg number (in particular thymic-derived Treg) in a transplantation model[449]. This piece of evidence was further supported by work from Charbonnier et al who showed that the deleterious effect of CTLA-4Ig on Treg development and function was CD28-dependent[464]. Belatacept treatment has also been found to inhibit human Treg generation *ex vivo*[559]. In

contrast, a more recent report challenged this concept that CTLA-4Ig did not affect Treg proliferation and function at least *in vitro*[560]. The authors proposed that effector T cells were more reliant on CD28/B7 costimulation than Treg. Vogel et al also showed that CTLA-4Ig preferentially inhibits the proliferation of conventional T cells compared to Treg *in vitro*[561]. Furthermore, CTLA-4Ig was reported to inhibit the frequency of nTreg, but the suppressive function of nTreg was preserved in patients with rheumatoid arthritis treated with abatacept[562]. In EAE model, Vogel et al showed that CTLA4-Ig exacerbated autoimmunity by transiently suppressing endogeneous Treg function and proliferative marker[563].

CTLA-4Ig can act upon on T cells via a CD28-dependent and a CD28-independent manner. The former would explain that in the presence of Treg, which may compete with effector T cells for CD28-B7 signalling, Howver, already activated T cells are less dependent on CD28 signalling and thus not affected by exogenous CTLA-4Ig, whereas nTreg require activation and compete for engagement with B7. As we have shown in ***Figure 5.2.5.2.i*** that non-Treg upregulate CTLA-4 significantly upon expansion. Thus, intrinsic suppressive mechanism of effector T cells could also be dampened by the presence of CTLA-4Ig engagement with B7 on APC, thus aggravated effector function. The accelerated rejection phenomen seen might be explained by the lack of blocking of CTLA-4 on the effector population.

At the molecular level, CTLA-4Ig activity could work in both ways in terms of effector T cells and APC. As shown by Mayer et al that at the time of T-DC interaction, CTLA-4Ig effectively exert their effect to inhibit T cell proliferation. On the other hand, when DC were pre-cultured with CTLA-4Ig, they were still capable to stimulate T cells. This demonstrated that CTLA-4Ig does not act solely on the activity of DC via IDO alone[564].

Why would then activated nTreg fare better than other two nTreg preparations in terms of suppressive function in the presence of abatacept is difficult to dissect with limited information. Future work could include an assessment of the cellular interactions between freshly-isolated nTreg, activated nTreg and expanded nTreg and APC following incubation with CTLA-4Ig *in vitro*. Using confocal microscopy, one might be able to demonstrate the influence of abatacept or belatacept on the intricate engagement of CD28/CTLA-4 and B7 molecules between these cells and APC, and to ask if these interactions contribute to the detrimental effect on Treg activity.

Chapter 6 Novel bio-imaging for the evaluation of graft outcome

6.1 Introduction

The heterotopic model for heart transplantation in mice was pioneered by Corry et al[565] in the 1973 follow by a simplified modification by Niimi[566] and a number of modifications of this technique have been reported over the years[567]. The conventional method of assessing graft function is carried out by bi-manual abdominal palpation of the heterotopic heart graft[447]. Although alternative methods have been described such as electrocardiogram[568-570], echocardiography[571], ultrasound Doppler[572] and MR imaging[573-577], histological examination has remained the gold standard for confirmatory assessment of the degree of rejection by means of chronic vascular arteriopathy[578-581]. Newer approaches for the detection of rejection have also been reported such as intravital multi-fluorescence microscopy[582] and bioluminescence imaging[583]. However, the evaluation of the functional aspects of graft outcome in mice with heterotopically transplanted heart graft has been limited[584,585].

While we continued to search for a reliable protocol to expand IFN-γ Treg, we interrogated the dosing strategies and optimal delivery for IFN-γ Treg in the presence of a low-dose costimulation blockade-abatacept, using our heterotopic heart transplant model ***(Chapter 3.2.5)***. In addition, we aimed to investigate the possibility of employing a novel non-invasive method to monitor

and assess graft functional outcome in recipients following Treg therapy using *in vivo* MR imaging in our experimental heart transplant model.

6.2 Results

6.2.1 Magnetic resonance imaging in experimental heterotopic heart transplantation

The use of Magnetic Resonance Imaging (MRI) for the evaluation of heterotopic heart graft began with the studies of graft rejection carried out in rat[586] and canine[587] models in the mid-1980s. Subsequent developments included the incorporation of nuclear magnetic resonance (NMR)[588], gadolinium contrast[589] and the use of superparamagnetic iron oxide (SPIO) particles[590] for the study of reperfusion injury in experimental ischaemic heart model. SPIO have also been used to label and track immune cells in the context of rejection mediated by the innate immune system[591,592]. Christen et al reported the use of MR molecular imaging technique for the study of the innate immune response in transplant rejection in mice[593].

In the last decade, more patients with end-stage heart failure who have been put on left ventricular assist device as a bridge to heart transplant. While the volume of the ventricle is unloaded by the ventricular assist device, a potential reversal modelling of the diseased myocardium could occur. NMR and MRI are important tools for the study of myocardial

remodelling following the unloading of the left ventricle in heterotopic heart transplant models, which mirrors the clinical situation[594].

6.2.2 Rationale of non-invasive graft assessment technique

We have established some convincing data demonstrating that *in vitro* generated IFN-γ Treg could attenuate alloresponses in lymphorepleted recipients with the aid of an adjunctive sub-optimal costimulation blockade regimen ***(Chapter 3.2.5)***. Graft survival was determined by the presence or absence of a pulsating vascularized heart graft using conventional bi-manual palpation technique. Rejection was then confirmed by definitive laparotomy. Bi-manual palpation of the heterotopic heart graft has remained the method of choice offering a non-invasive monitoring tool to assess graft outcome in a longitudinal study. In clinical transplantation, rejection is usually diagnosed by various clinical parameters followed by a histological confirmation of biopsied specimens. However, biopsy is not practically applicable in small rodent heart transplant models because taking an adequate amount of tissues for proper histological tests would lead to massive haemorrhage and render the death of the animals. Besides, regular examination under direct vision is not feasible as interval laparotomies are not ethically approved. Hence, we aimed to develop a new non-invasive technique that could provide a detailed assessment of graft outcome. In collaboration with the group of Prof. Clarke from the Cardiac Metabolism Research Group, Department of Physiology Anatomy and Genetics at our University, we proposed to evaluate the possibility of using *in vivo* MRI to determine graft outcome in our experimental heart transplant model.

6.2.3 *In vivo* MRI experimental set up

The experimental set up for the *in vivo* MRI is illustrated in a schematic diagram shown in ***Figure 6.2.3.1***. A mouse heart transplant recipient was given gaseous general anaesthesia and placed in the supine position within a specially designed plastic cradle. Prior to the commencement of MRI, an initial electrocardiogram (ECG) was performed to determine the heart rate and contractility of the implanted heart graft and a separate electrode wire loop was attached to the chest wall for the monitoring of respiration. Adjustment of the percutaneously placed ECG probes might be required to ensure accurate capturing of cardiac impulses generated by the heterotopic heart graft ***(Figure 6.2.3.2)***. The recipient was then delivered into the core of the MR system, which was attached to a Bruker console for image processing with continuous ECG and respiratory monitoring. After initial scouting images for the location of graft in the abdomen, multiple high-resolution ECG-gated still MR slides (1mm each in thickness) were captured along the long axis of the graft to expose the right and left ventricles ***(Figure 6.2.3.3)***. These contiguous slides were then computerized to generate Cine MR images for real-time examination of the ventricular contraction and dilatation. Epicardial and endocardial areas at the end-systolic and end-diastolic phase could be outlined using an image processor. Various biological parameters such as end-diastolic volume, stroke volume, ejection fraction and cardiac output of each ventricle could then be calculated using the sum of 3-4 cross-sectional slides along the long axis of the graft. An example of a single MR slide in the axial plane taken at the mid-level between the base and the apex of the heart graft is shown in ***Figure 6.2.3.4*** demonstrating its relationship with the recipient's abdominal aorta and inferior vena cava (IVC) in the lower abdomen.

Figure 6.2.3.1. *In vivo* MRI set up for the functional assessment of heterotopic heart graft in mice

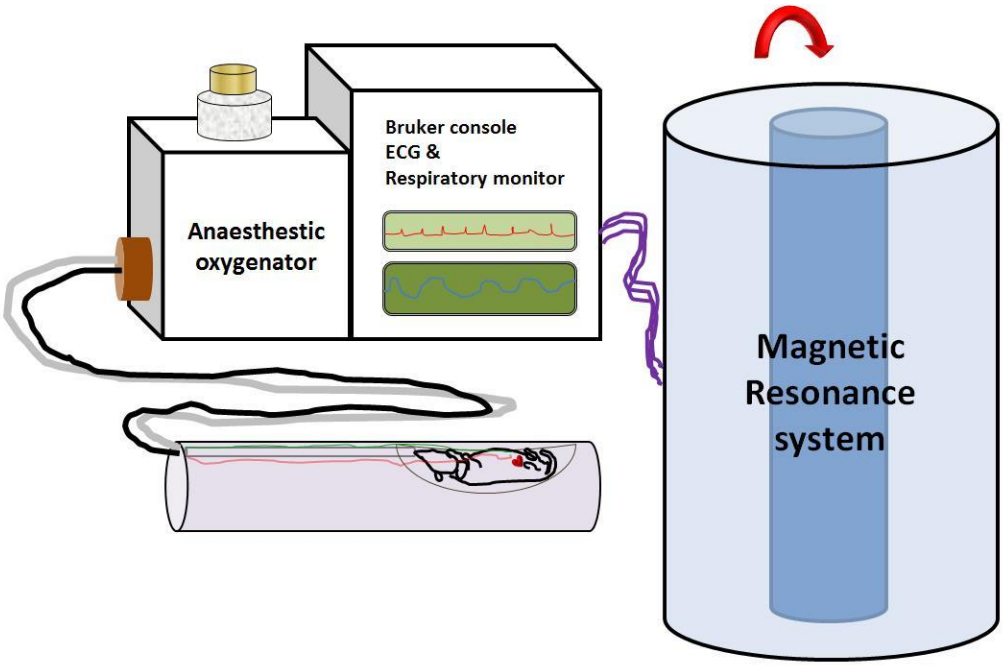

Figure 6.2.3.1. *In vivo* MRI set up for the functional assessment of heterotopic heart graft in mice. Schematic diagram illustrates the crude experimental set up of *in vivo* MRI. Mouse heterotopic heart transplant recipients were given gaseous general anaesthestics and positioned in a designated cradle in supine position with temperature control. Electrocardiogram (ECG) electrodes were inserted percutaneously in the lower ventral abdominal wall adjacent to the heterotopically implanted heart allograft. A separate respiratory loop wire was placed and taped across the recipient's chest to monitor respiration. The cradle was then lowered into the vertical bore 500 MHz, 1.7 Tesla Magnetic Resonance system connected to the Bruker console. ECG and respiratory trigger levels were adjusted at the same point of the cardiac cycle of the heart graft prior to MR scanning. Scout images were obtained for the localisation of heart graft for optimal true short axis images acquisition. Cine-MR images were acquired in 6-8 contiguous slices in the short-axis orientation. At the end of the procedure, the cradle was elevated and the recipient was removed from cradle and placed in a designated chamber for recovery. Data images were processed and analysed using the ImageJ® software. (see ***Chapter 2.4*** for more detailed description on the methodology of *in vivo* MRI)

Figure 6.2.3.2. *In vivo* MRI scan acquisition using ECG gating to capture cardiac cycle of the graft

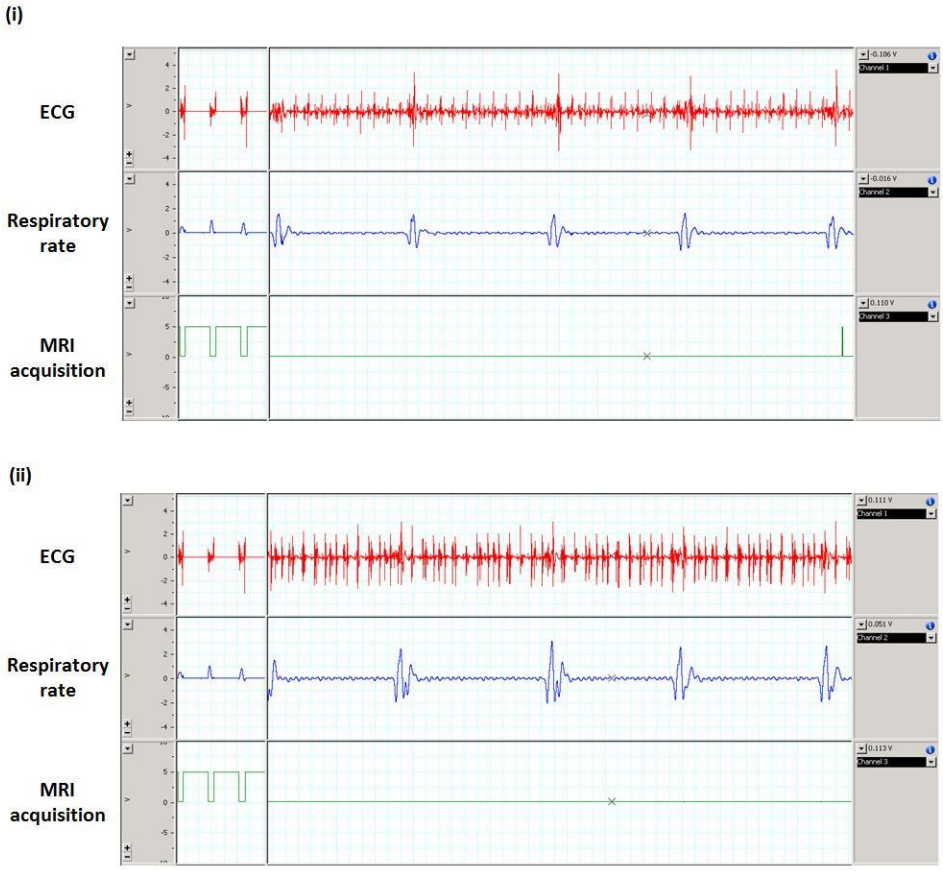

Figure 6.2.3.2. *In vivo* MRI scan acquisition using ECG gating to capture cardiac cycle of the graft.
(i) Cardiac gating for Cine MRI image capture. ECG traces **(red)** were determined by percutaneous needles placed adjacent to the heterotopic heart graft in the lower abdomen. A separate wire was placed on the thorax to determine the respiratory rate **(blue)**. Respiratory trigger levels were adjusted at the same point of the cardiac cycle of the heart graft prior to MR scanning. Acquisition of MRI of at each cardiac cycle was monitored **(green)**. At rest, a uniform ECG tracing confirmed the correct capturing of cardiac impulses from the heterotopic graft implanted in the lower abdomen. **(ii)** ECG tracing of percutaneous probes applied further away from heterotopic heart graft. ECG from both graft and the native heart were demonstrated. Polymorphic ECG tracing of different heart rates and QRS complexes of the graft and native heart were superimposed on each other. In such instances, ECG probes were readjusted, placed closer in proximity of the heterotopic graft ensuring the correct acquisition prior to high resolution MR imaging.

Figure 6.2.3.3. Generation of cardiovascular functional parameters using *in vivo* MRI to assess graft outcome in the heterotopic heart transplant model

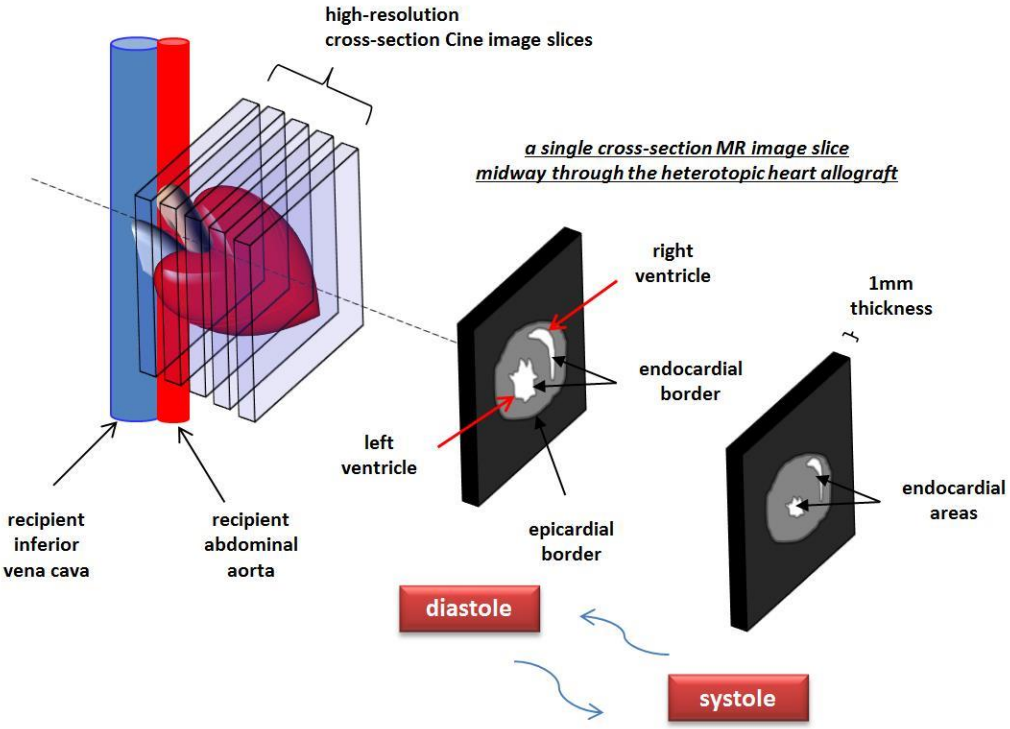

Figure 6.2.3.3. Generation of cardiovascular functional parameters using *in vivo* MRI to assess the graft outcome in the heterotopic heart transplant model. Initial low-resolution (128 x 128 pixels) scout images were performed to locate the heterotopically transplanted heart graft in the abdomen, in addition to formulate the 3-dimensional orientation and margins for subsequent true imaging. Multiple high-resolution (256 x 256 pixels) Cine slices (4-10) were captured to include the base and the apex of the graft. A cross-section MR image is depicted above showing the left and right ventricle, as well as the epicardial and endocardial borders of the graft. Dynamic changes of the graft during the entire cardiac cycle were captured by ECG-triggered Cine images over time. The endocardial luminal areas of each ventricle were measured with the aid of an image software (ImageJ®). The end-diastolic (EDV) and end-systolic (ESV) volumes of each ventricle were determined by the summation of multiple endocardial luminal volumes of each slice of the MR image (1mm in thickness) at the end-diastolic and end-systolic phase of the cardiac cycle, respectively. Stroke volume (SV) of each ventricle was calculated according to the difference between the end-diastolic and end-systolic volume (EDV - ESV). Ejection fraction of each ventricle was calculated by the following equation: (EDV - ESV) / EDV and expressed in percentage. The cardiac output of each ventricle was determined by the product of stroke volume and heart rate (CO=SV x HR). Due to the unloaded left heart in this model, we would focus on the functional parameters of the right ventricle only.

Figure 6.2.3.4. ***In vivo*** **MRI provided fundamental anatomical features of heterotopically transplanted heart graft in mice**

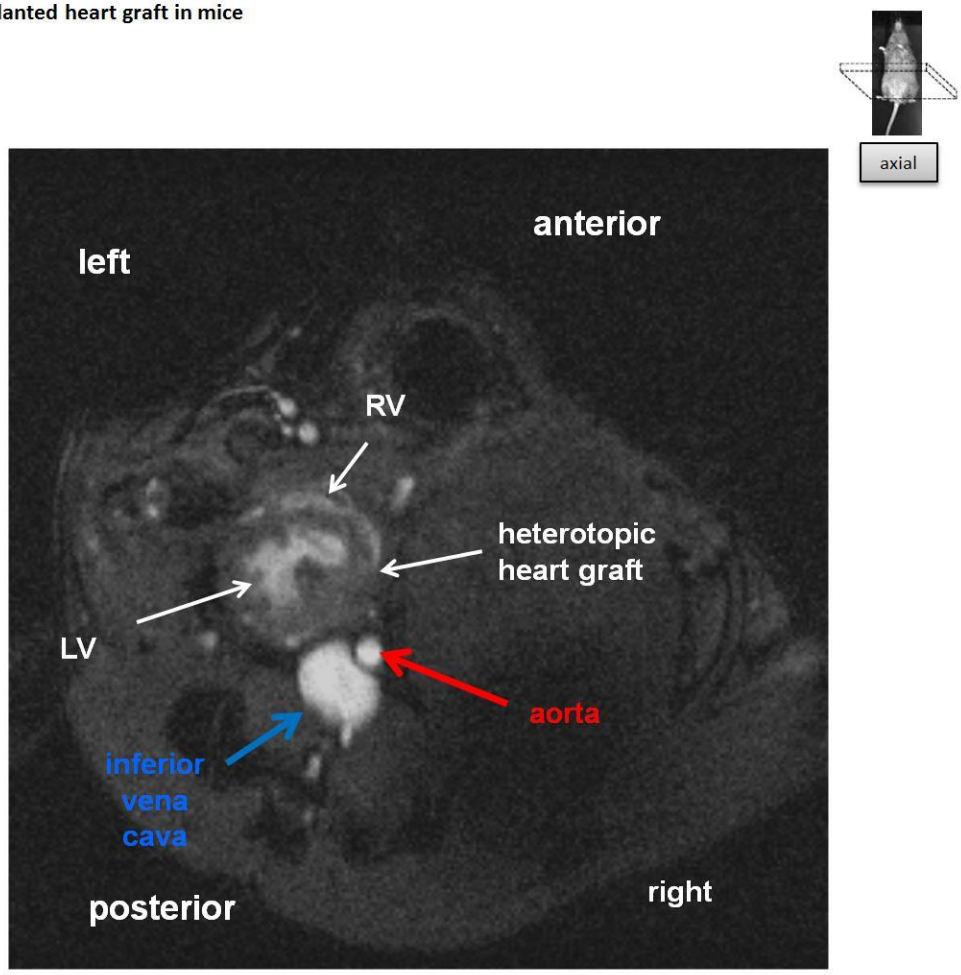

Figure 6.2.3.4. ***In vivo*** **MRI provided fundamental anatomical features of heterotopically transplanted heart graft in mice.** A single slice of MR image was obtained by scanning through the axial plane of the lower abdomen of the mouse heterotopic heart transplant recipient using the experimental set up mentioned above ***(Figure 6.2.3.1-2)***. A T2-weighted MR image demonstrates the recipient abdominal aorta and inferior vena cava, to which the donor aorta and pulmonary artery of the heterotopic heart graft were anastomosed to. In the axial plane, the chambers of the left (LV) and right ventricle (RV) of the graft were clearly demonstrated by the tissue and blood interface. The above slice was taken during the diastolic phase of the cardiac cycle showing ventricular relaxation and filling, which was captured using the incorporated ECG triggering system.

An important caveat in considering the measurement of the cardiovascular parameters of the heterotopic heart graft was the blood flow system leading to an unloaded left ventricle. Normal physiological blood flow in a normal heart is shown in ***Figure 6.2.3.5.i***. Venous blood is collected in the right atrium (RA) via the superior vena cava (SVC) and inferior vena cava (IVC) , and is then delivered to the lungs from the right ventricle (RV) through the pulmonary artery (PA). Arterial blood is collected in the left atrium (LA) via the pulmonary veins (PV) and delivered from the left ventricle (LV) to the systemic circulation via the aorta. In contrast, the heterotopic heart model served as a simple two-chamber system ***(Figure 6.2.3.5.ii)***. As the SVC, IVC, and PV were ligated the RA and LA were made redundant. The graft tooks its arterial blood supplies from the recipient's abdominal aorta, through the root of the donor aorta and retrograde into the coronary arteries. The graft was then perfused and venous blood was drained into the right atrium via the coronary sinus and was pumped into the right ventricle and then via the pulmonary artery into the recipient's inferior vena cava. As a result, the left ventricle was unloaded and not considered for any measurable parameters for this study. The right ventricle is only partially loaded with the output arising solely from the donor myocardium. The contractility of the right ventricle is thus reflecting the perfusion of the graft alone. Hence the contractile functional parameters of the right ventricle simply serve as surrogate markers for the viability of the graft and bear no real physiological means. Using the functional MR imaging technique, we examined the contractility of the right ventricles of the heterotopic heart graft and to compare the surrogate contractile parameters of the right ventricles such as the right ventricular end diastolic volume (RVEDV), right ventricular stroke volume (RVSV), right ventricular ejection fraction (RVEF) and right ventricular cardidac output (RVCO) in mouse recipients receiving different treatment.

Figure 6.2.3.5. Blood circulation of the heterotopic heart graft

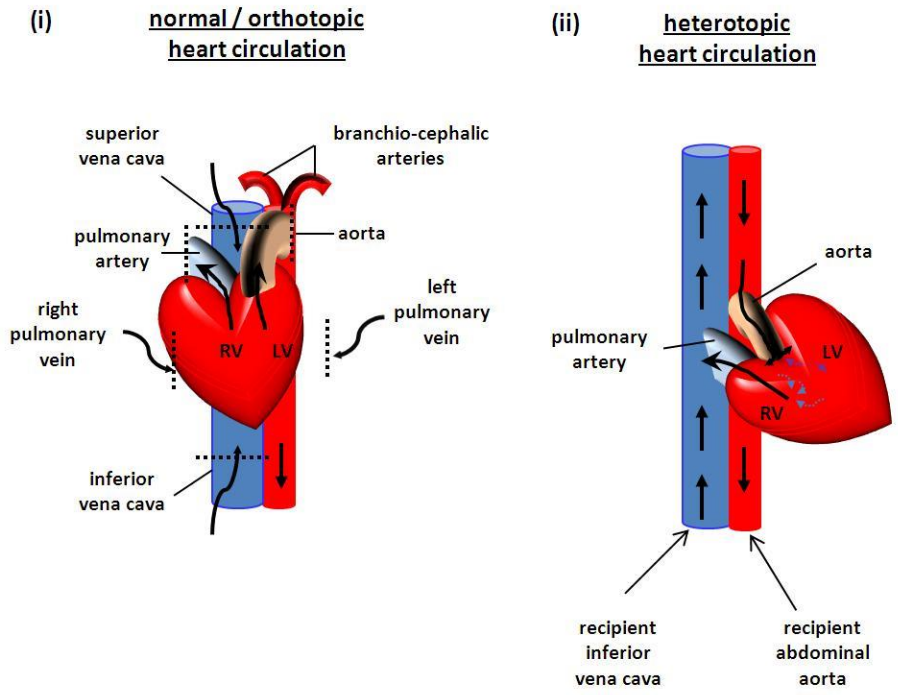

Figure 6.2.3.5. Blood circulation of the heterotopic heart graft. (i) Normal circulation of the heart: venous blood is collected in the right atrium via the superior vena cava and inferior vena cava then delivered to the lungs from the right ventricle through the pulmonary artery. Arterial blood is collected in the left atrium via the pulmonary veins and delivered from the left ventricle to the systemic circulation via the aorta. In an orthotopic transplanted graft, the circulation would follow the physiological blood flow. **(ii)** In the heterotopic heart transplant model, it serves as a simple two-chambers, in-and-out flow system. The inferior vena cava, superior vena cava and pulmonary veins are ligated and divided. Blood supply to the graft is delivered from the recipient's aorta through the coronary arteries at the root of the donor heart aorta when the aortic valves are closed. Deoxygenated blood is then collected from the cardiac capillaries which converge into small veins that drain into the coronary sinus, which is drained into the right atrium and then pumped into the right ventricle. Venous blood is then delivered into the recipient's inferior vena cava via the donor pulmonary artery. The left ventricle is unloaded as no pulmonary circulation is delivered to the left heart and it would become hypotrophic over time. The left ventricle is unloaded and not considered for any measurable parameters for this study. The right ventricle is only partially loaded with the output arising solely from the donor myocardium. The contractility of the right ventricle is thus reflecting the perfusion of the graft alone. The contractile functional parameters of the right ventricle serve as surrogate markers for the viability of the graft with no real physiological means. Using functional MR scanning, the contractile parameters of the right ventricle of the heterotopic heart graft: RVEDV, RVSV, RVEF and RVCO were determined and compared to those in mice receiving different treatment.

6.2.4. Pilot *in vivo* MRI of heterotopic heart allograft

A pilot study was carried out to test the applicability of MR imaging of two groups of mice. First, we elected to use B6 isografts as a positive control on the basis of a heart from this inbred mouse strain being transplanted in our experimental B6-to-CBA strain combination.

B6 mice which were transplanted with a B6 isograft were rested for 2 weeks for full recovery prior to the first MRI scan. The positive finding at this time point also served as a quality control. As shown in ***Figure 6.2.4.1, left panel***, the scanning of the isograft on week 2 was successful with a clear demonstration of contraction of the RV. A second scan was carried out on week 5, which was the time-frame deliberately chosen for the comparison between other experimental groups. We chose to use week 5 because according to historical data, all of the grafts would not be rejected in all of the planned experimental groups ***(see Chapter 3.2.4, 3.2.5)***. More importantly, this time frame was 2 to 3 weeks away from the typical MST of the abatacept control group (MST of 40-55 days). The scan of the isograft on week 5 demonstrated that the post-surgical changes did not affect the quality of MRI ***(Figure 6.2.4.1, middle panel)***. A further scan was carried out on week 8 to determine if it would be possible to carry out proper gated cine MR images as the size of the graft began to involute overtime. Importantly, as shown in ***Figure 6.2.4.1, right panel***, this approach was able to produce high quality of MR images of the isograft.

In order to evaluate the optimal scanning of the allograft, we also performed scanning In 3 different planes on week 5. ***Figure 6.2.4.2.i*** illustrates the isograft in the axial plane. It demonstrated an excellent view of the right and left ventricle and their relationship with other anatomical structures such as the recipient abdominal aorta and IVC. In the Cine video image, it demonstrated the diastolic and systolic phase of the cardiac cycle effectively. In the coronal

plane ***(Figure 6.2.4.2.ii)*** it also demonstrated both chambers clearly. In addition, it showed the bidirectional blood flow occurring between the LV and the aorta. In the sagittal plane ***(Figure 6.2.4.2.iii)***, the bidirectional blood flow between the LV and aorta was again demonstrated. However, the images of the LV and RV were more obscure. Taken together, we elected to use the axial plane for the remaining study for the calculation of the cardiovascular parameters.

Figure 6.2.4.1. Pilot study of *in vivo* MRI of heterotopic heart isograft from week 2 to week 8

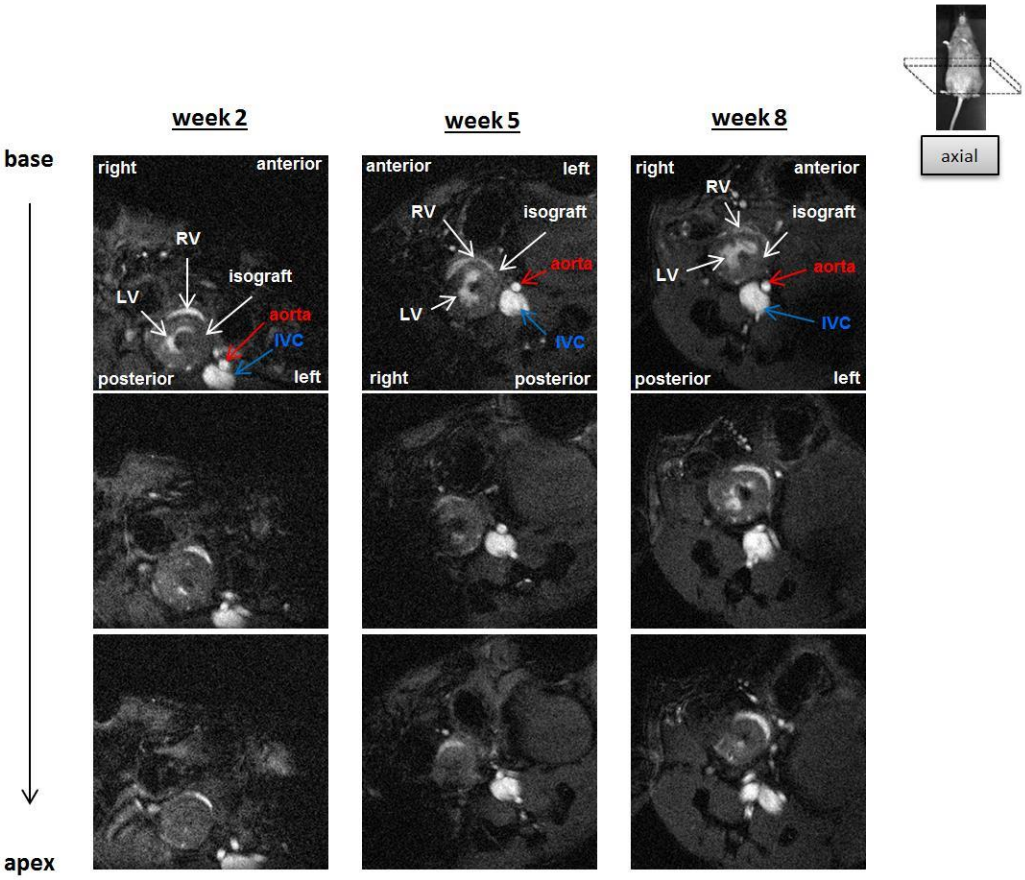

Figure 6.2.4.1. Pilot study of *in vivo* MRI of heterotopic heart isograft from week 2 to week 8. B6 mice were transplanted with a B6 heart isograft heterotopically and underwent *in vivo* MRI on week 2, 5 and 8. MR slides shown above were captured in the axial plane at 3 different levels from the base to the apex of the isograft. The first serial scans confirmed that recipients were physically fit to undergo MRI after 2 weeks of full recovery from transplant surgery. It also provided a quality control scan prior to the proper scanning on week 5. The scanning of B6 isograft on week 5 demonstrated that a positive control scan could be readily obtained to compare amongst different experimental groups. The week 8 scans showed that a pulsating graft could be evaluated at a later time-point, if required. Data above are representative of results obtained from two mice.

Figure 6.2.4.2.i. ***In vivo*** **MR image of a heterotopic heart isograft on week 5 in the axial plane**

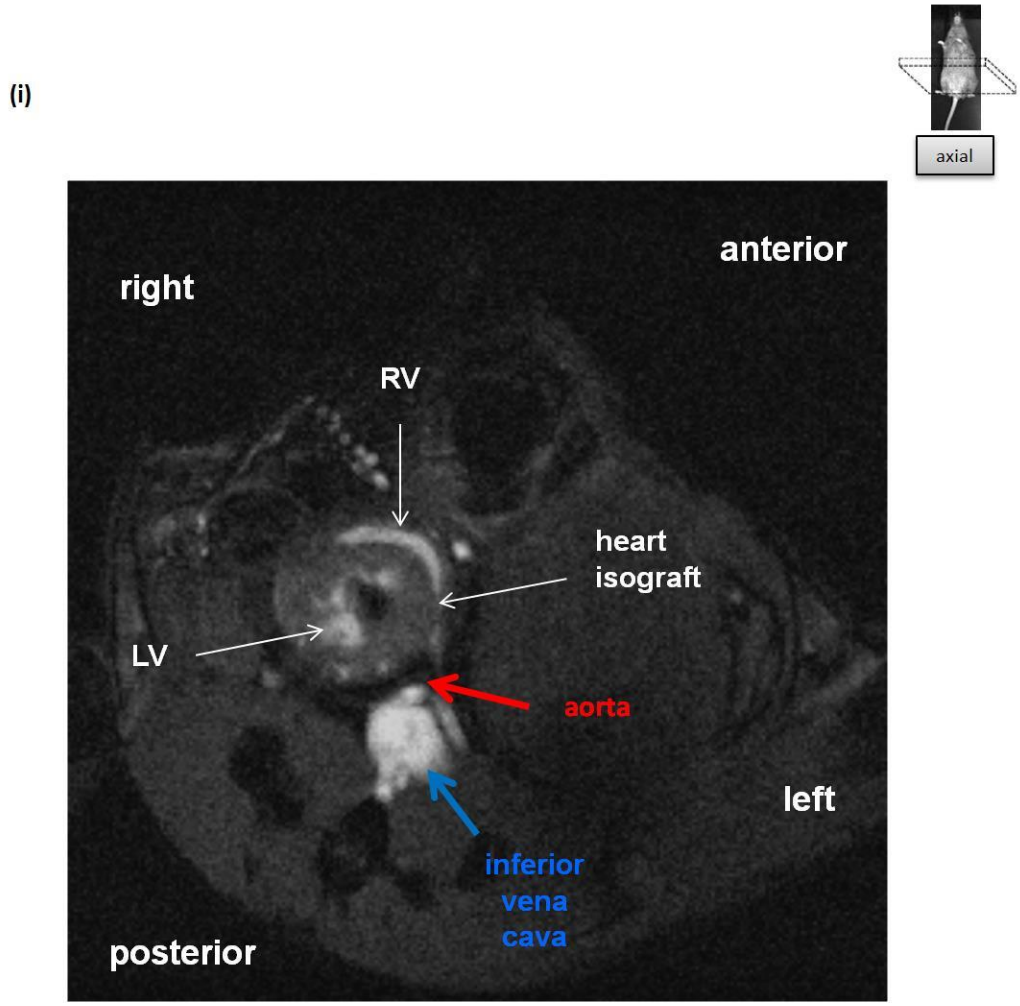

Figure 6.2.4.2.i. ***In vivo*** **MR image of a heterotopic heart isograft on week 5 in the axial plane.** B6 mice were transplanted with a B6 heart isograft heterotopically. *In vivo* MR image above demonstrated a functional isograft 5 weeks post-transplantation. An axial plane image across the recipient's lower abdomen shows the isograft in relation to the recipient aorta and inferior vena cava anteriorly. During the diastolic phase of the cardiac cycle, ventricular blood filling into the left (LV) and right ventricle (RV) is observed.

Figure 6.2.4.2.ii. ***In vivo*** **MR image of a heterotopic heart isograft on week 5 in the coronal plane**

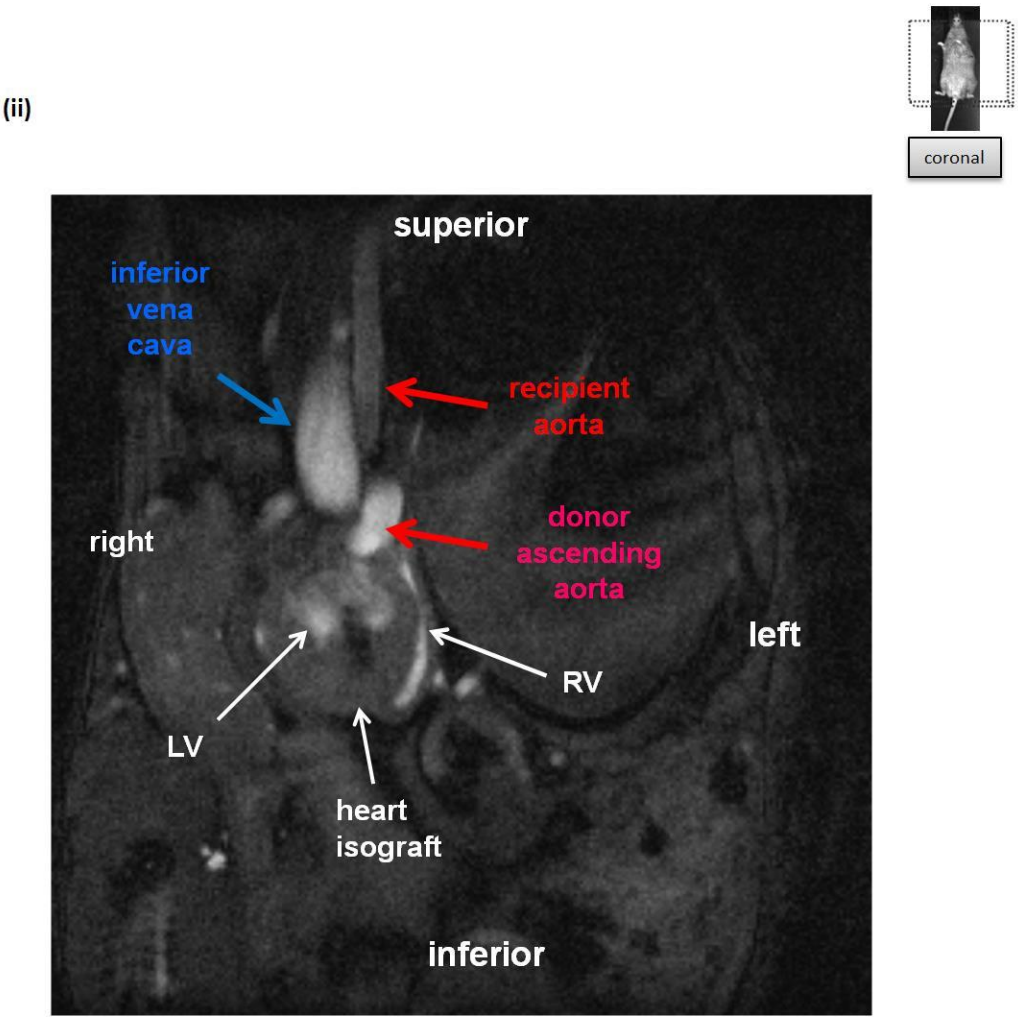

Figure 6.2.4.2.ii. ***In vivo*** **MR image of a heterotopic heart isograft on week 5 in the coronal plane.** B6 mice were transplanted with a B6 heart isograft heterotopically. *In vivo* MR image above demonstrated a functional isograft 5 weeks post-transplantation. In the coronal view, the isograft is shown in relation to the recipient's aorta and inferior vena cava inferiorly. During the diastolic phase of the cardiac cycle, left and right ventricular filling is demonstrated. The isograft receives its blood supply through the coronary arteries at the root of the donor ascending aorta. Incompetent donor aortic valves led to arterial blood regurgitation back into donor ascending aorta and the recipient abdominal aorta from the left ventricle.

Figure 6.2.4.2.iii. ***In vivo*** **MR image of a heterotopic heart isograft on week 5 in the sagittal plane**

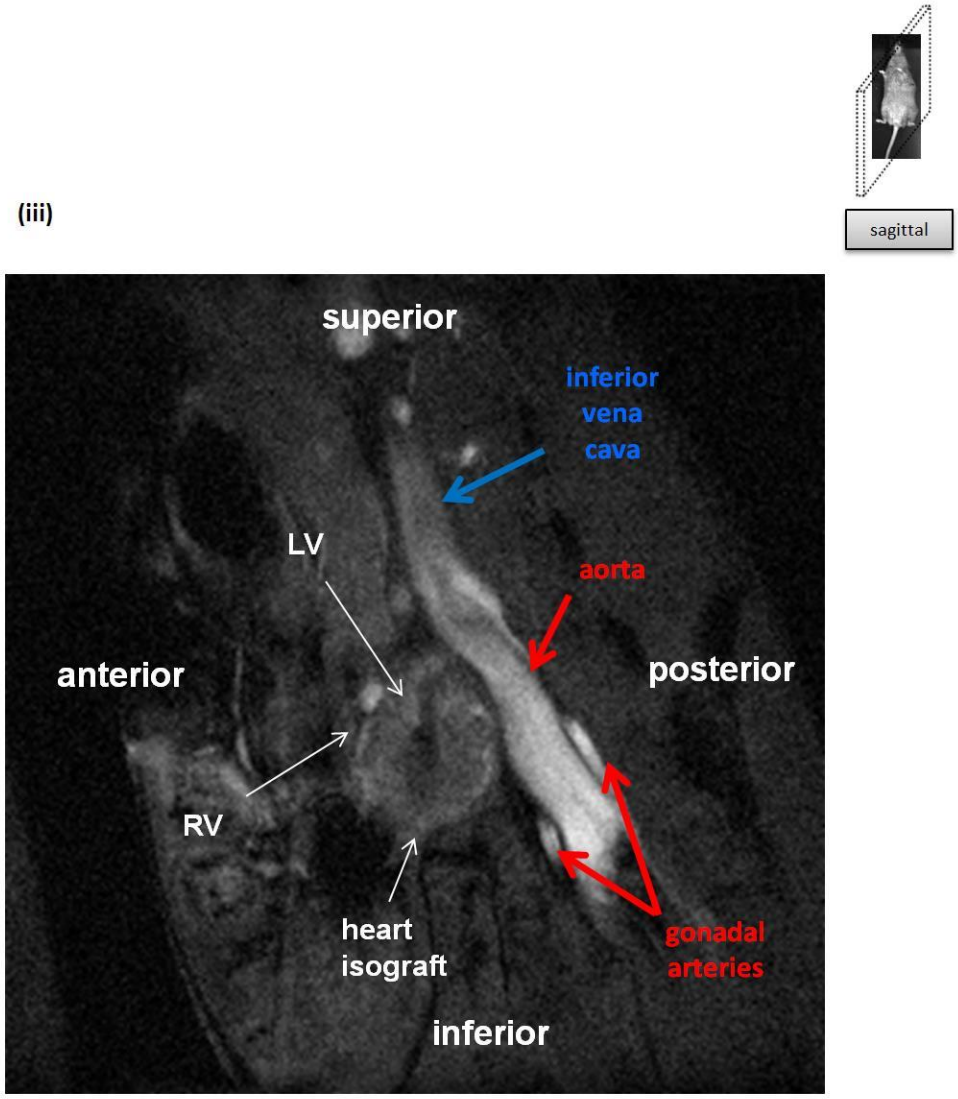

Figure 6.2.4.2.iii. ***In vivo*** **MR image of a heterotopic heart isograft on week 5 in the sagittal plane.** B6 mice were transplanted with a B6 heart isograft heterotopically. *In vivo* MR image above demonstrated a functional isograft 5 weeks post-transplantation. In the sagittal view, the isograft is shown in relation to the recipient's aorta and inferior vena cava anteriorly. During the diastolic phase of the cardiac cycle, left and right ventricular filling is demonstrated. The right ventricle is less readily identifiable in this still image compared to the Cine video images (not shown). Regurgitation of arterial blood through donor ascending aorta into the recipient abdominal aorta is observed due to incompetent donor aortic valves.

As part of the pilot study, we also carried out scanning of the allograft which had accepted an allogeneic heart transplant long-term, i.e. ≥100 days post-transplant. CBA mice transplanted with a B6 allograft which were treated with a sub-optimal abatacept combined with IFN-γ Treg therapy with a palpable graft 100 days post-transplant were recruited. As shown in ***Figure 6.2.4.3*** (axial plane), there was dramatic involution of the LV mass because of the volume unloading phenomenon. The RV was still visible; however, it is more difficult to define, suggesting that the scanning of an allograft at this time-point could be technically challenging due to the poor ECG-gated imaging. We also confirmed that by scanning the allograft in 3 different planes. As shown in ***Figure 6.2.4.4.i***, it demonstrated the LV and RV contraction in the axial plane. In ***Figure 6.2.4.4.ii*** (coronal plane), a slit of RV was clearly demonstrated. However, in the Cine video image, the contraction of the RV was not clearly illustrated. In ***Figure 6.2.4.4.iii*** (sagittal plane), the LV was clearly identified but the RV was more difficult to define, similar to that of the isograft above. Collectively, these data suggest that the involution of the allograft over time had a significant impact on the quality of *in vivo* MR imaging to obtain ECG-synchronized high quality Cine video imaging to demonstrate the contraction of the RV due to the poor ECG-gating. Hence, we concluded that using cine MR imaging it will not be possible to determine the changes of the allograft of this time-scale, thus long-term graft survivors beyond 100 days.

Figure 6.2.4.3. *In vivo* MR images of a heterotopic heart allograft tolerized by abatacept plus IFN-γ Treg 100 days post-transplant

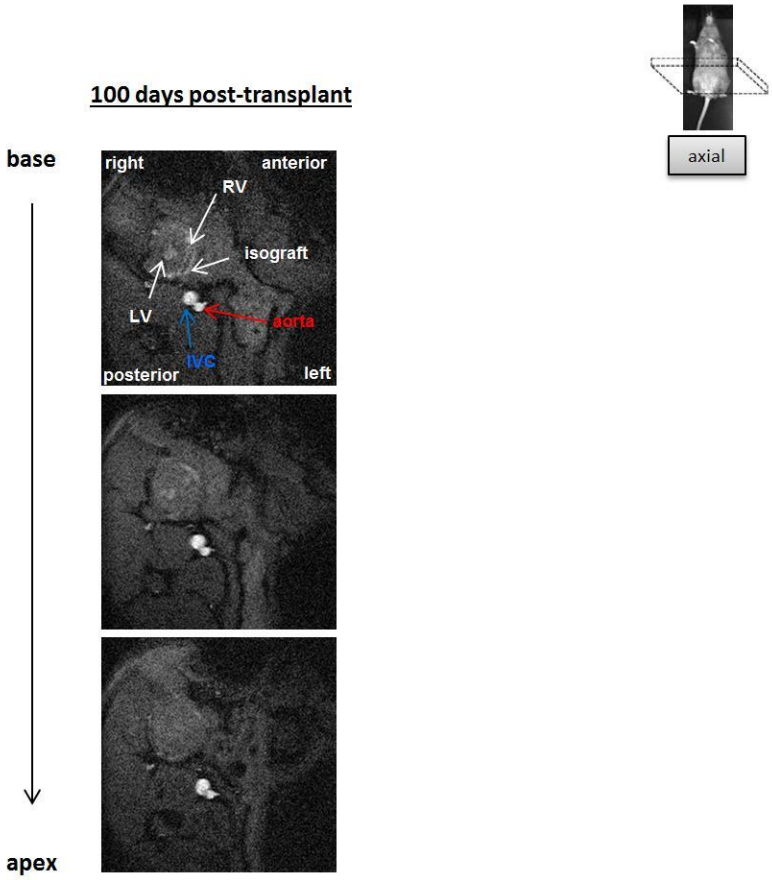

Figure 6.2.4.3. *In vivo* MR images of a heterotopic heart allograft tolerized by abatacept plus IFN-γ Treg 100 days post-transplant. A pilot scan illustrates the acceptance of an allograft using *in vivo* MRI. CBA mouse was given $2x10^6$ IFN-γ Treg one day before the transplant of a B6 heterotopic heart allograft, plus a peri-operative sub-optimal abatacept (i.v. 25 μg day 0, 1 and 5). Survival of the B6 heart allograft was determined by conventional palpation at regular intervals. B6 heart allograft was tolerized by abatacept plus IFN-γ Treg therapy as confirmed by a pulsating graft on day 100 post-transplant. Graft outcome was assessed additionally by *in vivo* MRI on day 100. MR slides shown above were captured during the end-diastolic phase of the cardiac cycle in the axial plane at 3 different levels of the allograft from the base to the apex.

Figure 6.2.4.4.i. ***In vivo*** **MR image of a heterotopic heart allograft tolerized by abatacept and IFN-γ Treg 100 days post-transplant- the axial plane**

(i)

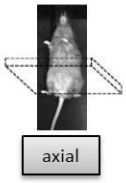

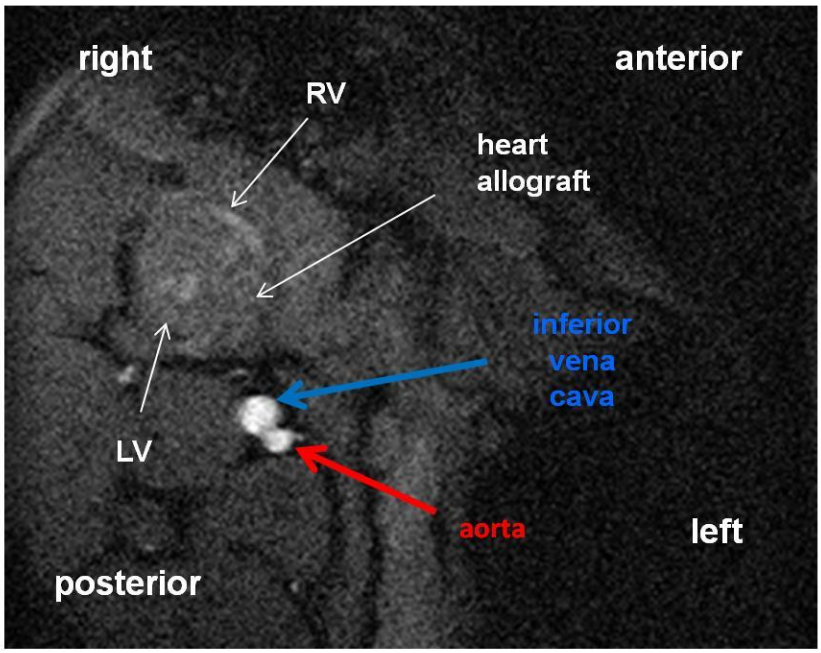

Figure 6.2.4.4.i. ***In vivo*** **MR image of a heterotopic heart allograft tolerized by abatacept and IFN-γ Treg 100 days post-transplant- the axial plane.** A pilot scan illustrates the acceptance of an allograft using *in vivo* MRI. CBA mouse was given $2x10^6$ IFN-γ Treg one day before the transplant of a B6 heterotopic heart allograft plus a peri-operative sub-optimal abatacept (i.v. 25 μg day 0, 1 and 5). An axial plane image across the recipient's lower abdomen shows the allograft in relation to the recipient's aorta and inferior vena cava. During the diastolic phase of the cardiac cycle, left and right ventricular filling of the allograft was demonstrated.

Figure 6.2.4.4.ii. *In vivo* MR image of a heterotopic heart allograft tolerized by abatacept and IFN-γ Treg 100 days post-transplant- the coronal plane

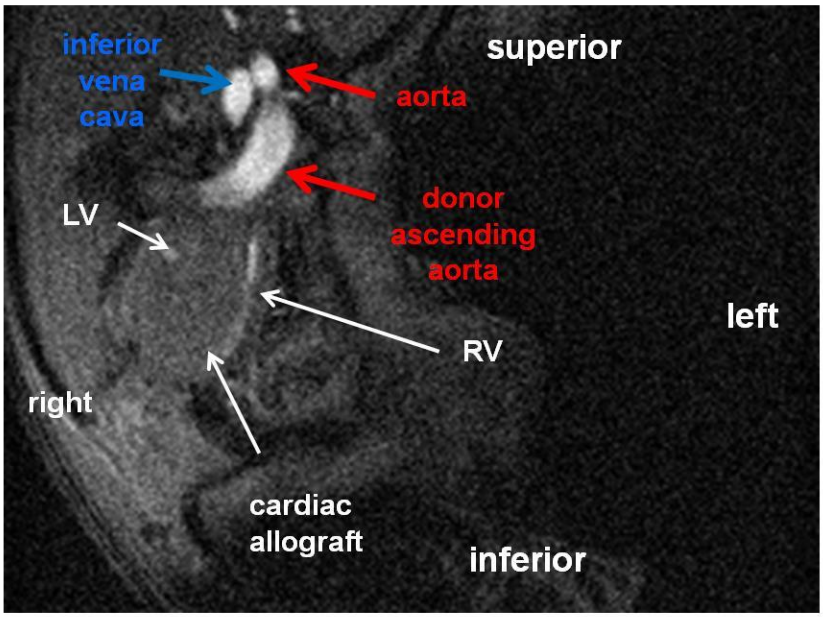

Figure 6.2.4.4.ii. *In vivo* MR image of a heterotopic heart allograft tolerized by abatacept and IFN-γ Treg 100 days post-transplant- the coronal plane. A pilot scan illustrates the acceptance of an allograft using *in vivo* MRI. CBA mouse was given $2x10^6$ IFN-γ Treg one day before the transplant of a B6 heterotopic heart allograft, plus a peri-operative sub-optimal abatacept (i.v. 25 μg day 0, 1 and 5). A coronal plane image across the recipient's lower abdomen shows the allograft in relation to the recipient's aorta and inferior vena cava. During the diastolic phase of the cardiac cycle, left and right ventricular filling of the allograft was demonstrated. Regurgitation was observed at the root of the donor ascending aorta due to the incompetent donor aortic valves of the left ventricle.

Figure 6.2.4.4.iii. *In vivo* MR image of a heterotopic heart allograft tolerized by abatacept and IFN-γ Treg 100 days post-transplant- the sagittal plane

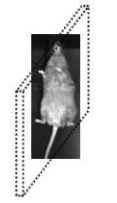

(iii)

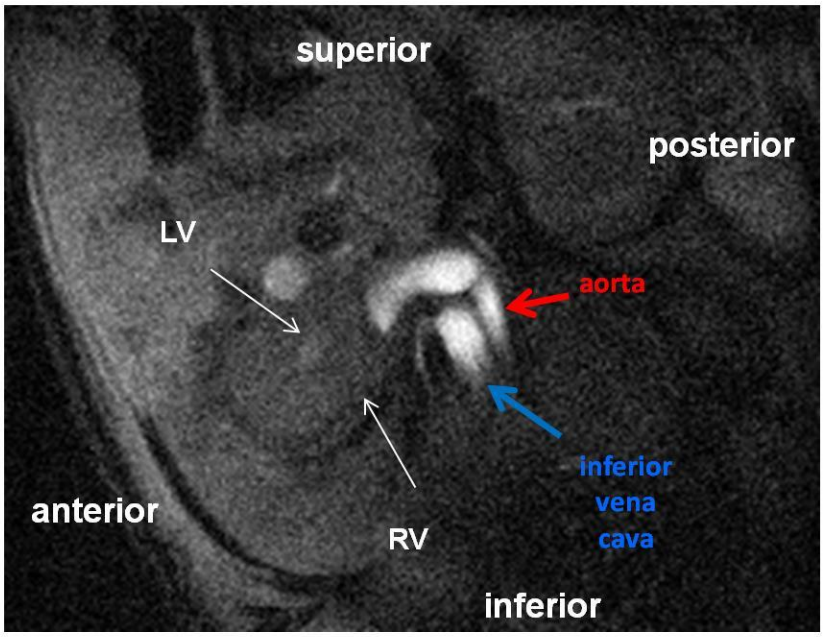

Figure 6.2.4.4.iii. *In vivo* MR image of a heterotopic heart allograft tolerized by abatacept and IFN-γ Treg 100 days post-transplant- the sagittal plane. A pilot scan illustrates the acceptance of an allograft using *in vivo* MRI. CBA mouse was given $2x10^6$ IFN-γ Treg one day before the transplant of a B6 heterotopic heart allograft, plus a peri-operative sub-optimal abatacept (i.v. 25 μg day 0,1 and 5). A sagittal plane image across the recipient's lower abdomen shows the allograft in relation to the recipient's aorta and inferior vena cava. During the diastolic phase of the cardiac cycle, left and right ventricular filling of the allograft was demonstrated. The right ventricle was less readily identifiable in this still image compared to the Cine video image. Regurgitation was observed at the root of the donor ascending aorta due to the incompetent donor aortic valves of the left ventricle.

6.2.5 IFN-γ Treg therapy preserved right ventricular function of allograft in a dose-dependent manner

In our first set of experiments, we looked at the subtle differences between the RV contractility between 4 experimental groups and compared to their respective palpation scores on week 5 after transplantation ***(Figure 6.2.5.1)***. CBA mice were transplanted with a B6 heart allograft plus an established tolerizing anti-CD4 (50μg/dose) / anti-CD8 (100μg/dose) antibody protocol which served as a positive control. This protocol was designed with reference to our own experience in the laboratory and studies from other groups which showed that anti-CD4/CD8 antibody could induce tolerance *in vivo*[595]. A second control group included CBA mice which were transplanted with a B6 heart allograft and given a peri-operative sub-optimal abatacept treatment (i.v. 25μg day 0, 1 and 5), in which historical data demonstrated consistently that it delayed allograft survivals with a MST of ~50 days ***(Chapter 3.2.4)***. Lastly, CBA mice transplanted with a B6 heart allograft received either $5x10^5$ or $2x10^6$ IFN-γ Treg 3 days prior to the transplant plus the sub-optimal abatacept treatment. We hypothesized that Treg therapy plus abatacept conferred a superior graft outcome compared to abatacept alone at the early phase post-transplantation. These subtle differences might be reflected by their differential RV functional parameters derived from *in vivo* MRI, but not by bi-manual palpation.

Representative MR scan images of the heterotopic heart allografts taken at week 2 and week 5 post-transplantation in mice treated with anti-CD4/CD8 antibody ***(Figure 6.2.5.2)***, sub-optimal abatacept ***(Figure 6.2.5.3)***, abatacept + $5x10^5$ IFN-γ Treg ***(Figure 6.2.5.4)*** and abatacept + $2x10^6$ IFN-γ Treg ***(Figure 6.2.5.5)*** are shown.

Figure 6.2.5.1. IFN-γ Treg therapy preserved the right ventricular function of allograft in a dose-dependent manner as shown by *in vivo* MRI

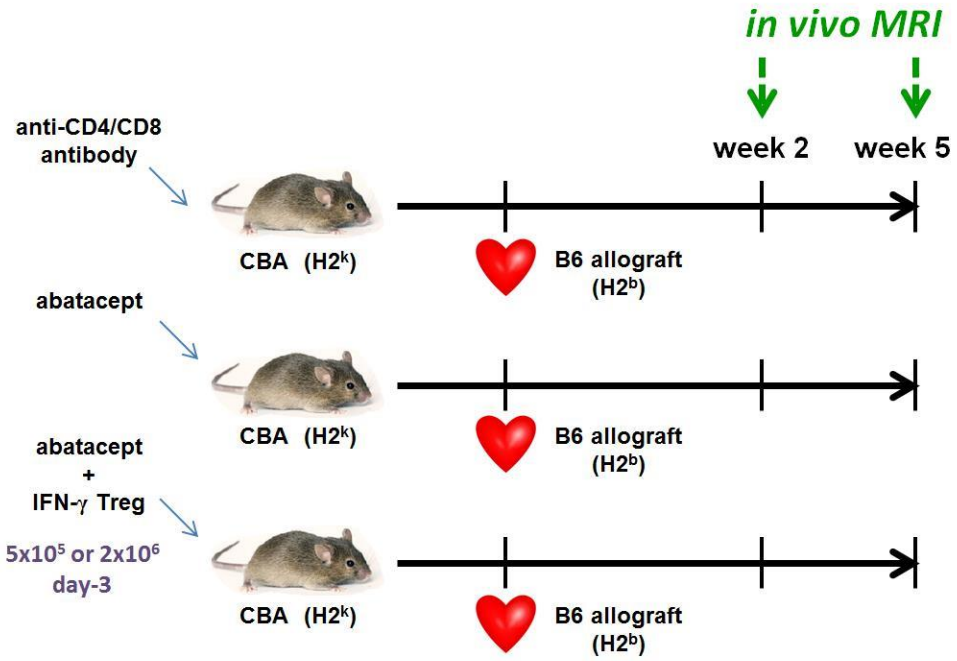

Figure 6.2.5.1. IFN-γ Treg therapy preserved the right ventricular function of allograft in a dose-dependent manner as shown by *in vivo* MRI. CBA IFN-γ Treg were generated *in vitro* by stimulating $CD4^+$ T cells with B6 alloantigens in the presence of IFN-γ as described in ***Chapter 2.8.1***. $5x10^5$ or $2x10^6$ IFN-γ Treg were given to CBA mice 3 days prior to the transplant of a B6 heterotopic heart allograft in addition to a sub-optimal abatacept protocol (i.v. 25μg day 0, 1 and 5). Two weeks after transplantation, these recipients underwent *in vivo* MRI with the set up as described in ***Figure 6.2.3.1***, on week 2 and 5 for the assessment of graft functional outcome. These groups of mice were compared to mice that received a peri-operative anti-CD4 (i.v. 50μg) and anti-CD8 (i.v. 100μg) antibody protocol or the sub-optimal abatacept protocol alone. Data retrieved from MRI were processed using the ImageJ® software for the calculation of various cardiovascular functional parameters as described in ***Chapter 2.4***. Bi-manual palpation scores were recorded for each graft at regular intervals.

Figure 6.2.5.2. ***In vivo*** **MR images of B6 allograft in CBA recipients treated with anti-CD4/CD8 antibody between week 2 and week 5**

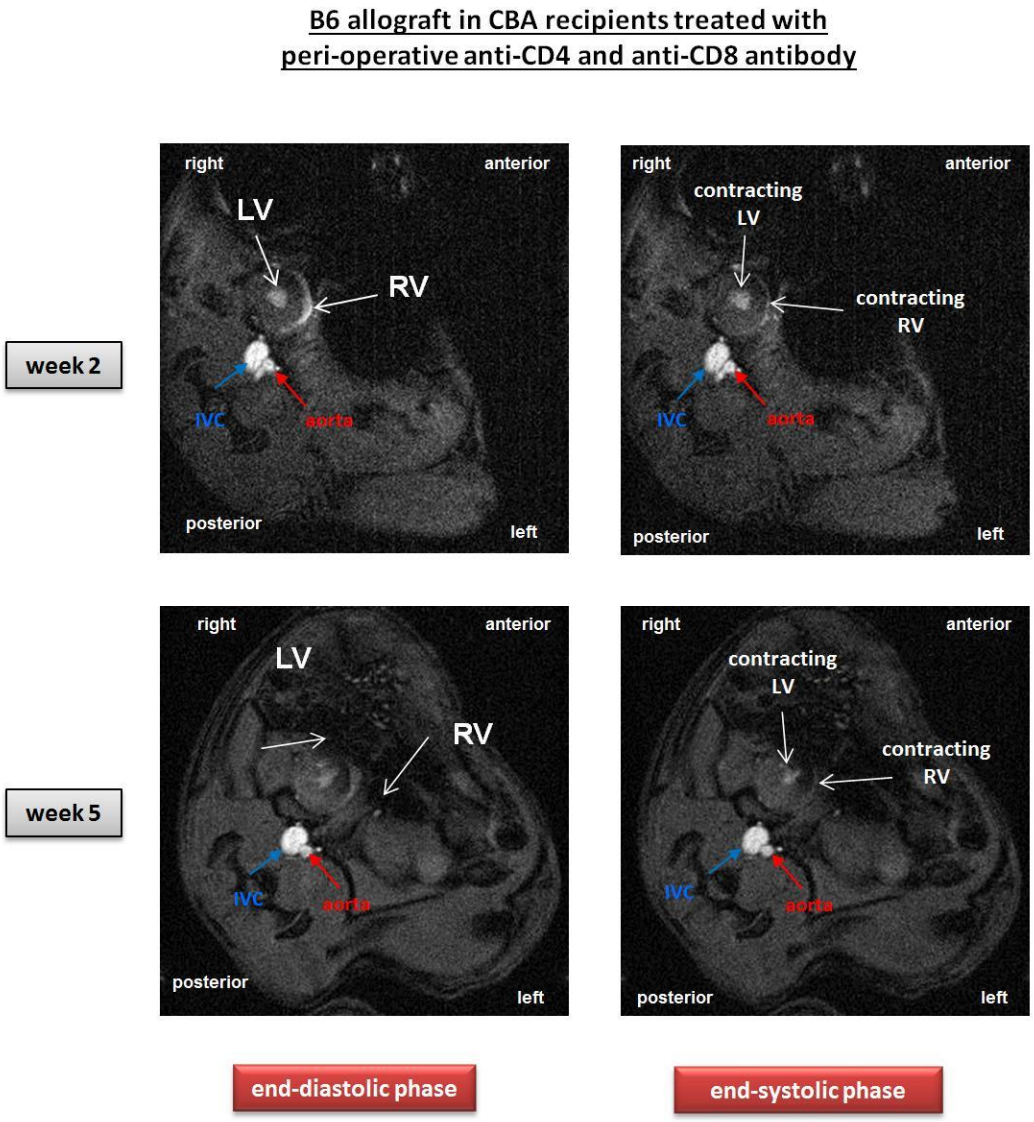

Figure 6.2.5.2. ***In vivo*** **MR images of B6 allograft in CBA recipients treated with anti-CD4/CD8 antibody between week 2 and week 5.** Cross-sectional images of heterotopically transplanted B6 allograft in CBA recipient at the end-diastolic and end-systolic phase are shown with the relevant anatomical features. Peri-operative anti-CD4 and anti-CD8 antibody treatment delayed allograft rejection long-term and used as a positive control. The right ventricular contractility was preserved between week2 and week 5. Data above are representative of results obtained from 3 mice.

Figure 6.2.5.3. ***In vivo*** **MR images of B6 allograft in CBA recipients treated with sub-optimal abatacept between week 2 and week 5**

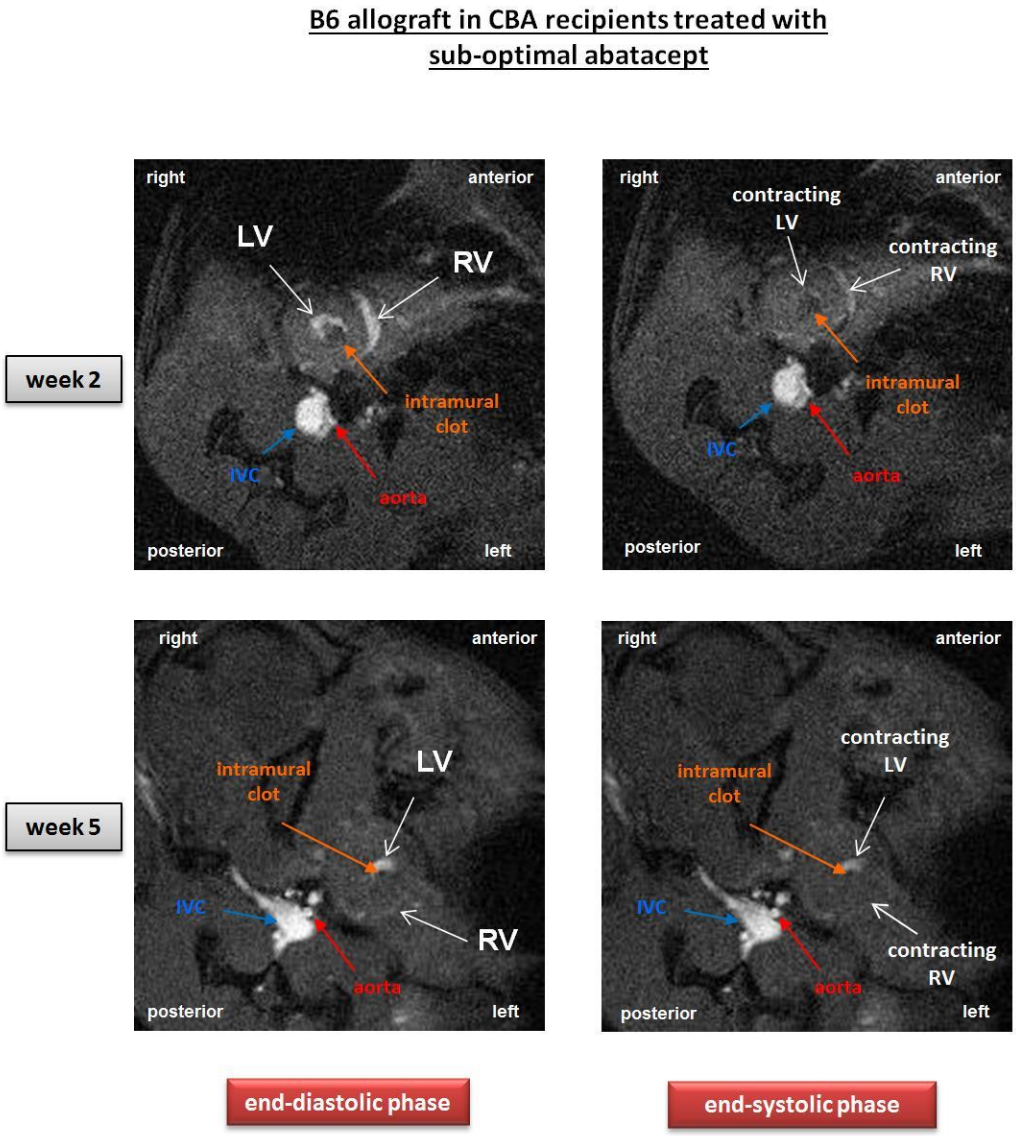

Figure 6.2.5.3. ***In vivo*** **MR images of B6 allograft in CBA recipients treated with sub-optimal abatacept between week 2 and week 5.** Cross-sectional images of heterotopically transplanted B6 allograft in CBA recipient treated with a peri-operative sub-optimal abatacept at the end-diastolic and end-systolic phase are shown with the relevant anatomical features. A sub-optimal abatacept protocol delayed allograft rejection with a MST around 50 days according to historical controls. Good ventricular contractility was seen at week 2, which declined significantly on week 5 as shown by the poorly perfused right ventricle. Data above are representative of results obtained from 6 mice.

Figure 6.2.5.4. ***In vivo*** **MR images of B6 allograft in CBA recipients treated with sub-optimal abatacept plus IFN-γ Treg 5x10^5 between week 2 and week 5**

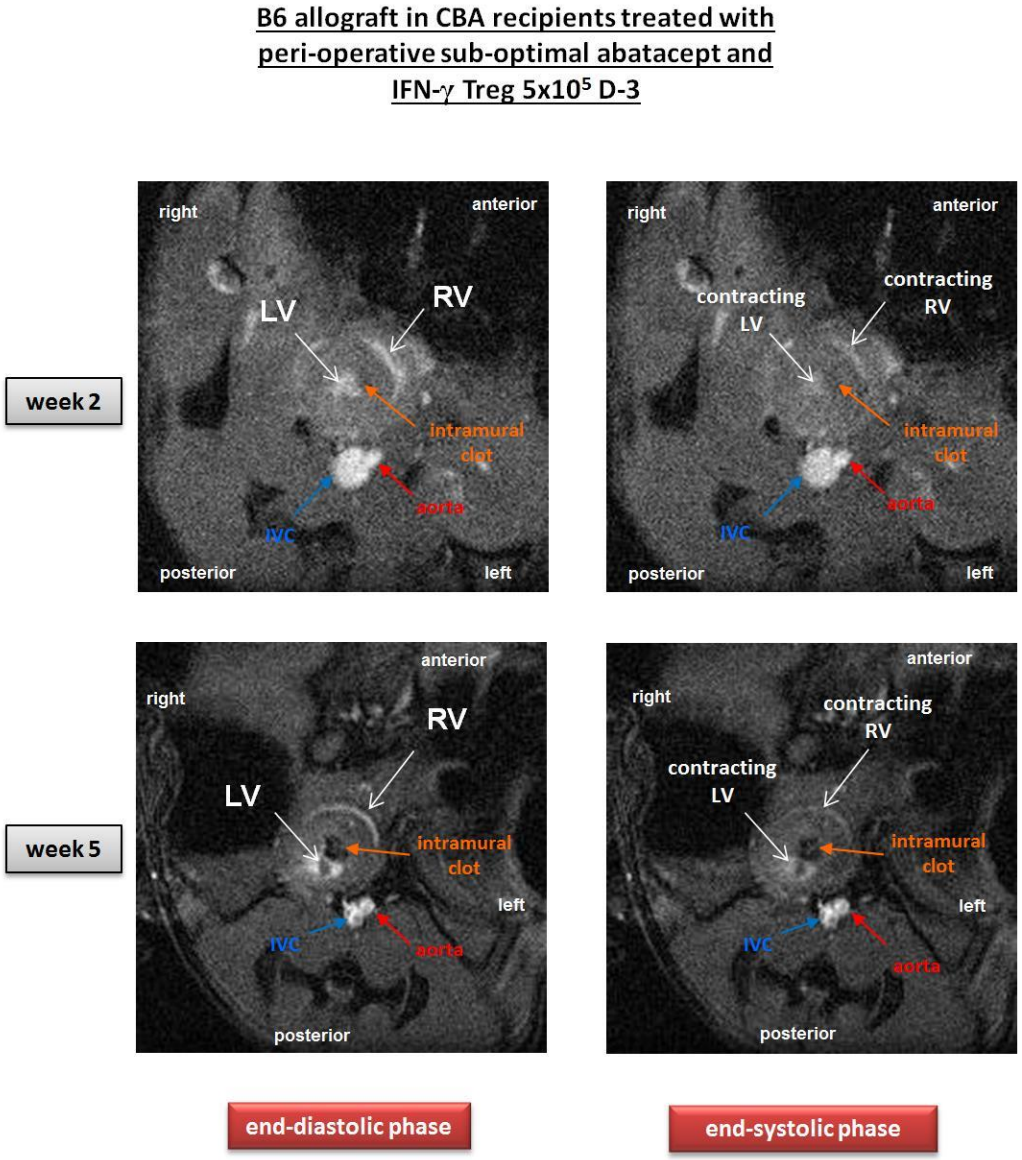

Figure 6.2.5.4. ***In vivo*** **MR images of B6 allograft in CBA recipients treated with sub-optimal abatacept plus IFN-γ Treg 5x10^5 between week 2 and week 5.** Cross-sectional images of heterotopically transplanted B6 allograft in CBA recipient treated with abatacept plus 5x10^5 IFN-γ Treg at the end-diastolic and end-systolic phase are shown with the relevant anatomical features. IFN-γ Treg therapy preserved right ventricular contractility of allograft between week 2 and week 5 post-transplantation. Data above are representative of results obtained from 4 mice.

Figure 6.2.5.5. ***In vivo*** **MR images of B6 allograft in CBA recipients treated with sub-optimal abatacept plus IFN-γ Treg 2x10^6 between week 2 and week 5**

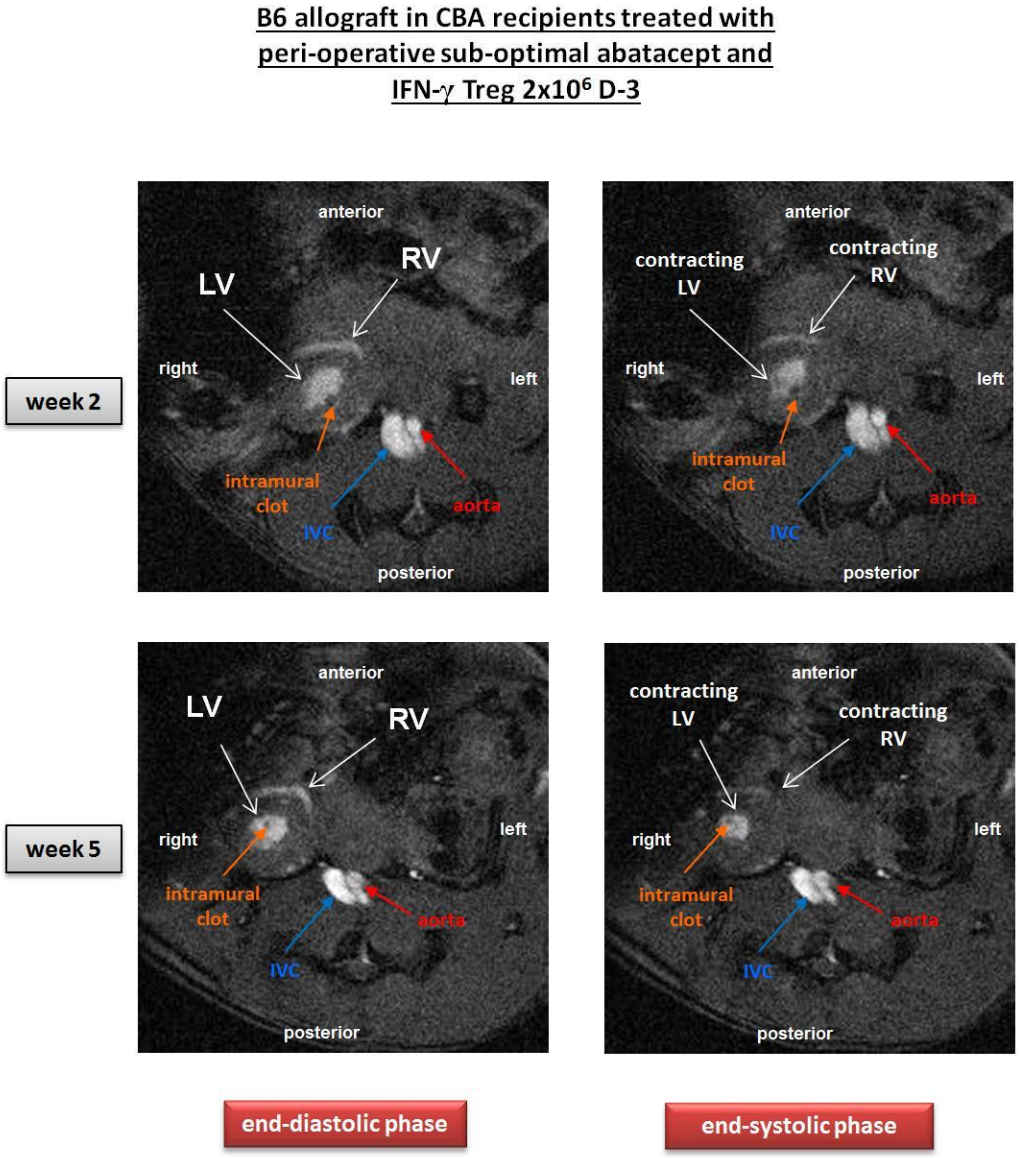

Figure 6.2.5.5. ***In vivo*** **MR images of B6 allograft in CBA recipients treated with sub-optimal abatacept plus IFN-γ Treg 2x10^6 between week 2 and week 5.** Cross-sectional images of heterotopically transplanted B6 allograft in CBA recipient treated with abatacept plus 2x10^6 IFN-γ Treg at the end-diastolic and end-systolic phase are shown with the relevant anatomical features. IFN-γ Treg given at a dose of 2x10^6 also appeared to preserve good ventricular contractility between week 2 and week 5 post-transplantation. Data above are representative of results obtained from 5 mice.

Contractile parameters were derived from *in vivo* MRI scanning at week 5. Firstly, the Right ventricular end-diastolic volume (RVEDV) is a functional parameter to determine the preload of the right ventricle of the transplanted allograft, which is ultimately related to the stroke volume. The mean RVEDV of allografts in mice treated with abatacept plus $2x10^6$ IFN-γ Treg (3.91±1.16μl, n=5) remained significantly higher than those treated with abatacept alone (1.99±1.22μl, n=4; *p*=0.0473), however, the low-dose IFN-γ Treg treatment group (4.17±1.60μl, n=5) remained no different from the abatacept only group (*p*=0.0604). Both IFN-γ Treg groups had a similar RVEDV compared to the anti-CD4/CD8 antibody group (3.71±1.87μl, n=6; *p*=0.6777 and *p*=0.8449, respectively) ***(Figure 6.2.5.6.i)***.

The right ventricular stroke volume (RVSV) is the volume of blood that was ejected at each stroke of heart beat. It was calculated from the difference between the right ventricular end-diastolic volume and the end-systolic volume, i.e. RVSV=RVEDV-RVESV. the mean RVSV of allografts in mice treated with abatacept plus $5x10^5$ IFN-γ Treg (1.74±0.89μl, n=5) and $2x10^6$ IFN-γ Treg (1.99±1.07μl, n=5) were significantly higher than those treated with abatacept alone (0.39±0.26μl, n=4; *p*=0.0231 and *p*=0.0240, respectively), but remained no different from the anti-CD4/CD8 antibody group (2.31±1.54μl, n=6; *p*=0.4833 and *p*=0.707, respectively) ***(Figure 6.2.5.6.ii)***.

The right ventricular ejection fraction (RVEF) is a functional parameter which correlates with the intrinsic contractility of the right ventricle. RVEF denotes the efficiency of the right ventricle to empty its diastolic volume (RVEF=RVEDV-RVESV/RVEDV*100%). the mean RVEF of allografts in mice treated with abatacept plus $5x10^5$ IFN-γ Treg (40±9.49%, n=5) and $2x10^6$ IFN-γ Treg (49.6±17.9%, n=5) were significantly higher than those treated with abatacept alone (19.5±7.65%, n=4; *p*=0.0099 and *p*=0.0171, respectively), but remained no different from the

anti-CD4/CD8 antibody group (58.3±18.5% , n=6; p=0.0785 and *p*=0.4329, respectively) ***(Figure 6.2.5.6.iii, right panel)***.

The right ventricular cardiac outputs (RVCO) is the product of the stroke volume and heart rate (CO= SV x HR). HR was recorded using the ECG tracing for each recipient. The mean RVCO of allografts in mice treated with abatacept plus $5x10^5$ IFN-γ Treg (0.56±0.31ml/min, n=5) and $2x10^6$ IFN-γ Treg (0.56±0.24ml/min, n=5) were significantly higher than those treated with abatacept alone (0.08±0.06ml/min, n=4; *p*=0.0202 and *p*=0.0063, respectively), but remained no different from the anti-CD4/CD8 antibody group (0.58±0.27ml/min, n=6; p=0.9203 and *p*=0.8801, respectively) ***(Figure 6.2.5.6.iv)***.

Conventionally, the assessment of graft outcome in the heterotopic heart transplant model is carried out by interval bi-manual palpation for the impulse generated by the pulsating graft in the abdomen. According to the intensity of the impulses generated, a Pulsation Score (PS) from 0-4 is assigned to reflect the status of the graft. 0= no pulsation (rejected); 1= definitive but very weak impulses; 2= weak but regular rhythmic impulses; 3= strong but sub-optimal pulsation; and 4= forceful impulses. The PS of allografts in mice treated with $5x10^5$ IFN-γ Treg (3.0±0.7, n=5) was not significantly different from those treated with abatacept (2.0±0.8, n=4; *p*=0.0892) or anti-CD4/CD8 antibody (2.7±0.8, n=6; *p*=0.4927). On the other hand, the PS in mice treated with $2x10^6$ IFN-γ Treg (3.2±0.4, n=5) was significantly higher than the abatacept group (*p*=0.0255), but not the anti-CD4/CD8 antibody group (*p*=0.2260) ***(Figure 6.2.5.7)***. Graft assessment by both MRI and bi-manual palpation revealed the superior allograft function in the higher-dose ($2x10^6$) IFN-γ Treg group compared to the abatacept control ***(Figure 6.2.5.6 versus 6.2.5.7)***. However, PS failed to detect the functional differences between the lower-dose ($5x10^5$) IFN-γ Treg group compared to the abatacept control, whilst MRI could detect these subtle

differences. Collectively, these data suggest that *in vivo* MRI could reveal subtle differences in terms of the graft function between these experimental groups, more sensitive than the crude way of measurement by palpation.

Figure 6.2.5.6. Comparison of right ventricular function of allografts treated with 2 different doses of IFN-γ Treg at week 5 using *in vivo* MRI

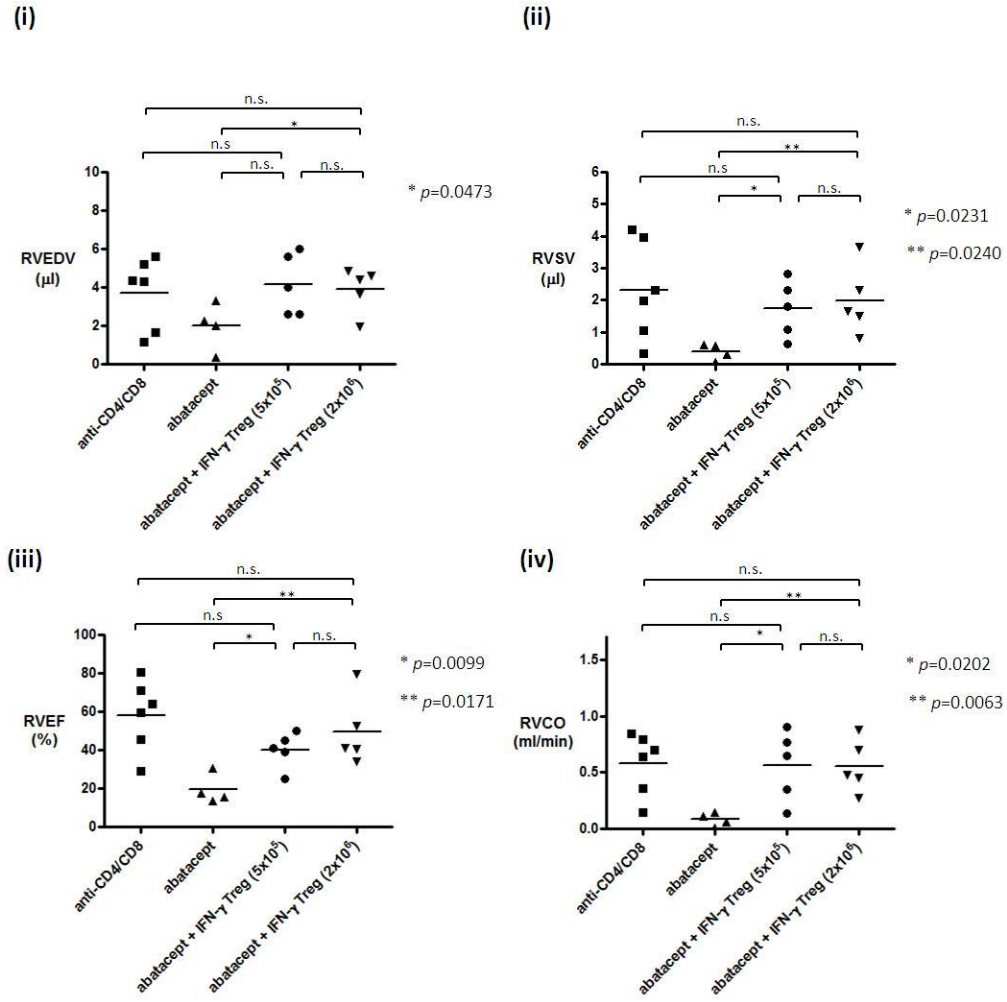

Figure 6.2.5.6. Comparison of right ventricular function of allografts treated with 2 different doses of IFN-γ Treg at week 5 using *in vivo* MRI. (i) RVEDV: Mice treated with $2x10^6$ (but not $5x10^5$) IFN-γ Treg remained significantly higher than the abatacept group (p=0.0473) and similar to the anti-CD4/CD8 antibody group (p>0.05). **(ii) RVSV:** Mice treated with either $5x10^5$ or $2x10^6$ IFN-γ Treg was significantly higher than the abatacept group (p=0.0231 and p=0.0240, respectively), but remained similar to the anti-CD4/CD8 antibody group (p>0.05). **(iii) RVEF:** Both IFN-γ Treg groups had a higher RVSV compared to the abatacept group (p=0.0099 and p=0.0171, respectively), but indifferent from the anti-CD4/CD8 antibody group (p>0.05). **(iv) RVCO:** Mice treated with abatacept plus either $5x10^5$ or $2x10^6$ IFN-γ Treg had a significantly higher RVCO compared to abatacept alone (p=0.0202 and p=0.0063, respectively), but similar to the anti-CD4/CD8 antibody group (p>0.05). Student's t-tests were used for statistical comparisons. (p<0.05 denotes statistically significant)

Figure 6.2.5.7. Assessment of allograft pulsation using bi-manual palpation

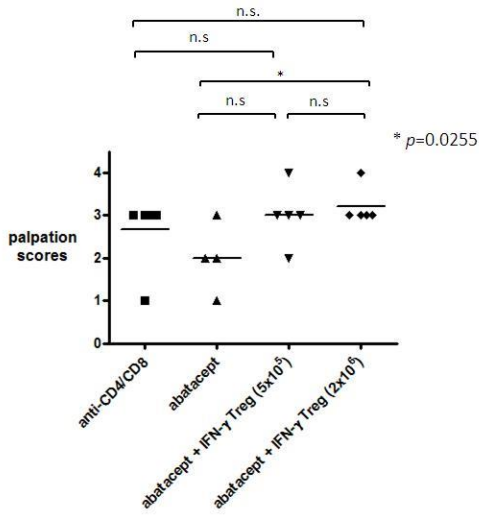

Figure 6.2.5.7. Assessment of allograft pulsation using bi-manual palpation at week 5. The pulsation scores (PS) of the heterotopic heart grafts in each experimental group are illustrated above. There were no differences in the PS between mice treated with $5x10^5$ IFN-γ Treg and abatacept (p=0.0892) or anti-CD4/CD8 antibody (p=0.4927). Mice given a higher IFN-γ Treg dose ($2x10^6$) showed a significantly higher PS compared to the abatacept control (p=0.0255), but similar to the anti-CD4/CD8 antibody group (p=0.2260). Student's t-tests were used for statistical comparisons. (p<0.05 denotes statistically significant)

6.2.6 IFN-γ Treg therapy preserved right ventricular function of allograft when delivered at optimal timing

In a separate set of experiments, we aimed to compare the allograft function in mice given the same dose of IFN-γ Treg at different time points ***(Figure 6.2.6.1)***. We devised the study to include B6 isografts as a group of positive controls for the purpose of subsequent histopathological assessment. Similar to the previous set of experiments, a group of CBA mice were transplanted with a B6 heart allograft and received a peri-operative anti-CD4/anti-CD8 antibody. A third group of CBA mice were transplanted with a B6 heart allograft and received the sub-optimal abatacept protocol. Lastly, instead of comparing the cell dose, we compared the timing of IFN-γ Treg delivery in which CBA mice transplanted with a B6 allograft treated with abatacept plus $5x10^5$ IFN-γ Treg either on day-3 or day-7. We have previously shown that IFN-γ Treg given on day-1 or day-3 could delay allograft rejection at a given cell dose ***(Chapter 3.2.6.2)***. We hypothesized that IFN-γ Treg given closer to the transplant would allow better suppressive effects and therefore preserve graft architecture more effectively.

Representative MR scan images of the heterotopic heart B6 isografts ***(Figure 6.2.6.2)*** and allografts taken at week 2 and week 5 post-transplantation in mice treated with anti-CD4/CD8 antibody ***(Figure 6.2.6.3)***, sub-optimal abatacept ***(Figure 6.2.6.4)***, abatacept + $5x10^5$ IFN-γ Treg day-3 ***(Figure 6.2.5.4)*** and abatacept + $5x10^5$ IFN-γ Treg day-7 ***(Figure 6.2.5.5)*** are shown.

Figure 6.2.6.1. Compare and contrast the assessment of graft outcome using *in vivo* MRI and histopathological examination following IFN-γ Treg therapy

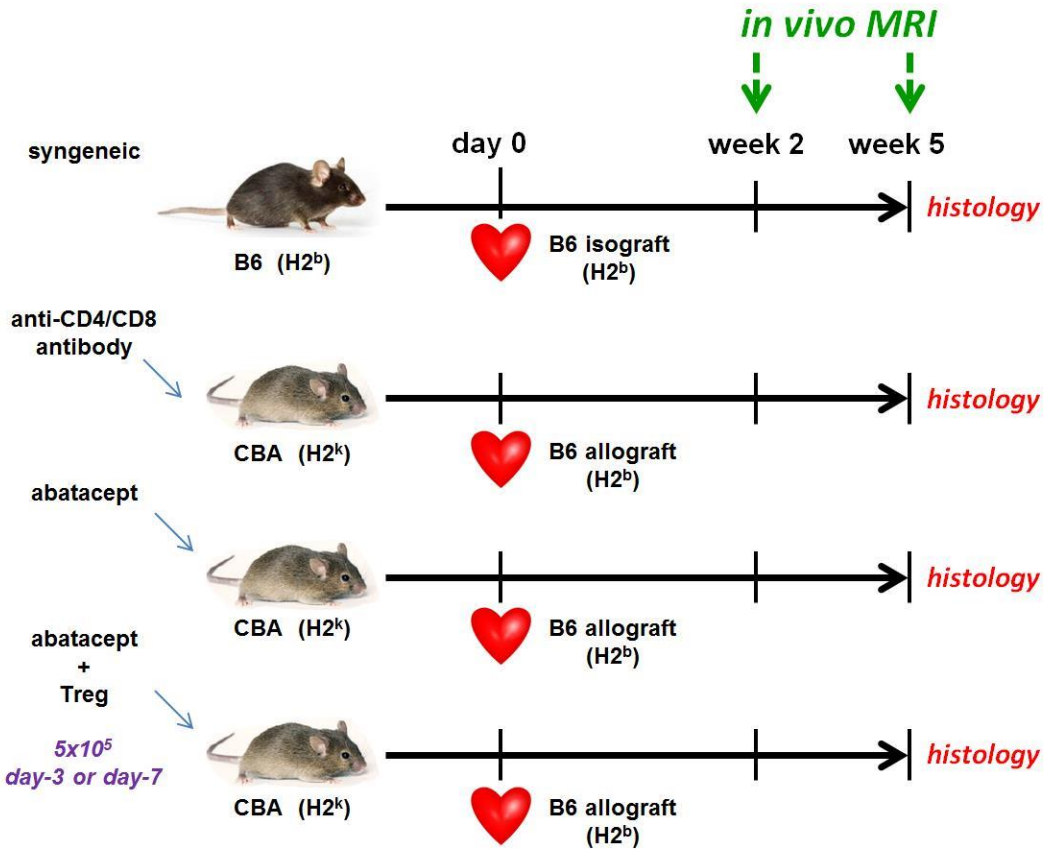

Figure 6.2.6.1. Compare and contrast the assessment of graft outcome using *in vivo* MRI and histopathological examination following IFN-γ Treg therapy. CBA IFN-γ Treg were generated by the IFN-γ protocol using the B6 to CBA donor to recipient strain combination as described in ***Chapter 2.8.1***. $5x10^5$ IFN-γ Treg were given either on day-3 or day-7 to CBA recipients of B6 heterotopic heart allograft in addition to the sub-optimal abatacept protocol (i.v. 25μg day 0, 1 and 5). These groups of mice were compared to recipients treated with a peri-operative sub-optimal abatacept protocol alone, or anti-CD4 (i.v. 50μg) and anti-CD8 (i.v. 100μg) antibody protocol. In addition, B6 syngeneic heart transplants were used as controls for the graft and histological examination. All heart transplant recipients were rested for 2 weeks and underwent *in vivo* MRI on week 2 and week 5 for the comparison of graft outcome prior to necropsy for histopathological examination, which was performed immediately after the last MRI scan on week 5. Data retrieved from MRI were processed using the ImageJ® software for the calculation of various cardiovascular functional parameters as described in ***Chapter 2.4***. Bi-manual palpation scores were recorded for each graft at regular intervals.

Figure 6.2.6.2. *In vivo* MR Images of B6 isografts on week 2 and week 5

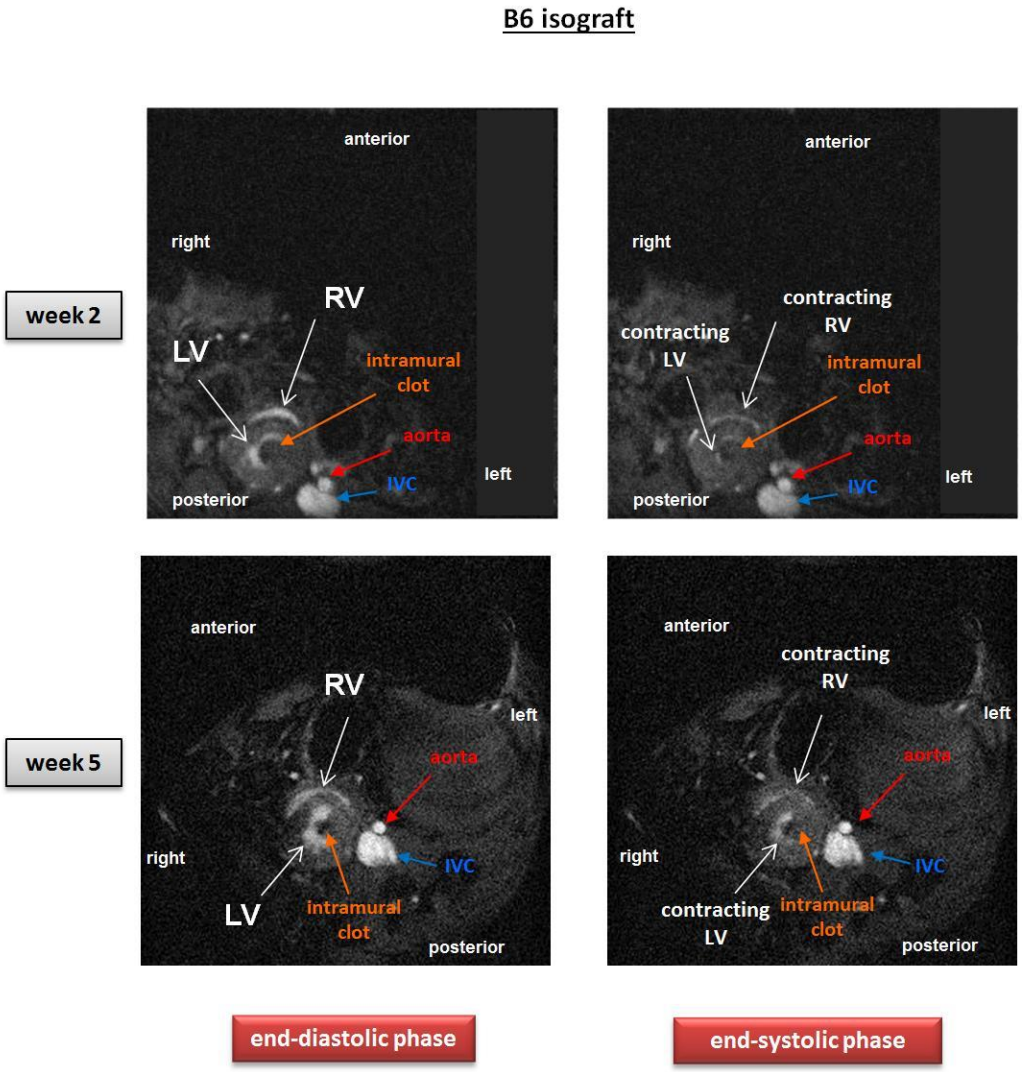

Figure 6.2.6.2. *In vivo* MR images of B6 isografts on week 2 and 5. Cross-sectional images of heterotopically transplanted B6 isograft at the end-diastolic and end-systolic phase are shown with the relevant anatomical features. Isograft showed persistent adequate left (LV) and right ventricular (RV) contractility from week 2 to week 5. Data above are representative of results obtained from 2 mice.

Figure 6.2.6.3. ***In vivo*** **MR Images of allografts in recipients treated with anti-CD4/CD8 antibody on week 2 and week 5**

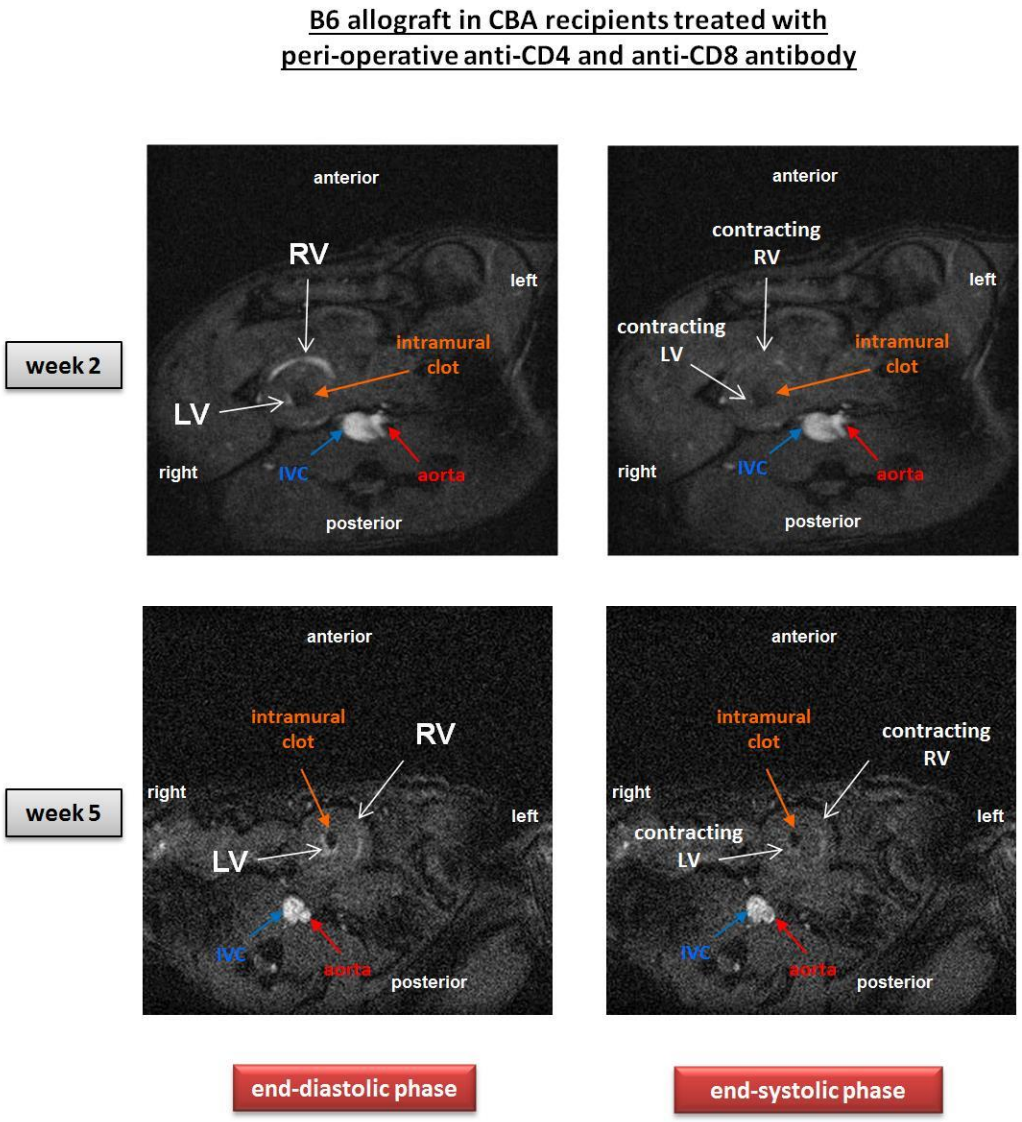

Figure 6.2.6.3. ***In vivo*** **MR Images of allografts in recipients treated with anti-CD4/CD8 antibody on week 2 and week 5.** Cross-sectional images of heterotopically transplanted B6 allograft in CBA recipients at the end-diastolic and end-systolic phase are shown with the relevant anatomical features. Peri-operative anti-CD4 and anti-CD8 antibody treatment delayed allograft rejection. There was no significant changes in the right ventricular contractility in mice treated with anti-CD4/CD8 antibody between week 2 and week 5. Data above are representative of results obtained from 3 mice.

Figure 6.2.6.4. ***In vivo*** **MR Images of allografts in recipients treated with sub-optimal abatacept on week 2 and week 5**

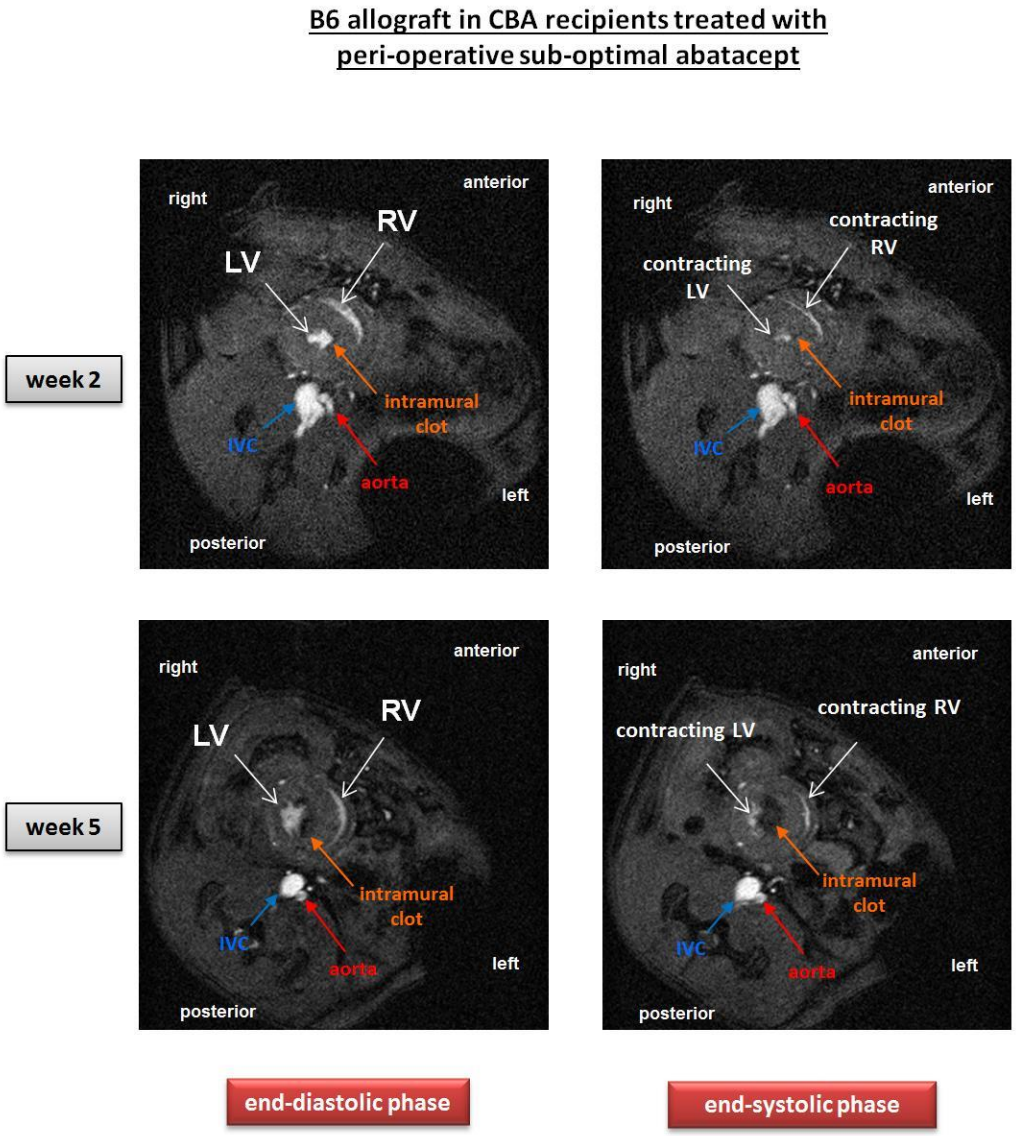

Figure 6.2.6.4. ***In vivo*** **MR images of B6 allograft in CBA recipients treated with sub-optimal abatacept on week 2 and week 5.** Cross-sectional images of heterotopically transplanted B6 allograft in CBA recipient treated with a peri-operative sub-optimal abatacept at the end-diastolic and end-systolic phase are shown with the relevant anatomical features. A sub-optimal abatacept protocol delayed allograft rejection with a MST around 50 days according to historical controls. Good right ventricular function was seen on week 2. However, there was a significant decline of the right ventricular function on week 5. Data above are representative of results obtained from 6 mice.

Figure 6.2.6.5. ***In vivo*** **MR images of B6 allograft in CBA recipients treated with sub-optimal abatacept plus IFN-γ Treg given on day-3 on week 2 and week 5**

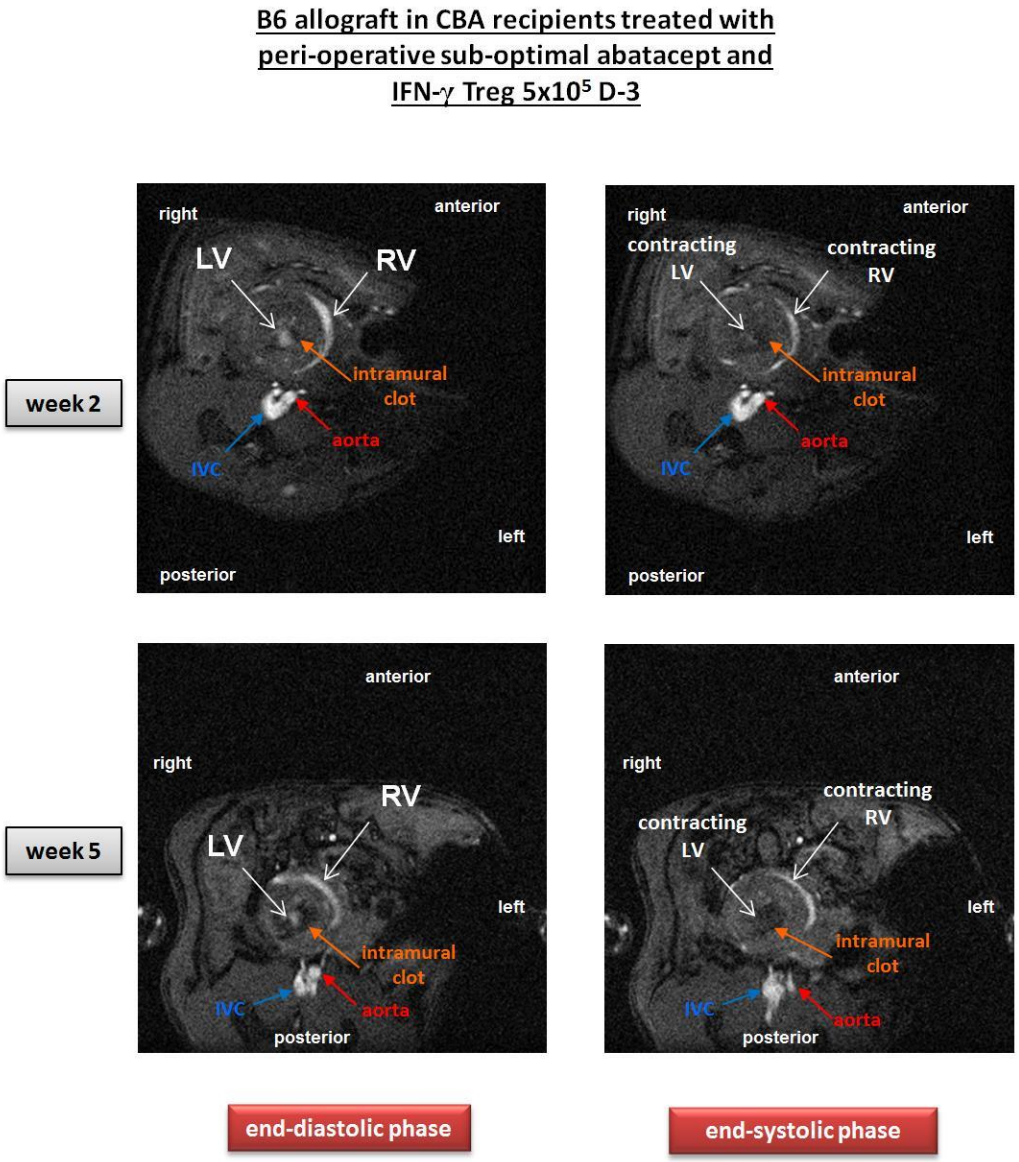

Figure 6.2.6.5. ***In vivo*** **MR images of B6 allograft in CBA recipients treated with sub-optimal abatacept plus IFN-γ Treg given on day-3 on week 2 and week 5.** Cross-sectional images of heterotopically transplanted B6 allograft in CBA recipient treated with abatacept plus 5x10^5 IFN-γ Treg on day-3 at the end-diastolic and end-systolic phase are shown with the relevant anatomical features. IFN-γ Treg therapy preserved right ventricular contractility on week 5 post-transplantation. Data above are representative of results obtained from 4 mice.

Figure 6.2.6.6. ***In vivo*** **MR images of B6 allograft in CBA recipients treated with sub-optimal abatacept plus IFN-γ Treg given on day-7 on week 2 and week 5**

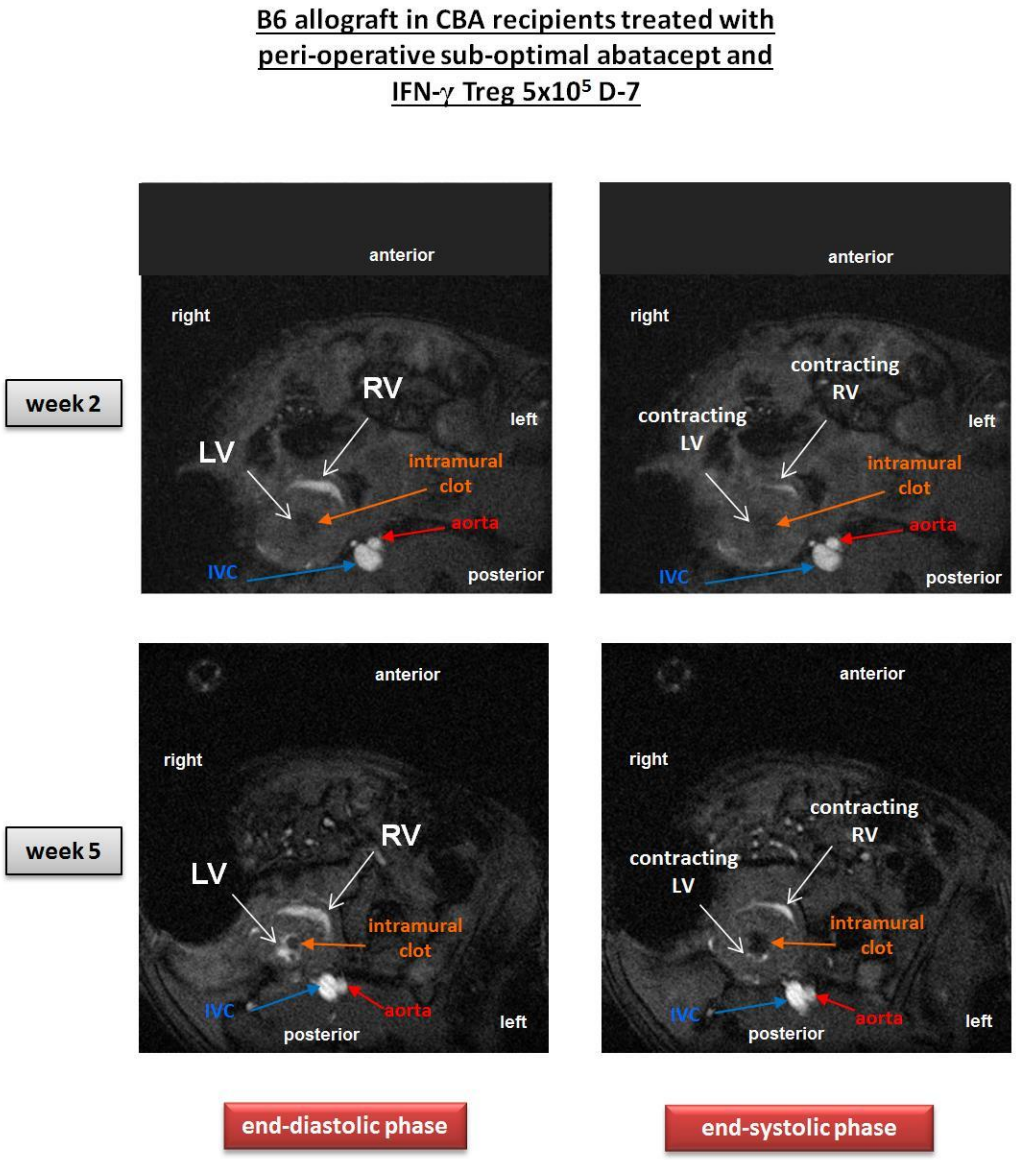

Figure 6.2.6.6. ***In vivo*** **MR images of B6 allograft in CBA recipients treated with sub-optimal abatacept plus IFN-γ Treg given on day-7 on week 2 and week 5.** Cross-sectional images of heterotopically transplanted B6 allograft in CBA recipient treated with abatacept plus 5x10^5 IFN- Treg on day-7 at the end-diastolic and end-systolic phase are shown with the relevant anatomical features. IFN-γ Treg given on day-7 preserved the right ventricular contractility on week 5 post-transplantation. Data above are representative of results obtained from 5 mice.

Figure 6.2.6.7. Serial MR images of allografts in CBA mice treated with abatacept compared to abatacept plus IFN-γ Treg in a complete cardiac cycle

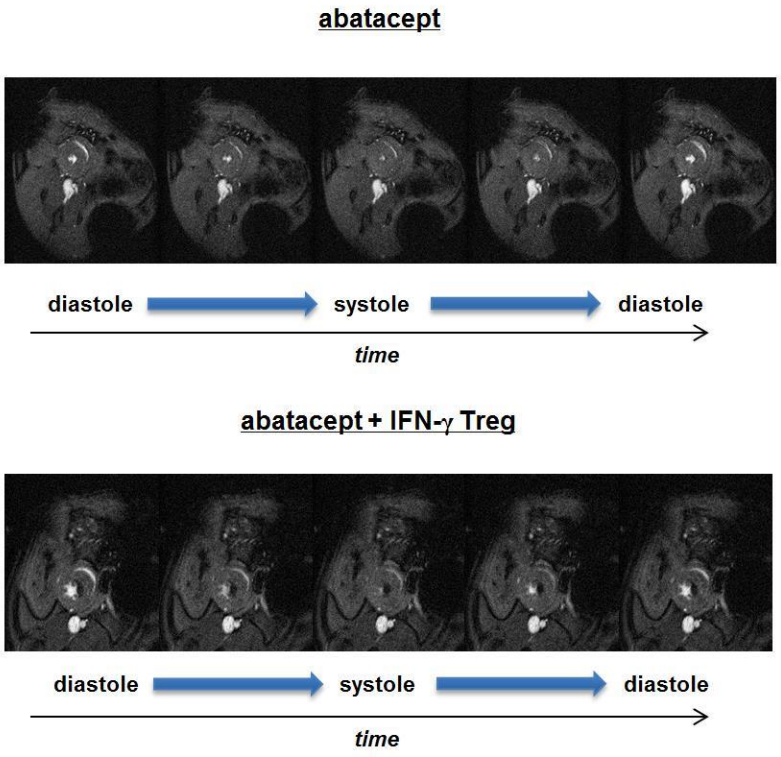

Figure 6.2.6.7. Serial MR images of allografts in CBA mice treated with abatacept compared to abatacept plus IFN-γ Treg in a complete cardiac cycle. Cine MR images were reconstructed and processed to obtain still images at different part of the cardiac cycle (at 25 frames per cardiac cycle). Selected images are displayed above to illustrate the ventricular contractility of allografts in recipients treated with abatacept alone and those treated with abatacept plus $5x10^5$ IFN-γ Treg on day-3. Allografts in CBA mice treated with abatacept plus IFN-γ Treg appeared to have a superior ventricular emptying compared to that of allografts in CBA mice treated with abatacept alone on week 5.

The RVEDV of allografts in mice treated with abatacept plus $5x10^5$ IFN-γ Treg on day-3 (4.71±0.99μl, n=4) remained significantly higher than those treated with abatacept alone (2.27±1.07μl, n=6; *p*=0.0065). The RVEDV of allografts in mice treated with IFN-γ Treg given on day-7 (2.36±1.28μl, n=5) remained no different from the abatacept only group (*p*=0.8976). Both IFN-γ Treg groups had a similar RVEDV compared to the anti-CD4/CD8 antibody group (3.41±1.69μl, n=3; *p*=0.2513 and *p*=0.3528, respectively) and B6 isografts (3.29±1.10μl, n=2; *p*=0.1811 and *p*=0.4149, respectively) ***(Figure 6.2.6.8.i)***.

The RVSV of allografts in mice treated with abatacept plus $5x10^5$ IFN-γ Treg on day-3 (1.72±1.18μl, n=4) was significantly higher RVSV compared to abatacept alone (0.42±0.18μl, n=6; *p*=0.0254), but no different from the anti-CD4/CD8 antibody group (1.04±0.43μl, n=3; *p*=0.3924) and B6 isografts (1.70±0.49μl, n=2; *p*=0.9972). On the other hand, the RVSV of allografts in mice treated with abatacept plus $5x10^5$ IFN-γ Treg on day-7 (0.80±0.78μl, n=5) remained no different from those treated with abatacept (*p*=0.2819), anti-CD4/CD8 antibody (*p*=0.6423) and B6 isografts (*p*=0.2044) ***(Figure 6.2.6.8.ii)***.

The RVEF of allografts treated with abatacept plus IFN-γ Treg on day-3 (35.0±22.0%, n=4) or day-7 (30.3±14.3%, n=5) remained no different from those received abatacept alone (18.9±1.38%, n=6; *p*=0.1012 and *p*=0.0794, respectively), anti-CD4/CD8 antibody (36.0±24.5%, n=3; *p*=0.9545 and *p*=0.6848, respectively) and B6 isografts (52.0±2.5%, n=2; *p*=0.3607 and *p*=0.0996, respectively) ***(Figure 6.2.6.8.iii)***.

The RVCO of allografts in mice treated with IFN-γ Treg on day-3 (0.70±0.43ml/min, n=4) was persistently higher than those treated with abatacept alone (0.17±0.06ml/min, n=6; *p*=0.0156), but indifferent from those treated with anti-CD4/CD8 antibody (0.42±0.15ml/min, n=3; *p*=0.3390) or B6 isografts (0.49±0.35ml/min, n=2; *p*=0.5843). On the other hand, the RVCO of

allografts in mice treated with IFN-γ Treg on day-7 (0.37±0.35ml/min, n=5) was no different from those treated with abatacept alone (*p*=0.1985), anti-CD4/CD8 antibody (*p*=0.8236) and B6 isograft (*p*=0.7006) ***(Figure 6.2.6.8.iv)***.

The Palpation Scores (PS) of allografts in mice treated with $5x10^5$ IFN-γ Treg given on day-3 (1.8±0.5, n=4) and day-7 (1.6±0.4, n=5) were not significantly different from those treated with abatacept (2.2±1.3, n=6; *p*=0.5716 and *p*=0.3985, respectively). However, the PS of allografts in mice treated with IFN-γ Treg given on day-3 and day-7 were significantly lower than those treated with anti-CD4/CD8 antibody (3.3±0.6, n=3; *p*=0.0115 and *p*=0.0053, respectively), but no different from B6 isografts (2.5±0.7, n=2; *p*=0.1963 and *p*=0.1244, respectively ***(Figure 6.2.6.9)***.

Graft functional assessment carried out by MRI scanning indicated that allografts treated with $5x10^5$ IFN-γ Treg given on day-3 had a superior RV functional profile compared to the abatacept alone group. Moreover, it also demonstrated that the delivery of Treg on day-3 was more favourable in achieving a better graft outcome compared to day-7. ***(Figure 6.2.6.8)*** However, bi-manual palpation was unable to reveal these differences ***(Figure 6.2.6.9)***. Collectively, these data suggest that *in vivo* MRI could reveal subtle differences in terms of the graft function between these experimental groups, and is a more sensitive approach to determining graft function than measurement by palpation.

Figure 6.2.6.8. Comparison of right ventricular function of allografts treated with IFN-γ Treg given at different time points at week 5 using *in vivo* MRI

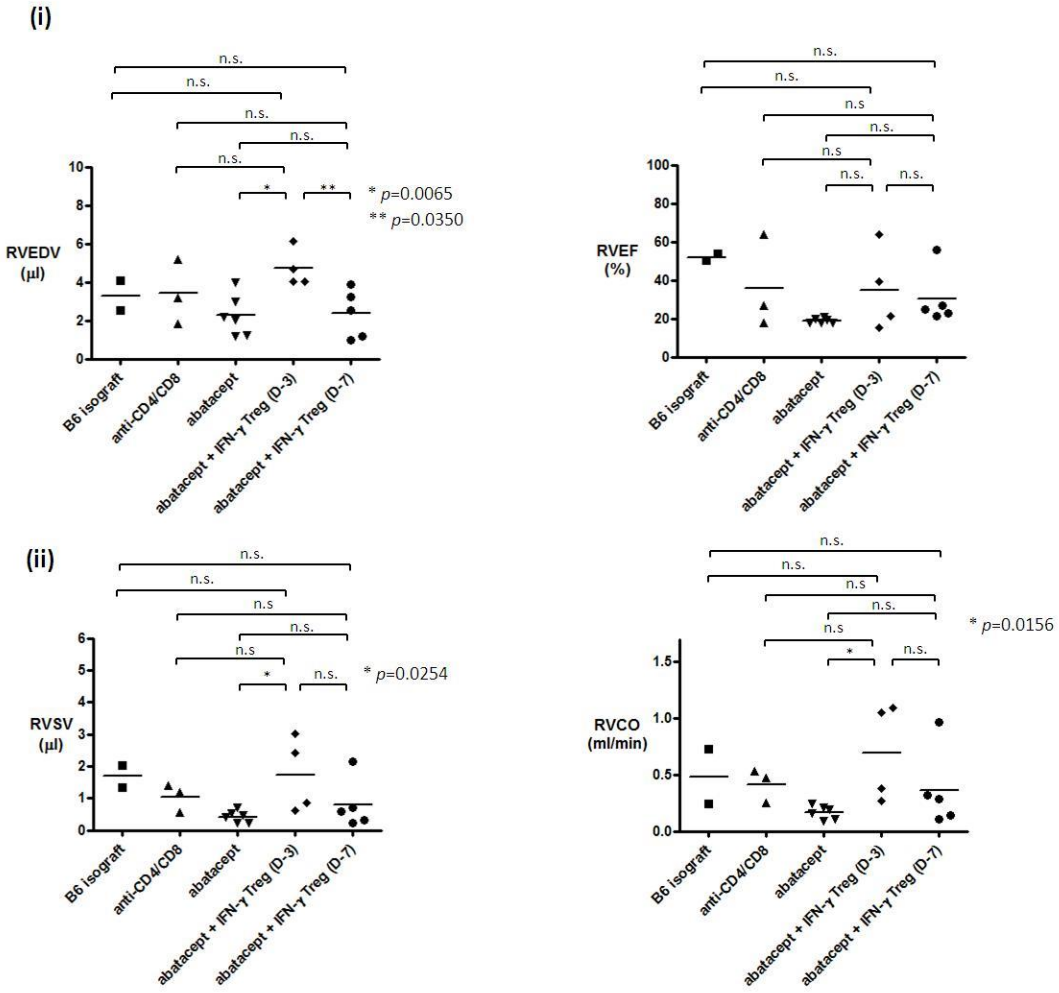

Figure 6.2.6.8. Comparison of right ventricular function of allografts treated with IFN-γ Treg given at different time points at week 5 using *in vivo* MRI. (i) RVEDV: Both IFN-γ Treg day-3 and day-7 groups showed a higher RVEDV compared to abatacept (p=0.0065 and p=0.0350, respectively). **(ii) RVSV:** Mice treated with abatacept plus 5x10^5 IFN-γ Treg on day-3 (but not day-7) showed a significantly higher RVSV compared to abatacept alone (p=0.0254). The RVEDV and RVSV of allografts treated with abatacept plus IFN-γ Treg were not significantly different from those treated with anti-CD4/CD8 antibody or B6 isografts (p>0.05). **(iii) RVEF:** Mice treated with both IFN-γ Treg groups showed no differences amongst other groups (p>0.05). **(iv) RVCO:** Mice treated with abatacept plus 5x10^5 IFN-γ Treg on day-3 (but not for those given on day-7) showed a significantly higher RVCO compared to those received abatacept alone (p=0.0156). Student's t-tests were used for statistical comparisons. (p<0.05 denotes statistically significant)

Figure 6.2.6.9. Assessment of graft outcome using bi-manual palpation at week 5 following heterotopic heart transplantation

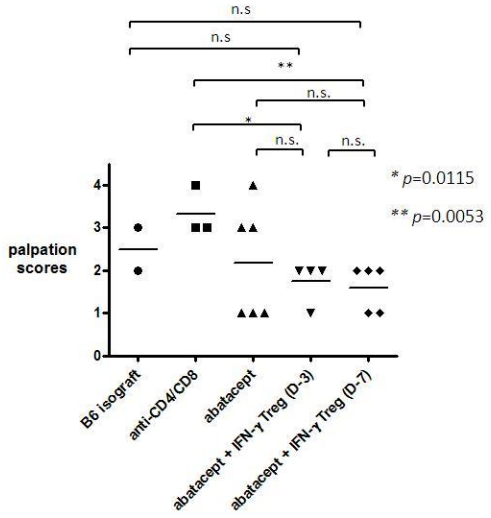

Figure 6.2.6.9. Assessment of graft outcome using bi-manual palpation at week 5 following heterotopic heart transplantation. Palpation scores (PS) of allografts in mice treated with $5x10^5$ IFN-γ Treg given on day-3 and day-7 were not significantly different from those treated with abatacept (p=0.5716 and p=0.3985, respectively). However, the PS of allografts in mice treated with IFN-γ Treg given on day-3 and day-7 were significantly lower than those treated with anti-CD4/CD8 antibody (p=0.0115 and p=0.0053, respectively), but indifferent from B6 isografts (p=0.1963 and p=0.1244, respectively). Student's t-tests were used for statistical comparisons. (p<0.05 denotes statistically significant)

6.2.7 Comparison *in vivo* MR imaging versus traditional histopathological assessment of graft outcome

6.2.7.1 Haematoxylin & Eosin staining

Initial histopathological assessment of all grafts was carried out using haematoxylin & eosin (H&E) staining of frozen sections of all heterotopic heart grafts on week 5 following MR scanning. The inclusion of B6 isografts served as negative control for any pathological changes. Histological analyses were performed in collaboration with pathologists with expertise in mouse histology led by Dr Wang Lai Mun, Consultant Pathologist at the Department of Cellular Pathology, John Radcliffe Hospital, Oxford. Representative H&E slides are shown as follow: In ***Figure 6.2.7.1.1.i***, B6 isografts showed mild myocardial scarring and inflammatory changes secondary to surgery. In contrast, B6 heart allografts transplanted into CBA mice receiving anti-CD4/CD8 antibody treatment showed moderate myocardial inflammation, scarring with moderate cellular infiltrates ***(Figure 6.2.7.1.1.ii)***. At a sub-optimal dose, abatacept treatment led to marked myocardial inflammation with vasculopathic changes in B6 allografts as shown in ***Figure 6.2.7.1.1.iii***. On the other hand, B6 heart allografts transplanted in CBA mice receiving abatacept plus $5x10^5$ IFN-γ Treg given on day-3 showed marked myocardial inflammation, cellular infiltrates with mild vasculopathic changes ***(Figure 6.2.7.1.1.iv)***. Similarly, B6 allografts in CBA mice receiving abatacept plus $5x10^5$ IFN-γ Treg given on day-7 also showed moderate myocardial inflammation and scarring with mild vasculopathic changes ***(Figure 6.2.7.1.1.v)***. These data suggest that infused IFN-γ Treg could lead to marked inflammatory responses in the

grafts 5 weeks post-transplant, despite the fact that they exhibited superior graft function macroscopically when compared to mice receiving the sub-optimal abatacept protocol alone.

Figure 6.2.7.1.1. Histological assessment of graft outcome by haematoxylin and eosin staining

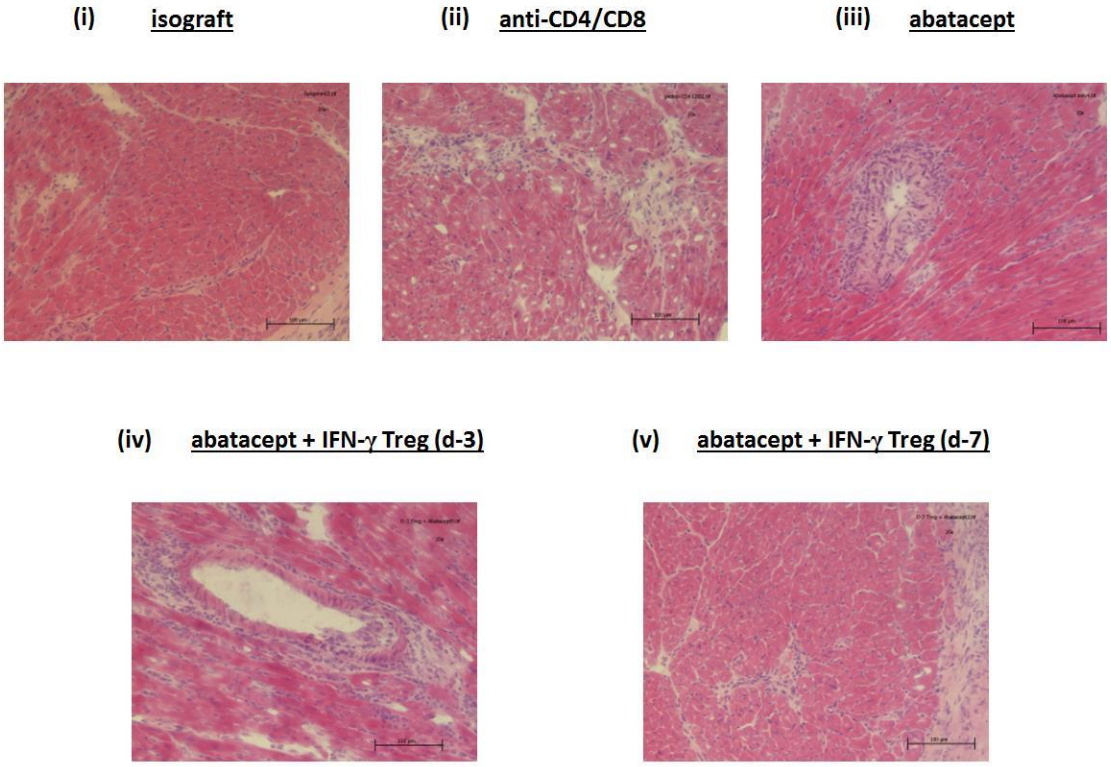

Figure 6.2.7.1.1. Histological assessment of graft outcome by haematoxylin and eosin staining. Representative photomicrographs (20x magnification) of haematoxylin & eosin (H&E) staining (see staining methodology in ***Chapter 2.5.4.2***) of frozen sections of heterotopically transplanted heart grafts illustrate pathological features on week 5 post-transplantation in each experimental group. **(i)** B6 heart graft transplanted into B6 recipients showed mild myocardial scarring and inflammatory changes. **(ii)** B6 heart graft transplanted into CBA mice receiving anti-CD4/CD8 antibody treatment showed moderate myocardial inflammation, scarring with moderate cellular infiltrates. **(iii)** B6 heart graft transplanted into CBA mice receiving a sub-optimal abatacept treatment showed marked myocardial inflammation and vasculopathic changes. **(iv)** B6 heart graft transplanted into CBA mice receiving abatacept plus IFN-γ Treg (day-3) showed marked myocardial inflammation, cellular infiltrates and mild vasculopathic changes. **(v)** B6 heart graft transplanted into CBA mice receiving abatacept plus IFN-γ Treg (day-7) showed moderate myocardial inflammation and scarring with mild vasculopathic changes. Data above are representatives of results obtained from 2-6 mice from each group.

6.2.7.2 Chronic allograft vasculopathy

Vasculopathy is classically manifested in chronic rejection of vascularized allografts. We aimed to determine if IFN-γ Treg treatment could prevent or delay the development of chronic allograft vasculopathy (CAV) in our model. Heterotopic heart grafts were sectioned and evaluated for vasculopathic changes using elastin Van Gieson staining on week 5 post-transplantation in each experimental group mentioned above. As shown in ***Figure 6.2.7.2.1.i***, EVG staining revealed patent arterioles in B6 isografts with no evidence of CAV. In contrast, all allografts regardless of their treatment modality presented with various degrees of CAV as shown in ***Figure 6.2.7.2.1.ii-v***. In addition, various degree of CAV occurred within the same graft, hence the overall vasculopathy status was determined by taking the means of luminal occlusion at multiple levels (≥ 5 sections devoid of the apex and the base) of each graft using the formula as shown in ***Figure 6.2.7.2.2***. Allografts treated with IFN-γ Treg given on day-3 (32.4±13.1%, n=4) showed a similar level of luminal occlusion compared to those treated with abatacept alone (22.6.±4.1%, n=6; p=0.0590) and anti-CD4/CD8 antibody (27.8±6.6%, n=3; p=0.3000); but significantly higher than that of B6 isografts (6.8±6.4%, n=2; p=0.0328). Similarly, allografts treated with IFN-γ Treg given on day-7 (23.9±10.1%, n=5) showed a similar level of luminal occlusion compared to those treated with abatacept alone (p=0.3914) and anti-CD4/CD8 antibody (p=0.2917); but significantly higher than that of B6 isografts (p=0.0412). Moreover, the vasculopathy status of allografts treated with IFN-γ Treg on day-3 and day-7 were not statistically different (p=0.1524). Collectively, these data suggest that the prolongation of allograft survivals in this model using different treatment modalities invariably led to a significant level of CAV.

Figure 6.2.7.2.1. Assessment of chronic allograft vasculopathy by elastin Van Gieson staining

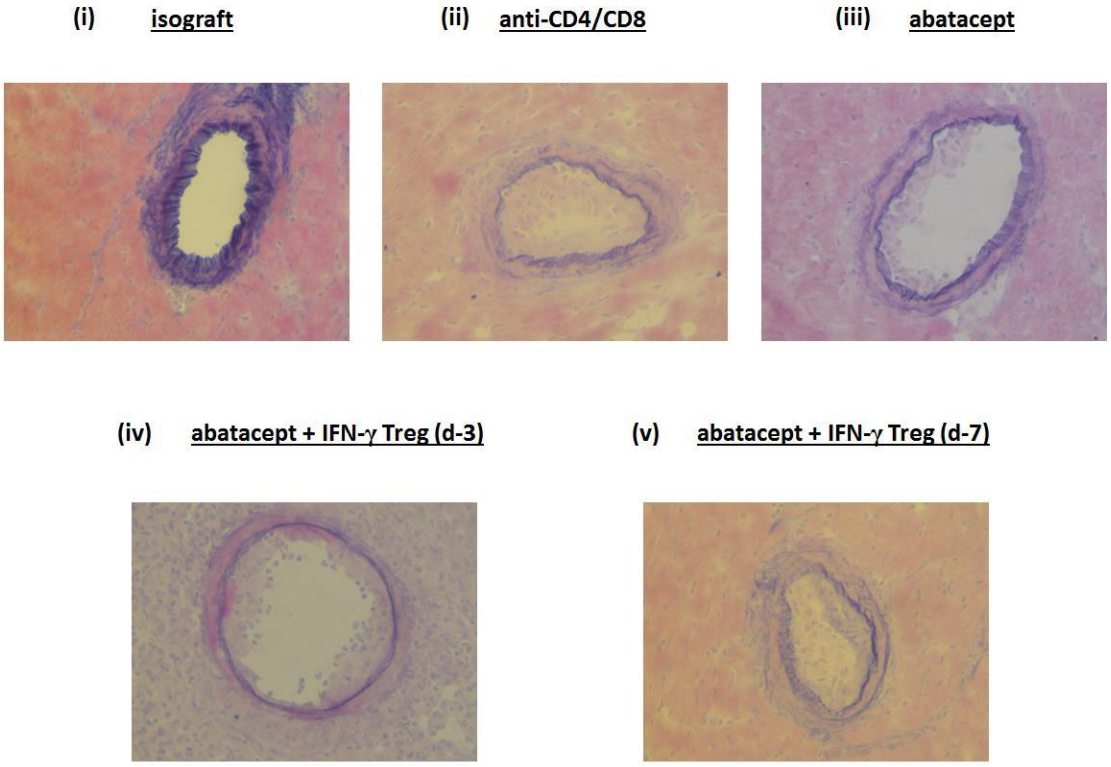

Figure 6.2.7.2.1. Assessment of chronic allograft vasculopathy by elastin Van Gieson staining. Representative photomicrographs (20x magnification) of elastin Van Gieson staining (see staining methodology in ***Chapter 2.5.4.3***) of frozen sections of heterotopically transplanted heart grafts illustrate features of chronic allograft vasculopathy (CAV) on week 5 post-transplantation in each experimental group. **(i)** Patent vessel showed with no evidence of CAV in B6 isografts. Various degrees of CAV was observed in allografts treated with **(ii)** anti-CD4/CD8 antibody, **(iii)** abatacept, **(iv)** abatacept plus $5x10^5$ IFN-γ Treg given on day-3 and **(v)** abatacept plus $5x10^5$ IFN-γ Treg given on day-7. Data above are representatives of results obtained from 2-6 mice from each group.

Figure 6.2.7.2.2. Quantitative assessment of chronic allograft vasculopathy by elastin Van Gieson staining

(i) EVG staining of coronary arteriole of transplanted heart graft

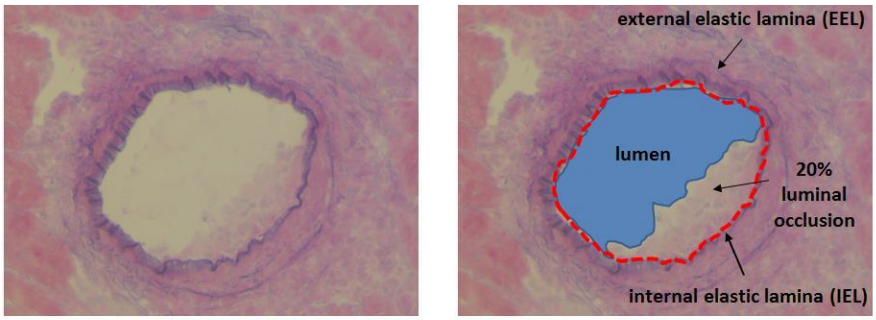

$$\% \text{ luminal occlusion} = \frac{\text{internal elastic lamina (IEL) area} - \text{luminal area}}{\text{internal elastic lamina (IEL) area}} \times 100$$

(ii)

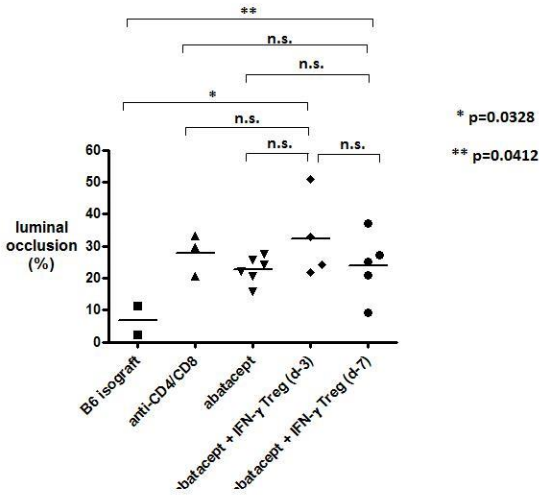

Figure 6.2.7.2.2. Quantitative assessment of chronic allograft vasculopathy by elastin Van Gieson staining. (i) A sample section of EVG stained arteriole of transplanted heart allograft illustrating the internal and external elastic lamina and signs of chronic allograft vasculoapathy (CAV). The degree of vasculopathy is denoted by the percentage of luminal occlusion as calculated by the formula shown. **(ii)** The degree of CAV of each experimental group is represented by the percentage of luminal occlusion (average of ≥5 different levels in each graft) on week 5 post-transplantation. Allografts treated with abatacept plus IFN-γ Treg given on either d-3 or d-7 showed no significant differences in their vasculopathy status compared to those treated with abatacept alone or anti-CD4/CD8 antibody; but significantly higher than B6 isografts (p=0.0328 and p=0.0412, respectively). The vasculopathy status in those treated with IFN-γ Treg on day-3 was not significantly different from that of day-7 (p=0.1524). Student t-tests were used for statistical comparisons. (p<0.05 denotes statistically significant)

6.2.7.3 Immunohistochemistry

Infiltration of $CD3^+$ T cells, $CD8^+$ T cells and $Foxp3^+$ T cells were analyzed by immunohistochemical staining of heterotopic heart grafts in the aforementioned experimental groups 5 weeks post-transplantation. Enumeration of $CD3^+$, $CD8^+$ and $Foxp3^+$ cells were done manually at original magnification x400 in 3 separate sections defined by a graticule, the sum of cell counts from 5 high power fileds in each 3 sections were recorded and compared to unstained controls. Representative IHC slides stained for CD3, CD8 and Foxp3 are shown in ***Figure 6.2.7.3.1***, ***6.2.7.3.2*** and ***6.2.7.3.3***, respectively.

There was negligible staining of $CD3^+$, $CD8^+$ and $Foxp3^+$ T cells in B6 isografts. In the anti-CD4/CD8 antibody group, a small number of $CD3^+$ and $CD8^+$ T cells were present but not $Foxp3^+$ T cells. In the sub-optimal abatacept treatment group, a significant number of $CD3^+$ and $CD8^+$ T cells were present; however, no $Foxp3^+$ T cells were detected. In the IFN-γ Treg treatment groups (day-3 or day-7), a significant number of $CD3^+$ and $CD8^+$ T cells were present, but a number of $Foxp3^+$ T cells were also detected.

The number of $CD3^+$, $CD8^+$ and $Foxp3^+$ T cell infiltrates in grafts from each group was summarized in ***Figure 6.2.7.3.4***. Allografts treated with abatacept plus $5x10^5$ IFN-γ Treg given on day-3 (245±7, n=4) had a significantly higher number of $CD3^+$ T cells compared to those treated with abatacept alone (188±15, n=6; $p<0.0001$), anti-CD4/CD8 antibody (96±9, n=3; $p<0.0001$) and B6 isografts (8±6, n=2; $p<0.0001$). On the other hand, allografts treated with abatacept plus $5x10^5$ IFN-γ Treg given on day-7 (169±31, n=5) had a similar number of $CD3^+$ T cell infiltrates compared to those treated with abatacept alone ($p=0.2193$); however, it was significantly higher than the anti-CD4/CD8 antibody group ($p=0.0084$) and B6 isografts ($p=0.0010$). Moreover, the

number of $CD3^+$ T cell infiltrates was significantly higher in the IFN-γ Treg day-3 group compared to day-7 group (p=0.0023).

Figure 6.2.7.3.1. Histological assessment of graft outcome by immunohistochemistry – CD3

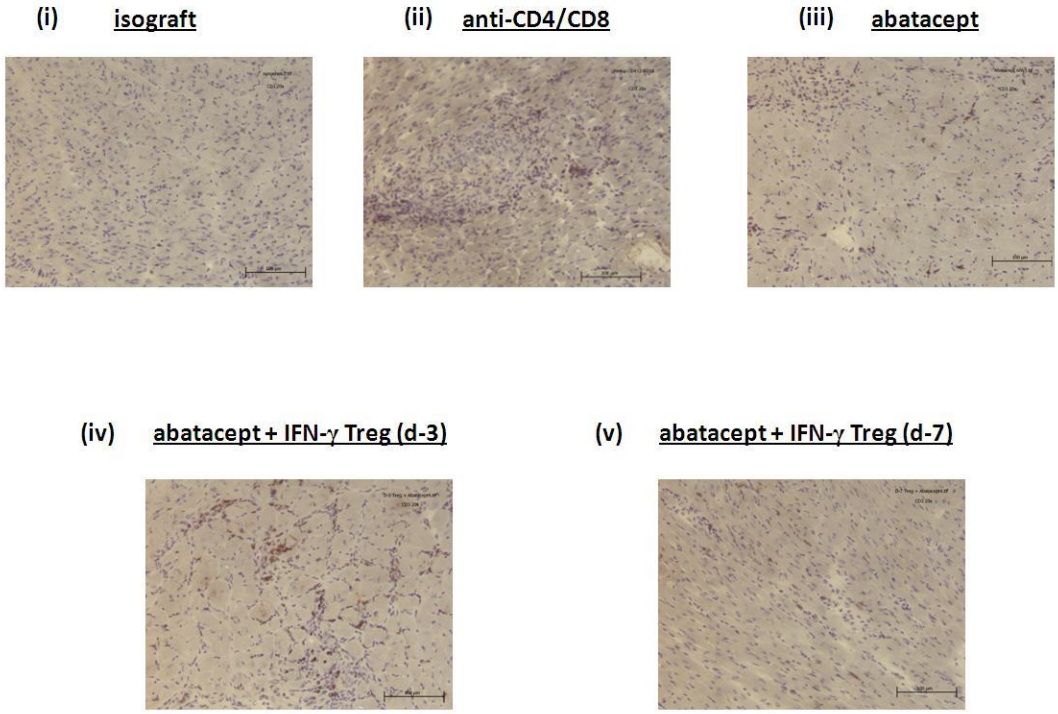

Figure 6.2.7.3.1. Histological assessment of graft outcome by immunohistochemistry – CD3. B6 heart grafts were transplanted heterotopically into **(i)** syngeneic recipients or into CBA recipients treated with anti-CD4/CD8 antibody treatment **(ii)**, or abatacept **(iii)** or abatacept plus IFN-γ Treg on day -3 **(iv)** or day-7 **(v)**. Transplanted grafts were harvested and snapped frozen in liquid nitrogen for histological assessment on week 5 immediately after the final *in vivo* MRI. Frozen sections of grafts were prepared by cryostat and stained for CD3 using immunohistochemical technique as described in ***Chapter 2.5.4.4***. Representative photomicrographs (original magnification x400) from each group of mice illustrate the degree of lymphocytic infiltration of $CD3^+$cells in heterotopically transplanted heart grafts. Syngeneic isografts showed no lymphocytic infiltration. An anti-CD4/CD8 antibody protocol led to a low level of $CD3^+$ cell infiltrates. Mice treated with sub-optimal abatacept showed significant $CD3^+$ cell infiltrates. Mice treated with abatacept plus IFN-γ Treg on day-3 showed significant higher level of $CD3^+$ infiltrates compared to mice treated with abatacept alone. Mice treated with IFN-γ Treg on day-7 plus abatacept showed a demonstrable of $CD3^+$ cells infiltrates. Data above represent results obtained from 2 to 5 mice from each experimental group.

Figure 6.2.7.3.2. Histological assessment of graft outcome by immunohistochemistry – CD8

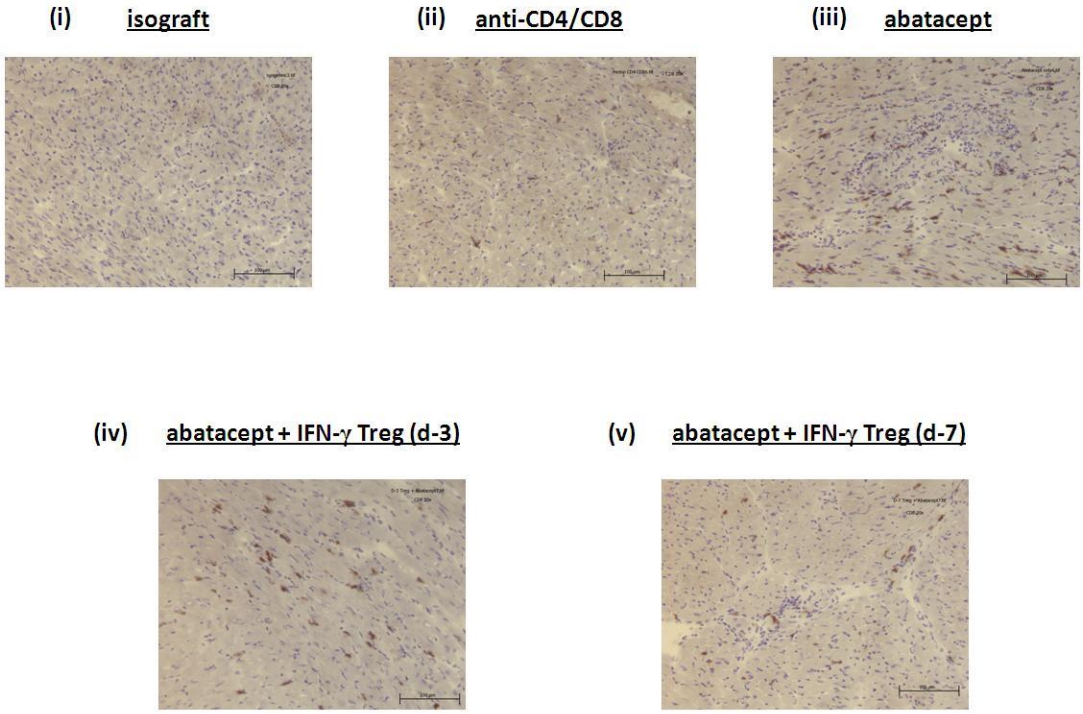

Figure 6.2.7.3.2. Histological assessment of graft outcome by immunohistochemistry – CD8. B6 heart grafts were transplanted heterotopically into **(i)** syngeneic recipients or into CBA recipients treated with anti-CD4/CD8 antibody treatment **(ii)**, or abatacept **(iii)** or abatacept plus IFN-γ Treg on day -3 **(iv)** or day-7 **(v)**. Transplanted grafts were harvested and snapped frozen in liquid nitrogen for histological assessment on week 5 immediately after the final *in vivo* MRI. Frozen sections of grafts were prepared by cryostat and stained for CD8 using immunohistochemical technique as described in ***Chapter 2.5.4.4***. Representative photomicrographs (original magnification x400) from each group of mice illustrate the degree of lymphocytic infiltration of $CD8^+$ cells in heterotopically transplanted heart grafts. Syngeneic isografts showed no lymphocytic infiltration. An anti-CD4/CD8 antibody protocol led to a low level of $CD8^+$ T cell infiltrates but not $Foxp3^+$ cells. Mice treated with sub-optimal abatacept showed significant $CD8^+$ cellular infiltrates. Mice treated with abatacept plus IFN-γ Treg on day-3 showed significant higher level of $CD3^+$ infiltrates within the graft compared to mice treated with abatacept alone. Mice treated with IFN-γ Treg on day-7 plus abatacept showed a demonstrable of $CD8^+$ infiltrates. Data above represent results obtained from 2 to 5 mice from each experimental group.

Figure 6.2.7.3.3. Histological assessment of graft outcome by immunohistochemistry – Foxp3

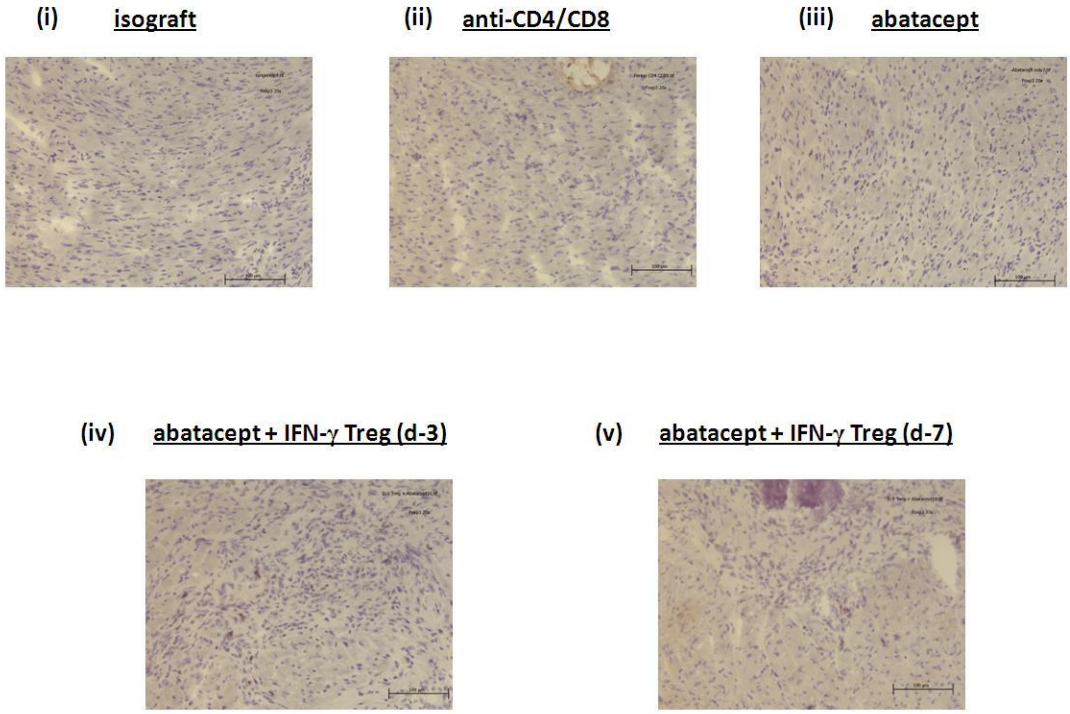

Figure 6.2.7.3.3. Histological assessment of graft outcome by immunohistochemistry – Foxp3. B6 heart grafts were transplanted heterotopically into **(i)** syngeneic recipients or into CBA recipients treated with anti-CD4/CD8 antibody treatment **(ii)**, or abatacept **(iii)** or abatacept plus IFN-γ Treg on day -3 **(iv)** or day-7 **(v)**. Transplanted grafts were harvested and snapped frozen in liquid nitrogen for histological assessment on week 5 immediately after the final *in vivo* MRI. Frozen sections of grafts were prepared by cryostat and stained for intracellullar Foxp3 using immunohistochemical technique as described in ***Chapter 2.5.4.4***. Representative photomicrographs (original magnification x400) from each group of mice illustrate the degree of lymphocytic infiltration of $Foxp3^+$ cells in heterotopically transplanted heart grafts. Syngeneic isografts showed no infiltrates of $Foxp3^+$ cells . An anti-CD4/CD8 antibody protocol did not led to any $Foxp3^+$ cells. Mice treated with sub-optimal abatacept also showed no significant number of $Foxp3^+$ cells. Mice treated with abatacept plus IFN-γ Treg on day-3 showed a demonstrable number of $Foxp3^+$ T cells within the graft compared to mice treated with abatacept alone. Mice treated with IFN-γ Treg on day-7 plus abatacept showed a limited number of $Foxp3^+$ cells. Data above represent results obtained from 2 to 5 mice from each experimental group.

Interestingly, the number of $CD8^+$ T cell infiltrates in recipients treated with abatacept plus $5x10^5$ IFN-γ Treg given on day-3 (60±14, n=4) was lower than those treated with abatacept alone (100±7; *p*=0.0003), but no different from the anti-CD4/CD8 antibody group (48±10, n=3; *p*=0.2596) and B6 isografts (28±14, n=2; *p*=0.0562). On the other hand, the number of $CD8^+$ infiltrates in recipients treated with abatacept plus $5x10^5$ IFN-γ Treg given on day-7 (135±14, n=5) was significantly higher than the abatacept only group (*p*=0.0004), anti-CD4/CD8 antibody group (*p*<0.0001) and B6 isograft group (*p*=0.0003). Moreover, the number of $CD8^+$ T cell infiltrates was significantly higher in allografts receiving IFN-γ Treg on day-7 compared to day-3 (*p*<0.0001).

The number of $Foxp3^+$ T cells were significantly higher in the allografts treated with abatacept plus $5x10^5$ IFN-γ Treg given on day-3 (50±4, n=4) compared to those treated with abatacept alone (18±4, n=6; *p*<0.0001), anti-CD4/CD8 antibody (12±9, n=3; *p*=0.0005) and B6 isografts (6±3, n=2; *p*=0.0002). On the other hand, the number of $Foxp3^+$ T cell infiltrates in allografts treated with abatacept plus $5x10^5$ IFN-γ Treg given on day-7 was not significantly different from the abatacept only group (*p*=0.1653), anti-CD4/CD8 antibody group (*p*=0.1129) and B6 isografts (*p*=0.0550). More importantly, the number of $Foxp3^+$ T cell infiltrates was significantly higher in allografts treated with IFN-γ Treg given on day-3 compared to day-7 (*p*=0.0020).

Figure 6.2.7.3.4. Quantitative histological assessment of graft outcome by immunohistochemistry

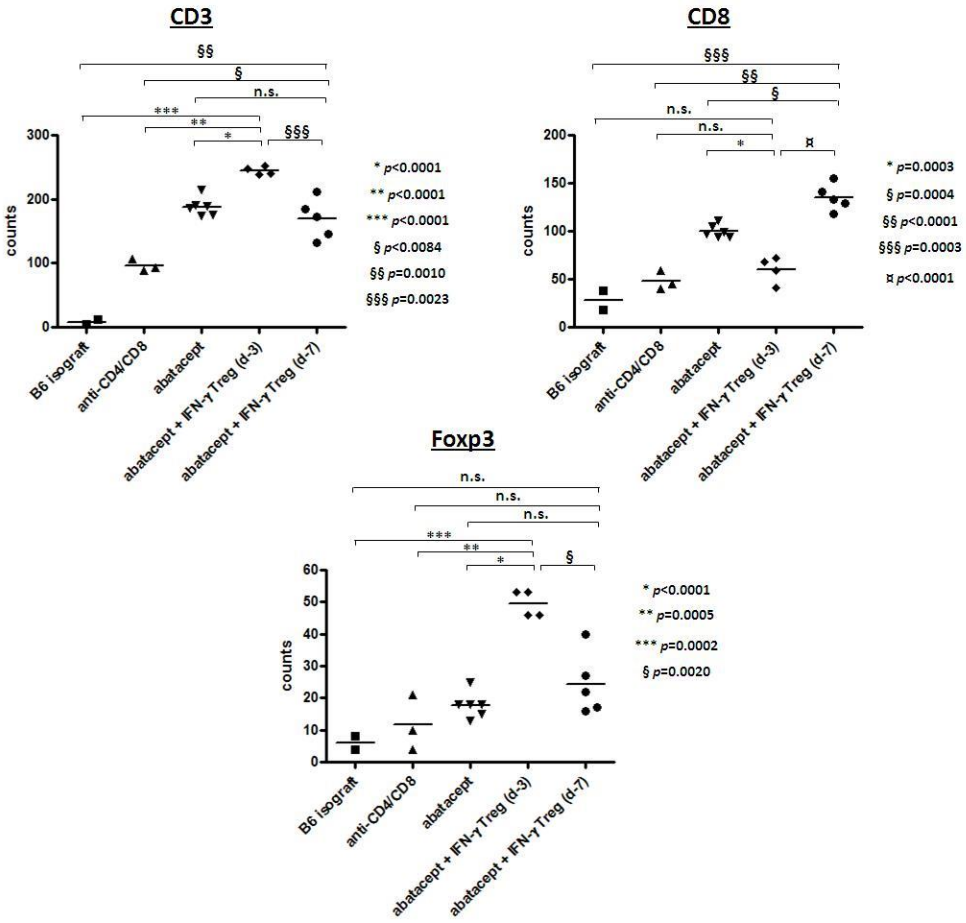

Figure 6.2.7.3.4. Quantitative histological assessment of graft outcome by immunohistochemistry. Frequencies of lymphocytic infiltrates on week 5 post-transplant are shown above. **(i)** ***CD3:*** Mice received abatacept plus IFN-γ Treg given on day-3 showed a higher number of $CD3^+$ infiltrates compared to abatacept ($p<0.0001$), anti-CD4/CD8 antibody ($p<0.0001$), and B6 isografts ($p<0.0001$). IFN-γ Treg given on day-7 led to a similar number of $CD3^+$ infiltrates compared to the abatacept group ($p=0.2193$), but a higher number than the anti-CD4/CD8 antibody group ($p=0.0084$) and B6 isografts ($p=0.0010$). Treg delivery on day-3 led to a higher number of $CD3^+$ infiltrates compared to day-7 ($p=0.0023$) **(ii)** ***CD8:*** IFN-γ Treg given on day-3 led to a lower number of $CD8^+$ infiltrates compared to the abatacept group ($p=0.0003$), but indifferent from the anti-CD4/CD8 antibody group ($p=0.2596$) and B6 isografts ($p=0.0562$). IFN-γ Treg given on day-7 led to a higher number of $CD8^+$ infiltrates compared to the abatacept ($p=0.0004$), anti-CD4/CD8 antibody ($p<0.0001$) and B6 isograft group ($p=0.0003$). Treg delivery on day-3 led to a lower $CD8^+$ infiltrates than day-7 ($p=0.0001$) **(iii)** ***Foxp3:*** IFN-γ Treg delivery on day-3, but not day-7 led to a statistically higher number of $Foxp3^+$ infiltrates compared to the abatacept ($p<0.0001$ versus $p=0.1653$), anti-CD4/CD8 antibody ($p=0.0005$ versus $p=0.1129$) and B6 isograft group ($p=0.0002$ versus $p=0.1129$). Treg delivery on day-3 yielded a significantly higher number of $Foxp3^+$ infiltrates compared to day-7 ($p=0.0020$). Student t-tests were used for statistical comparisons. ($p<0.05$ denotes statistically significant)

Collectively, these data suggest that infused Treg migrate to the allograft and could be detected 5 weeks post-transplantation. More importantly, the combination of a highest count of $CD3^+$ $Foxp3^+$ infiltrates in the IFN-γ Treg day-3 group suggest that IFN-γ Treg delivery closer to the time of transplantation yielded a higher number of graft-infiltrating $Foxp3^+$ Treg, which might have implications for their ability to control allograft rejection and hence a superior RV function compared to those delivered on day-7. Furthermore, an early Treg delivery (day-7) led to a higher count of $CD8^+$ T cell infiltrate compared to the day-3 group suggesting that optimal Treg delivery might also be implicated in the control of $CD8^+$ T cell mediated rejection.

6.3 Discussion

Diagnosis of graft rejection in clinical solid organ transplantation is usually guided by various clinical parameters followed by a histological confirmation of biopsied specimens. Biopsy is not applicable to small rodent heterotopic heart transplant models and the confirmation of graft rejection is usually carried out at necropsy at the end of the experiment. Bi-manual palpation of the heart graft has remained the method of choice for non-invasive monitoring graft outcome in rodent models. However, this crude method might not be able to detect the subtle differences between experimental groups in which the graft outcomes are marginal. We therefore aimed to develop new tools to improve the assessment of graft outcome. The heterotopic heart graft in our model has a unique blood flow system leading to an unloaded left and partially loaded right ventricle. Hence, only the right ventricular function was considered in this study. This non-invasive tool has enabled us to objectively assess the contractility of the graft which is directly proportional to the viability of the graft, rather than its cardiophydiological features as it does not provide the cardiac output for the entire body of the recipient. Using the MR imaging we found that there were significant differences in the graft contractile parameters between the IFN-γ Treg groups and the abatacept control groups ***(Figure 6.2.5.6 & 6.2.6.8)***, which could not otherwise be detected using palpation scores ***(Figure 6.2.5.7 & 6.2.6.9)***.

The data obtained from our MRI analysis concurred with the notion that Treg with direct specificity could control acute rejection effectively. However, the presence of cellular infiltration suggestive of chronic allograft rejection indicated that our Treg therapy was able to delay graft rejection effectively in the presence of a costimulation blockade, but might not able to induce rejection free long-term allograft survival per se. Other groups have demonstrated that Treg therapy with indirect allospecificity or better with dual allospecificities, could control chronic

allograft rejection[428,429]. Hence, transduction of TCR with both direct and indirect allospecificities might confer tolerance in this model. Recently, the generation of Treg bearing chimeric antigen receptors directed against HLA class I molecules have been reported[341,596]. This technology might pave the way in which future 'designer Treg' with specific allospecificities could be engineered. Another approach to be considered would be the combination of a prolonged course of low-dose costimulation blockade agents, such as belatacept.

Non-invasive graft outcome monitoring tools could be extended using bioimaging to locate labelled Treg. To further this approach, we could attempt to label Treg with a compatible contrast material or superparamanetic iron oxide (SPIO) conjugates to incorporate into Treg in order tracking the fate of Treg and compare to that with the functional parameters obtained from the MR imaging concurrently. Gadolinium is a heavy element that represents another alternative for tracking Treg *in vivo* using MR imaging. Many gadolinium compounds are GMP-certified and are already being used as contrast medium in clinical MR scanning. By using gadolinium compound would greatly enhance its translational potential from bench to clinic. However, one should bear in mind of the toxicity of which the risk of systemic nephrogenic fibrosis is a main consideration in the application of such techniques to patients with impaired renal function. Details regarding T cell labelling will be further discussed in the next Chapter.

Chapter 7 General discussion

We acknowledge that the experimental data were completed 6 years ago that interpretation of these data in the context of this fast-growing Treg therapy field can be limited. The aim of this thesis is to investigate the translational potential of Treg therapy in transplantation using an experimental model to mimic the clinical scenario. We have provided data for proof-of-concept in utilizing Treg therapy as an adjunct to a current immunosuppressive agent *in vivo*. Treg therapy controls allograft rejection in an anticipated dose-dependent manner. The potency of Treg therapy is also dependent on the precursor frequency of alloantigen-specific Treg. However, the choice between using polyclonal versus alloantigen-reactive Treg has remained uncertain. Both polyclonal and donor alloantigen reactive Treg have been envisaged to be safe in the use of post renal transplant in recent trials ***(discussed in Chapter 1.4.6)***. Circumstantial evidence in the literature suggested the superiority of alloreactive Treg over nTreg. Our data appeared to mirror these pieces of evidence in the literature that we were able to demonstrate that donor alloantigen-experienced Treg were superior to nTreg and expanded nTreg in our model using CTLA-4Ig as the immunosuppressant, although we have not demonstrated alloreactivity or allospecificity in any of the experiments carried out above. Supplemetary experiments using third party cells/grafts with a serial cell titration experiment with CTLA-4 Ig in different strain combination might reveal the true differences between nTreg and alloantigen-driven Treg. On the other hand, the activation status of Treg could be vitally important at the time of Treg delivery as we also demonstrated that nTreg activated over a short period of time by a polyclonal stimulus *in vitro* could also equip them with potency similar to alloreactive Treg on a cell-to-cell basis. As we have demonstrated that CTLA-4 plays a non-redundant role in both

alloreactive Treg and nTreg function *in vivo*, the expression of CTLA-4 at the time of Treg delivery, as well as their expression after Treg homing to the site of action would be an interesting area to explore further using advance molecular imaging. For example, SPIO – super paramagnetic iron oxide particles have been used to tag macrophages in the interrogation of innate response *in vivo*. However, owing to the fact that T cells lack phagocytosis feature, difficulties were encountered for labelling these cells with larger compounds. Smaller molecules, such as heavy elements or metals have been proposed to be an alternative for tagging T cells. In fact, we had collaboration with the Department of Chemistry at the Loughborough Univerwsity to investigate such approach. Human $CD4^+$ T cells were labelled with gadolinium-based GMP-certified contrast medium. Interestingly, these cells were shown to retain gadolinium-based contrast material 10 days after labelling by laser ablation inductively coupled plasma mass spectrometry[597]. Clinically relevant materials such as radioactive deuterium have also been used to study T cells *in vivo* kinetics. Bollyky et al showed that the administration of deuterium oxide could be used to study the kinetics of various T cell subsets in type 1 diabetes patients[598]. Furthermore, deuterium labelling technique has also been included in one of the Treg cell trial in transplantation mentioned in ***Chapter 1.4.6***[599]. Other established and potential Treg labelling technique including fluorescent protein-based reporters, forester resonance energy-transfer-based photoactivatable reporters, gene-transfer-free cell-labelling, lipophilic dye labelling, antibody and aptamer labelling is comphrehsively summarized in a review article elsewhere[600].

We propose a model of long-term allograft survival leading to the development of operational tolerance using Treg and an immunosuppressive drug ***(Figure 7.1)***. A pre-operative delivery of fully activated alloreactive Treg into systemic circulation allows time for their distribution and homing to secondary lymphoid tissue preparing them to suppress alloresponses against an allograft. Shortly after the transplant of an allograft, the inflammatory stimuli trigger both innate and adaptive immunity. Exogenous and endogenous Treg as well as effector T cells are being attracted to the site of action. The CTLA-4 domain of abatacept blocks the CD28/B7 axis, thereby limiting the number of CD80 and CD86 available to propagate T cell responses. As mentioned above, the action of abatacept has a preferential effect on dampening the costimulation of effector T cells due to a lower threshold of activation[561]. Surveying nTreg might be affected by the reduced number of B7 for full activation to mediate suppression. However, the infused Treg that have already been fully activated *in vitro* are unlikely to be affected by abatacept. These potent exogenous Treg can then exert their suppressive function in synergy with abatacept in this setting as the latter further reduces the number of CD80/CD86 on APC. Although the effect of abatacept is designed to be short-lived in this model, the suppressive effect of Treg is long-lasting and some of these Treg take residence within the allograft to ascertain local control as well as mediate linked suppression and infectious tolerance ***(Figure 7.2)***.

Figure 7.1 Operational transplant tolerance achieved by Treg therapy plus low dose immunosuppressant

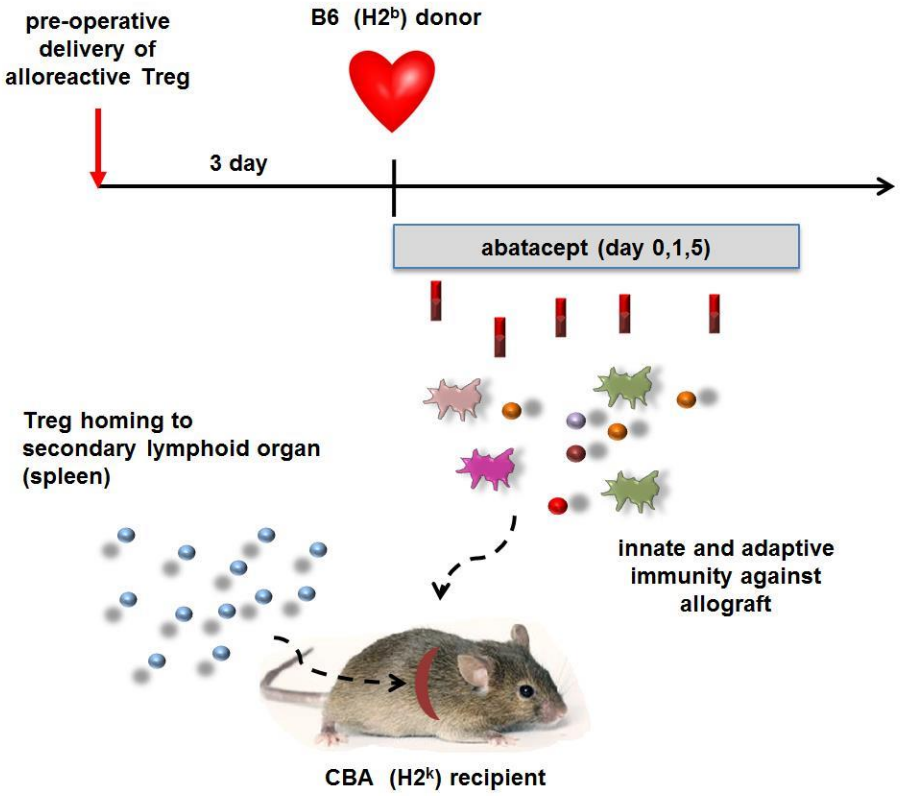

Figure 7.1. Operational transplant tolerance achieved by Treg therapy plus low dose immunosuppressant. Pre-transplant intravenous delivery of fully functional alloreactive Treg take their residence in the draining secondary lymphoid tissue, the spleen in the case of this heterotopic heart transplant model. These therapeutic Treg were enriched *in vitro* for alloreactivity by means of exposure to donor-specific alloantigens for 2 weeks. Transplant of a full MHC mismatched heart allograft triggers an array of innate and adaptive immunue responses against alloantigens. In the presence of a peri-operative sub-optimal costimulation blockade treatment- abatacept (i.v. 25µg day 0, 1 and 5), Treg control allograft rejection effectively when given at the optimal cell dose and timing ***(see Chapter 3.2.5 and 6.2.1)***.

Figure 7.2. Modulation of alloresponses by Treg and abatacept

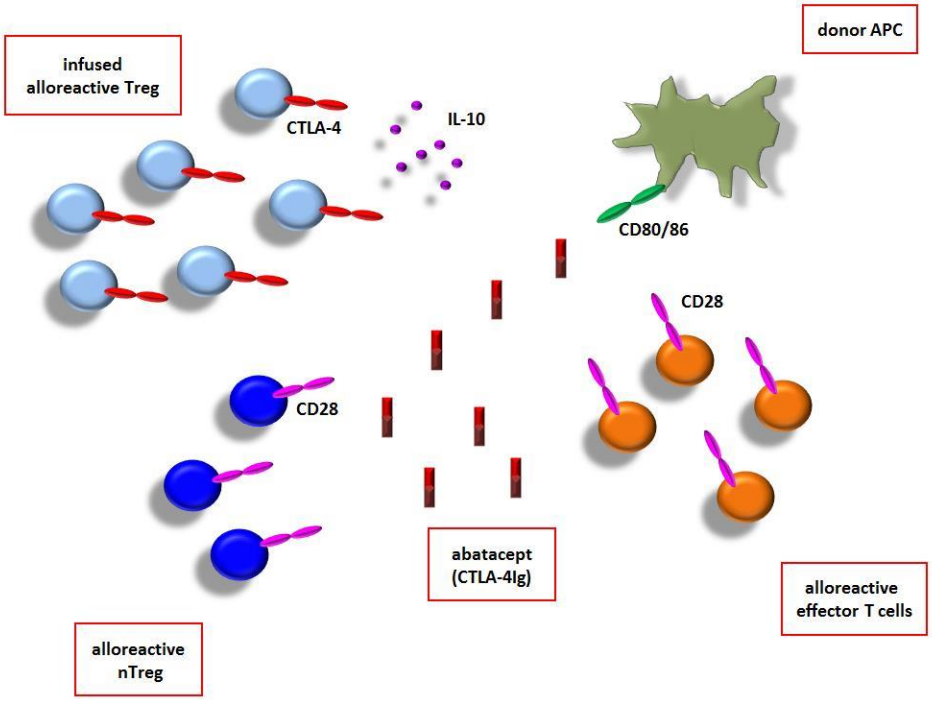

Figure 7.2. Modulation of alloresponses by Treg and abatacept. A given precursor frequency of alloreactive Treg is required to elicit a full control of allograft rejection mediated by alloreactive effector T cells. The CTLA-4 domain of abatacept blocks the CD27/B7 axis and limits the number of CD80 and CD86 available to propagate T cell responses. However, the action of abatacept has a preferential effect on dampening the costimulation of effector T cells because of a lower level of threshold for CD28/B7 dependent activation compared to nTreg and infused Treg. Although, endogenous surveying nTreg might be affected by the reduced number of CD80/CD86 molecules for full activation to mediate their suppressive effect, infused alloreactive Treg which had already been fully activated *in vitro* are likely to be spared by the action of abatacept. In addition to CTLA-4, infused Treg could mediate their suppressive effect via the secretion of IL-10 ***(Chapter 4.2.1 & 4.2.2)***. Infused alloreactive Treg could mediate long-term suppressive effect by taking residence within the allograft to ascertain local control, as well as mediate linked suppression and infectious tolerance ***(Chapter 4.2.4)***.

Invariably, Treg cell dose plays an integral part to ensure that the number of alloreactive T cells is covered. Our data showed that Treg therapy was dose-dependent. Experiments carried out using immunodeficient mice indicated that the number required to provide adequate suppressive function is approximately 30% of the number of alloreactive T cells. Another important factor in determining outcome using Treg therapy was the timing of Treg delivery related to the transplant. We have shown that Treg given prior to the transplant unequivocally led to long-term graft survivals, but not after the transplant. We believe that the time allowed for Treg trafficking and homing reveals this striking difference. More importantly, consistent with other reports, Treg are less efficient to control allograft rejection in sensitized individuals, compared to naïve individuals. Cell doses could be a main reason for such inadequate control, however further experiments addressing these issues are warranted.

We could also consider that our transplant model mimics drug minimization strategies in clinical transplantation. Using immunocompetent mice, we demonstrated that allografts were accepted long-term after immunosuppressive drugs were withdrawn completely from the first week of transplant in the presence of a single dose pre-operative Treg therapy. Currently minimizing calcineurin inhibitors and withdrawal of corticosteroids use are being studied in several clinical trials in the last decade. CTLA-4Ig has been put forward to replace CNI with the advantage that it lacks nephrotoxic side-effects. Undoubtedly, as the development of Treg therapy in transplantation becomes mature, the rationale of the selection of appropriate immunosuppressive drugs to support Treg therapy would become more apparent. The impact of a number of immunosuppressive drugs on Treg has been reviewed extensively elsewhere[601-604]. There had been a consensus about the negative relationship between CNI and Treg expansion, survival and function, but recent findings suggested that its effect on Treg could be beneficial at low-dose. Rapamycin had been shown to be the drug of choice to compliment Treg

therapy given the data based on Treg development *in vitro* and *in vivo*. The detrimental effect of CTLA-4Ig on Treg could be specific to naïve Treg, but not activated Treg, which were less dependent on B7 for activation as discussed above[449]. The potential action of CTLA4-Ig that may affect Treg activity was discussed in ***Chapter 5.3***. More specifically, the impact of several conventional immunosuppressive drugs such as tacrolimus, MMF and corticosteroids were tested for their impact on *ex vivo* expanded human Treg in a recent study. Scotta et al demonstrated that tacrolimus and MMF were negatively related to the function of Treg *in vitro* and *in vivo* using a humanized GVHD model[553]. On the other hand, rapamycin appeared to be permissive to Treg therapy as it preserved Treg frequency and function. Ongoing studies will provide us more insights into the optimal choice of Treg-sparing immunosuppressive drug.

Circumstantial evidence suggests that alloreactive Treg are superior to polyclonal nTreg in controlling allograft rejection *in vivo*. In addition, alloreactive Treg appear to have a higher potency in a cell-to-cell basis compared to the polyclonal nTreg. Direct comparison between these two types of Treg will be revealed by the pilot trials under the ONE study. The logistic issue of obtaining allogeneic tissues and the generation of large number of alloreactive Treg are major considerations. Recent advances in evolution of protocols for the *in vitro* generation of human alloreactive Treg have made it plausible. Peters et al initially reported a GMP-compatible MACS sorting method to isolate highly pure human Treg and expanded using a combination of allogeneic PBMC and anti-CD3/CD28 antibody-coated beads. These expanded human Treg showed allospecific suppression *in vitro*[498]. Putnam et al described another GMP-compatible method to generate alloreactive human Treg by stimulating PBMC with allogeneic B cells and then expanded them using anti-CD3/CD28 polyclonal stimuli. These alloreactive Treg were shown to be superior to polyclonal nTreg in the control of skin allograft rejection in a humanized mouse model[605]. Our group also recently described a GMP-compatible method to generate

human alloreactive Treg by using allogeneic B cell bank obtained from a pooled local population[606]. Expanded human nTreg using this approach were shown to be more potent to the polyclonally-expanded nTreg in a humanized skin transplant model. Genetically-engineered allospecific Treg or so-called 'designer Treg' may not be far from reality. Tsang et al previously showed that Treg transduced with TCR specific for both direct and indirect allospecificity could efficiently control chronic allograft rejection *in vivo*[428]. Employing the technology of retroviral transfection of chimeric antigen receptors into human T cells, which has been used in engineering tumour antigen-specific T cells in cancer immunotherapy[607]. Chimeric antigen receptor T cells (CAR T cells) have been developed and tested to target CD22+ leukaemic cells in end-stage lymphoblastic leukaemia. Applying a similar principle, Boardman et al took this further to generate human alloreactive Treg that possess a chimeric antigen receptor (CAR) that regulate alloresponses in a humanized skin transplant model[608]. CAR T cells have the advantage that it theoretically elicit antigen-specific response. However, translational from bench-to-clinic is still far from reality. As shown by the set back in the recent trials, bystander activity in human tissues bearing the same antigen could lead to detrimental effect. The huge cost involved to build a state-of-the-art clinical cell culture facility could deem such therapy to be limited in certain healthcare systems. As it is the case for most novel therapeutics, the costs always pose a challenging issue in translating cell therapy with its complex technological set up. In the hope of minimizing the costs required for the reliance on long-term immunosuppressive drug therapy and the management of morbidities associated with drugs, Treg therapy might be envisaged as a better trade off in the long run. In terms of Treg, in which a specific cell surface marker is yet to be identified, a rescue therapy may not be feasible once CAR Treg therapy is being administered, unlike bondafide CAR T cells, in which corticosteroids may be used to arrest cell therapy action.

Plasticity and stability of Treg function has become a topical debate in recent years. Plasticity is defined as the complete change of function of Treg upon stimulation. For instance, it has been reported that Treg change their phenotype into a Th17 subset in various studies[286,609,610]. The mechanism of plasticity is often linked to the epigenome control of Foxp3 expression ***(Figure 1.3.2.3.1)***. Rudensky et al demonstrated that the phenotypic profile of Treg could be tracked if these cells ever expressed Foxp3 using an irreversible genetic tagging technology in an 'ex-Treg' model[611]. Using Cre recombinase expression under the control of Foxp3 with a fluorescent reporter protein, they provided the experimental evidence that Treg could change their regulatory phenotypes into effector T cells which mediated autoimmunity in a NOD mice model. By employing this approach, we might be able to ascertain that the $Foxp3^-$ cells that emerged in our expansion cultures ***(Chapter 5)*** were expanding contaminants or cells that have lost their Foxp3 expression due to plasticity.

Stability of Treg function can be described as the tendency of the loss of Treg function when Treg are being subjected in certain microenvironment. It has been suggested that the change of Treg phenotype could be attributed by DNA methylation in TSDR region of the Foxp3 locus[612]. We have previously reported that TSDR demethylation played a critical role in the function of our *in vitro* generated Treg driven by alloantigen and cilostamide[451]. Whilst non-Treg exhibited high level of methylation in the TSDR region of the Foxp3 locus, these *in vitro* generated alloreactive Treg showed a lower level of methylated TSDR in the same region. Functionally, these alloreactive Treg maintained their Foxp3 phenotype and controlled allograft rejection in an adoptive transfer skin graft model.

The cause of plasticity and stability of Treg function has been addressed by a number of experiments examining the epigenome status between nTreg and conventional T cells[613].

H3K4me3 (histone H3 lysine 4 trimethylation) is one of the permissive epigenome studied between nTreg and conventional T cells[614]. TSDR with H3K4me3 modification were found to be present in a number of Treg-associated genes such as Foxp3, CTLA-4, IL-2Ra, and TNFRSF18. Upon *in vitro* activation with anti-CD3/CD28 antibody and IL-2, expanded Treg showed a reduction in the amount of H3K4me3 leading to down-regulation of these Treg-associated genes[615]. Interestingly, this was replaced by a dominant up-regulation of Th2-associated genes. This study demonstrated that *in vitro* polyclonal stimulation of Treg led to the instability of Foxp3 expression and conversion of Treg to Th2 phenotype.

Questions remain as to what potential problems associated with the contamination of alloreactive conventional T cells within the Treg preparations and their effect on allografts. Given the plasticity potential of Treg to convert to conventional T cells under inflammatory conditions ***(Chapter 1.3.2.3)***, it would be important to address these issues in future studies, with particular attention to devise a methodology to effectively identify and remove the contaminated effector population, or minimize the emergence of such effector phenotypes in cultures.

A consistent finding is the relationship between CTLA-4 and Treg function. However, new insights into the molecular interaction in the CD28/CTLA-4/B7 axis have provided new avenues for further studies. Treg have been shown to use trans-endocytosis to capture surface molecules on neighbourhood cells, more importantly via CTLA-4 and CD80 and CD86[393]. Captured CD80 and CD86 from APC are internalized and metabolized in lyzosome. The reduced number of CD80 and CD86 render fewer available costimulation ligands for T cell activation. This would apply to both effector T cells and Treg which would be affected, which might provide the explanation that CTLA-4Ig was detrimental to circulating nTreg. In our model, however, we observed that *in*

vitro alloantigen driven IFN-γ Treg were fully activated upon harvest. They expressed high levels of surface CD25, GITR and intracellular CTLA-4. Hence, IFN-γ Treg as well as activated nTreg are ready to function *in vivo* upon transfer, as opposed to freshly-isolated nTreg.

In order to take this protocol forward, we could advance this into a humanized model in which we could prepare alloreactive IFN-γ Treg using PBMC. A similar approach was carried out using the cilostamide protocol, in which human alloantigen-driven Treg showed potent suppressive function in a humanized mouse model using the branches of the internal mammary artery as an interpositional graft.

Pre-transplant Treg delivery appears to favour graft outcome. One possible avenue worth exploring would be the administration of Treg during pre-transplant organ conditioning using machine perfusion. In theory, this will shorten the time for Treg trafficking and homing in order to create an environment that maximal Treg-mediated immunomodulation could take place at the earliest time point possible. Pre-transplant organ perfusion technique has advanced rapidly over the years. Different types of perfusion machines are now commercially available. These technologies have been spun off from the basic research carried out with an aim to tackle ischaemic-reperfusion injury. Latest findings suggest that normothermic perfusion is better than hypothermic perfusion in terms of tissue repair and function. So far, no studies regarding the administration of cell therapy during pre-transplant organ pre-conditioning have been reported.

We would propose the 'ideal Treg' protocol based on the data generated in this thesis. We believe that alloantigen-driven Treg would offer better control of allograft rejection at a given cell dose. In the living donor renal transplant setting for instance, we could potentially generate donor alloantigen specific Treg which could be safely cryopreserved. Prior to the planned living donor renal transplant, intead of using depletion therapy, we could infuse a single (the number

of cells used in human trials has been extrapolated from in vivo study to be in the range of 100-500 x10^6 cells per dose per patient) of pre-activated donor-antigen specific Treg in advance, and employ a suboptimal costimulation blockade in which we have shown that abatacept was not detrimental to pre-activated nTreg, nor alloantigen-driven Treg. Subsequently, conventional immunosuppressive therapy could be weaned off with an aim to achieve operational tolerance.

Chapter 8 Conclusions

Treg therapy has evolved rapidly over the last few years. It has embarked its first milestone in clinical transplantation by completing the first trial in living renal transplantation under the umbrella of the ONE study. A vast amount of clinical data will emerge as these first initial trials are nearing completion. Answers may be provided for some but more questions will be generated. In the same instance, discovery of novel immunosuppressive drugs are also in the pipelines and studies on combinatorial therapies involving cell therapy and novel immunomodulating strategies will continue to fuel the advancement of transplant immunology.

Chapter 9 References

1. Hamilton D: **A history of organ transplantation. 1st Edition.** *University of Pittsburgh Press, USA* 2012.
2. Barker CF, Markmann JF: **Historical overview of transplantation**. *Cold Spring Harb Perspect Med* 2013, **3**:a014977.
3. Dutkowski P, de Rougemont O, Clavien PA: **Alexis Carrel: genius, innovator and ideologist**. *Am J Transplant* 2008, **8**:1998-2003.
4. Matevossian E, Kern H, Huser N, Doll D, Snopok Y, Nahrig J, Altomonte J, Sinicina I, Friess H, Thorban S: **Surgeon Yurii Voronoy (1895-1961) - a pioneer in the history of clinical transplantation: in memoriam at the 75th anniversary of the first human kidney transplantation**. *Transpl Int* 2009, **22**:1132-1139.
5. Schultheiss D, Jardin A: **Rene Kuss (1913-2006)-a transplant pioneer in Paris**. *Transplant Proc* 2013, **45**:1220-1223.
6. Palmer J: **Of the Freemartin, p.34-43.** *The Works of John Hunter, F.R.S. with Notes, Volume IV* 1837.
7. Lillie FR: **The Theory of the Free-Martin**. *Science* 1916, **43**:611-613.
8. Owen RD: **Immunogenetic Consequences of Vascular Anastomoses between Bovine Twins**. *Science* 1945, **102**:400-401.
9. Billingham RE, Brent L, Medawar PB: **Actively acquired tolerance of foreign cells**. *Nature* 1953, **172**:603-606.
10. Guild WR, Harrison JH, Merrill JP, Murray J: **Successful homotransplantation of the kidney in an identical twin**. *Trans Am Clin Climatol Assoc* 1955, **67**:167-173.
11. Murray JE: **The first successful organ transplants in man**. *J Am Coll Surg* 2005, **200**:5-9.
12. Groth CG, Brent LB, Calne RY, Dausset JB, Good RA, Murray JE, Shumway NE, Schwartz RS, Starzl TE, Terasaki PI, et al.: **Historic landmarks in clinical transplantation: conclusions from the consensus conference at the University of California, Los Angeles**. *World J Surg* 2000, **24**:834-843.
13. Dealy JB, Jr., Dammin GJ, Murray JE, Merrill JP: **Total body irradiation in man: tissue patterns observed in attempts to increase the receptivity of renal homografts**. *Ann N Y Acad Sci* 1960, **87**:572-585.
14. Najarian JS, Ferguson RM, Sutherland DE, Slavin S, Kim T, Kersey J, Simmons RS: **Fractionated total lymphoid irradiation as preparative immunosuppression in high risk renal transplantation: clinical and immunological studies**. *Ann Surg* 1982, **196**:442-452.
15. Field EH, Strober S: **Tolerance, mixed chimerism and protection against graft-versus-host disease after total lymphoid irradiation**. *Philos Trans R Soc Lond B Biol Sci* 2001, **356**:739-748.
16. Kim TH, Shank BM, Vallera DA, Travis EL, Song CW: **Immunosuppressive techniques using radiation**. *Am J Clin Oncol* 1988, **11**:362-367.
17. Schwartz R, Dameshek W: **The effects of 6-mercaptopurine on homograft reactions**. *J Clin Invest* 1960, **39**:952-958.
18. Calne RY: **The rejection of renal homografts. Inhibition in dogs by 6-mercaptopurine**. *Lancet* 1960, **1**:417-418.

19. Calne RY, Evans DB, Herbertson BM, Joysey V, McMillan R, Maginn RR, Millard PR, Pena JR, Salaman JR, White HJ, et al.: **Survival after renal transplantation in man: an interim report on 54 consecutive transplants**. *BMJ* 1968, **2**:404-406.
20. Starzl TE, Marchioro TL, Porter KA, Iwasaki Y, Cerilli GJ: **The use of heterologous antilymphoid agents in canine renal and liver homotransplantation and in human renal homotransplantation**. *Surg Gynecol Obstet* 1967, **124**:301-308.
21. Borel JF, Feurer C, Magnee C, Stahelin H: **Effects of the new anti-lymphocytic peptide cyclosporin A in animals**. *Immunology* 1977, **32**:1017-1025.
22. Calne RY, White DJ: **The use of cyclosporin A in clinical organ grafting**. *Ann Surg* 1982, **196**:330-337.
23. Merion RM, White DJ, Thiru S, Evans DB, Calne RY: **Cyclosporine: five years' experience in cadaveric renal transplantation**. *N Engl J Med* 1984, **310**:148-154.
24. Kahan BD: **Forty years of publication of transplantation proceedings--the second decade: the cyclosporine revolution**. *Transplant Proc* 2009, **41**:1423-1437.
25. Ponticelli C: **Steroid-sparing strategies**. *Transplant Proc* 2005, **37**:3597-3599.
26. Zhang X, Huang H, Han S, Fu S, Wang L: **Is it safe to withdraw steroids within seven days of renal transplantation?** *Clin Transplant* 2013, **27**:1-8.
27. Knoll GA, Bell RC: **Tacrolimus versus cyclosporin for immunosuppression in renal transplantation: meta-analysis of randomised trials**. *BMJ* 1999, **318**:1104-1107.
28. Webster A, Woodroffe RC, Taylor RS, Chapman JR, Craig JC: **Tacrolimus versus cyclosporin as primary immunosuppression for kidney transplant recipients**. *Cochrane Database Syst Rev* 2005:CD003961.
29. Penninga L, Moller CH, Gustafsson F, Steinbruchel DA, Gluud C: **Tacrolimus versus cyclosporine as primary immunosuppression after heart transplantation: systematic review with meta-analyses and trial sequential analyses of randomised trials**. *Eur J Clin Pharmacol* 2010, **66**:1177-1187.
30. Penninga L, Penninga EI, Moller CH, Iversen M, Steinbruchel DA, Gluud C: **Tacrolimus versus cyclosporin as primary immunosuppression for lung transplant recipients**. *Cochrane Database Syst Rev* 2013:CD008817.
31. Muduma G, Saunders R, Odeyemi I, Pollock RF: **Systematic Review and Meta-Analysis of Tacrolimus versus Ciclosporin as Primary Immunosuppression After Liver Transplant**. *PLoS One* 2016, **11**:e0160421.
32. Meier-Kriesche HU, Steffen BJ, Hochberg AM, Gordon RD, Liebman MN, Morris JA, Kaplan B: **Mycophenolate mofetil versus azathioprine therapy is associated with a significant protection against long-term renal allograft function deterioration**. *Transplantation* 2003, **75**:1341-1346.
33. Wang K, Zhang H, Li Y, Wei Q, Li H, Yang Y, Lu Y: **Efficacy of mycophenolate mofetil versus azathioprine after renal transplantation: a systematic review**. *Transplant Proc* 2004, **36**:2071-2072.
34. Knight SR, Russell NK, Barcena L, Morris PJ: **Mycophenolate mofetil decreases acute rejection and may improve graft survival in renal transplant recipients when compared with azathioprine: a systematic review**. *Transplantation* 2009, **87**:785-794.
35. Wagner M, Earley AK, Webster AC, Schmid CH, Balk EM, Uhlig K: **Mycophenolic acid versus azathioprine as primary immunosuppression for kidney transplant recipients**. *Cochrane Database Syst Rev* 2015:CD007746.
36. Webster AC, Lee VW, Chapman JR, Craig JC: **Target of rapamycin inhibitors (TOR-I; sirolimus and everolimus) for primary immunosuppression in kidney transplant recipients**. *Cochrane Database Syst Rev* 2006:CD004290.

37. Kauffman HM, Cherikh WS, Cheng Y, Hanto DW, Kahan BD: **Maintenance immunosuppression with target-of-rapamycin inhibitors is associated with a reduced incidence of de novo malignancies**. *Transplantation* 2005, **80**:883-889.
38. Murakami N, Riella LV, Funakoshi T: **Risk of metabolic complications in kidney transplantation after conversion to mTOR inhibitor: a systematic review and meta-analysis**. *Am J Transplant* 2014, **14**:2317-2327.
39. Su L, Tam N, Deng R, Chen P, Li H, Wu L: **Everolimus-based calcineurin-inhibitor sparing regimens for kidney transplant recipients: a systematic review and meta-analysis**. *Int Urol Nephrol* 2014, **46**:2035-2044.
40. Tang CY, Shen A, Wei XF, Li QD, Liu R, Deng HJ, Wu YZ, Wu ZJ: **Everolimus in de novo liver transplant recipients: a systematic review**. *Hepatobiliary Pancreat Dis Int* 2015, **14**:461-469.
41. de Paula MI, Medina Pestana JO, Nicolau Ferreira A, Pontello Cristelli M, Fabiano Franco M, Aguiar WF, Tedesco-Silva H, Rosso Felipe C: **Long-Term Follow-Up of De Novo Use of mTOR and Calcineurin Inhibitors After Kidney Transplantation**. *Ther Drug Monit* 2016, **38**:22-31.
42. Pengel LH, Liu LQ, Morris PJ: **Do wound complications or lymphoceles occur more often in solid organ transplant recipients on mTOR inhibitors? A systematic review of randomized controlled trials**. *Transpl Int* 2011, **24**:1216-1230.
43. Webster AC, Ruster LP, McGee R, Matheson SL, Higgins GY, Willis NS, Chapman JR, Craig JC: **Interleukin 2 receptor antagonists for kidney transplant recipients**. *Cochrane Database Syst Rev* 2010:CD003897.
44. Liu Y, Zhou P, Han M, Xue CB, Hu XP, Li C: **Basiliximab or antithymocyte globulin for induction therapy in kidney transplantation: a meta-analysis**. *Transplant Proc* 2010, **42**:1667-1670.
45. Morgan RD, O'Callaghan JM, Knight SR, Morris PJ: **Alemtuzumab induction therapy in kidney transplantation: a systematic review and meta-analysis**. *Transplantation* 2012, **93**:1179-1188.
46. Penninga L, Moller CH, Penninga EI, Iversen M, Gluud C, Steinbruchel DA: **Antibody induction therapy for lung transplant recipients**. *Cochrane Database Syst Rev* 2013:CD008927.
47. Zhang Y, Jin W, Cai X: **Anti-interleukin-2 receptor antibodies for the prevention of rejection in liver transplant recipients: a systematic review and meta-analysis**. *Ann Med* 2016:1-33.
48. Shah N, Meouchy J, Qazi Y: **Bortezomib in kidney transplantation**. *Curr Opin Organ Transplant* 2015, **20**:652-656.
49. Macklin PS, Morris PJ, Knight SR: **A systematic review of the use of rituximab for desensitization in renal transplantation**. *Transplantation* 2014, **98**:794-805.
50. Lo P, Sharma A, Craig JC, Wyburn K, Lim W, Chapman JR, Palmer SC, Strippoli GF, Wong G: **Preconditioning Therapy in ABO-Incompatible Living Kidney Transplantation: A Systematic Review and Meta-Analysis**. *Transplantation* 2016, **100**:933-942.
51. Tedla FM, Roche-Recinos A, Brar A: **Intravenous immunoglobulin in kidney transplantation**. *Curr Opin Organ Transplant* 2015, **20**:630-637.
52. Keith DS: **Therapeutic apheresis in renal transplantation; current practices**. *J Clin Apher* 2014, **29**:206-210.
53. Roberts DM, Jiang SH, Chadban SJ: **The treatment of acute antibody-mediated rejection in kidney transplant recipients-a systematic review**. *Transplantation* 2012, **94**:775-783.
54. Amore A: **Antibody-mediated rejection**. *Curr Opin Organ Transplant* 2015, **20**:536-542.

55. Fishman JA: **Infection in solid-organ transplant recipients**. *N Engl J Med* 2007, **357**:2601-2614.
56. Grim SA, Clark NM: **Management of infectious complications in solid-organ transplant recipients**. *Clin Pharmacol Ther* 2011, **90**:333-342.
57. Martin-Gandul C, Mueller NJ, Pascual M, Manuel O: **The Impact of Infection on Chronic Allograft Dysfunction and Allograft Survival After Solid Organ Transplantation**. *Am J Transplant* 2015, **15**:3024-3040.
58. Geissler EK: **Post-transplantation malignancies: here today, gone tomorrow?** *Nat Rev Clin Oncol* 2015, **12**:705-717.
59. Tufaro AP, Azoury SC, Crompton JG, Straughan DM, Reddy S, Prasad NB, Shi G, Fischer AC: **Rising incidence and aggressive nature of cutaneous malignancies after transplantation: An update on epidemiology, risk factors, management and surveillance**. *Surg Oncol* 2015, **24**:345-352.
60. Morscio J, Tousseyn T: **Recent insights in the pathogenesis of post-transplantation lymphoproliferative disorders**. *World J Transplant* 2016, **6**:505-516.
61. Jardine AG, Gaston RS, Fellstrom BC, Holdaas H: **Prevention of cardiovascular disease in adult recipients of kidney transplants**. *Lancet* 2011, **378**:1419-1427.
62. Bamgbola O: **Metabolic consequences of modern immunosuppressive agents in solid organ transplantation**. *Ther Adv Endocrinol Metab* 2016, **7**:110-127.
63. De Bleser L, Matteson M, Dobbels F, Russell C, De Geest S: **Interventions to improve medication-adherence after transplantation: a systematic review**. *Transpl Int* 2009, **22**:780-797.
64. Prendergast MB, Gaston RS: **Optimizing medication adherence: an ongoing opportunity to improve outcomes after kidney transplantation**. *Clin J Am Soc Nephrol* 2010, **5**:1305-1311.
65. Lieber SR, Helcer J, Shemesh E: **Monitoring drug adherence**. *Transplant Rev (Orlando)* 2015, **29**:73-77.
66. Cooper M, Salvadori M, Budde K, Oppenheimer F, Sollinger H, Zeier M: **Enteric-coated mycophenolate sodium immunosuppression in renal transplant patients: efficacy and dosing**. *Transplant Rev (Orlando)* 2012, **26**:233-240.
67. Guada M, Beloqui A, Kumar MN, Preat V, Dios-Vieitez Mdel C, Blanco-Prieto MJ: **Reformulating cyclosporine A (CsA): More than just a life cycle management strategy**. *J Control Release* 2016, **225**:269-282.
68. Singh N, Von Visger J, Zachariah M: **Extended release once a day tacrolimus**. *Curr Opin Organ Transplant* 2015, **20**:657-662.
69. Patel N, Cook A, Greenhalgh E, Rech MA, Rusinak J, Heinrich L: **Overview of extended release tacrolimus in solid organ transplantation**. *World J Transplant* 2016, **6**:144-154.
70. Halleck F, Friedersdorff F, Fuller TF, Matz M, Huber L, Durr M, Schutz M, Budde K: **New perspectives of immunosuppression**. *Transplant Proc* 2013, **45**:1224-1231.
71. Hardinger KL, Brennan DC: **Novel immunosuppressive agents in kidney transplantation**. *World J Transplant* 2013, **3**:68-77.
72. Busque S, Cantarovich M, Mulgaonkar S, Gaston R, Gaber AO, Mayo PR, Ling S, Huizinga RB, Meier-Kriesche HU: **The PROMISE study: a phase 2b multicenter study of voclosporin (ISA247) versus tacrolimus in de novo kidney transplantation**. *Am J Transplant* 2011, **11**:2675-2684.
73. Waldner M, Fantus D, Solari M, Thomson AW: **New perspectives on mTOR inhibitors (rapamycin, rapalogs and TORKinibs) in transplantation**. *Br J Clin Pharmacol* 2016, **82**:1158-1170.

74. Li XC, Rothstein DM, Sayegh MH: **Costimulatory pathways in transplantation: challenges and new developments**. *Immunol Rev* 2009, **229**:271-293.
75. Ford ML, Larsen CP: **Translating costimulation blockade to the clinic: lessons learned from three pathways**. *Immunol Rev* 2009, **229**:294-306.
76. Kinnear G, Jones ND, Wood KJ: **Costimulation blockade: current perspectives and implications for therapy**. *Transplantation* 2013, **95**:527-535.
77. Vincenti F, Larsen CP, Alberu J, Bresnahan B, Garcia VD, Kothari J, Lang P, Urrea EM, Massari P, Mondragon-Ramirez G, et al.: **Three-year outcomes from BENEFIT, a randomized, active-controlled, parallel-group study in adult kidney transplant recipients**. *Am J Transplant* 2012, **12**:210-217.
78. Rostaing L, Vincenti F, Grinyo J, Rice KM, Bresnahan B, Steinberg S, Gang S, Gaite LE, Moal MC, Mondragon-Ramirez GA, et al.: **Long-term belatacept exposure maintains efficacy and safety at 5 years: results from the long-term extension of the BENEFIT study**. *Am J Transplant* 2013, **13**:2875-2883.
79. Masson P, Henderson L, Chapman JR, Craig JC, Webster AC: **Belatacept for kidney transplant recipients**. *Cochrane Database Syst Rev* 2014:CD010699.
80. Vincenti F, Rostaing L, Grinyo J, Rice K, Steinberg S, Gaite L, Moal MC, Mondragon-Ramirez GA, Kothari J, Polinsky MS, et al.: **Belatacept and Long-Term Outcomes in Kidney Transplantation**. *N Engl J Med* 2016, **374**:333-343.
81. Durrbach A, Pestana JM, Florman S, Del Carmen Rial M, Rostaing L, Kuypers D, Matas A, Wekerle T, Polinsky M, Meier-Kriesche HU, et al.: **Long-Term Outcomes in Belatacept- Versus Cyclosporine-Treated Recipients of Extended Criteria Donor Kidneys: Final Results From BENEFIT-EXT, a Phase III Randomized Study**. *Am J Transplant* 2016, **16**:3192-3201.
82. Riella LV, Sayegh MH: **T-cell co-stimulatory blockade in transplantation: two steps forward one step back!** *Expert Opin Biol Ther* 2013, **13**:1557-1568.
83. Krummey SM, Ford ML: **New insights into T-cell cosignaling in allograft rejection and survival**. *Curr Opin Organ Transplant* 2015, **20**:43-48.
84. Goldwater R, Keirns J, Blahunka P, First R, Sawamoto T, Zhang W, Kowalski D, Kaibara A, Holman J: **A phase 1, randomized ascending single-dose study of antagonist anti-human CD40 ASKP1240 in healthy subjects**. *Am J Transplant* 2013, **13**:1040-1046.
85. Stegall MD, Diwan T, Raghavaiah S, Cornell LD, Burns J, Dean PG, Cosio FG, Gandhi MJ, Kremers W, Gloor JM: **Terminal complement inhibition decreases antibody-mediated rejection in sensitized renal transplant recipients**. *Am J Transplant* 2011, **11**:2405-2413.
86. Biglarnia AR, Nilsson B, Nilsson T, von Zur-Muhlen B, Wagner M, Berne C, Wanders A, Magnusson A, Tufveson G: **Prompt reversal of a severe complement activation by eculizumab in a patient undergoing intentional ABO-incompatible pancreas and kidney transplantation**. *Transpl Int* 2011, **24**:e61-66.
87. Stewart ZA, Collins TE, Schlueter AJ, Raife TI, Holanda DG, Nair R, Reed AI, Thomas CP: **Case report: Eculizumab rescue of severe accelerated antibody-mediated rejection after ABO-incompatible kidney transplant**. *Transplant Proc* 2012, **44**:3033-3036.
88. Gaber AO, Mulgaonkar S, Kahan BD, Woodle ES, Alloway R, Bajjoka I, Jensik S, Klintmalm GB, Patton PR, Wiseman A, et al.: **YSPSL (rPSGL-Ig) for improvement of early renal allograft function: a double-blind, placebo-controlled, multi-center Phase IIa study**. *Clin Transplant* 2011, **25**:523-533.
89. Budde K, Sommerer C, Becker T, Asderakis A, Pietruck F, Grinyo JM, Rigotti P, Dantal J, Ng J, Barten MJ, et al.: **Sotrastaurin, a novel small molecule inhibiting protein kinase C: first clinical results in renal-transplant recipients**. *Am J Transplant* 2010, **10**:571-581.

90. Matz M, Naik M, Mashreghi MF, Glander P, Neumayer HH, Budde K: **Evaluation of the novel protein kinase C inhibitor sotrastaurin as immunosuppressive therapy after renal transplantation**. *Expert Opin Drug Metab Toxicol* 2011, **7**:103-113.
91. Tedesco-Silva H, Kho MM, Hartmann A, Vitko S, Russ G, Rostaing L, Budde K, Campistol JM, Eris J, Krishnan I, et al.: **Sotrastaurin in calcineurin inhibitor-free regimen using everolimus in de novo kidney transplant recipients**. *Am J Transplant* 2013, **13**:1757-1768.
92. Busque S, Leventhal J, Brennan DC, Steinberg S, Klintmalm G, Shah T, Mulgaonkar S, Bromberg JS, Vincenti F, Hariharan S, et al.: **Calcineurin-inhibitor-free immunosuppression based on the JAK inhibitor CP-690,550: a pilot study in de novo kidney allograft recipients**. *Am J Transplant* 2009, **9**:1936-1945.
93. Vincenti F, Tedesco Silva H, Busque S, O'Connell P, Friedewald J, Cibrik D, Budde K, Yoshida A, Cohney S, Weimar W, et al.: **Randomized phase 2b trial of tofacitinib (CP-690,550) in de novo kidney transplant patients: efficacy, renal function and safety at 1 year**. *Am J Transplant* 2012, **12**:2446-2456.
94. Vincenti F, Mendez R, Pescovitz M, Rajagopalan PR, Wilkinson AH, Butt K, Laskow D, Slakey DP, Lorber MI, Garg JP, et al.: **A phase I/II randomized open-label multicenter trial of efalizumab, a humanized anti-CD11a, anti-LFA-1 in renal transplantation**. *Am J Transplant* 2007, **7**:1770-1777.
95. Di Lernia V: **Progressive multifocal leukoencephalopathy and antipsoriatic drugs: assessing the risk of immunosuppressive treatments**. *Int J Dermatol* 2010, **49**:631-635.
96. Chandrasekharan D, Issa F, Wood KJ: **Achieving operational tolerance in transplantation: how can lessons from the clinic inform research directions?** *Transpl Int* 2013, **26**:576-589.
97. Dugast E, Chesneau M, Soulillou JP, Brouard S: **Biomarkers and possible mechanisms of operational tolerance in kidney transplant patients**. *Immunol Rev* 2014, **258**:208-217.
98. Sarwal MM: **Fingerprints of transplant tolerance suggest opportunities for immunosuppression minimization**. *Clin Biochem* 2016, **49**:404-410.
99. Sawitzki B, Reinke P, Pascher A, Volk HD: **State of the art on the research for biomarkers allowing individual, tailor-made minimization of immunosuppression**. *Curr Opin Organ Transplant* 2010, **15**:691-696.
100. Turka LA, Wood K, Bluestone JA: **Bringing transplantation tolerance into the clinic: lessons from the ITN and RISET for the Establishment of Tolerance consortia**. *Curr Opin Organ Transplant* 2010, **15**:441-448.
101. Gokmen R, Hernandez-Fuentes MP: **Biomarkers of tolerance**. *Curr Opin Organ Transplant* 2013, **18**:416-420.
102. Viklicky O, Hribova P, Brabcova I: **Molecular markers of rejection and tolerance: lessons from clinical research**. *Nephrol Dial Transplant* 2013, **28**:2701-2708.
103. Schlickeiser S, Boes D, Streitz M, Sawitzki B: **The use of novel diagnostics to individualize immunosuppression following transplantation**. *Transpl Int* 2015, **28**:911-920.
104. Sawitzki B, Schlickeiser S, Reinke P, Volk HD: **Monitoring tolerance and rejection in organ transplant recipients**. *Biomarkers* 2011, **16 Suppl 1**:S42-50.
105. Baron D, Giral M, Brouard S: **Reconsidering the detection of tolerance to individualize immunosuppression minimization and to improve long-term kidney graft outcomes**. *Transpl Int* 2015, **28**:938-959.
106. Girmanova E, Hruba P, Viklicky O: **Circulating biomarkers of tolerance**. *Transplant Rev (Orlando)* 2016, **29**:68-72.

107. Chowdhury P, Hernandez-Fuentes MP: **Non-invasive biomarkers to guide management following renal transplantation: the need for a multiplatform approach**. *Curr Opin Organ Transplant* 2013, **18**:1-5.
108. Eng HS, Leffell MS: **Histocompatibility testing after fifty years of transplantation**. *J Immunol Methods* 2011, **369**:1-21.
109. Tait BD, Susal C, Gebel HM, Nickerson PW, Zachary AA, Claas FH, Reed EF, Bray RA, Campbell P, Chapman JR, et al.: **Consensus guidelines on the testing and clinical management issues associated with HLA and non-HLA antibodies in transplantation**. *Transplantation* 2013, **95**:19-47.
110. Brockmann JG, Vaidya A, Reddy S, Friend PJ: **Retrieval of abdominal organs for transplantation**. *Br J Surg* 2006, **93**:133-146.
111. Hameed AM, Hawthorne WJ, Pleass HC: **Advances in organ preservation for transplantation**. *ANZ Journal of Surgery* 2016:n/a-n/a.
112. Piros L, Langer RM: **Laparoscopic donor nephrectomy techniques**. *Curr Opin Organ Transplant* 2012, **17**:401-405.
113. NHS Blood and Transplant: **Organ Donation and Transplantation Activity Report 2015/2016**. *http://www.odt.nhs.uk/pdf/activity-report/activity_report_2015_16.pdf* 2016.
114. Giacomoni A, Di Sandro S, Lauterio A, Concone G, Buscemi V, Rossetti O, De Carlis L: **Robotic nephrectomy for living donation: surgical technique and literature systematic review**. *Am J Surg* 2016, **211**:1135-1142.
115. Tzvetanov I, Bejarano-Pineda L, Giulianotti PC, Jeon H, Garcia-Roca R, Bianco F, Oberholzer J, Benedetti E: **State of the art of robotic surgery in organ transplantation**. *World J Surg* 2013, **37**:2791-2799.
116. Sharfuddin A: **Renal relevant radiology: imaging in kidney transplantation**. *Clin J Am Soc Nephrol* 2014, **9**:416-429.
117. Issa F: **Vascularized composite allograft-specific characteristics of immune responses**. *Transpl Int* 2016, **29**:672-681.
118. Kueckelhaus M, Fischer S, Seyda M, Bueno EM, Aycart MA, Alhefzi M, ElKhal A, Pomahac B, Tullius SG: **Vascularized composite allotransplantation: current standards and novel approaches to prevent acute rejection and chronic allograft deterioration**. *Transpl Int* 2016, **29**:655-662.
119. Moreau A, Varey E, Anegon I, Cuturi MC: **Effector mechanisms of rejection**. *Cold Spring Harb Perspect Med* 2013, **3**.
120. Vadori M, Cozzi E: **Immunological challenges and therapies in xenotransplantation**. *Cold Spring Harb Perspect Med* 2014, **4**:a015578.
121. Land WG, Agostinis P, Gasser S, Garg AD, Linkermann A: **Transplantation and Damage-Associated Molecular Patterns (DAMPs)**. *Am J Transplant* 2016, **16**:3338-3361.
122. Salehi S, Reed EF: **The divergent roles of macrophages in solid organ transplantation**. *Curr Opin Organ Transplant* 2015, **20**:446-453.
123. Lo DJ, Weaver TA, Kleiner DE, Mannon RB, Jacobson LM, Becker BN, Swanson SJ, Hale DA, Kirk AD: **Chemokines and their receptors in human renal allotransplantation**. *Transplantation* 2011, **91**:70-77.
124. Schnickel GT, Bastani S, Hsieh GR, Shefizadeh A, Bhatia R, Fishbein MC, Belperio J, Ardehali A: **Combined CXCR3/CCR5 blockade attenuates acute and chronic rejection**. *J Immunol* 2008, **180**:4714-4721.

125. Kakuta Y, Okumi M, Miyagawa S, Tsutahara K, Abe T, Yazawa K, Matsunami K, Otsuka H, Takahara S, Nonomura N: **Blocking of CCR5 and CXCR3 suppresses the infiltration of macrophages in acute renal allograft rejection**. *Transplantation* 2012, **93**:24-31.
126. Sheen JH, Heeger PS: **Effects of complement activation on allograft injury**. *Curr Opin Organ Transplant* 2015, **20**:468-475.
127. Farrar CA, Sacks SH: **Mechanisms of rejection: role of complement**. *Curr Opin Organ Transplant* 2014, **19**:8-13.
128. Saidi RF, Rajeshkumar B, Shariftabrizi A, Dresser K, Walter O: **Human C1 inhibitor attenuates liver ischemia-reperfusion injury and promotes liver regeneration**. *J Surg Res* 2014, **187**:660-666.
129. Raedler H, Vieyra MB, Leisman S, Lakhani P, Kwan W, Yang M, Johnson K, Faas SJ, Tamburini P, Heeger PS: **Anti-complement component C5 mAb synergizes with CTLA4Ig to inhibit alloreactive T cells and prolong cardiac allograft survival in mice**. *Am J Transplant* 2011, **11**:1397-1406.
130. Cravedi P, Leventhal J, Lakhani P, Ward SC, Donovan MJ, Heeger PS: **Immune cell-derived C3a and C5a costimulate human T cell alloimmunity**. *Am J Transplant* 2013, **13**:2530-2539.
131. Strainic MG, Shevach EM, An F, Lin F, Medof ME: **Absence of signaling into CD4(+) cells via C3aR and C5aR enables autoinductive TGF-beta1 signaling and induction of Foxp3(+) regulatory T cells**. *Nat Immunol* 2013, **14**:162-171.
132. van der Touw W, Cravedi P, Kwan WH, Paz-Artal E, Merad M, Heeger PS: **Cutting edge: Receptors for C3a and C5a modulate stability of alloantigen-reactive induced regulatory T cells**. *J Immunol* 2013, **190**:5921-5925.
133. Baldwin WM, 3rd, Valujskikh A, Fairchild RL: **Antibody-mediated rejection: emergence of animal models to answer clinical questions**. *Am J Transplant* 2010, **10**:1135-1142.
134. Benichou G, Yamada Y, Aoyama A, Madsen JC: **Natural killer cells in rejection and tolerance of solid organ allografts**. *Curr Opin Organ Transplant* 2011, **16**:47-53.
135. Rajalingam R: **The Impact of HLA Class I-Specific Killer Cell Immunoglobulin-Like Receptors on Antibody-Dependent Natural Killer Cell-Mediated Cytotoxicity and Organ Allograft Rejection**. *Front Immunol* 2016, **7**:585.
136. Klein J: **Seeds of time: fifty years ago Peter A. Gorer discovered the H-2 complex**. *Immunogenetics* 1986, **24**:331-338.
137. Benacerraf B: **Role of MHC gene products in immune regulation**. *Science* 1981, **212**:1229-1238.
138. Dansset J: **The Nobel Lectures in Immunology. The Nobel Prize for Physiology or Medicine, 1980. The major histocompatibility complex in man. Past, present, and future concepts**. *Scand J Immunol* 1992, **36**:145-157.
139. Snell GD: **The Nobel Lectures in Immunology. Lecture for the Nobel Prize for Physiology or Medicine, 1980: Studies in histocompatibility**. *Scand J Immunol* 1992, **36**:513-526.
140. Doherty PC: **The Nobel Lectures in Immunology. The Nobel Prize for Physiology or Medicine, 1996. Cell mediated immunity in virus infections**. *Scand J Immunol* 1997, **46**:527-540.
141. Zinkernagel RM: **The Nobel Lectures in Immunology. The Nobel Prize for Physiology or Medicine, 1996. Cellular immune recognition and the biological role of major transplantation antigens**. *Scand J Immunol* 1997, **46**:421-436.
142. Ali JM, Bolton EM, Bradley JA, Pettigrew GJ: **Allorecognition pathways in transplant rejection and tolerance**. *Transplantation* 2013, **96**:681-688.

143. Marino J, Paster J, Benichou G: **Allorecognition by T Lymphocytes and Allograft Rejection**. *Front Immunol* 2016, **7**:582.
144. Pietra BA, Wiseman A, Bolwerk A, Rizeq M, Gill RG: **CD4 T cell-mediated cardiac allograft rejection requires donor but not host MHC class II**. *J Clin Invest* 2000, **106**:1003-1010.
145. Boardman DA, Jacob J, Smyth LA, Lombardi G, Lechler RI: **What Is Direct Allorecognition?** *Curr Transplant Rep* 2016, **3**:275-283.
146. Lechler RI, Batchelor JR: **Restoration of immunogenicity to passenger cell-depleted kidney allografts by the addition of donor strain dendritic cells**. *J Exp Med* 1982, **155**:31-41.
147. Lechler RI, Batchelor JR: **Immunogenicity of retransplanted rat kidney allografts. Effect of inducing chimerism in the first recipient and quantitative studies on immunosuppression of the second recipient**. *J Exp Med* 1982, **156**:1835-1841.
148. Benichou G, Takizawa PA, Olson CA, McMillan M, Sercarz EE: **Donor major histocompatibility complex (MHC) peptides are presented by recipient MHC molecules during graft rejection**. *J Exp Med* 1992, **175**:305-308.
149. Auchincloss H, Jr., Lee R, Shea S, Markowitz JS, Grusby MJ, Glimcher LH: **The role of "indirect" recognition in initiating rejection of skin grafts from major histocompatibility complex class II-deficient mice**. *Proc Natl Acad Sci U S A* 1993, **90**:3373-3377.
150. Smyth LA, Lechler RI, Lombardi G: **Continuous Acquisition of MHC:Peptide Complexes by Recipient Cells Contributes to the Generation of Anti-Graft CD8+ T Cell Immunity**. *Am J Transplant* 2016, **17**:60-68.
151. Smyth LA, Hervouet C, Hayday T, Becker PD, Ellis R, Lechler RI, Lombardi G, Klavinskis LS: **Acquisition of MHC:peptide complexes by dendritic cells contributes to the generation of antiviral CD8+ T cell immunity in vivo**. *J Immunol* 2012, **189**:2274-2282.
152. Thery C, Duban L, Segura E, Veron P, Lantz O, Amigorena S: **Indirect activation of naive CD4+ T cells by dendritic cell-derived exosomes**. *Nat Immunol* 2002, **3**:1156-1162.
153. Marino J, Babiker-Mohamed MH, Crosby-Bertorini P, Paster JT, LeGuern C, Germana S, Abdi R, Uehara M, Kim JI, Markmann JF, et al.: **Donor exosomes rather than passenger leukocytes initiate alloreactive T cell responses after transplantation**. *Sci Immunol* 2016, **1**.
154. Brown K, Sacks SH, Wong W: **Coexpression of donor peptide/recipient MHC complex and intact donor MHC: evidence for a link between the direct and indirect pathways**. *Am J Transplant* 2011, **11**:826-831.
155. Harper SJ, Ali JM, Wlodek E, Negus MC, Harper IG, Chhabra M, Qureshi MS, Mallik M, Bolton E, Bradley JA, et al.: **CD8 T-cell recognition of acquired alloantigen promotes acute allograft rejection**. *Proc Natl Acad Sci U S A* 2015, **112**:12788-12793.
156. Morelli AE, Bracamonte-Baran W, Burlingham WJ: **Donor-derived exosomes: the trick behind the semidirect pathway of allorecognition**. *Curr Opin Organ Transplant* 2017, **22**:46-54.
157. Brown K, Sacks SH, Wong W: **Extensive and bidirectional transfer of major histocompatibility complex class II molecules between donor and recipient cells in vivo following solid organ transplantation**. *FASEB J* 2008, **22**:3776-3784.
158. Gonzalez-Nolasco B, Wang M, Prunevieille A, Benichou G: **Emerging role of exosomes in allorecognition and allograft rejection**. *Curr Opin Organ Transplant* 2018, **23**:22-27.
159. Guy CS, Vignali DA: **Organization of proximal signal initiation at the TCR:CD3 complex**. *Immunol Rev* 2009, **232**:7-21.
160. Liu JO: **Calmodulin-dependent phosphatase, kinases, and transcriptional corepressors involved in T-cell activation**. *Immunol Rev* 2009, **228**:184-198.

161. Franklin RA, Tordai A, Patel H, Gardner AM, Johnson GL, Gelfand EW: **Ligation of the T cell receptor complex results in activation of the Ras/Raf-1/MEK/MAPK cascade in human T lymphocytes**. *J Clin Invest* 1994, **93**:2134-2140.
162. Brezar V, Tu WJ, Seddiki N: **PKC-Theta in Regulatory and Effector T-cell Functions**. *Front Immunol* 2015, **6**:530.
163. Schwartz RH: **A cell culture model for T lymphocyte clonal anergy**. *Science* 1990, **248**:1349-1356.
164. Jenkins MK, Schwartz RH: **Antigen presentation by chemically modified splenocytes induces antigen-specific T cell unresponsiveness in vitro and in vivo**. *J Exp Med* 1987, **165**:302-319.
165. Appleman LJ, Boussiotis VA: **T cell anergy and costimulation**. *Immunol Rev* 2003, **192**:161-180.
166. Schwartz RH: **T cell anergy**. *Annu Rev Immunol* 2003, **21**:305-334.
167. Delgoffe GM, Powell JD: **Feeding an army: The metabolism of T cells in activation, anergy, and exhaustion**. *Mol Immunol* 2015, **68**:492-496.
168. Zheng Y, Delgoffe GM, Meyer CF, Chan W, Powell JD: **Anergic T cells are metabolically anergic**. *J Immunol* 2009, **183**:6095-6101.
169. Peter C, Waldmann H, Cobbold SP: **mTOR signalling and metabolic regulation of T cell differentiation**. *Curr Opin Immunol* 2010, **22**:655-661.
170. Gajewski TF, Qian D, Fields P, Fitch FW: **Anergic T-lymphocyte clones have altered inositol phosphate, calcium, and tyrosine kinase signaling pathways**. *Proc Natl Acad Sci U S A* 1994, **91**:38-42.
171. Gajewski TF, Fields P, Fitch FW: **Induction of the increased Fyn kinase activity in anergic T helper type 1 clones requires calcium and protein synthesis and is sensitive to cyclosporin A**. *Eur J Immunol* 1995, **25**:1836-1842.
172. Gamper CJ, Powell JD: **Genetic and biochemical regulation of CD4 T cell effector differentiation: insights from examination of T cell clonal anergy**. *Immunol Res* 2010, **47**:162-171.
173. Sharpe AH: **Mechanisms of costimulation**. *Immunol Rev* 2009, **229**:5-11.
174. Nurieva RI, Liu X, Dong C: **Yin–Yang of costimulation: crucial controls of immune tolerance and function**. *Immunol Rev* 2009, **229**:88-100.
175. Pentcheva-Hoang T, Corse E, Allison JP: **Negative regulators of T-cell activation: potential targets for therapeutic intervention in cancer, autoimmune disease, and persistent infections**. *Immunol Rev* 2009, **229**:67-87.
176. Yamane H, Paul WE: **Cytokines of the gamma(c) family control CD4+ T cell differentiation and function**. *Nat Immunol* 2012, **13**:1037-1044.
177. Read KA, Powell MD, McDonald PW, Oestreich KJ: **IL-2, IL-7, and IL-15: Multistage regulators of CD4(+) T helper cell differentiation**. *Exp Hematol* 2016, **44**:799-808.
178. Altomare DA, Khaled AR: **Homeostasis and the importance for a balance between AKT/mTOR activity and intracellular signaling**. *Curr Med Chem* 2012, **19**:3748-3762.
179. Liu Z, Fan H, Jiang S: **CD4(+) T-cell subsets in transplantation**. *Immunol Rev* 2013, **252**:183-191.
180. Askar M: **T helper subsets & regulatory T cells: rethinking the paradigm in the clinical context of solid organ transplantation**. *Int J Immunogenet* 2014, **41**:185-194.
181. Barbara JA, Turvey SE, Kingsley CI, Spriewald BM, Hara M, Witzke O, Morris PJ, Wood KJ: **Islet allograft rejection can be mediated by CD4+, alloantigen experienced, direct pathway T cells of TH1 and TH2 cytokine phenotype**. *Transplantation* 2000, **70**:1641-1649.

182. Tay SS, Plain KM, Bishop GA: **Role of IL-4 and Th2 responses in allograft rejection and tolerance**. *Curr Opin Organ Transplant* 2009, **14**:16-22.
183. Chadha R, Heidt S, Jones ND, Wood KJ: **Th17: contributors to allograft rejection and a barrier to the induction of transplantation tolerance?** *Transplantation* 2011, **91**:939-945.
184. Sullivan JA, Adams AB, Burlingham WJ: **The emerging role of TH17 cells in organ transplantation**. *Transplantation* 2014, **97**:483-489.
185. Zhao P, Xiao X, Ghobrial RM, Li XC: **IL-9 and Th9 cells: progress and challenges**. *Int Immunol* 2013, **25**:547-551.
186. Conley JM, Gallagher MP, Berg LJ: **T Cells and Gene Regulation: The Switching On and Turning Up of Genes after T Cell Receptor Stimulation in CD8 T Cells**. *Front Immunol* 2016, **7**:76.
187. Swain SL, Bradley LM: **Helper T cell memory: more questions than answers**. *Semin Immunol* 1992, **4**:59-68.
188. Budd RC, Van Houten N, Clements J, Mixter PF: **Parallels in T lymphocyte development between lpr and normal mice**. *Semin Immunol* 1994, **6**:43-48.
189. Haluszczak C, Akue AD, Hamilton SE, Johnson LD, Pujanauski L, Teodorovic L, Jameson SC, Kedl RM: **The antigen-specific CD8+ T cell repertoire in unimmunized mice includes memory phenotype cells bearing markers of homeostatic expansion**. *J Exp Med* 2009, **206**:435-448.
190. Berard M, Tough DF: **Qualitative differences between naive and memory T cells**. *Immunology* 2002, **106**:127-138.
191. Sener A, Tang AL, Farber DL: **Memory T-cell predominance following T-cell depletional therapy derives from homeostatic expansion of naive T cells**. *Am J Transplant* 2009, **9**:2615-2623.
192. Brook MO, Wood KJ, Jones ND: **The impact of memory T cells on rejection and the induction of tolerance**. *Transplantation* 2006, **82**:1-9.
193. Hickman SP, Turka LA: **Homeostatic T cell proliferation as a barrier to T cell tolerance**. *Philos Trans R Soc Lond B Biol Sci* 2005, **360**:1713-1721.
194. Nicosia M, Valujskikh A: **Total Recall: Can We Reshape T Cell Memory by Lymphoablation?** *Am J Transplant* 2016.
195. Espinosa JR, Samy KP, Kirk AD: **Memory T cells in organ transplantation: progress and challenges**. *Nat Rev Nephrol* 2016, **12**:339-347.
196. Sprent J, Surh CD: **Normal T cell homeostasis: the conversion of naive cells into memory-phenotype cells**. *Nat Immunol* 2011, **12**:478-484.
197. Smith K, Seddon B, Purbhoo MA, Zamoyska R, Fisher AG, Merkenschlager M: **Sensory adaptation in naive peripheral CD4 T cells**. *J Exp Med* 2001, **194**:1253-1261.
198. Ge Q, Rao VP, Cho BK, Eisen HN, Chen J: **Dependence of lymphopenia-induced T cell proliferation on the abundance of peptide/ MHC epitopes and strength of their interaction with T cell receptors**. *Proc Natl Acad Sci U S A* 2001, **98**:1728-1733.
199. Wang Q, Strong J, Killeen N: **Homeostatic competition among T cells revealed by conditional inactivation of the mouse Cd4 gene**. *J Exp Med* 2001, **194**:1721-1730.
200. Lantz O, Grandjean I, Matzinger P, Di Santo JP: **Gamma chain required for naive CD4+ T cell survival but not for antigen proliferation**. *Nat Immunol* 2000, **1**:54-58.
201. Mackall CL, Fry TJ, Gress RE: **Harnessing the biology of IL-7 for therapeutic application**. *Nat Rev Immunol* 2011, **11**:330-342.

202. Ploix C, Lo D, Carson MJ: **A ligand for the chemokine receptor CCR7 can influence the homeostatic proliferation of CD4 T cells and progression of autoimmunity**. *J Immunol* 2001, **167**:6724-6730.
203. Attridge K, Walker LS: **Homeostasis and function of regulatory T cells (Tregs) in vivo: lessons from TCR-transgenic Tregs**. *Immunol Rev* 2014, **259**:23-39.
204. Cho BK, Rao VP, Ge Q, Eisen HN, Chen J: **Homeostasis-stimulated proliferation drives naive T cells to differentiate directly into memory T cells**. *J Exp Med* 2000, **192**:549-556.
205. Tan JT, Ernst B, Kieper WC, LeRoy E, Sprent J, Surh CD: **Interleukin (IL)-15 and IL-7 jointly regulate homeostatic proliferation of memory phenotype CD8+ cells but are not required for memory phenotype CD4+ cells**. *J Exp Med* 2002, **195**:1523-1532.
206. Boyman O, Letourneau S, Krieg C, Sprent J: **Homeostatic proliferation and survival of naive and memory T cells**. *Eur J Immunol* 2009, **39**:2088-2094.
207. Murali-Krishna K, Lau LL, Sambhara S, Lemonnier F, Altman J, Ahmed R: **Persistence of memory CD8 T cells in MHC class I-deficient mice**. *Science* 1999, **286**:1377-1381.
208. Gudmundsdottir H, Turka LA: **A closer look at homeostatic proliferation of CD4+ T cells: costimulatory requirements and role in memory formation**. *J Immunol* 2001, **167**:3699-3707.
209. Murali-Krishna K, Ahmed R: **Cutting edge: naive T cells masquerading as memory cells**. *J Immunol* 2000, **165**:1733-1737.
210. Tchao NK, Turka LA: **Lymphodepletion and homeostatic proliferation: implications for transplantation**. *Am J Transplant* 2012, **12**:1079-1090.
211. McFarland RD, Douek DC, Koup RA, Picker LJ: **Identification of a human recent thymic emigrant phenotype**. *Proc Natl Acad Sci U S A* 2000, **97**:4215-4220.
212. Heeger PS, Greenspan NS, Kuhlenschmidt S, Dejelo C, Hricik DE, Schulak JA, Tary-Lehmann M: **Pretransplant frequency of donor-specific, IFN-gamma-producing lymphocytes is a manifestation of immunologic memory and correlates with the risk of posttransplant rejection episodes**. *J Immunol* 1999, **163**:2267-2275.
213. Padovan E, Casorati G, Dellabona P, Meyer S, Brockhaus M, Lanzavecchia A: **Expression of two T cell receptor alpha chains: dual receptor T cells**. *Science* 1993, **262**:422-424.
214. Adams AB, Williams MA, Jones TR, Shirasugi N, Durham MM, Kaech SM, Wherry EJ, Onami T, Lanier JG, Kokko KE, et al.: **Heterologous immunity provides a potent barrier to transplantation tolerance**. *J Clin Invest* 2003, **111**:1887-1895.
215. Montgomery RA, Cozzi E, West LJ, Warren DS: **Humoral immunity and antibody-mediated rejection in solid organ transplantation**. *Semin Immunol* 2011, **23**:224-234.
216. Resch T, Fabritius C, Ebner S, Ritschl P, Kotsch K: **The Role of Natural Killer Cells in Humoral Rejection**. *Transplantation* 2015, **99**:1335-1340.
217. Sun Q, Yang Y: **Late and chronic antibody-mediated rejection: main barrier to long term graft survival**. *Clin Dev Immunol* 2013, **2013**:859761.
218. Becker LE, Morath C, Suesal C: **Immune mechanisms of acute and chronic rejection**. *Clin Biochem* 2016, **49**:320-323.
219. Baldwin WM, III, Valujskikh A, Fairchild RL: **Mechanisms of antibody-mediated acute and chronic rejection of kidney allografts**. *Curr Opin Organ Transplant* 2016, **21**:7-14.
220. Smith RN, Colvin RB: **Chronic alloantibody mediated rejection**. *Semin Immunol* 2012, **24**:115-121.
221. Philogene MC, Jackson AM: **Non-HLA antibodies in transplantation: when do they matter?** *Curr Opin Organ Transplant* 2016, **21**:427-432.

222. Sicard A, Chen CC, Morelon E, Thaunat O: **Alloimmune-induced intragraft lymphoid neogenesis promotes B-cell tolerance breakdown that accelerates chronic rejection**. *Curr Opin Organ Transplant* 2016, **21**:368-374.
223. Merola J, Jane-wit DD, Pober JS: **Recent advances in allograft vasculopathy**. *Curr Opin Organ Transplant* 2017, **22**:1-7.
224. Subramanian V, Mohanakumar T: **Chronic rejection: a significant role for Th17-mediated autoimmune responses to self-antigens**. *Expert Rev Clin Immunol* 2012, **8**:663-672.
225. Djamali A, Kaufman DB, Ellis TM, Zhong W, Matas A, Samaniego M: **Diagnosis and management of antibody-mediated rejection: current status and novel approaches**. *Am J Transplant* 2014, **14**:255-271.
226. Schinstock CA, Stegall M, Cosio F: **New insights regarding chronic antibody-mediated rejection and its progression to transplant glomerulopathy**. *Curr Opin Nephrol Hypertens* 2014, **23**:611-618.
227. Schatz DG, Ji Y: **Recombination centres and the orchestration of V(D)J recombination**. *Nat Rev Immunol* 2011, **11**:251-263.
228. Bluestone JA: **Mechanisms of tolerance**. *Immunol Rev* 2011, **241**:5-19.
229. Metzger TC, Anderson MS: **Control of central and peripheral tolerance by Aire**. *Immunol Rev* 2011, **241**:89-103.
230. Daniely D, Kern J, Cebula A, Ignatowicz L: **Diversity of TCRs on natural Foxp3+ T cells in mice lacking Aire expression**. *J Immunol* 2010, **184**:6865-6873.
231. Zhao B, Chang L, Fu H, Sun G, Yang W: **The Role of Autoimmune Regulator (AIRE) in Peripheral Tolerance**. *J Immunol Res* 2018, **2018**:3930750.
232. Rudensky AY: **Regulatory T cells and Foxp3**. *Immunological Reviews* **241**:260-268.
233. Gershon RK, Kondo K: **Cell interactions in the induction of tolerance: the role of thymic lymphocytes**. *Immunology* 1970, **18**:723-737.
234. Gershon RK, Cohen P, Hencin R, Liebhaber SA: **Suppressor T cells**. *J Immunol* 1972, **108**:586-590.
235. Waksman BH: **Tolerance, the thymus, and suppressor T cells**. *Clin Exp Immunol* 1977, **28**:363-374.
236. Hutchinson IV: **Suppressor T cells in allogeneic models**. *Transplantation* 1986, **41**:547-555.
237. Dorf ME, Kuchroo VK, Collins M: **Suppressor T cells: some answers but more questions**. *Immunol Today* 1992, **13**:241-243.
238. Hall BM, Pearce NW, Gurley KE, Dorsch SE: **Specific unresponsiveness in rats with prolonged cardiac allograft survival after treatment with cyclosporine. III. Further characterization of the CD4+ suppressor cell and its mechanisms of action**. *J Exp Med* 1990, **171**:141-157.
239. Sakaguchi S, Fukuma K, Kuribayashi K, Masuda T: **Organ-specific autoimmune diseases induced in mice by elimination of T cell subset. I. Evidence for the active participation of T cells in natural self-tolerance; deficit of a T cell subset as a possible cause of autoimmune disease**. *J Exp Med* 1985, **161**:72-87.
240. Powrie F, Mason D: **OX-22high CD4+ T cells induce wasting disease with multiple organ pathology: prevention by the OX-22low subset**. *J Exp Med* 1990, **172**:1701-1708.
241. Sakaguchi S, Sakaguchi N, Asano M, Itoh M, Toda M: **Immunologic self-tolerance maintained by activated T cells expressing IL-2 receptor alpha-chains (CD25). Breakdown of a single mechanism of self-tolerance causes various autoimmune diseases**. *J Immunol* 1995, **155**:1151-1164.
242. Asano M, Toda M, Sakaguchi N, Sakaguchi S: **Autoimmune disease as a consequence of developmental abnormality of a T cell subpopulation**. *J Exp Med* 1996, **184**:387-396.

243. Thornton AM, Shevach EM: **CD4+CD25+ immunoregulatory T cells suppress polyclonal T cell activation in vitro by inhibiting interleukin 2 production**. *J Exp Med* 1998, **188**:287-296.
244. Takahashi T, Kuniyasu Y, Toda M, Sakaguchi N, Itoh M, Iwata M, Shimizu J, Sakaguchi S: **Immunologic self-tolerance maintained by CD25+CD4+ naturally anergic and suppressive T cells: induction of autoimmune disease by breaking their anergic/suppressive state**. *Int Immunol* 1998, **10**:1969-1980.
245. Baecher-Allan C, Brown JA, Freeman GJ, Hafler DA: **CD4+CD25high regulatory cells in human peripheral blood**. *J Immunol* 2001, **167**:1245-1253.
246. Dieckmann D, Plottner H, Berchtold S, Berger T, Schuler G: **Ex vivo isolation and characterization of CD4(+)CD25(+) T cells with regulatory properties from human blood**. *J Exp Med* 2001, **193**:1303-1310.
247. Jonuleit H, Schmitt E, Stassen M, Tuettenberg A, Knop J, Enk AH: **Identification and functional characterization of human CD4(+)CD25(+) T cells with regulatory properties isolated from peripheral blood**. *J Exp Med* 2001, **193**:1285-1294.
248. Ng WF, Duggan PJ, Ponchel F, Matarese G, Lombardi G, Edwards AD, Isaacs JD, Lechler RI: **Human CD4(+)CD25(+) cells: a naturally occurring population of regulatory T cells**. *Blood* 2001, **98**:2736-2744.
249. Taams LS, Smith J, Rustin MH, Salmon M, Poulter LW, Akbar AN: **Human anergic/suppressive CD4(+)CD25(+) T cells: a highly differentiated and apoptosis-prone population**. *Eur J Immunol* 2001, **31**:1122-1131.
250. Levings MK, Sangregorio R, Roncarolo MG: **Human CD25(+)CD4(+) t regulatory cells suppress naive and memory T cell proliferation and can be expanded in vitro without loss of function**. *J Exp Med* 2001, **193**:1295-1302.
251. Read S, Malmstrom V, Powrie F: **Cytotoxic T lymphocyte-associated antigen 4 plays an essential role in the function of CD25(+)CD4(+) regulatory cells that control intestinal inflammation**. *J Exp Med* 2000, **192**:295-302.
252. Takahashi T, Tagami T, Yamazaki S, Uede T, Shimizu J, Sakaguchi N, Mak TW, Sakaguchi S: **Immunologic self-tolerance maintained by CD25(+)CD4(+) regulatory T cells constitutively expressing cytotoxic T lymphocyte-associated antigen 4**. *J Exp Med* 2000, **192**:303-310.
253. Shimizu J, Yamazaki S, Takahashi T, Ishida Y, Sakaguchi S: **Stimulation of CD25(+)CD4(+) regulatory T cells through GITR breaks immunological self-tolerance**. *Nat Immunol* 2002, **3**:135-142.
254. Bushell A, Wood K: **GITR ligation blocks allograft protection by induced CD25+CD4+ regulatory T cells without enhancing effector T-cell function**. *Am J Transplant* 2007, **7**:759-768.
255. Ermann J, Hoffmann P, Edinger M, Dutt S, Blankenberg FG, Higgins JP, Negrin RS, Fathman CG, Strober S: **Only the CD62L+ subpopulation of CD4+CD25+ regulatory T cells protects from lethal acute GVHD**. *Blood* 2005, **105**:2220-2226.
256. Feng G, Wood KJ, Bushell A: **Interferon-gamma conditioning ex vivo generates CD25+CD62L+Foxp3+ regulatory T cells that prevent allograft rejection: potential avenues for cellular therapy**. *Transplantation* 2008, **86**:578-589.
257. Bennett CL, Christie J, Ramsdell F, Brunkow ME, Ferguson PJ, Whitesell L, Kelly TE, Saulsbury FT, Chance PF, Ochs HD: **The immune dysregulation, polyendocrinopathy, enteropathy, X-linked syndrome (IPEX) is caused by mutations of FOXP3**. *Nat Genet* 2001, **27**:20-21.

258. Godfrey VL, Wilkinson JE, Russell LB: **X-linked lymphoreticular disease in the scurfy (sf) mutant mouse**. *Am J Pathol* 1991, **138**:1379-1387.
259. Fontenot JD, Gavin MA, Rudensky AY: **Foxp3 programs the development and function of CD4+CD25+ regulatory T cells**. *Nat Immunol* 2003, **4**:330-336.
260. Hori S, Nomura T, Sakaguchi S: **Control of regulatory T cell development by the transcription factor Foxp3**. *Science* 2003, **299**:1057-1061.
261. Khattri R, Cox T, Yasayko SA, Ramsdell F: **An essential role for Scurfin in CD4+CD25+ T regulatory cells**. *Nat Immunol* 2003, **4**:337-342.
262. Battaglia M, Gregori S, Bacchetta R, Roncarolo M-G: **Tr1 cells: From discovery to their clinical application**. *Semin Immunol* 2006, **18**:120-127.
263. Carrier Y, Yuan J, Kuchroo VK, Weiner HL: **Th3 cells in peripheral tolerance. I. Induction of Foxp3-positive regulatory T cells by Th3 cells derived from TGF-beta T cell-transgenic mice**. *J Immunol* 2007, **178**:179-185.
264. Carrier Y, Yuan J, Kuchroo VK, Weiner HL: **Th3 cells in peripheral tolerance. II. TGF-beta-transgenic Th3 cells rescue IL-2-deficient mice from autoimmunity**. *J Immunol* 2007, **178**:172-178.
265. Sage PT, Sharpe AH: **T follicular regulatory cells**. *Immunol Rev* 2016, **271**:246-259.
266. Vuddamalay Y, van Meerwijk JP: **CD28- and CD28lowCD8+ Regulatory T Cells: Of Mice and Men**. *Front Immunol* 2017, **8**:31.
267. Thomson CW, Lee BP, Zhang L: **Double-negative regulatory T cells: non-conventional regulators**. *Immunol Res* 2006, **35**:163-178.
268. Kabelitz D, Peters C, Wesch D, Oberg H-H: **Regulatory functions of γδT cells**. *Int Immunopharmacol* 2013, **16**:382-387.
269. Rosser EC, Mauri C: **Regulatory B Cells: Origin, Phenotype, and Function**. *Immunity* 2015, **42**:607-612.
270. Berzins SP, Ritchie DS: **Natural killer T cells: drivers or passengers in preventing human disease?** *Nat Rev Immunol* 2014, **14**:640-646.
271. Lees JR, Azimzadeh AM, Bromberg JS: **Myeloid derived suppressor cells in transplantation**. *Curr Opin Immunol* 2011, **23**:692-697.
272. Casiraghi F, Noris M, Remuzzi G: **Immunomodulatory effects of mesenchymal stromal cells in solid organ transplantation**. *Curr Opin Organ Transplant* 2010, **15**:731-737.
273. Ligocki AJ, Niederkorn JY: **Advances on Non-CD4 + Foxp3+ T Regulatory Cells: CD8+, Type 1, and Double Negative T Regulatory Cells in Organ Transplantation**. *Transplantation* 2015, **99**:1553-1559.
274. Zhou X, Bailey-Bucktrout S, Jeker LT, Bluestone JA: **Plasticity of CD4(+) FoxP3(+) T cells**. *Curr Opin Immunol* 2009, **21**:281-285.
275. Lu L, Barbi J, Pan F: **The regulation of immune tolerance by FOXP3**. *Nat Rev Immunol* 2017, **17**:703-717.
276. Wu Y, Borde M, Heissmeyer V, Feuerer M, Lapan AD, Stroud JC, Bates DL, Guo L, Han A, Ziegler SF, et al.: **FOXP3 controls regulatory T cell function through cooperation with NFAT**. *Cell* 2006, **126**:375-387.
277. Ono M, Yaguchi H, Ohkura N, Kitabayashi I, Nagamura Y, Nomura T, Miyachi Y, Tsukada T, Sakaguchi S: **Foxp3 controls regulatory T-cell function by interacting with AML1/Runx1**. *Nature* 2007, **446**:685-689.
278. Li B, Samanta A, Song X, Iacono KT, Bembas K, Tao R, Basu S, Riley JL, Hancock WW, Shen Y, et al.: **FOXP3 interactions with histone acetyltransferase and class II histone deacetylases are required for repression**. *Proc Natl Acad Sci U S A* 2007, **104**:4571-4576.

279. Tao R, de Zoeten EF, Ozkaynak E, Chen C, Wang L, Porrett PM, Li B, Turka LA, Olson EN, Greene MI, et al.: **Deacetylase inhibition promotes the generation and function of regulatory T cells**. *Nat Med* 2007, **13**:1299-1307.
280. Zheng Y, Josefowicz S, Chaudhry A, Peng XP, Forbush K, Rudensky AY: **Role of conserved non-coding DNA elements in the Foxp3 gene in regulatory T-cell fate**. *Nature* 2010, **463**:808-812.
281. Tai X, Cowan M, Feigenbaum L, Singer A: **CD28 costimulation of developing thymocytes induces Foxp3 expression and regulatory T cell differentiation independently of interleukin 2**. *Nat Immunol* 2005, **6**:152-162.
282. Salomon B, Lenschow DJ, Rhee L, Ashourian N, Singh B, Sharpe A, Bluestone JA: **B7/CD28 costimulation is essential for the homeostasis of the CD4+CD25+ immunoregulatory T cells that control autoimmune diabetes**. *Immunity* 2000, **12**:431-440.
283. Thornton AM, Donovan EE, Piccirillo CA, Shevach EM: **Cutting edge: IL-2 is critically required for the in vitro activation of CD4+CD25+ T cell suppressor function**. *J Immunol* 2004, **172**:6519-6523.
284. Schlenner SM, Weigmann B, Ruan Q, Chen Y, von Boehmer H: **Smad3 binding to the foxp3 enhancer is dispensable for the development of regulatory T cells with the exception of the gut**. *J Exp Med* 2012, **209**:1529-1535.
285. O'Malley JT, Sehra S, Thieu VT, Yu Q, Chang HC, Stritesky GL, Nguyen ET, Mathur AN, Levy DE, Kaplan MH: **Signal transducer and activator of transcription 4 limits the development of adaptive regulatory T cells**. *Immunology* 2009, **127**:587-595.
286. Heidt S, Segundo DS, Chadha R, Wood KJ: **The impact of Th17 cells on transplant rejection and the induction of tolerance**. *Curr Opin Organ Transplant* 2010, **15**:456-461.
287. Smigiel KS, Srivastava S, Stolley JM, Campbell DJ: **Regulatory T-cell homeostasis: steady-state maintenance and modulation during inflammation**. *Immunol Rev* 2014, **259**:40-59.
288. Apostolou I, Verginis P, Kretschmer K, Polansky J, Huhn J, von Boehmer H: **Peripherally induced Treg: mode, stability, and role in specific tolerance**. *J Clin Immunol* 2008, **28**:619-624.
289. Weissler KA, Caton AJ: **The role of T-cell receptor recognition of peptide:MHC complexes in the formation and activity of Foxp3+ regulatory T cells**. *Immunol Rev* 2014, **259**:11-22.
290. Morikawa H, Sakaguchi S: **Genetic and epigenetic basis of Treg cell development and function: from a FoxP3-centered view to an epigenome-defined view of natural Treg cells**. *Immunol Rev* 2014, **259**:192-205.
291. Kerdiles YM, Stone EL, Beisner DR, McGargill MA, Ch'en IL, Stockmann C, Katayama CD, Hedrick SM: **Foxo transcription factors control regulatory T cell development and function**. *Immunity* 2010, **33**:890-904.
292. Luo CT, Li MO: **Transcriptional control of regulatory T cell development and function**. *Trends Immunol* 2013, **34**:531-539.
293. Sakaguchi S, Vignali DA, Rudensky AY, Niec RE, Waldmann H: **The plasticity and stability of regulatory T cells**. *Nat Rev Immunol* 2013, **13**:461-467.
294. Bettini ML, Vignali DA: **Development of thymically derived natural regulatory T cells**. *Ann N Y Acad Sci* 2010, **1183**:1-12.
295. Haljasorg U, Dooley J, Laan M, Kisand K, Bichele R, Liston A, Peterson P: **Irf4 Expression in Thymic Epithelium Is Critical for Thymic Regulatory T Cell Homeostasis**. *J Immunol* 2017.

296. Chen Z, Benoist C, Mathis D: **How defects in central tolerance impinge on a deficiency in regulatory T cells**. *Proc Natl Acad Sci U S A* 2005, **102**:14735-14740.
297. Liston A, Lesage S, Wilson J, Peltonen L, Goodnow CC: **Aire regulates negative selection of organ-specific T cells**. *Nat Immunol* 2003, **4**:350-354.
298. Hinterberger M, Aichinger M, Prazeres da Costa O, Voehringer D, Hoffmann R, Klein L: **Autonomous role of medullary thymic epithelial cells in central CD4(+) T cell tolerance**. *Nat Immunol* 2010, **11**:512-519.
299. Yang S, Fujikado N, Kolodin D, Benoist C, Mathis D: **Immune tolerance. Regulatory T cells generated early in life play a distinct role in maintaining self-tolerance**. *Science* 2015, **348**:589-594.
300. Kekalainen E, Lehto MK, Smeds E, Miettinen A, Meri S, Jarva H, Arstila TP: **Defective central tolerance in Aire-deficient mice is not sufficient to induce symptomatic autoimmunity during lymphopenia-induced T cell proliferation**. *Scand J Immunol* 2011, **74**:71-79.
301. Liang S, Alard P, Zhao Y, Parnell S, Clark SL, Kosiewicz MM: **Conversion of CD4+ CD25- cells into CD4+ CD25+ regulatory T cells in vivo requires B7 costimulation, but not the thymus**. *J Exp Med* 2005, **201**:127-137.
302. Kretschmer K, Apostolou I, Hawiger D, Khazaie K, Nussenzweig MC, von Boehmer H: **Inducing and expanding regulatory T cell populations by foreign antigen**. *Nat Immunol* 2005, **6**:1219-1227.
303. Gao W, Lu Y, El Essawy B, Oukka M, Kuchroo VK, Strom TB: **Contrasting effects of cyclosporine and rapamycin in de novo generation of alloantigen-specific regulatory T cells**. *Am J Transplant* 2007, **7**:1722-1732.
304. Qin S, Cobbold SP, Pope H, Elliott J, Kioussis D, Davies J, Waldmann H: **"Infectious" transplantation tolerance**. *Science* 1993, **259**:974-977.
305. Kendal AR, Chen Y, Regateiro FS, Ma J, Adams E, Cobbold SP, Hori S, Waldmann H: **Sustained suppression by Foxp3+ regulatory T cells is vital for infectious transplantation tolerance**. *J Exp Med* 2011, **208**:2043-2053.
306. Bluestone JA, Abbas AK: **Natural versus adaptive regulatory T cells**. *Nat Rev Immunol* 2003, **3**:253-257.
307. Horwitz DA, Zheng SG, Gray JD: **Natural and TGF-beta-induced Foxp3(+)CD4(+) CD25(+) regulatory T cells are not mirror images of each other**. *Trends Immunol* 2008, **29**:429-435.
308. Curotto de Lafaille MA, Lafaille JJ: **Natural and adaptive foxp3+ regulatory T cells: more of the same or a division of labor?** *Immunity* 2009, **30**:626-635.
309. Bilate AM, Lafaille JJ: **Induced CD4+Foxp3+ regulatory T cells in immune tolerance**. *Annu Rev Immunol* 2012, **30**:733-758.
310. Shevach EM, Thornton AM: **tTregs, pTregs, and iTregs: similarities and differences**. *Immunol Rev* 2014, **259**:88-102.
311. Thornton AM, Korty PE, Tran DQ, Wohlfert EA, Murray PE, Belkaid Y, Shevach EM: **Expression of Helios, an Ikaros transcription factor family member, differentiates thymic-derived from peripherally induced Foxp3+ T regulatory cells**. *J Immunol* 2010, **184**:3433-3441.
312. Singh K, Hjort M, Thorvaldson L, Sandler S: **Concomitant analysis of Helios and Neuropilin-1 as a marker to detect thymic derived regulatory T cells in naive mice**. *Sci Rep* 2015, **5**:7767.
313. Sugita K, Hanakawa S, Honda T, Kondoh G, Miyachi Y, Kabashima K, Nomura T: **Generation of Helios reporter mice and an evaluation of the suppressive capacity of Helios(+) regulatory T cells in vitro**. *Exp Dermatol* 2015, **24**:554-556.

314. Getnet D, Grosso JF, Goldberg MV, Harris TJ, Yen HR, Bruno TC, Durham NM, Hipkiss EL, Pyle KJ, Wada S, et al.: **A role for the transcription factor Helios in human CD4(+)CD25(+) regulatory T cells**. *Mol Immunol* 2010, **47**:1595-1600.
315. Zabransky DJ, Nirschl CJ, Durham NM, Park BV, Ceccato CM, Bruno TC, Tam AJ, Getnet D, Drake CG: **Phenotypic and functional properties of Helios+ regulatory T cells**. *PLoS One* 2012, **7**:e34547.
316. Takatori H, Kawashima H, Matsuki A, Meguro K, Tanaka S, Iwamoto T, Sanayama Y, Nishikawa N, Tamachi T, Ikeda K, et al.: **Helios Enhances Treg Cell Function in Cooperation With FoxP3**. *Arthritis Rheumatol* 2015, **67**:1491-1502.
317. Sebastian M, Lopez-Ocasio M, Metidji A, Rieder SA, Shevach EM, Thornton AM: **Helios Controls a Limited Subset of Regulatory T Cell Functions**. *J Immunol* 2016, **196**:144-155.
318. Akimova T, Beier UH, Wang L, Levine MH, Hancock WW: **Helios expression is a marker of T cell activation and proliferation**. *PLoS One* 2011, **6**:e24226.
319. Himmel ME, MacDonald KG, Garcia RV, Steiner TS, Levings MK: **Helios+ and Helios- cells coexist within the natural FOXP3+ T regulatory cell subset in humans**. *J Immunol* 2013, **190**:2001-2008.
320. Ross EM, Bourges D, Hogan TV, Gleeson PA, van Driel IR: **Helios defines T cells being driven to tolerance in the periphery and thymus**. *Eur J Immunol* 2014, **44**:2048-2058.
321. Elkord E, Abd Al Samid M, Chaudhary B: **Helios, and not FoxP3, is the marker of activated Tregs expressing GARP/LAP**. *Oncotarget* 2015, **6**:20026-20036.
322. Szurek E, Cebula A, Wojciech L, Pietrzak M, Rempala G, Kisielow P, Ignatowicz L: **Differences in Expression Level of Helios and Neuropilin-1 Do Not Distinguish Thymus-Derived from Extrathymically-Induced CD4+Foxp3+ Regulatory T Cells**. *PLoS One* 2015, **10**:e0141161.
323. Madakamutil LT, Maricic I, Sercarz EE, Kumar V: **Immunodominance in the TCR Repertoire of αTCR Peptide-Specific CD4$^+$ Treg Population That Controls Experimental Autoimmune Encephalomyelitis**. *J Immunol* 2008, **180**:4577-4585.
324. Huang H, Ma Y, Dawicki W, Zhang X, Gordon JR: **Comparison of induced versus natural regulatory T cells of the same TCR specificity for induction of tolerance to an environmental antigen**. *J Immunol* 2011, **191**:1136-1143.
325. Sakaguchi S, Sakaguchi N, Shimizu J, Yamazaki S, Sakihama T, Itoh M, Kuniyasu Y, Nomura T, Toda M, Takahashi T: **Immunologic tolerance maintained by CD25+ CD4+ regulatory T cells: their common role in controlling autoimmunity, tumor immunity, and transplantation tolerance**. *Immunol Rev* 2001, **182**:18-32.
326. Huang H, Ma Y, Dawicki W, Zhang X, Gordon JR: **Comparison of induced versus natural regulatory T cells of the same TCR specificity for induction of tolerance to an environmental antigen**. *J Immunol* 2013, **191**:1136-1143.
327. Karlsson F, Martinez NE, Gray L, Zhang S, Tsunoda I, Grisham MB: **Therapeutic evaluation of ex vivo-generated versus natural regulatory T-cells in a mouse model of chronic gut inflammation**. *Inflamm Bowel Dis* 2013, **19**:2282-2294.
328. Haribhai D, Williams JB, Jia S, Nickerson D, Schmitt EG, Edwards B, Ziegelbauer J, Yassai M, Li SH, Relland LM, et al.: **A requisite role for induced regulatory T cells in tolerance based on expanding antigen receptor diversity**. *Immunity* 2011, **35**:109-122.
329. Kong N, Lan Q, Chen M, Wang J, Shi W, Horwitz DA, Quesniaux V, Ryffel B, Liu Z, Brand D, et al.: **Antigen-specific transforming growth factor beta-induced Treg cells, but not natural Treg cells, ameliorate autoimmune arthritis in mice by shifting the Th17/Treg cell balance from Th17 predominance to Treg cell predominance**. *Arthritis Rheum* 2012, **64**:2548-2558.

330. Fu S, Zhang N, Yopp AC, Chen D, Mao M, Chen D, Zhang H, Ding Y, Bromberg JS: **TGF-beta induces Foxp3 + T-regulatory cells from CD4 + CD25 - precursors**. *Am J Transplant* 2004, **4**:1614-1627.
331. Fantini MC, Becker C, Tubbe I, Nikolaev A, Lehr HA, Galle P, Neurath MF: **Transforming growth factor beta induced FoxP3+ regulatory T cells suppress Th1 mediated experimental colitis**. *Gut* 2006, **55**:671-680.
332. Benson MJ, Pino-Lagos K, Rosemblatt M, Noelle RJ: **All-trans retinoic acid mediates enhanced T reg cell growth, differentiation, and gut homing in the face of high levels of co-stimulation**. *J Exp Med* 2007, **204**:1765-1774.
333. Singh AK, Horvath KA, Mohiuddin MM: **Rapamycin promotes the enrichment of CD4(+)CD25(hi)FoxP3(+) T regulatory cells from naive CD4(+) T cells of baboon that suppress antiporcine xenogenic response in vitro**. *Transplant Proc* 2009, **41**:418-421.
334. Taylor AL, Llewelyn MJ: **Superantigen-induced proliferation of human CD4+CD25- T cells is followed by a switch to a functional regulatory phenotype**. *J Immunol* 2010, **185**:6591-6598.
335. Karim M, Feng G, Wood KJ, Bushell AR: **CD25+CD4+ regulatory T cells generated by exposure to a model protein antigen prevent allograft rejection: antigen-specific reactivation in vivo is critical for bystander regulation**. *Blood* 2005, **105**:4871-4877.
336. Szymczak-Workman AL, Workman CJ, Vignali DA: **Cutting edge: regulatory T cells do not require stimulation through their TCR to suppress**. *J Immunol* 2009, **182**:5188-5192.
337. Churlaud G, Jimenez V, Ruberte J, Amadoudji Zin M, Fourcade G, Gottrand G, Casana E, Lambrecht B, Bellier B, Piaggio E, et al.: **Sustained stimulation and expansion of Tregs by IL2 control autoimmunity without impairing immune responses to infection, vaccination and cancer**. *Clin Immunol* 2014, **151**:114-126.
338. Bonnet B, Vigneron J, Levacher B, Vazquez T, Pitoiset F, Brimaud F, Churlaud G, Klatzmann D, Bellier B: **Low-Dose IL-2 Induces Regulatory T Cell-Mediated Control of Experimental Food Allergy**. *J Immunol* 2016, **197**:188-198.
339. Masteller EL, Tang Q, Bluestone JA: **Antigen-specific regulatory T cells-Ex vivo expansion and therapeutic potential**. *Semin Immunol* 2006, **18**:103-110.
340. Hall BM, Verma ND, Tran GT, Hodgkinson SJ: **Distinct regulatory CD4+T cell subsets; differences between naive and antigen specific T regulatory cells**. *Curr Opin Immunol* 2011, **23**:641-647.
341. Hoeppli RE, MacDonald KG, Levings MK, Cook L: **How antigen specificity directs regulatory T-cell function: self, foreign and engineered specificity**. *HLA* 2016, **88**:3-13.
342. Fisson S, Djelti F, Trenado A, Billiard F, Liblau R, Klatzmann D, Cohen JL, Salomon BL: **Therapeutic potential of self-antigen-specific CD4+ CD25+ regulatory T cells selected in vitro from a polyclonal repertoire**. *Eur J Immunol* 2006, **36**:817-827.
343. Wise MP, Bemelman F, Cobbold SP, Waldmann H: **Linked suppression of skin graft rejection can operate through indirect recognition**. *J Immunol* 1998, **161**:5813-5816.
344. Semple K, Yu Y, Wang D, Anasetti C, Yu XZ: **Efficient and selective prevention of GVHD by antigen-specific induced Tregs via linked-suppression in mice**. *Biol Blood Marrow Transplant* 2011, **17**:309-318.
345. Ito T, Yamada A, Batal I, Yeung MY, McGrath MM, Sayegh MH, Chandraker A, Ueno T: **The Limits of Linked Suppression for Regulatory T Cells**. *Front Immunol* 2016, **7**:82.
346. Kendal AR, Waldmann H: **Infectious tolerance: therapeutic potential**. *Curr Opin Immunol* 2010, **22**:560-565.
347. Sojka DK, Huang YH, Fowell DJ: **Mechanisms of regulatory T-cell suppression - a diverse arsenal for a moving target**. *Immunology* 2008, **124**:13-22.

348. Long ET, Baker S, Oliveira V, Sawitzki B, Wood KJ: **Alpha-1,2-Mannosidase and Hence N-Glycosylation Are Required for Regulatory T Cell Migration and Allograft Tolerance in Mice**. *PLoS ONE* 2010, **5**:e8894.
349. Siegmund K, Feuerer M, Siewert C, Ghani S, Haubold U, Dankof A, Krenn V, Schon MP, Scheffold A, Lowe JB, et al.: **Migration matters: regulatory T-cell compartmentalization determines suppressive activity in vivo**. *Blood* 2005, **106**:3097-3104.
350. Dieckmann D, Plottner H, Dotterweich S, Schuler G: **Activated CD4+ CD25+ T cells suppress antigen-specific CD4+ and CD8+ T cells but induce a suppressive phenotype only in CD4+ T cells**. *Immunology* 2005, **115**:305-314.
351. Frimpong-Boateng K, van Rooijen N, Geiben-Lynn R: **Regulatory T Cells Suppress Natural Killer Cells during Plasmid DNA Vaccination in Mice, Blunting the CD8+ T Cell Immune Response by the Cytokine TGF-**. *PLoS One* 2010, **5**:e12281.
352. La Cava A, Van Kaer L, Fu Dong S: **CD4+CD25+ Tregs and NKT cells: regulators regulating regulators**. *Trends Immunol* 2006, **27**:322-327.
353. Iikuni N, Lourenco EV, Hahn BH, La Cava A: **Cutting edge: Regulatory T cells directly suppress B cells in systemic lupus erythematosus**. *J Immunol* 2009, **183**:1518-1522.
354. Onishi Y, Fehervari Z, Yamaguchi T, Sakaguchi S: **Foxp3+ natural regulatory T cells preferentially form aggregates on dendritic cells in vitro and actively inhibit their maturation**. *Proc Natl Acad Sci U S A* 2008, **105**:10113-10118.
355. Yang J, Brook MO, Carvalho-Gaspar M, Zhang J, Ramon HE, Sayegh MH, Wood KJ, Turka LA, Jones ND: **Allograft rejection mediated by memory T cells is resistant to regulation**. *Proc Natl Acad Sci U S A* 2007, **104**:19954-19959.
356. Afzali B, Mitchell PJ, Scotta C, Canavan J, Edozie FC, Fazekasova H, Lord GM, John S, Barber LD, Hernandez-Fuentes MP, et al.: **Relative resistance of human CD4(+) memory T cells to suppression by CD4(+) CD25(+) regulatory T cells**. *Am J Transplant* 2011, **11**:1734-1742.
357. Kanai T, Tanimoto K, Nemoto Y, Fujii R, Makita S, Totsuka T, Watanabe M: **Naturally arising CD4+CD25+ regulatory T cells suppress the expansion of colitogenic CD4+CD44highCD62L- effector memory T cells**. *Am J Physiol Gastrointest Liver Physiol* 2006, **290**:G1051-1058.
358. Carvalho-Gaspar M, Jones ND, Luo S, Martin L, Brook MO, Wood KJ: **Location and time-dependent control of rejection by regulatory T cells culminates in a failure to generate memory T cells**. *J Immunol* 2008, **180**:6640-6648.
359. de Goer de Herve MG, Jaafoura S, Vallee M, Taoufik Y: **FoxP3(+) regulatory CD4 T cells control the generation of functional CD8 memory**. *Nat Commun* 2012, **3**:986.
360. Murakami M, Sakamoto A, Bender J, Kappler J, Marrack P: **CD25+CD4+ T cells contribute to the control of memory CD8+ T cells**. *Proc Natl Acad Sci U S A* 2002, **99**:8832-8837.
361. Dai Z, Li Q, Wang Y, Gao G, Diggs LS, Tellides G, Lakkis FG: **CD4+CD25+ regulatory T cells suppress allograft rejection mediated by memory CD8+ T cells via a CD30-dependent mechanism**. *J Clin Invest* 2004, **113**:310-317.
362. Tadokoro CE, Shakhar G, Shen S, Ding Y, Lino AC, Maraver A, Lafaille JJ, Dustin ML: **Regulatory T cells inhibit stable contacts between CD4+ T cells and dendritic cells in vivo**. *J Exp Med* 2006, **203**:505-511.
363. Tang Q, Adams JY, Tooley AJ, Bi M, Fife BT, Serra P, Santamaria P, Locksley RM, Krummel MF, Bluestone JA: **Visualizing regulatory T cell control of autoimmune responses in nonobese diabetic mice**. *Nat Immunol* 2006, **7**:83-92.
364. Shevach EM, McHugh RS, Piccirillo CA, Thornton AM: **Control of T-cell activation by CD4+ CD25+ suppressor T cells**. *Immunol Rev* 2001, **182**:58-67.

365. Sojka DK, Hughson A, Sukiennicki TL, Fowell DJ: **Early kinetic window of target T cell susceptibility to CD25+ regulatory T cell activity**. *J Immunol* 2005, **175**:7274-7280.
366. Sukiennicki TL, Fowell DJ: **Distinct molecular program imposed on CD4+ T cell targets by CD4+CD25+ regulatory T cells**. *J Immunol* 2006, **177**:6952-6961.
367. DiPaolo RJ, Glass DD, Bijwaard KE, Shevach EM: **CD4+CD25+ T cells prevent the development of organ-specific autoimmune disease by inhibiting the differentiation of autoreactive effector T cells**. *J Immunol* 2005, **175**:7135-7142.
368. Wing K, Onishi Y, Prieto-Martin P, Yamaguchi T, Miyara M, Fehervari Z, Nomura T, Sakaguchi S: **CTLA-4 control over Foxp3+ regulatory T cell function**. *Science* 2008, **322**:271-275.
369. Liang B, Workman C, Lee J, Chew C, Dale BM, Colonna L, Flores M, Li N, Schweighoffer E, Greenberg S, et al.: **Regulatory T cells inhibit dendritic cells by lymphocyte activation gene-3 engagement of MHC class II**. *J Immunol* 2008, **180**:5916-5926.
370. Puccetti P, Grohmann U: **IDO and regulatory T cells: a role for reverse signalling and non-canonical NF-kappaB activation**. *Nat Rev Immunol* 2007, **7**:817-823.
371. Fallarino F, Grohmann U: **Using an ancient tool for igniting and propagating immune tolerance: IDO as an inducer and amplifier of regulatory T cell functions**. *Curr Med Chem* 2011, **18**:2215-2221.
372. Reinwald S, Wiethe C, Westendorf AM, Breloer M, Probst-Kepper M, Fleischer B, Steinkasserer A, Buer J, Hansen W: **CD83 expression in CD4+ T cells modulates inflammation and autoimmunity**. *J Immunol* 2008, **180**:5890-5897.
373. Kreiser S, Eckhardt J, Kuhnt C, Stein M, Krzyzak L, Seitz C, Tucher C, Knippertz I, Becker C, Gunther C, et al.: **Murine CD83-positive T cells mediate suppressor functions in vitro and in vivo**. *Immunobiology* 2015, **220**:270-279.
374. Garin MI, Chu CC, Golshayan D, Cernuda-Morollon E, Wait R, Lechler RI: **Galectin-1: a key effector of regulation mediated by CD4+CD25+ T cells**. *Blood* 2007, **109**:2058-2065.
375. Grossman WJ, Verbsky JW, Barchet W, Colonna M, Atkinson JP, Ley TJ: **Human T regulatory cells can use the perforin pathway to cause autologous target cell death**. *Immunity* 2004, **21**:589-601.
376. Gondek DC, Lu LF, Quezada SA, Sakaguchi S, Noelle RJ: **Cutting edge: contact-mediated suppression by CD4+CD25+ regulatory cells involves a granzyme B-dependent, perforin-independent mechanism**. *J Immunol* 2005, **174**:1783-1786.
377. Daniel V, Sadeghi M, Wang H, Opelz G: **CD4+ CD25+ Foxp3+ IFNgamma+ CD178+ human induced Treg (iTreg) contribute to suppression of alloresponses by apoptosis of responder cells**. *Hum Immunol* 2013, **74**:151-162.
378. Li MO, Wan YY, Sanjabi S, Robertson AK, Flavell RA: **Transforming growth factor-beta regulation of immune responses**. *Annu Rev Immunol* 2006, **24**:99-146.
379. Asseman C, Mauze S, Leach MW, Coffman RL, Powrie F: **An essential role for interleukin 10 in the function of regulatory T cells that inhibit intestinal inflammation**. *J Exp Med* 1999, **190**:995-1004.
380. Whitehead GS, Wilson RH, Nakano K, Burch LH, Nakano H, Cook DN: **IL-35 production by inducible costimulator (ICOS)-positive regulatory T cells reverses established IL-17-dependent allergic airways disease**. *J Allergy Clin Immunol* 2012, **129**:207-215 e201-205.
381. Barthlott T, Moncrieffe H, Veldhoen M, Atkins CJ, Christensen J, O'Garra A, Stockinger B: **CD25+ CD4+ T cells compete with naive CD4+ T cells for IL-2 and exploit it for the induction of IL-10 production**. *Int Immunol* 2005, **17**:279-288.

382. Bopp T, Becker C, Klein M, Klein-Hessling S, Palmetshofer A, Serfling E, Heib V, Becker M, Kubach J, Schmitt S, et al.: **Cyclic adenosine monophosphate is a key component of regulatory T cell-mediated suppression**. *J Exp Med* 2007, **204**:1303-1310.
383. Deaglio S, Dwyer KM, Gao W, Friedman D, Usheva A, Erat A, Chen J-F, Enjyoji K, Linden J, Oukka M, et al.: **Adenosine generation catalyzed by CD39 and CD73 expressed on regulatory T cells mediates immune suppression**. *J Exp Med* 2007, **204**:1257-1265.
384. Walunas TL, Lenschow DJ, Bakker CY, Linsley PS, Freeman GJ, Green JM, Thompson CB, Bluestone JA: **CTLA-4 can function as a negative regulator of T cell activation**. *Immunity* 1994, **1**:405-413.
385. Krummel MF, Allison JP: **CD28 and CTLA-4 have opposing effects on the response of T cells to stimulation**. *J Exp Med* 1995, **182**:459-465.
386. Tivol EA, Borriello F, Schweitzer AN, Lynch WP, Bluestone JA, Sharpe AH: **Loss of CTLA-4 leads to massive lymphoproliferation and fatal multiorgan tissue destruction, revealing a critical negative regulatory role of CTLA-4**. *Immunity* 1995, **3**:541-547.
387. Waterhouse P, Penninger JM, Timms E, Wakeham A, Shahinian A, Lee KP, Thompson CB, Griesser H, Mak TW: **Lymphoproliferative disorders with early lethality in mice deficient in Ctla-4**. *Science* 1995, **270**:985-988.
388. Bachmann MF, Kohler G, Ecabert B, Mak TW, Kopf M: **Cutting edge: lymphoproliferative disease in the absence of CTLA-4 is not T cell autonomous**. *J Immunol* 1999, **163**:1128-1131.
389. Homann D, Dummer W, Wolfe T, Rodrigo E, Theofilopoulos AN, Oldstone MB, von Herrath MG: **Lack of intrinsic CTLA-4 expression has minimal effect on regulation of antiviral T-cell immunity**. *J Virol* 2006, **80**:270-280.
390. Davis PM, Nadler SG, Stetsko DK, Suchard SJ: **Abatacept modulates human dendritic cell-stimulated T-cell proliferation and effector function independent of IDO induction**. *Clin Immunol* 2008, **126**:38-47.
391. Carman JA, Davis PM, Yang WP, Zhu J, Chang H, He A, Truong A, Suchard SJ, Nadler SG: **Abatacept does not induce direct gene expression changes in antigen-presenting cells**. *J Clin Immunol* 2009, **29**:479-489.
392. Holmgaard RB, Zamarin D, Munn DH, Wolchok JD, Allison JP: **Indoleamine 2,3-dioxygenase is a critical resistance mechanism in antitumor T cell immunotherapy targeting CTLA-4**. *J Exp Med* 2013, **210**:1389-1402.
393. Qureshi OS, Zheng Y, Nakamura K, Attridge K, Manzotti C, Schmidt EM, Baker J, Jeffery LE, Kaur S, Briggs Z, et al.: **Trans-endocytosis of CD80 and CD86: a molecular basis for the cell-extrinsic function of CTLA-4**. *Science* 2011, **332**:600-603.
394. Wang CJ, Kenefeck R, Wardzinski L, Attridge K, Manzotti C, Schmidt EM, Qureshi OS, Sansom DM, Walker LSK: **Cutting Edge: Cell-Extrinsic Immune Regulation by CTLA-4 Expressed on Conventional T Cells**. *J Immunol* 2012, **189**:1118-1122.
395. Ansari AW, Khan MA, Schmidt RE, Broering DC: **Harnessing the immunotherapeutic potential of T-lymphocyte co-signaling molecules in transplantation**. *Immunol Lett* 2017, **183**:8-16.
396. Bardhan K, Anagnostou T, Boussiotis VA: **The PD1:PD-L1/2 Pathway from Discovery to Clinical Implementation**. *Front Immunol* 2016, **7**:550.
397. Ozkaynak E, Wang L, Goodearl A, McDonald K, Qin S, O'Keefe T, Duong T, Smith T, Gutierrez-Ramos JC, Rottman JB, et al.: **Programmed death-1 targeting can promote allograft survival**. *J Immunol* 2002, **169**:6546-6553.
398. Tao R, Wang L, Han R, Wang T, Ye Q, Honjo T, Murphy TL, Murphy KM, Hancock WW: **Differential effects of B and T lymphocyte attenuator and programmed death-1 on**

acceptance of partially versus fully MHC-mismatched cardiac allografts. *J Immunol* 2005, **175**:5774-5782.
399. Yang J, Popoola J, Khandwala S, Vadivel N, Vanguri V, Yuan X, Dada S, Guleria I, Tian C, Ansari MJ, et al.: **Critical role of donor tissue expression of programmed death ligand-1 in regulating cardiac allograft rejection and vasculopathy**. *Circulation* 2008, **117**:660-669.
400. Guo Y, Wang AY: **Novel Immune Check-Point Regulators in Tolerance Maintenance**. *Front Immunol* 2015, **6**:421.
401. Yamaura K, Watanabe T, Boenisch O, Yeung M, Yang S, Magee CN, Padera R, Datta S, Schatton T, Kamimura Y, et al.: **In vivo function of immune inhibitory molecule B7-H4 in alloimmune responses**. *Am J Transplant* 2010, **10**:2355-2362.
402. Leach DR, Krummel MF, Allison JP: **Enhancement of antitumor immunity by CTLA-4 blockade**. *Science* 1996, **271**:1734-1736.
403. Hodi FS, O'Day SJ, McDermott DF, Weber RW, Sosman JA, Haanen JB, Gonzalez R, Robert C, Schadendorf D, Hassel JC, et al.: **Improved survival with ipilimumab in patients with metastatic melanoma**. *N Engl J Med* 2010, **363**:711-723.
404. Eggermont AM, Chiarion-Sileni V, Grob JJ, Dummer R, Wolchok JD, Schmidt H, Hamid O, Robert C, Ascierto PA, Richards JM, et al.: **Prolonged Survival in Stage III Melanoma with Ipilimumab Adjuvant Therapy**. *N Engl J Med* 2016, **375**:1845-1855.
405. Pardoll DM: **The blockade of immune checkpoints in cancer immunotherapy**. *Nat Rev Cancer* 2012, **12**:252-264.
406. Topalian SL, Hodi FS, Brahmer JR, Gettinger SN, Smith DC, McDermott DF, Powderly JD, Carvajal RD, Sosman JA, Atkins MB, et al.: **Safety, activity, and immune correlates of anti-PD-1 antibody in cancer**. *N Engl J Med* 2012, **366**:2443-2454.
407. Brahmer JR, Tykodi SS, Chow LQ, Hwu WJ, Topalian SL, Hwu P, Drake CG, Camacho LH, Kauh J, Odunsi K, et al.: **Safety and activity of anti-PD-L1 antibody in patients with advanced cancer**. *N Engl J Med* 2012, **366**:2455-2465.
408. Topalian SL, Sznol M, McDermott DF, Kluger HM, Carvajal RD, Sharfman WH, Brahmer JR, Lawrence DP, Atkins MB, Powderly JD, et al.: **Survival, durable tumor remission, and long-term safety in patients with advanced melanoma receiving nivolumab**. *J Clin Oncol* 2014, **32**:1020-1030.
409. Postow MA, Chesney J, Pavlick AC, Robert C, Grossmann K, McDermott D, Linette GP, Meyer N, Giguere JK, Agarwala SS, et al.: **Nivolumab and ipilimumab versus ipilimumab in untreated melanoma**. *N Engl J Med* 2015, **372**:2006-2017.
410. Mason D, Powrie F: **Control of immune pathology by regulatory T cells**. *Curr Opin Immunol* 1998, **10**:649-655.
411. Sakaguchi S: **Regulatory T cells: key controllers of immunologic self-tolerance**. *Cell* 2000, **101**:455-458.
412. Shevach EM: **Regulatory T cells in autoimmmunity***. *Annu Rev Immunol* 2000, **18**:423-449.
413. Karim M, Bushell AR, Wood KJ: **Regulatory T cells in transplantation**. *Curr Opin Immunol* 2002, **14**:584-591.
414. Cohen JL, Salomon BL: **Therapeutic potential of CD4+ CD25+ regulatory T cells in allogeneic transplantation**. *Cytotherapy* 2005, **7**:166-170.
415. Bluestone JA: **Regulatory T-cell therapy: is it ready for the clinic?** *Nat Rev Immunol* 2005, **5**:343-349.
416. June CH, Blazar BR: **Clinical application of expanded CD4+25+ cells**. *Semin Immunol* 2006, **18**:78-88.

417. Waldmann H, Chen TC, Graca L, Adams E, Daley S, Cobbold S, Fairchild PJ: **Regulatory T cells in transplantation**. *Semin Immunol* 2006, **18**:111-119.
418. Roncarolo MG, Battaglia M: **Regulatory T-cell immunotherapy for tolerance to self antigens and alloantigens in humans**. *Nat Rev Immunol* 2007, **7**:585-598.
419. Sagoo P, Lombardi G, Lechler RI: **Regulatory T cells as therapeutic cells**. *Curr Opin Organ Transplant* 2008, **13**:645-653.
420. Feng G, Chan T, Wood KJ, Bushell A: **Donor reactive regulatory T cells**. *Curr Opin Organ Transplant* 2009, **14**:432-438.
421. Riley JL, June CH, Blazar BR: **Human T regulatory cell therapy: take a billion or so and call me in the morning**. *Immunity* 2009, **30**:656-665.
422. Bushell A, Jones E, Gallimore A, Wood K: **The generation of CD25+ CD4+ regulatory T cells that prevent allograft rejection does not compromise immunity to a viral pathogen**. *J Immunol* 2005, **174**:3290-3297.
423. Taylor PA, Lees CJ, Blazar BR: **The infusion of ex vivo activated and expanded CD4+CD25+ immune regulatory cells inhibits graft-versus-host disease lethality**. *Blood* 2002, **99**:3493-3499.
424. Hoffmann P, Eder R, Kunz-Schughart LA, Andreesen R, Edinger M: **Large-scale in vitro expansion of polyclonal human $CD4^{+}CD25^{high}$ regulatory T cells**. *Blood* 2004, **104**:895-903.
425. Zheng SG, Meng L, Wang JH, Watanabe M, Barr ML, Cramer DV, Gray JD, Horwitz DA: **Transfer of regulatory T cells generated ex vivo modifies graft rejection through induction of tolerogenic CD4+CD25+ cells in the recipient**. *Int Immunol* 2006, **18**:279-289.
426. Xia G, He J, Leventhal JR: **Ex vivo-expanded natural CD4+CD25+ regulatory T cells synergize with host T-cell depletion to promote long-term survival of allografts**. *Am J Transplant* 2008, **8**:298-306.
427. Joffre O, Santolaria T, Calise D, Al Saati T, Hudrisier D, Romagnoli P, van Meerwijk JP: **Prevention of acute and chronic allograft rejection with CD4+CD25+Foxp3+ regulatory T lymphocytes**. *Nat Med* 2008, **14**:88-92.
428. Tsang JY, Tanriver Y, Jiang S, Xue SA, Ratnasothy K, Chen D, Stauss HJ, Bucy RP, Lombardi G, Lechler R: **Conferring indirect allospecificity on CD4+CD25+ Tregs by TCR gene transfer favors transplantation tolerance in mice**. *J Clin Invest* 2008, **118**:3619-3628.
429. Tsang JY, Tanriver Y, Jiang S, Leung E, Ratnasothy K, Lombardi G, Lechler R: **Indefinite mouse heart allograft survival in recipient treated with CD4(+)CD25(+) regulatory T cells with indirect allospecificity and short term immunosuppression**. *Transpl Immunol* 2009, **21**:203-209.
430. Gliwinski M, Iwaszkiewicz-Grzes D, Trzonkowski P: **Cell-Based Therapies with T Regulatory Cells**. *BioDrugs* 2017, **31**:335-347.
431. Trzonkowski P, Bieniaszewska M, Juscinska J, Dobyszuk A, Krzystyniak A, Marek N, Mysliwska J, Hellmann A: **First-in-man clinical results of the treatment of patients with graft versus host disease with human ex vivo expanded CD4+CD25+CD127- T regulatory cells**. *Clin Immunol* 2009, **133**:22-26.
432. Romano M, Tung SL, Smyth LA, Lombardi G: **Treg therapy in transplantation: a general overview**. *Transpl Int* 2017, **30**:745-753.
433. Leslie M: **Immunology. Regulatory T cells get their chance to shine**. *Science* 2011, **332**:1020-1021.
434. Tang Q, Vincenti F: **Transplant trials with Tregs: perils and promises**. *J Clin Invest* 2017, **127**:2505-2512.

435. Zwang NA, Leventhal JR: **Cell Therapy in Kidney Transplantation: Focus on Regulatory T Cells**. *J Am Soc Nephrol* 2017, **28**:1960-1972.
436. Mathew JM, J HV, LeFever A, Konieczna I, Stratton C, He J, Huang X, Gallon L, Skaro A, Ansari MJ, et al.: **A Phase I Clinical Trial with Ex Vivo Expanded Recipient Regulatory T cells in Living Donor Kidney Transplants**. *Sci Rep* 2018, **8**:7428.
437. Feng S: **Spontaneous and induced tolerance for liver transplant recipients**. *Curr Opin Organ Transplant* 2016, **21**:53-58.
438. Todo S, Yamashita K, Goto R, Zaitsu M, Nagatsu A, Oura T, Watanabe M, Aoyagi T, Suzuki T, Shimamura T, et al.: **A pilot study of operational tolerance with a regulatory T-cell-based cell therapy in living donor liver transplantation**. *Hepatology* 2016, **64**:632-643.
439. Todo S, Yamashita K: **Anti-donor regulatory T cell therapy in liver transplantation**. *Hum Immunol* 2018, **79**:288-293.
440. Feng G, Gao W, Strom TB, Oukka M, Francis RS, Wood KJ, Bushell A: **Exogenous IFN-gamma ex vivo shapes the alloreactive T-cell repertoire by inhibition of Th17 responses and generation of functional Foxp3+ regulatory T cells**. *Eur J Immunol* 2008, **38**:2512-2527.
441. MiltenyiBiotec: **Treg Expansion Kit (mouse)**. *Product Data Sheet, Miltenyi Biotec GmbH, Bergisch Gladbach, Germany* 2010.
442. Kruisbeek AM, Shevach E, Thornton AM: **Proliferative Assays for T Cell Function**. In *Current Protocols in Immunology*. Edited by: John Wiley & Sons, Inc.; 2001.
443. Yamazaki S, Patel M, Harper A, Bonito A, Fukuyama H, Pack M, Tarbell KV, Talmor M, Ravetch JV, Inaba K, et al.: **Effective expansion of alloantigen-specific Foxp3+ CD25+ CD4+ regulatory T cells by dendritic cells during the mixed leukocyte reaction**. *Proc Natl Acad Sci U S A* 2006, **103**:2758-2763.
444. Raimondi G, Sumpter TL, Matta BM, Pillai M, Corbitt N, Vodovotz Y, Wang Z, Thomson AW: **Mammalian target of rapamycin inhibition and alloantigen-specific regulatory T cells synergize to promote long-term graft survival in immunocompetent recipients**. *J Immunol* 2010, **184**:624-636.
445. Bhattacharya P, Gopisetty A, Ganesh BB, Sheng JR, Prabhakar BS: **GM-CSF-induced, bone-marrow-derived dendritic cells can expand natural Tregs and induce adaptive Tregs by different mechanisms**. *J Leukoc Biol* 2011, **89**:235-249.
446. Jones ND, Turvey SE, Van Maurik A, Hara M, Kingsley CI, Smith CH, Mellor AL, Morris PJ, Wood KJ: **Differential susceptibility of heart, skin, and islet allografts to T cell-mediated rejection**. *J Immunol* 2001, **166**:2824-2830.
447. Martins PNA: **Assessment of graft function in rodent models of heart transplantation**. *Microsurgery* 2008, **28**:565-570.
448. Warnecke G, Feng G, Goto R, Nadig SN, Francis R, Wood KJ, Bushell A: **CD4+ regulatory T cells generated in vitro with IFN-{gamma} and allogeneic APC inhibit transplant arteriosclerosis**. *Am J Pathol* 2010, **177**:464-472.
449. Riella LV, Liu T, Yang J, Chock S, Shimizu T, Mfarrej B, Batal I, Xiao X, Sayegh MH, Chandraker A: **Deleterious effect of CTLA4-Ig on a Treg-dependent transplant model**. *Am J Transplant* 2012, **12**:846-855.
450. Kingsley CI, Karim M, Bushell AR, Wood KJ: **CD25+CD4+ regulatory T cells prevent graft rejection: CTLA-4- and IL-10-dependent immunoregulation of alloresponses**. *J Immunol* 2002, **168**:1080-1086.
451. Feng G, Nadig SN, Backdahl L, Beck S, Francis RS, Schiopu A, Whatcott A, Wood KJ, Bushell A: **Functional regulatory T cells produced by inhibiting cyclic nucleotide phosphodiesterase type 3 prevent allograft rejection**. *Sci Transl Med* 2011, **3**:83ra40.

452. Chai JG, Tsang JY, Lechler R, Simpson E, Dyson J, Scott D: **CD4+CD25+ T cells as immunoregulatory T cells in vitro**. *Eur J Immunol* 2002, **32**:2365-2375.
453. Godfrey WR, Ge YG, Spoden DJ, Levine BL, June CH, Blazar BR, Porter SB: **In vitro-Expanded human CD4^{+}CD25^{+} T-regulatory cells can markedly inhibit allogeneic dendritic cell-stimulated MLR cultures**. *Blood* 2004, **104**:453-461.
454. Zheng SG, Gray JD, Ohtsuka K, Yamagiwa S, Horwitz DA: **Generation ex vivo of TGF-beta-producing regulatory T cells from CD4+CD25- precursors**. *J Immunol* 2002, **169**:4183-4189.
455. Peters JH, Hilbrands LB, Koenen HJ, Joosten I: **Ex vivo generation of human alloantigen-specific regulatory T cells from CD4(pos)CD25(high) T cells for immunotherapy**. *PLoS One* 2008, **3**:e2233.
456. Turner MS, Kane LP, Morel PA: **Dominant role of antigen dose in CD4+Foxp3+ regulatory T cell induction and expansion**. *J Immunol* 2009, **183**:4895-4903.
457. Thomson AW, Turnquist HR, Zahorchak AF, Raimondi G: **Tolerogenic dendritic cell-regulatory T-cell interaction and the promotion of transplant tolerance**. *Transplantation* 2009, **87**:S86-90.
458. Landwehr-Kenzel S, Issa F, Luu SH, Schmuck M, Lei H, Zobel A, Thiel A, Babel N, Wood K, Volk HD, et al.: **Novel GMP-compatible protocol employing an allogeneic B cell bank for clonal expansion of allospecific natural regulatory T cells**. *Am J Transplant* 2014, **14**:594-606.
459. Litjens NH, Boer K, Zuijderwijk JM, Klepper M, Peeters AM, Prens EP, Verschoor W, Kraaijeveld R, Ozgur Z, van den Hout-van Vroonhoven MC, et al.: **Allogeneic Mature Human Dendritic Cells Generate Superior Alloreactive Regulatory T Cells in the Presence of IL-15**. *J Immunol* 2015, **194**:5282-5293.
460. Zeiser R, Nguyen VH, Beilhack A, Buess M, Schulz S, Baker J, Contag CH, Negrin RS: **Inhibition of CD4+CD25+ regulatory T-cell function by calcineurin-dependent interleukin-2 production**. *Blood* 2006, **108**:390-399.
461. Wekerle T: **T-regulatory cells-what relationship with immunosuppressive agents?** *Transplant Proc* 2008, **40**:S13-16.
462. San Segundo D, Fernandez-Fresnedo G, Gago M, Beares I, Ruiz-Criado J, Gonzalez M, Ruiz JC, Gomez-Alamillo C, Arias M, Lopez-Hoyos M: **Number of peripheral blood regulatory T cells and lymphocyte activation at 3 months after conversion to mTOR inhibitor therapy**. *Transplant Proc* 2010, **42**:2871-2873.
463. Carroll RP, Hester J, Wood KJ, Harden PN: **Conversion to sirolimus in kidney transplant recipients with squamous cell cancer and changes in immune phenotype**. *Nephrol Dial Transplant* 2013, **28**:462-465.
464. Charbonnier LM, Vokaer B, Lemaitre PH, Field KA, Leo O, Le Moine A: **CTLA4-Ig restores rejection of MHC class-II mismatched allografts by disabling IL-2-expanded regulatory T cells**. *Am J Transplant* 2012, **12**:2313-2321.
465. Caridade M, Graca L, Ribeiro RM: **Mechanisms Underlying CD4+ Treg Immune Regulation in the Adult: From Experiments to Models**. *Front Immunol* 2013, **4**:378.
466. Vignali DA, Collison LW, Workman CJ: **How regulatory T cells work**. *Nat Rev Immunol* 2008, **8**:523-532.
467. Schmetterer KG, Neunkirchner A, Pickl WF: **Naturally occurring regulatory T cells: markers, mechanisms, and manipulation**. *FASEB J* 2012, **26**:2253-2276.
468. Walker LS: **Treg and CTLA-4: two intertwining pathways to immune tolerance**. *J Autoimmun* 2013, **45**:49-57.

469. Alegre ML, Noel PJ, Eisfelder BJ, Chuang E, Clark MR, Reiner SL, Thompson CB: **Regulation of surface and intracellular expression of CTLA4 on mouse T cells**. *J Immunol* 1996, **157**:4762-4770.
470. Juvet SC, Sanderson S, Hester J, Wood KJ, Bushell A: **Quantification of CD4(+) T Cell Alloreactivity and Its Control by Regulatory T Cells Using Time-Lapse Microscopy and Immune Synapse Detection**. *Am J Transplant* 2016, **16**:1394-1407.
471. Juvet SC, Moshkelgosha S, Sanderson S, Hester J, Wood KJ, Bushell A: **Measurement of T Cell Alloreactivity Using Imaging Flow Cytometry**. *J Vis Exp* 2017.
472. Waldmann H, Cobbold S: **How do monoclonal antibodies induce tolerance? A role for infectious tolerance?** *Annu Rev Immunol* 1998, **16**:619-644.
473. Kinnear G, Wood KJ, Fallah-Arani F, Jones ND: **A diametric role for OX40 in the response of effector/memory CD4+ T cells and regulatory T cells to alloantigen**. *J Immunol* 2013, **191**:1465-1475.
474. Wang L, Han R, Hancock WW: **Programmed cell death 1 (PD-1) and its ligand PD-L1 are required for allograft tolerance**. *Eur J Immunol* 2007, **37**:2983-2990.
475. Tanaka K, Albin MJ, Yuan X, Yamaura K, Habicht A, Murayama T, Grimm M, Waaga AM, Ueno T, Padera RF, et al.: **PDL1 is required for peripheral transplantation tolerance and protection from chronic allograft rejection**. *J Immunol* 2007, **179**:5204-5210.
476. del Rio ML, Buhler L, Gibbons C, Tian J, Rodriguez-Barbosa JI: **PD-1/PD-L1, PD-1/PD-L2, and other co-inhibitory signaling pathways in transplantation**. *Transpl Int* 2008, **21**:1015-1028.
477. Gao W, Demirci G, Strom TB, Li XC: **Stimulating PD-1-negative signals concurrent with blocking CD154 co-stimulation induces long-term islet allograft survival**. *Transplantation* 2003, **76**:994-999.
478. Truong W, Plester JC, Hancock WW, Merani S, Murphy TL, Murphy KM, Kaye J, Anderson CC, Shapiro AM: **Combined coinhibitory and costimulatory modulation with anti-BTLA and CTLA4Ig facilitates tolerance in murine islet allografts**. *Am J Transplant* 2007, **7**:2663-2674.
479. Hara M, Kingsley CI, Niimi M, Read S, Turvey SE, Bushell AR, Morris PJ, Powrie F, Wood KJ: **IL-10 Is Required for Regulatory T Cells to Mediate Tolerance to Alloantigens In Vivo**. *J Immunol* 2001, **166**:3789-3796.
480. Roncarolo MG, Gregori S, Battaglia M, Bacchetta R, Fleischhauer K, Levings MK: **Interleukin-10-secreting type 1 regulatory T cells in rodents and humans**. *Immunol Rev* 2006, **212**:28-50.
481. Allan SE, Broady R, Gregori S, Himmel ME, Locke N, Roncarolo MG, Bacchetta R, Levings MK: **CD4+ T-regulatory cells: toward therapy for human diseases**. *Immunol Rev* 2008, **223**:391-421.
482. Yao Y, Vent-Schmidt J, McGeough MD, Wong M, Hoffman HM, Steiner TS, Levings MK: **Tr1 Cells, but Not Foxp3+ Regulatory T Cells, Suppress NLRP3 Inflammasome Activation via an IL-10-Dependent Mechanism**. *J Immunol* 2015, **195**:488-497.
483. Mayer CT, Sparwasser T: **Assessing the suppressive activity of Foxp3(+) regulatory T cells**. *Methods Mol Biol* 2014, **1193**:85-96.
484. Azimi M, Aslani S, Mortezagholi S, Salek A, Javan MR, Rezaiemanesh A, Ghaedi M, Gholamzad M, Salehi E: **Identification, Isolation, and Functional Assay of Regulatory T Cells**. *Immunol Invest* 2016, **45**:584-602.
485. Brusko TM, Hulme MA, Myhr CB, Haller MJ, Atkinson MA: **Assessing the in vitro suppressive capacity of regulatory T cells**. *Immunol Invest* 2007, **36**:607-628.

486. Kataoka M, Margenthaler JA, Ku G, Eilers M, Flye MW: **"Infectious tolerance" develops after the spontaneous acceptance of Lewis-to-Dark Agouti rat liver transplants**. *Surgery* 2003, **134**:227-234.
487. Tang Q, Henriksen KJ, Bi M, Finger EB, Szot G, Ye J, Masteller EL, McDevitt H, Bonyhadi M, Bluestone JA: **In Vitro-Expanded Antigen-specific Regulatory T Cells Suppress Autoimmune Diabetes**. *J Exp Med* 2004, **199**:1455-1465.
488. Battaglia M, Stabilini A, Roncarolo MG: **Rapamycin selectively expands CD4+CD25+FoxP3+ regulatory T cells**. *Blood* 2005, **105**:4743-4748.
489. Tarbell KV, Yamazaki S, Olson K, Toy P, Steinman RM: **$CD25^+CD4^+$ T Cells, Expanded with Dendritic Cells Presenting a Single Autoantigenic Peptide, Suppress Autoimmune Diabetes**. *J Exp Med* 2004, **199**:1467-1477.
490. Nishimura E, Sakihama T, Setoguchi R, Tanaka K, Sakaguchi S: **Induction of antigen-specific immunologic tolerance by in vivo and in vitro antigen-specific expansion of naturally arising Foxp3+CD25+CD4+ regulatory T cells**. *Int Immunol* 2004, **16**:1189-1201.
491. Golshayan D, Jiang S, Tsang J, Garin MI, Mottet C, Lechler RI: **In vitro-expanded donor alloantigen-specific $CD4^+CD25^+$ regulatory T cells promote experimental transplantation tolerance**. *Blood* 2007, **109**:827-835.
492. Ma A, Qi S, Wang Z, Massicotte E, Dupuis M, Daloze P, Chen H: **Combined therapy of CD4+CD25+ regulatory T cells with low-dose sirolimus, but not calcineurin inhibitors, preserves suppressive function of regulatory T cells and prolongs allograft survival in mice**. *Int Immunopharmacol* 2009, **9**:553-563.
493. Matta BM, Lott JM, Mathews LR, Liu Q, Rosborough BR, Blazar BR, Turnquist HtR: **IL-33 Is an Unconventional Alarmin That Stimulates IL-2 Secretion by Dendritic Cells To Selectively Expand IL-33R/$ST2^+$ Regulatory T Cells**. *J Immunol* 2014, **193**:4010-4020.
494. Moore C, Tejon G, Fuentes C, Hidalgo Y, Bono MR, Maldonado P, Fernandez R, Wood KJ, Fierro JA, Rosemblatt M, et al.: **Alloreactive regulatory T cells generated with retinoic acid prevent skin allograft rejection**. *Eur J Immunol* 2015, **45**:452-463.
495. Matta BM, Turnquist HtR: **Expansion of Regulatory T Cells In Vitro and In Vivo by IL-33**. In *Suppression and Regulation of Immune Responses: Methods and Protocols, Volume II*. Edited by Cuturi MC, Anegon I: Springer New York; 2016:29-41.
496. Levings MK, Sangregorio R, Roncarolo M-G: **Human $CD25^+CD4^+$ T Regulatory Cells Suppress Naive and Memory T Cell Proliferation and Can Be Expanded in Vitro without Loss of Function**. *The Journal of Experimental Medicine* 2001, **193**:1295-1302.
497. Earle KE, Tang Q, Zhou X, Liu W, Zhu S, Bonyhadi ML, Bluestone JA: **In vitro expanded human CD4+CD25+ regulatory T cells suppress effector T cell proliferation**. *Clinical Immunology* 2005, **115**:3-9.
498. Peters JH, Hilbrands LB, Koenen HJPM, Joosten I: **Ex Vivo Generation of Human Alloantigen-Specific Regulatory T Cells from CD4posCD25high T Cells for Immunotherapy**. *PLOS ONE* 2008, **3**:e2233.
499. Peters JH, Preijers FW, Woestenenk R, Hilbrands LB, Koenen HJPM, Joosten I: **Clinical Grade Treg: GMP Isolation, Improvement of Purity by CD127pos Depletion, Treg Expansion, and Treg Cryopreservation**. *PLoS One* 2008, **3**:e3161.
500. Nadig SN, Wieckiewicz J, Wu DC, Warnecke G, Zhang W, Luo S, Schiopu A, Taggart DP, Wood KJ: **In vivo prevention of transplant arteriosclerosis by ex vivo-expanded human regulatory T cells**. *Nat Med* 2010, **16**:809-813.
501. Wu DC, Hester J, Nadig SN, Zhang W, Trzonkowski P, Gray D, Hughes S, Johnson P, Wood KJ: **Ex Vivo Expanded Human Regulatory T Cells Can Prolong Survival of a Human Islet Allograft in a Humanized Mouse Model**. *Transplantation* 2013, **96**:707-716.

502. Issa F, Hester J, Goto R, Nadig S, Goodacre TE, Wood K: **Ex vivo-expanded human regulatory T cells prevent the rejection of skin allografts in a humanised mouse model()**. *Transplantation* 2010, **90**:1321-1327.
503. Invitrogen: **Dynabeads® Mouse CD3/CD28 T cell Expander**. *Product Datasheet, Invitrogen Dnyal AS, Oslo, Norway* 2008.
504. Masteller EL, Warner MR, Tang Q, Tarbell KV, McDevitt H, Bluestone JA: **Expansion of functional endogenous antigen-specific CD4+CD25+ regulatory T cells from nonobese diabetic mice**. *J Immunol* 2005, **175**:3053-3059.
505. Ring S, Thome M, Pretsch L, Enk AH, Mahnke K: **Expanded murine regulatory T cells: Analysis of phenotype and function in contact hypersensitivity reactions**. *J Immunol Methods* 2007, **326**:10-21.
506. Liu C, Wang Q, Liu F, Li H, Zhu F, Wang X, Guo C, Ma C, Zhang L: **The allogeneic but not syngeneic dendritic cells effectively generated regulatory T cells from total CD4+ population without exogenous cytokines**. *Scand J Immunol* 2010, **71**:12-19.
507. Inaba K, Inaba M, Romani N, Aya H, Deguchi M, Ikehara S, Muramatsu S, Steinman RM: **Generation of large numbers of dendritic cells from mouse bone marrow cultures supplemented with granulocyte/macrophage colony-stimulating factor**. *J Exp Med* 1992, **176**:1693-1702.
508. Smith KA: **T-Cell Growth Factor**. *Immunol Rev* 1980, **51**:337-357.
509. Kilburn DG, Anaka R: **Antigen-specific helper factors present in the supernatant of concanavalin A-induced spleen cell cultures**. *J Immunol* 1981, **127**:702-705.
510. Kohama Y, Shinoda S, Hagihara K, Hashimoto T, Yamaguchi A, Nakamura A, Tsuchiya T, Tsujikawa K, Yamamoto H: **Isolation of proliferation factor of immature T-cell clone in concanavalin A-stimulated splenocyte culture supernatant**. *Immunology* 2003, **109**:209-216.
511. Beeton C, Chandy KG: **Preparing T Cell Growth Factor from Rat Splenocytes**. *J Vis Exp* 2007:402.
512. Sredni B, Kalechman Y, Michlin H, Rozenszajn LA: **Development of colonies in vitro of mitogen-stimulated mouse T lymphocytes**. *Nature* 1976, **259**:130-132.
513. Suntharalingam G, Perry MR, Ward S, Brett SJ, Castello-Cortes A, Brunner MD, Panoskaltsis N: **Cytokine storm in a phase 1 trial of the anti-CD28 monoclonal antibody TGN1412**. *N Engl J Med* 2006, **355**:1018-1028.
514. Kenter MJ, Cohen AF: **Establishing risk of human experimentation with drugs: lessons from TGN1412**. *Lancet* 2006, **368**:1387-1391.
515. Elkord E: **Frequency of human T regulatory cells in peripheral blood is significantly reduced by cryopreservation**. *J Immunol Methods* 2009, **347**:87-90.
516. Daniele N, Scerpa MC, Landi F, Caniglia M, Miele MJ, Locatelli F, Isacchi G, Zinno F: **Treg cells: Collection, processing, storage and clinical use**. *Pathology - Research and Practice* 2010, **207**:209-215.
517. Van Hemelen D, Oude Elberink JN, Heimweg J, van Oosterhout AJ, Nawijn MC: **Cryopreservation does not alter the frequency of regulatory T cells in peripheral blood mononuclear cells**. *J Immunol Methods* 2010, **353**:138-140.
518. Florek M, Schneidawind D, Pierini A, Baker J, Armstrong R, Pan Y, Leveson-Gower D, Negrin R, Meyer E: **Freeze and Thaw of CD4+CD25+Foxp3+ Regulatory T Cells Results in Loss of CD62L Expression and a Reduced Capacity to Protect against Graft-versus-Host Disease**. *PLoS One* 2015, **10**:e0145763.

519. Suchin EJ, Langmuir PB, Palmer E, Sayegh MH, Wells AD, Turka LA: **Quantifying the frequency of alloreactive T cells in vivo: new answers to an old question**. *J Immunol* 2001, **166**:973-981.
520. Malek TR: **The biology of interleukin-2**. *Annu Rev Immunol* 2008, **26**:453-479.
521. Zheng SG, Wang J, Wang P, Gray JD, Horwitz DA: **IL-2 is essential for TGF-beta to convert naive CD4+CD25- cells to CD25+Foxp3+ regulatory T cells and for expansion of these cells**. *J Immunol* 2007, **178**:2018-2027.
522. Vang KB, Yang J, Mahmud SA, Burchill MA, Vegoe AL, Farrar MA: **IL-2, -7, and -15, but not thymic stromal lymphopoeitin, redundantly govern CD4+Foxp3+ regulatory T cell development**. *J Immunol* 2008, **181**:3285-3290.
523. Wuest TY, Willette-Brown J, Durum SK, Hurwitz AA: **The influence of IL-2 family cytokines on activation and function of naturally occurring regulatory T cells**. *J Leukoc Biol* 2008, **84**:973-980.
524. Mazzucchelli R, Hixon JA, Spolski R, Chen X, Li WQ, Hall VL, Willette-Brown J, Hurwitz AA, Leonard WJ, Durum SK: **Development of regulatory T cells requires IL-7Ralpha stimulation by IL-7 or TSLP**. *Blood* 2008, **112**:3283-3292.
525. Bayer AL, Lee JY, de la Barrera A, Surh CD, Malek TR: **A function for IL-7R for CD4+CD25+Foxp3+ T regulatory cells**. *J Immunol* 2008, **181**:225-234.
526. Fantini MC, Dominitzki S, Rizzo A, Neurath MF, Becker C: **In vitro generation of CD4+CD25+ regulatory cells from murine naive T cells**. *Nat Protocols* 2007, **2**:1789-1794.
527. Tacke M, Hanke G, Hanke T, Hunig T: **CD28-mediated induction of proliferation in resting T cells in vitro and in vivo without engagement of the T cell receptor: evidence for functionally distinct forms of CD28**. *Eur J Immunol* 1997, **27**:239-247.
528. Lin CH, Hunig T: **Efficient expansion of regulatory T cells in vitro and in vivo with a CD28 superagonist**. *Eur J Immunol* 2003, **33**:626-638.
529. Kitazawa Y, Fujino M, Li XK, Xie L, Ichimaru N, Okumi M, Nonomura N, Tsujimura A, Isaka Y, Kimura H, et al.: **Superagonist CD28 antibody preferentially expanded Foxp3-expressing nTreg cells and prevented graft-versus-host diseases**. *Cell Transplant* 2009, **18**:627-637.
530. Chen J, Xie L, Toyama S, Hunig T, Takahara S, Li XK, Zhong L: **The effects of Foxp3-expressing regulatory T cells expanded with CD28 superagonist antibody in DSS-induced mice colitis**. *Int Immunopharmacol* 2011, **11**:610-617.
531. Singh N, Yamamoto M, Takami M, Seki Y, Takezaki M, Mellor AL, Iwashima M: **$CD4^+CD25^+$ Regulatory T Cells Resist a Novel Form of CD28- and Fas-Dependent p53-Induced T Cell Apoptosis**. *J Immunol* 2010, **184**:94-104.
532. Thornton AM, Shevach EM: **Suppressor effector function of CD4+CD25+ immunoregulatory T cells is antigen nonspecific**. *J Immunol* 2000, **164**:183-190.
533. Li J, Bracht M, Shang X, Radewonuk J, Emmell E, Griswold DE, Li L: **Ex vivo activated OVA specific and non-specific CD4+CD25+ regulatory T cells exhibit comparable suppression to OVA mediated T cell responses**. *Cell Immunol* 2006, **241**:75-84.
534. Miyara M, Wing K, Sakaguchi S: **Therapeutic approaches to allergy and autoimmunity based on FoxP3+ regulatory T-cell activation and expansion**. *J Allergy Clin Immunol* 2009, **123**:749-755; quiz 756-747.
535. Chen X, Oppenheim JJ: **Resolving the identity myth: key markers of functional CD4+FoxP3+ regulatory T cells**. *Int Immunopharmacol* 2011, **11**:1489-1496.
536. Firan M, Dhillon S, Estess P, Siegelman MH: **Suppressor activity and potency among regulatory T cells is discriminated by functionally active CD44**. *Blood* 2006, **107**:619-627.

537. Bollyky PL, Falk BA, Long SA, Preisinger A, Braun KR, Wu RP, Evanko SP, Buckner JH, Wight TN, Nepom GT: **CD44 costimulation promotes FoxP3+ regulatory T cell persistence and function via production of IL-2, IL-10, and TGF-beta**. *J Immunol* 2009, **183**:2232-2241.
538. Allan SE, Crome SQ, Crellin NK, Passerini L, Steiner TS, Bacchetta R, Roncarolo MG, Levings MK: **Activation-induced FOXP3 in human T effector cells does not suppress proliferation or cytokine production**. *Int Immunol* 2007, **19**:345-354.
539. Pillai V, Ortega SB, Wang CK, Karandikar NJ: **Transient regulatory T-cells: A state attained by all activated human T-cells**. *Clin Immunol* 2007, **123**:18-29.
540. Wang J, Ioan-Facsinay A, van der Voort EI, Huizinga TW, Toes RE: **Transient expression of FOXP3 in human activated nonregulatory CD4+ T cells**. *Eur J Immunol* 2007, **37**:129-138.
541. Gottschalk RA, Corse E, Allison JP: **Expression of Helios in peripherally induced Foxp3+ regulatory T cells**. *J Immunol* 2012, **188**:976-980.
542. Bynoe MS, Viret C: **Foxp3+CD4+ T cell-mediated immunosuppression involves extracellular nucleotide catabolism**. *Trends Immunol* 2008, **29**:99-102.
543. Zhou Q, Yan J, Putheti P, Wu Y, Sun X, Toxavidis V, Tigges J, Kassam N, Enjyoji K, Robson SC, et al.: **Isolated CD39 expression on CD4+ T cells denotes both regulatory and memory populations**. *Am J Transplant* 2009, **9**:2303-2311.
544. Sauer AV, Brigida I, Carriglio N, Jofra Hernandez R, Scaramuzza S, Clavenna D, Sanvito F, Poliani PL, Gagliani N, Carlucci F, et al.: **Alterations in the adenosine metabolism and CD39/CD73 adenosinergic machinery cause loss of Treg cell function and autoimmunity in ADA-deficient SCID**. *Blood* 2012, **119**:1428-1439.
545. Fletcher JM, Lonergan R, Costelloe L, Kinsella K, Moran B, O'Farrelly C, Tubridy N, Mills KHG: **$CD39^{+}Foxp3^{+}$ Regulatory T Cells Suppress Pathogenic Th17 Cells and Are Impaired in Multiple Sclerosis**. *J Immunol* 2009, **183**:7602-7610.
546. Boenisch O, D'Addio F, Watanabe T, Elyaman W, Magee CN, Yeung MY, Padera RF, Rodig SJ, Murayama T, Tanaka K, et al.: **TIM-3: A Novel Regulatory Molecule of Alloimmune Activation**. *J Immunol* 2010, **185**:5806-5819.
547. Gautron AS, Dominguez-Villar M, de Marcken M, Hafler DA: **Enhanced suppressor function of TIM-3+ FoxP3+ regulatory T cells**. *Eur J Immunol* 2014, **44**:2703-2711.
548. Huang CT, Workman CJ, Flies D, Pan X, Marson AL, Zhou G, Hipkiss EL, Ravi S, Kowalski J, Levitsky HI, et al.: **Role of LAG-3 in regulatory T cells**. *Immunity* 2004, **21**:503-513.
549. Haudebourg T, Dugast AS, Coulon F, Usal C, Triebel F, Vanhove B: **Depletion of LAG-3 positive cells in cardiac allograft reveals their role in rejection and tolerance**. *Transplantation* 2007, **84**:1500-1506.
550. McHugh RS, Whitters MJ, Piccirillo CA, Young DA, Shevach EM, Collins M, Byrne MC: **CD4(+)CD25(+) immunoregulatory T cells: gene expression analysis reveals a functional role for the glucocorticoid-induced TNF receptor**. *Immunity* 2002, **16**:311-323.
551. Beeston T, Smith TR, Maricic I, Tang X, Kumar V: **Involvement of IFN-gamma and perforin, but not Fas/FasL interactions in regulatory T cell-mediated suppression of experimental autoimmune encephalomyelitis**. *J Neuroimmunol* 2010, **229**:91-97.
552. Cao X, Cai SF, Fehniger TA, Song J, Collins LI, Piwnica-Worms DR, Ley TJ: **Granzyme B and perforin are important for regulatory T cell-mediated suppression of tumor clearance**. *Immunity* 2007, **27**:635-646.
553. Scotta C, Fanelli G, Hoong SJ, Romano M, Lamperti EN, Sukthankar M, Guggino G, Fazekasova H, Ratnasothy K, Becker PD, et al.: **Impact of immunosuppressive drugs on the therapeutic efficacy of ex vivo expanded human regulatory T cells**. *Haematologica* 2016, **101**:91-100.

554. Hippen KL, Merkel SC, Schirm DK, Sieben CM, Sumstad D, Kadidlo DM, McKenna DH, Bromberg JS, Levine BL, Riley JL, et al.: **Massive ex vivo expansion of human natural regulatory T cells (T(regs)) with minimal loss of in vivo functional activity**. *Sci Transl Med* 2011, **3**:83ra41.
555. Golab K, Leveson-Gower D, Wang XJ, Grzanka J, Marek-Trzonkowska N, Krzystyniak A, Millis JM, Trzonkowski P, Witkowski P: **Challenges in cryopreservation of regulatory T cells (Tregs) for clinical therapeutic applications**. *Int Immunopharmacol* 2013, **16**:371-375.
556. Weinberg A, Song LY, Wilkening C, Sevin A, Blais B, Louzao R, Stein D, Defechereux P, Durand D, Riedel E, et al.: **Optimization and limitations of use of cryopreserved peripheral blood mononuclear cells for functional and phenotypic T-cell characterization**. *Clin Vaccine Immunol* 2009, **16**:1176-1186.
557. Hattori Y, Kato H, Nitta M, Takamoto S: **Decrease of L-selectin expression on human CD34+ cells on freeze-thawing and rapid recovery with short-term incubation**. *Exp Hematol* 2001, **29**:114-122.
558. Taylor PA, Panoskaltsis-Mortari A, Swedin JM, Lucas PJ, Gress RE, Levine BL, June CH, Serody JS, Blazar BR: **L-Selectin(hi) but not the L-selectin(lo) CD4+25+ T-regulatory cells are potent inhibitors of GVHD and BM graft rejection**. *Blood* 2004, **104**:3804-3812.
559. Levitsky J, Miller J, Huang X, Chandrasekaran D, Chen L, Mathew JM: **Inhibitory effects of belatacept on allospecific regulatory T-cell generation in humans**. *Transplantation* 2013, **96**:689-696.
560. Ahmadi SM, Holzl MA, Mayer E, Wekerle T, Heitger A: **CTLA4-Ig preserves thymus-derived T regulatory cells**. *Transplantation* 2014, **98**:1158-1164.
561. Vogel I, Verbinnen B, Maes W, Boon L, Van Gool SW, Ceuppens JL: **Foxp3+ regulatory T cells are activated in spite of B7-CD28 and CD40-CD40L blockade**. *Eur J Immunol* 2013, **43**:1013-1023.
562. Alvarez-Quiroga C, Abud-Mendoza C, Doniz-Padilla L, Juarez-Reyes A, Monsivais-Urenda A, Baranda L, Gonzalez-Amaro R: **CTLA-4-Ig therapy diminishes the frequency but enhances the function of Treg cells in patients with rheumatoid arthritis**. *J Clin Immunol* 2011, **31**:588-595.
563. Vogel I, Kasran A, Cremer J, Kim YJ, Boon L, Van Gool SW, Ceuppens JL: **CD28/CTLA-4/B7 costimulatory pathway blockade affects regulatory T-cell function in autoimmunity**. *Eur J Immunol* 2015, **45**:1832-1841.
564. Mayer E, Holzl M, Ahmadi S, Dillinger B, Pilat N, Fuchs D, Wekerle T, Heitger A: **CTLA4-Ig immunosuppressive activity at the level of dendritic cell/T cell crosstalk**. *Int Immunopharmacol* 2013, **15**:638-645.
565. Corry RJ, Winn HJ, Russell PS: **PRIMARILY VASCULARIZED ALLOGRAFTS OF HEARTS IN MICE: THE ROLE OF H-2D, H-2K, AND NON-H-2 ANTIGENS IN REJECTION**. *Transplantation* 1973, **16**:343-350.
566. Niimi M: **The technique for heterotopic cardiac transplantation in mice: experience of 3000 operations by one surgeon**. *J Heart Lung Transplant* 2001, **20**:1123-1128.
567. Plenter RJ, Zamora MR, Grazia TJ: **Four Decades of Vascularized Heterotopic Cardiac Transplantation in the Mouse**. *J Invest Surg* 2013, **26**:223-228.
568. Superina RA, Peugh WN, Wood KJ, Morris PS: **Assessment of primary vascularized cardiac allografts in mice**. *Transplantation* 1986, **42**:226-227.
569. Koizumi H, Konoeda Y, Kobayashi S, Koizumi H, Tamaki T, Tanioka Y: **Comparison of Methods to Evaluate Acute Rejection in Heterotopic Heart Transplantation in Rats**. *Experimental Animals* 1996, **45**:217-225.

570. Mottram PL, Smith JA, Mason A, Mirisklavos A, Dumble LJ, Clunie GJ: **Electrocardiographic monitoring of cardiac transplants in mice**. *Cardiovasc Res* 1988, **22**:315-321.
571. Scherrer-Crosbie M, Glysing-Jensen T, Fry SJ, Vançon A-C, Gadiraju S, Picard MH, Russell ME: **Echocardiography improves detection of rejection after heterotopic mouse cardiac transplantation**. *J Am Soc Echocardiol* 2002, **15**:1315-1320.
572. Zhou Y-Q, Bishay R, Feintuch A, Tao K, Golding F, Zhu W, West LJ, Henkelman RM: **Morphological and Functional Evaluation of Murine Heterotopic Cardiac Grafts Using Ultrasound Biomicroscopy**. *Ultrasound in Med and Biol* 2007, **33**:870-879.
573. Sasaguri S, LaRaia PJ, Fabri BM, Fallon JT, Ayelsworth CA, D'Ambra MN, Newell JB, Brady TJ, Buckley MJ: **Early detection of cardiac allograft rejection with proton nuclear magnetic resonance**. *Circulation* 1985, **72**:II231-236.
574. Aherne T, Tscholakoff D, Finkbeiner W, Sechtem U, Derugin N, Yee E, Higgins CB: **Magnetic resonance imaging of cardiac transplants: the evaluation of rejection of cardiac allografts with and without immunosuppression**. *Circulation* 1986, **74**:145-156.
575. Konstam MA, Aronovitz MJ, Runge VM, Kaufman DM, Brockway BA, Isner JM, Katzen NA, Dresdale AR, Diehl JT, Kaplan E, et al.: **Magnetic resonance imaging with gadolinium-DTPA for detecting cardiac transplant rejection in rats**. *Circulation* 1988, **78**:III87-94.
576. Penno E, Johansson L, Ahlstrom H, Johnsson C: **Ultrasmall iron oxide particle contrast agent and MRI can be used to monitor the effect of anti-rejection treatment**. *Transplantation* 2007, **84**:374-379.
577. Figueiredo JL, Nahrendorf M, Sosnovik DE, Weissleder R: **MRI of a novel murine working heart transplant model**. *Circ Heart Fail* 2009, **2**:272-274.
578. Armstrong AT, Strauch AR, Starling RC, Sedmak DD, Orosz CG: **MORPHOMETRIC ANALYSIS OF NEOINTIMAL FORMATION IN MURINE CARDIAC ALLOGRAFTS: II. Rate and Location of Lesion Development 1, 2**. *Transplantation* 1997, **64**:322-328.
579. Hirozane T, Matsumori A, Furukawa Y, Sasayama S: **Experimental Graft Coronary Artery Disease in a Murine Heterotopic Cardiac Transplant Model**. *Circulation* 1995, **91**:386-392.
580. Hasegawa T, Visovatti SH, Hyman MC, Hayasaki T, Pinsky DJ: **Heterotopic vascularized murine cardiac transplantation to study graft arteriopathy**. *Nat Protoc* 2007, **2**:471-480.
581. Armstrong AT, Strauch AR, Starling RC, Sedmak DD, Orosz CG: **MORPHOMETRIC ANALYSIS OF NEOINTIMAL FORMATION IN MURINE CARDIAC ALLOGRAFTS 1**. *Transplantation* 1997, **63**:941-947.
582. Schramm R, Menger MD, Kirsch S, Langer F, Harder Y, Hamacher J, Schafers H-J: **The subepicardial microcirculation in heterotopically transplanted mouse hearts: An intravital multifluorescence microscopy study**. *J Thoracic Cardiovas Surg* 2007, **134**:210-217.e211.
583. Tanaka M, Swijnenburg R-J, Gunawan F, Cao Y-A, Yang Y, Caffarelli AD, de Bruin JL, Contag CH, Robbins RC: **In Vivo Visualization of Cardiac Allograft Rejection and Trafficking Passenger Leukocytes Using Bioluminescence Imaging**. *Circulation* 2005, **112**:I-105-I-110.
584. Yoshida S, Dodd SJ, del Nido PJ, Williams DS, Ho C: **Cardiac function of transplanted rat hearts using a working heart model assessed by magnetic resonance imaging**. *J Heart Lung Transplant* 1999, **18**:1054-1064.
585. Wu YL, Ye Q, Sato K, Foley LM, Hitchens TK, Ho C: **Noninvasive evaluation of cardiac allograft rejection by cellular and functional cardiac magnetic resonance**. *JACC Cardiovasc Imaging* 2009, **2**:731-741.

586. Eugene M, Lechat P, Hadjiisky P, Teillac A, Grosgogeat Y, Cabrol C: **Nuclear magnetic resonance and proton relaxation times in experimental heterotopic heart transplantation**. *J Heart Transplant* 1986, **5**:39-45.
587. Tscholakoff D, Aherne T, Yee ES, Derugin N, Higgins CB: **Cardiac transplantations in dogs: evaluation with MR**. *Radiology* 1985, **157**:697-702.
588. Sasaki H, Sada M, Nishimura T, Yutani C, Nakatani H, Yaku H, Yamaguchi T, Kawazoe K, Amemiya H, Fujita T: **The expanded scope of effectiveness of nuclear magnetic resonance imaging to determine cardiac allograft rejection**. *Transplant Proc* 1987, **19**:1062-1064.
589. Nishimura T, Sada M, Sasaki H, Amemiya H, Kozuka T, Fujita T, Akutsu T, Manabe H: **Cardiac transplantation in dogs: evaluation with gated MRI and Gd-DTPA contrast enhancement**. *Heart Vessels* 1987, **3**:141-145.
590. Rozenman Y, Zou XM, Kantor HL: **Magnetic resonance imaging with superparamagnetic iron oxide particles for the detection of myocardial reperfusion**. *Magn Reson Imaging* 1991, **9**:933-939.
591. Kanno S, Wu YJ, Lee PC, Dodd SJ, Williams M, Griffith BP, Ho C: **Macrophage accumulation associated with rat cardiac allograft rejection detected by magnetic resonance imaging with ultrasmall superparamagnetic iron oxide particles**. *Circulation* 2001, **104**:934-938.
592. Ye Q, Wu YL, Foley LM, Hitchens TK, Eytan DF, Shirwan H, Ho C: **Longitudinal tracking of recipient macrophages in a rat chronic cardiac allograft rejection model with noninvasive magnetic resonance imaging using micrometer-sized paramagnetic iron oxide particles**. *Circulation* 2008, **118**:149-156.
593. Christen T, Nahrendorf M, Wildgruber M, Swirski FK, Aikawa E, Waterman P, Shimizu K, Weissleder R, Libby P: **Molecular imaging of innate immune cell function in transplant rejection**. *Circulation* 2009, **119**:1925-1932.
594. Fu X, Segiser A, Carrel TP, Tevaearai Stahel HT, Most H: **Rat Heterotopic Heart Transplantation Model to Investigate Unloading-Induced Myocardial Remodeling**. *Front Cardiovasc Med* 2016, **3**:34.
595. Cobbold SP, Martin G, Waldmann H: **The induction of skin graft tolerance in major histocompatibility complex-mismatched or primed recipients: primed T cells can be tolerized in the periphery with anti-CD4 and anti-CD8 antibodies**. *Eur J Immunol* 1990, **20**:2747-2755.
596. MacDonald KG, Hoeppli RE, Huang Q, Gillies J, Luciani DS, Orban PC, Broady R, Levings MK: **Alloantigen-specific regulatory T cells generated with a chimeric antigen receptor**. *J Clin Invest* 2016, **126**:1413-1424.
597. Managh AJ, Edwards SL, Bushell A, Wood KJ, Geissler EK, Hutchinson JA, Hutchinson RW, Reid HJ, Sharp BL: **Single cell tracking of gadolinium labeled CD4+ T cells by laser ablation inductively coupled plasma mass spectrometry**. *Anal Chem* 2013, **85**:10627-10634.
598. Bollyky JB, Long SA, Fitch M, Bollyky PL, Rieck M, Rogers R, Samuels PL, Sanda S, Buckner JH, Hellerstein MK, et al.: **Evaluation of in vivo T cell kinetics: use of heavy isotope labelling in type 1 diabetes**. *Clin Exp Immunol* 2013, **172**:363-374.
599. Gregori S, Passerini L, Roncarolo MG: **Clinical Outlook for Type-1 and FOXP3(+) T Regulatory Cell-Based Therapy**. *Front Immunol* 2015, **6**:593.
600. Progatzky F, Dallman MJ, Lo Celso C: **From seeing to believing: labelling strategies for in vivo cell-tracking experiments**. *Interface Focus* 2013, **3**:20130001.

601. Demirkiran A, Hendrikx TK, Baan CC, van der Laan LJ: **Impact of immunosuppressive drugs on CD4+CD25+FOXP3+ regulatory T cells: does in vitro evidence translate to the clinical setting?** *Transplantation* 2008, **85**:783-789.
602. Lim DG, Koo SK, Park YH, Kim Y, Kim HM, Park CS, Kim SC, Han DJ: **Impact of immunosuppressants on the therapeutic efficacy of in vitro-expanded CD4+CD25+Foxp3+ regulatory T cells in allotransplantation**. *Transplantation* 2010, **89**:928-936.
603. Wu T, Zhang L, Xu K, Sun C, Lei T, Peng J, Liu G, Wang R, Zhao Y: **Immunosuppressive drugs on inducing Ag-specific CD4(+)CD25(+)Foxp3(+) Treg cells during immune response in vivo**. *Transpl Immunol* 2012, **27**:30-38.
604. Furukawa A, Wisel SA, Tang Q: **Impact of Immune-Modulatory Drugs on Regulatory T Cell**. *Transplantation* 2016, **100**:2288-2300.
605. Putnam AL, Safinia N, Medvec A, Laszkowska M, Wray M, Mintz MA, Trotta E, Szot GL, Liu W, Lares A, et al.: **Clinical grade manufacturing of human alloantigen-reactive regulatory T cells for use in transplantation**. *Am J Transplant* 2013, **13**:3010-3020.
606. Landwehr-Kenzel S, Issa F, Luu SH, Schmück M, Lei H, Zobel A, Thiel A, Babel N, Wood K, Volk HD, et al.: **Novel GMP-Compatible Protocol Employing an Allogeneic B Cell Bank for Clonal Expansion of Allospecific Natural Regulatory T Cells**. *American Journal of Transplantation* 2014, **14**:594-606.
607. Figueroa JA, Reidy A, Mirandola L, Trotter K, Suvorava N, Figueroa A, Konala V, Aulakh A, Littlefield L, Grizzi F, et al.: **Chimeric antigen receptor engineering: a right step in the evolution of adoptive cellular immunotherapy**. *Int Rev Immunol* 2015, **34**:154-187.
608. Boardman DA, Philippeos C, Fruhwirth GO, Ibrahim MAA, Hannen RF, Cooper D, Marelli-Berg FM, Watt FM, Lechler RI, Maher J, et al.: **Expression of a Chimeric Antigen Receptor Specific for Donor HLA Class I Enhances the Potency of Human Regulatory T Cells in Preventing Human Skin Transplant Rejection**. *Am J Transplant* 2017, **17**:931-943.
609. Lee YK, Mukasa R, Hatton RD, Weaver CT: **Developmental plasticity of Th17 and Treg cells**. *Curr Opin Immunol* 2009, **21**:274-280.
610. Mitchell P, Afzali B, Lombardi G, Lechler RI: **The T helper 17-regulatory T cell axis in transplant rejection and tolerance**. *Curr Opin Organ Transplant* 2009, **14**:326-331.
611. Rudensky AY: **Regulatory T cells and Foxp3**. *Immunol Rev* 2011, **241**:260-268.
612. Floess S, Freyer J, Siewert C, Baron U, Olek S, Polansky J, Schlawe K, Chang HD, Bopp T, Schmitt E, et al.: **Epigenetic control of the foxp3 locus in regulatory T cells**. *PLoS Biol* 2007, **5**:e38.
613. Huehn J, Beyer M: **Epigenetic and transcriptional control of Foxp3+ regulatory T cells**. *Semin Immunol* 2015, **27**:10-18.
614. Tian Y, Jia Z, Wang J, Huang Z, Tang J, Zheng Y, Tang Y, Wang Q, Tian Z, Yang D, et al.: **Global mapping of H3K4me1 and H3K4me3 reveals the chromatin state-based cell type-specific gene regulation in human Treg cells**. *PLoS One* 2011, **6**:e27770.
615. He H, Ni B, Tian Y, Tian Z, Chen Y, Liu Z, Yang X, Lv Y, Zhang Y: **Histone methylation mediates plasticity of human FOXP3(+) regulatory T cells by modulating signature gene expressions**. *Immunology* 2014, **141**:362-376.